Low-Calcium Pyroxene - Melt Equilibria at 1 bar: An Experimental Study in Natural Systems.

Kathryn M. Dearing

Doctor of Philosophy
University of Edinburgh
1985

I declare that the work described in this thesis
is my own, except where otherwise stated.

ABSTRACT

Equilibrium experiments carried out at atmospheric pressure using 13 samples of boninitic composition have produced 80 new pairs of low-calcium pyroxene - glass analyses. Of the low-calcium pyroxenes 55 were orthopyroxene (Mg/(Mg+Fe)=0.66-0.86) and 25 were pigeonite (Mg/(Mg+Fe)=0.47-0.82); in addition 4 analyses of proto-pyroxene (Mg/(Mg+Fe)=0.85), inverted to clinoenststite, were obtained from disequilibrium experiments. These new analyses were combined with 111 pairs of low-calcium pyroxene - glass analyses taken from a literature search; of these low-calcium pyroxenes 34 were orthopyroxene (Mg/(Mg+Fe)=0.45-0.87) and 77 were pigeonite (Mg/(Mg+Fe)=0.27-0.85). These two data sets covered a temperature range of 300°C (1050-1350°C).

The new low-calcium pyroxene - glass data base was used to examine previously described low-calcium pyroxene - melt equilibria models. In all cases the orthopyroxene and pigeonite data were considered separately; this had not been the case in any of the original models, principally due to the lack of data. In addition new regular solution mixing models for both the low-calcium pyroxene and the liquid were tested. However, none of the regular solution models was particularly successful, probably because there are insufficient data for the accurate calculation of interaction parameters.

The model that best describes low-calcium pyroxene - melt equilibria is that using the modified Bottinga-Weill polymer melt model of Nielsen & Dungan (1983) and ideally mixing pyroxene components the site occupancy of which was determined by an adaptation of the method of Ghiorso et al. (1983). This model, used as a geothermometer, was able to reproduce the experimental temperatures of the data set to within 35°C (2σ) for orthopyroxene - liquid pairs and 57°C (2σ) for pigeonite - liquid pairs. Used as a liquidus temperature equation it was able to reproduce the experimental temperatures of the data set to within 30°C (2σ) for both orthopyroxene - and pigeonite - liquid pairs. At the same time it was able to reproduce the enstatite activity in the orthopyroxene to within 7.5% (2σ) and in the pigeonite to within 32% (2σ). For the other quadrilateral components the activities calculated were only within 50% (2σ) of the original values.

CONTENTS

CHAPTER 1

INTRODUCTION

The term low-calcium pyroxene is used to describe the four structurally and compositionally distinct pyroxenes containing less than 10 wt% CaO - protopyroxene, clinoenstatite, orthopyroxene and pigeonite. Protopyroxene has orthorhombic symmetry and is stable at high temperatures and Mg/(Mg+Fe) ratios, and low (<0.5 wt%) CaO contents. On cooling it often partially inverts to clinoenstatite which has monoclinic symmetry. Clinoenstatite is rarely found in rocks (e.g. Dallwitz et al., 1966; Hensen & Gray, 1979; Shiraki et al., 1980; Crawford, 1980). Orthopyroxene has orthorhombic symmetry and is stable over a wide range of Mg/(Mg+Fe) ratios, it may contain up to 3.5 wt% CaO. It is a common constituent of ultrabasic rocks and the cumulate sequences of layered basic intrusions. It is occasionally found as a phenocryst in volcanic rocks. Pigeonite has monoclinic symmetry and is stable over a wide range of Mg/(Mg+Fe) ratios but in rocks it is rarely more magnesian than Mg/(Mg+Fe) = 0.80. It may contain up to 10 wt% CaO, although if formed metastably, i.e. by rapid cooling, higher CaO contents are possible. It is a common constituent of the cumulate sequences of layered intrusions and is often found as a microphenocryst or groundmass constituent of volcanic rocks.

Although low-calcium pyroxenes are comparatively rare in terrestrial basalts they are important in the generation and subsequent evolution of basaltic magmas. Orthopyroxene is a major constituent of the ultramafic nodules brought up from the mantle by alkaline mafic lavas and kimberlites, and is the second most common mineral in the mantle (Wyllie, 1971, p120). Experimental studies have shown that large volumes of basaltic liquid can be generated by partial melting of lherzolite and peridotite between 20 and 35kb (Mysen & Kushiro, 1977; Scarfe et al., 1979) and that orthopyroxene is always present in the residue. At very high pressures (>35kb) orthopyroxene may be the liquidus phase in mantle compositions (Mysen & Kushiro, 1977).

Experimental studies of MORB have shown that with increasing pressure the orthopyroxene primary phase volume expands, principally at the expense of olivine (Stolper, 1980; Elthon & Scarfe, 1984). However, primitive MORB compositions never actually lie on the olivine + orthopyroxene cotectic (Stolper, 1980) and therefore must have evolved by fractionation from a parental liquid generated by partial melting in the mantle. Most MORBs lie close to the 1 atmosphere olivine + clinopyroxene + plagioclase cotectic and must therefore have undergone low pressure fractionation (Stolper, 1980). However, the most primitive MORBs lie close to the 10kb olivine + clinopyroxene + spinel cotectic which indicates that they may have undergone high pressure fractionation (Elthon & Scarfe, 1984). This is supported by the presence in some primitive basalts of an olivine + orthopyroxene + clinopyroxene + spinel invariant point at 10kb, which originally led to the hypothesis that basaltic liquids could be generated by partial melting of peridotite at 10kb (Fujii & Bougault, 1983). A more likely interpretation of these high pressure invariant points is that a basaltic liquid generated by partial melting between 20 and 35kb continually reequilibrates to lower pressure invariant points as it ascends (Elthon et al., 1982; Elthon & Scarfe, 1984). The presence of orthopyroxenes in the cumulate sequences of some ophiolite complexes (Cameron et al., 1979; Elthon et al., 1982) provides further evidence for their importance in the high pressure fractionation of basaltic liquids.

At low pressures low-calcium pyroxenes are found in large layered intrusions such as the Bushveld and Skaergaard, and in boninites. Boninites generally occur as lava flows (Dallwitz et al., 1966; Shiraki et al., 1980; Wood, 1980) but some intrusive equivalents are recognised (Crawford, 1980), they are also compositionally similar to proposed initial liquids for the large layered intrusions (Sharpe & Irvine, 1983). Boninites are characterised by high MgO, Cr and Ni, intermediate SiO_2 and low TiO_2, Al_2O_3, CaO and Na_2O. They contain phenocrysts of one or more varieties of pyroxene; in many cases all three high temperature low-calcium pyroxenes; some or all of which exhibit quench textures, in a glassy matrix. Magnesiochromite and minor amounts of olivine are common, amphibole or laths of plagioclase are rare. Major and trace element geochemistry suggest that boninites are primitive liquids derived by

partial melting of an incompatible-element-depleted lherzolite in the presence of a hydrous incompatible-element-enriched fluid derived from a subducting slab (Cameron et al., 1983). Although it is now recognised that the processes involved in the formation of layered intrusions are far more complex than the fractional crystallisation of a boninitic parental liquid, the ability to predict crystallisation sequences of parental liquids is still essential to the understanding of such intrusions as a whole (Irvine et al., 1983).

The modelling of the evolution of magmatic liquids by processes such as differentiation and fractionation has been approached in three ways. Initially experimental studies were carried out in simple synthetic systems containing the common igneous minerals (e.g. Bowen & Schairer, 1935; Kushiro, 1969). Secondly the behaviour of naturally occurring compositions have been studied, generally by determination of equilibrium phase relations (e.g. Tilley et al., 1964; Thompson, 1972). Recently the large amount of data generated by these experimental studies have been used to produce equations to describe the relationships between a liquid composition, the compositions of coexisting phases and the temperatures at which they are in equilibrium. In theory, given sufficient thermodynamic data, it would be possible to calculate the phase relations of a liquid under whatever pressure and temperature conditions were of interest. However, thermodynamic data and models, particularly regarding liquid behaviour, are not yet sufficient to adequately describe behaviour in natural systems although some progress has been made in simple synthetic systems (Berman & Brown, 1984).

Two types of model have been described in which the composition of a liquid in equilibrium with a given phase is related to temperature. French (1971), Nathan & Van Kirk (1978), Ford & Russell (1981) and French & Cameron (1981) used equations of the form:-

$$T°C = a_1X_1^L + a_2X_2^L + \ldots a_nX_n^L$$

where T°C is the temperature at which a crystalline phase (olivine for example) is in equilibrium with the liquid, a_1 to a_n are constants, different for each phase considered, produced by linear regression and X_1^L to X_n^L are the concentrations of the oxides (MgO,

SiO_2, etc) in the liquid. Roeder & Emslie (1970), Drake (1976), Nielsen & Drake (1979), Ford et al. (1983), Ghiorso et al. (1983), Nielsen & Dungan(1983) used equations of the form:-

$$\ln K = A/T + B$$

where A and B are the slope and intercept of a line fitted to the data by linear regression and K is a distribution coefficient, for example for the reaction:-

$$2MgO + SiO_2 = Mg_2SiO_4$$

$$K = \frac{a^{Ol}_{Mg_2SiO_4}}{(a^{L}_{MgO})^2(a^{L}_{SiO_2})}$$

where $a^{Ol}_{MgSiO_3}$, a^{L}_{MgO}, $a^{L}_{SiO_2}$ are the activities of the components ($MgSiO_3$ etc) in the phases of interest (Ol, L). Further details of the models are given in chapter 5.

In both types of model the constants are calculated by linear regression on a data base of analyses from experimental studies, in the first type of model it is only necessary to know the liquid composition and what phases are in equilibrium with it. In the second type of model it is necessary to have analyses of both the liquid and the phase under consideration, which must have attained equilibrium in the course of the experiment. Once equations have been produced for the phases of interest they are used to calculate the temperature at which the phases will first appear in a given liquid composition. The phase with the highest temperature of first appearance being the liquidus phase. With the second type of model the composition of the phase under consideration is also calculated and fractional crystallisation can be modelled by extracting small amounts of the liquidus phase from the liquid and recalculating the temperature and composition of the liquidus phase for the new liquid composition.

The ability of these models to accurately predict crystallisation sequences depends on the size and compositional range of the data base for the phases concerned. As the equations are

produced by fitting a line to the available data, extrapolation to compositions outwith the data base may lead to deviations from reality. Previously described low-calcium pyroxene - liquid equilibria models (Nathan & Van Kirk, 1978; Nielsen & Drake, 1979; Nielsen & Dungan, 1983; Ghiorso et al., 1983) have been based on data sets of less than 50 pairs of analyses, whereas olivine - and plagioclase - liquid equilibria models (e.g. Ford et al., 1983; Ghiorso et al.,1983) have been based on data sets of over 200 pairs of analyses. The principal reason for the comparative lack of low-calcium pyroxene - liquid data is that most melting studies have been concerned with the origins of basaltic samples which, as discussed above, do not often contain low-calcium pyroxenes at atmospheric pressure.

Experimental studies of low-calcium pyroxenes at atmospheric pressure have been carried out for over fifty years (Bowen & Schairer, 1935). Most of these studies have been in synthetic systems where advances are still being made; e.g. the occurrence of orthopyroxene as a liquidus phase in the system enstatite - diopside was not recognised until 1980 (Longhi & Boudreau, 1980). Partial melting studies of single pyroxene crystals separated from igneous and metamorphic rocks of terrestrial and lunar origin suggest a natural pyroxene phase diagram comparable to that of synthetic systems (Huebner & Turnock, 1980). Although low-calcium pyroxenes have occasionally been reported from experimental studies of natural systems, particularly in studies of lunar basalts (chapter 3.4, Basaltic Volcanism Study Project, 1981), no experimental study in natural systems has been aimed specifically at low-calcium pyroxenes.

The aims of this thesis were firstly to enlarge the low-calcium pyroxene - liquid data base and secondly to use this data, in conjunction with that available in the literature, to produce a model for low-calcium pyroxene - liquid equilibria at atmospheric pressure. Although an understanding of low-calcium pyroxene -liquid equilibria at elevated pressure is necessary to model the processes involved in the generation and evolution of basaltic liquids it is essential to define low-calcium pyroxene - liquid relationships at atmospheric pressure before considering the effects of increasing pressure. In order to obtain analyses of low-calcium pyroxene in

equilibrium with a liquid, samples of boninitic compostion were chosen for study as such compositions are most likely to produce low-calcium pyroxenes under experjmental conditions at atmospheric pressure. Details of the samples used in this study are given in appendix I.

CHAPTER 2

EXPERIMENTAL METHOD

2.1 INTRODUCTION

Information on the design and operation of the furnaces used in the Edinburgh laboratories has been published elsewhere. The important points are outlined below, followed by details of techniques particular to this project.

Atmospheric pressure experiments were carried out in vertical "quenching" furnaces (Biggar & O'Hara, 1969). Up to July 1984 the controllers were Viscount potentiometric controllers with the ability to keep the control thermocouple within $\pm 0.14°C$ of a set point for the duration of an experiment. In July 1984 the Viscounts were replaced by Eurotherm type 812 programmable controllers which are able to hold the control thermocouple within $\pm 0.50°C$ of a set point.

The probe assembly used to carry the samples is similar to that described in Biggar & O'Hara (1969). Two sample assemblies were used. For experiments at the nickel-nickel oxide (NNO) and cobalt-cobalt oxide (CCO) buffers, samples were suspended on PtFe wires. Four such wires were hung from a Pt cage with the buffer assemblage on a hook in the centre. For experiments at the iron-wustite (IW) buffer, samples were loaded into molybdenum capsules which were then placed in a Pt bucket. The wire cage or bucket was then suspended from the probe assembly by fine Pt quench wires.

Each furnace was operated with a H_2-CO_2 gas supply as described in Biggar (1974), with the mixed gas flowing down the furnace. Thermal profiles of furnaces were determined following the method given by Humphries (1975) prior to carrying out any experiments. Profiles obtained from furnaces used in this study are given in fig. 2.1.

Two types of experiment were carried out. In heating experiments the probe assembly was lowered into a furnace already at the run temperature. In cooling experiments the probe assembly was lowered into a furnace set at an initial, higher, temperature. After the

selected time the furnace temperature was lowered at a steady rate to a second temperature for the duration of the experiment.

2.2 PREPARATION OF SAMPLES

Samples 17M, 170, 120, B4, B5, K1, K6 and T2 were supplied in powder form. Samples M1, C2, C5, C11 and 295 were provided as rock chips and ground in a tema disc mill. All starting materials had a grain size of less than 200um.

In early experiments samples from the Bonin Islands (M1, C2, C5 and C11) did not reach equilibrium (as defined in section 3.1.3.1) whilst samples from the Eagle Brick Quarry (17M, 170 and 120) did. The Eagle Brick Quarry samples come from a greenschist facies metamorphic belt (Cawthorn et al., 1979) and did not contain any pyroxenes (appendix I). The presence of relict pyroxene crystals in the Bonin Islands samples together with the slow diffusion rate in pyroxenes (Freer et al., 1982) may explain why the pyroxenes in these samples failed to equilibrate under experimental conditions.

To destroy the pyroxene crystals present, the Bonin Islands samples were artificially metamorphosed prior to use in atmospheric pressure experiments. This was done by placing 100mg of ground sample in a gold capsule with 10mg of distilled water. Two capsules were placed in a "Tuttle" cold seal pressure vessel (Luth & Tuttle, 1963) and held at 650°C under 2kb pressure for 10-15 days. X-ray diffraction charts of the products confirmed the destruction of pyroxene within the detection limit of the apparatus. Samples treated in this way are distinguished from the original in the text, tables etc. by the suffix -MET.

2.3 SAMPLE CONTAINERS

In the experimental study of natural samples a container has to be chosen that gives the best conditions for recovery of the original bulk composition. The major problems being loss of iron to the sample container (Ford, 1978; O'Hara & Humpries, 1977) and volatilization of sodium to the furnace atmosphere (Donaldson, 1979; Corrigan & Gibb, 1979). Furthermore the melting point of the container must be above the temperature of the experiments.

Wire loops have the advantage over capsules in that the surface area in contact with the sample is minimal thus reducing iron loss. However, the surface exposed to the atmosphere is maximal, increasing the extent of sodium loss (Corrigan & Gibb, 1979). Quartz normative glasses are less likely to lose sodium than olivine normative glasses (Biggar, pers. comm.). As most of the samples used in this study were quartz normative platinum wire hooks were used, experimental results confirmed negligible sodium losses (table 2.1). During microprobe analyses sodium migration is observed in the form of decreasing sodium count rates. In the samples used in this study no such losses were observed suggesting that quartz normative samples are more stable than olivine normative samples under the electron beam. In each sample as the experimental temperature fell and the proportion of ferromagnesian crystals increased, the sodium content of the glasses increased. This steady rise in sodium content with falling temperature, but differing run duration, suggests there was no significant sodium loss from the samples during experiments. Comparison of all-glass charges with XRF analyses of the samples (table 2.1) shows a sodium recovery greater than 95%.

In some samples the sodium content of the all-glass charge was greater than that given in the XRF analysis. In such cases the sodium content of the glass also rose steadily in lower temperature experiments. If this extra sodium was due to furnace contamination (Biggar, 1981a) such a pattern would not be expected over runs of differing durations. It thus seems probable that either the XRF analysis was inaccurate or there was some difference between the samples used for experiments and XRF analysis.

Iron loss to a platinum wire hook can be restricted by pre-doping the hook with iron and using it repeatedly (Russell, 1981). PtFe hooks were prepared by electroplating iron onto pre-formed Pt hooks from a solution of 87.5g ferrous ammonium sulphate in 250cc H_2O (Johannes & Bode, 1978 & pers. comm.) . The pre-formed Pt hooks formed the cathode and a current of 20-25mA was passed through the solution. The Fe coating was observed by eye and checked by weight. After electroplating, the hooks were transferred directly to a furnace and annealed for 16 hours at 1200°C in an atmosphere close to the IW buffer. Probe analysis of these hooks showed that the edges contained 1.5 wt% Fe and

the centres had 1.0 wt% Fe. As the PtFe hooks are brittle and cannot withstand repeated bending, a length of Pt wire was welded to the hook so that it could be attached to the Pt cage, allowing up to ten experiments to be carried out on the same PtFe hook before failure. Microprobe analysis of a hook used for 9 experiments at the NNO buffer showed some increases in iron content, 6 wt% Fe being present throughout the hook. However, most of this gain is believed to have occurred during the first experiment on the hook. Iron recovery in experiments at NNO and CCO was greater than 90% (table 2.1).

Experiments at IW were initially carried out on PtFe hooks but the hooks proved to be very brittle, breaking after only one experiment. Microprobe analysis of such a hook showed the presence of 11 wt% Fe in its margin; the glass from that sample contained only 1 wt% FeO, an iron recovery of only 13% of the original (table 2.1). Further experiments at the IW buffer were carried out in molybdenum capsules which do not absorb iron provided that the oxygen fugacity is maintained close to the IW buffer (Biggar, 1970). Iron recovery from experiments in molybdenum capsules was greater than 85%; sodium recovery was greater than 80% (table 2.1).

2.4 TEMPERATURE CALIBRATION

Temperature was measured from the e.m.f. of an axial, sheathed, Pt13%Rh thermocouple (Humphries, 1975). All thermocouples drift with use due to diffusion of the metals involved. Thus the temperature recorded by the axial, sheathed thermocouple needs to be calibrated against known melting points which fall in the temperature range to be used in experiments. In this study calibrations have been made using the following compounds (Humphries, 1975):-

Gold	1064.43°C
Lithium Metasilicate	1208°C
Anorthite-Wollastonite-Gehlenite	1276°C
Diopside	1395.3°C

After calibration, temperature measurements were believed to be accurate to ±2°C.

2.5 OXYGEN FUGACITY CONTROL

The oxygen fugacity within the furnace was calibrated against a buffer for which the T-X-fO_2 conditions are known. The buffers used in this study were nickel-nickel oxide (NNO), cobalt-cobalt oxide (CCO) and iron-wustite (IW), the equations for which (fig. 2.2) are taken from Myers & Gunter (1979).

Before commencing an experiment the buffer fO_2 was calculated for the temperature of interest using the appropriate equation; this fO_2 was translated into a $\%H_2$ using the tables of Deines et al. (1974). This $\%H_2$ could then be obtained in the gas mix by adjusting the dip-tubes for the H_2-CO_2 supply and observing the reading on a Katharometer. The presence of the buffer assemblage in the furnace indicates whether or not the $\%H_2$ on the Katharometer is the same as the $\%H_2$ in the furnace. According to the Katharometer, the NNO buffer was found to lie at more reducing conditions than indicated by the buffer equation (fig. 2.2). This difference is probably due to errors in the Katharometer when considering small amounts of H_2. There was no obvious error in the position of the CCO and IW buffers due to the greater amount of H_2 in the gas mix.

2.6 RUN PROCEDURE

For each experiment the furnace temperature was set in advance, preferably overnight, to allow the furnace to settle at the desired temperature (Biggar & O'Hara, 1969). The samples were suspended from the probe assembly with the appropriate buffer and lowered stepwise into the furnace. The gas supply was adjusted to the required mixture while the probe was near the top of the furnace so as to avoid oxidation of iron in the sample. The probe was lowered 4cm every 20 minutes until it was 2cm from the run depth determined by the thermal profile. It was then lowered 1cm, left for 20 minutes and then twice lowered by 0.5cm after 15 minutes so as to avoid overheating the sample. The duration of the experiment was calculated from the time the probe reached the run depth. In reversal experiments the run was started as above but after an initial time at the higher temperature the furnace temperature was lowered. With the Viscount controllers this could only be done approximately, thus for 20°C/hr cooling the controller was turned down 5°C every 15 minutes. On reaching the

final experimental temperature the samples were left for the required period of time.

2.7 IDENTIFICATION OF PHASES

After quenching, the sample assembly was removed from the quench flask and allowed to dry. The glass beads were removed from the PtFe wires by crushing. The sample was ground under acetone, leaving some shards larger than 1mm for making probe slides. The finer part of the sample was mounted on a glass slide, the remainder being retained for making XRD slides. Initial identification of phases was by transmitted light microscopy. For reflected light microscopy the visibility of silicate phases was enhanced by buffing on a cloth lap to induce relief between the crystals and the glass. As X-ray diffraction examination can only detect a phase when it comprises at least 10% of the material on the X-ray slide, this technique was most often used when crystal abundance made optical identification difficult.

Since the crystals grown were generally smaller than 50um in diameter microscopic identification had to rely on easily discernible properties such as crystal habit, relief, birefringence, extinction angle and twinning. In some samples the microprobe was used to confirm optical identifications. Details of microprobe operating conditions, accuracy and precision are given in appendix II. The descriptions given below relate to properties observed in this series of experiments.

Protoenstatite (Pr) was readily identified by the polysynthetic twinning and perpendicular cracks caused by inversion to clinoenstatite on cooling (fig. 2.3). Crystals observed were generally less than 15um long and elongate with irregular fractured ends, high relief, low birefringence and irregular extinction angles due to the polysynthetic twinning.

Orthopyroxene (Opx) occurred as 30-40um long crystals with good euhedral form, high relief, low birefringence and extinction parallel to the long axis (fig. 2.4). Orthopyroxenes are distinguished from olivines by the lower birefringence of the former.

Pigeonite (Pig) occurred as rounded, globular crystals 10-20um in diameter with high relief, moderate birefringence and an extinction angle of 10-15° (fig. 2.5). Twinning is rare.

Augite (Cpx) was difficult to identify optically due to its occurrence well below the liquidus in these samples. However, its XRD peaks are readily identifiable, and on the microprobe the high CaO and low Al_2O_3 contents distinguish it from the other phases.

Olivine (Ol) occurred as small, rounded grains less than 10um in diameter at lower temperatures and euhedral crystals up to 25um in diameter in near-liquidus experiments. Crystals have high relief and moderate birefringence.

Plagioclase (Plag) occurred as tabular crystals less than 10um long with very low relief and low birefringence. In reflected light it is readily distinguished by its darker grey colour in comparison to the glass and pyroxene crystals.

Opaque Oxides (Sp) usually occurred as brown 1um cubic crystals throughout the glass. In some charges "strings" of rounded, paler crystals were found (fig 2.6), these are probably a quench phase (Biggar pers. comm.).

TABLE 2.1

Sodium and iron recoveries from experiments at NNO and IW. The glass (GL) composition was taken from an all-glass charge or the highest temperature charge whe no all-liquid charge was available. The original rock composition (WR) was taken from the published XRF analysis (appendix I).

A) Experiments at NNO

Sample	WR Na_2O	GL Na_2O	%Recovery	WR FeO	GL FeO	%Recovery
295	1.69	1.60	95	9.53	9.65	101
120	1.63	2.14	131	9.66	8.32	86
170	2.74	2.84	104	8.47	7.88	93
17M	1.19	1.50	126	12.11	10.70	88
K1	1.42	1.38	97	8.99	8.55	95
K6	1.77	1.75	99	8.56	8.60	100
C2	0.96	2.13	222	8.40	8.39	100
C5	1.60	1.87	117	7.28	7.16	98
C11	1.69	1.80	107	7.84	7.66	98
M1	1.46	2.26	156	8.79	8.41	96
B4	2.02	1.99	98	8.78	8.64	98
B5	2.21	2.68	121	10.06	7.87	78
T2	3.10	3.23	104	10.30	9.40	91

B) Experiments at IW - PtFe Hooks

Sample	WR Na_2O	GL Na_2O	%Recovery	WR FeO	GL FeO	%Recovery
295	1.69	1.84	109	9.53	3.07	32
120	1.63	1.89	116	9.66	5.43	56
170	2.74	2.63	96	8.47	1.10	13
17M	1.19	1.99	167	12.11	6.13	51

C) Experiments at IW - Molybdenum Capsules

Sample	WR Na_2O	GL Na_2O	%Recovery	WR FeO	GL FeO	%Recovery
295	1.69	1.58	93	9.53	9.01	95
120	1.63	2.19	134	9.66	8.38	87
170	2.74	2.25	82	8.47	7.59	90
17M	1.19	1.51	127	12.11	10.23	84

Figure 2.1 (see p. 18)

Thermal profiles of furnaces used in this study. Each curve is identified by the run number, e.g. 4/207, controller temperature in °C, e.g. C1200, and the furnace atmosphere for that profile, e.g. NNO. Vertical dashed lines indicate the run depth used for subsequent experiments. The y-axis, AS-C, is the difference between the e.m.f.'s of the control (C) and axial, sheathed (AS) thermocouples.

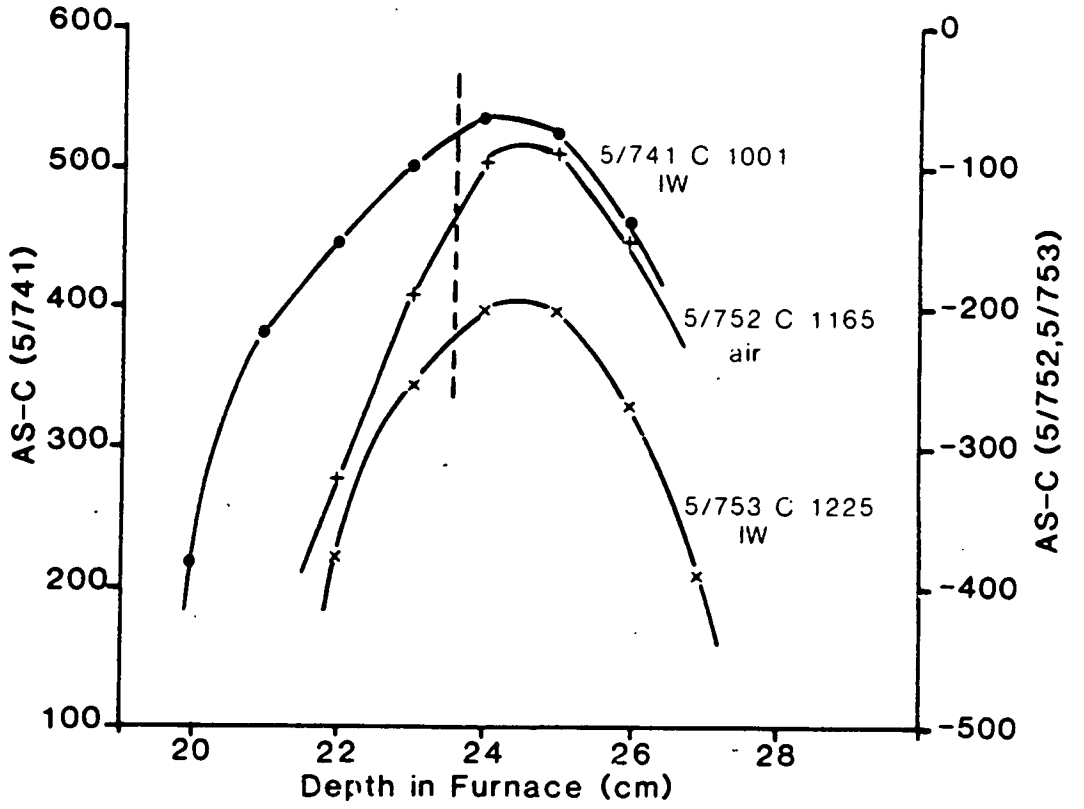
600
500
400
300
200
100
AS-C (5/741)
0
-100
-200
-300
-400
-500
AS-C (5/752,5/753)
5/741 C 1001
IW
5/752 C 1165
air
5/753 C 1225
IW
20
22
24
26
28
Depth in Furnace (cm)

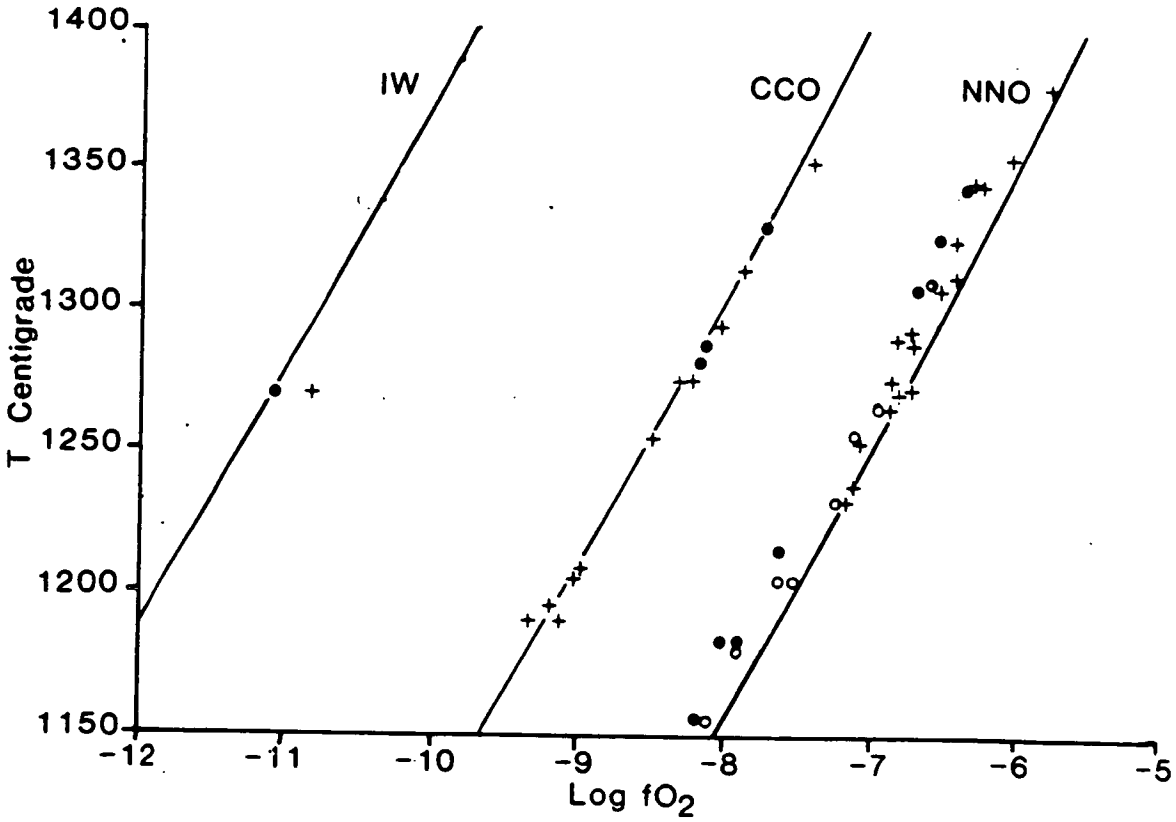
1400
1350
1300
1250
1200
1150
T Centigrade
IW
CCO
NNO
-12
-11
-10
-9
-8
-7
-6
-5
Log fO2

Figure 2:1 cont (see p. 16)

Figure 2:2 (see p. 16)

Results of buffer calibrations used in this study. The theoretical buffer curves are from the equations given in Myers & Gunter (1979). The calibration results are indicated by:-

- ● metal
- + metal oxide
- o mixture of metal and metal oxide

NNO	$\log fO_2 = 9.346 - 24920 / T°K$
CCO	$\log fO_2 = 7.936 - 25070 / T°K$
IW	$\log fO_2 = 7.184 - 28040 / T°K$

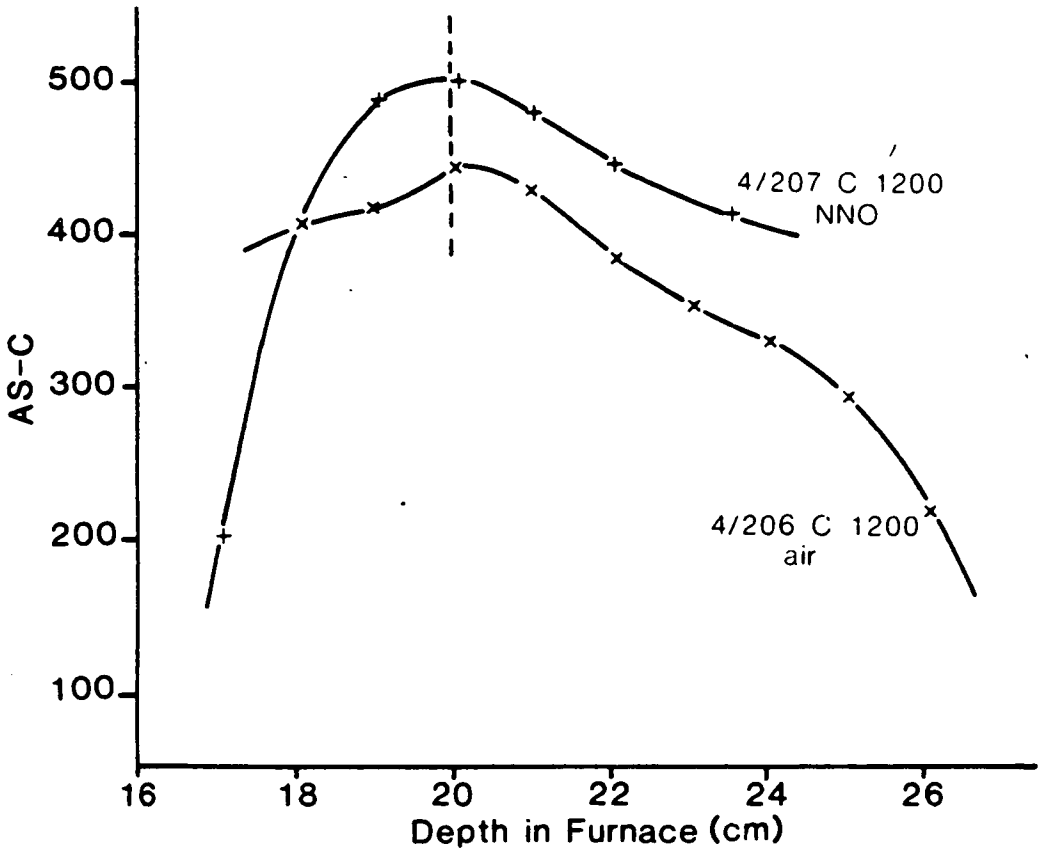
500
400
300
200
100
AS-C
4/207 C 1200
NNO
4/206 C 1200
air
16
18
20
22
24
26
Depth in Furnace (cm)

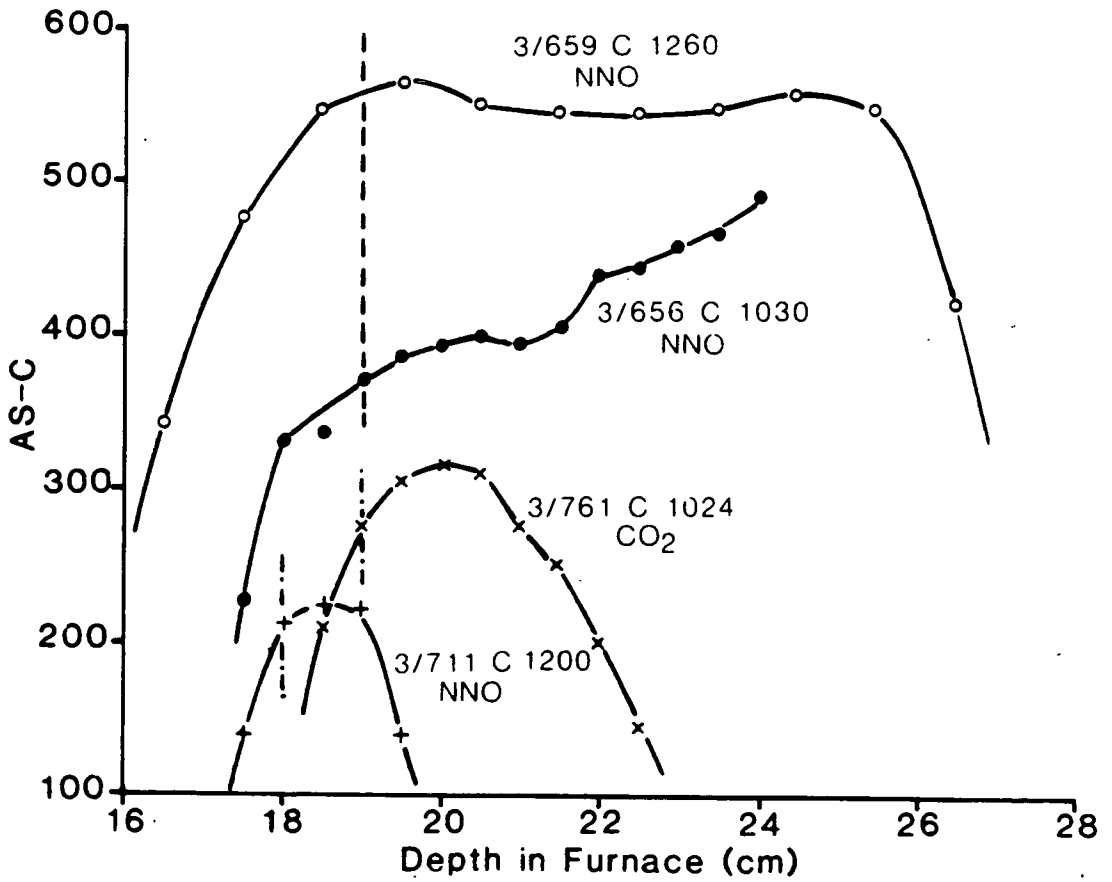
600
500
400
300
200
100
AS-C
3/659 C 1260
NNO
3/656 C 1030
NNO
3/761 C 1024
CO_2
3/711 C 1200
NNO
16
18
20
22
24
26
28
Depth in Furnace (cm)

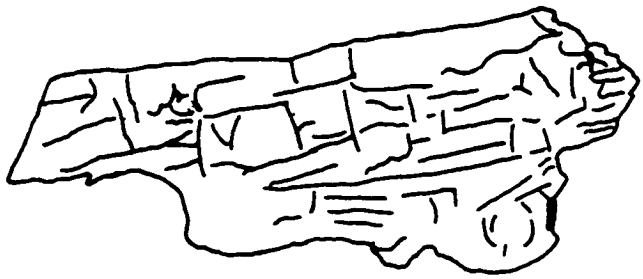

Figure 2.3
Protoenstatite crystal inverted to clinoenstatite, from sample 17M experiment 4/238

Figure 2.4
Orthopyroxene crystals from sample 120 experiment 3/685

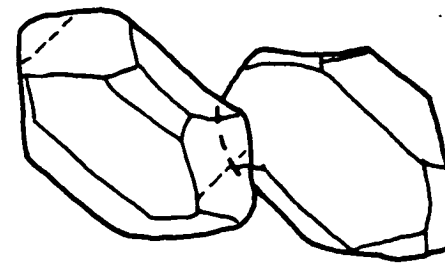

Figure 2.5
Pigeonite crystals from sample 120 experiment 3/703

Figure 2.6
"Strings" of opaque oxides from sample 120 experiment 3/681

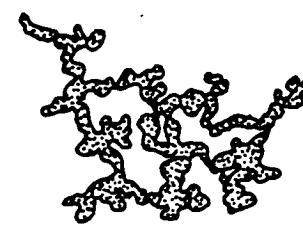

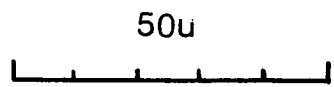

CHAPTER 3

MINERAL CHEMISTRY

3.1 LOW-CALCIUM PYROXENES

3.1.1 Previous Work

A comprehensive review of the subject has been given in Huebner (1980). The main points are outlined below using the simplified nomenclature and quadrilateral presentation scheme given therein.

3.1.1.1 Experimental Work in Synthetic Systems

Pure enstatite ($MgSiO_3$) has three polymorphs, protopyroxene which is stable at high temperatures, orthopyroxene which is stable at low temperatures and clinoenstatite which forms when protopyroxene is cooled rapidly. The inversion from protopyroxene to orthopyroxene occurs at 985°C (Atlas, 1952). Orthopyroxene is the only pyroxene that preserves orthorhombic symmetry and is readily distinguished optically. Protopyroxene is rarely preserved to room temperature although its former presence can be inferred from the inversion product, clinoenstatite, which has polysynthetic twinning and fracturing perpendicular to the twinning. A fourth low-calcium pyroxene, pigeonite, could be confused with protopyroxene as it may exhibit polysynthetic twinning, however, pigeonite lacks the fracturing associated with protopyroxene and is not a polymorph of pure enstatite.

In the calcium-bearing system, enstatite-diopside, protopyroxene was the only recognised low-calcium pyroxene at high temperatures and was considered to be stable in the presence of diopside (Boyd & Schairer, 1964). in the early 1970's "iron-free pigeonite" was recognised in the En-Di join (Kushiro, 1972; Yang, 1973). Pigeonite is a monoclinic low-calcium pyroxene that when found in natural rocks has a Mg/(Mg+Fe) ratio no greater than 0.80 (Huebner, 1980). Closer examination of the phase descriptions given in Kushiro (1972) and Yang (1973) reveals that the phase Kushiro

called pigeonite had orthorhombic symmetry and the phase Yang called protopyroxene had no polysynthetic twinning or cracks (except in the highest temperature experiment). On this basis Ross & Huebner (1979) revised Kushiro's phases to protopyroxene + orthopyroxene and Yang's to orthopyroxene + pigeonite and proposed a high temperature stability field for orthopyroxene, which until then had only been considered stable at low temperatures. This was confirmed experimentally by Longhi & Boudreau (1980) who defined liquidus fields for protopyroxene, orthopyroxene and pigeonite in the low-calcium part of the En-Di join. The subsolidus relationships of these low-calcium pyroxenes is unclear but Huebner's (1980) adaptation of Longhi & Boudreau's diagram (their fig. 3) is the most likely interpretation - fig. 3.1 (after fig. 7b of Huebner, 1980).

In the system enstatite-ferrosilite the polymorphism of enstatite was not recognised in early experimental studies (Bowen & Schairer, 1935). A reinvestigation of the join by Huebner & Turnock (1980) showed that protopyroxene, orthopyroxene and pigeonite are stable liquidus phases (fig. 3.2). At low Mg/(Mg+Fe) ratios olivine and silica are stable rather than pyroxene.

A thorough study of phase relations in the pyroxene quadrilateral (En-Di-Fs-Hd) was undertaken by Huebner & Turnock (1980). Their liquidus and solidus diagrams are given (fig. 3.3) with the addition of a protopyroxene field after fig. 21 of Huebner (1980).

3.1.1.2 Naturally Occurring Pyroxenes

Analyses of pyroxenes that were in equilibrium with a melt produce a generalised solidus diagram, fig. 3.4a (Huebner, 1980). Protopyroxene has recently been recognised in some natural lavas; these analyses are plotted in the pyroxene quadrilateral in fig. 3.4b. The point at which pigeonite becomes stable and orthopyroxene + augite cease to coexist shows considerable variation. In basaltic rocks pigeonite is found with Mg/(Mg+Fe) ratios up to 0.73, although the orthopyroxene + augite assemblage may persist with Mg/(Mg+Fe) ratios down to 0.55; in andesites orthopyroxene + augite coexist with Mg/(Mg+Fe) ratios as low as 0.24 (Huebner, 1980).

3.1.1.3 Experimental Work in Natural Systems

A literature search of experimental data at atmospheric pressure has revealed 77 pigeonite and 34 orthopyroxene analyses for which a coexisting liquid composition is also known(appendix III.2). Details of references are given in table 3.1 and the analyses are plotted in the pyroxene quadrilateral in fig. 3.5. There is some overlap between calcium-rich orthopyroxenes and calcium-poor pigeonites. However, as none of these overlapping analyses originate from the same sample there is no conflict with the generalised quadrilateral given in fig. 3.4.

Protopyroxene has only been recorded twice in experimental studies of natural systems. Tilley et al. (1964) found protopyroxene as the liquidus phase in a melting study of a boninite from Cape Vogel, Papua New Guinea (Dallwitz et al., 1966). Unfortunately chemical analysis of experimental products was not possible at that time, but the presence of polysynthetic twinning confirms the phase identification. Biggar et al. (1971) recorded protopyroxene coexisting with olivine and pigeonite near the liquidus of a lunar basalt. In the light of recent work and the high CaO content given in the analysis this phase is not now considered to be protopyroxene (Biggar, pers. comm.).

In considering experimental results from synthetic and natural systems it is important to be aware of the possi bility of growing metastable phases in the course of an experiment. Many authors working with synthetic low-calcium pyroxenes have commented on the different results achieved from experiments of different durations (Bowen & Schairer, 1935; Yang, 1973; Longhi & Boudreau, 1980). Biggar (pers. comm.) in a series of experiments currently in progress has found that, from some gel starting materials, pigeonite compositions nucleate initially and persist through two or three episodes of heating, quenching and crushing over 12 to 17 days but finally transform to orthopyroxene.

As as result of the confusion in low-calcium pyroxene identification, names used in the literature should be treated with caution and checked against the composition and phase description. In the synthetic system CaO-MgO-SiO_2 protopyroxene contains less than 1 wt% CaO, orthopyroxene 1.4 - 2.2 wt% CaO and pigeonite 3-6

wt% CaO (Biggar, 1984a). In more complex synthetic and natural systems a similar relationship between CaO content and mineralogy is observed, although calcium-rich orthopyroxenes (3 wt% CaO) could be confused with calcium-poor pigeonites (Biggar, 1984a).

3.1.2 Site Occupancy and the Pyroxene Structure

The general pyroxene formula together with site occupancy and ionic radii details are given in table 3.2. A review of the pyroxene structure has been given in Cameron & Papike (1980); the main points are outlined below. The tetrahedral Z site (table 3.2) contains mostly Si cations and can be considered as two distinct sites, Si(A) and Si(B), on the basis of crystal structure and atomic bond lengths. The octahedral M sites (table 3.2) are also structurally distinct, the M2 site being larger and more distorted. The size of the M2 site is directly related to the crystal structure, being smallest in protopyroxene, intermediate in orthopyroxene and pigeonite and largest in augite.

Calcium, magnesium and iron are the principal occupants of the M sites in igneous pyroxenes. In a simple system $Ca^{2+} + Mg^{2+} + Fe^{2+} = 2$. In natural systems elements such as Ti^{4+}, $Cr^{3+/4+}$, Mn^{2+}, Na^{+} and Al^{3+} are also found so $Ca^{2+} + Mg^{2+} + Fe^{2+} < 2$. Calcium is restricted to the M2 site because of its large atomic radius. Iron and magnesium are able to occupy both M sites, however, iron shows a strong preference for M2 because it has a larger ionic radius than magnesium and being a transition metal ion it is more stable in a distorted environment (Walsh et al., 1974). Mossbauer studies of orthopyroxenes have shown that nearly all the M2 site is taken up by iron (Bancroft et al., 1967; Zverev et al., 1971) and in high magnesium orthopyroxenes it is possible to consider all iron to be present in the M2 site (Davidson, 1968). In protopyroxenes iron has a greater preference for the M2 site than in orthopyroxenes (Smyth, 1974). There is not yet sufficient data to determine the variation in iron and magnesium content over the M sites with changing pressure, temperature and oxygen fugacity. As the magnesium content of pyroxenes falls so the iron and calcium contents rise. The increase in calcium and iron from protopyroxene through to augite is related to the size of the M2 site (Virgo & Hafner, 1969) and is, at

least in part, responsible for the transitions from protopyroxene to orthopyroxene, orthopyroxene to pigeonite and pigeonite to augite.

Manganese is found in both M1 and M2 sites. In natural pyroxenes it shows a preference for the M2 site due to its large ionic radius (table 3.2) (Snellenburg, 1975; Bancroft et al., 1967). In pyroxenes quenched from high temperatures, manganese shows no preference for M2 and is equally divided between M1 and M2 (Bohlen et al., 1980; Fleet, 1974). As manganese is only found as a divalent ion in igneous rocks there is no need to consider charge balance.

One other ion commonly found in the M2 site is sodium, which is restricted to M2 because of its large ionic radius (table 3.2). The amount of sodium a pyroxene crystal can accommodate is related to its crystal structure; the M2 site in augite being larger than the M2 site in low-calcium pyroxenes leads to a concentration of sodium in clinopyroxene (Campbell & Borely, 1974). The difference in sodium content between orthopyroxene and pigeonite is also attributable to a larger M2 site in the pigeonite structure. As sodium is a monovalent cation a coupled substitution such as Na^{+}-Al^{iv}, Na^{+}-Al^{vi}, Na^{+}-Cr^{3+} or Na^{+}-Fe^{3+} is necessary to maintain charge balance.

The M1 site is occupied principally by Mg^{2+} and any excess Fe^{2+} and Mn^{2+} from the M2 site, the remaining space being occupied by Cr^{3+}, Ti^{4+} and Al^{3+}. Pyroxenes contain comparatively large amounts of Cr^{3+} and Ti^{4+} because the structure is able to accommodate them and the Na^{+} or Al^{3+} needed to maintain charge balance (Campbell & Borely, 1974; Huebner et al., 1976). Common coupled substitutions include Cr^{3+}-Al^{iv}, Al^{iv}-Al^{vi} and Ti^{4+}-$2Al^{iv}$. Although Ti^{4+}:Al ratios of 1:2 or 1:4 are often found in lunar samples (Grove et al., 1973), in terrestrial samples the range is 1:1 to 1:10 (Verhoogen, 1962).

Of the two tetrahedral site only Si(B) is involved in substitution of Al^{3+} and as there can be no Al-O-Al bonds (Ganguly & Ghose, 1979) no more than 50% of Si(B) and 25% of SiO_2 can be replaced by Al_2O_3. As the relative size and distortion of the Si(B) site is related to the M2 site it is possible to have more Al_2O_3 in a pigeonite structure than an orthopyroxene structure (Campbell & Borely, 1974; Fleet, 1974).

3.1.3 Experimental Work; This Study

3.1.3.1 Attainment of Equilibrium

Equilibrium is considered to have been achieved when several probe analyses of a phase from a single charge are distinguishable from analyses of the same phase at higher and lower temperatures (fig. 3.6). It is not possible to determine whether such an occurrence represents true or metastable equilibrium. Olivines are known to equilibrate with the melt within 5 hours at near liquidus temperatures (Russell, pers. comm.), however, pyroxenes and feldspars require longer, feldspars being notoriously difficult to equilibrate (Grove et al., 1982; Walker et al., 1979).

Initial experiments of five hours duration at the CCO buffer produced analyses with compositional variation in both crystals and glass. Experiments of 24, 48, 72 and 102 hours using samples 17M and 120 (24 and 48 hours only) were carried out at 1315°C. There was a marked decrease in compositional variation of the glasses between 5 and 24 hour experiments and a further slight decrease in longer experiments on sample 17M (table 3.3). In addition four samples (120, 295, M1MET and C5MET) run for 477 hours at 1224C produced results identical to or better than those from experiments of 24 or 48 hours at a similar temperature (fig. 3.7 and table 3.4). On this basis 24 hours was considered to be sufficient for samples to reach equilibrium at 1300°C; at lower temperatures experiments were of longer duration.

Cooling experiments were carried out on sample 17M (table 3.5). In both experiments two charges were loaded and each gave a different result (fig 3.8 and table 3.5). This is attributable to minor sample inhomogeneity and/or the kinetics of cooling experiments. However, the orthopyroxene compositions are comparable to results from heating experiments.

Although in many of the experiments the microprobe analyses suggested that the pigeonites were in equilibrium there are two points worth noting. Firstly the "granular" texture exhibited by pigeonite crystals (fig. 2.5) suggests that they are unstable. Secondly, the appearance of pigeonite is related to the duration of the experiment. For example, in sample 120 the first appearance of pigeonite in 5 hour experiments is at 1314°C, in 24 hour experiments at 1265°C, in 48 hour experiments between 1245°C and 1206°C; whilst

in the 477 hour experiment orthopyroxene and pigeonite coexist at 1224°C (appendix III.3). Recent experiments carried out on synthetic systems by Biggar (pers. comm.) suggest that orthopyroxene is stable to higher temperatures than previously considered and that protopyroxene or pigeonite initially form metastably and only invert to orthopyroxene after some time.

Further evidence for the preferential growth of pigeonite comes from the early experiments at IW carried out on PtFe hooks. These charges lost large amounts of iron to the wire during the experiments. In some charges a multiply twinned phase, originally identified as protopyroxene, was found. In sample 170, experiment 5/751, the microprobe analysis confirmed the presence of protopyroxene; fig. 3.9, table 3.6. However, in sample 295 , experiment 5/751, the microprobe analysis showed that the "protopyroxene" had more CaO than the coexisting orthopyroxene; fig. 3.9, table 3.6; and is therefore pigeonite. It is likely that the presence of protopyroxene and pigeonite in these experiments has been promoted by compositional changes during the experiment - i.e. severe iron loss.

3.1.3.2 Experimental Results

This study has produced 55 analyses of orthopyroxene,Mg/(Mg+Fe) between 0.66 and 0.86; 25 analyses of pigeonite,Mg/(Mg+Fe) between 0.47 and 0.82; and 4 analyses of protopyroxene, Mg/(Mg+Fe) of 0.85, (appendix III.4). A "good" pyroxene analysis has a total between 99% and 100% and when the formula is calculated on the basis of six oxygens the cations sum lies in the range 3.95 - 4.05 (fig. 3.10). In an experiment that has reached equilibrium all the "good" pyroxene analyses have a narrow compositional range and are distinguishable from pyroxenes in experiments at higher and lower temperatures (fig. 3.6a). In an experiment that has not reached equilibrium the "good" pyroxene analyses cover a wide compositional range and cannot be distinguished from those in experiments at different temperatures (fig 3.6b). Although many more experiments produced low-calcium pyroxenes (appendix III.3) only those meeting the criteria for equilibrium given above are considered here; such analyses are shown in the pyroxene quadrilateral in fig. 3.11.

As it is not possible to analyse for Fe_2O_3 using the microprobe the Fe_2O_3 content of pyroxenes can only be determined by manipulation of the pyroxene formula on the assumption that charge balance is achieved. Lindsley & Anderson (1983) calculate charge balance on the assumption that Na-Al^{vi}, Cr-Al^{iv}, Ti-2Al and Fe^{3+}-Al^{iv} are the only substitutions occurring. This produces the following equation:

$$Fe^{3+} = (Al^{iv} + Na) - (Al^{vi} + Cr + Ti)$$

However, in the high temperature, low pressure igneous low-calcium pyroxenes produced in this study Al_2O_3 contents are low and coupled with low Na_2O and high Cr_2O_3 contents; the amount of Fe_2O_3 calculated is usually negative. Alternatively, Fe_2O_3 can be calculated by adjusting the formula such that with O=6 cations=4; Robinson (1980) used a variation by calculating the pyroxene formula to cations=4 and then adjusting the Fe_2O_3:FeO ratio until O=6. All of these methods are sensitive to errors in measurement of major elements, especially SiO_2, and the calculated Fe_2O_3 contents show no variation with iron content, temperature or oxygen fugacity, but a strong correlation with the SiO_2 content (fig. 3.12). As none of the above mentioned Fe_2O_3 calculation methods produced reasonable results no attempt has been made to calculate the Fe_2O_3 contents of pyroxenes produced in this study.

Protopyroxene was analysed from three cooling experiments and from a heating experiment at IW where iron recovery was less than 20%. Heating experiments carried out between the temperatures of the cooling period of cooling experiments failed to produce protopyroxene crystals. Protopyroxene is not considered to be an equilibrium phase in these samples. However, as no other experiments in natural systems have produced analyses of protopyroxene these 4 analyses are plotted in the pyroxene quadrilateral in fig. 3.11. The presence of protopyroxene in these four experiments suggests that the growth of protopyroxene in natural samples is encouraged by rapid changes in temperature or composition.

In orthopyroxene and pigeonite $Ca^{2+} + Fe^{2+} + Mg^{2+} < 2$ cations per six oxygens (fig. 3.13) and as Mg^{2+} contents decrease so Ca^{2+} and Fe^{2+} contents increase. These compositional changes are in part related to temperature, figs. 3.14 to 3.16. However, the com-

position of the coexisting liquid is also a factor hence the broad range of Fs contents for a given temperature (fig. 3.16). Mineral - melt relationships are discussed in chapter 4. Manganese contents are low but there is a tendency for Mn^{2+} to increase with increasing Fe^{2+} content (fig. 3.17). Sodium contents are also low but are significantly higher in pigeonite than orthopyroxene (fig. 3.18) as predicted by structural differences. As sodium contents are low there is no obvious correlation between Na^{+} and Al^{3+}, Ti^{4+} or Cr^{3+} so the nature of the coupled substitution could not be determined. There is, however, a tendency for Na^{+} content to increase with Fe^{2+} content (fig. 3.18). Titanium contents are low and show no obvious correlation with Al^{3+}, the Ti:Al ratio being in the range 1:1 to 1:100 (fig. 3.19) which is comparable to the range reported in natural rocks (Verhoogen, 1962). Although chromium contents are significant (0.5 wt% Cr_2O_3) the nature of the coupled substitution is unclear. Generally Si + Al > 2 cations per six oxygens (fig. 3.20) so some octahedral Al^{3+} must be present, but there is no evidence for a coupled Al^{iv}-Al^{vi} substitution (fig. 3.21).

3:2 OLIVINES

Olivines were produced in experiments at NNO, CCO and IW; although the crystals were small analyses were obtained from most samples. A typical olivine analysis contains only trace amounts of calcium and aluminium, any analysis containing more than 0.5 wt% CaO or Al_2O_3 was considered to be contaminated with glass. Where no glass-free olivine analysis was obtained that with the lowest wt% CaO content is presented (appendix III.5).

The forsterite content of olivines falls from Fo_{90} at 1345°C to Fo_{83} at 1181°C (fig. 3.22), this is in agreement with the trend given in Roeder & Emslie (1970) and Russell (1985). The forsterite content also varies with fO_2 (Roeder & Emslie, 1970); experiments at IW carried out in molybdenum capsules produced olivines with Fo contents slightly lower than those produced at NNO at a similar temperature. The IW experiments carried out on PtFe hooks produced anomalously high Fo olivines; this was due to low iron recovery (less than 40%) from the samples which is reflected in the crystal compositions. Experiments at CCO would be expected to produce

olivines with Fo contents between those from IW and NNO. However, the high CaO content, due to contamination by glass, of these analyses led to lower Fo contents than expected in some cases (fig. 3.22).

The olivines analysed were essentially pure $(Mg,Fe)_2SiO_4$ with $CaO + MnO + Al_2O_3 < 1$wt% (appendix III.5). The major compositional change is a substitution of Fe^{2+} for Mg^{2+} maintaining $Mg^{2+}+Fe^{2+} < 2$ cations per four oxygens (fig. 3.23). There is a slight increase in Ca^{2+} and Mn^{2+} with falling temperature (figs. 3.24 & 3.25).

3.3 AUGITE

Clinopyroxenes of augite composition are found well below the liquidus in some samples (fig. 3.26), however, the wide spread of compositions obtained from a single experiment indicates that equilibrium has not been reached (appendix III.6). If glass contamination had been a factor then the calcium content would decrease as the aluminium content increased, however, no such relationship is seen (appendix III.6).

The Kopi boninite is the only sample in which augite analyses are available from both the original sample (Wood, 1980) and these experiments. The augite analyses given in Wood (1980) cover a fairly broad compositional span (appendix III.6), fig. 3.26) especially with respect to calcium (Wo_{33-41}). The experimental results suggest a sharp fall in Ca^{2+} with decreasing temperature (fig 3.26) which is in contrast with the gradual changes found in natural crystallization trends e.g. the Skaergaard (Deer et al. 1966, fig. 47). Sharp drops in Ca^{2+} contents of augites have been attributed to quench processes (Smith & Lindsley, 1971) and further supports the hypothesis that these augites are not in equilibrium with the melt.

3.4 PLAGIOCLASE

In eight of the samples plagioclase feldspars are found well below the liquidus in experiments at the NNO buffer. Glass contamination can be assessed by the MgO content which is typically less than 0.2 wt%. Where several poor analyses were obtained that with the lowest MgO content is presented; if MgO contents were low or equally high in several analyses an averaged analysis is given

(appendix III.7). Most analyses fall into two groups (fig. 3.28), those with An_{70-80} from samples K1, K6, 295, C2 and C11; and those with An_{50-60} from samples T2, B4 and B5. As feldspars are known to be difficult to equilibrate under experimental conditions (Grove et al., 1982; Walker et al., 1979) it is unlikely that any of the analyses presented represents a composition that was in equilibrium with the coexisting melt. The Kopi boninite, samples K1 & K6, is recorded as containing quenched groundmass plagioclase in the range An_{67-79} (Wood, 1980). This is comparable to the range of experimental feldspar analyses and indicates that either relict crystals have survived or this is close to the equilibrium composition. Sample T2 contains plagioclase in the range An_{37-49} (Baxter, pers. comm.) which does not coincide with the experimental range of An_{50-60}. The plagioclase - melt equation of Nielsen & Dungan (1983) predicts plagioclase compositions of An_{60-70} to be in equilibrium with the melt in the appropriate temperature range which suggests that plagioclases in sample T2 are approaching equilibrium.

3.5 OPAQUE OXIDES

Although present in most experimental products at the NNO buffer, opaque oxides were usually too small to give reliable analyses. Glass contamination can be assessed by the SiO_2 content, which is typically less than 0.1 wt%. The opaque oxides analyses that were obtained from heating experiments contained at least 1.0 wt% SiO_2 (appendix III.8). Formula calculations and estimates of Fe_2O_3 contents are impracticable due to the high SiO_2 contents. The analyses indicate that the opaque oxides belong to the chromite series and have Mg/(Mg+Fe) ratios between 0.50 and 0.60; and Cr/(Cr+Al) ratios between 0.70 and 0.75.

Two opaque oxide analyses with SiO_2 contents less than 0.12 wt% were obtained from a reversal experiment (appendix III.8, analyses 1 & 2). These oxides belong to the chromite series and have Mg/(Mg+Fe) ratios of 0.38 and Cr/(Cr+Al) ratios of 0.80, after recalculation of the formula to allow for Fe_2O_3. As analyses of opaque oxides are not available from more than one experiment on any given sample it is not possible to determine whether there is any systematic variation with changing composition or temperature.

3.6 MINERAL - MINERAL DISTRIBUTION COEFFICIENTS

3.6.1 X^{OPX} / X^{OL}

The distribution of Mg^{2+} and Fe^{2+} between orthopyroxene and olivine is roughly equal; $D_{Mg} = 0.98 \pm 0.02$, $D_{Fe} = 0.92 \pm 0.02$ and $K_D^{Fe/Mg} = 0.95 \pm 0.05$ (table 3.7); which is in agreement with the findings of Matsui & Nishizawa (1974) and Walker et al. (1973). There is no detectable change with temperature or composition. Manganese prefers orthopyroxene to olivine giving a D_{Mn} of 1.0 to 1.75 (table 3.7). Aluminium, calcium and chromium are only trace constituents of olivines and there is always more in a coexisting orthopyroxene. When the calcium or manganese content of an olivine increases so does the calcium or manganese content of the coexisting orthopyroxene (fig. 3.28).

3.6.2 X^{PIG} / X^{OPX}

There is always slightly less Mg^{2+} and more Fe^{2+} in a pigeonite than in a coexisting orthopyroxene; $D_{Mg} = 0.95 \pm 0.03$, $D_{Fe} = 1.04 \pm 0.04$ and $K_D^{Fe/Mg} = 1.09 \pm 0.02$ (table 3.8). Manganese shows no preference for pigeonite or orthopyroxene, $D_{Mn} = 1.0 \pm 0.08$ (table 3.8); this supports the suggestion (Bohlen et al., 1980; Fleet et al., 1974) that at high temperatures there is no preference of Mn^{2+} for M2 otherwise it would be concentrated in pigeonite. Chromium appears to be concentrated in orthopyroxene when it coexists with pigeonite, $D_{Cr} = 0.4$ to 1.0 (table 3.8), however, the chromium content of pigeonites is not generally distinguishable from the chromium content of orthopyroxenes (fig. 3.29). There is, however, an increase in the chromium content of pyroxenes with decreasing fO_2 (Stolper, 1977), fig. 3.29. Titanium tends to be concentrated in pigeonite, $D_{Ti} = 0.8$ to 2.0 (table 3.8), this is a result of the increased size of the Si(B) site in pigeonite which enables it to accommodate the Al^{3+} necessary for charge balance (Campbell & Borely, 1974) - hence the tendency for Al^{3+} to be concentrated in pigeonite $D_{Al} = 0.6$ to 1.4 (table 3.8). Calcium is concentrated in pigeonite, $D_{Ca} = 1.5 \pm 0.3$ (table 3.8) and as the calcium content of the orthopyroxene rises so does that of pigeonite, fig. 3.30.

TABLE 3.1

Sources of Low-Calcium Pyroxene - Melt Data from the Literature Search

Reference	Opx-Gl pairs	Pig-GL pairs	T range	fO_2	Rock type
Huebner et al. (1976)	6	4	1332 - 1151	IW	Partial melting of lunar pyroxene crystals & heating of synthetic lunar basalts.
Biggar et al. (1971)	1	6	1179 - 1114	IW	Lunar protohypersthene basalts.
Grove et al. (1982)	6	12	1153 - 1059	IW	Calc-alkaline high-alumina basalts/andesites.
Weill & McKay (1975)	5		1320 - 1220	IW	Lunar ferromagnesian basalt.
Huebner & Turnock (1980)	5	8	1300 - 1123	IW	Partial melting of lunar and terresrial pyroxene crystals.
Neilsen & Drake (1979)	6	3	1241 - 1134	IW	Lunar basalts.
Mitchell (pers. comm.)	5	1	1210 - 1160	QFM	High Fe-Ti terrestrial basalts doped with pyroxene gel.
Walker et al. (1976)		4	1176 - 1150	IW	Lunar picritic basalt.
Grove & Bence (1977)		4	1194 - 1123	IW	Lunar quartz-normative basalt.
O'Hara et al. (1974)		1	1133	IW	Lunar high-Ti basalt.
Stolper (1977)		4	1171	IW	Eucrite meteorites.
Walker et al. (1977)		10	1225 - 1124	IW	Lunar microgabbros.
Rhodes et al.(1979)		4	1150 - 1125	IW	Lunar ilmenite basalt.
Grove & Raudsepp (1978)		3	1099 - 1071	IW	Lunar microgabbros.
Grove & Beaty (1980)		4	1146 - 1113	IW	Lunar high-K basalts.
Hess et al. (1978)		3	1180 - 1080	IW	Lunar LKFM basalt.
Grove & Bryan (1983)		6	1167 - 1137	QFM	Pyroxene-phyric MORB.

* N.B. 6 of the analyses from Huebner & Turnock (1980) were later omitted from the data base because of their high MnO contents.

TABLE 3.2

General pyroxene formula:-

$$M1\ M2\ Z_2O_6$$

Site occupancy and atomic radii:-

M1

Cr^{3+}	0.63Å
Al^{3+}	0.51Å
Ti^{4+}	0.68Å
Fe^{3+}	0.64Å
Mg^{2+}	0.66Å
Mn^{2+}	0.80Å
Fe^{2+}	0.74Å

M2

Mg^{2+}	0.66Å
Mn^{2+}	0.80Å
Fe^{2+}	0.74Å
Ca^{2+}	0.99Å
Na^{+}	0.97Å

Z

Si^{4+}	0.42Å
Al^{3+}	0.51Å

TABLE 3.3a

Coefficients of Variation for "Time Trial" Experiments on Sample 17M

Oxide	5 hr	24 hr	48 hr	72 hr	102 hr
Na_2O	0.0654	0.0241	0.0103	0.0073	0.0220
MgO	0.0491	0.0195	0.0152	0.0102	0.0035
Al_2O_3	0.0425	0.0088	0.0158	0.0066	0.0050
SiO_2	0.0018	0.0026	0.0121	0.0055	0.0053
K_2O	0.1435	0.0456	0.0555	0.0656	0.0168
CaO	0.0229	0.0132	0.0154	0.0058	0.0051
TiO_2	0.0571	0.0276	0.0225	0.0199	0.0145
MnO	0.1230	0.0721	0.0667	0.0495	0.0275
FeO	0.0165	0.0359	0.0269	0.0130	0.0039

TABLE 3.3b

Coefficients of Variation for "Time Trials" Experiments on Sample 120

Oxide	5 hr	24 hr	48 hr
Na_2O	0.0321	0.0103	0.0121
MgO	0.0225	0.0070	0.0069
Al_2O_3	0.0234	0.0089	0.0081
SiO_2	0.0042	0.0052	0.0011
K_2O	1.4142	0.0435	0.0597
CaO	0.0134	0.0056	0.0089
TiO_2	0.0760	0.0151	0.0240
MnO	1.4142	0.0435	0.0828
FeO	0.0124	0.0056	0.0061

coefficient of variation = standard deviation / wt% oxide

TABLE 3.4

Comparison of Glasses from 477 and 24/48 Hour Experiments

Oxide	120	120	295	295	M1MET	M1MET	C5MET	C5
SiO_2	59.76	59.01	53.89	55.23	61.65	59.95	59.28	59.31
TiO_2	1.30	1.20	0.70	0.62	0.14	0.12	0.19	0.15
Al_2O_3	11.07	10.41	14.50	13.12	11.69	11.44	14.31	14.00
FeO	7.16	8.46	8.32	8.56	6.56	7.97	6.26	6.41
MnO	0.11	0.13	0.17	0.16	0.17	0.17	0.12	0.11
MgO	6.62	8.09	8.11	8.47	6.38	6.55	6.41	6.65
CaO	9.42	8.99	9.77	9.00	9.73	9.49	8.48	8.29
Na_2O	1.97	2.86	1.56	2.11	1.50	1.81	1.85	2.56
K_2O	0.27	0.11	0.62	0.74	0.58	0.62	1.21	1.52
P_2O_5	0.25	0.12	0.07	0.04	0.04	0.05	0.12	0.18
total	97.95	99.39	97.72	98.04	98.43	98.17	98.23	99.19
temp	1224	1236	1224	1235	1224	1215	1224	1215
time	477	23.66	477	24	477	48	477	48

* slight losses of sodium and iron in the 477 hour experiments causes apparent increases in the other elements

TABLE 3:5a

Experimental Details of Cooling Experiments

Expt.	Ti	ti	cooling rate	Tf	tf	fO_2	Phases
4/237	1365°C	1 Hr	30°/Hr	1304°C	69 Hr	-7.90	GL+OL+SP
4/237A	1365°C	1 hr	30°/hr	1304°C	69 hr	-7.90	GL+OL+OPX+PROTO
4/238	1327°C	1 hr	20°/hr	1307°C	70 hr	-7.90	GL+OPX+PROTO
4/238A	1327°C	1 hr	20°/hr	1307°C	70 hr	-7.90	GL+OPX+PROTO

TABLE 3:5b

Products of Cooling Experiments

Oxide	4:237 GL	4:237 OL	4:237A GL	4:237A OL	4:237A OPX	4:237A PROTO	4:238 GL	4:238 OPX	4:238 PROTO	4:238A GL	4:238A OPX	4:238 PROT
SiO_2	56.02	40.41	57.79	41.56	58.64	58.96	55.41	56.65	55.33	57.25	58.20	58.0
TiO_2	1.08	-	1.12	0.0	0.09	0.09	1.17	0.12	0.07	1.16	0.11	0.0
Al_2O_3	9.72	0.06	9.90	0.06	0.68	0.49	10.64	0.68	0.54	10.49	0.70	0.6
Cr_2O_3	-	-	-	0.21	0.62	0.42	0.03	0.57	0.47	-	0.61	0.4
FeO	9.28	11.40	9.06	11.27	7.53	6.73	7.79	7.00	6.36	7.75	7.02	6.0
MnO	0.19	0.15	0.17	0.19	0.14	0.11	0.19	0.16	0.12	0.17	0.15	0.1
NiO	-	0.22	-	-	-	-	-	-	-	-	-	-
MgO	12.38	47.12	12.55	48.76	33.65	34.57	12.31	33.22	35.19	12.78	34.24	34.7
CaO	7.97	0.21	8.16	0.22	0.93	0.45	8.66	0.93	0.43	8.43	0.91	0.4
Na_2O	1.36	-	1.35	0.02	0.04	0.02	1.18	0.04	0.03	1.24	0.04	0.0
K_2O	0.30	-	0.32	-	-	-	0.25	-	-	0.30	-	-
total	98.30	99.57	100.43	102.29	102.31	101.84	97.62	99.36	98.54	99.58	101.97	100.5
Ti	1365	1365	1365	1365	1365	1365	1327	1327	1327	1327	1327	132
Tf	1304	1304	1304	1304	1304	1304	1307	1307	1307	1307	1307	130

TABLE 3.6

Pyroxene Analyses from Experiments at IW carried out on PtFe Hooks

Oxide	17M 5:750 OPX	17M 5:751 OPX	120 5:750 OPX	120 5:751 OPX	170 5:750 PROTO	170 5:750 OPX	170 5:751 OPX	295 5:751 OPX	295 5:751 PIG
SiO_2	56.89	56.05	56.66	56.87	56.93	57.02	56.60	56.20	55.74
TiO_2	0.13	0.14	0.10	0.19	0.09	0.12	0.19	0.06	0.11
Al_2O_3	0.58	0.59	0.34	0.69	0.29	0.40	0.93	0.65	1.01
Cr_2O_3	0.47	0.44	0.46	0.76	0.41	0.49	0.57	0.59	0.76
FeO	5.21	7.47	6.29	3.33	1.67	3.64	5.27	6.84	5.86
MnO	0.13	0.16	0.13	0.16	0.10	0.14	0.32	0.19	0.23
MgO	33.28	32.17	33.49	34.83	36.74	35.18	33.68	32.65	32.67
CaO	1.03	1.40	1.13	1.55	0.49	1.02	1.51	1.39	1.79
Na_2O	0.03	0.03	0.05	0.05	0.04	0.05	0.05	0.03	0.04
total	97.76	98.45	98.65	98.43	96.76	98.05	99.12	98.60	98.21
temp	1307	1258	1307	1258	1307	1307	1258	1258	1258
time	24.5	45.5	24.5	45.5	24.5	24.5	45.5	45.5	45.5
WO	2.01	2.69	2.16	2.95	0.92	1.92	2.88	2.66	3.46
EN	90.08	86.09	88.52	92.11	96.61	92.70	89.29	87.10	87.71
FS	7.91	11.21	9.32	4.94	2.47	5.37	7.84	10.24	8.83

TABLE 3:7

Olivine - Orthopyroxene Distribution Coefficients

Sample	run no.	$K_D^{Fe/Mg}$	D_{Mg}	D_{Fe}	D_{Mn}
17M	3/677	0.932	0.975	0.909	1.333
17M	3/684	0.968	0.963	0.933	1.666
17M	3/692	0.911	0.991	0.903	1.666
K1	3/745	0.961	0.981	0.943	1.750
295	3/770	1.007	0.934	0.941	1.500
17M	4/239:2	0.917	0.987	0.905	1.333
17M	4/248	0.943	0.990	0.933	1.000
17M	4/245	0.899	1.004	0.903	1.333

TABLE 3:8

Orthopyroxene - Pigeonite Distribution Coefficients

Sample	run no.	$K_D^{Fe/Mg}$	D_{Mg}	D_{Fe}	D_{Mn}
17M	3/700	1.096	0.969	1.062	0.93
17M	3/754	1.103	0.974	1.075	0.93
17M	3/775	1.109	0.921	1.022	1.08
17M	3/743	1.084	0.981	1.064	1.08
120	3/770	1.087	0.949	1.031	1.08
120	3/693	1.073	0.961	1.031	1.18

Sample	run no.	D_{Cr}	D_{Ti}	D_{Al}	D_{Ca}
17M	3/700	0.666	1.25	1.236	1.385
17M	3/754	0.666	0.80	0.594	1.357
17M	3/775	0.714	1.60	1.396	1.763
17M	3/743	0.909	0.83	0.627	1.320
120	3/770	1.000	1.25	1.24	1.58
120	3/693	0.923	1.33	1.389	1.57

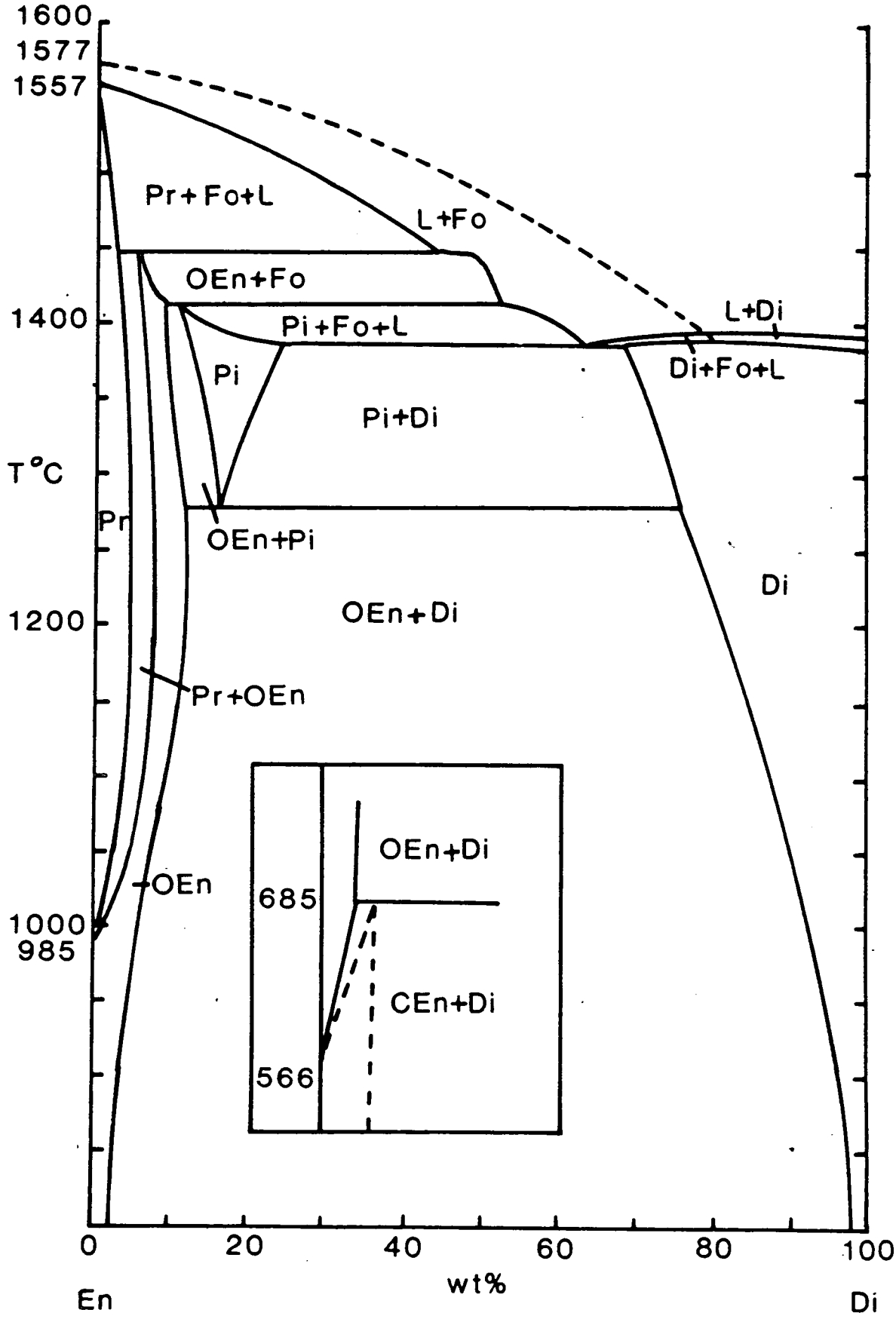

Figure 3.1

Phase diagram for the enstatite-diopside join, after fig. 7b of Huebner (1980)

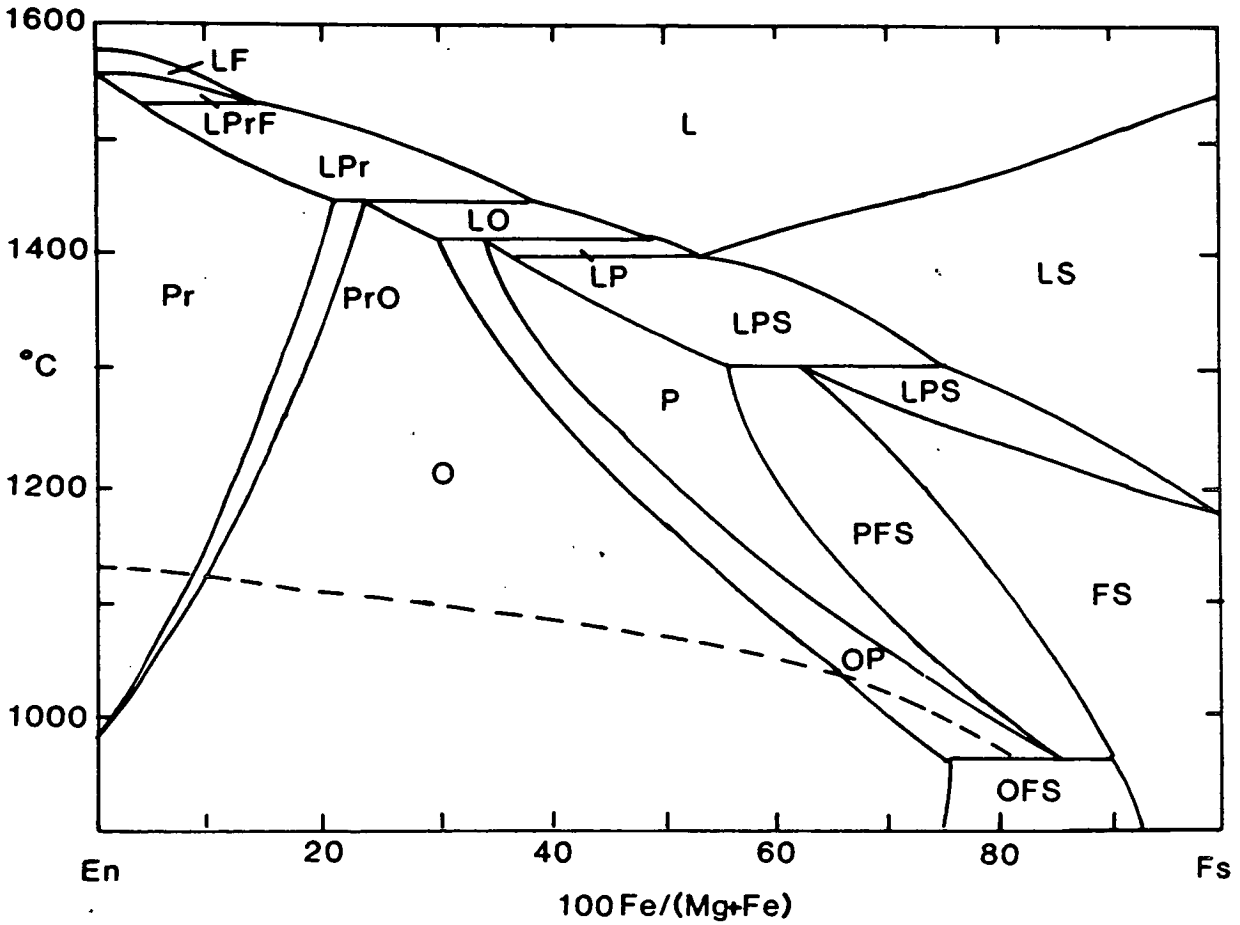

Figure 3.2

Phase diagram for the enstatite-ferrosilite join after fig.8 of Huebner (1980).

L - liquid, F - olivine, Pr - protopyroxene, O - orthopyroxene, P - pigeonite, S - silica

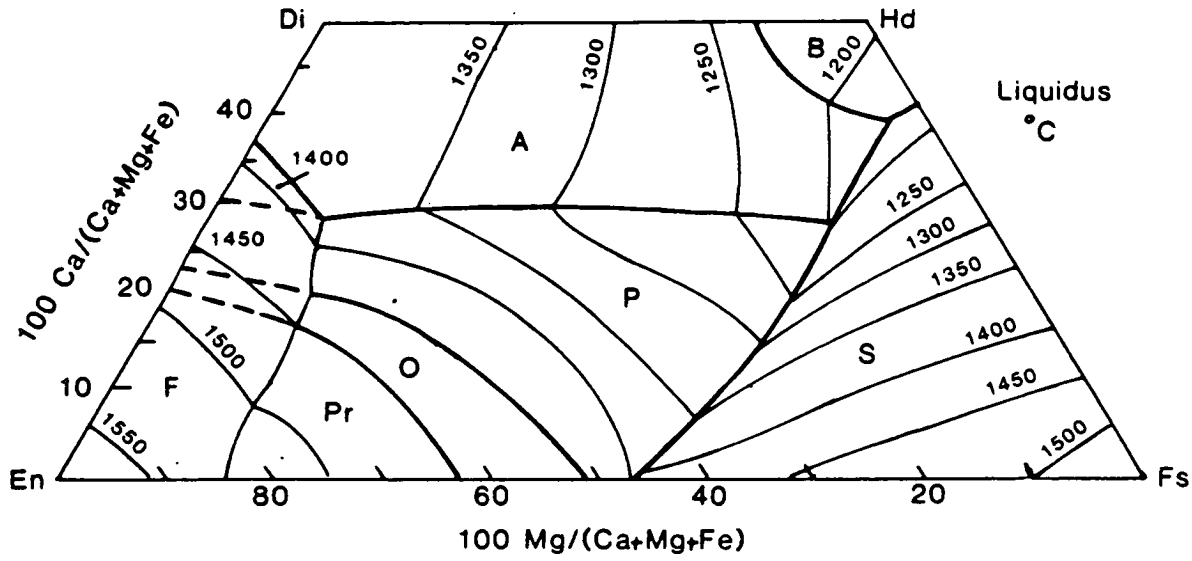

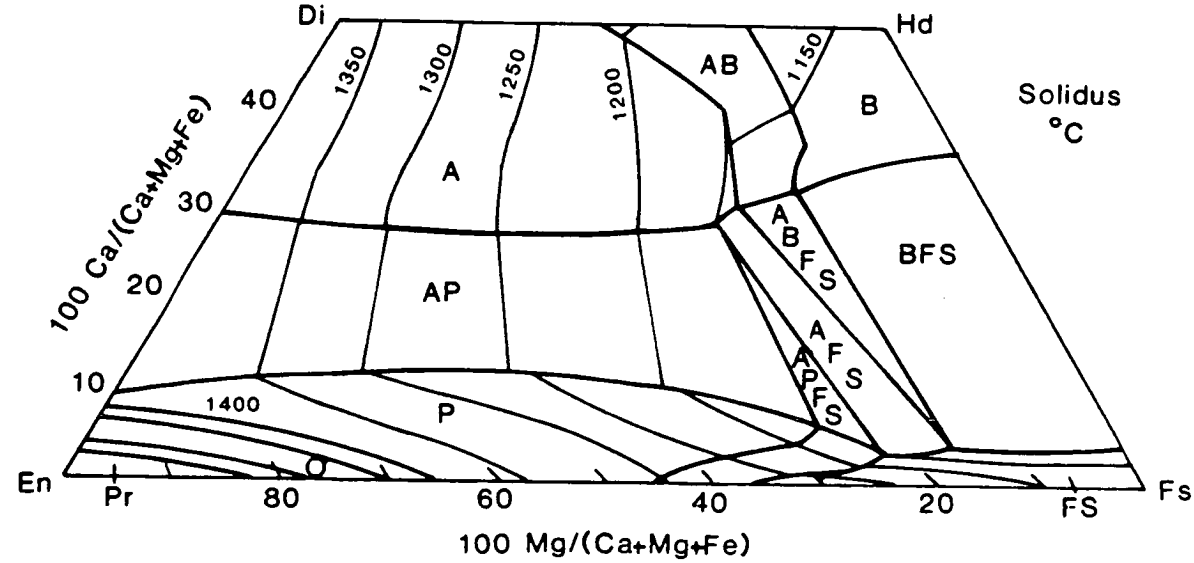

Figure 3.3

Liquidus (3.3a) and solidus (3.3b) diagrams for the pyroxene quadrilateral in synthetic systems after fig. 21 of Huebner (1980).

A - augite, F - olivine, Pr - protopyroxene, O - orthopyroxene, P - pigeonite, B - ferrobustamite, S - silica

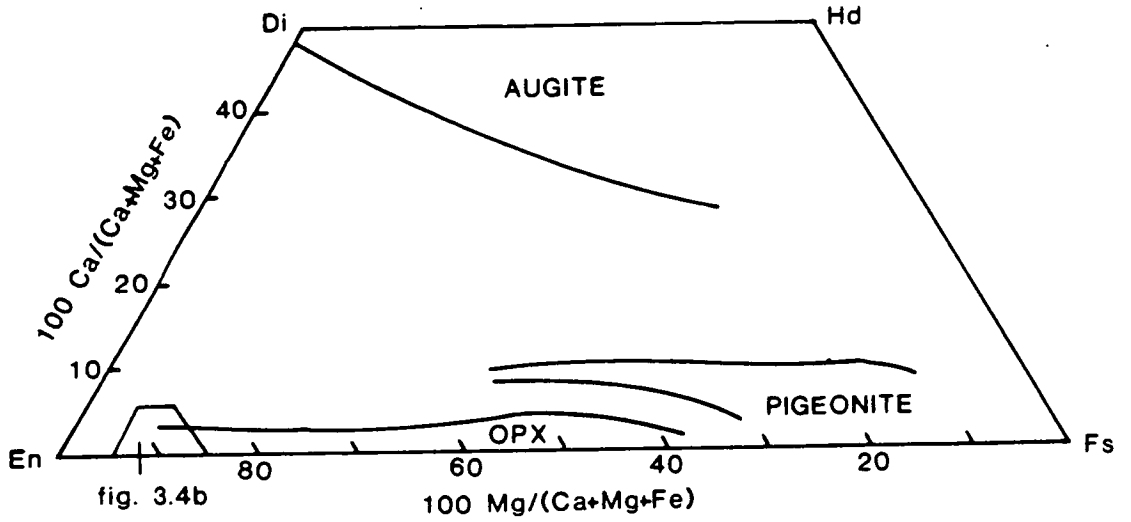

Figure 3.4

Generalized solidus diagram for the pyroxene quadrilateral in natural rocks (3.4a) after fig. 4 Huebner (1980). The proto-pyroxene analyses (3.4b) are taken from Crawford (1980), Komatsu (1980), Sameshima et al. (1983), Sharaskin et al. (1980), Shiraki et al. (1980); and are given in appendix III.1.

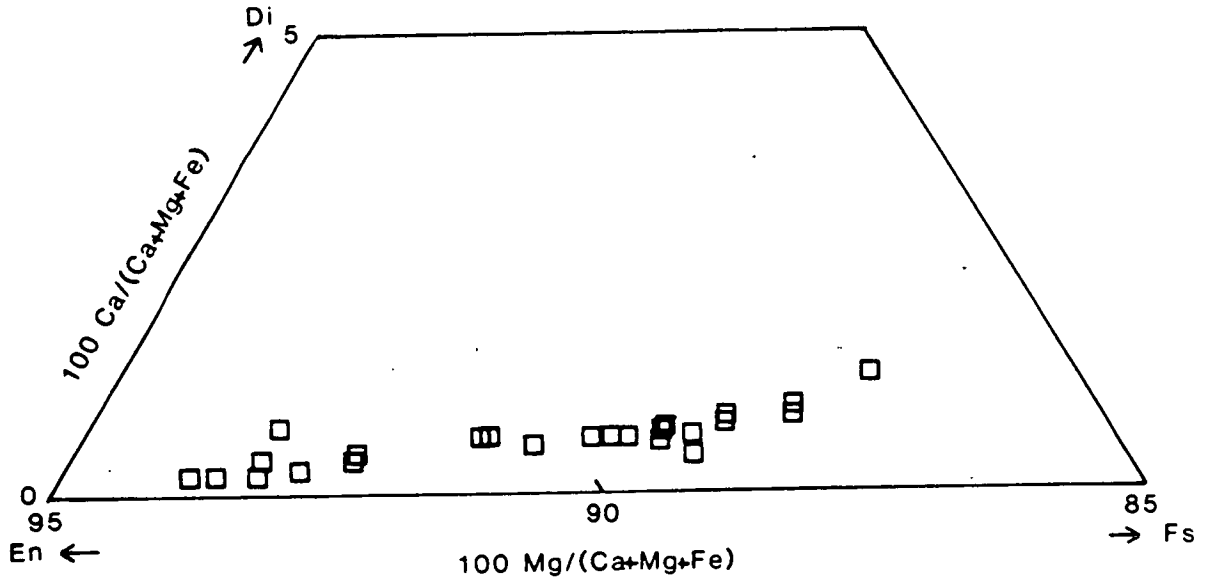

Figure 3.5

Orthopyroxene and pigeonite analyses from experiments on remelted rocks (table 3.1).

× orthopyroxene

□ pigeonite

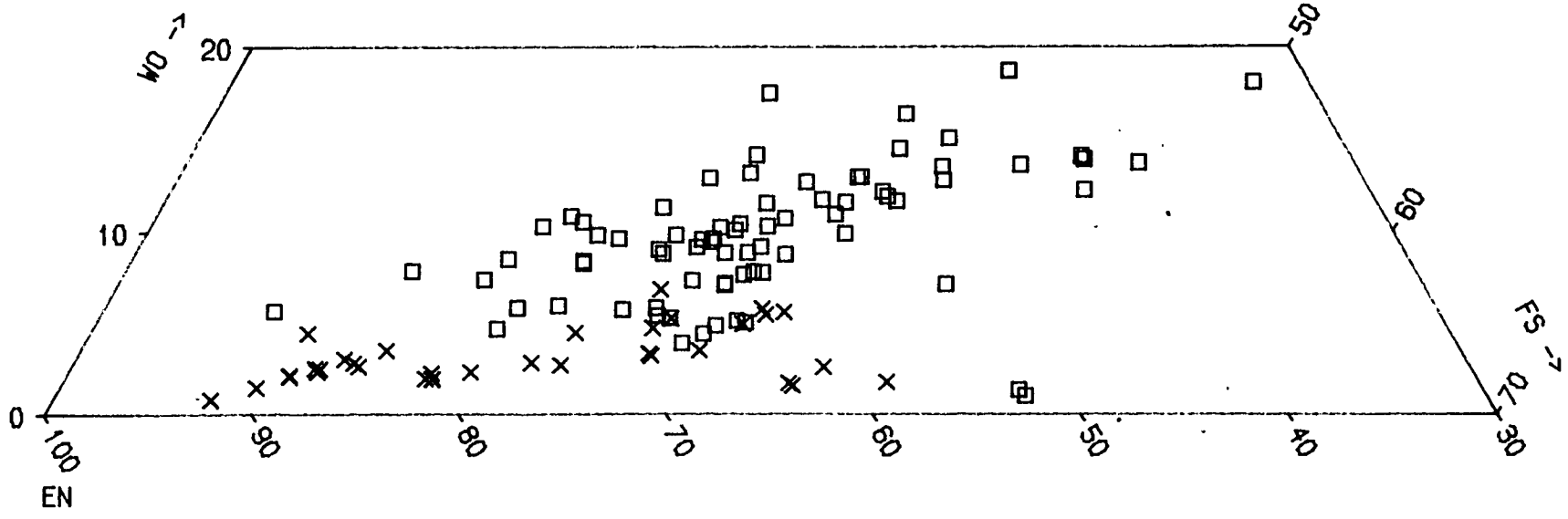

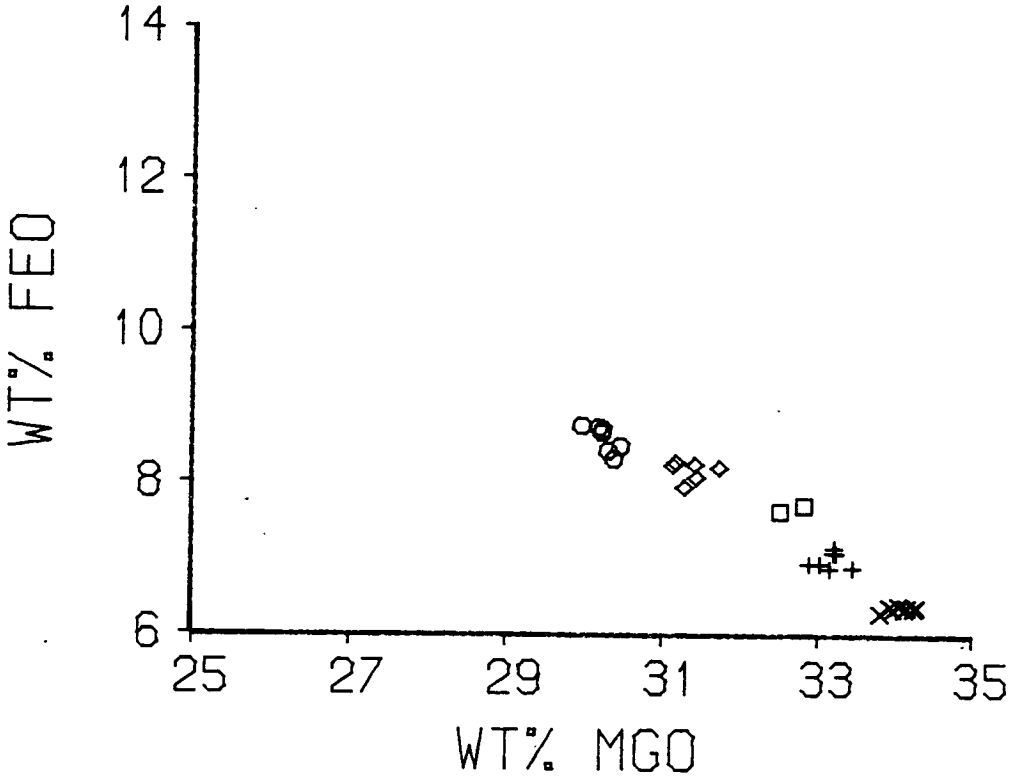
14
12
10
8
6
WT% FEO
25
27
29
31
33
35
WT% MGO

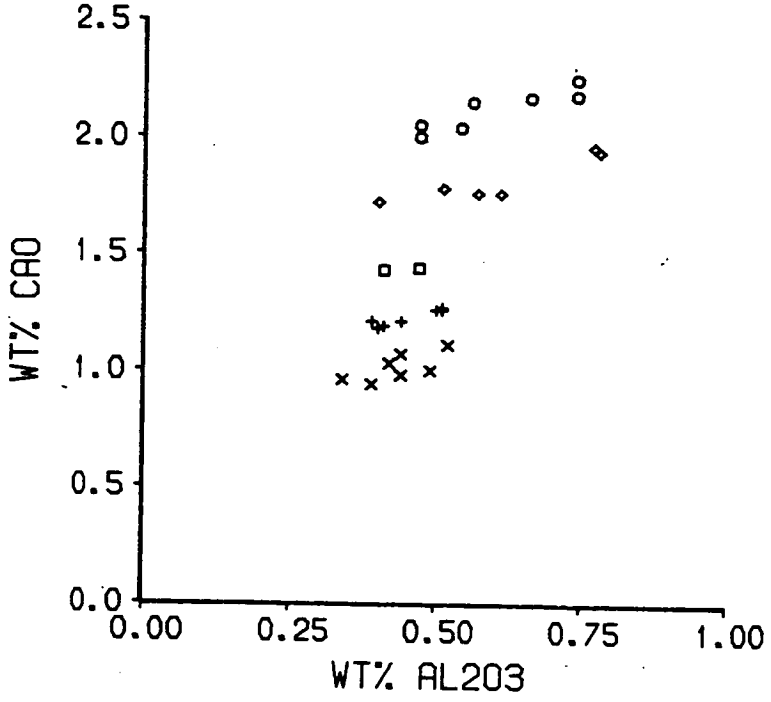
2.5
2.0
1.5
1.0
0.5
0.0
WT% CAO
0.00
0.25
0.50
0.75
1.00
WT% AL203

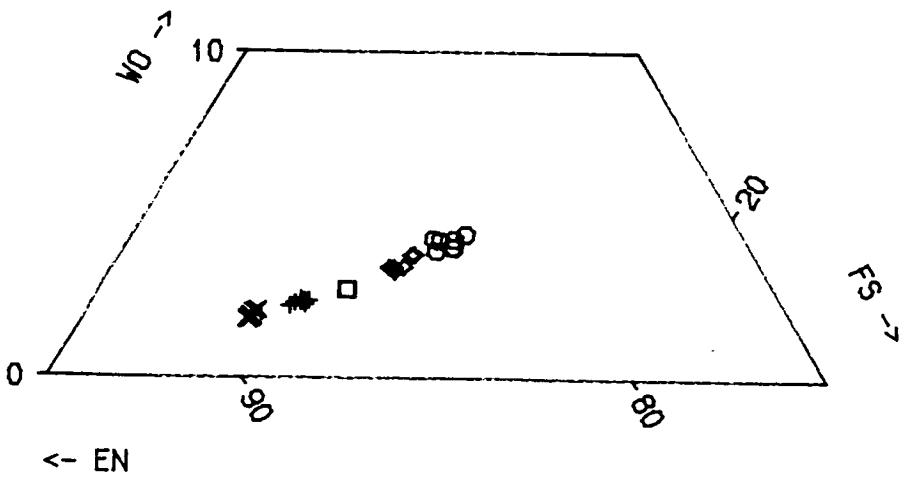
WO ->
10
20
FS ->
0
90
80
<- EN

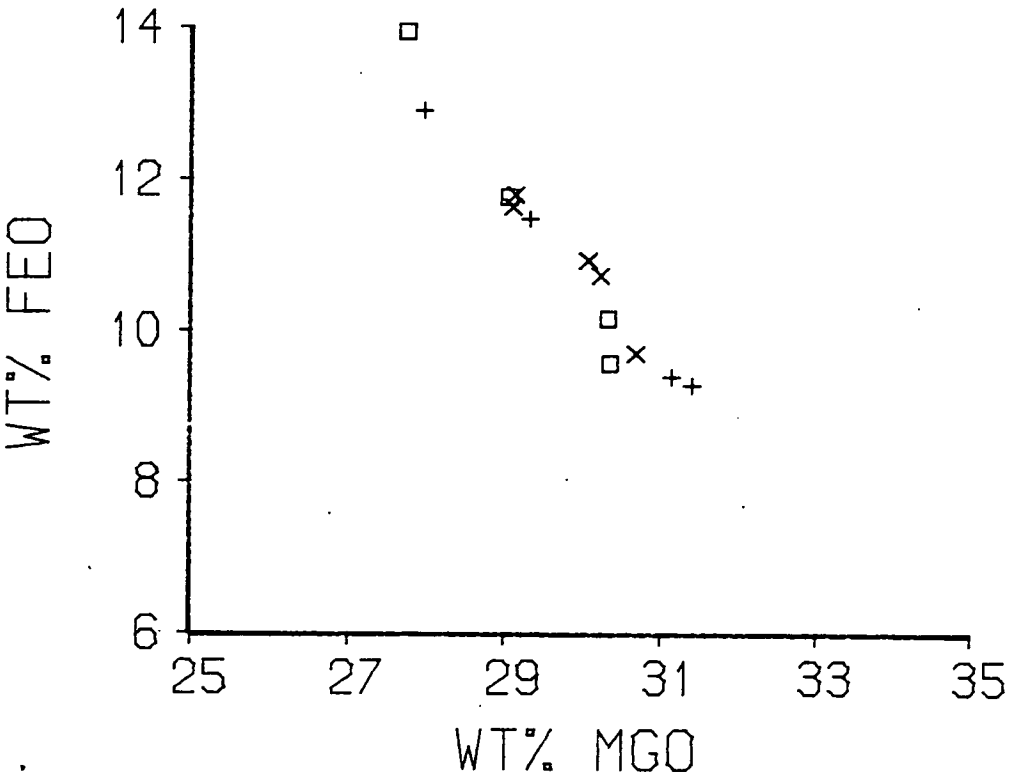
14
12
10
8
6
WT% FEO
25
27
29
31
33
35
WT% MGO

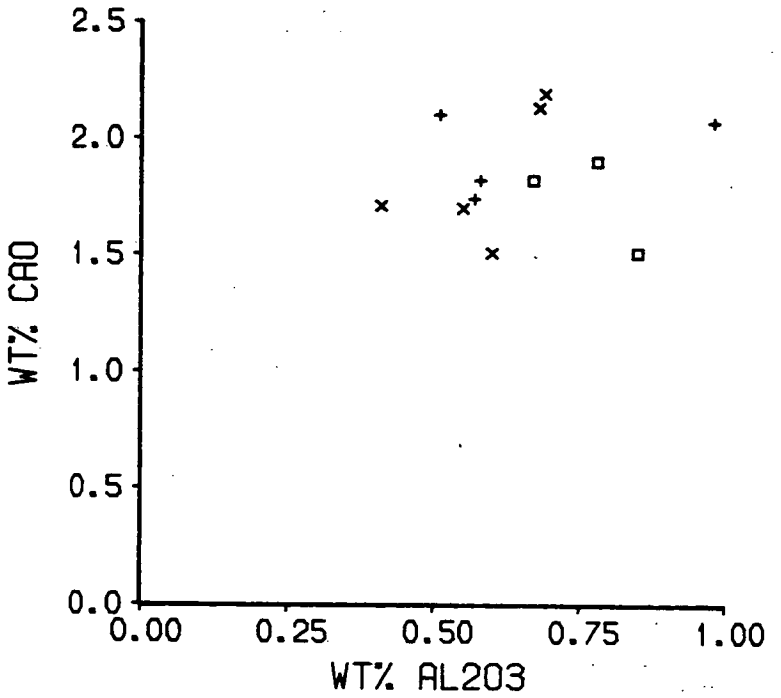
2.5
2.0
1.5
1.0
0.5
0.0
WT% CAO
0.00
0.25
0.50
0.75
1.00
WT% AL203

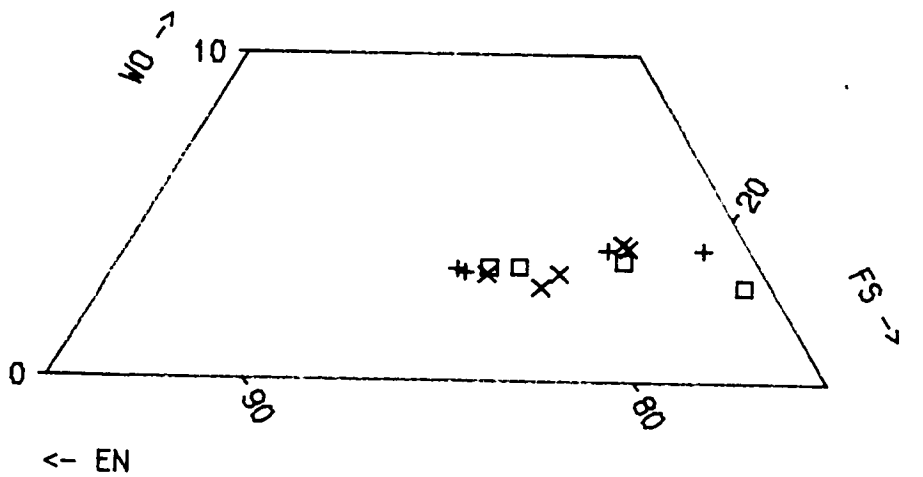
WO ->
10
20
FS ->
0
90
80
<- EN

Figure 3.7

Pyroxene analyses from long (477 hours) and short (24 or 48 hours) experiments on samples 295 (3.7a) and M1MET (3.7b). In the longer experiment both samples showed a more uniform ∔ composition with respect to iron and magnesium. That the pyroxenes from sample 295 became less magnesian in the longer experiment whilst those from sample M1MET became more magnesian probably reflects the composition of relict crystals in the two samples. There was no real improvement in homogeneity with respect to calcium and aluminium, however, pyroxenes in sample 295 have become more calcic whilst those in sample M1MET have become less calcic. These changes in calcium content combined with the changes in magnesium and iron contents suggests that relict crystals in sample 295 are nearer the enstatite corner of the quadrilateral than the equilibrium crystals at 1224°C. Likewise relict crystals in M1MET are further from the enstatite corner than crystals in equilibrium at 1224°C.

□ 477 hr
× 24 / 48 hr

fig. 3.7a sample 295

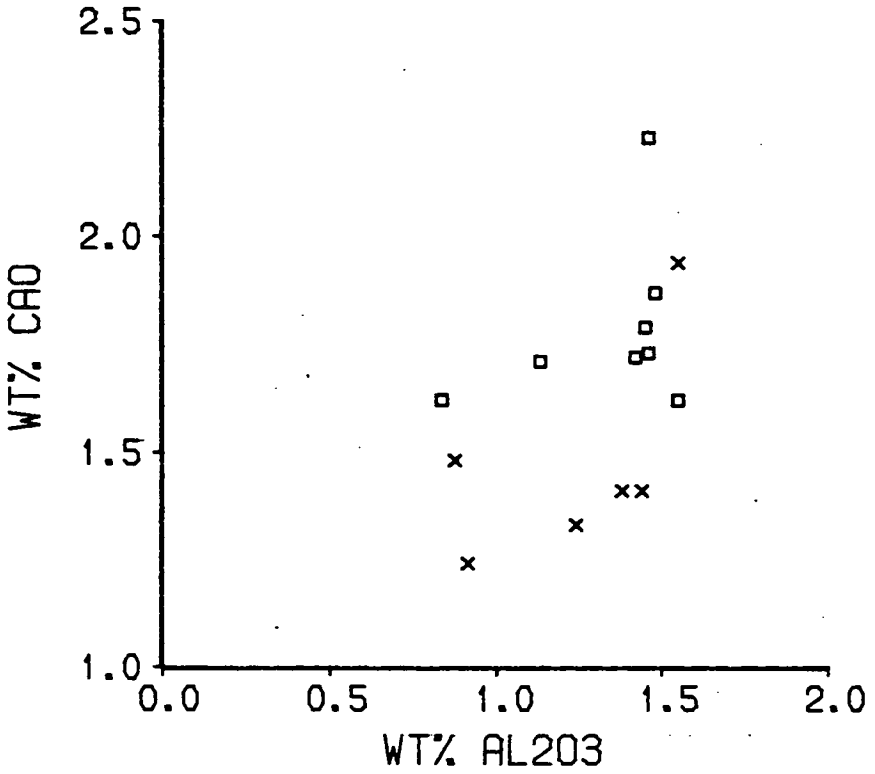

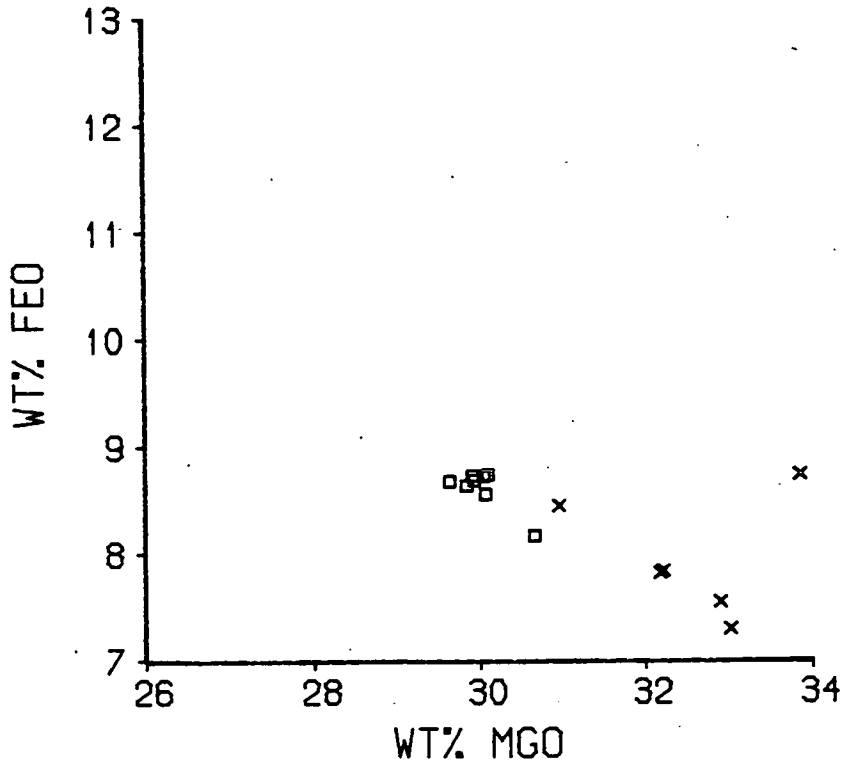

fig. 3.7b sample M1MET

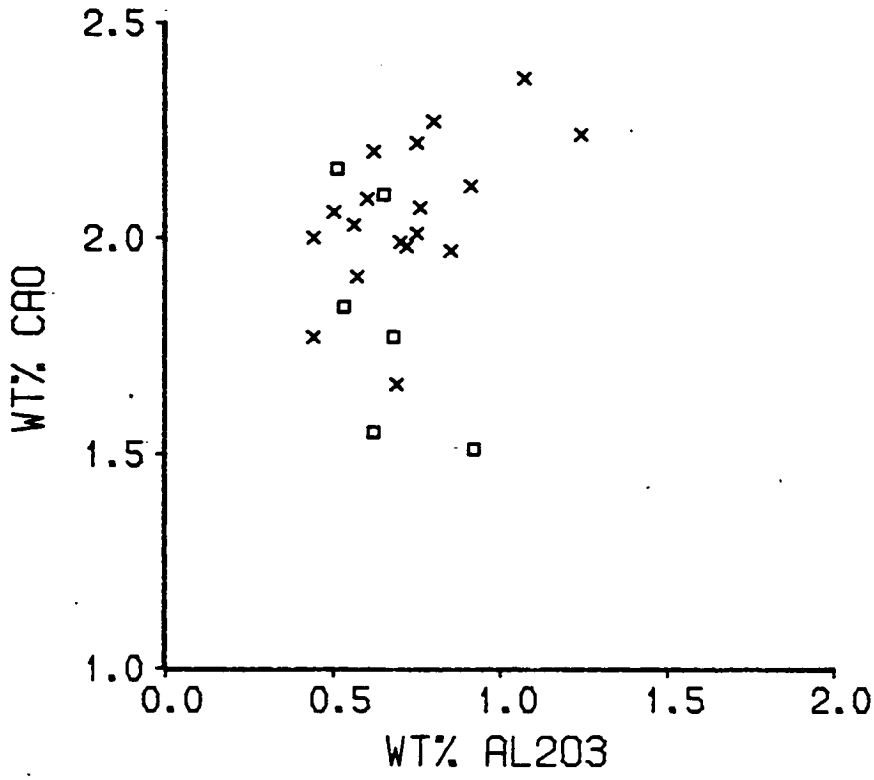

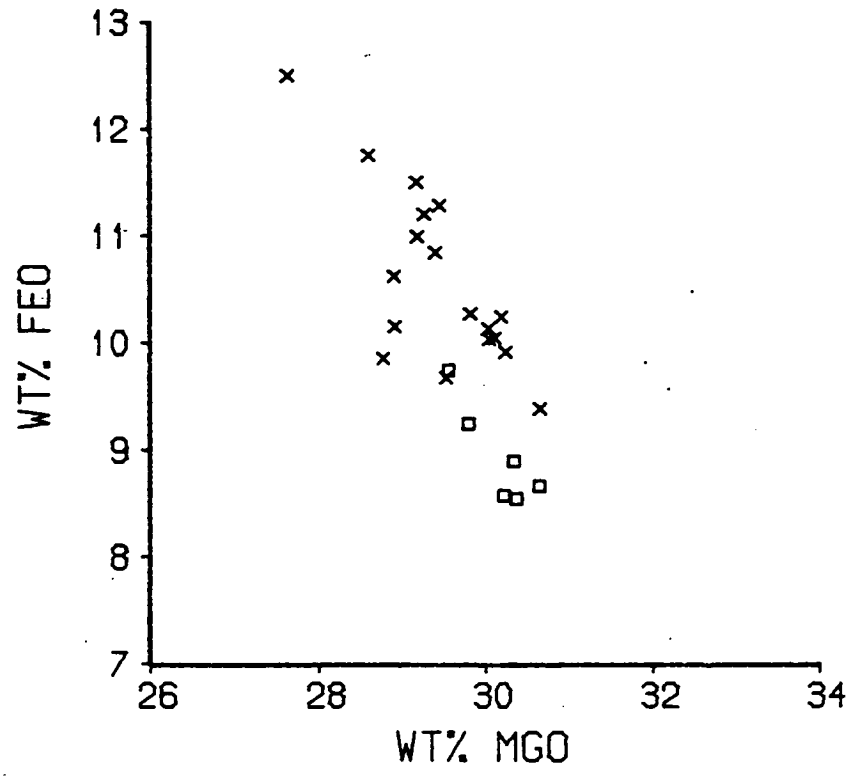

Figure 3.8

Protopyroxene and orthopyroxene analyses from cooling experiments carried out on sample 17M.

× 4:237A opx
\+ 4:237A proto
□ 4:238 opx
◇ 4:238 proto
○ 4:238A opx
△ 4:238A proto

Figure 3.9

Protopyroxene, orthopyroxene and pigeonite analyses from experiments at the IW buffer carried out on PtFe wire hooks.

● protopyroxene
▼ pigeonite

All other symbols represent orthopyroxenes.

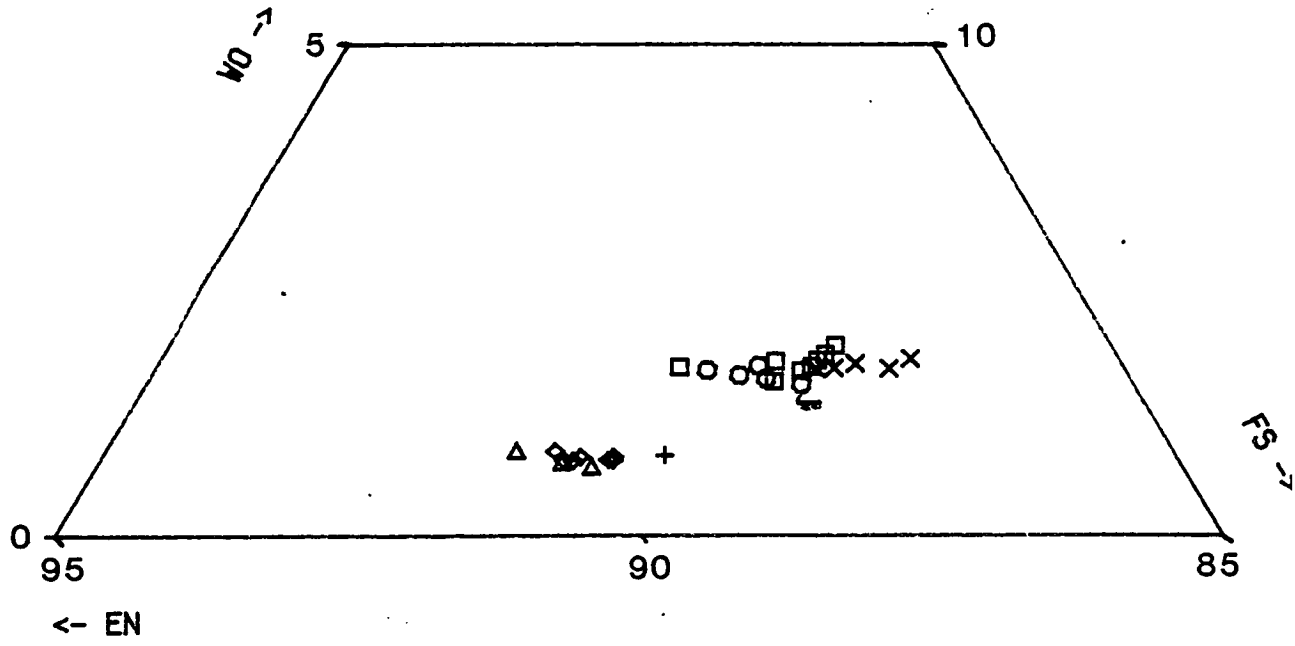
VO →
5
10
FS →
0
95
90
85
<- EN

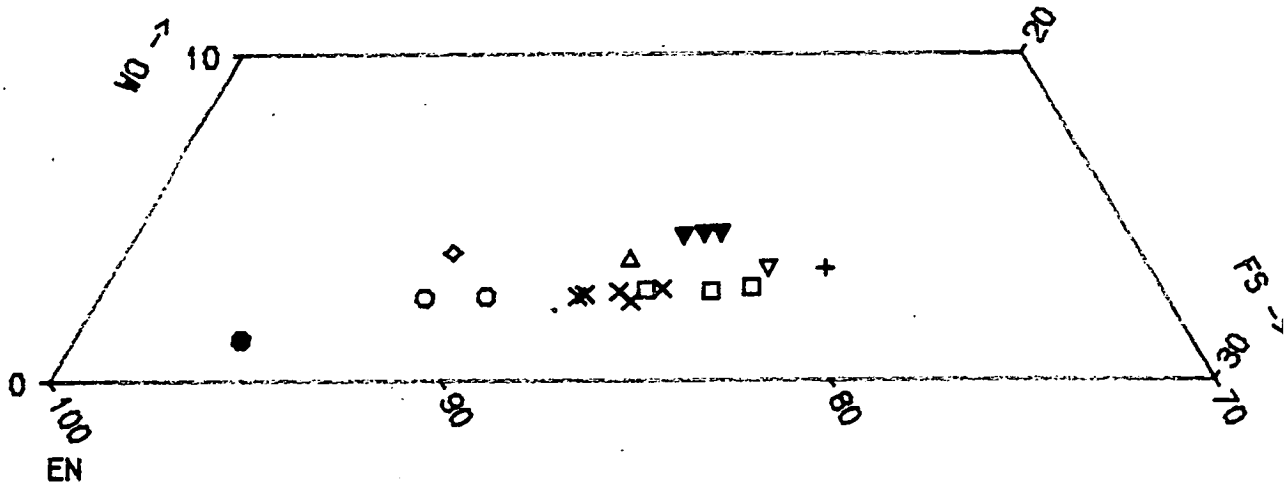
VO →
10
20
FS →
0
100
90
80
70
EN

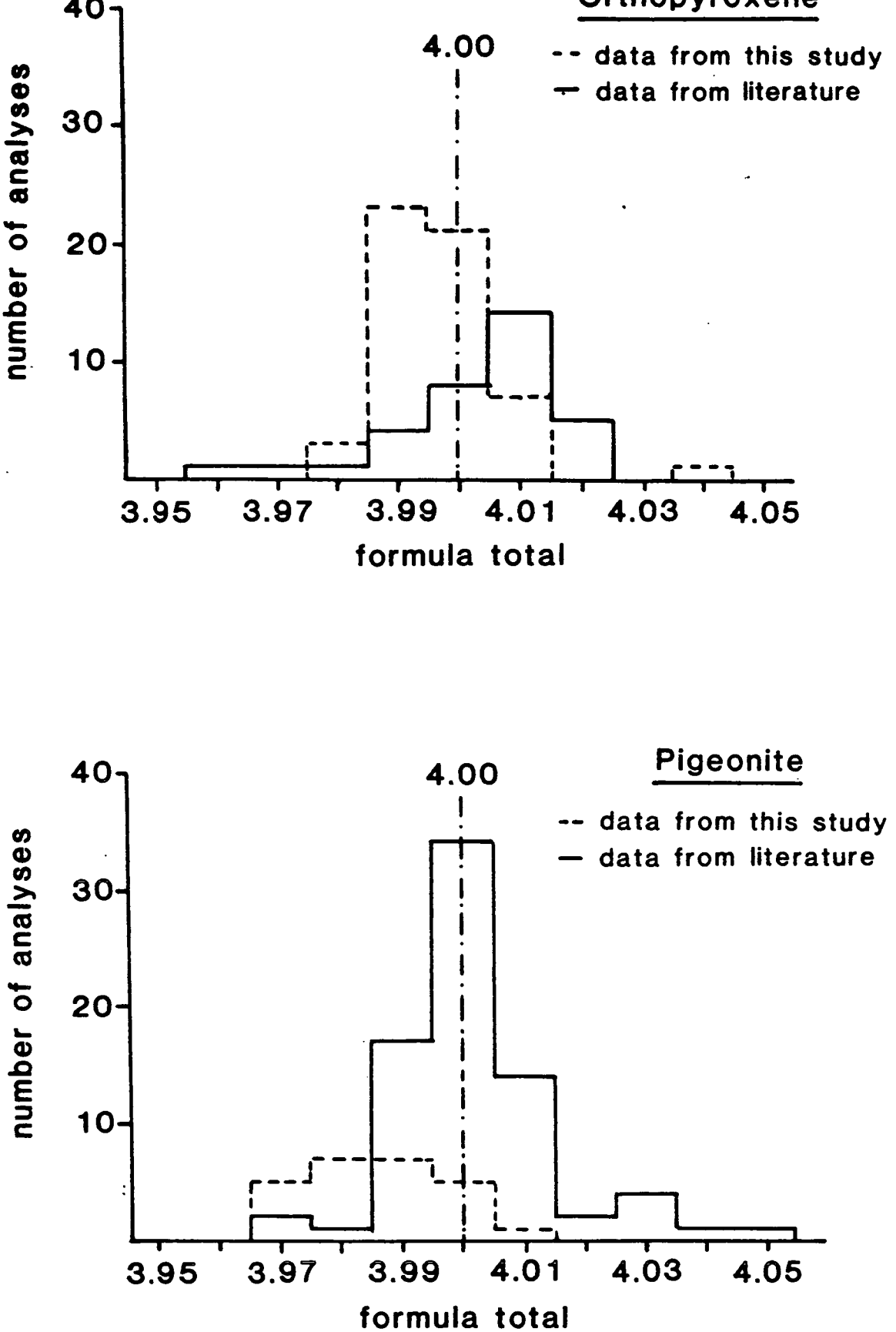

Figure 3.10

Histogram of formula totals for pyroxene analyses used in this study. The higher mean value for the literature data set reflects the greater proportion of analyses from experiments at the IW buffer where lower Fe_2O_3 contents lead to more accurate analyses (Russell pers. comm.).

Figure 3.11

Protopyroxene, orthopyroxene and pigeonite analyses from the experiments carried out in this study. The diagram is to the same scale as fig. 3.5 for comparison.

O protopyroxene
× orthopyroxene
□ pigeonite

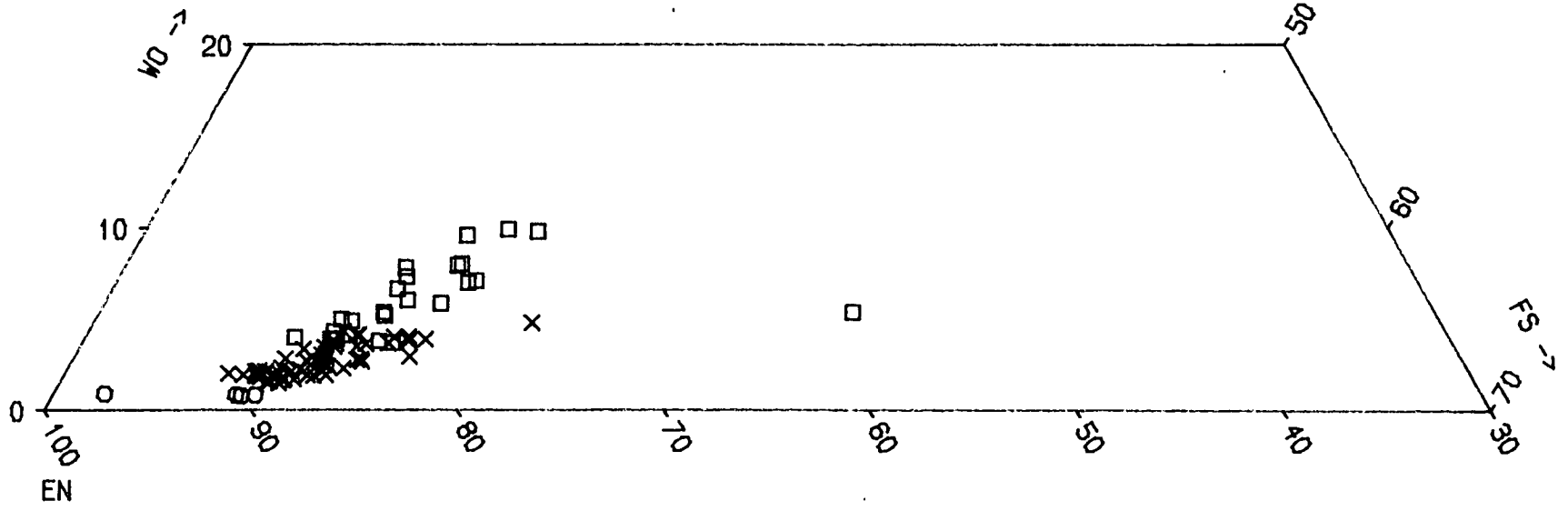

Figures 3.12 to 3.20 - the scale is in cations per six oxygens unless otherwise stated.

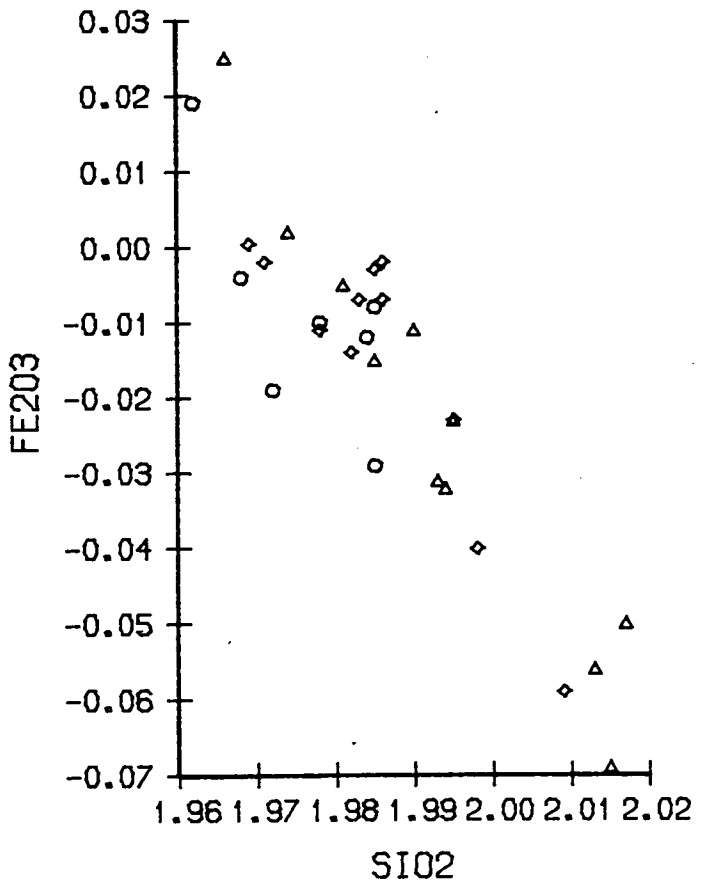

Figure 3.12

Fe_2O_3 calculations for some pyroxenes from experiments in this study.

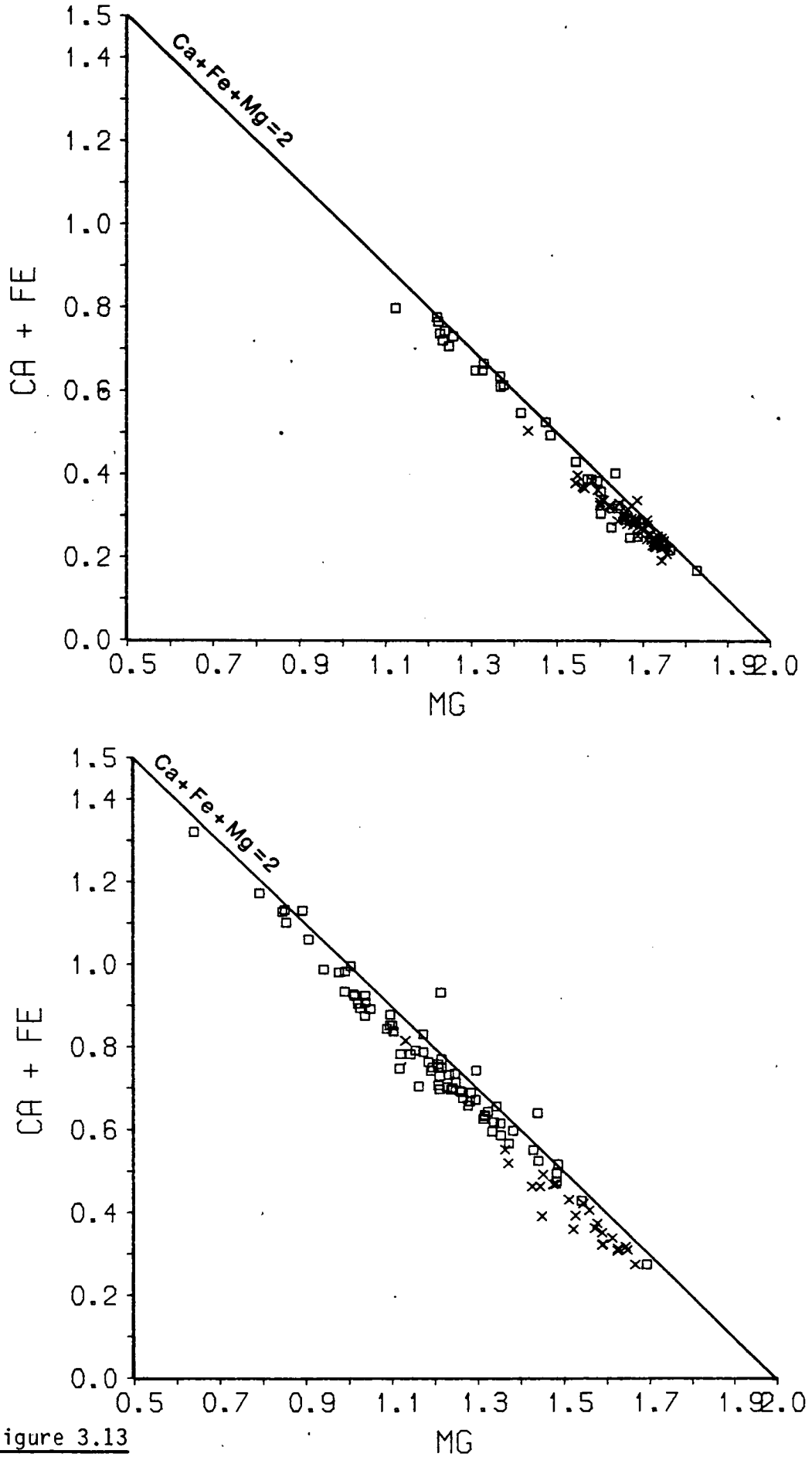

Figure 3.13

Mg:Ca:Fe relationships of orthopyroxenes (top diagram) and pigeonites (bottom diagram).

× this study

□ literature search

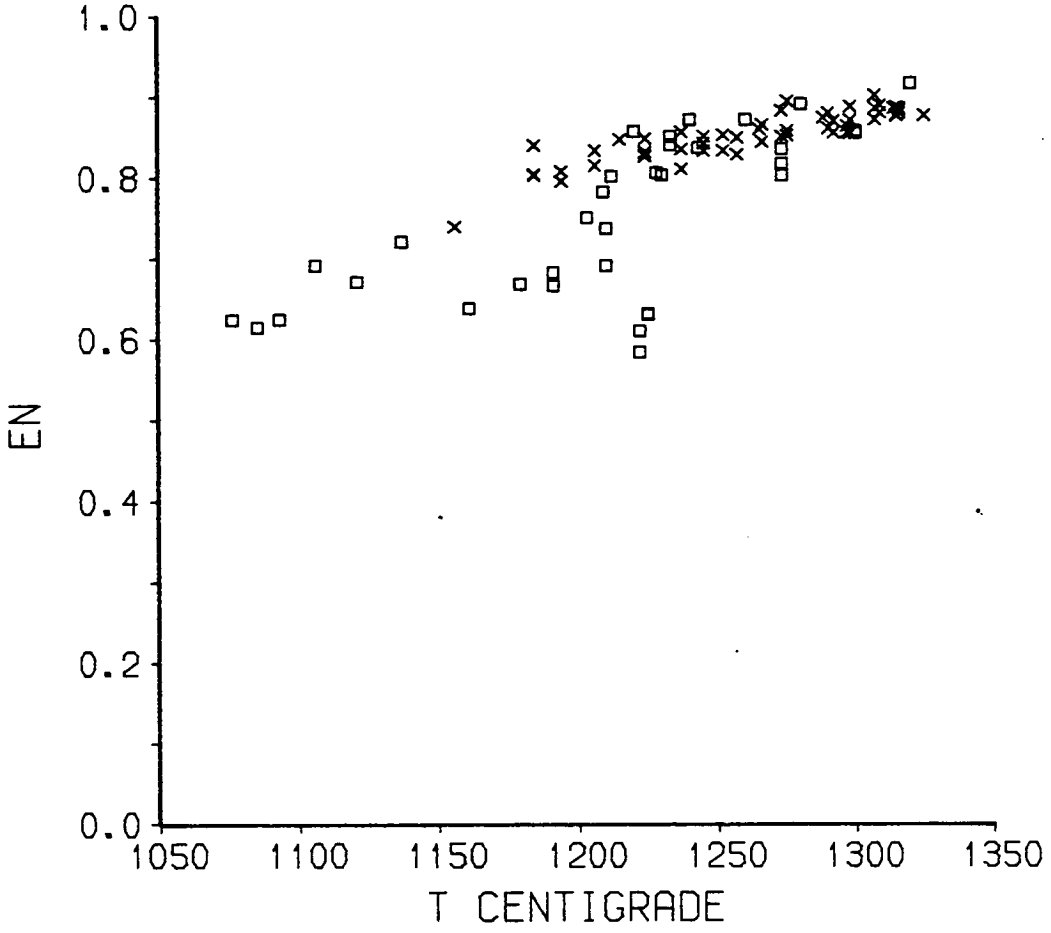
1.0
0.8
0.6
0.4
0.2
0.0
EN
1050
1100
1150
1200
1250
1300
1350
T CENTIGRADE

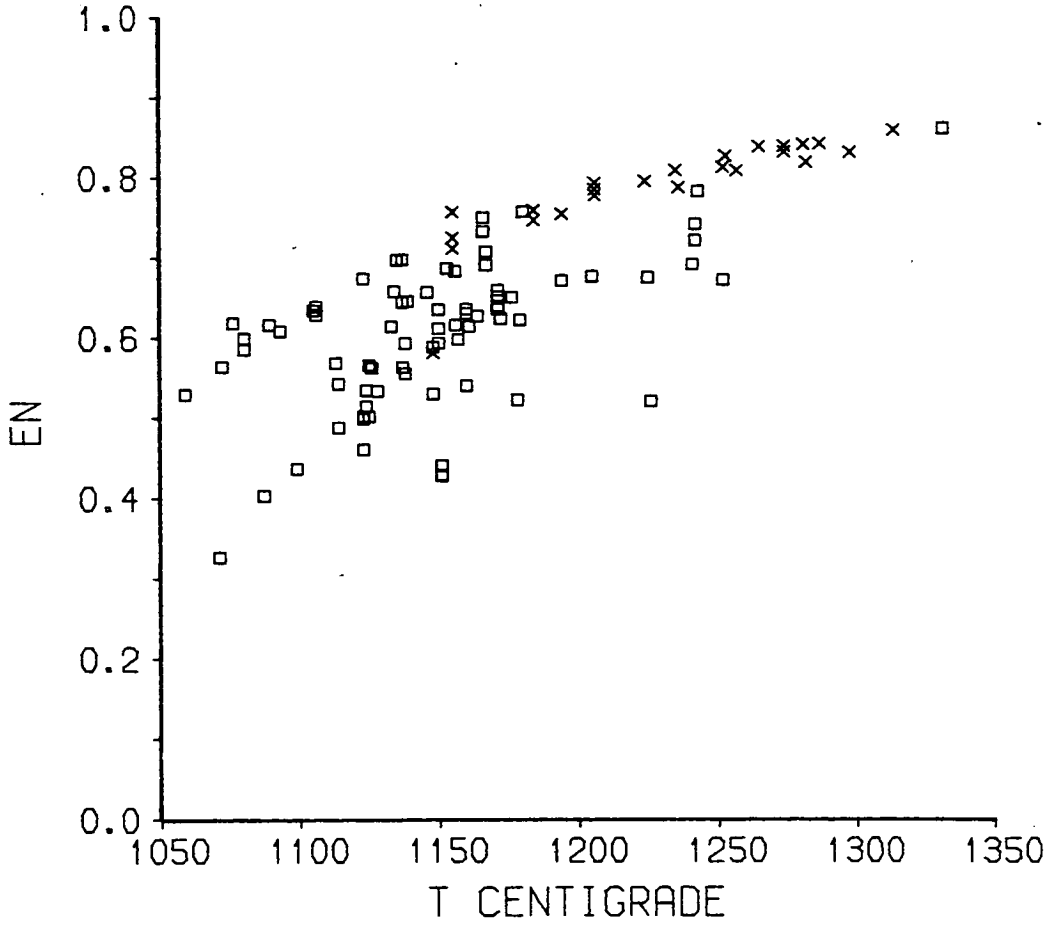
1.0
0.8
0.6
0.4
0.2
0.0
EN
1050
1100
1150
1200
1250
1300
1350
T CENTIGRADE

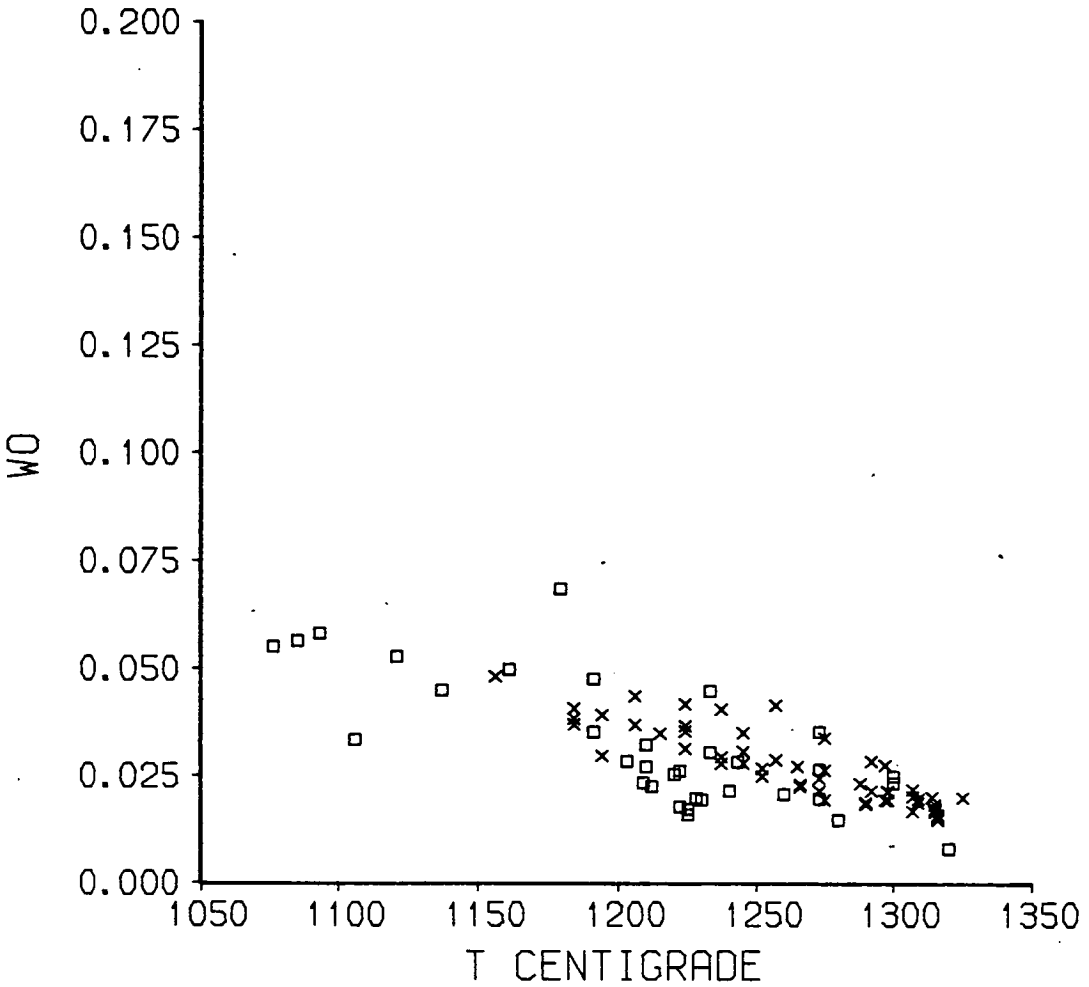
0.200
0.175
0.150
0.125
0.100
0.075
0.050
0.025
0.000
WO
1050
1100
1150
1200
1250
1300
1350
T CENTIGRADE

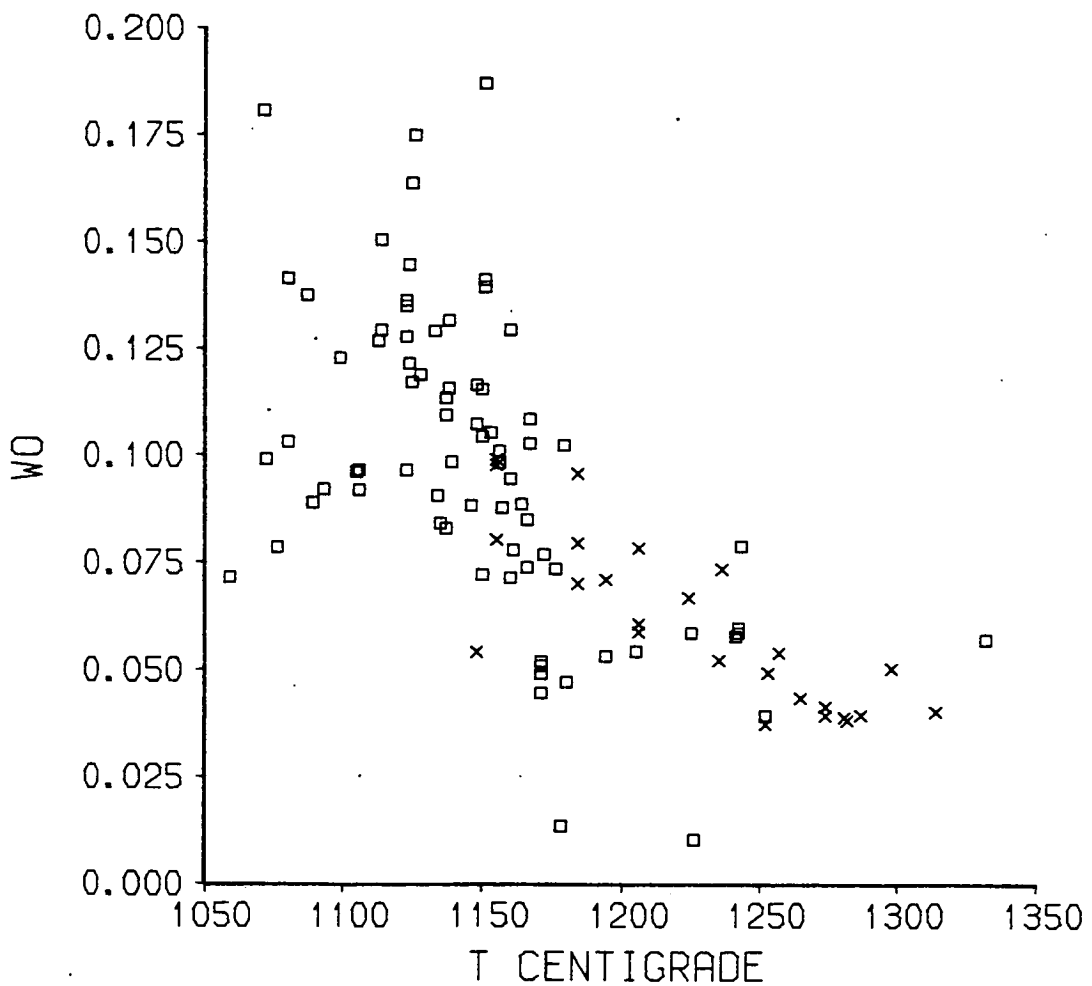
0.200
0.175
0.150
0.125
0.100
0.075
0.050
0.025
0.000
WO
1050
1100
1150
1200
1250
1300
1350
T CENTIGRADE

Figure 3.16

Changes in Fs content of orthopyroxenes (top diagram) and pigeonites (bottom diagram) with temperature. There is a wide range of Fs contents for a given temperature indicating that temperature is not the controlling factor and that other variables, such as liquid composition are involved.

× this study

□ literature search

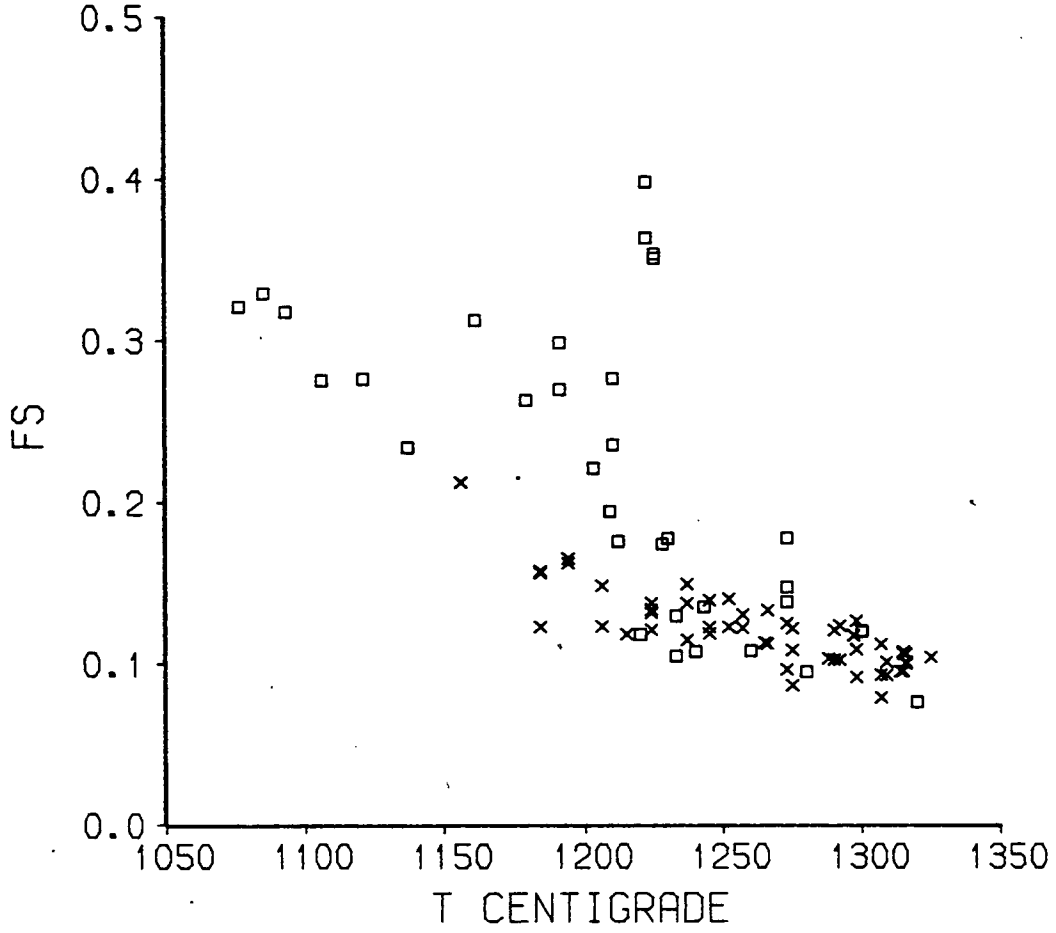
0.5
0.4
0.3
0.2
0.1
0.0
FS
1050
1100
1150
1200
1250
1300
1350
T CENTIGRADE

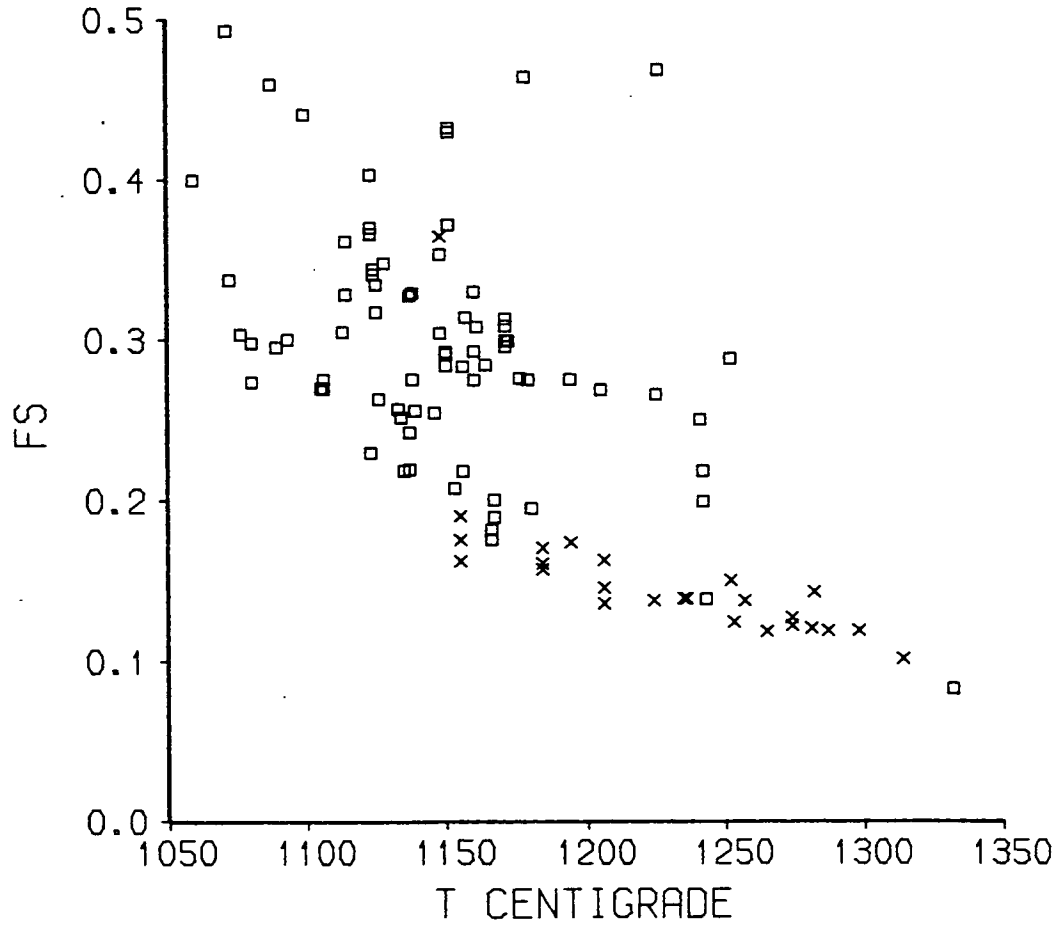
0.5
0.4
0.3
0.2
0.1
0.0
FS
1050
1100
1150
1200
1250
1300
1350
T CENTIGRADE

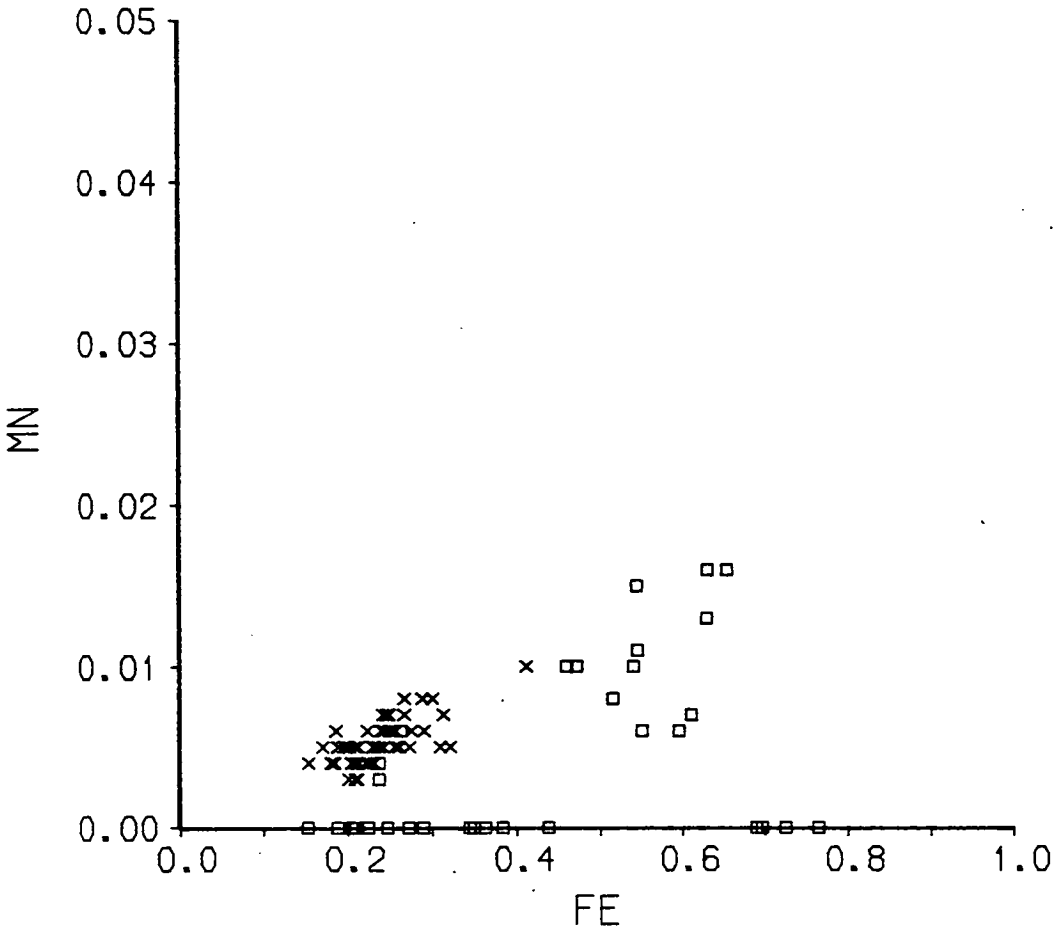
0.05
0.04
0.03
0.02
0.01
0.00
MN
0.0
0.2
0.4
0.6
0.8
1.0
FE

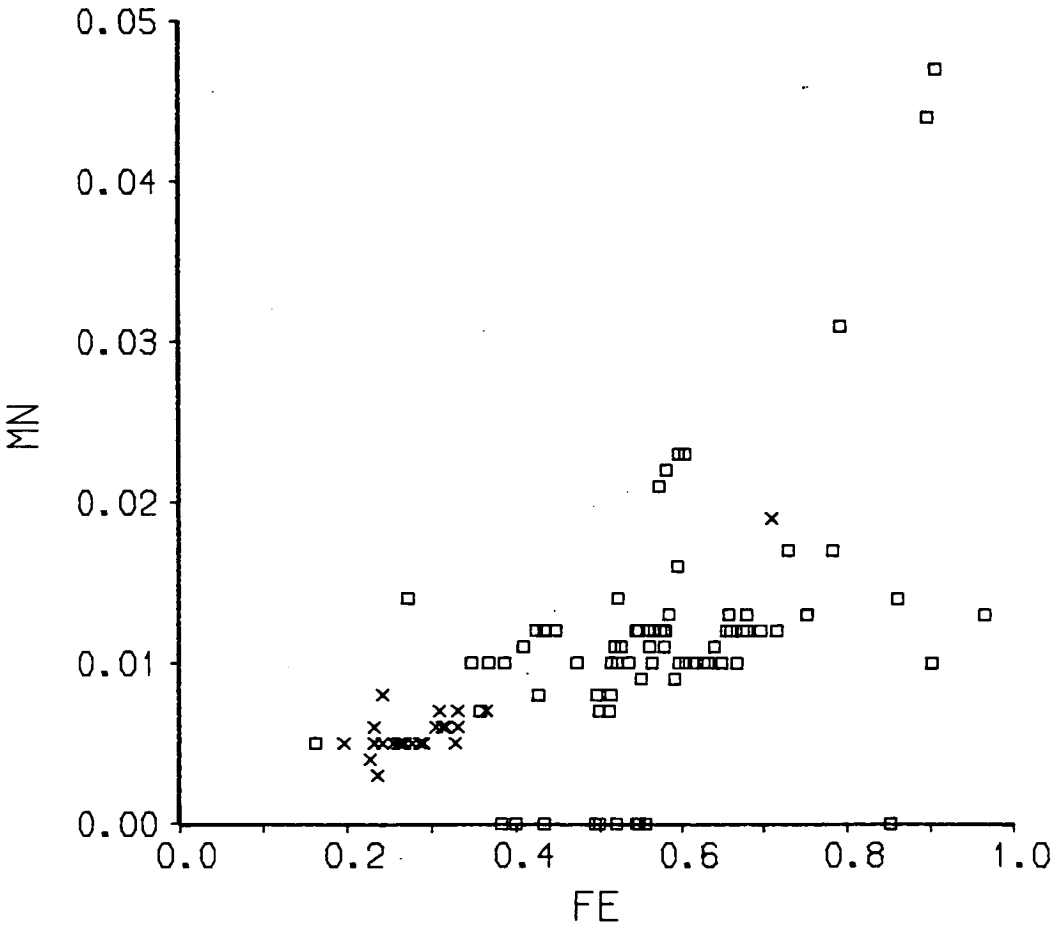
0.05
0.04
0.03
0.02
0.01
0.00
MN
0.0
0.2
0.4
0.6
0.8
1.0
FE

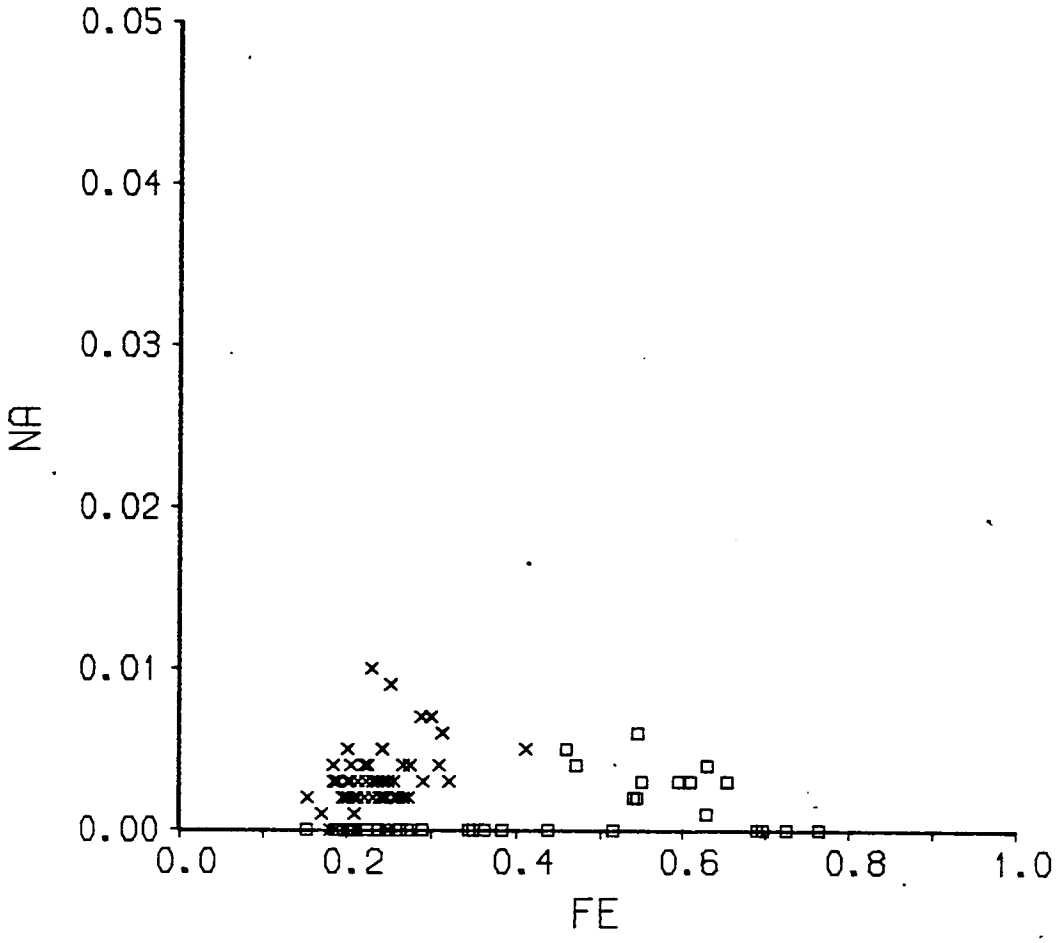
0.05
0.04
0.03
0.02
0.01
0.00
NA
0.0
0.2
0.4
0.6
0.8
1.0
FE

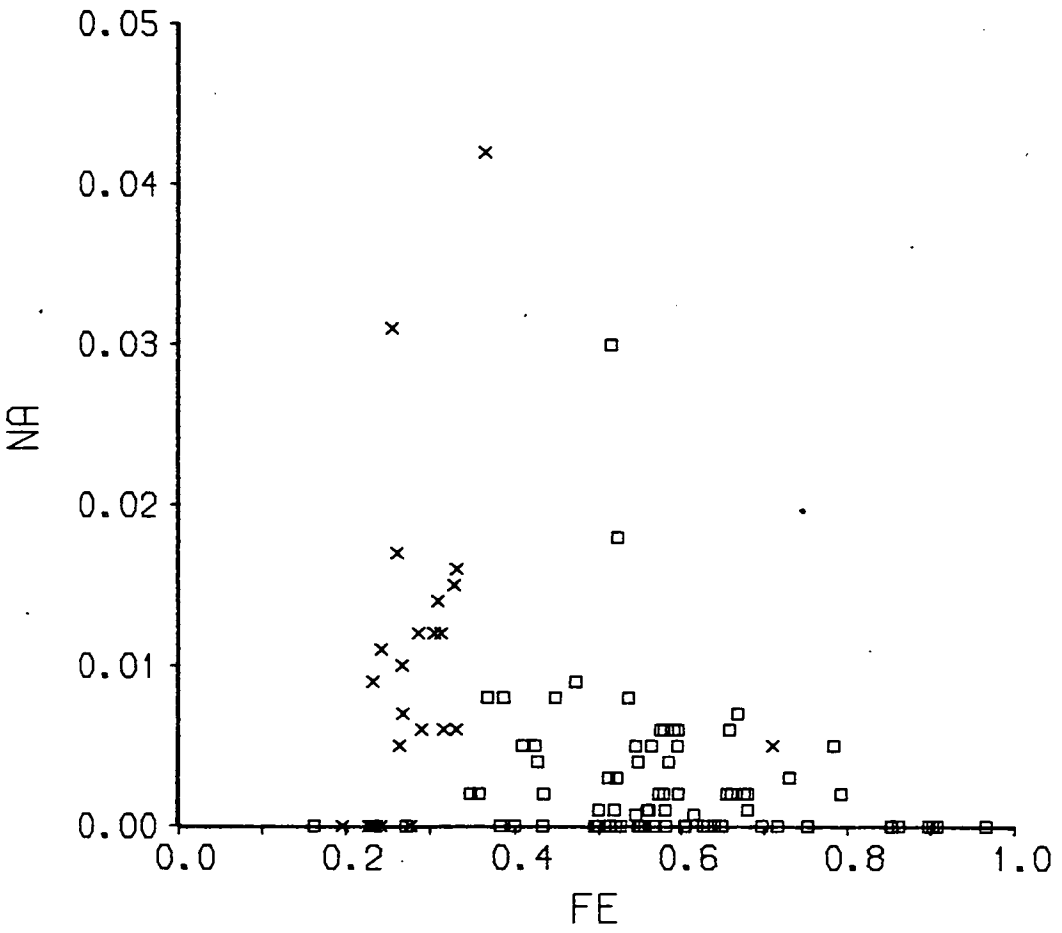
0.05
0.04
0.03
0.02
0.01
0.00
NA
0.0
0.2
0.4
0.6
0.8
1.0
FE

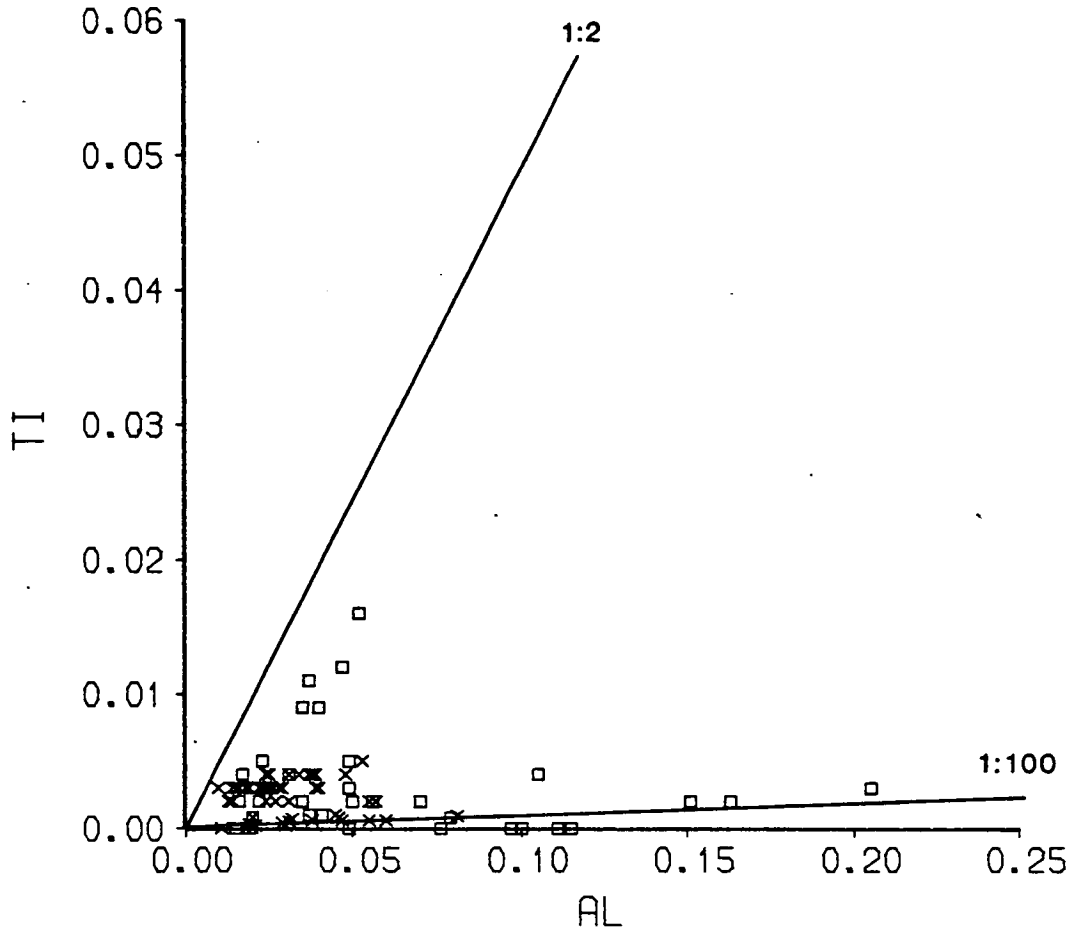
0.06
0.05
0.04
0.03
0.02
0.01
0.00
TI
1:2
1:100
0.00
0.05
0.10
0.15
0.20
0.25
AL

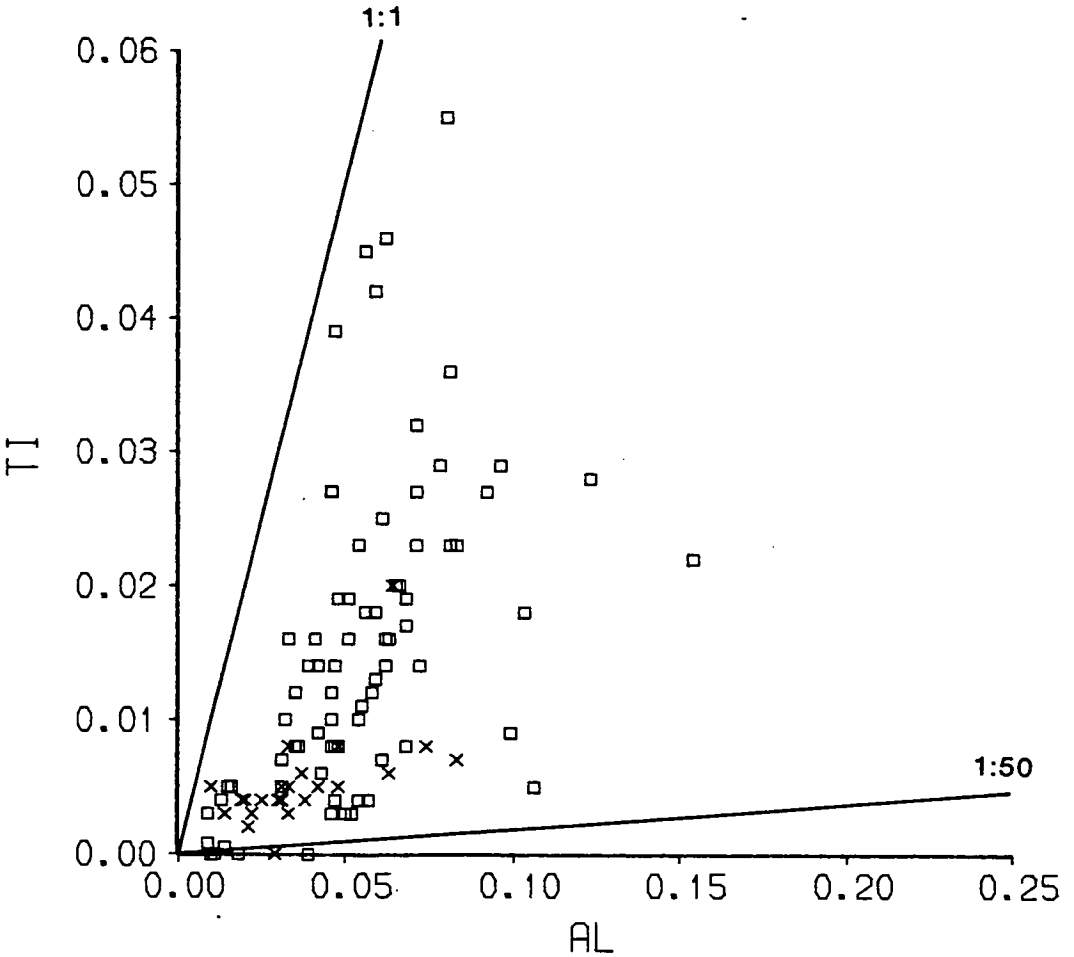
0.06
0.05
0.04
0.03
0.02
0.01
0.00
TI
1:1
1:50
0.00
0.05
0.10
0.15
0.20
0.25
AL

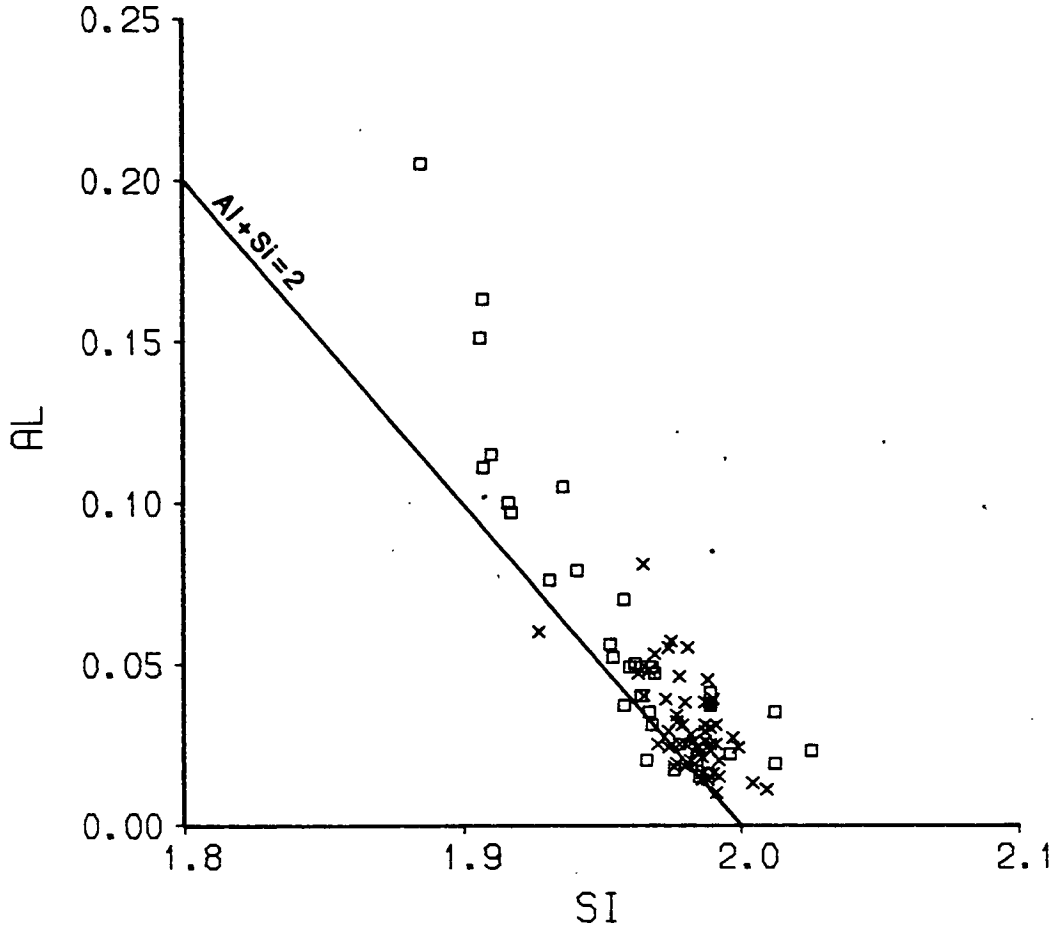
0.25
0.20
0.15
0.10
0.05
0.00
AL
Al+Si=2
1.8
1.9
2.0
2.1
SI

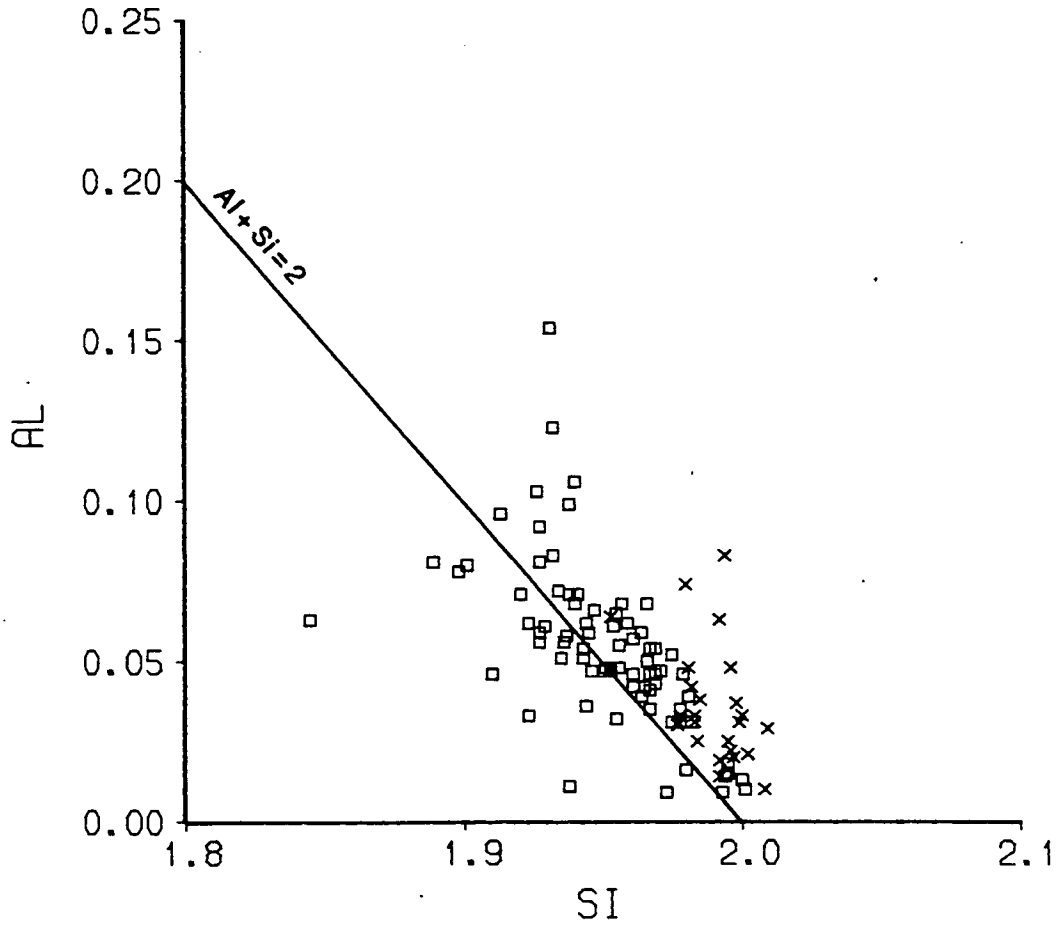
0.25
0.20
0.15
0.10
0.05
0.00
AL
Al+Si=2
1.8
1.9
2.0
2.1
SI

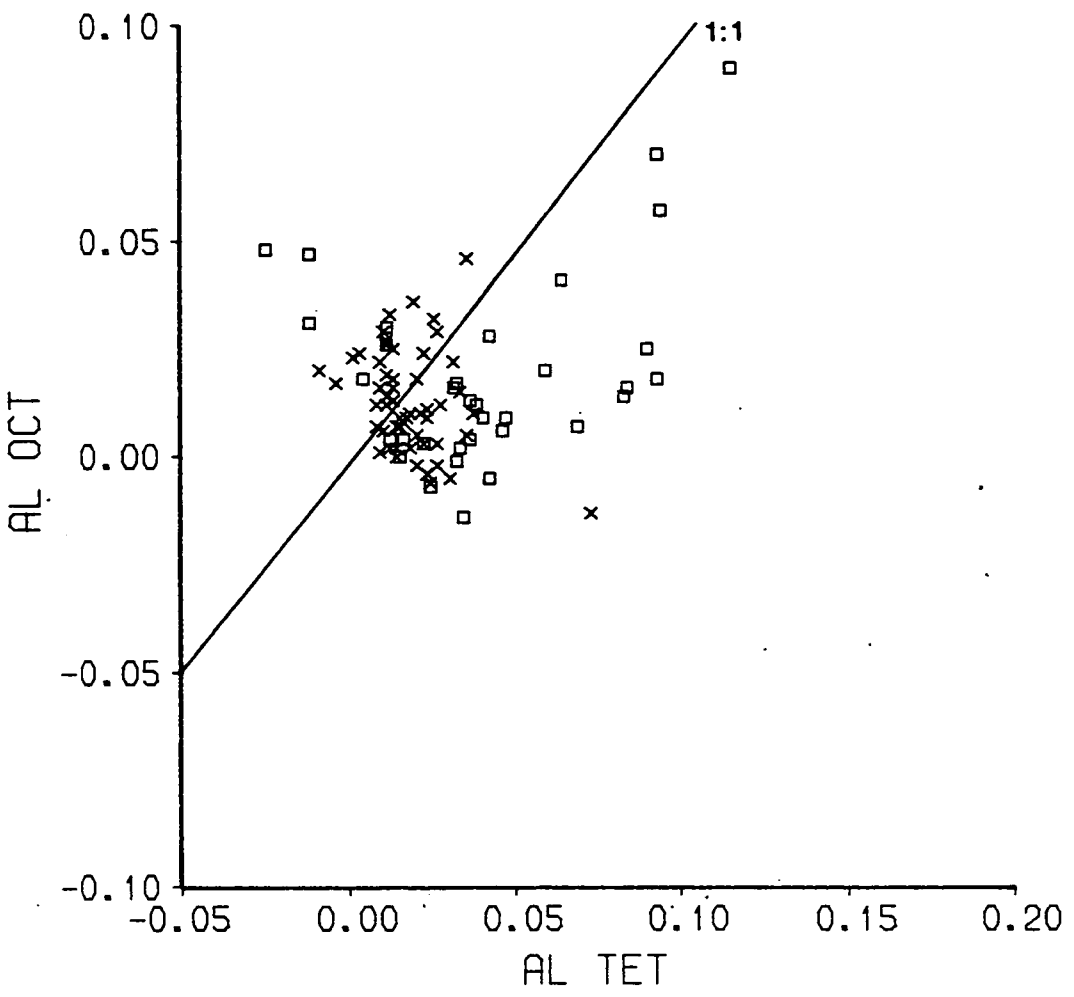
0.10
0.05
0.00
-0.05
-0.10
AL OCT
1:1
-0.05
0.00
0.05
0.10
0.15
0.20
AL TET

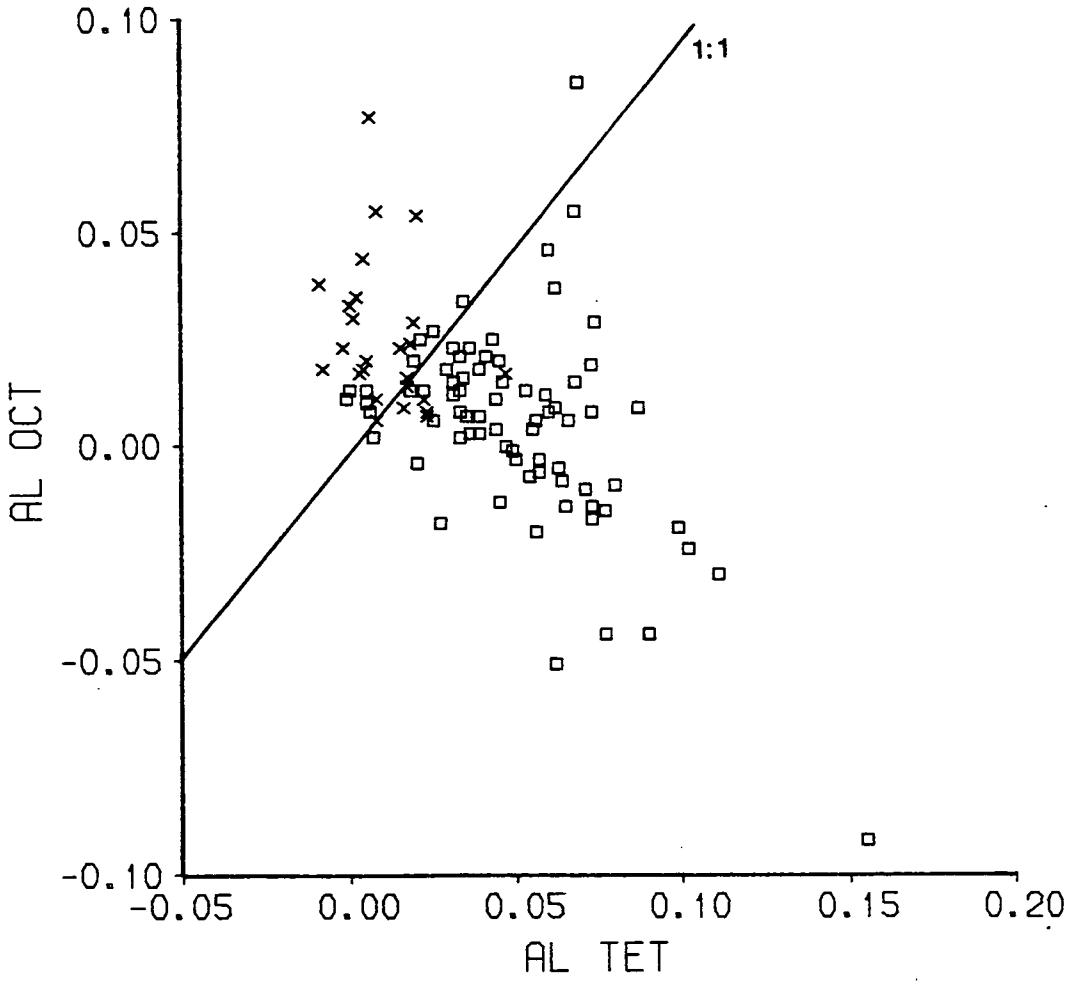
0.10
0.05
0.00
-0.05
-0.10
AL OCT
1:1
-0.05
0.00
0.05
0.10
0.15
0.20
AL TET

Figure 3.22

Forsterite content v temperature for olivines produced in this study. Although there is some scatter overall, each sample defines a single line of decreasing Fo with decreasing temperature e.g.

- – – . K1 & K6 at NNO
- –·– · 295 at NNO & IW
- –··– 17M at NNO & CCO

where

- × NNO
- □ CCO
- △ IW

Figures 3.23 to 3.25 - the scale is in cations per four oxygens.

Figure 3.23

Mg^{2+} v Fe^{2+} for olivines. $Mg^{2+} + Fe^{2+}$ is always less than 2, those analyses which deviate from the trend are contaminated by glass which results in an increase in Ca^{2+} content (fig. 3.24) and a loss in Mg^{2+} content. The Fe^{2+} content is not obviously affected as the olivines and glasses contain similar amounts of iron.

- × NNO
- □ CCO
- △ IW

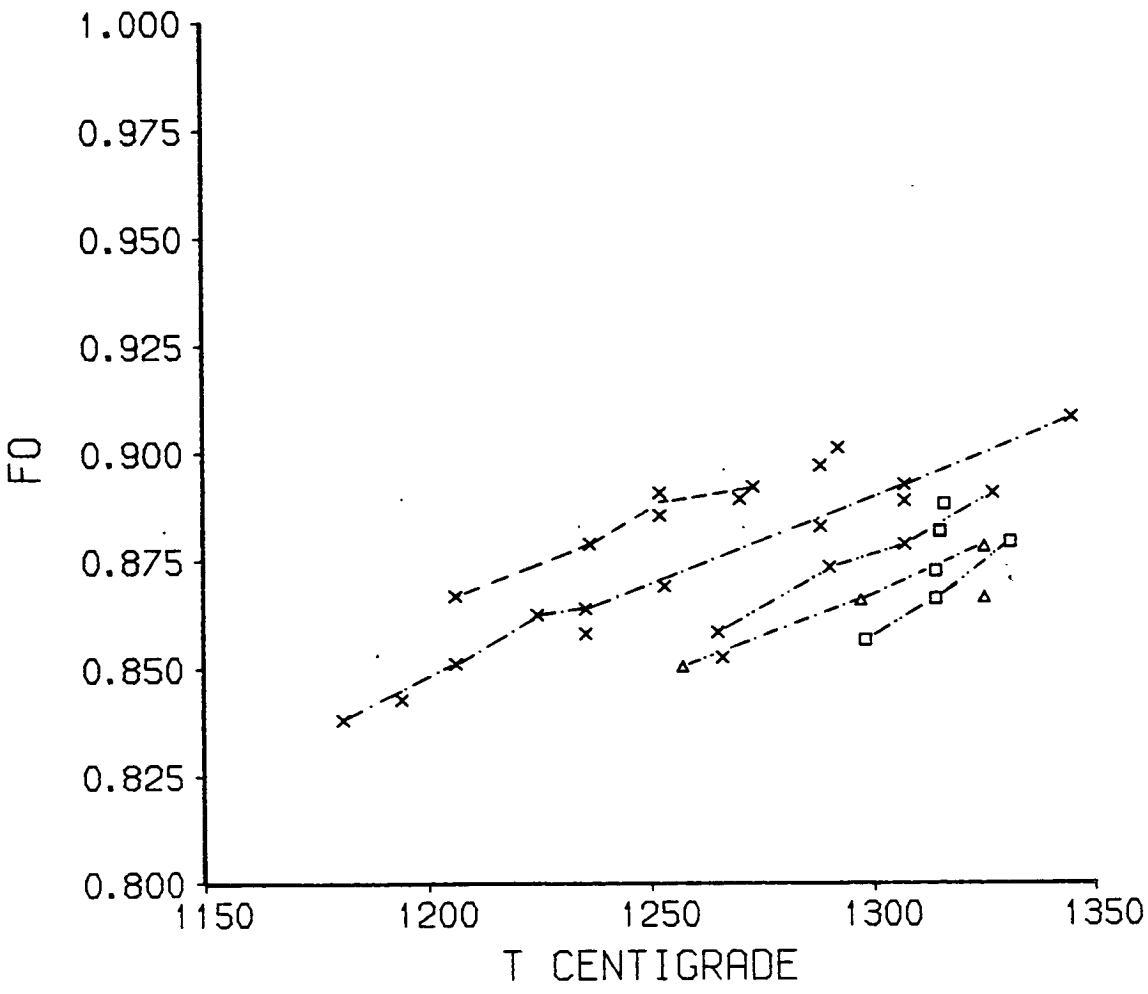
1.000
0.975
0.950
0.925
0.900
0.875
0.850
0.825
0.800
FO
1150
1200
1250
1300
1350
T CENTIGRADE

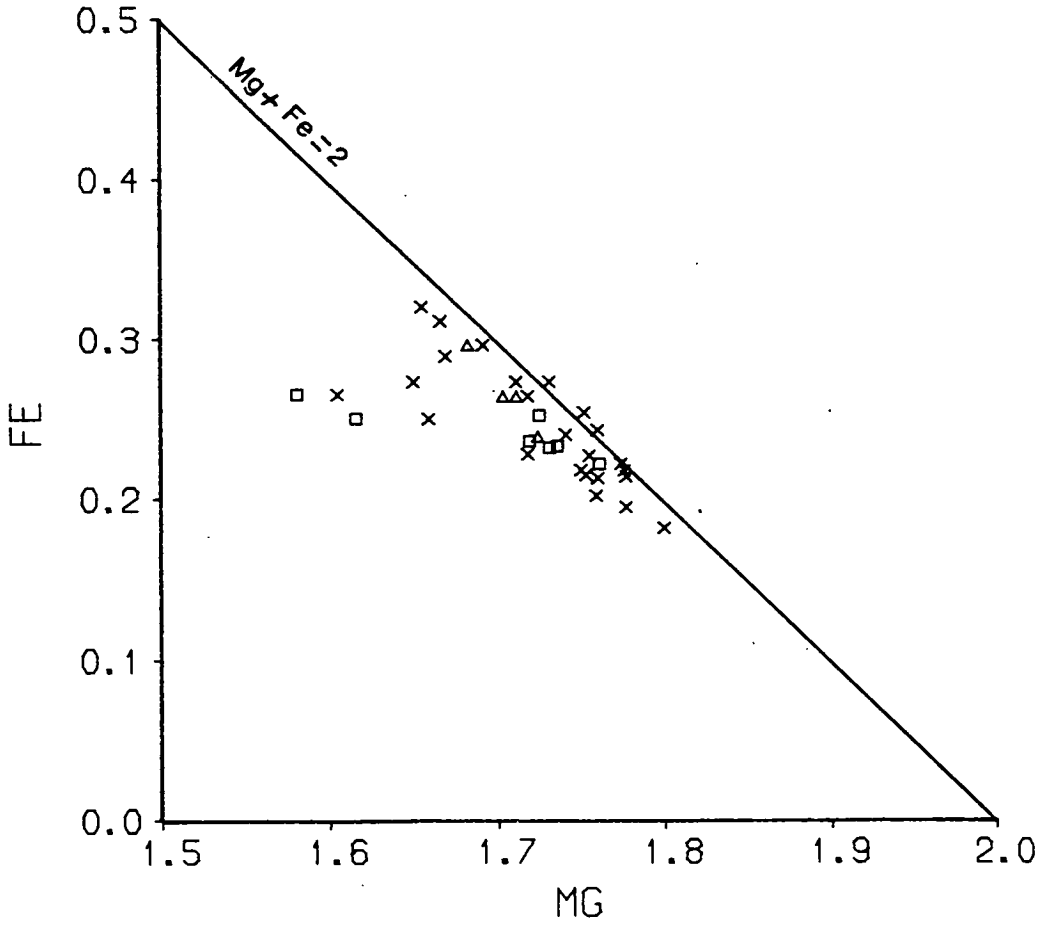
0.5
0.4
0.3
0.2
0.1
0.0
FE
Mg+Fe=2
1.5
1.6
1.7
1.8
1.9
2.0
MG

Figure 3:24

Ca^{2+} v temperature for olivines. Note the two high CaO analyses from experiments on sample 17M at CCO. In some samples the Ca^{2+} content rises with falling temperature, e.g. 295 & 17M at NNO, in others it remains steady, e.g. 295 at IW, or fluctuates, e.g. K1 at NNO.

- – – – K1 at NNO
- –·–· 295 at NNO & IW
- —·–· 17M at NNO

where

- × NNO
- □ CCO
- △ IW

Figure 3:25

Mn^{2+} v temperature for olivines.

- × NNO
- □ CCO
- △ IW

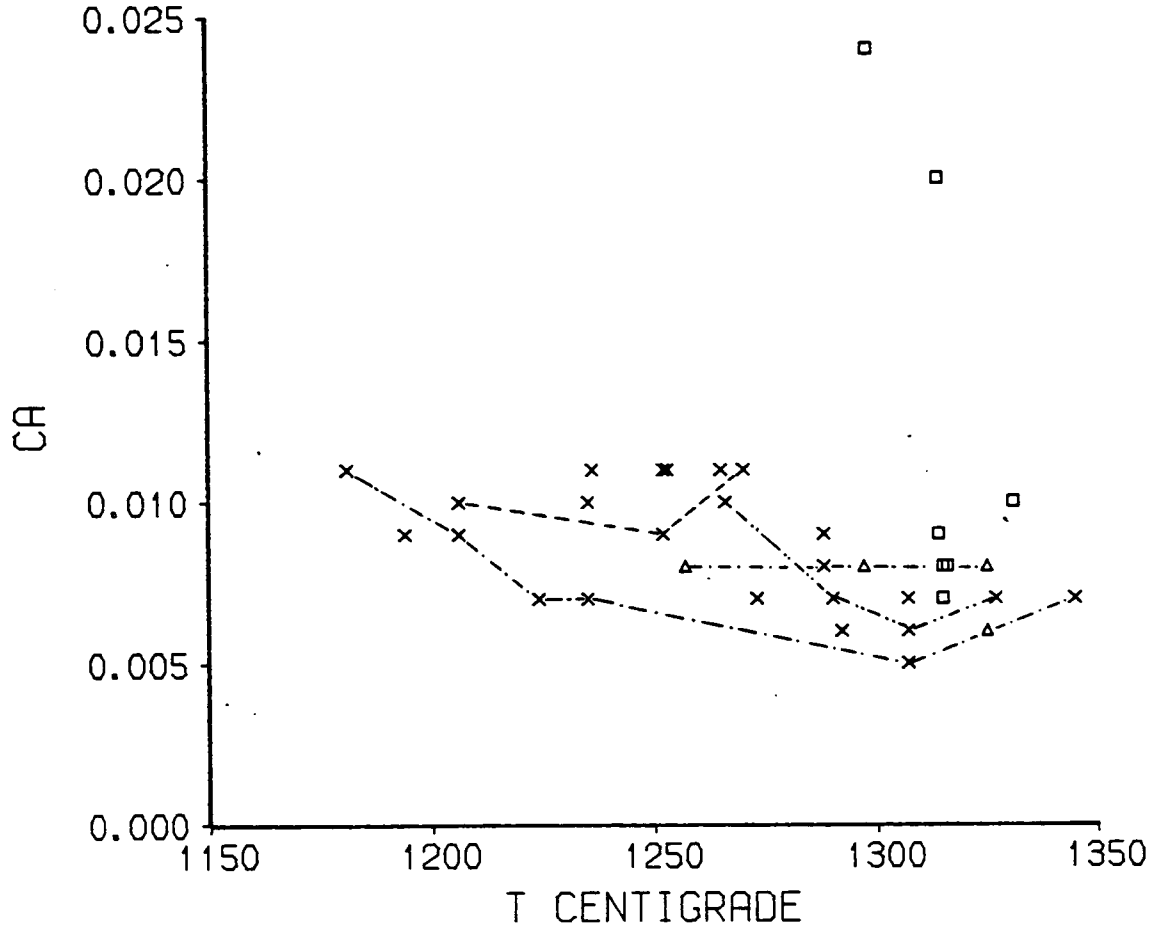
0.025
0.020
0.015
0.010
0.005
0.000
CA
1150
1200
1250
1300
1350
T CENTIGRADE

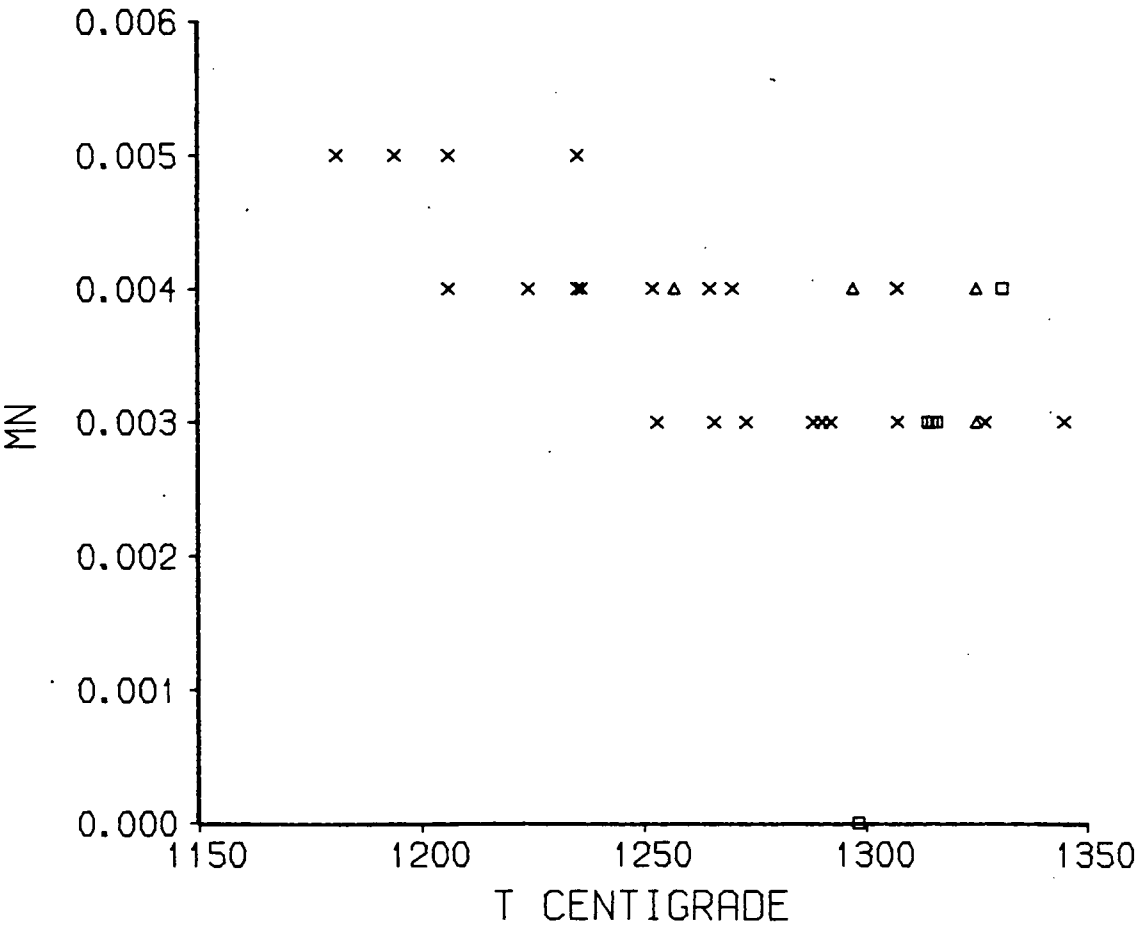
0.006
0.005
0.004
0.003
0.002
0.001
0.000
MN
1150
1200
1250
1300
1350
T CENTIGRADE

Figure 3.26

Augite analyses from these experiments and from Wood (1980).

◇ experimental results

◆ experimental results from sample K1

□ analyses from the original Kopi boninite (Wood, 1980)

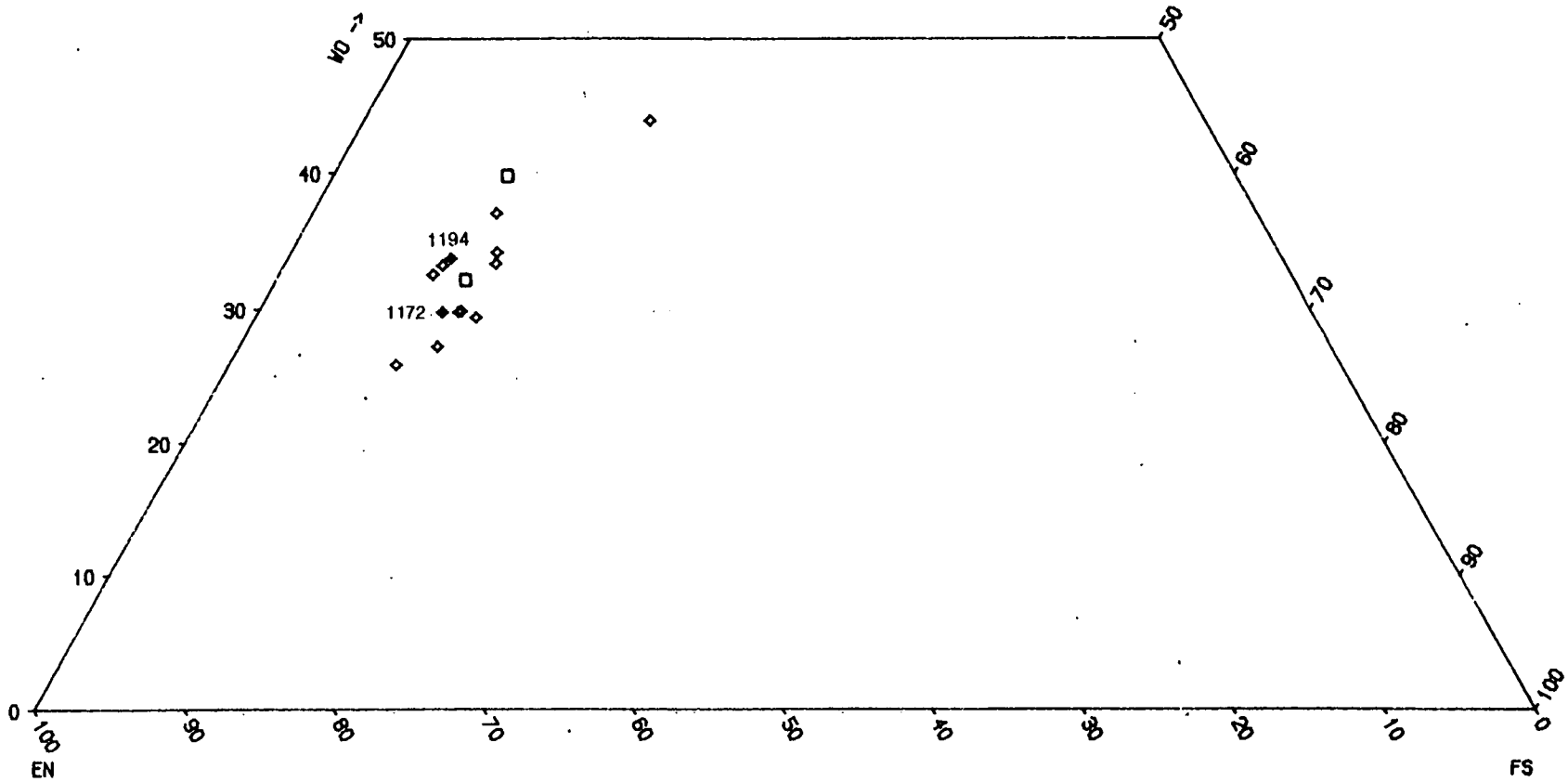

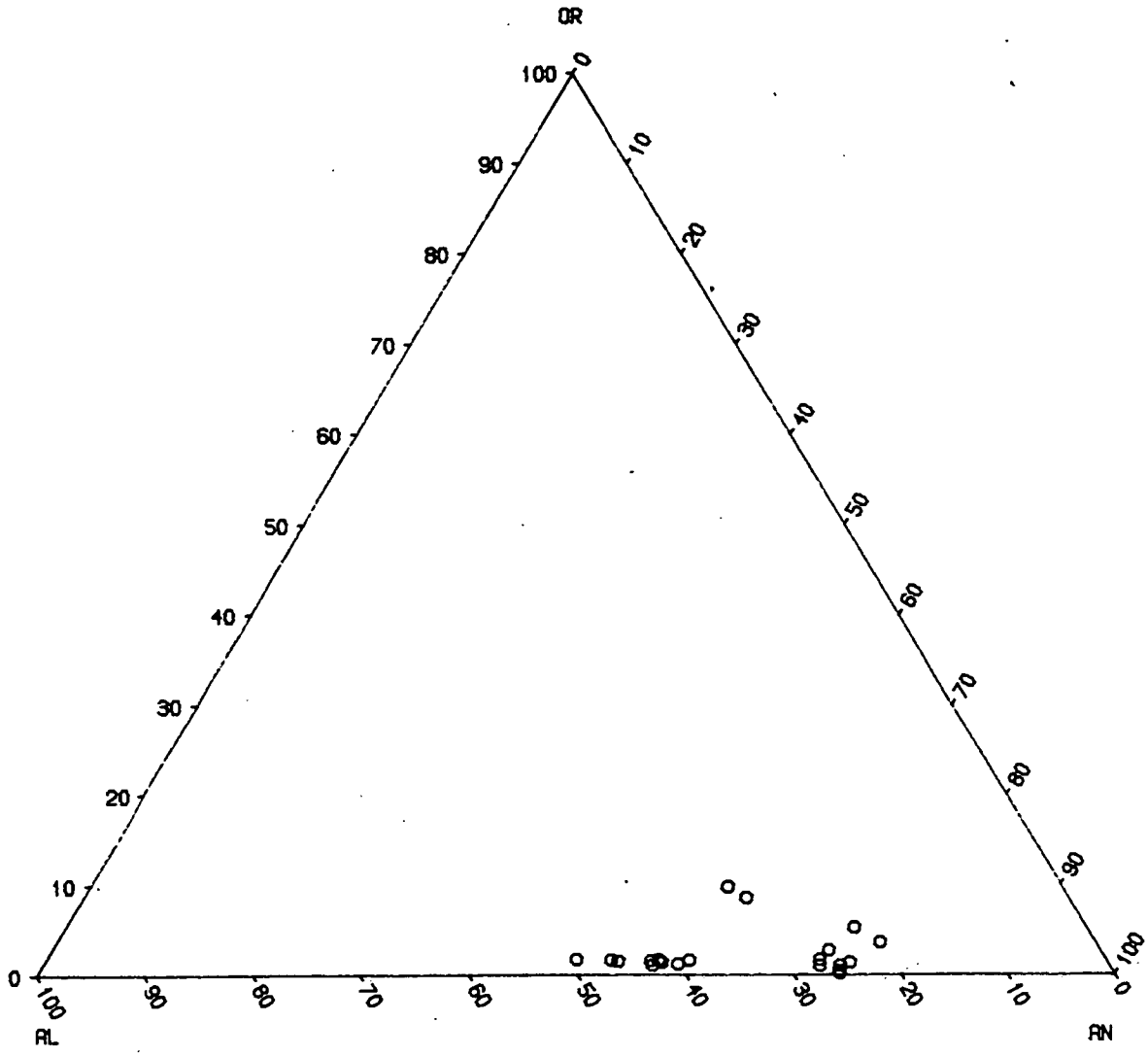

Figure 3:27

Plagioclase analyses from experiments carried out in this study.

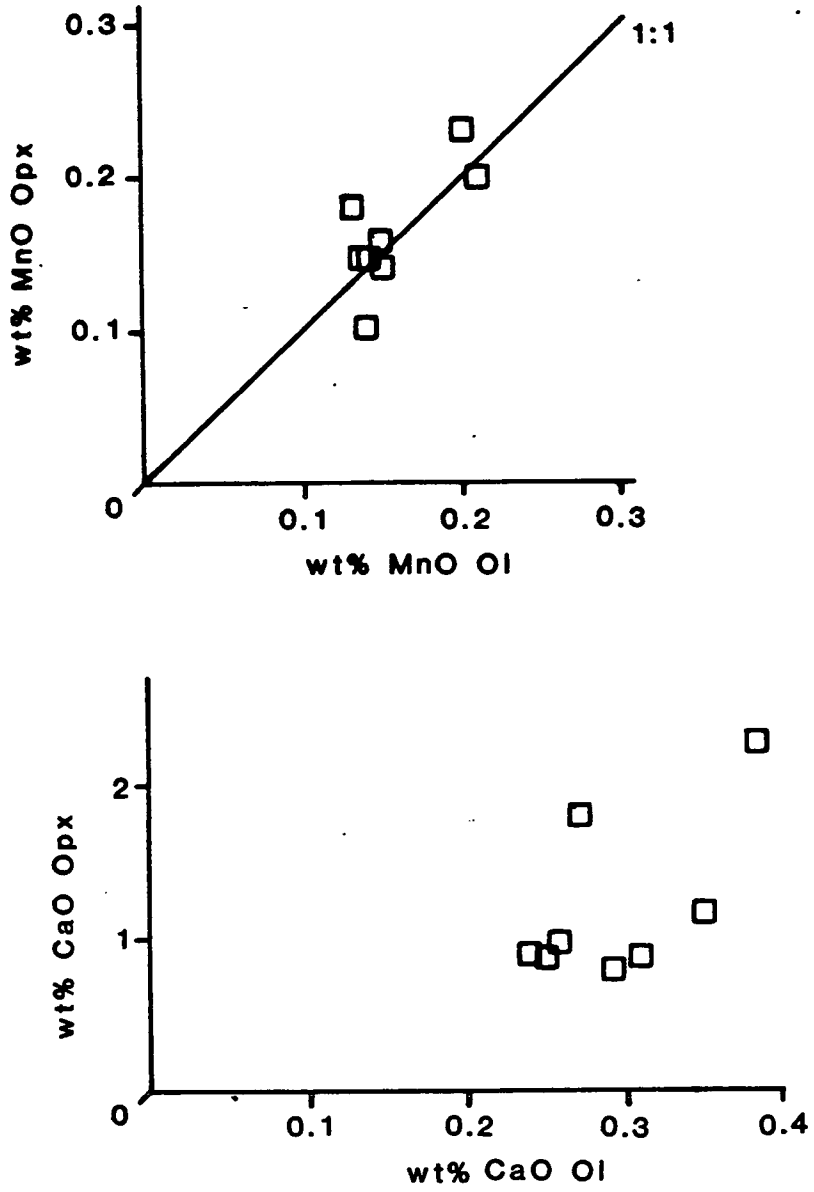

Figure 3.28

Distribution of MnO and CaO between coexisting olivine and orthopyroxene.

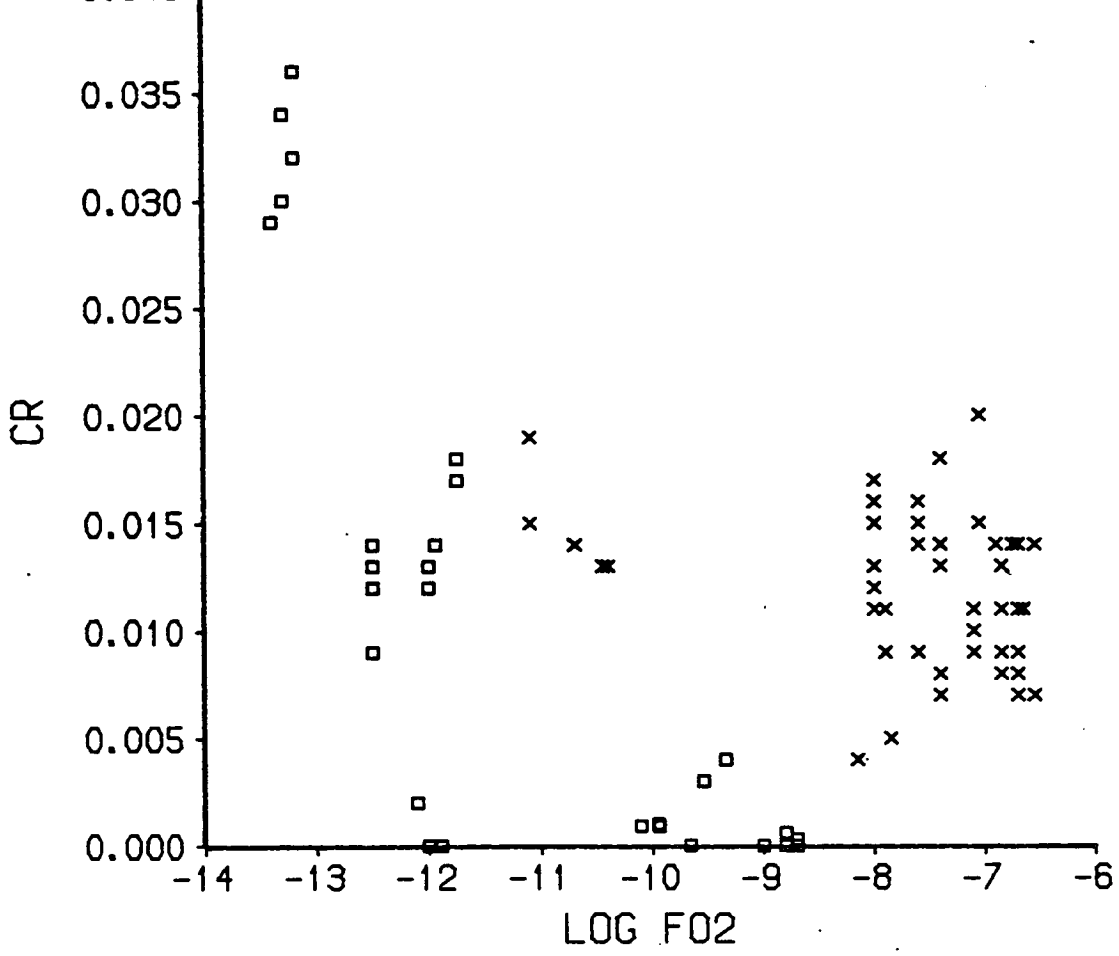
0.035
0.030
0.025
CR
0.020
0.015
0.010
0.005
0.000
-14
-13
-12
-11
-10
-9
-8
-7
-6
LOG FO2

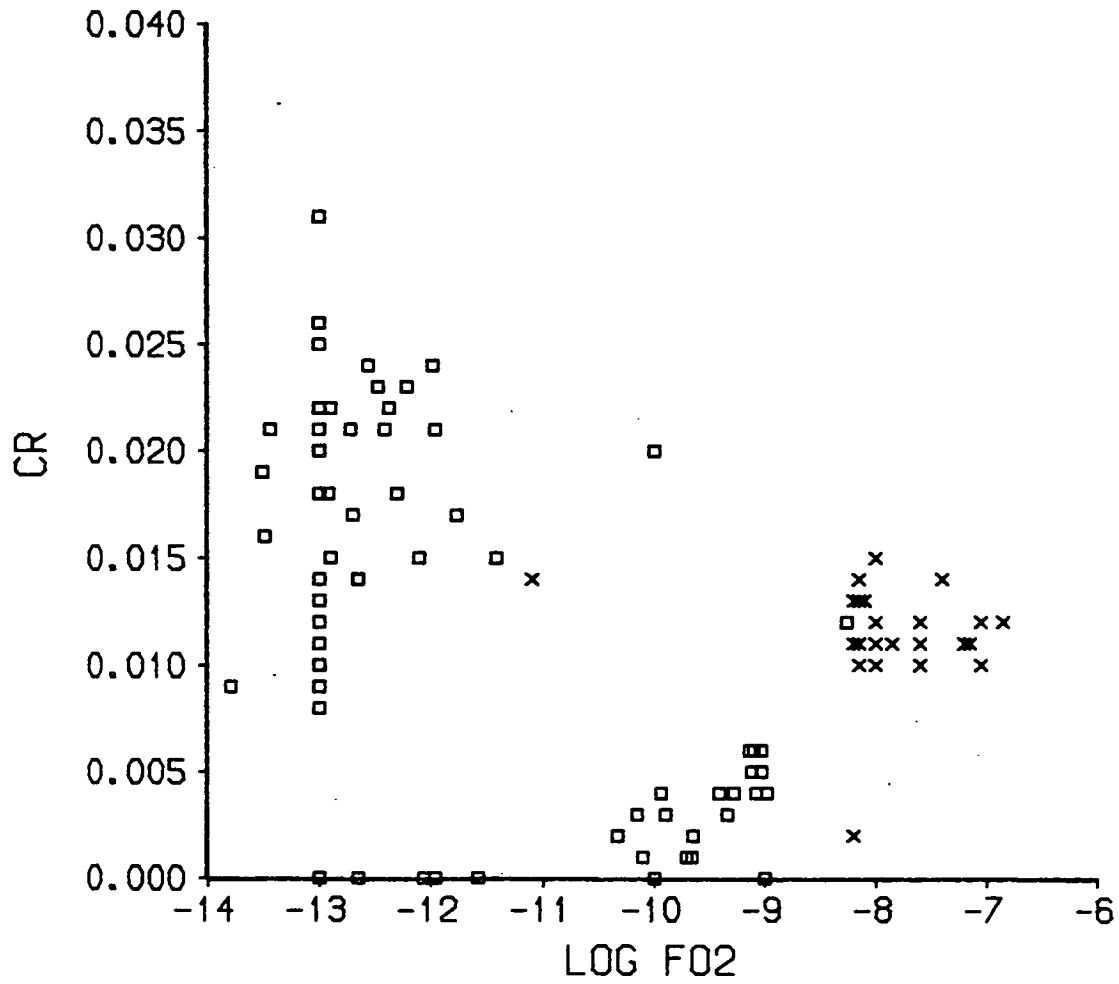
0.040
0.035
0.030
0.025
CR
0.020
0.015
0.010
0.005
0.000
-14
-13
-12
-11
-10
-9
-8
-7
-6
LOG FO2

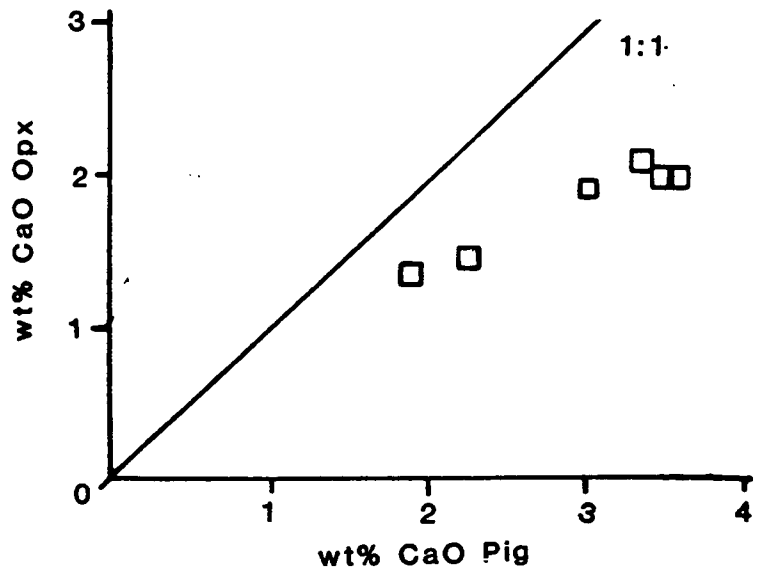

Figure 3.30

Distribution of CaO between coexisting orthopyroxene and pigeonite.

CHAPTER 4

MELT CHEMISTRY

4.1 THE CMAS PROJECTION SCHEME

In order to compare and contrast natural rocks or liquids with synthetic systems the analyses are projected into a pseudo-quaternary system, the apexes of which are defined as follows (O'Hara, 1968).

$$C = (CaO - 3\tfrac{1}{3}P_2O_5 + 2Na_2O + 2K_2O) \times 56.08$$

$$M = (MgO + FeO + MnO + NiO - TiO_2) \times 40.311$$

$$A = (Al_2O_3 + Cr_2O_3 + Fe_2O_3 + TiO_2 + Na_2O + K_2O) \times 101.961$$

$$S = (SiO_2 - 2Na_2O - 2K_2O) \times 60.085$$

Weight or mole percent values may be used, in this study all projections used are weight percent. The olivine solid solution series Mg_2SiO_4 - Fe_2SiO_4 plots at M_2S; the low-calcium pyroxene solid solution series $Mg_2Si_2O_6$ - $Fe_2Si_2O_6$ plots at MS and with increasing calcium content moves towards high-calcium pyroxene at CMS_2.

Two projections within the quadrilateral are considered in the following discussions, the olivine (M_2S) onto CS-MS-A and plagioclase (CAS_2) onto M_2S-CMS_2-S projections (fig 4.1). From fig 4.1 it can be seen that these two projections are approximately perpendicular to each other.

This projection scheme is particularly sensitive to some oxides, namely P_2O_5, K_2O, Na_2O and TiO_2, because they are multiplied, e.g. $3\tfrac{1}{3}P_2O_5$ in C, or used in more than one apex, e.g. Na_2O in C, A and S. It is unfortunate that the alkali elements, especially Na, are most likely to be lost under experimental conditions and thus contribute to deviations from cotectic lines which should, ideally, be smooth curves.

4.2 PREVIOUS WORK

4.2.1 Synthetic systems

In the system $CaO-MgO-Al_2O_3-SiO_2$ liquids in equilibrium with low-calcium pyroxenes and other phases define a series of primary crystallisation volumes, fig. 4.2 (Biggar, 1984b; Dearing and Biggar, 1984). As Na_2O replaces CaO so the equilibrium plag-ol-cpx -lq moves towards anorthite rich compositions, fig 4.2b (Biggar, 1984b).

4.2.2 Natural Systems

Liquids in equilibrium with the pigeonites and orthopyroxenes previously reported in the literature; table 3.1, appendix IV.1; are shown in the olivine onto CS-MS-A (fig 4.3a) and plagioclase onto CMS_2-M_2S-S (fig 4.4a) projections. They show broadly similar features to the synthetic system except that protopyroxene is suppressed and the pigeonite primary volume expands such that it meets the plagioclase volume. Those samples for which analyses at decreasing temperatures are available define segments of linesalong which, for example, ol+opx+lq, ol+opx+plag+lq, ol+pig+lq and ol+pig+plag+lq coexist (fig 4.4b).

Glasses in equilibrium with ilmenite ($FeTiO_3$) or containing more than 7 wt% TiO_2 are not included in figs. 4.3 and 4.4 because high TiO_2 contents cause contraction of the olivine phase volume in favour of pyroxene (Kushiro, 1975). This is especially evident in the projection plagioclase onto CMS_2-M_2S-S (fig. 4.5). Many lunar samples have been excluded from figs. 4.3 and 4.4 on this basis.

The samples studied in Grove et al. (1982) are high-alumina basalts, basaltic andesites and andesites of calc-alkaline affinity whereas the other samples are generally of a basaltic nature. These compositional differences result in the crystallisation of substantial amounts of plagioclase with minor amounts of olivine, prior to the crystallisation of low-calcium pyroxenes. This leads, with falling temperature, to the depletion of CaO from the liquid and the enrichment of SiO_2, causing the liquids to move towards the S apex in the plagioclase onto CMS_2-M_2S-S projection (fig. 4.4b). The other samples in the literature data set have olivine as the liquidus phase and only crystallise minor amounts of plagioclase, if

any, prior to the crystallisation of low-calcium pyroxenes. These liquids are enriched in CaO and depleted in SiO_2 (fig. 4.6) and do not move towards the S apex in the plagioclase projection (fig. 4.4b).

4.3 RESULTS FROM THIS STUDY

All the glass analyses from runs at the NNO buffer in this experimental study (appendix IV.2) are considered in this section, whether or not the crystals have reached equilibrium.

Temperature - composition diagrams for the thirteen rocks used in this study are presented in figs. 4.7 to 4.23. The results for the experimentally metamorphosed samples (-MET) are given on separate diagrams to their unmodified equivalents. In addition fig. 4.24 shows the similarity in glass chemistry of M1 and M1MET for the major elements. This shows that although the orthopyroxenes have failed to equilibrate (fig. 3.6) their margins are in local equilibrium with the glass. The bulk composition is probably maintained by changes in the amount of orthopyroxene present.

In all samples the MgO content falls and the CaO, Al_2O_3, Na_2O and K_2O contents rise with decreasing temperature. This is to be expected as the major crystalline phases are low-calcium pyroxenes and/or olivine both of which contain large amounts of magnesium and only minor amounts of alkalis and aluminium. The pattern for FeO is more complex as crystallisation of pyroxenes and olivines only causes its depletion in the liquid after the MgO has been depleted. Thus the FeO content often remains steady until the MgO content has fallen significantly e.g. figs. 4.7 and 4.9. As the Fe_2O_3 contents have been calculated according to the fO_2 of the experiment (Sack et al., 1980; Russell, 1985) they follow the same trend as the FeO contents. The behaviour of SiO_2 depends on the initial content, as pyroxenes and olivines contain 55-60 and 40 wt% SiO_2 respectively, any sample with pyroxene as a liquidus phase and more SiO_2 than that pyroxene will show an increase in SiO_2 content with decreasing temperature e.g. figs. 4.9 and 4.17. Likewise any sample crystallising substantial amounts of olivine will also show an increase in SiO_2 content with falling temperature e.g. fig. 4.15.

Iron losses from experiments on new hooks cause slight compositional changes, e.g. fig. 4.8 at 1245°C, as do combined iron and

sodium losses in the samples used in the 477 hour experiment at 1224°C (figs.4.9, 4.13, 4.17 and 4.20). In many samples the lowest temperature charge analysed deviates from the trend. There are two possible explanations. Firstly the high degree of crystallinity results in pools of glass that are too small to probe without contamination from surrounding phases and may prevent the liquid equilibrating throughout the charge. Secondly, in some samples, notably K1 and K6, quench crystals formed leaving very little clear glass to analyse.

The glass compositions are presented in the projections olivine onto CS-MS-A and plagioclase onto CMS_2-M_2S-S in figures 4.25 to 4.35. Individually the samples describe segments of a phase diagram comparable to the synthetic system (fig. 4.2). For example sample 17M (fig. 4.26) has olivine as the liquidus phase and the liquid composition moves across the olivine field away from olivine until it reaches the olivine + orthopyroxene primary crystallisation volume boundary where orthopyroxene begins to crystallise. The liquids then follow the olivine + orthopyroxene primary crystallisation volume boundary until olivine ceases to crystallise and pigeonite becomes stable, after which the liquids follow the orthopyroxene + pigeonite primary crystallisation volume boundary.

For these samples the overlap between the individual primary crystallisation volumes in the olivine projection (fig. 4.36) is too large to be simplified as in fig. 4.3. It is not possible to resolve this overlap by considering differences in magnesium number; sodium, titanium or total alkali content. In the plagioclase projection (fig. 4.36) a summary of the primary crystallisation volumes is possible (fig. 4.37) and is comparable to those found in synthetic and other natural systems (figs. 4.2 to 4.4).

4.4 MINERAL - MELT DISTRIBUTION COEFFICIENTS

4.4.1 The Use of Single Component Distribution Coefficients

Single component distribution coefficients of the form:-

$$D_{Mg} = Mg^{xtl} / Mg^{lq}$$

have been used to describe the relationship between coexisting crystal and liquid compositions. Such distribution coefficients tend to be dependent on temperature , pressure and liquid composition. Over a restricted compositional range plots of ln D v $^1/T$

and/or ln D v X^{lq} often produce straight line relationships. Because of their temperature and compositional dependence, distribution coefficients have been used in simple models of mineral - melt equilibria (Roeder & Emslie, 1970; Langmuir & Hanson, 1980; Nielsen & Dungan, 1983).

4.4.2 Low-calcium pyroxene - melt distribution coefficients

In this section only the pyroxene - glass pairs that have equilibrated are considered; the pyroxene analyses are given in appendix III.4, the co-existing glasses are in appendix IV.3.

The distribution coefficients for magnesium between both orthopyroxene & pigeonite and liquid lie in the range $D^{xtl/lq}$=2.30 to 6.00 (ln D=0.8 to 1.8) and increase with decreasing temperature (fig. 4.38a). This agrees with the distribution coefficients calculated from the data obtained in the literature search (fig. 4.38b). The distribution coefficients for iron (Fe^{2+}) between low calcium pyroxenes and liquid lie in the range $D^{xtl/lq}$=0.7 to 2.3 (ln D=-0.4 to 1.0) and increase with decreasing temperature (fig. 4.39a). At high temperature iron is concentrated in the melt, giving a distribution coefficient less than 1. However, as temperature falls so the melt becomes depleted in iron relative to the low-calcium pyroxenes and the distribution coefficient becomes greater than 1. The data from the literature search cover a similar range (fig. 4.39b). The coupled distribution coefficient $K_D^{Fe^{2+}/Mg}$ lies between 0.25 and 0.52 (ln K_D=-1.4 to -0.6) for both low-calcium pyroxenes with an average of $K_D^{Fe^{2+}/Mg}$= 0.337 for orthopyroxene and $K_D^{Fe^{2+}/Mg}$=0.355 for pigeonite. These values are similar to those given in the literature for pigeonite, $K_D^{Fe^{2+}/Mg}$=0.225 (Perfit & Fornari, 1983); $K_D^{Fe^{2+}/Mg}$=0.28 (Grove & Bence, 1977); $K_D^{Fe^{2+}/Mg}$=0.27 (Rhodes et al., 1979) and $K_D^{Fe^{2+}/Mg}$=0.30 (Stolper, 1977). There is a slight increase in $K_D^{Fe^{2+}/Mg}$ with rising temperature (fig. 4.40a and b) and Mg/(Mg + Fe) ratio (fig. 4.41a and b).

The pyroxene-liquid distribution coefficient for calcium lies in the range D=0.09 to 0.28 (ln D=-2.5 to -1.5) for orthopyroxene, and D=0.20 to 0.60 (ln D=-1.6 to -0.5) for pigeonite and increases with decreasing temperature (fig. 4.42a). At any given temperature $D^{pig/lq}$ is greater than $D^{opx/lq}$ which is to be expected as pigeonite

is able to accommodate more calcium in its structure. A similar relationship is seen in the data set from the literature search (fig. 4.42b).

The distribution coefficient for manganese lies in the range D=0.50 to 3.10 (ln D=-0.5 to 1.2) and shows some variation with temperature (fig. 4.43a). The distribution of manganese between low-calcium pyroxenes and melt exhibits a similar pattern to the distribution of iron - being concentrated in the melt at high temperature but in the crystals at lower temperatures; this could be related to the tendency for manganese content to be related to iron content in low-calcium pyroxenes (fig. 3.12). A similar range of distribution coefficients has been obtained from the literature data set (fig. 4.43b).

The distribution coefficient for silicon between low-calcium pyroxenes and liquid lies in the range D=0.80 to 0.97 (ln D=-0.20 to -0.03) and shows no variation with temperature (fig. 4.44a). The range of values obtained from the literature search is D=0.77 to 1.20 (ln D=-0.25 to 0.15). As the silica contents of low-calcium pyroxenes are constrained by stoichiometry any variation in the distribution coefficient must be related to the silicon content of the glass (fig. 4.45).

As sodium is a minor component of igneous, low-calcium pyroxenes it has a very low distribution coefficient, D=0.01 to 0.06 (ln D=-5.0 to -2.7) for orthopyroxenes and D=0.02 to 0.24 (ln D=-3.7 to -1.2) for pigeonites. There is no relationship between distribution coefficient and temperature for sodium (fig. 4.46a). There is very little overlap between the distribution coefficients of orthopyroxene and pigeonite either in this study or in the literature data set (fig. 4.46a & b). Sodium content is almost constant in low-calcium pyroxenes (fig. 4.47), thus the distribution coefficient should decrease as the sodium content of the glass increases. Such a relationship is discernible in the literature data set (fig. 4.48b) but not in the results from this study (fig. 4.48a).

The distribution coefficient for aluminium between low-calcium pyroxenes and liquid lies in the range D=0.025 to 0.18 (ln D=-3.7 to -1.6) which is comparable with the values previously reported for pigeonite; D=0.109 (Perfit & Fornari, 1983) and D=0.079 (Grove & Raudsepp, 1978); and with the values obtained from the literature

data set. There is some relationship between distribution coefficient and temperature in the present study (fig. 4.49a) but not in the literature data set (fig. 4.49b). Likewise there is some relationship between distribution coefficient and glass composition in this data set but not in the literature data set (fig. 4.50a & b) and similarly between Al contents of low-calcium pyroxenes and liquids (fig. 4.51). This is particularly evident where the Al contents in pyroxenes are below 1 cation % (0.01 in figures) and suggests that Al contents significantly above this level may not represent equilibrium.

The distribution coefficients for titanium between low-calcium pyroxenes and liquid lie in the range D=0.05 to 0.46 (ln D=-3.0 to -0.6), comparable to the value given by Perfit & Fornari (1983) of D=0.162. There is no obvious relationship between the distribution coefficient for titanium and temperature for this data set or the literature data set (fig. 4.52a & b). However, the distribution coefficient for titanium appears to be constant when compared to the titanium content of the glass, especially where the glass is richer in titanium (fig. 4.53b). Where the glass contains very little titanium there is a wide spread in values which is to be expected when taking a ratio of two small numbers. There is a good correlation between titanium contents in low-calcium pyroxenes and coexisting liquids (fig. 4.54a & b), analyses being clustered about a Ti crystal : Ti glass ratio of 1:6 (D=0.16, ln D= -1.80). In summary it seems likely that the distribution coefficient for titanium between low-calcium pyroxenes and liquid is approximately constant at D=0.16 (figs. 4.52 & 4.53).

The chromium contents of glasses in this study were not determined because routine microprobe analyses at low levels of concentration are not precise. Chromium contents of glasses are available for some of the literature data set and they give distribution coefficients in the range D=0.22 to 12.20 (ln D=-1.5 to 2.7) which show no variation with temperature (fig. 4.55). There is some variation in the distribution coefficient of chromium with changing atmospheric conditions. Schreiber & Haskin (1976) found D_{Cr}=2 to 3 at the IW buffer and D_{Cr}=4 to 7 at the NNO buffer. Stolper (1977) also found that D_{Cr} decreased with more reducing atmospheric conditions. These changes in distribution coefficient

are probably due to the increased amount of Cr^{2+} present at the IW buffer; Cr^{2+} does not substitute into pyroxene as readily as Cr^{3+}. As there is no means of determining the Cr^{3+}:Cr^{2+} ratio all Cr^{3+} in this study is treated as Cr^{3+}. A plot of Cr pyroxene : Cr glass indicates an average pyroxene : liquid ratio of 2:1 (fig. 4.56) giving a D_{Cr} of 2 which is comparable to previous values obtained from the IW buffer (Schreiber & Haskin, 1976). This is to be expected as nearly all the experiments in the literature data set were carried out at the IW buffer. This constant D_{Cr} is not obviously supported in the plot of ln D_{Cr} v 1/T (fig. 4.55); however, when the relationship between D_{Cr} and the Cr content of the glass is considered (fig. 4.57) it can be seen that most of the deviation occurs at low Cr concentrations where taking ratios of two small numbers leads to a lot of scatter.

4.4.3 Olivine - Melt Distribution Coefficients

There have been many previous studies of olivine-liquid relationships (Roeder & Emslie, 1970; French, 1971; French & Cameron, 1981; Ford et al., 1983; Russell, 1985) and the results obtained in this study are in agreement with previous results. Briefly, magnesium and iron (Fe^{2+}) are concentrated in the olivines relative to the melt giving distribution coefficients in the range D=2.91 to 5.16 (ln D=0.95 to 1.8) and D=0.97 to 1.74 (ln D=-0.05 to 0.7) respectively, both of which are related to temperature (figs. 4.58 and 4.59). The coupled distribution coefficient $K_D^{Fe^{2+}/Mg}$ lies in the range 0.32 to 0.37 and shows no variation with temperature or composition (figs. 4.60 and 4.61).

4.4.4 Clinopyroxene and Plagioclase Distribution Coefficients

The lack of equilibrium in these phases is evident in the wide range of distribution coefficients obtained for essential elements at a single temperature (figs. 4.62 to 4.67).

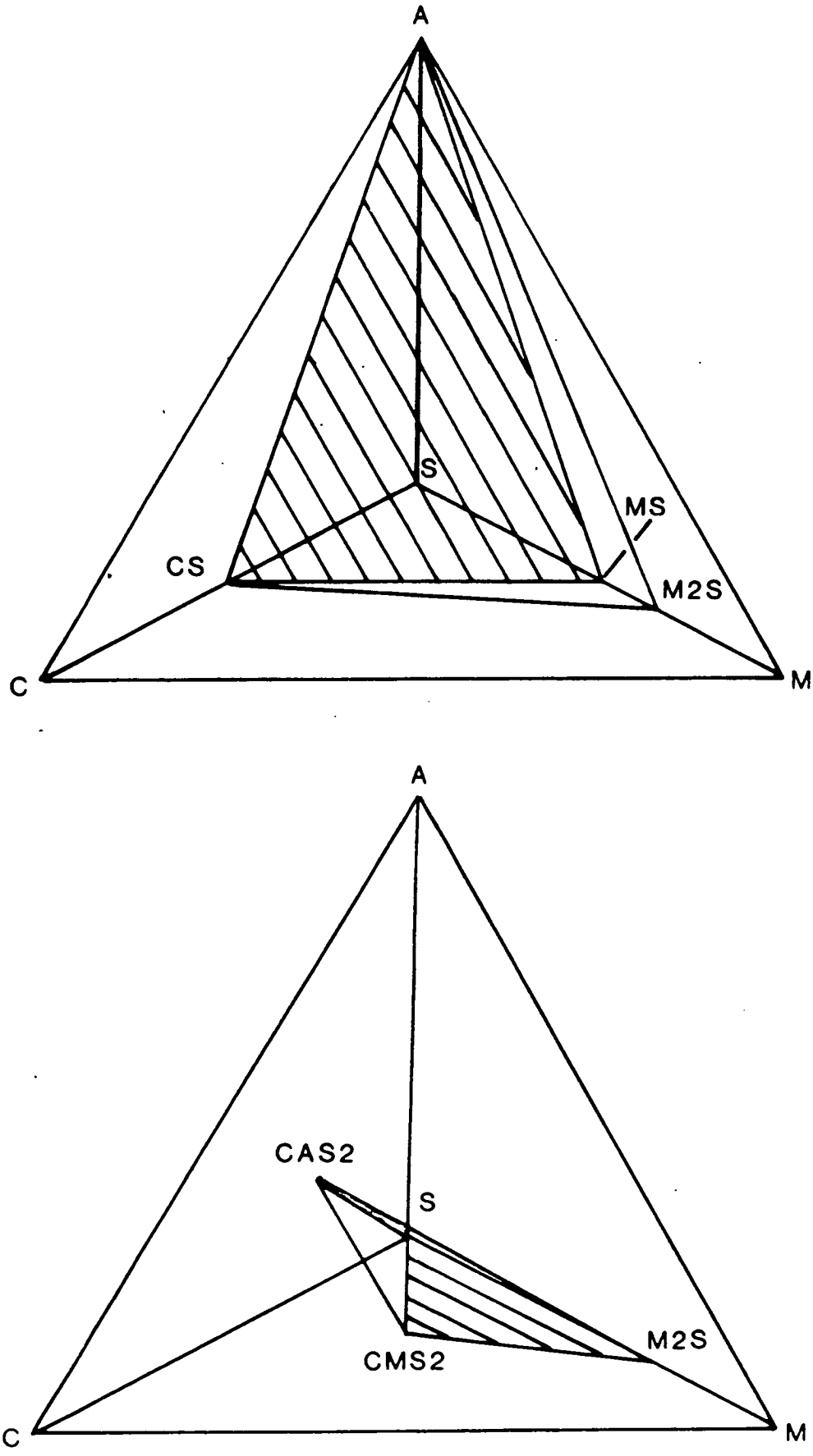

Figure 4.1

Projections from olivine onto CS-MS-A (4.1a) and plagioclase onto CMS_2-M_2S-S (4.1b) and their relationship to the CMAS psuedo-quaternary system.

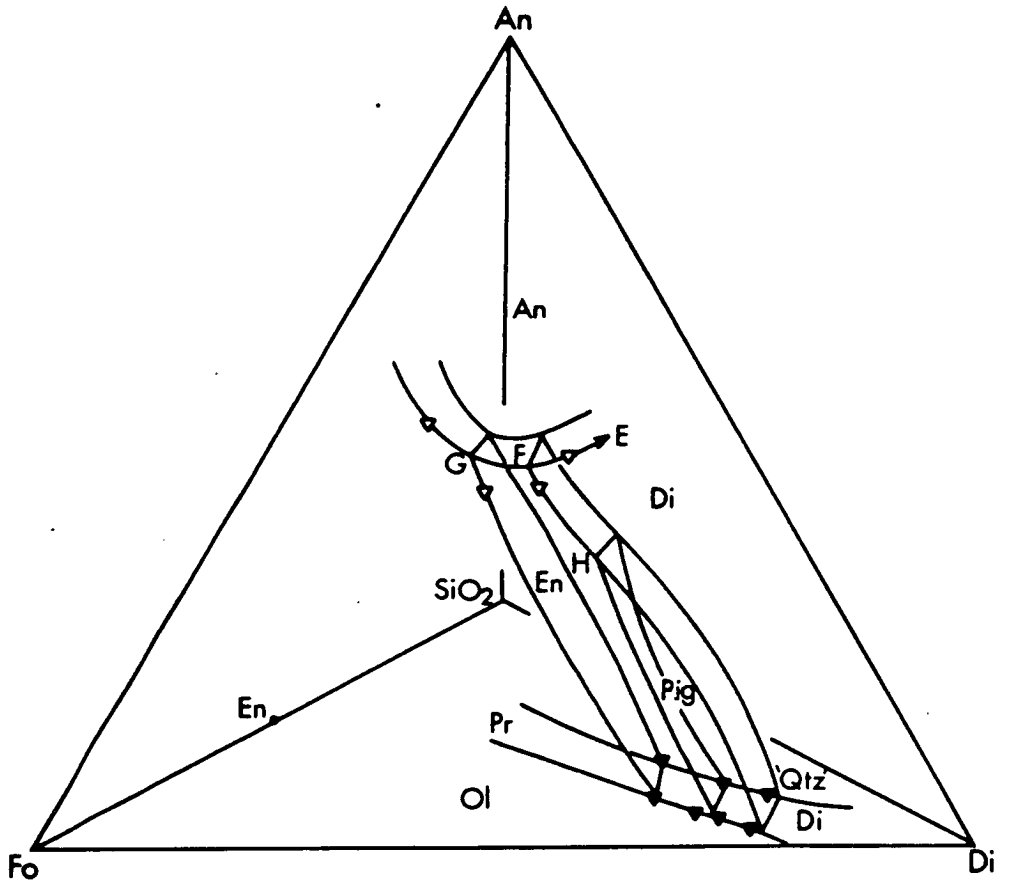

Figure 4:2a

Schematic three-dimensional view of pyroxene primary crystallisation volumes. Data sources are as follows:-

▽ Longhi (1978)

▼ Longhi & Boudreau (1980)

Figure 4.2b

Olivine onto CS-MS-A projection of liquids in the CMAS system coexisting with one or more pyroxenes. Data sources are as follows

▲ Presnall et al. (1978, 1979)
● Biggar (1984)
O Biggar CMAS + Na_2O (1984)
▽ Longhi (1978)
▼ Longhi & Boudreau (1980)

Figure 4.2c

Data from figure 4.2b shown in the plagioclase onto CMS_2-M_2S-S projection, those liquids not in equilibrium with plagioclase are omitted.

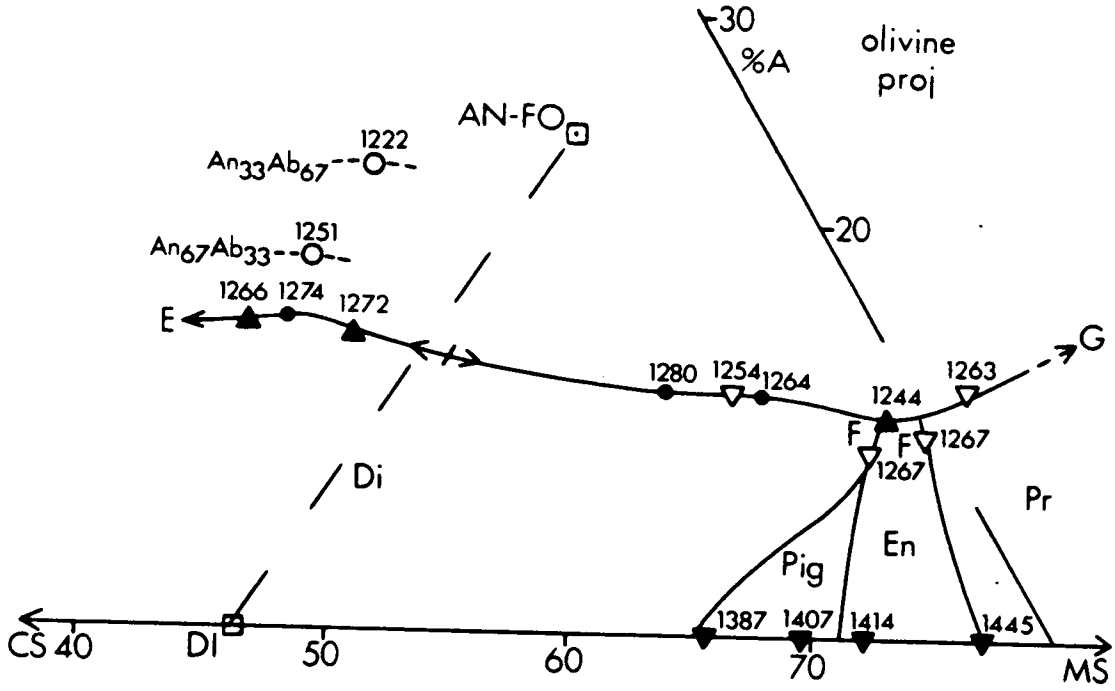
30
%A
olivine
proj
AN-FO
1222
An33Ab67
1251
An67Ab33
20
1266 1274 1272
E
G
1280 1254 1264
1244
1263
F
F
1267
1267
Di
Pr
En
Pig
1387 1407 1414 1445
CS 40
DI
50
60
70
MS

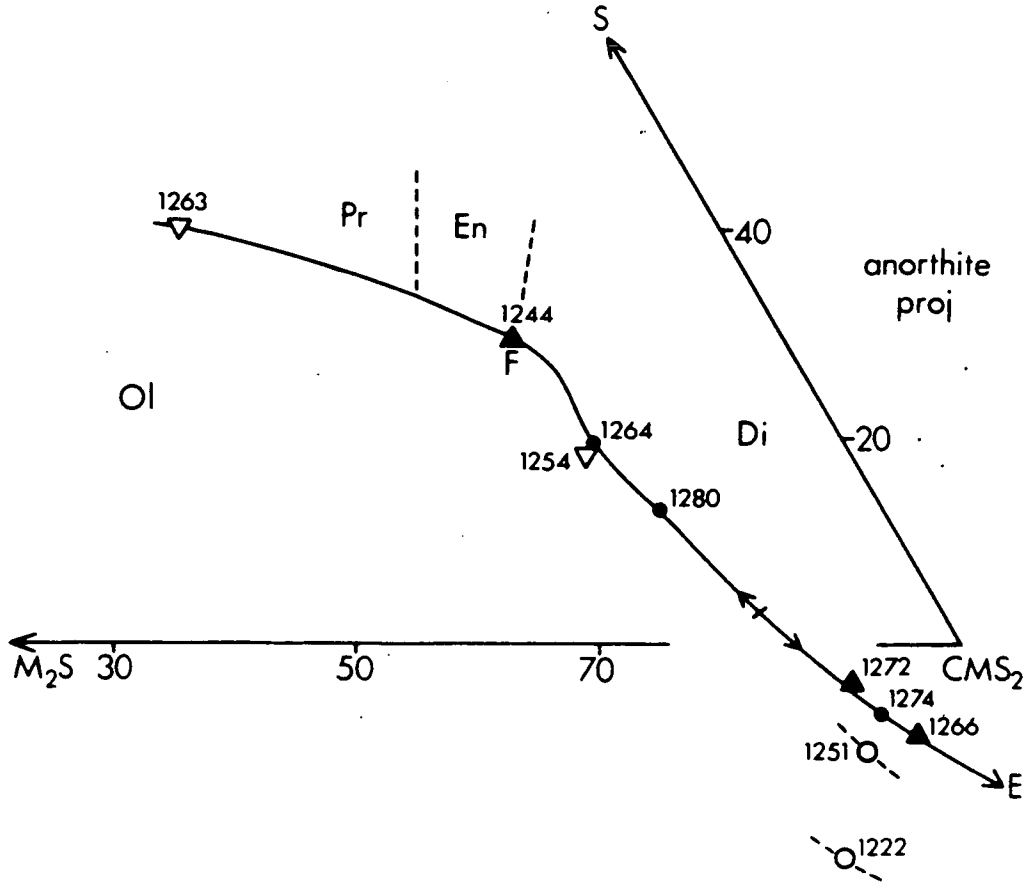
S
1263
Pr
En
40
anorthite
proj
1244
F
Ol
1264
Di
1254
20
1280
M2S 30
50
70
1272
CMS2
1274
1266
1251
E
1222

Figure 4.3a

Olivine onto CS-MS-A projection of liquids in equilibrium with one or more low-calcium pyroxenes ± olivine ± plagioclase ± augite.

× opx
+ pig
O opx + ol
□ pig + ol
● opx + ol + plag
■ pig + ol + plag
▽ opx + plag
▼ pig + plag
△ pig + cpx + ol
▲ pig + cpx + ol + plag
◆ pig + cpx + plag
— + qtz

Figure 4.3b

Schematic diagram to show the approximate position of primary crystallisation volume boundaries indicated by data in figure 4.3a. Grove et al.'s (1982) data lie along the dash - dotted line slightly nearer the A apex than the bulk of the rest of the data.

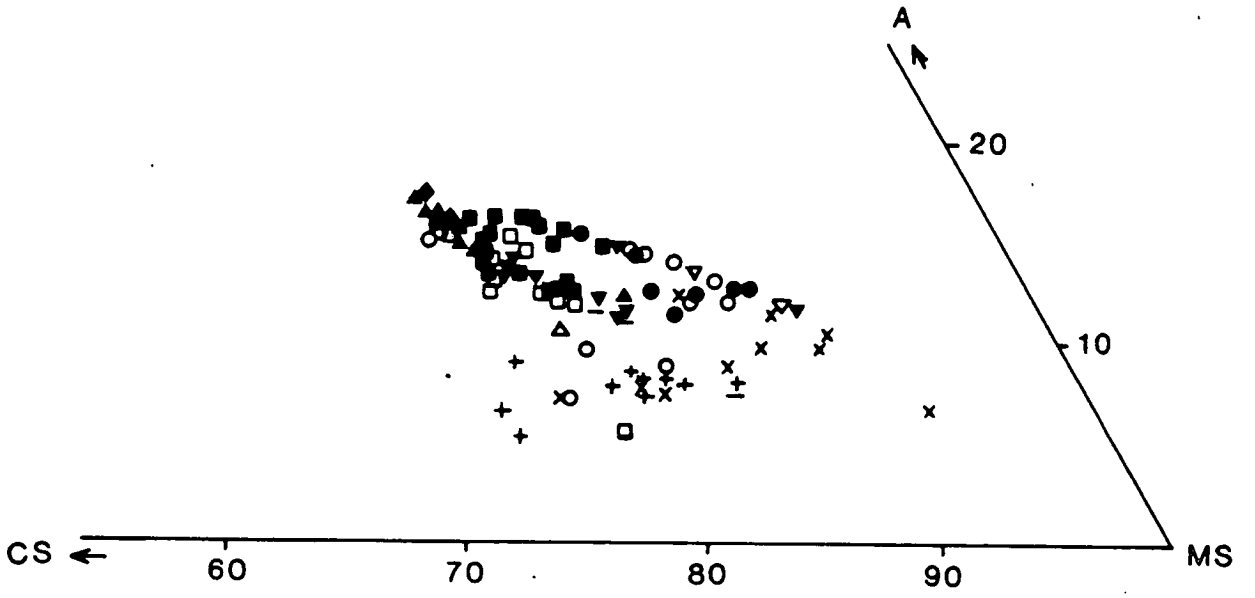
A
20
10
CS
60
70
80
90
MS

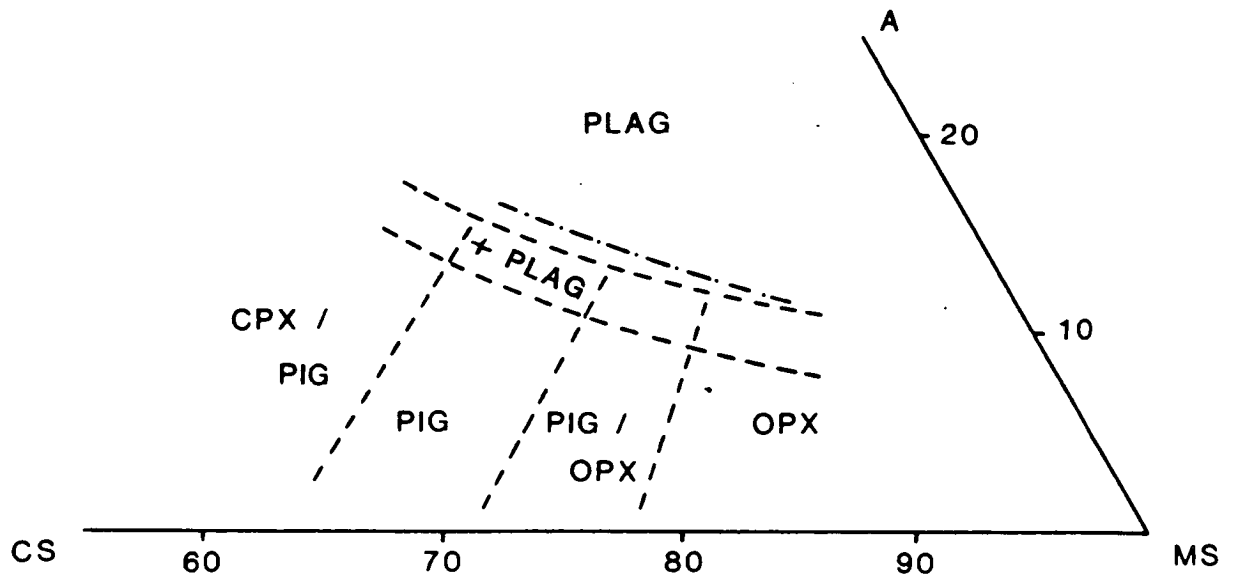
A
PLAG
20
+ PLAG
CPX /
PIG
PIG
PIG /
OPX
OPX
10
CS
60
70
80
90
MS

Figure 4.4a

Plagioclase onto CMS_2-M_2S-S projection of liquids in equilibrium with one or more low-calcium pyroxenes ± olivine ± plagioclase ± augite. Key as for fig. 4.3a.

Figure 4.4b

Schematic diagram to show approximate position of primary crystallisation volume boundaries indicated by data in fig. 4.4a. The continuous lines shown are the crystallisation paths described by samples from the following sources.

Sample a) Weill & McKay (1975); gl+opx+ol

b) Huebner et al. (1976); gl+opx, gl+opx+ol
gl+opx+ol+plag

c) Walker et al. (1976); gl+ol+pig, gl+ol+pig + plag

d) Grove & Bence (1977); gl+ol+pig, gl+ol+pig+plag
gl+pig+plag

Grove et al.'s (1982) data lie along the dash - dotted line and with decreasing temperature successive liquid analyses move toward the S apex.

The low-calcium pyroxenes coexisting with the liquids project into the shaded regions


orthopyroxene


pigeonite

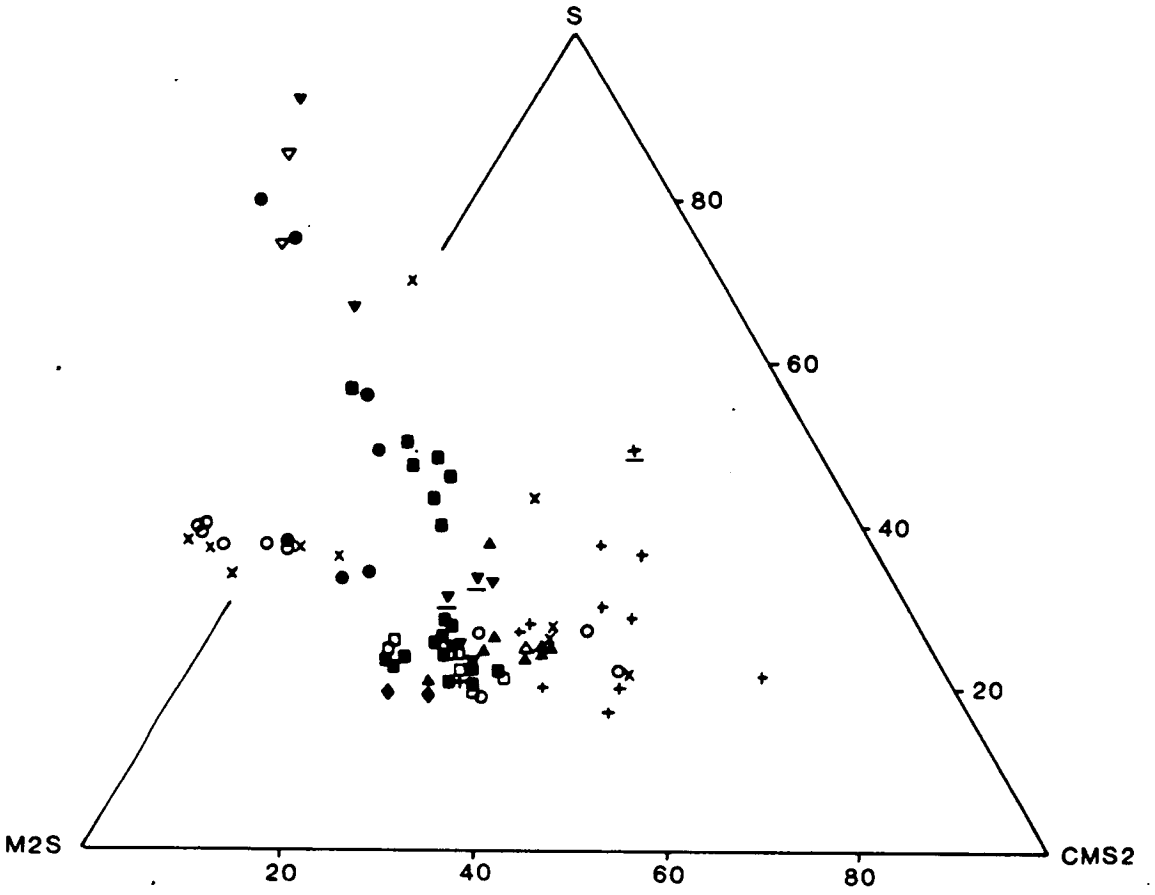
S
80
60
40
20
M2S
20
40
60
80
CMS2

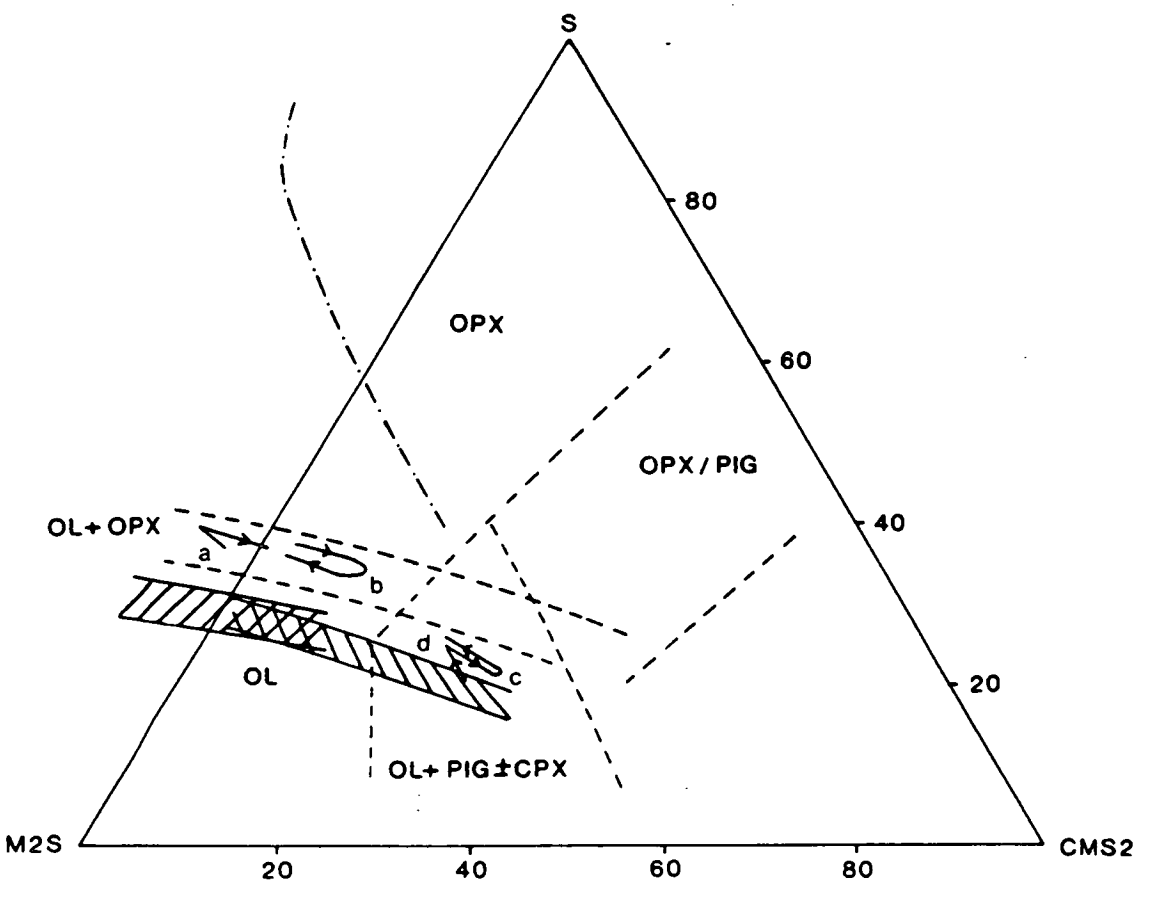
S
80
60
40
20
OPX
OPX / PIG
OL+ OPX
a
b
d
c
OL
OL+ PIG±CPX
M2S
20
40
60
80
CMS2

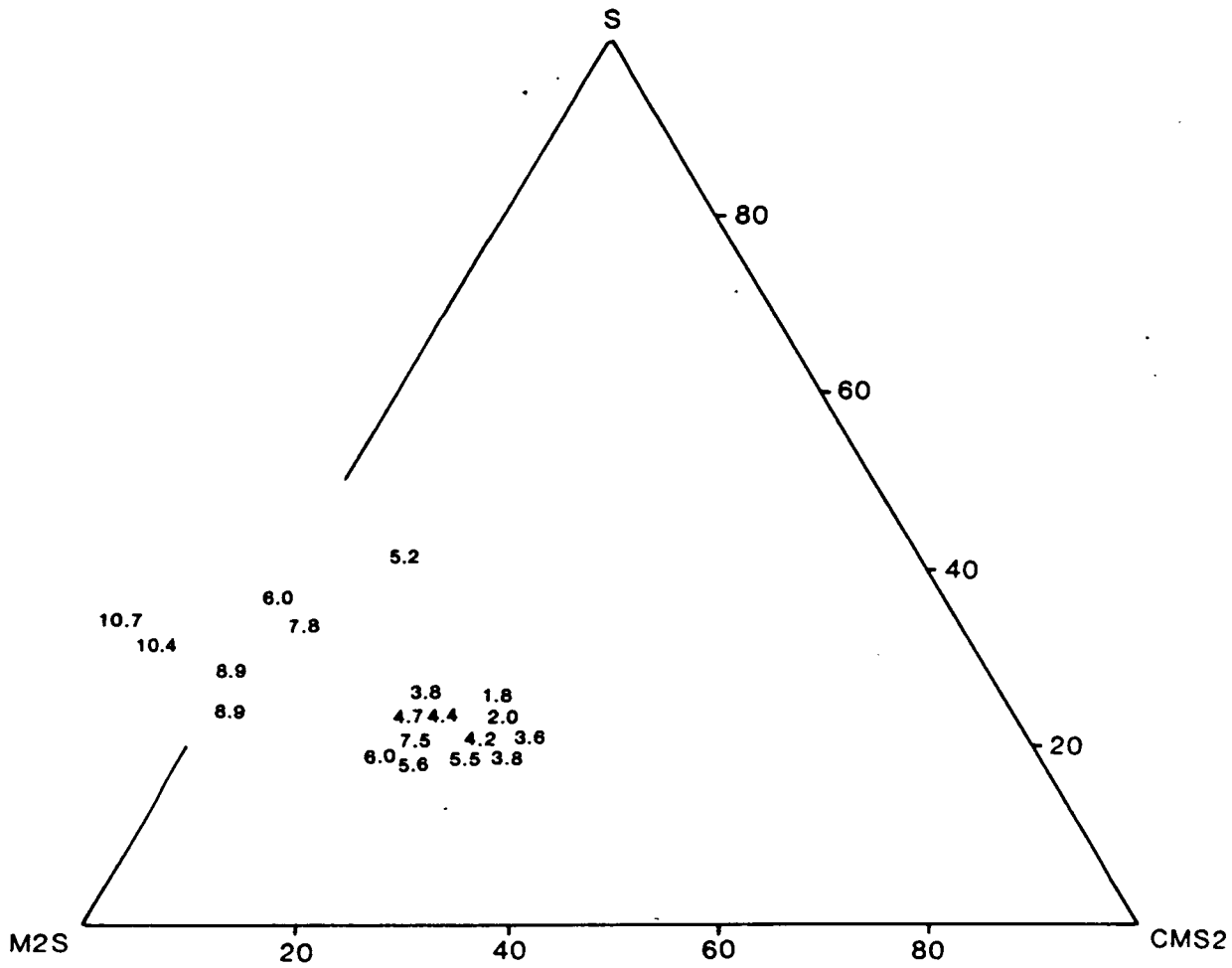

Figure 4.5

Plagioclase onto CMS_2-M_2S-S projection for high-titanium glasses. Points are indicated by the wt% TiO_2 in the glass rather than the actual phase assemblage (mostly ol+pig±others) to show the effect of TiO_2 content in the CMAS projection system.

Figure 4.6

CaO wt% v T°C (4.6a) and SiO_2 wt% v T°C (4.6b) for Grove et al.'s (1982) data and some others for which a series of analyses at decreasing temperatures is known.

× Grove et al. (1982); gl + pig ± others
O Grove et al. (1982); gl + opx ± others
Δ Weill & McKay (1975); gl + opx + ol
◇ Walker et al. (1976); gl + pig ± others
+ Walker et al. (1977); gl + pig ± others
□ Grove & Bryan (1983); gl + pig ± others

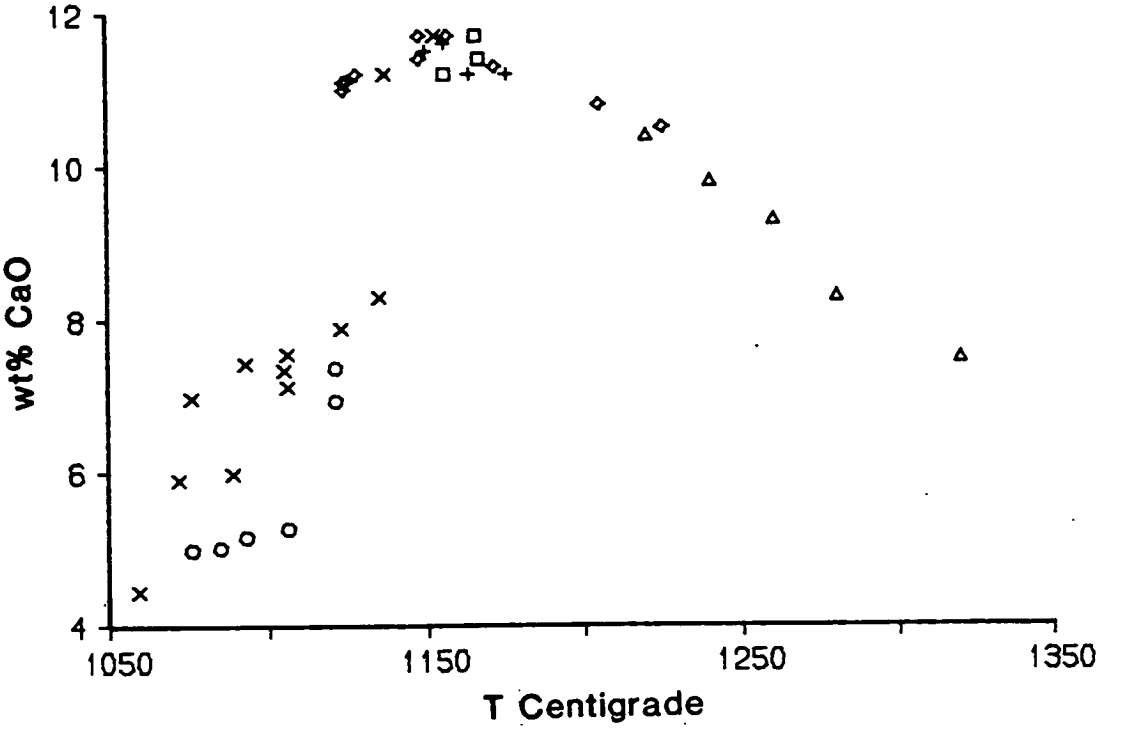
12
10
8
6
4
wt% CaO
1050
1150
1250
1350
T Centigrade

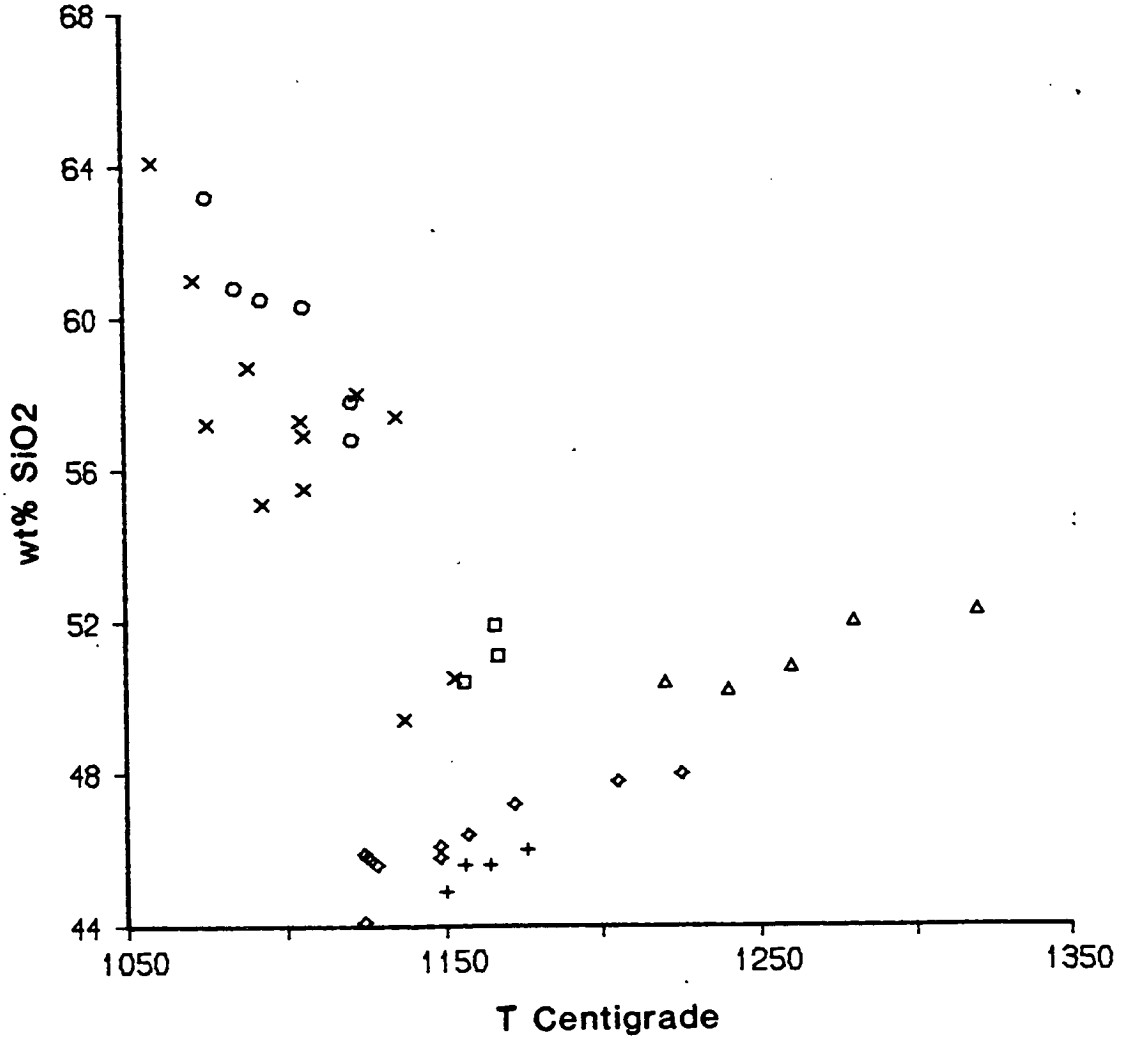
68
64
60
56
52
48
44
wt% SiO2
1050
1150
1250
1350
T Centigrade

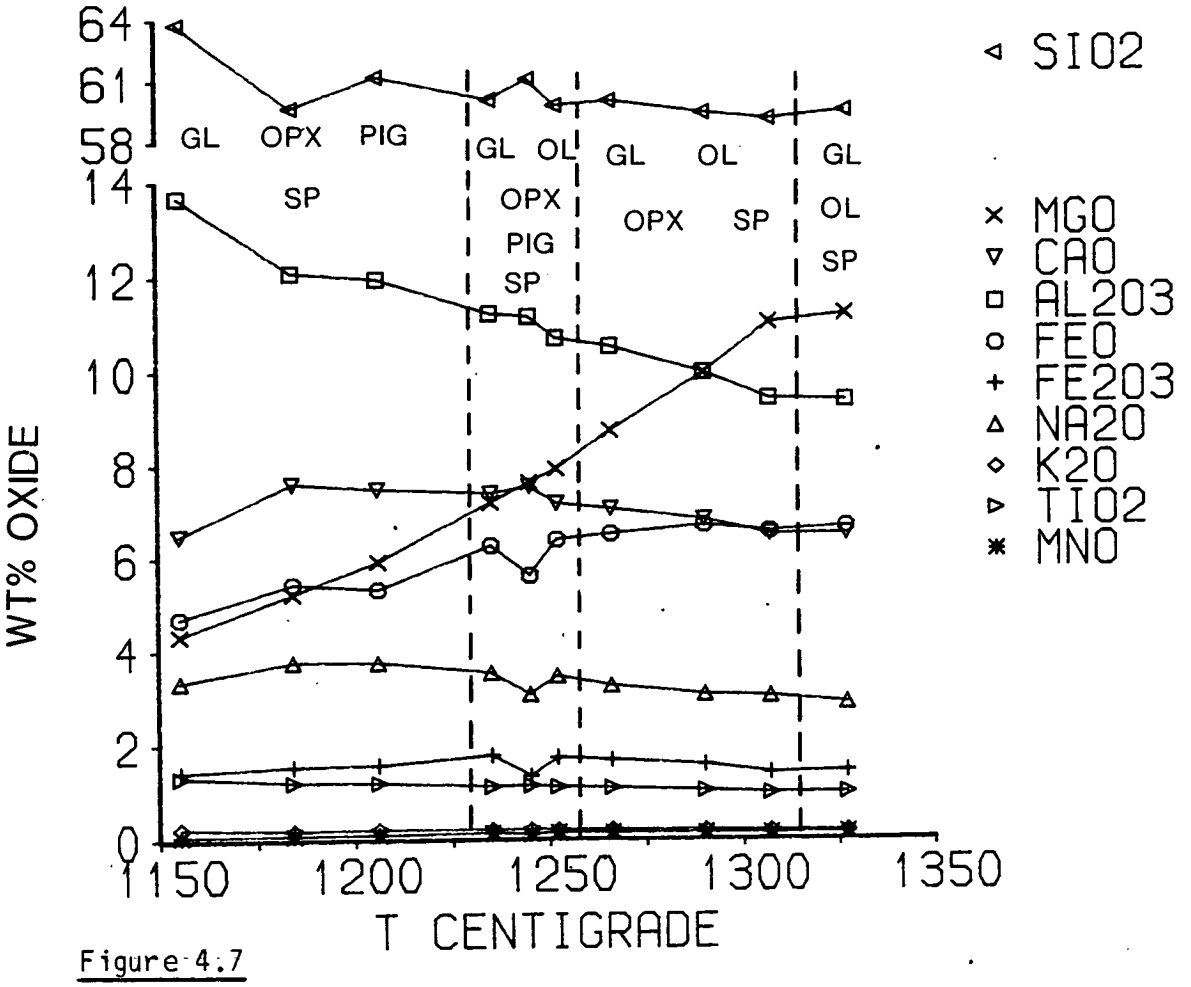

Figure 4.7

T - X diagram for sample 17M.

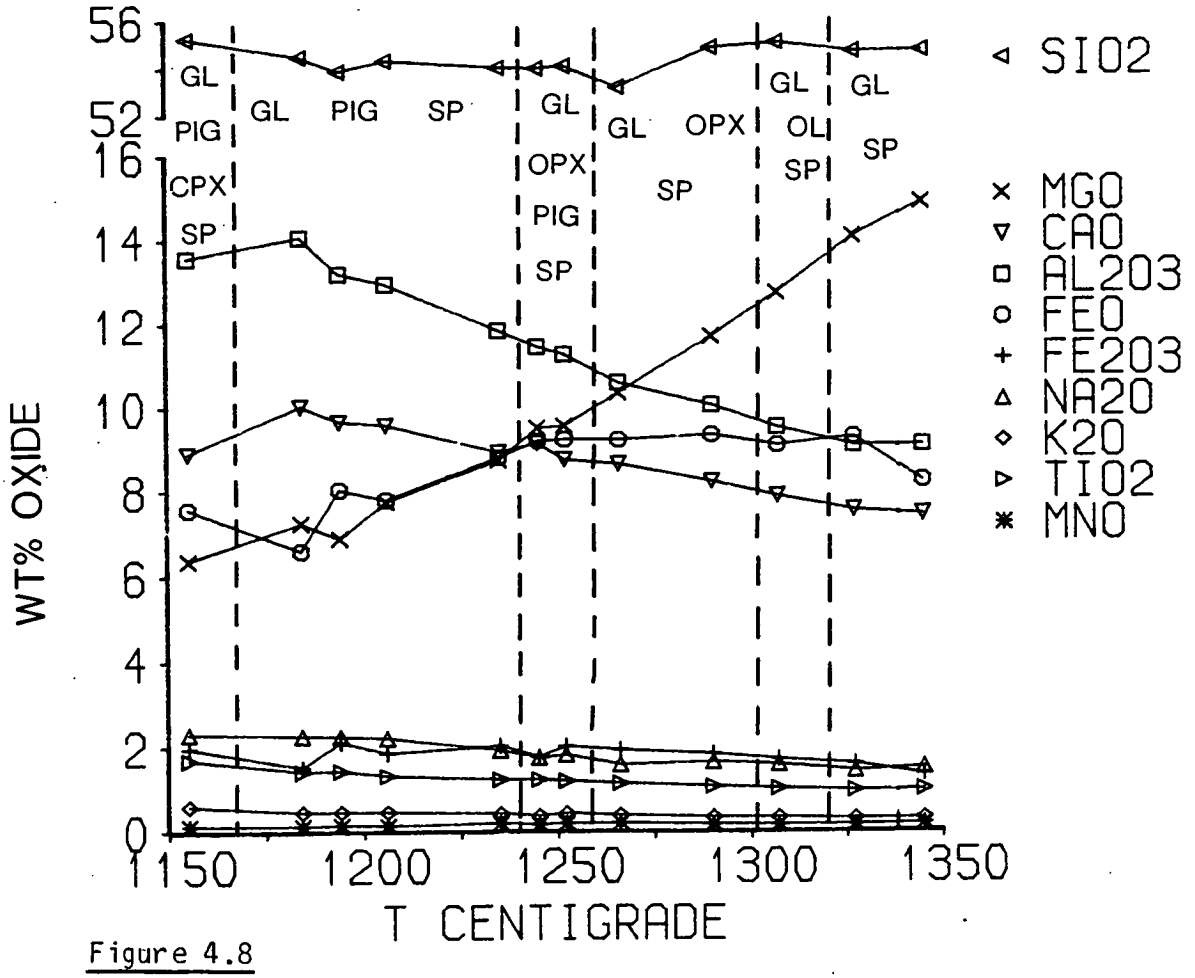

Figure 4.8

T - X diagram for sample 170.

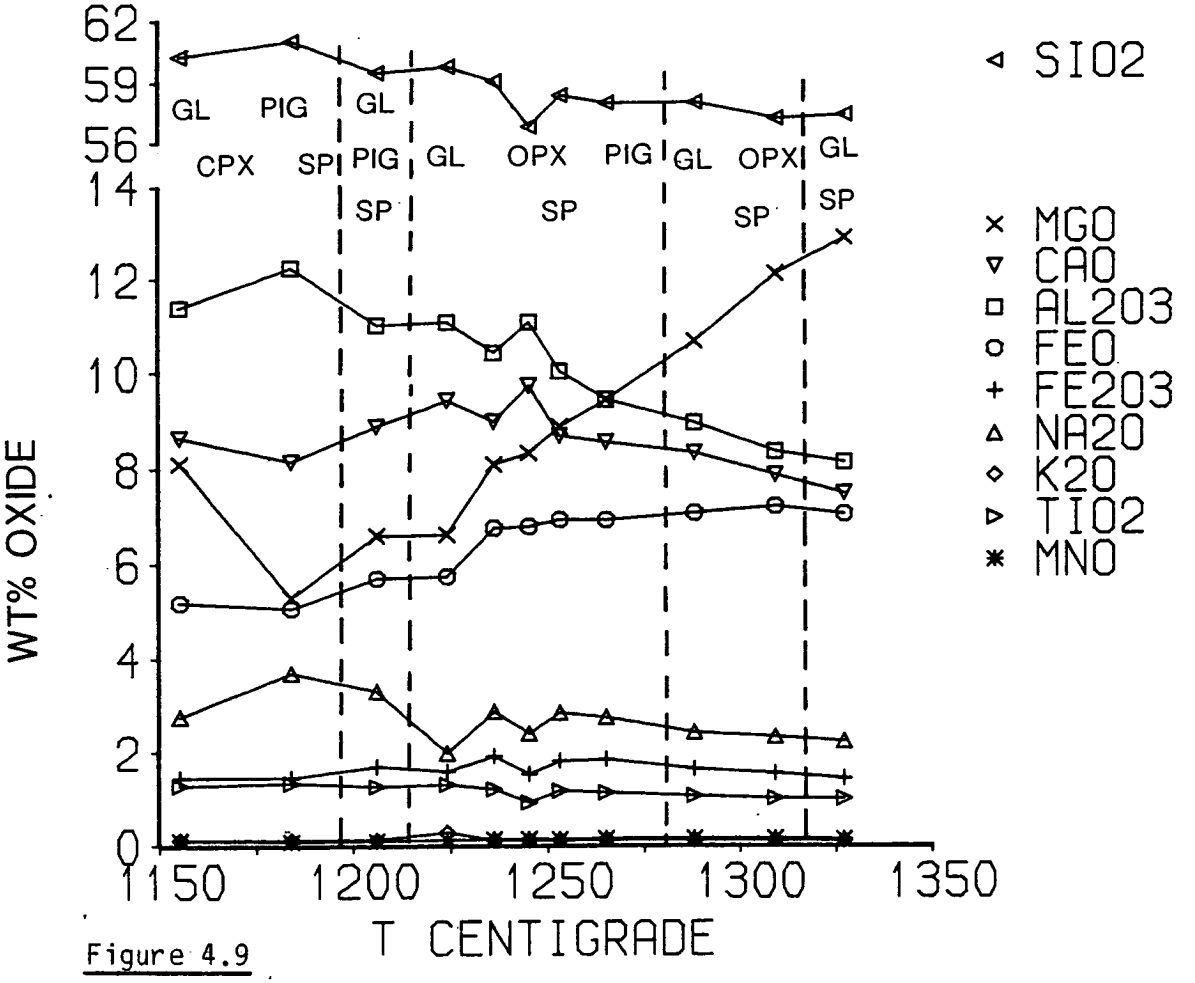

Figure 4.9

T - X diagram for sample 120.

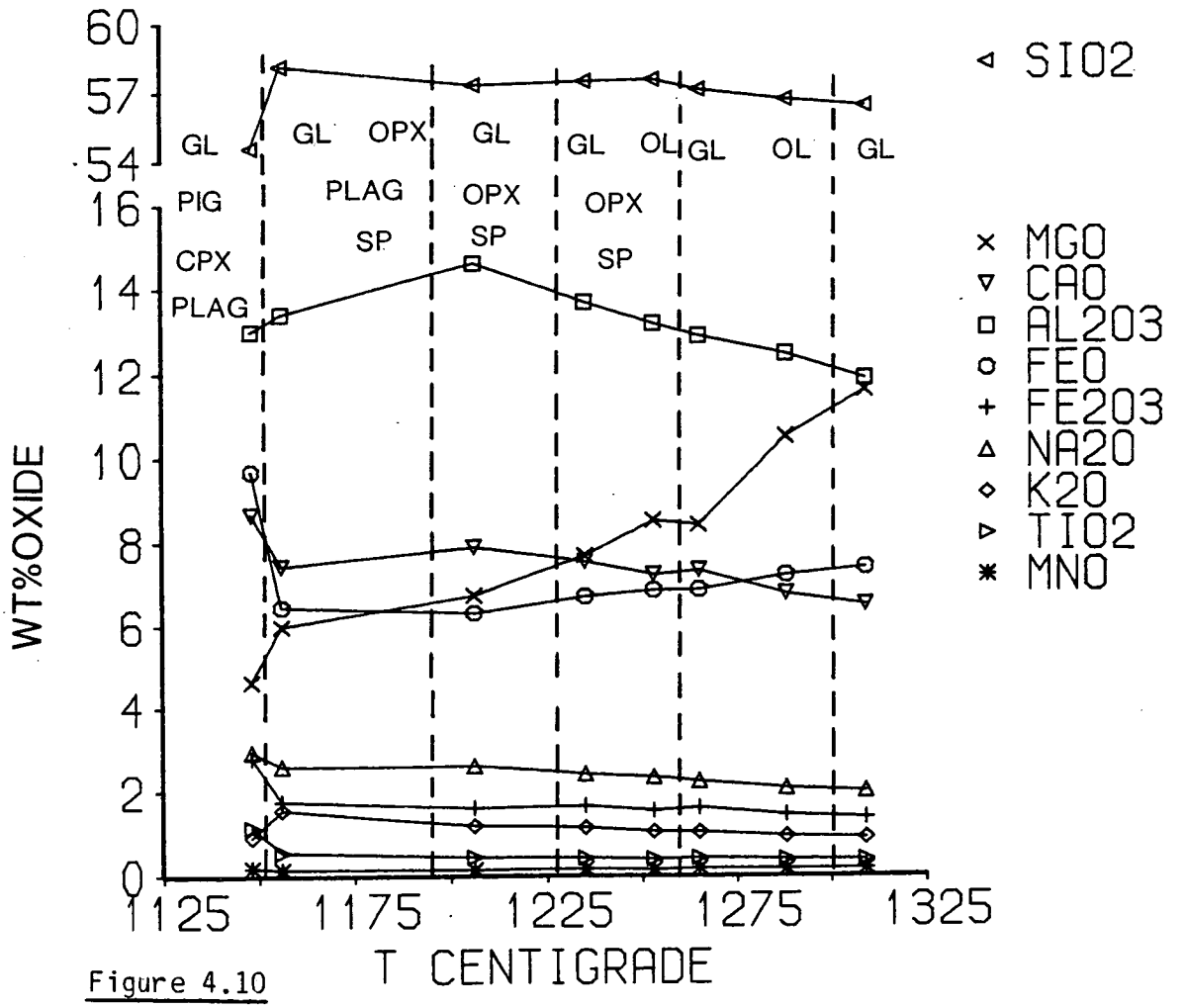

Figure 4.10

T - X diagram for sample B4

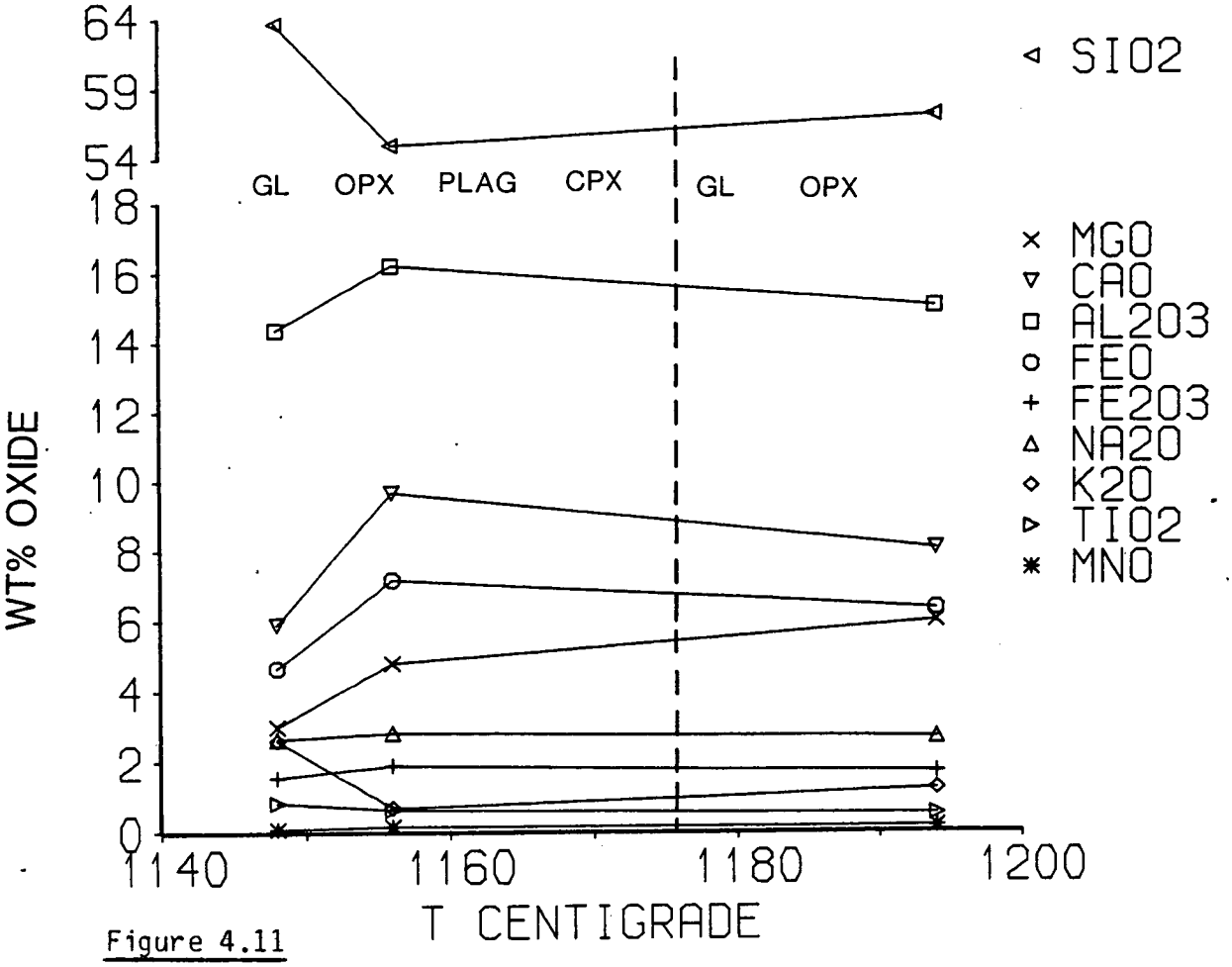

Figure 4.11

T - X diagram for sample B5.

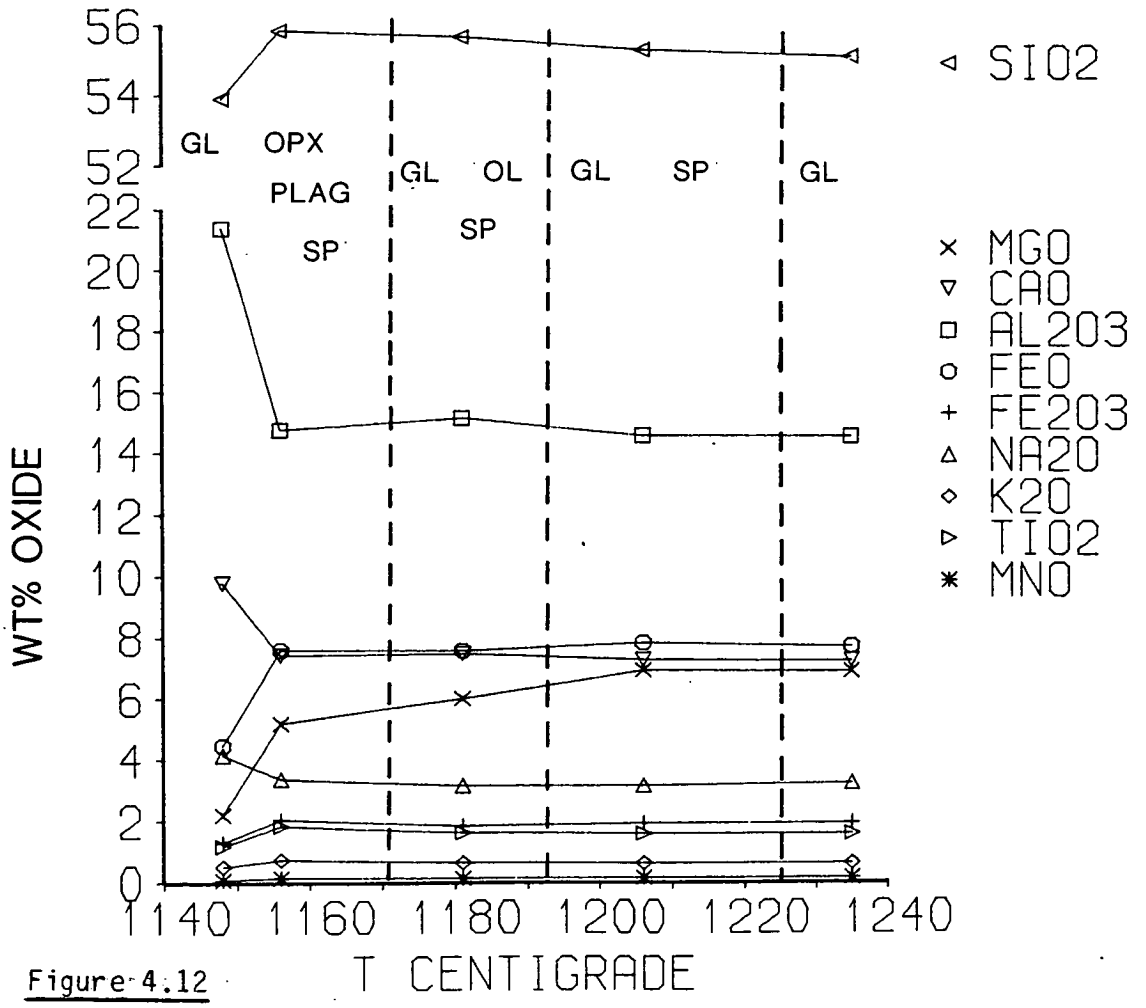

Figure 4.12

T - X diagram for sample T2

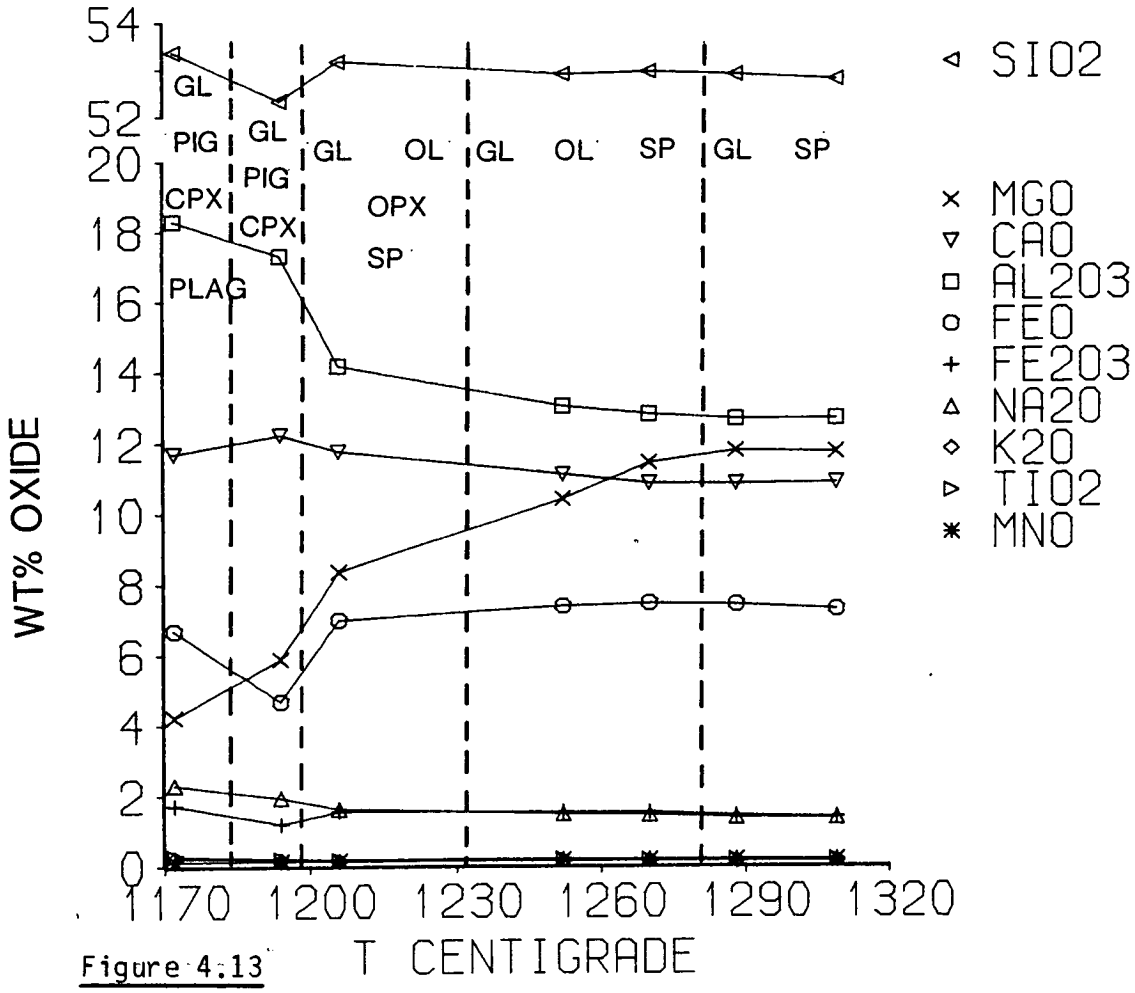

Figure 4.13

T - X diagram for sample K1.

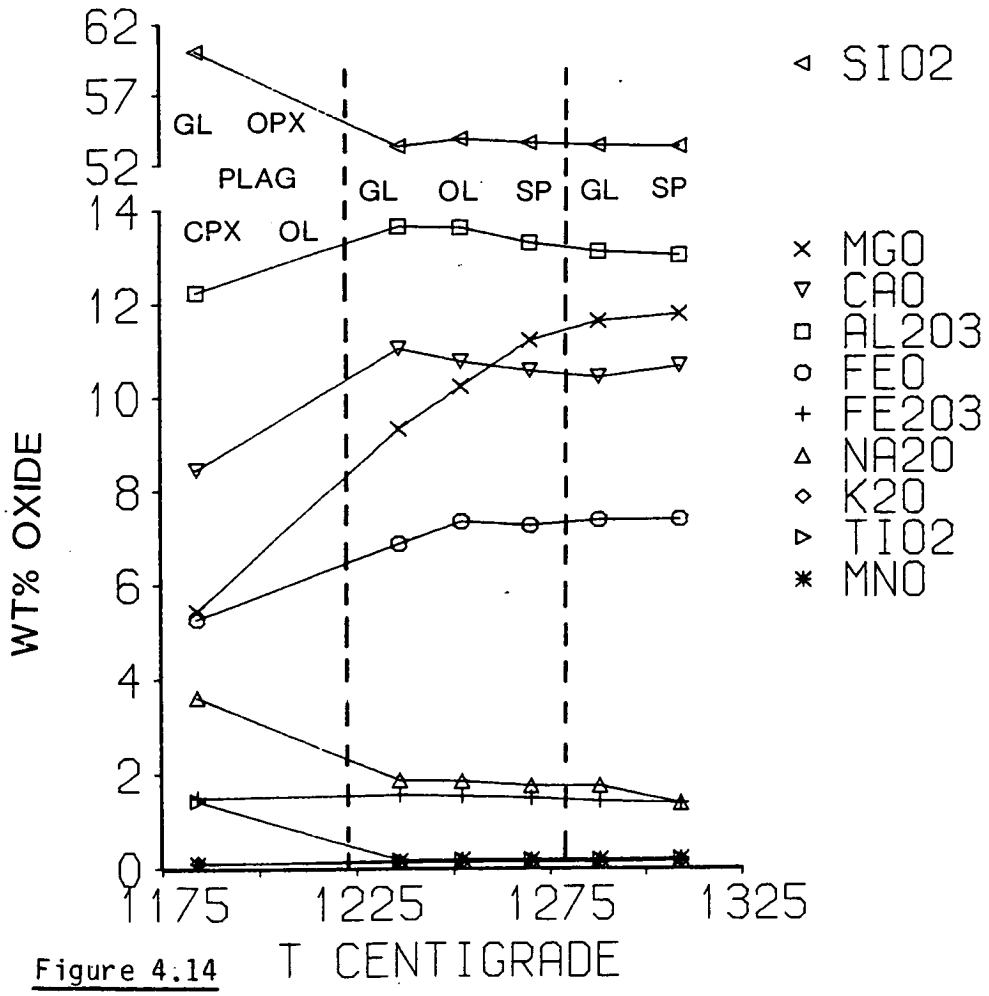

Figure 4.14

T - X diagram for sample K6

Figure 4.15

T - X diagram for sample 295.

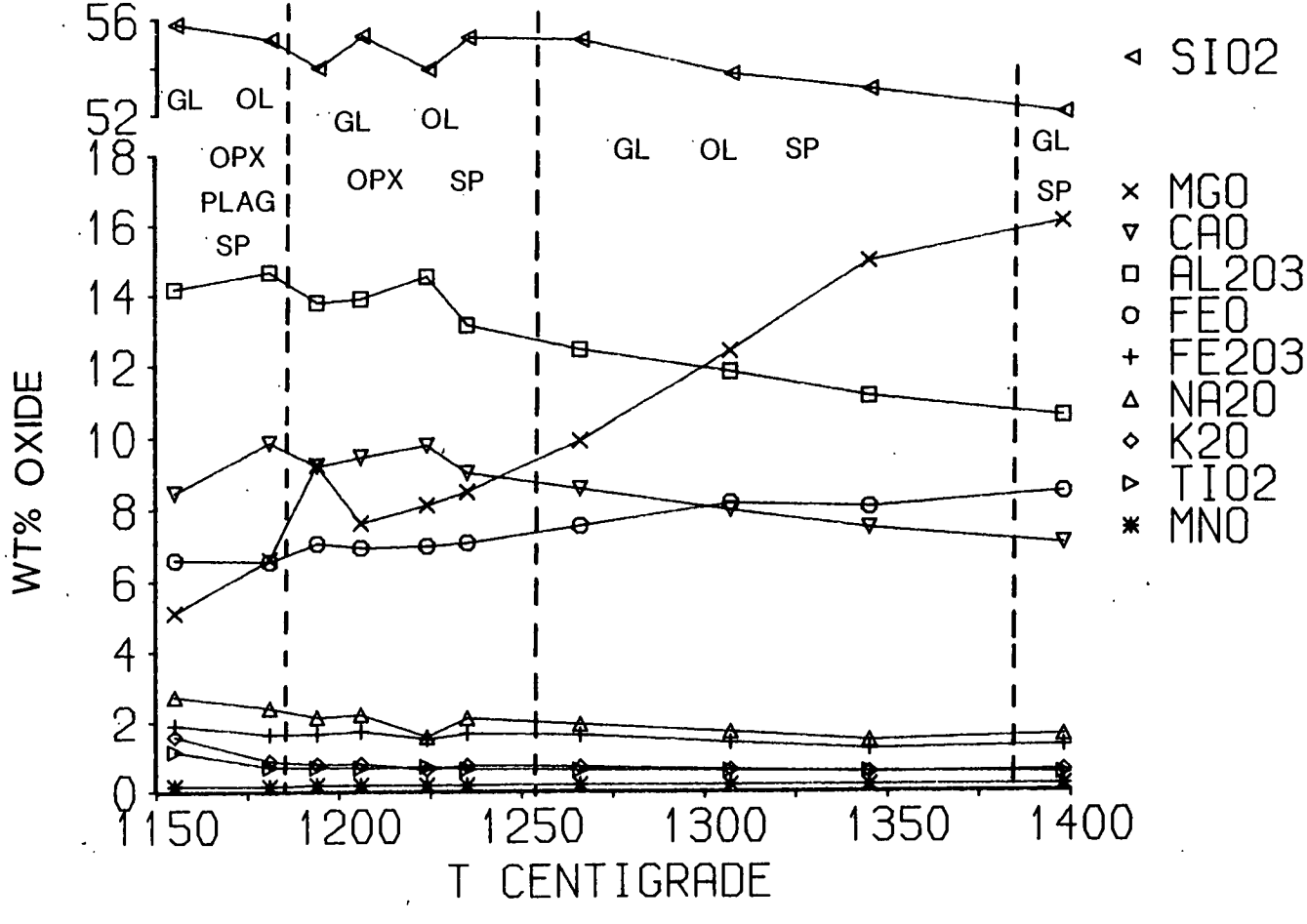

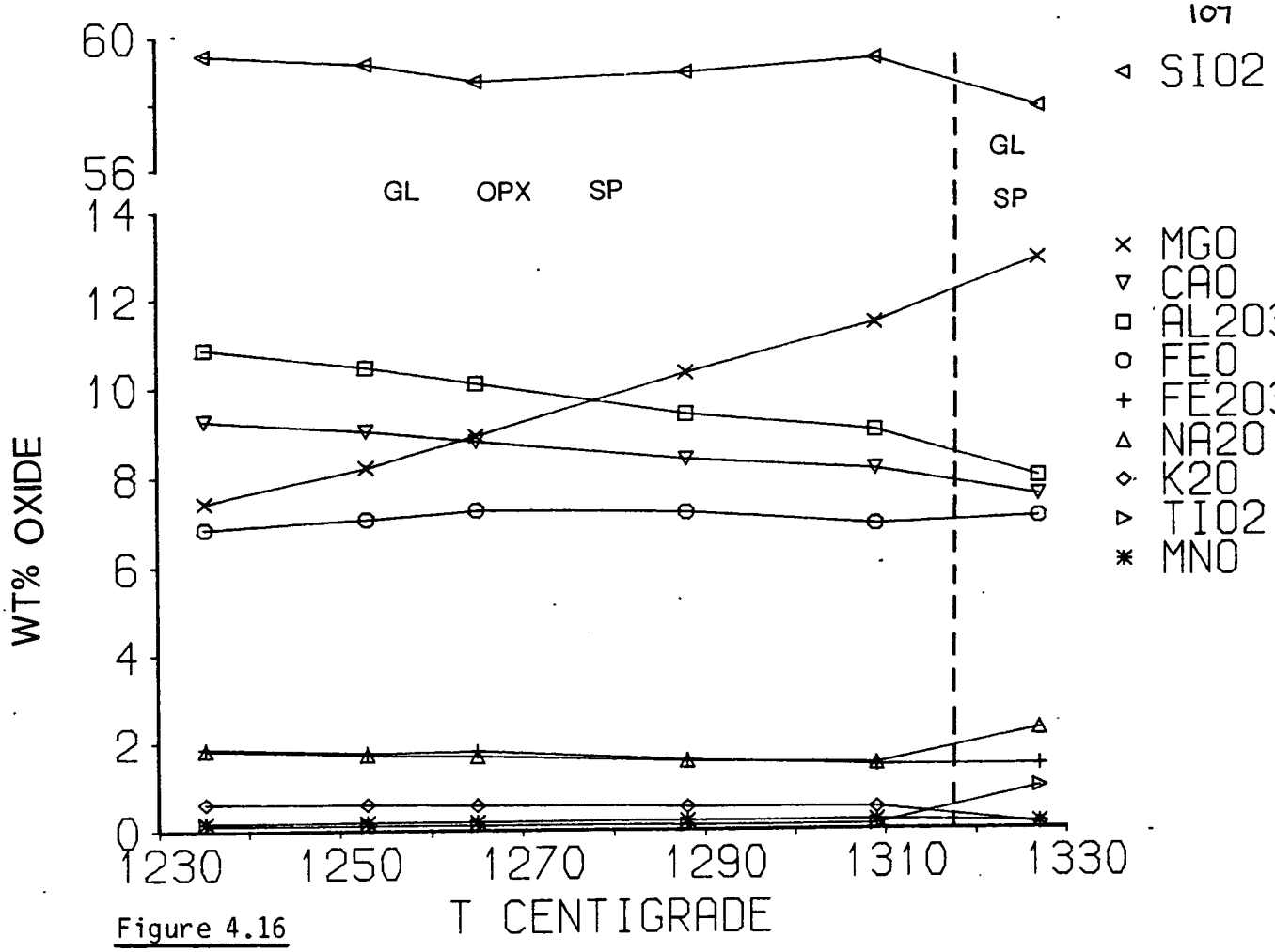

Figure 4.16

T - X diagram for sample M1.

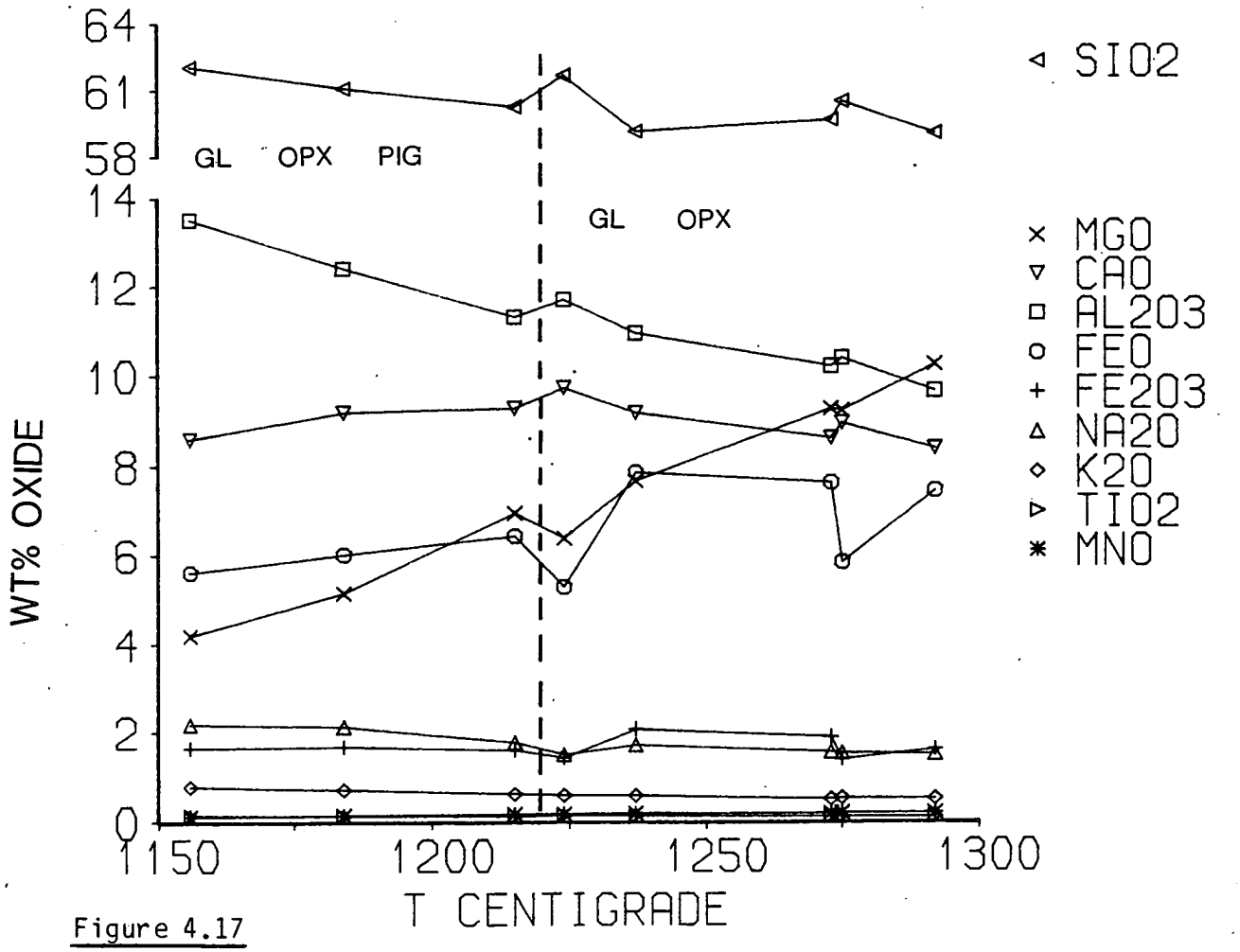

Figure 4.17

T - X diagram for sample M1MET.

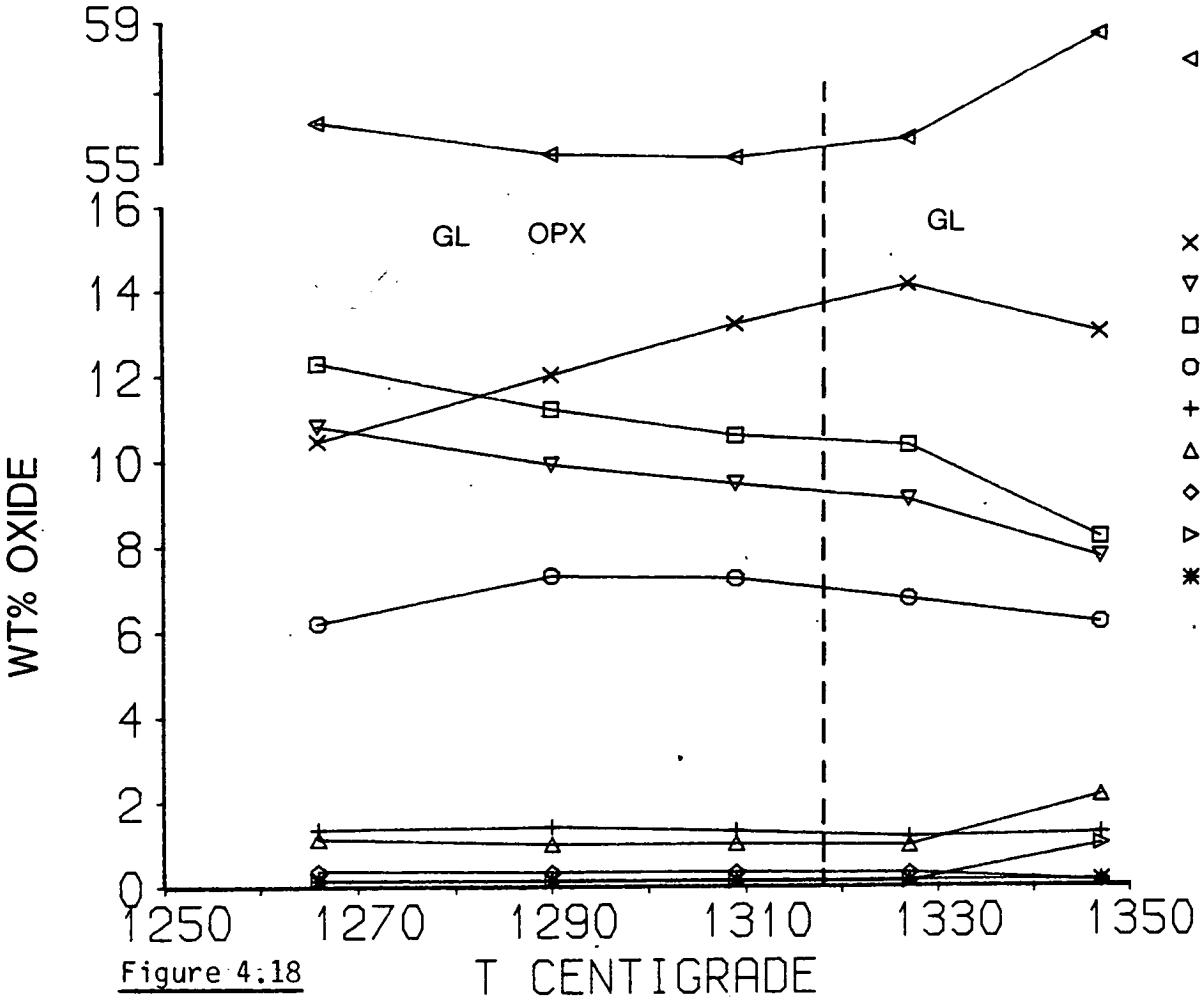

Figure 4:18

T - X diagram for sample C2.

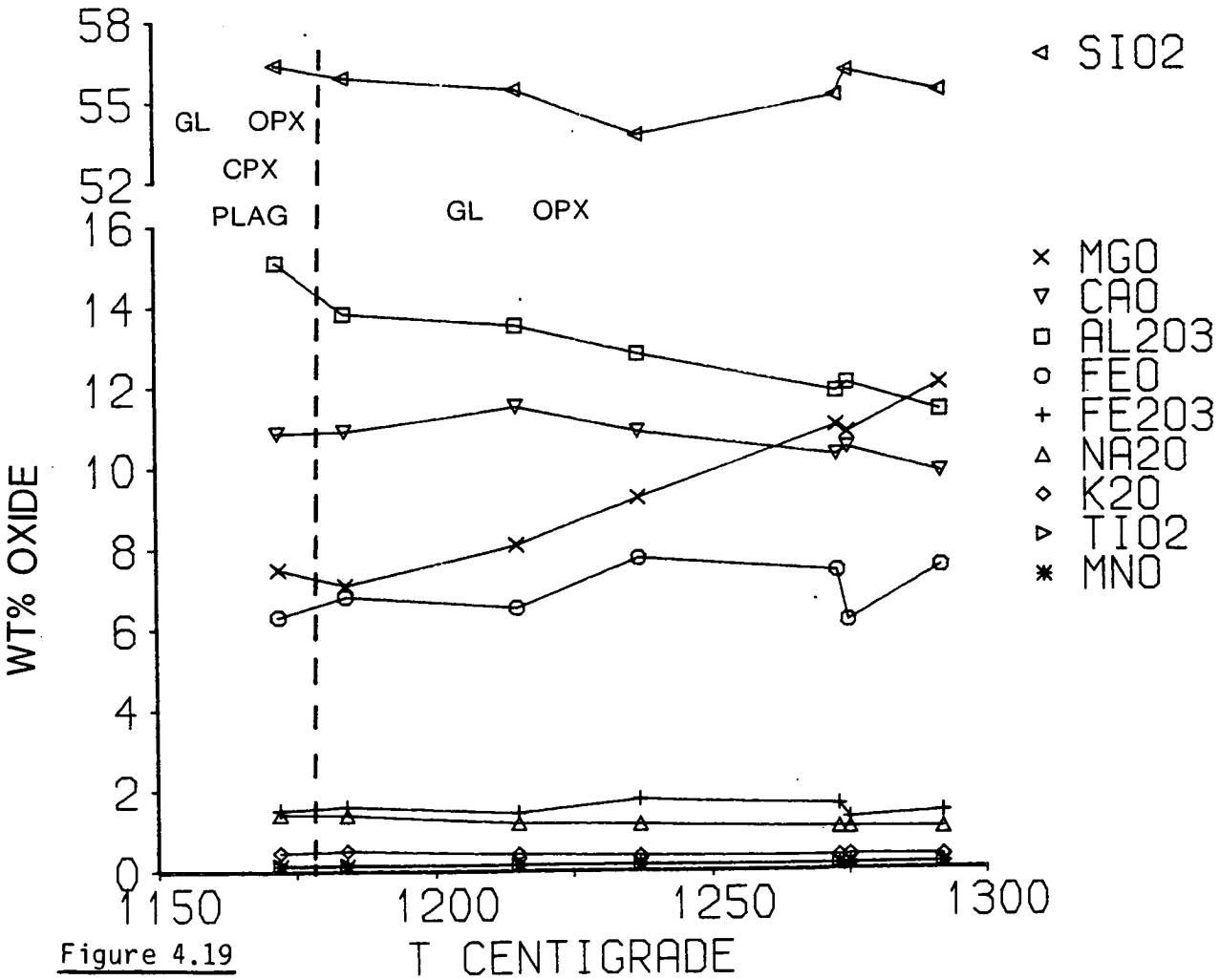

Figure 4.19

T - X diagram for sample C2MEI

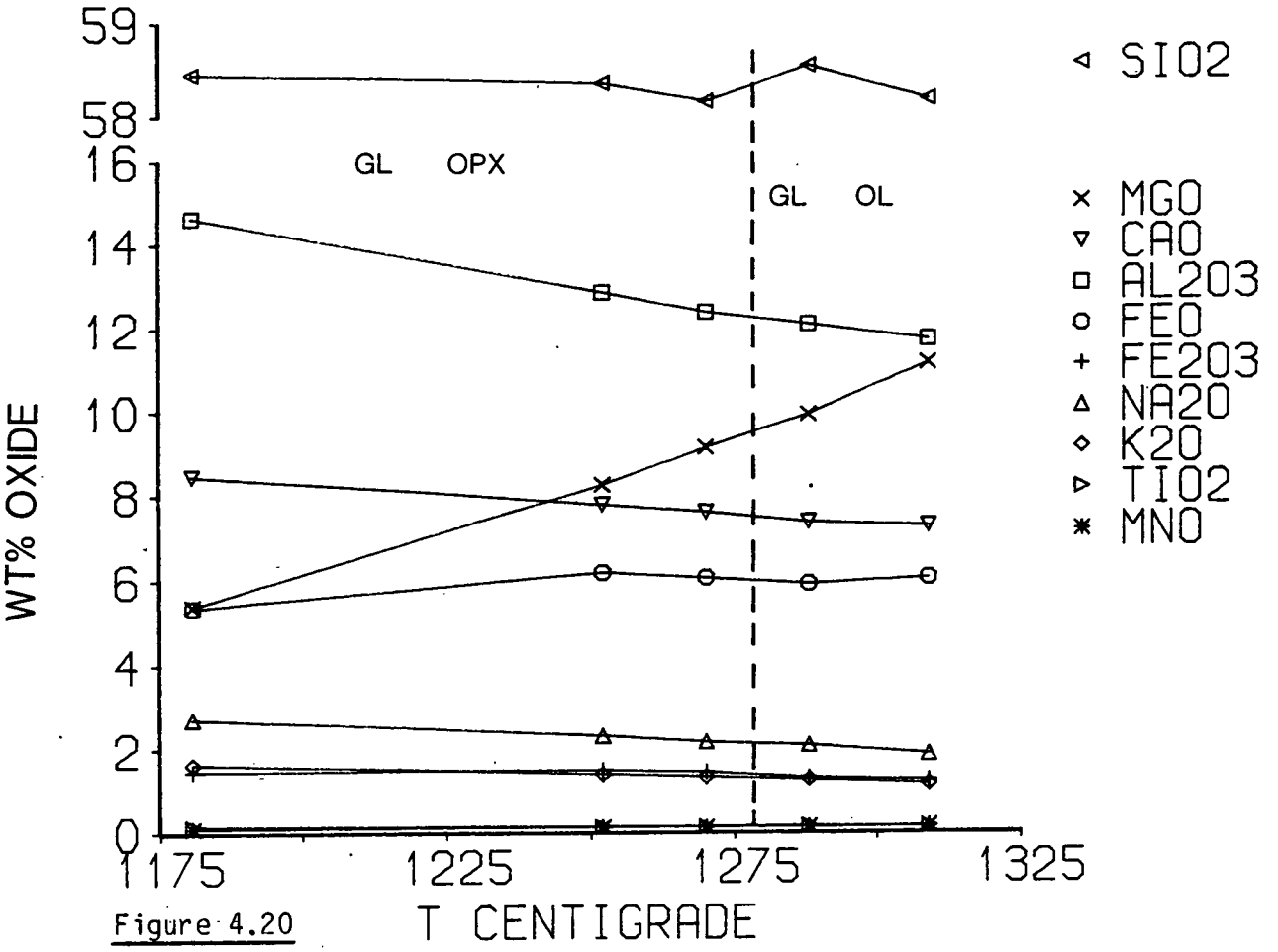

Figure 4.20

T - X diagram for sample C5.

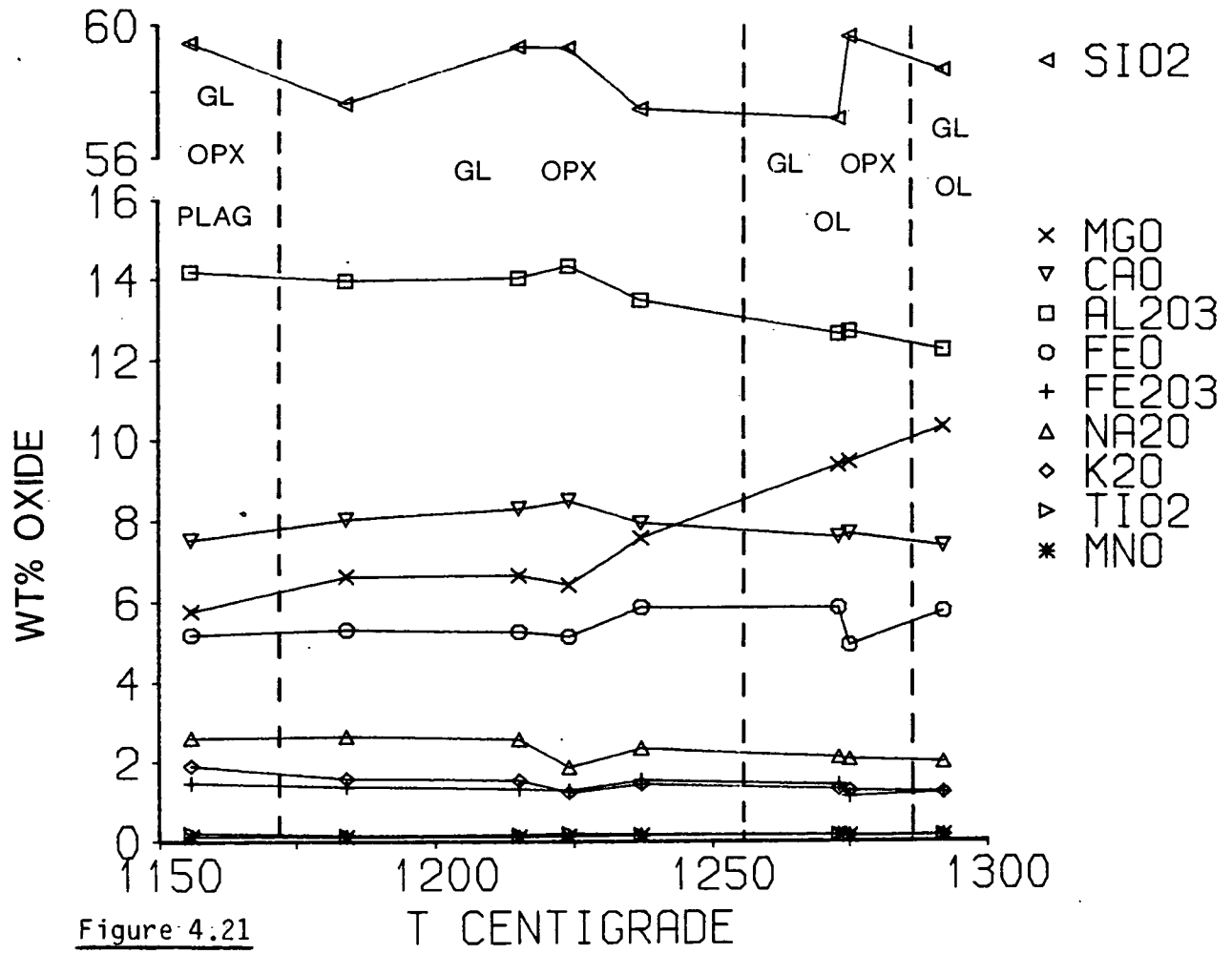

Figure 4.21

T - X diagram for sample C5MET.

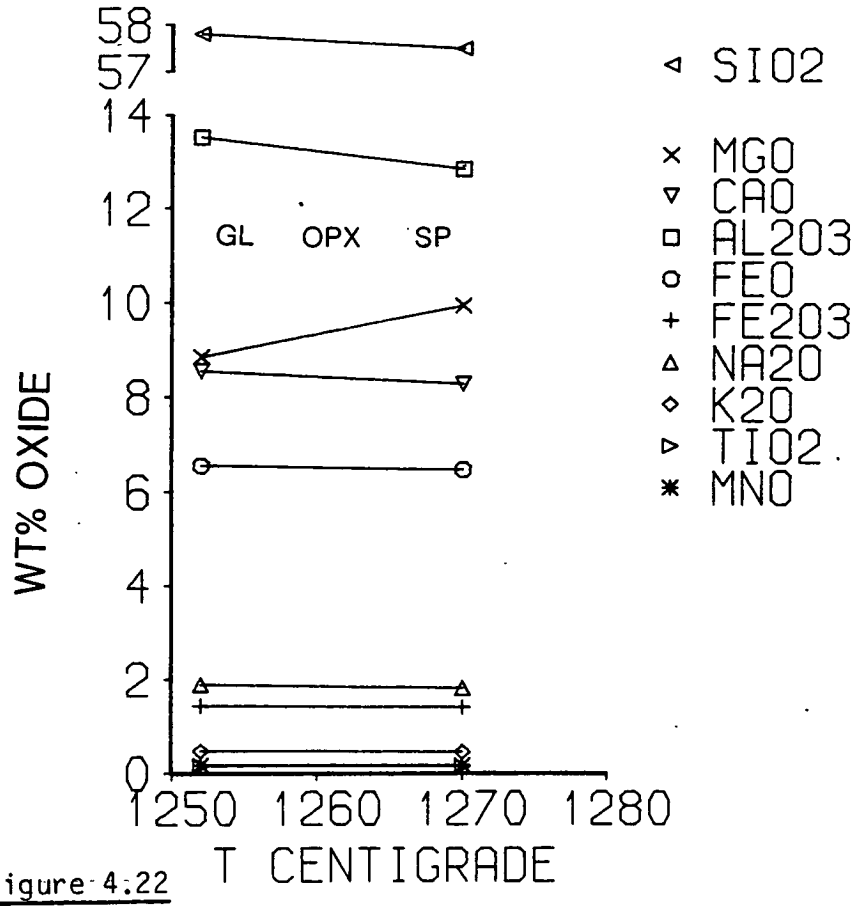

Figure 4:22

T - X diagram for sample C11.

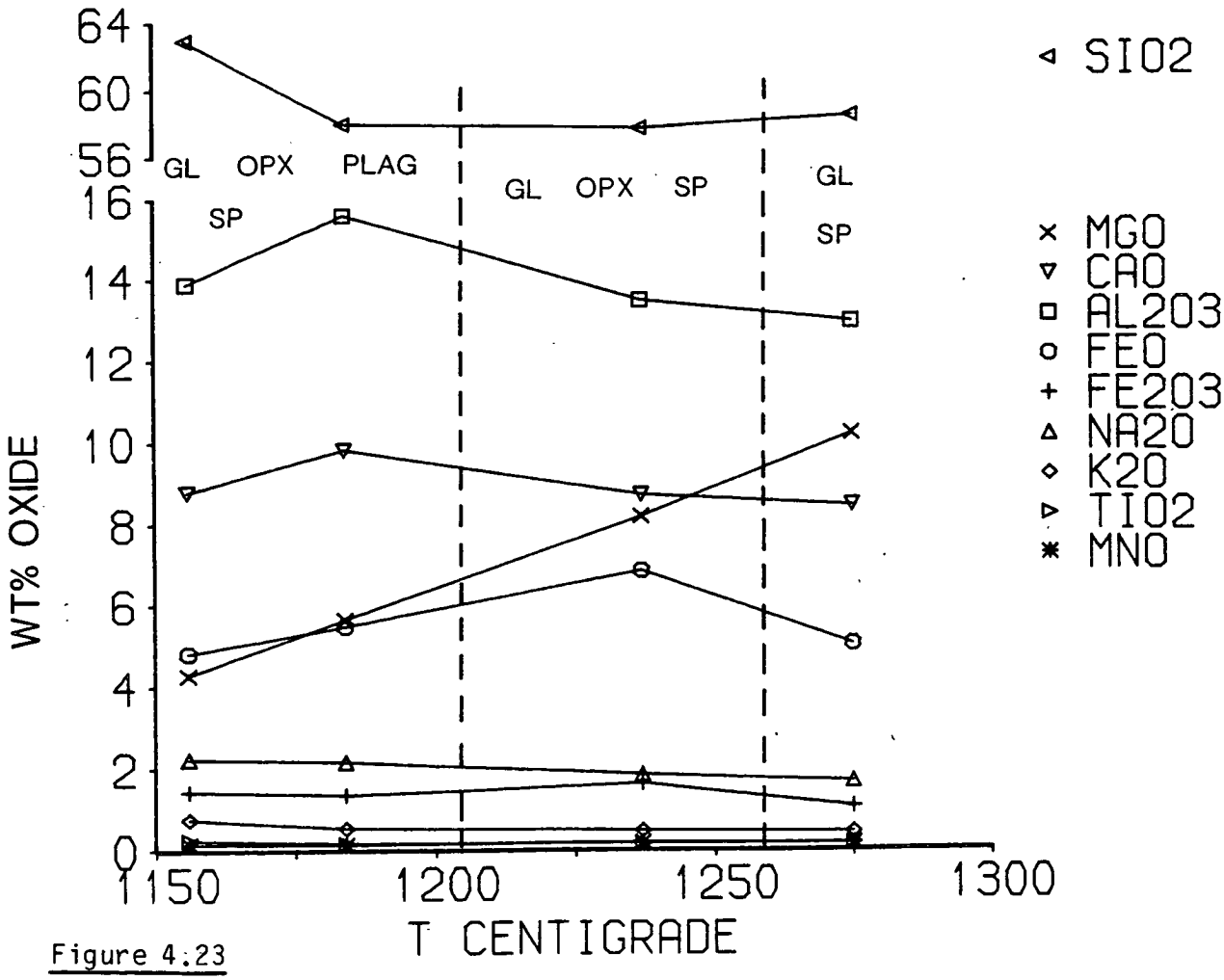

Figure 4:23

T - X diagram for sample C11MET.

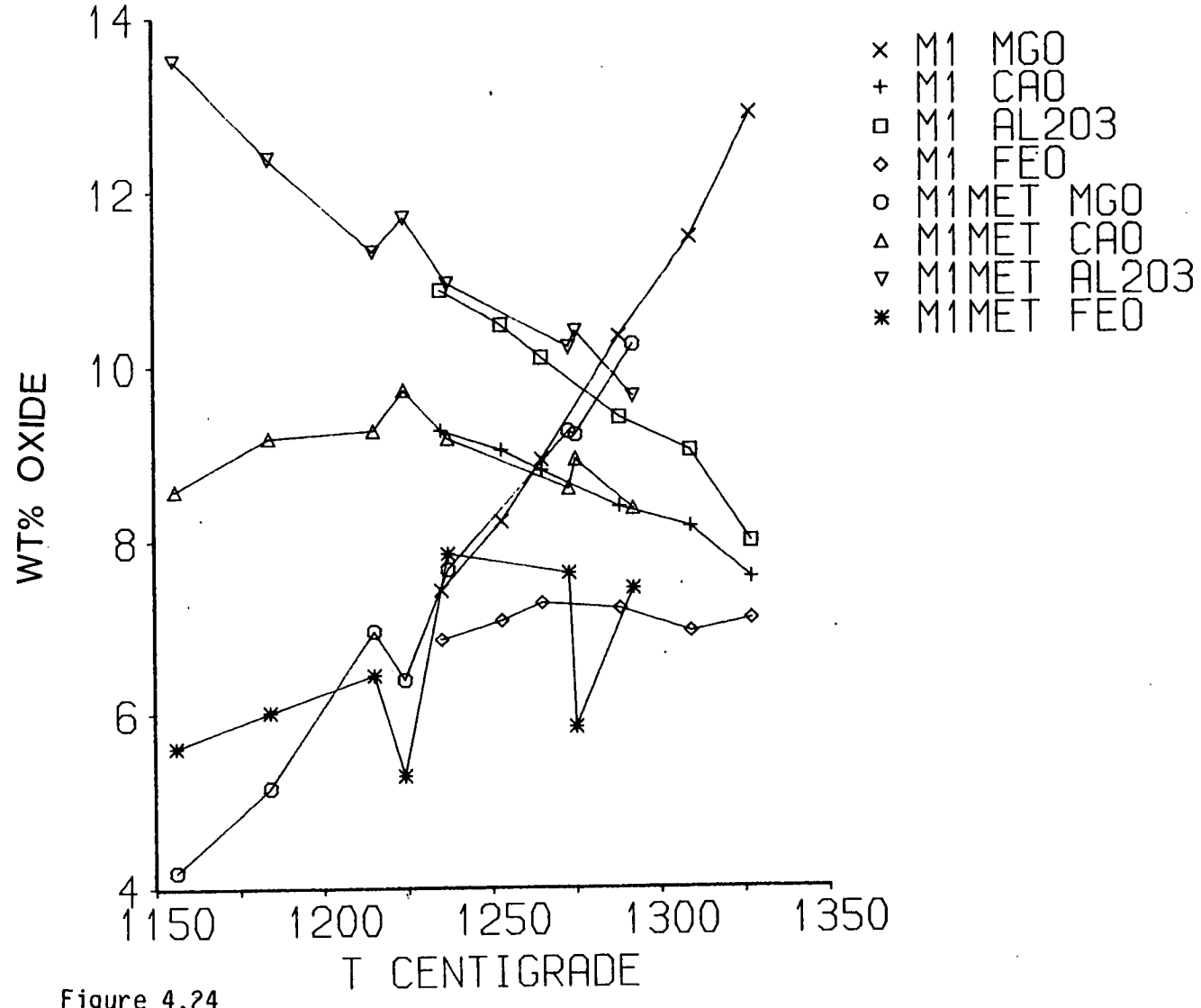

Figure 4.24

T - X diagram for major elements in M1 and M1MET.

Key for Figures 4.25 to 4.35

All data points have two numbers, the larger is the run temperature in °C, the smaller is the height above or below (-ve numbers) the plane of projection.

For all samples the olivine onto CS-MS-A projection is above the plagioclase onto CMS_2-M_2S-S projection.

- gl
- gl + ol
- gl + opx
- gl + opx + pig
- gl + pig
- gl + ol + opx
- gl + ol + opx + pig
- gl + ol + opx + plag
- gl + pig + plag
- gl + opx + pig + plag
- gl + pig + cpx + plag
- gl + opx + cpx + plag

Figure 4.25

Projections for sample 17O. Experiments carried out between 1327°C and 1235°C were of 24 hours, those between 1245°C and 1184°C were of 48 hours.

Figure 4.26

Projections for sample 17M. Experiments carried out between 1327°C and 1235°C were of 24 hours, those between 1245°C and 1184°C were of 48 or 96 hours. Although the experiment at 1155°C was of 96 hours it does not lie near the trend defined by the other experiments (see also fig. 4.7) and has probably failed to equilibrate.

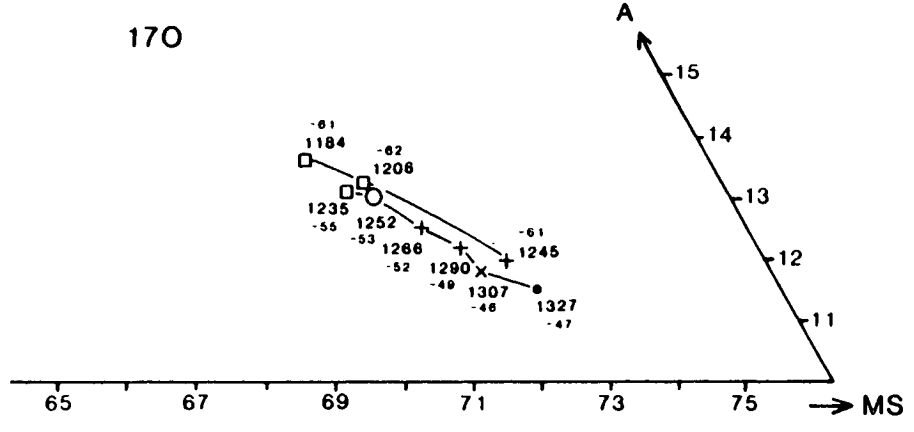
17O
A
15
14
13
12
11
-61
1184
-62
1206
1235
-55
1252
-53
1266
-52
1290
-49
1307
-46
-61
1245
1327
-47
65
67
69
71
73
75
MS

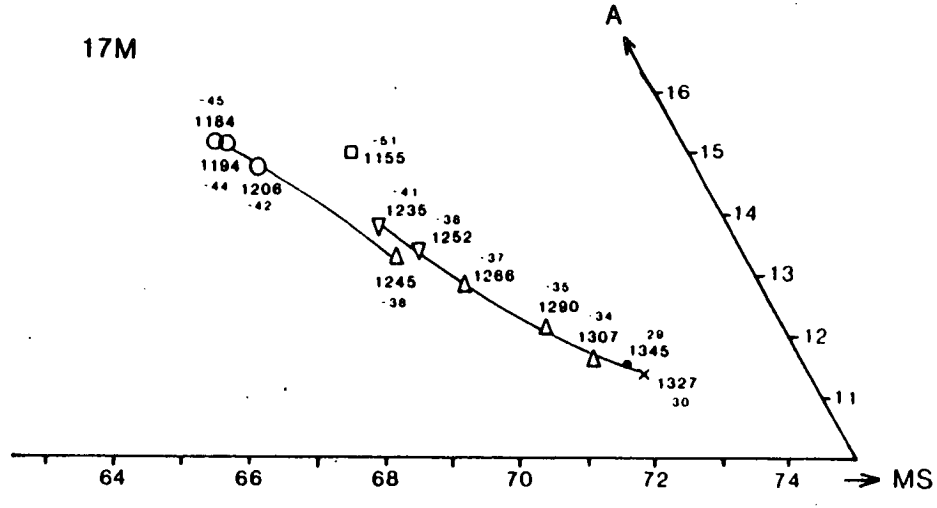
17M
A
16
15
14
13
12
11
-45
1184
1194
-44
-51
1155
1206
-42
-41
1235
-38
1252
1245
-38
-37
1266
-35
1290
-34
1307
29
1345
1327
30
64
66
68
70
72
74
MS

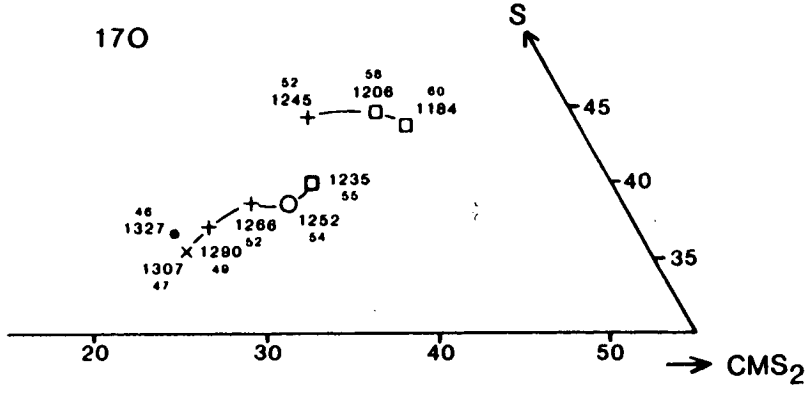
17O
S
45
40
35
52
1245
58
1206
60
1184
1235
55
46
1327
1266
52
1252
54
1290
49
1307
47
20
30
40
50
CMS2

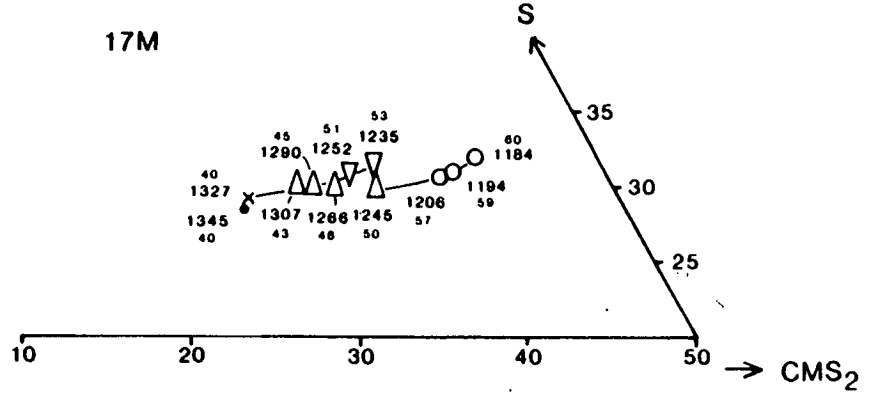
17M
S
35
30
25
45
1290
51
1252
53
1235
60
1184
40
1327
1345
40
1307
43
1266
46
1245
50
1206
57
1194
59
10
20
30
40
50
CMS2

Figure 4:27

Projections for sample B4. Experiments carried out between 1309°C and 1235°C were of 24 hours, those of 1206°C and 1156°C were of 48 hours. The apparent reversal of the crystallisation trend for 48 hour experiments in the olivine projection is due to the presence of quench phases in the 1156°C experiment which affect the glass composition, see also fig. 4.10.

Figure 4:28

Projections for sample 120. Experiments between 1327°C and 1253°C were of 24 hours, those between 1245°C and 1184°C were of 48 hours. The experiment at 1224°C was of 477 hours, although this analysis represents an equilibrium composition the losses of iron and sodium due to the increased length of the experiment cause it to plot off the trend defined by the shorter experiments.

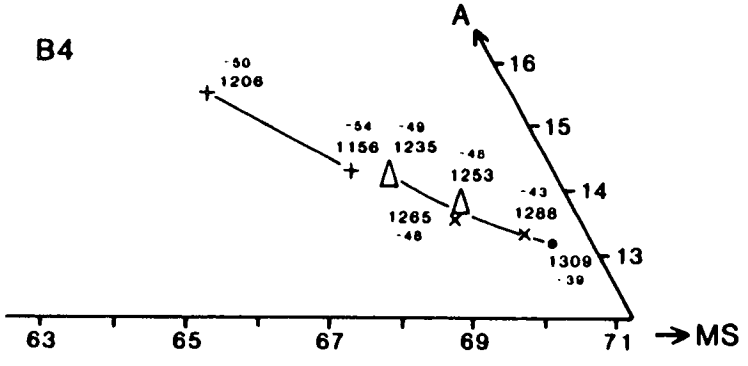
B4
A
16
15
14
13
-50
1206
-54
1156
-49
1235
-48
1253
-43
1288
1265
-48
1309
-39
63
65
67
69
71
→MS

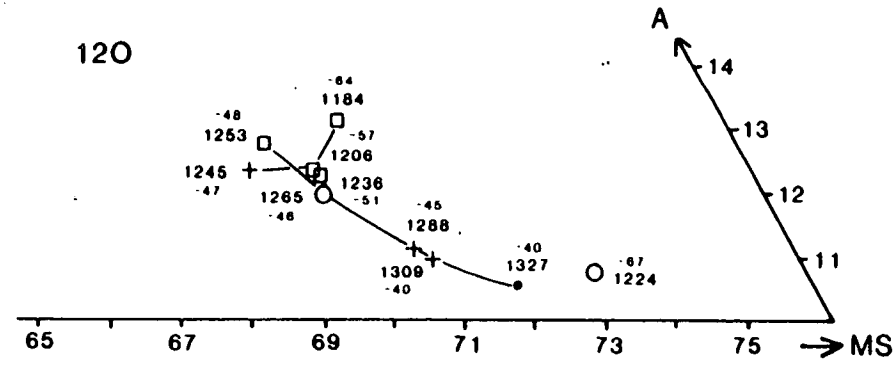
120
A
14
13
12
11
-64
1184
-48
1253
-57
1206
1245
-47
1236
-51
1265
-46
-45
1288
-40
1327
1309
-40
-67
1224
65
67
69
71
73
75
→MS

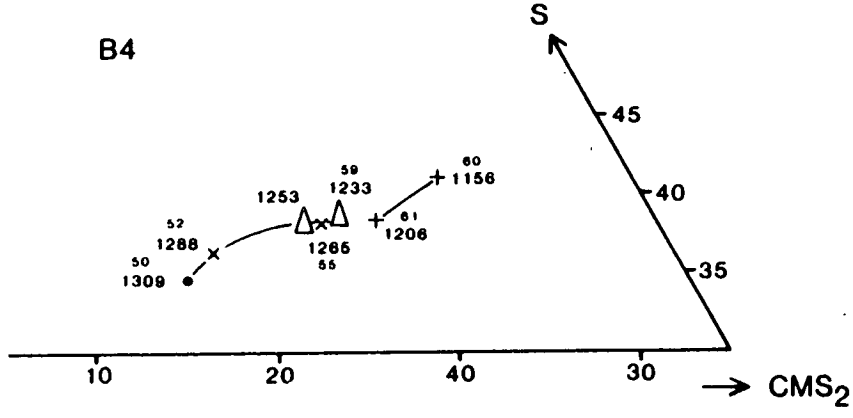
B4
S
45
40
35
59
1233
60
1156
1253
52
1288
61
1206
1265
55
50
1309
10
20
40
30
→CMS2

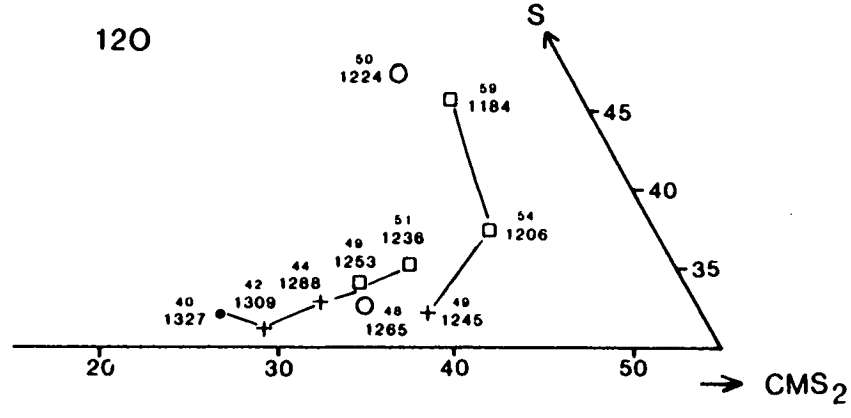
120
S
45
40
35
50
1224
59
1184
54
1206
51
1236
49
1253
44
1288
42
1309
40
1327
48
1265
49
1245
20
30
40
50
→CMS2

Figure 4.29

Projections for sample 295. Experiments between 1345°C and 1235°C were of 24 hours, those between 1206°C and 1155°C were of 48 or 96 hours. The glass from the 1194°C experiment deviates from the trend because of compositional changes (fig. 4.15) for which there is no obvious explanation. The glass from the long experiment (477 hours) at 1224°C deviates from the trend because of sodium losses (fig. 4.15).

Figure 4.30

Projections for sample T2.

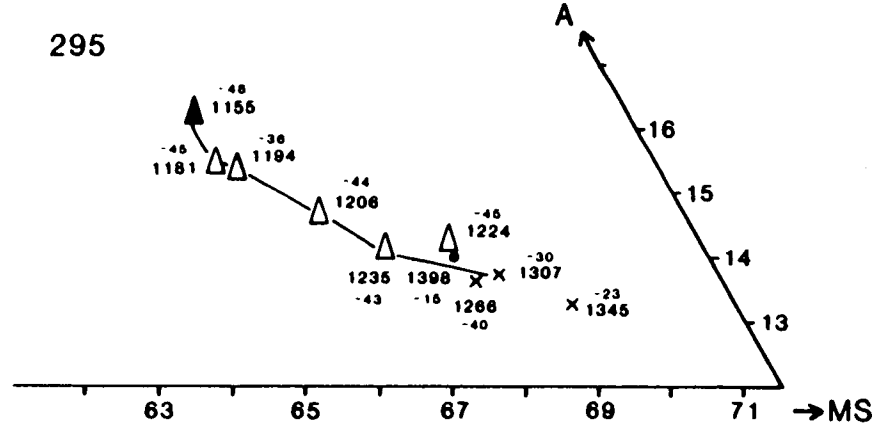
295
A
16
15
14
13
-48
1155
-45
1181
-36
1194
-44
1206
-45
1224
-30
1307
1235
-43
1398
-15
1266
-40
-23
1345
63
65
67
69
71
→MS

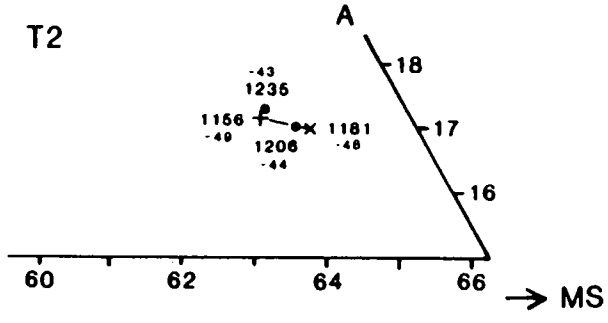
T2
A
18
17
16
-43
1235
1156
-49
1181
-48
1206
-44
60
62
64
66
→ MS

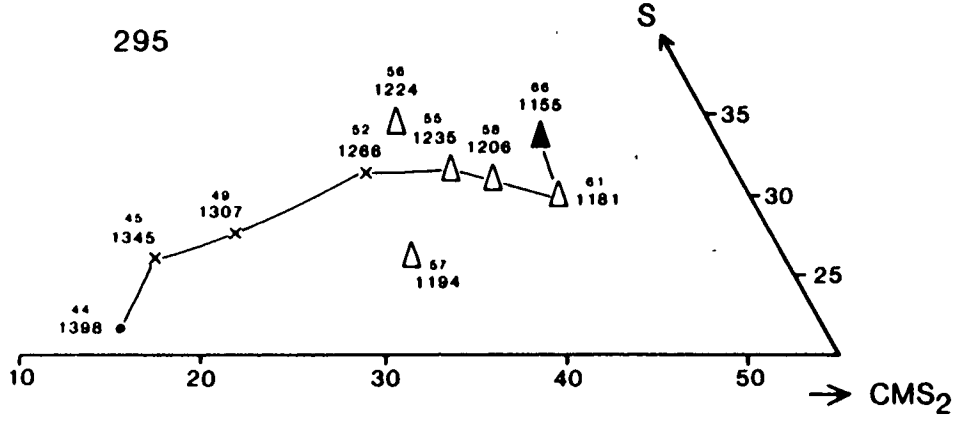
295
S
35
30
25
56
1224
66
1155
55
1235
52
1266
58
1206
61
1181
49
1307
45
1345
67
1194
44
1398
10
20
30
40
50
→ CMS2

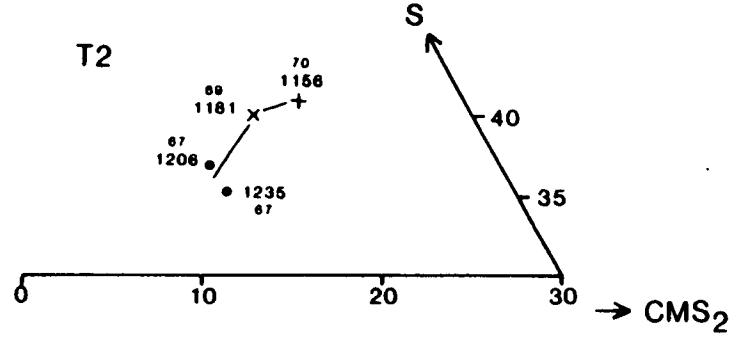
T2
S
40
35
70
1156
69
1181
67
1206
1235
67
0
10
20
30
→ CMS2

Figure 4.31

Projections for samples K1 and K6. Experiments between 1309°C and 1235°C were of 24 hours; those between 1206°C and 1172°C were of 48 or 96 hours. The glass from the experiment at 1172°C has been affected by quench phases (see also fig. 4.13) causing it to deviate from the trend.

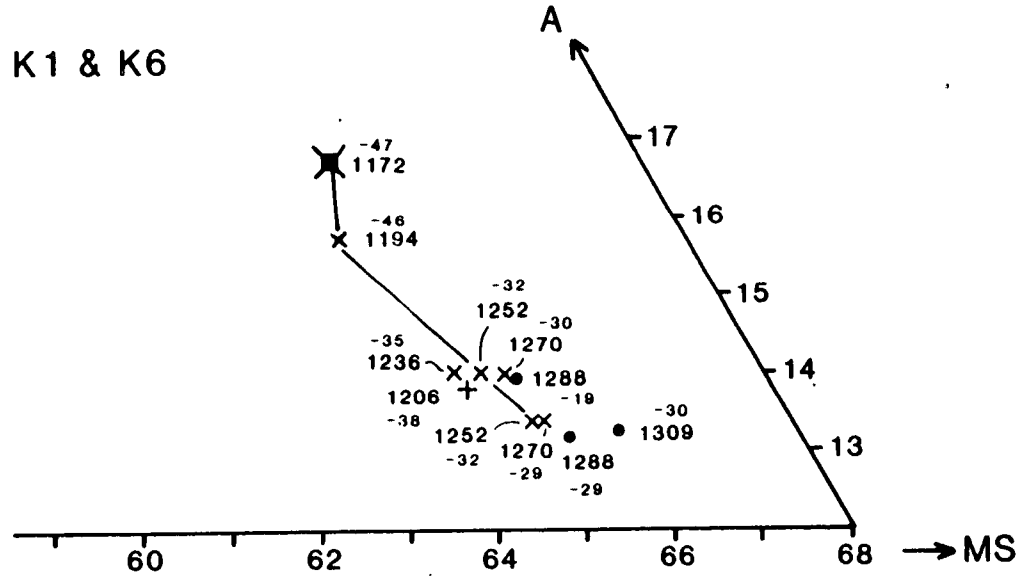
K1 & K6
A
17
16
15
14
13
-47
1172
-46
1194
-32
1252
-30
1270
-35
1236
1288
1206
-18
-38
-30
1309
1252
1270
1288
-32
-29
-29
60
62
64
66
68
MS

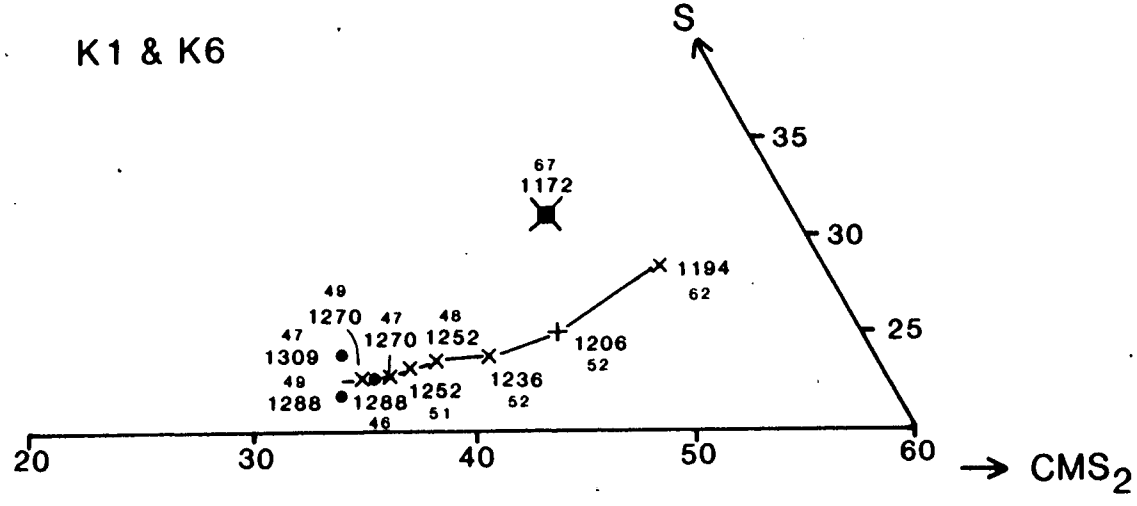
K1 & K6
S
35
30
25
67
1172
1194
62
49
1270
47
1270
48
1252
47
1309
1206
52
49
1288
1288
1252
1236
52
51
46
20
30
40
50
60
CMS2

Figure 4.32

Projections for samples M1 and M1MET. All experiments on sample M1 were of 24 hours, although the crystals in these charges did not equilibrate a good orthopyroxene crystallisation trend is defined. For sample M1MET all experiments except those at 1273°C and 1224°C were of 48 hours, the 1273°C experiment was of 24 hours. The 1224°C experiment was of 477 hours and due to losses of iron and sodium (see also fig. 4.17) deviates from the trend. This is not initially evident in the olivine projection, however, there is a large difference in the projection height, -73, compared with the other orthopyroxene bearing glasses, -61,-56 and -53.

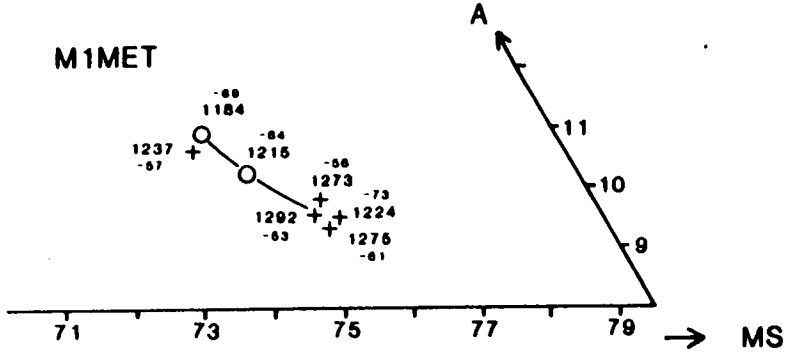
M1MET
A
11
10
9
71
73
75
77
79
MS
-69
1184
1237
-67
-64
1215
-66
1273
-73
1224
1292
-63
1275
-61

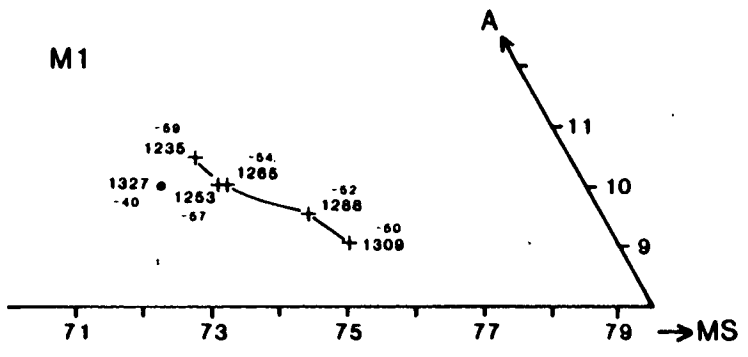
M1
A
11
10
9
71
73
75
77
79
MS
-69
1235
1327
-40
-64
1265
1253
-67
-62
1288
-60
1309

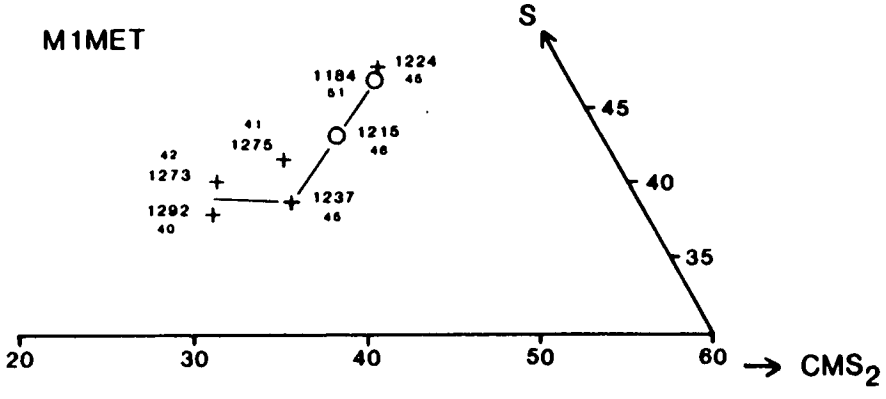
M1MET
S
45
40
35
20
30
40
50
60
CMS2
1184
51
1224
46
41
1275
1215
46
42
1273
1237
46
1292
40

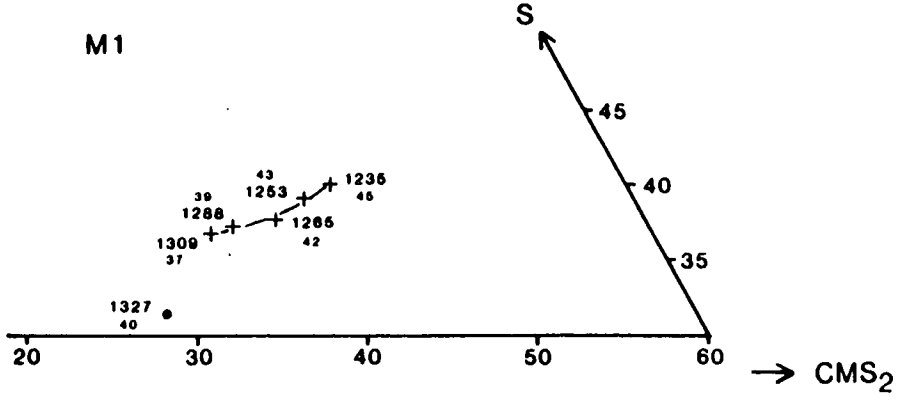
M1
S
45
40
35
20
30
40
50
60
CMS2
43
1253
1235
46
39
1288
1265
42
1309
37
1327
40

Figure 4.33

Projections for samples C2 and C2MET. All experiments on sample C2 were of 24 hours, although the crystals in these charges did not equilibrate a good orthopyroxene crystallisation trend is defined. Experiments on sample C2MET were of 48 hours, except the experiment at 1172°C which was of 93 hours. The 1275°C experiment plots slightly off the trend because of iron losses to a new PtFe hook (see also fig. 4.19). There is no obvious reason for the 1237°C experiment deviating from the trend.

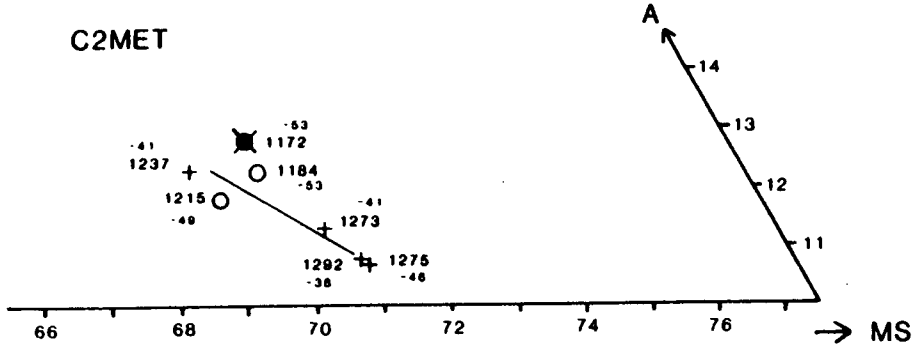
C2MET
A
14
13
12
11
-53
1172
-41
1237
1184
-53
1215
-48
-41
1273
1292
-38
1275
-46
66
68
70
72
74
76
MS

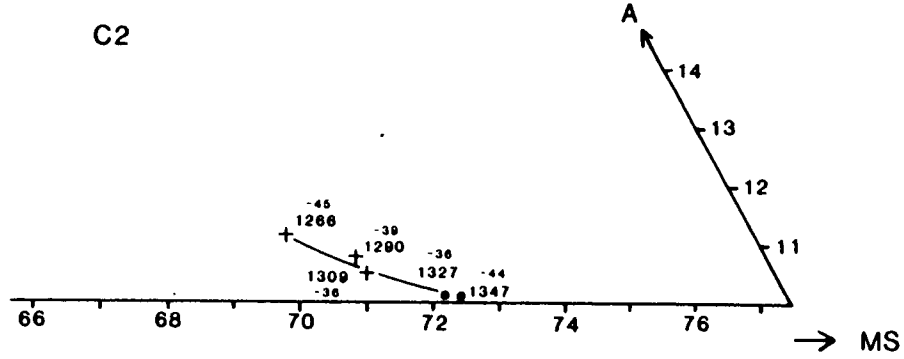
C2
A
14
13
12
11
-45
1266
-39
1290
-36
1327
-44
1347
1309
-36
66
68
70
72
74
76
MS

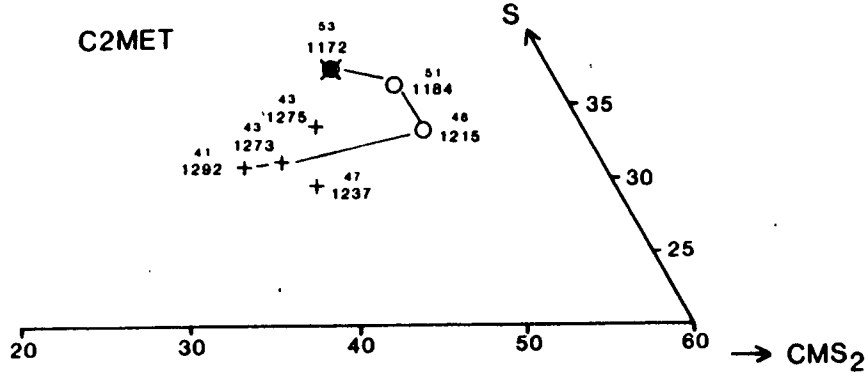
C2MET
S
35
30
25
53
1172
51
1184
43
1275
43
1273
41
1292
46
1215
47
1237
20
30
40
50
60
CMS2

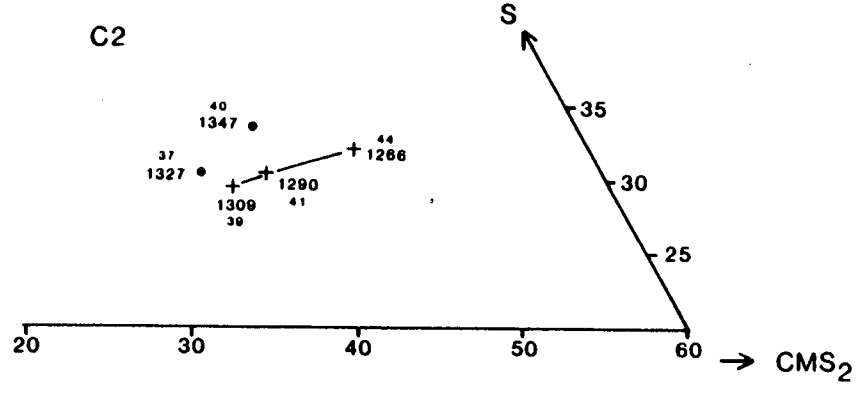
C2
S
35
30
25
40
1347
44
1266
37
1327
1290
41
1309
39
20
30
40
50
60
CMS2

Figure 4.34

Projections for samples C5 and C5MET. Experiments on sample C5 were of 24 hours with the exception of the experiment at 1181°C which was of 48 hours. Although the orthopyroxenes in these charges did not equilibrate a good crystallisation path is defined by the liquids. Experiments on sample C5MET were of 48 hours with the exception of the 477 hour experiment at 1224°C, which due to iron and sodium losses (fig. 4.21) deviates from the crystallisation path defined by the other liquids. Iron losses in the experiment at 1275°C, due to use of a new PtFe wire, cause it to deviate from the trend.

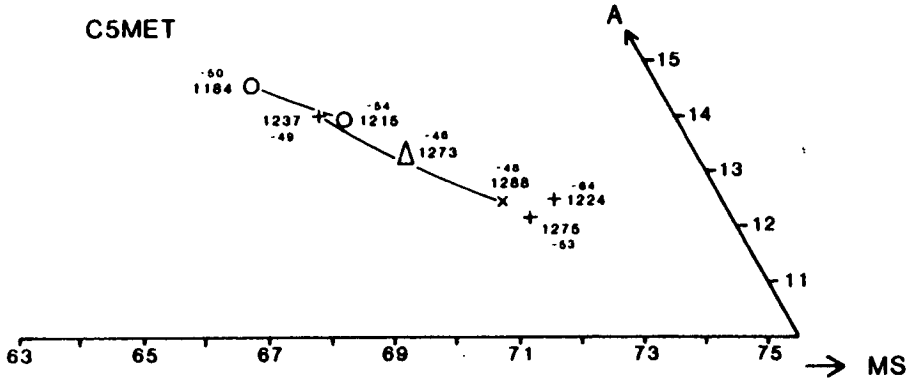
C5MET
A
15
14
13
12
11
63
65
67
69
71
73
75
MS
-50
1184
1237
-49
-54
1215
-48
1273
-48
1288
-64
1224
1275
-63

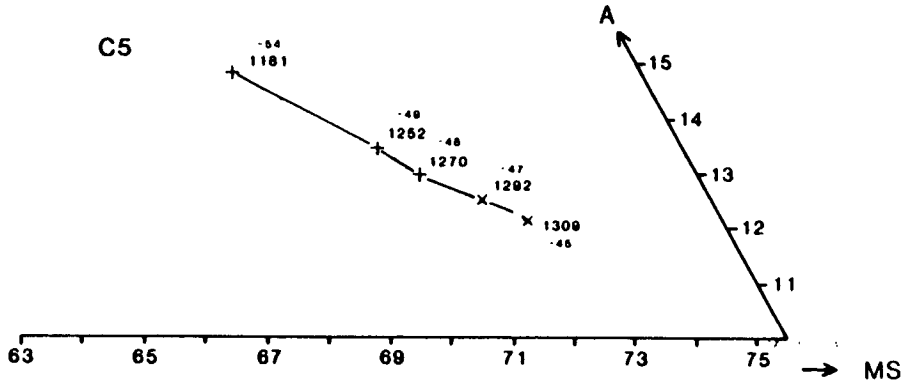
C5
A
15
14
13
12
11
63
65
67
69
71
73
75
MS
-54
1181
-49
1252
-48
1270
-47
1292
1309
-46

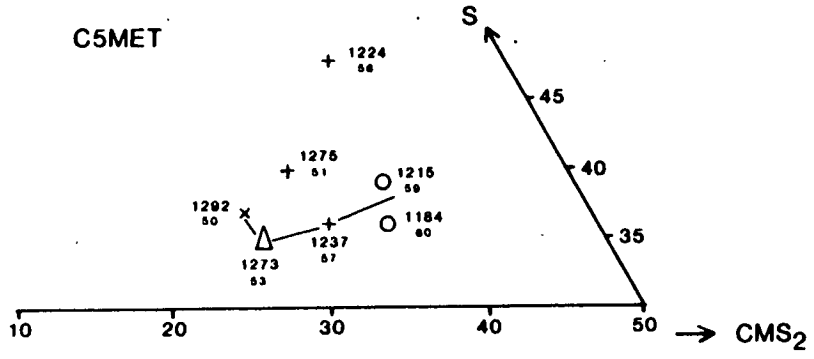
C5MET
S
45
40
35
10
20
30
40
50
CMS2
1224
56
1275
51
1215
59
1292
50
1184
60
1237
57
1273
53

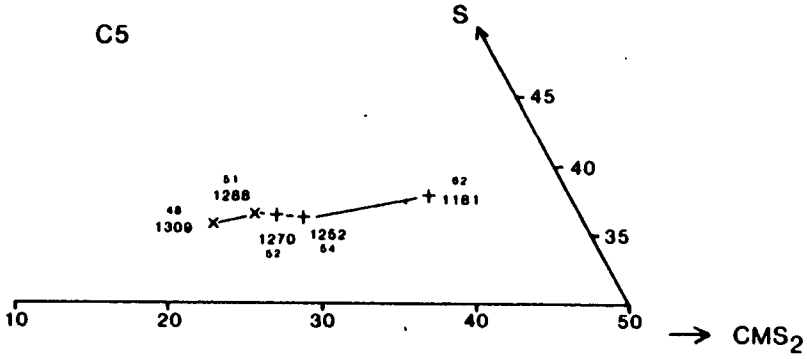
C5
S
45
40
35
10
20
30
40
50
CMS2
51
1288
62
1181
48
1309
1270
52
1252
54

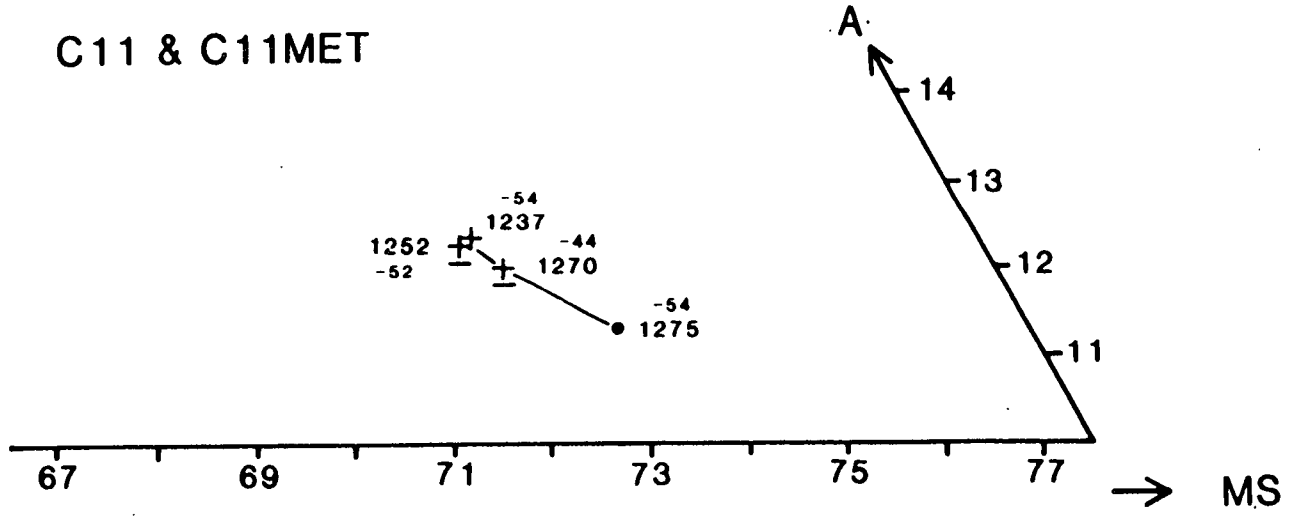

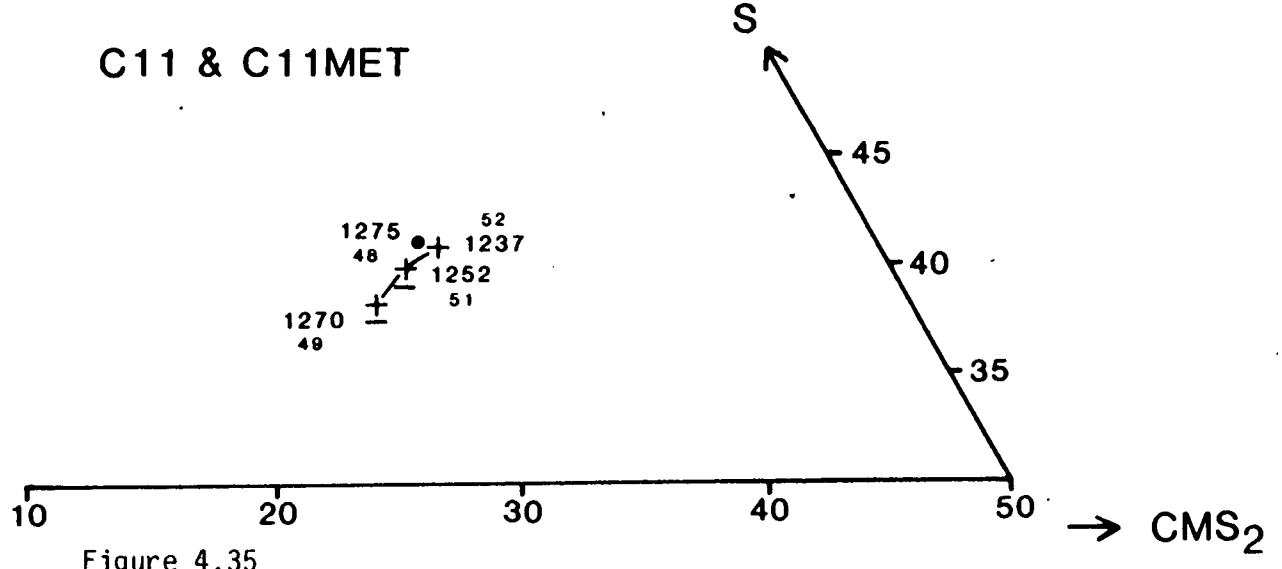

Figure 4.35

Projections for C11 and C11MET, underlined data points are from sample C11.

Figure 4.36

Projections of all the crystallisation paths from figures 4.25 to 4.35 with the exception of the unmetamorphosed boninites (C2, C5, C11, M1). For the olivine projection (top diagram) it is not possible to produce a summary comparable with fig. 4.3b; such a summary is given for the plagioclase projection (bottom diagram) in fig. 4.37.

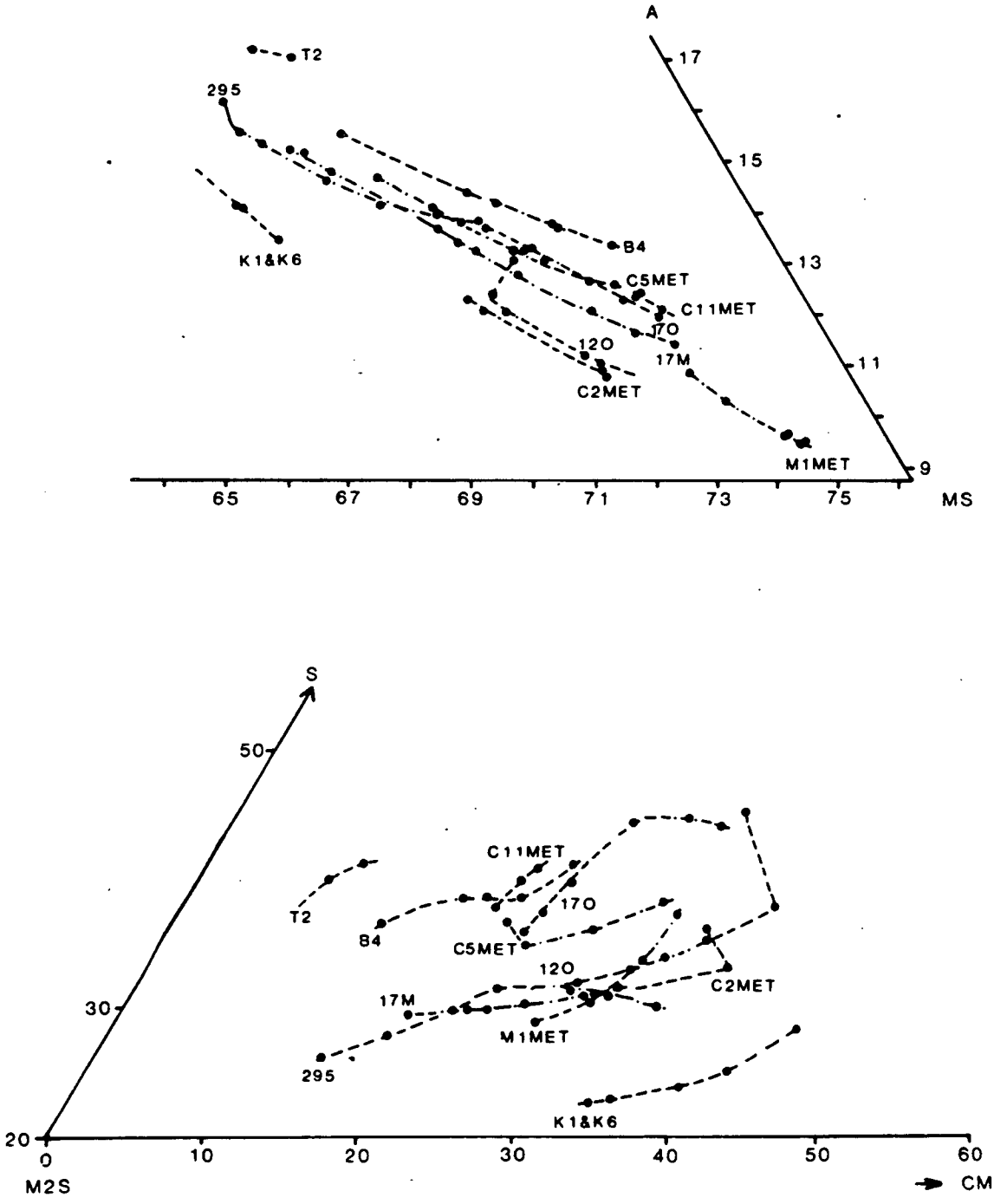

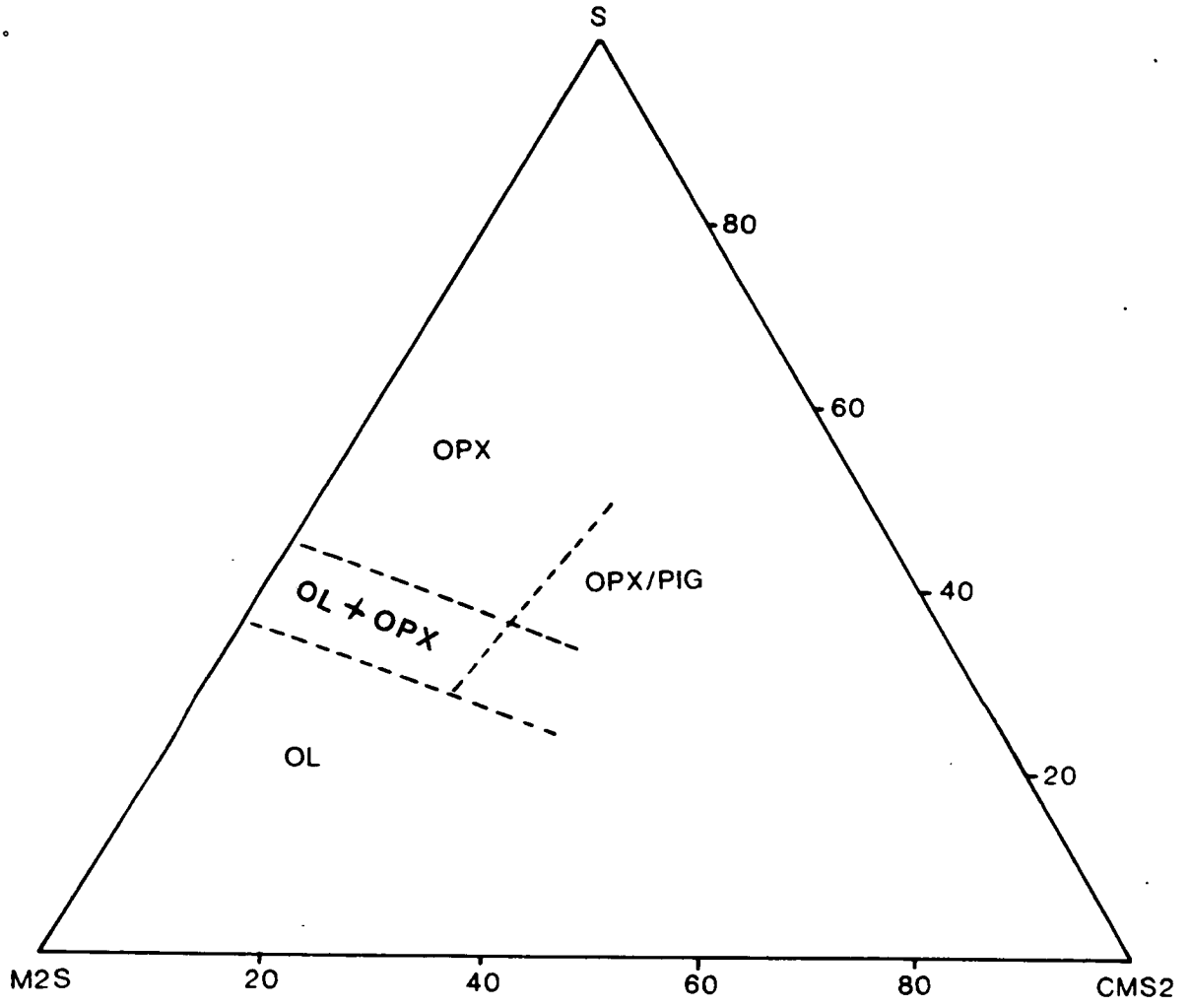

Figure 4.37

Approximate position of primary crystallisation volume boundaries indicated by experimental data from this study (fig. 4.36). This diagram is identical to that produced for data from the literature search (fig. 4.4b)

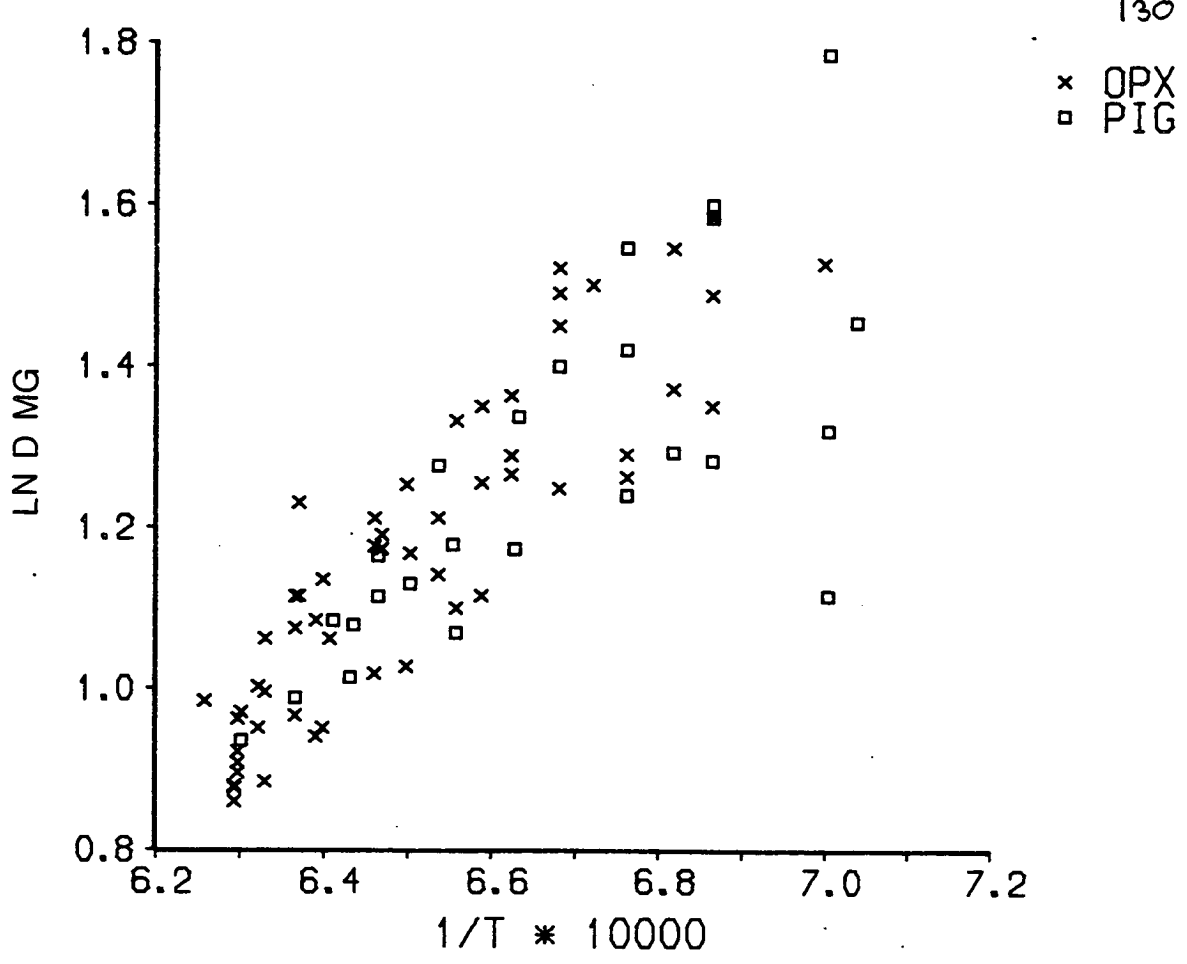

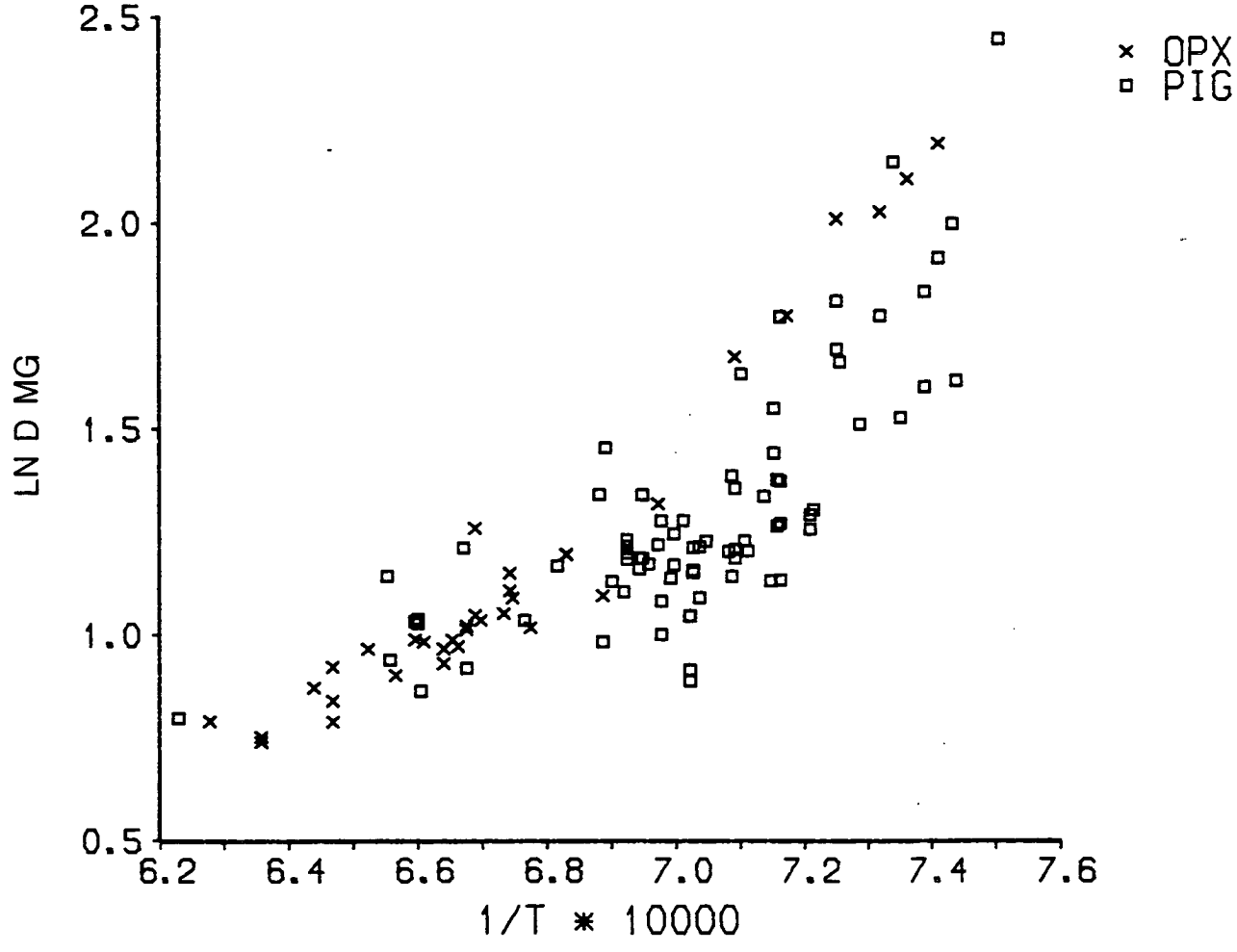

Figure 4.38

ln D_{Mg} v 1/T°K for low-calcium pyroxene - liquid pairs from this study (top diagram) and the literature search (bottom diagram)

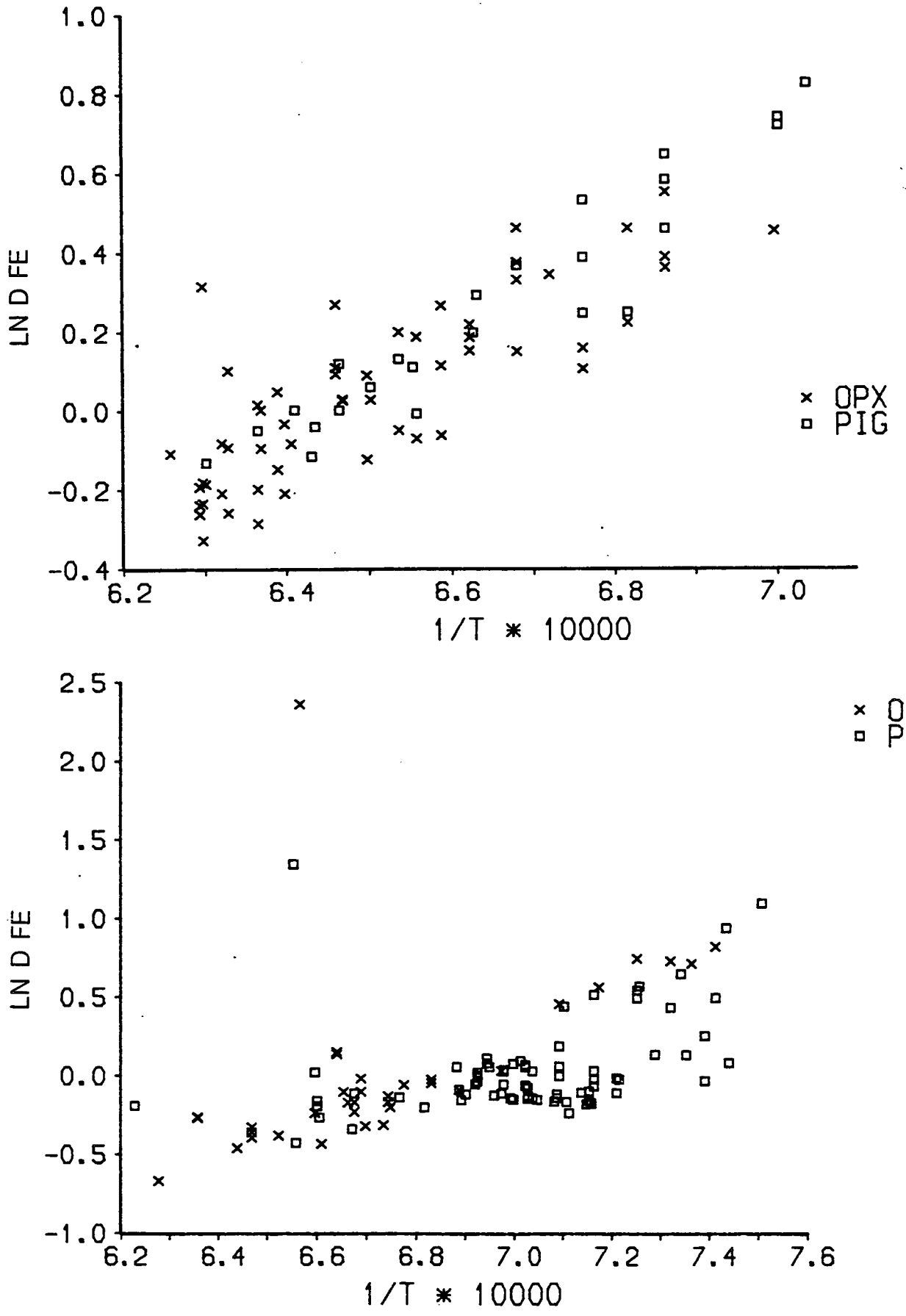

Figure 4.39

ln D_{Fe} v 1/T°K for low-calcium pyroxene - liquid pairs from this study (top diagram) and the literature search (bottom diagram)

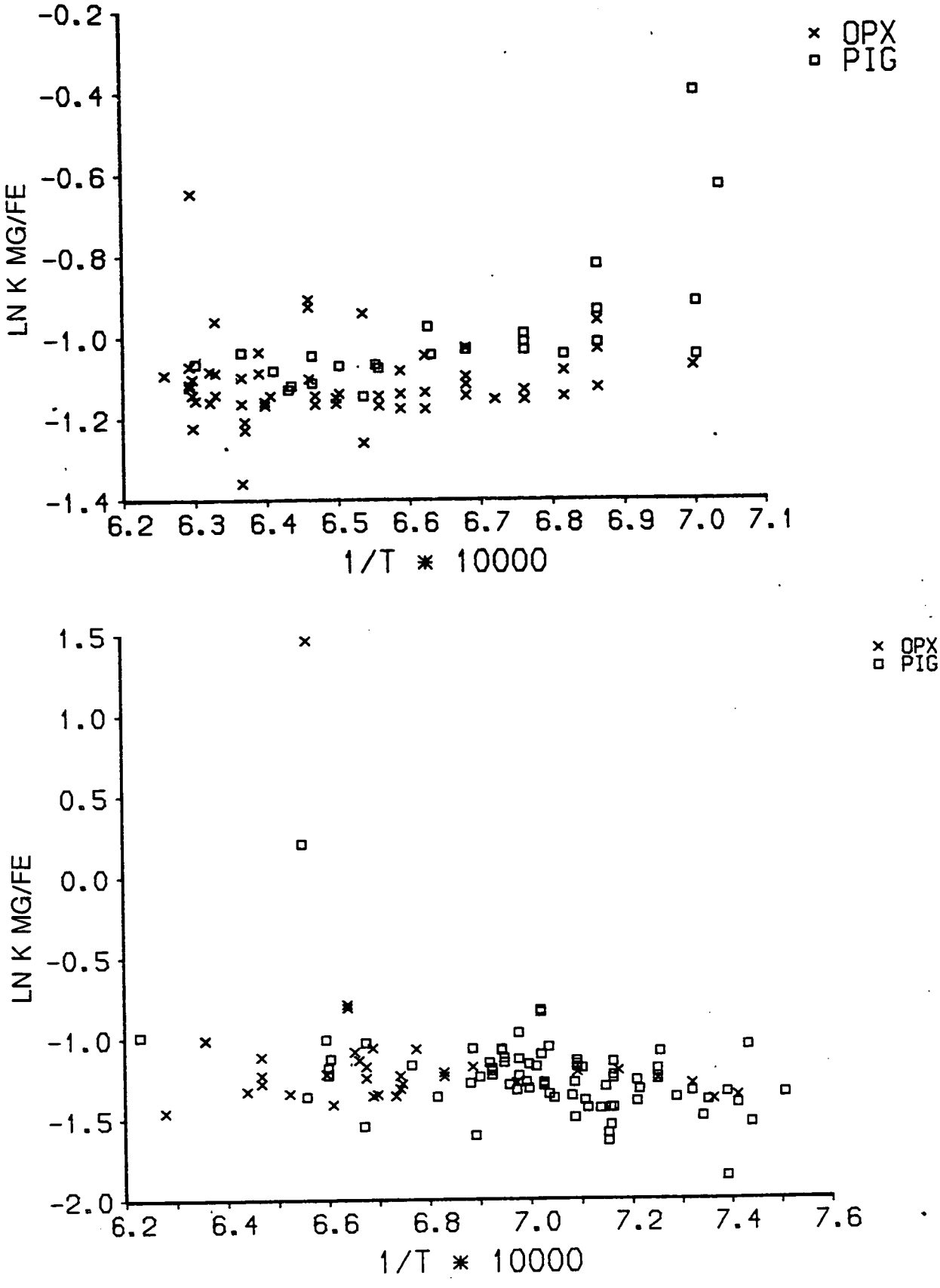

Figure 4.40

ln $K_D^{Fe^{2+}/Mg}$ v 1/T°K for low-calcium pyroxene - liquid pairs from this study (top diagram) and the literature search (bottom diagram)

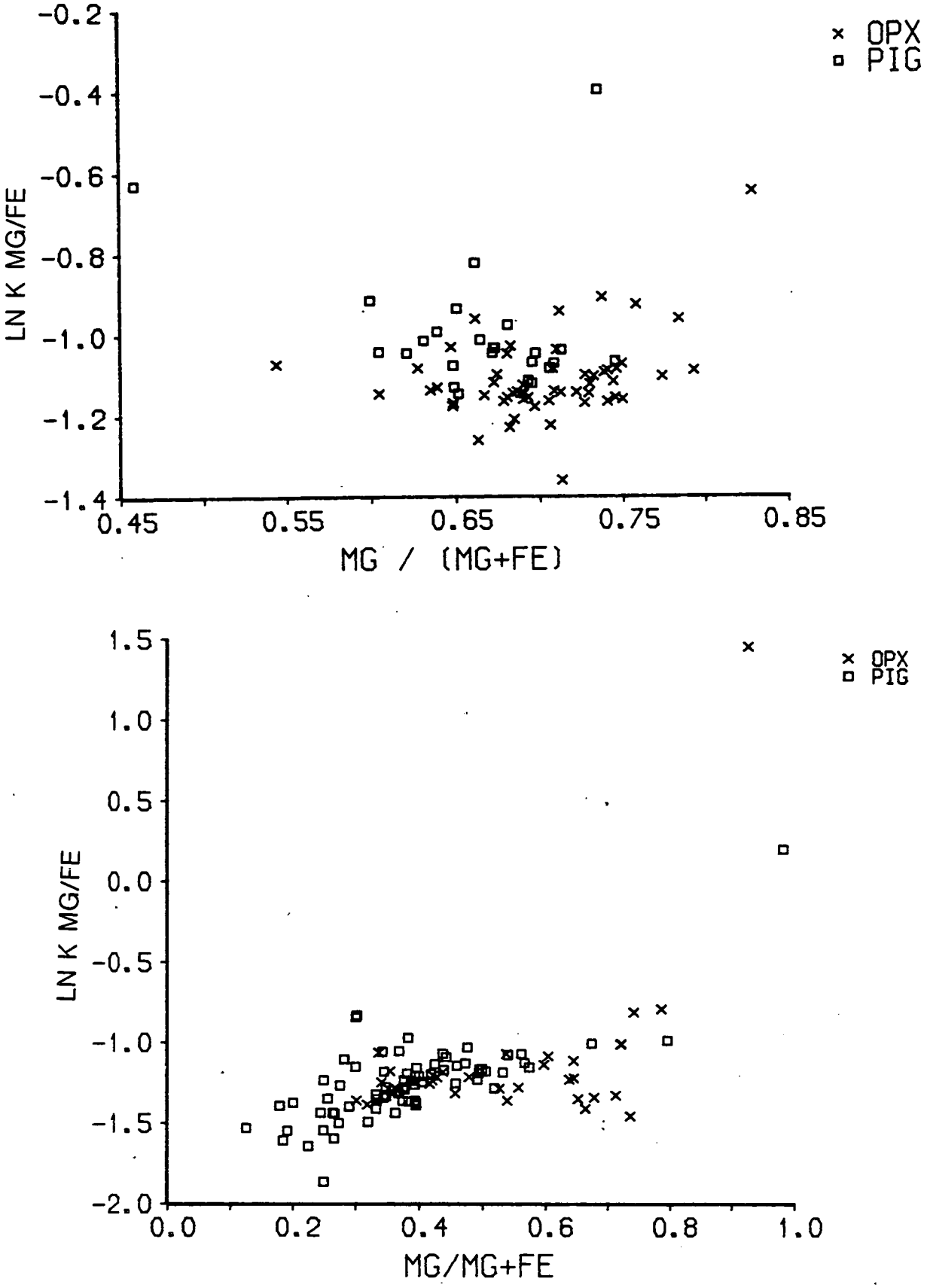

Figure 4.41

$\ln K_D^{Fe^{2+}/Mg}$ v Mg/(Mg + Fe) for low-calcium pyroxene - liquid pairs from this study (top diagram) and the literature search (bottom diagram)

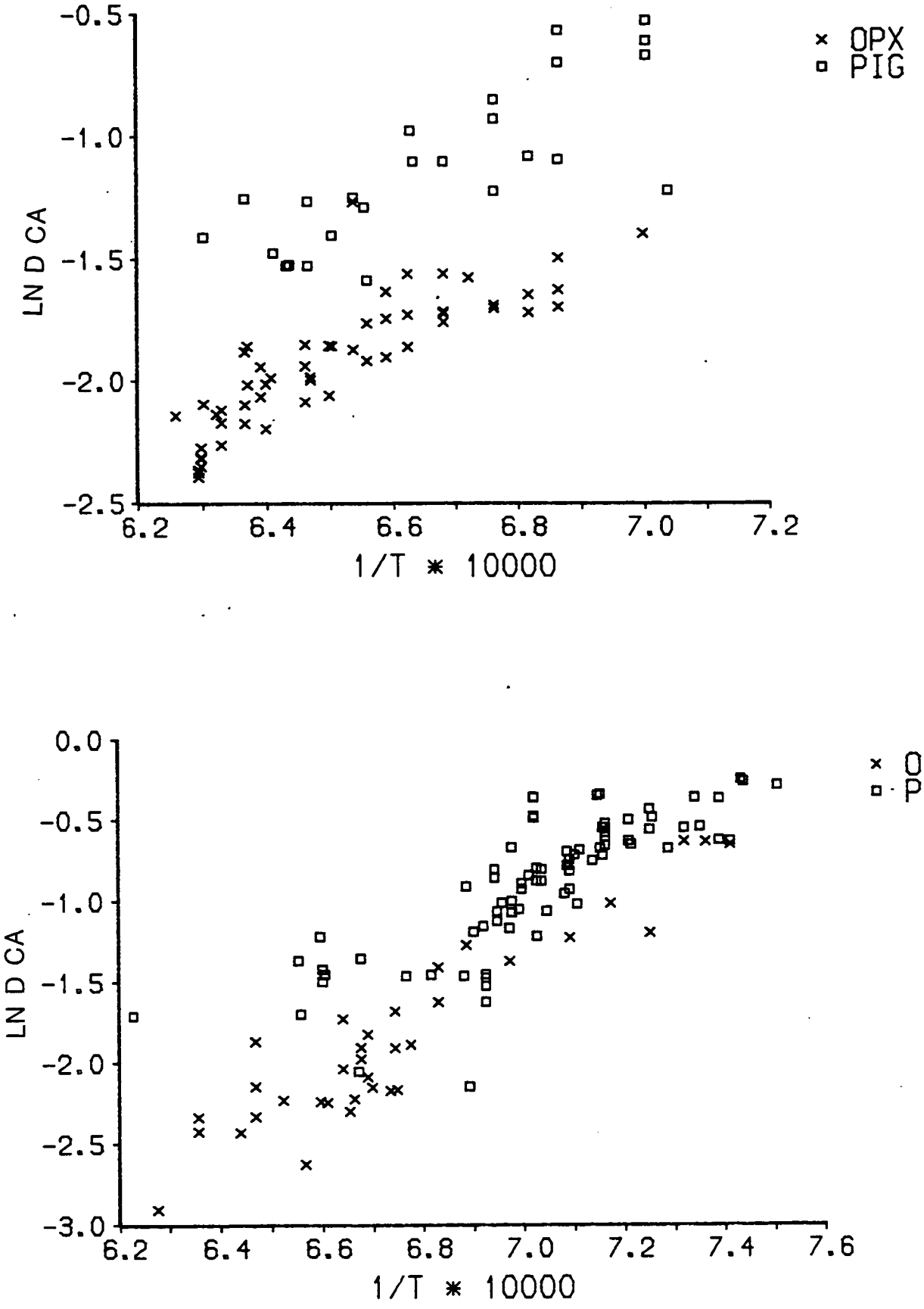

Figure 4:42

ln D_{Ca} v 1/T°K for low-calcium pyroxene - liquid pairs from this study (top diagram) and the literature search (bottom diagram). Orthopyroxenes and pigeonites from this study are clearly distinguishable on the basis of Ln D_{Ca} at a given temperature. A similar but less clear relationship is seen in the analyses from the literature data set.

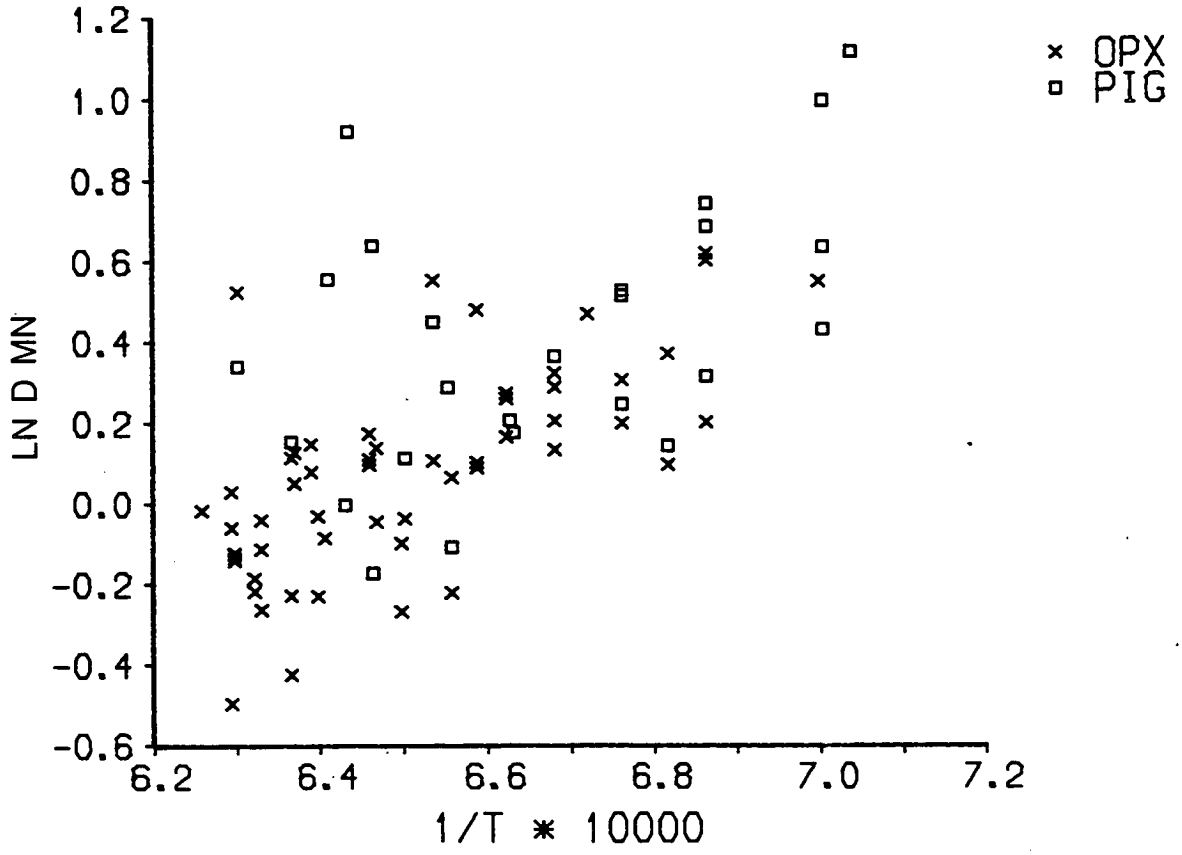

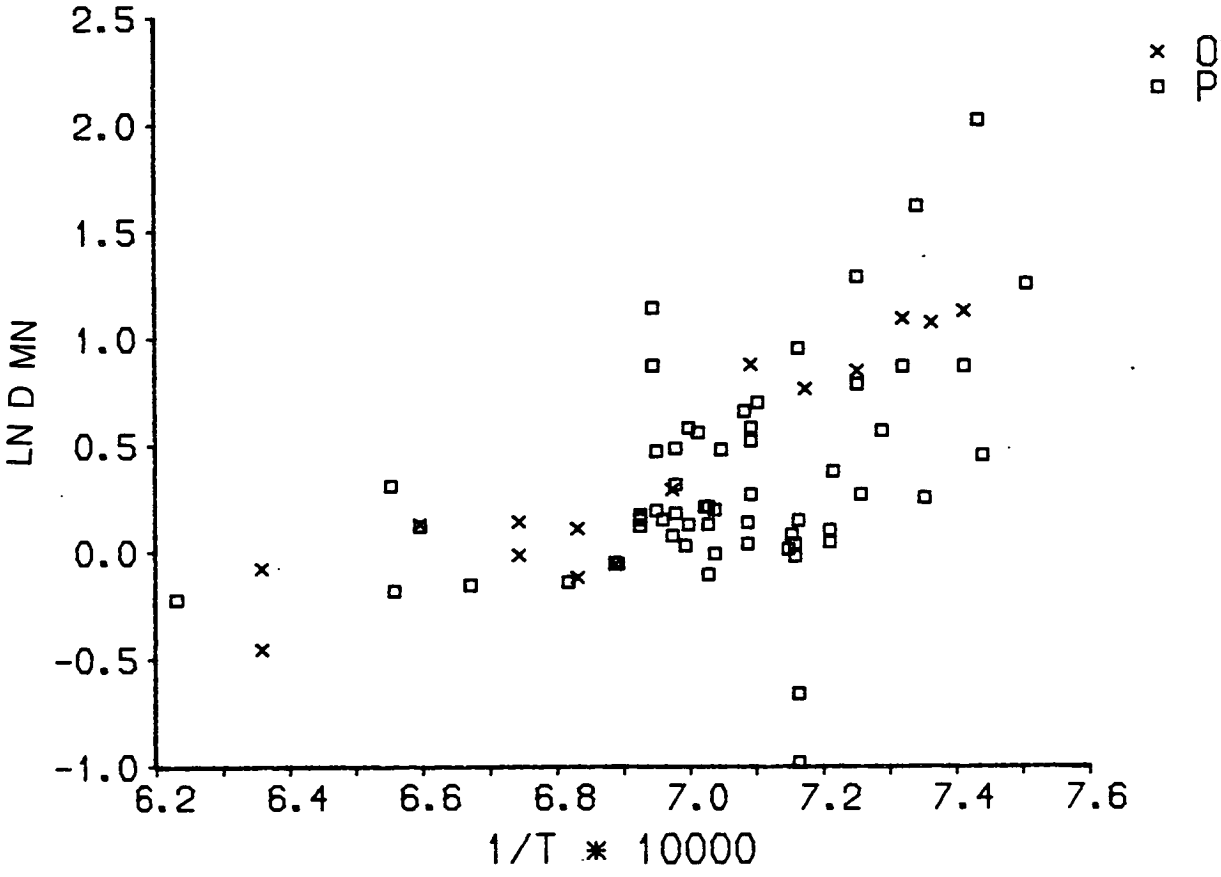

Figure 4.43

ln D_{Mn} v 1/T°K for low-calcium pyroxene - liquid pairs from this study (top diagram) and the literature search (bottom diagram).

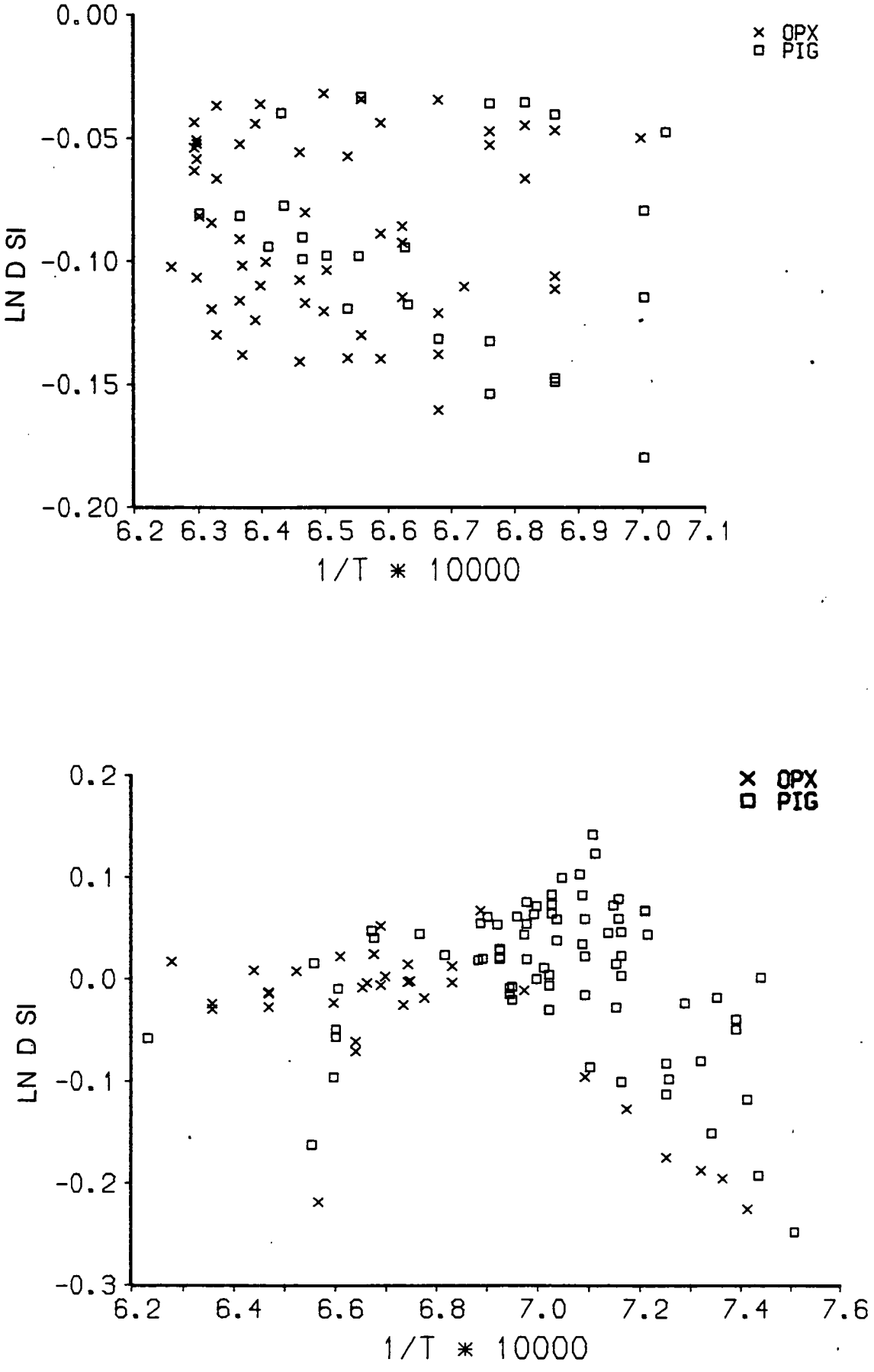

Figure 4.44

ln D_{Si} v 1/T°K for low-calcium pyroxene - liquid pairs from this study (top diagram) and the literature search (bottom diagram).

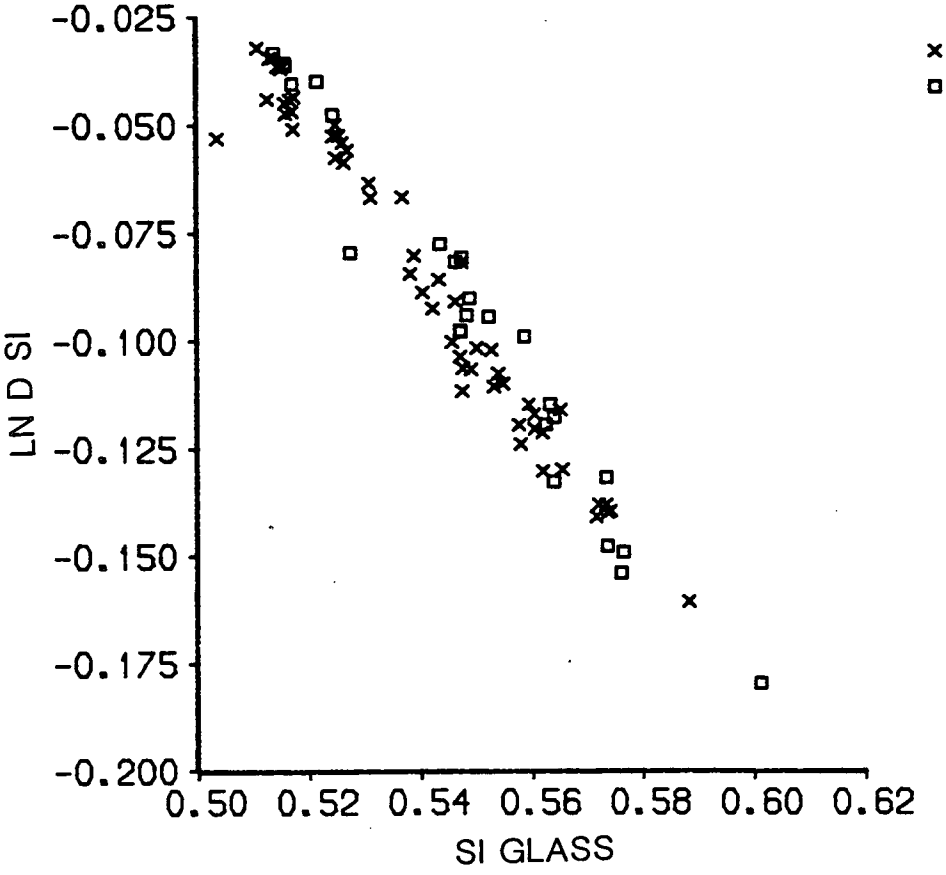

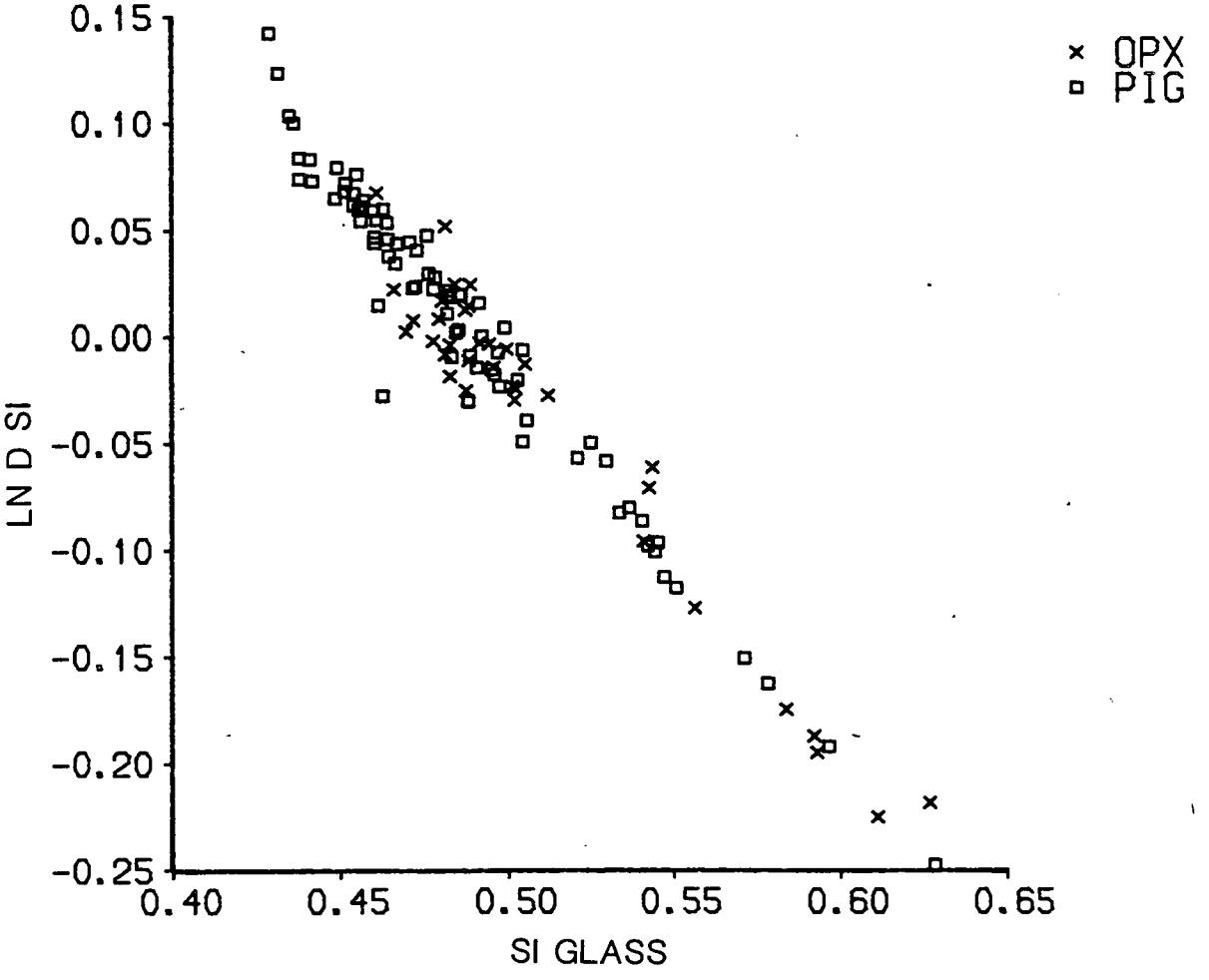

Figure 4.45

ln D_{Si} v Si glass for low-calcium pyroxene - liquid pairs from this study (top diagram) and the literature search (bottom diagram).

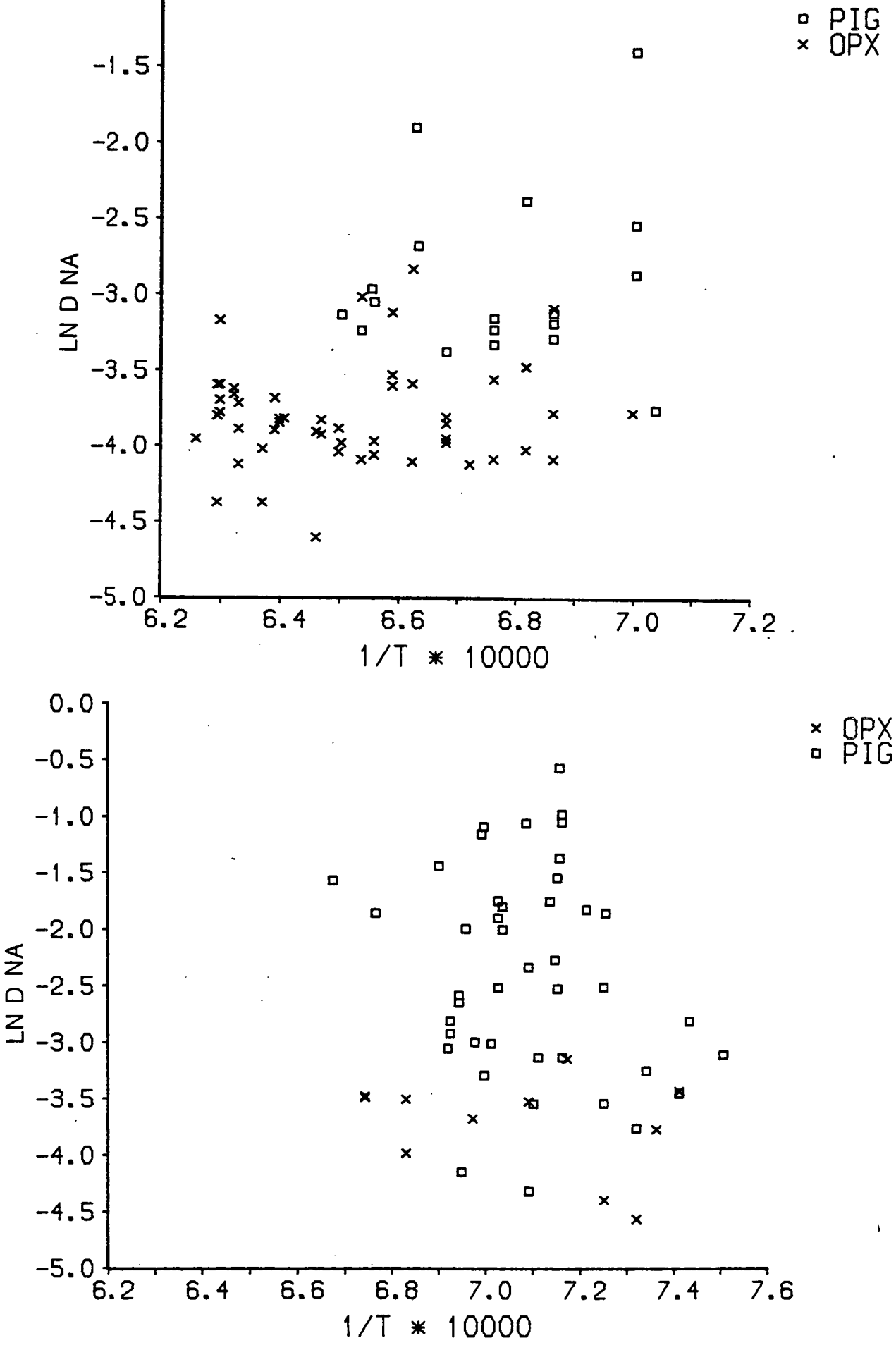

Figure 4.46

ln D_{Na} v 1/T°K for low-calcium pyroxene - liquid pairs from this study (top diagram) and the literature search (bottom diagram).

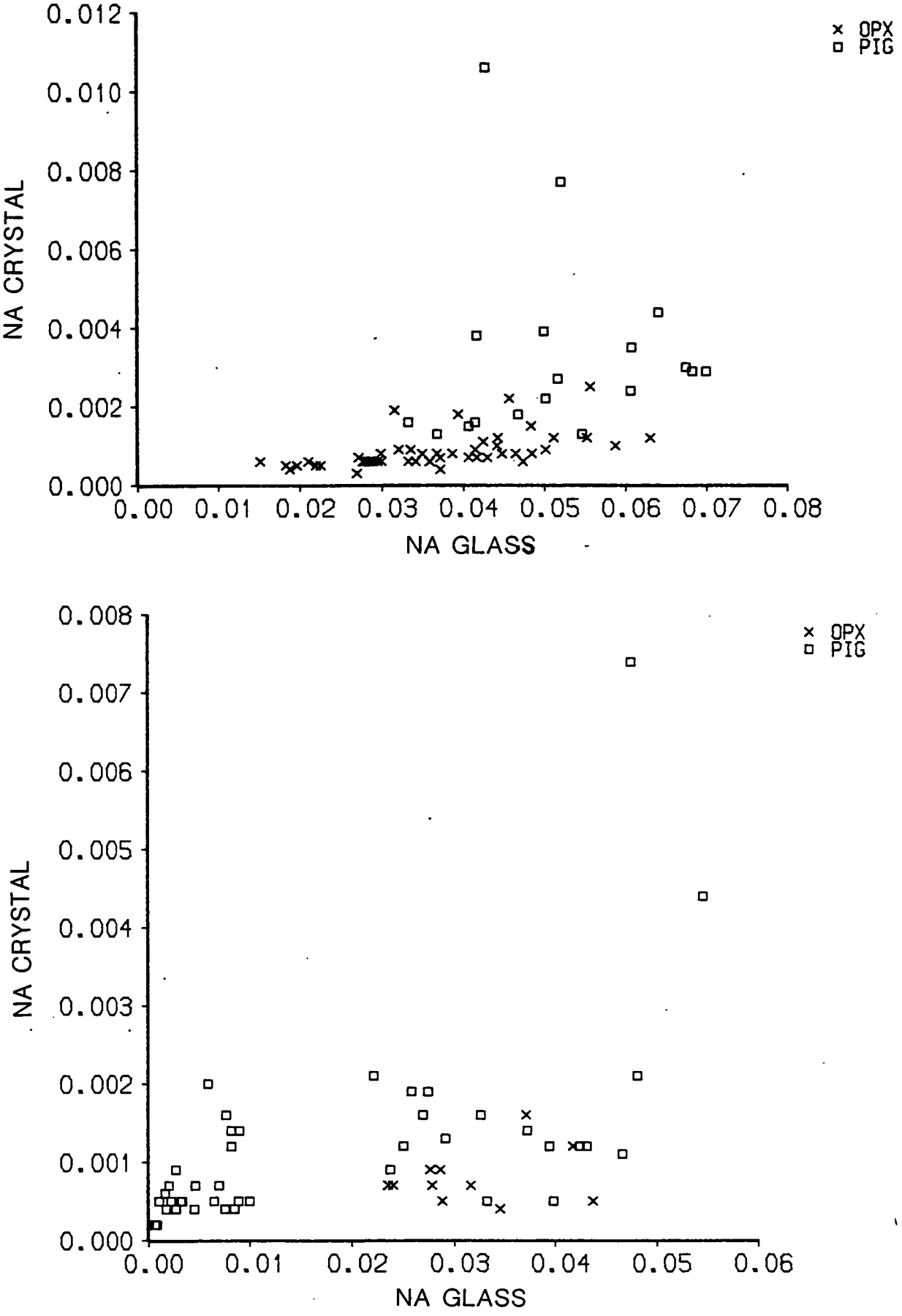

Figure 4.47

Na pyroxene v Na glass for low-calcium pyroxene - liquid pairs from this study (top diagram) and the literature search (bottom diagram).

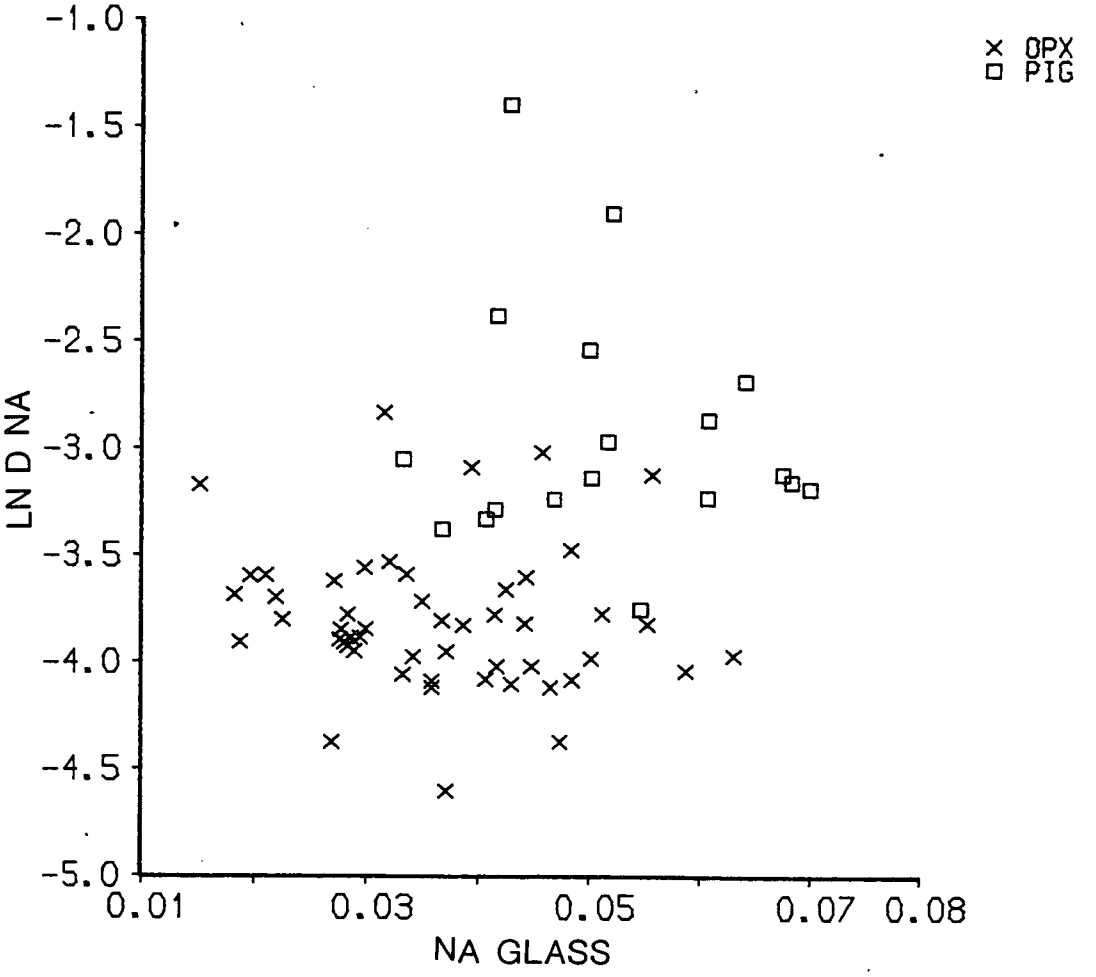

Figure 4.48a

ln D_{Na} v Na glass for low-calcium pyroxene - liquid pairs from this study.

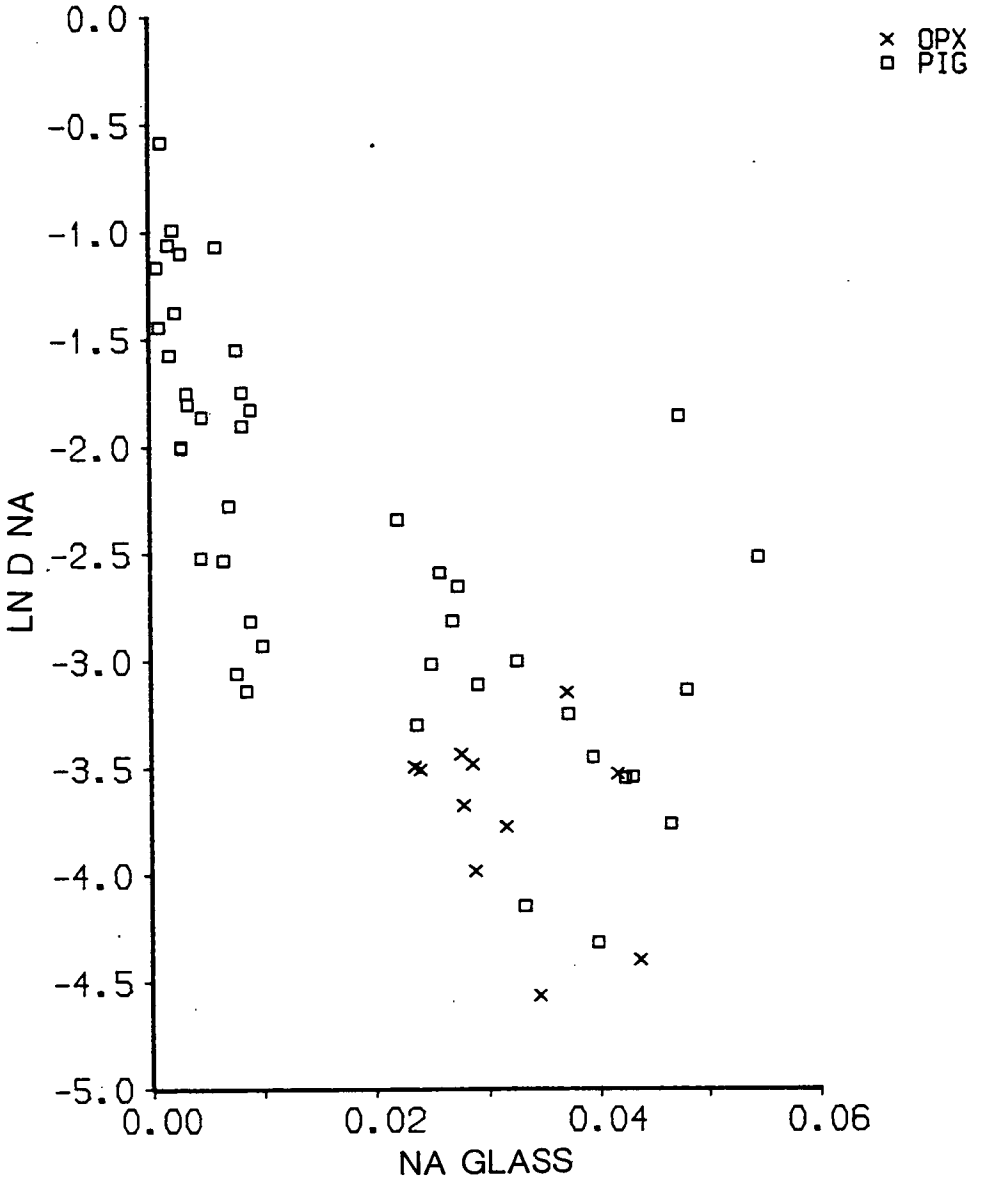

Figure 4:48b

ln D_{Na} v Na glass for low-calcium pyroxene - liquid pairs from the literature search.

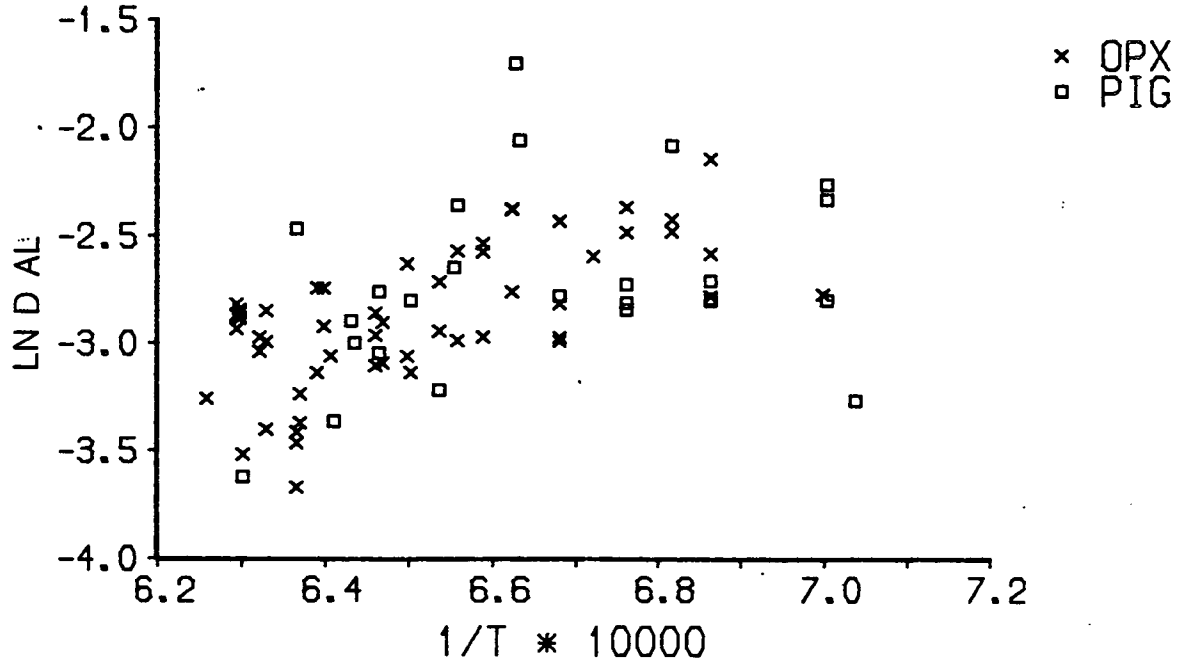

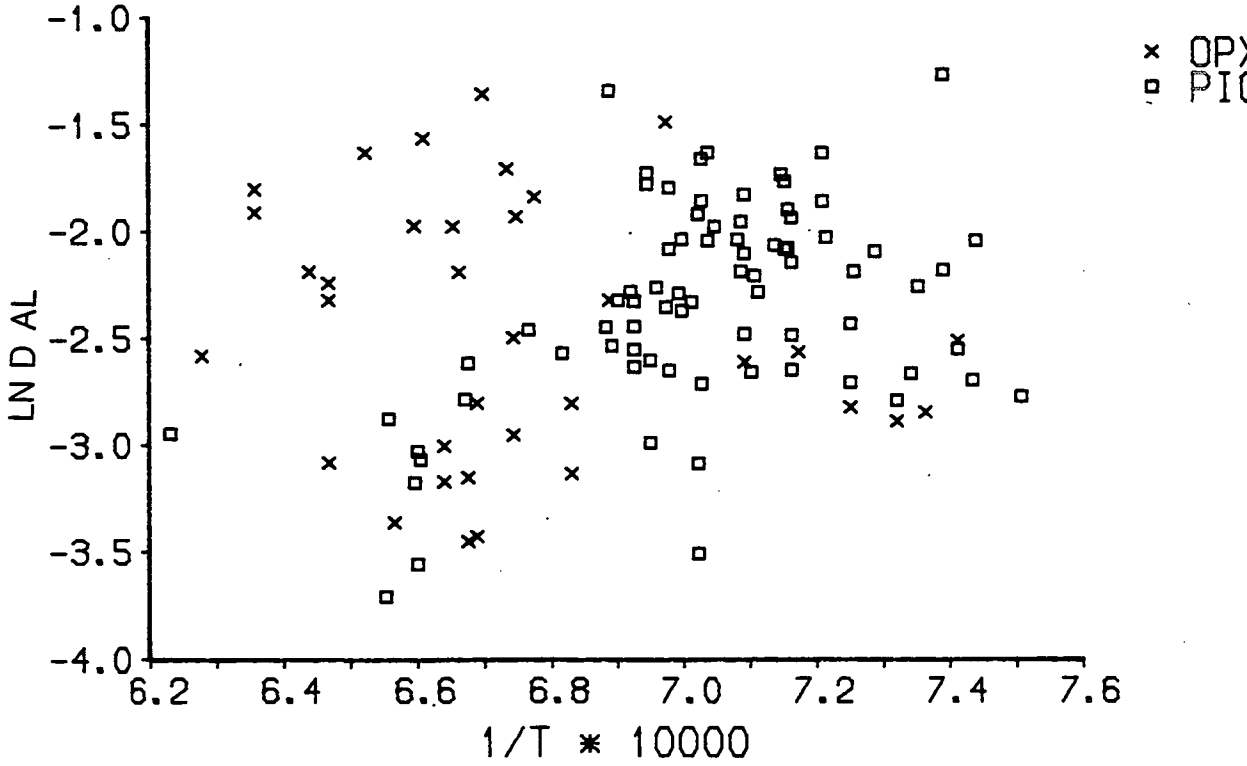

Figure 4.49

ln D_{Al} v 1/T°K for low-calcium pyroxene - liquid pairs from this study (top diagram) and from the literature search (bottom diagram).

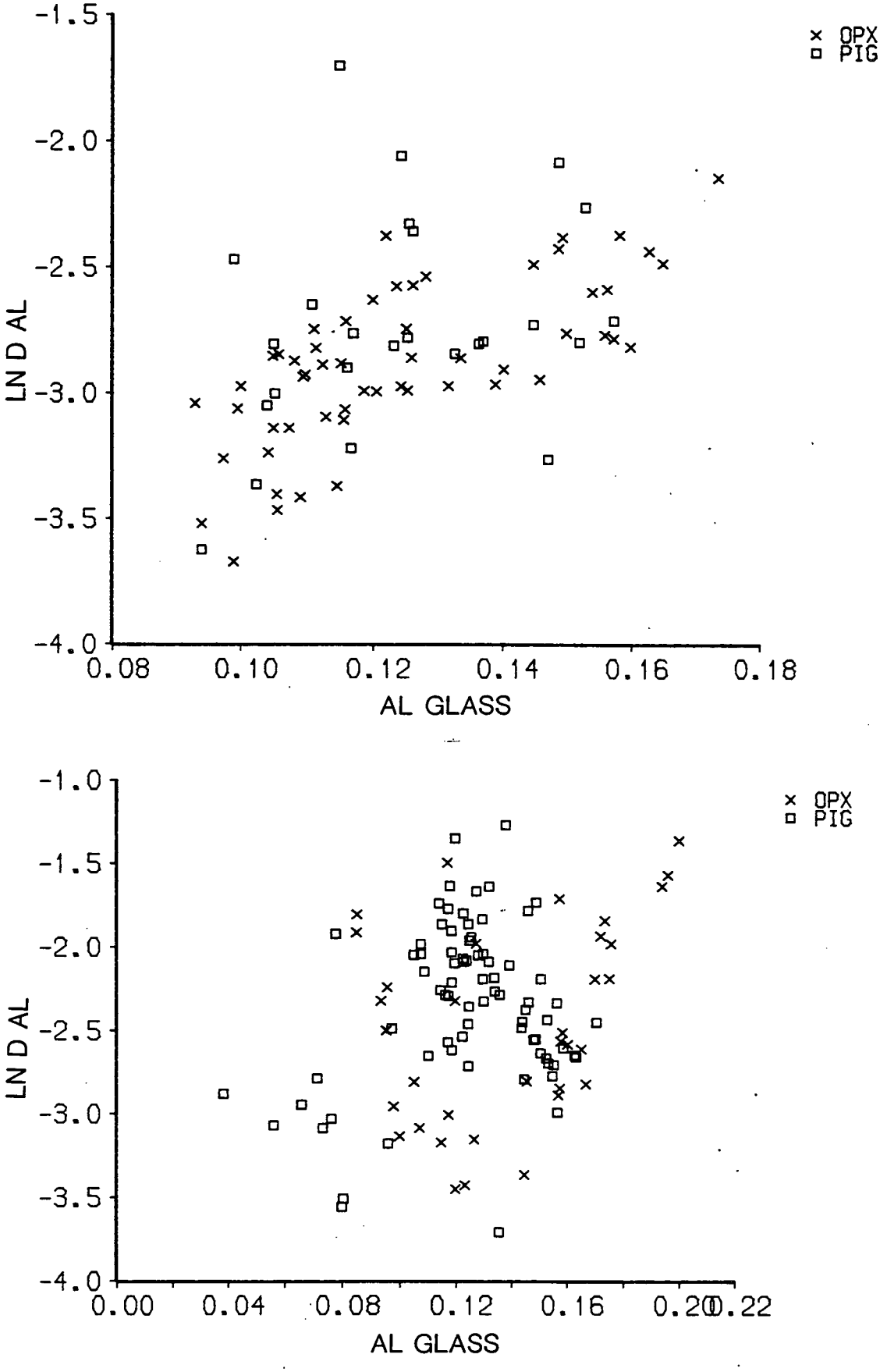

Figure 4.50

ln D_{Al} v Al glass for low-calcium pyroxene - liquid pairs from this study (top diagram) and from the literature search (bottom diagram).

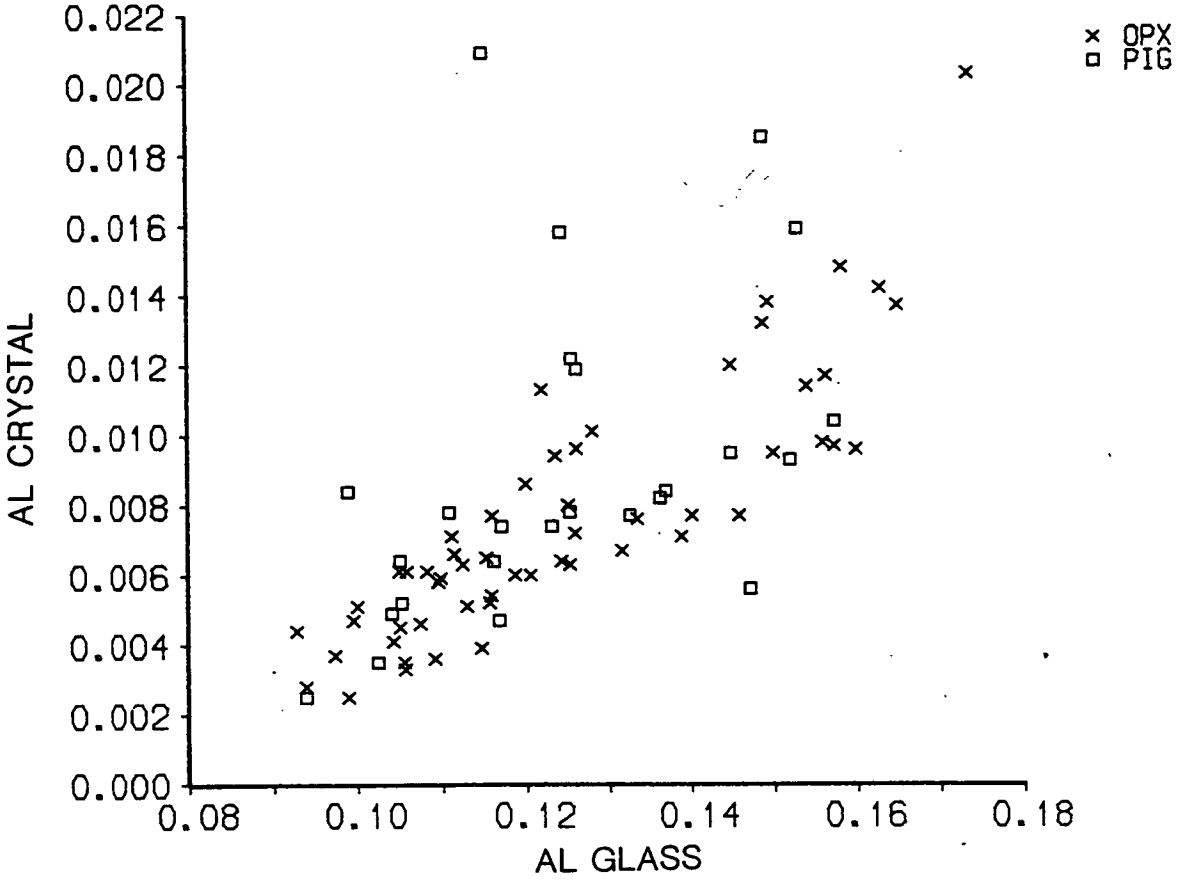

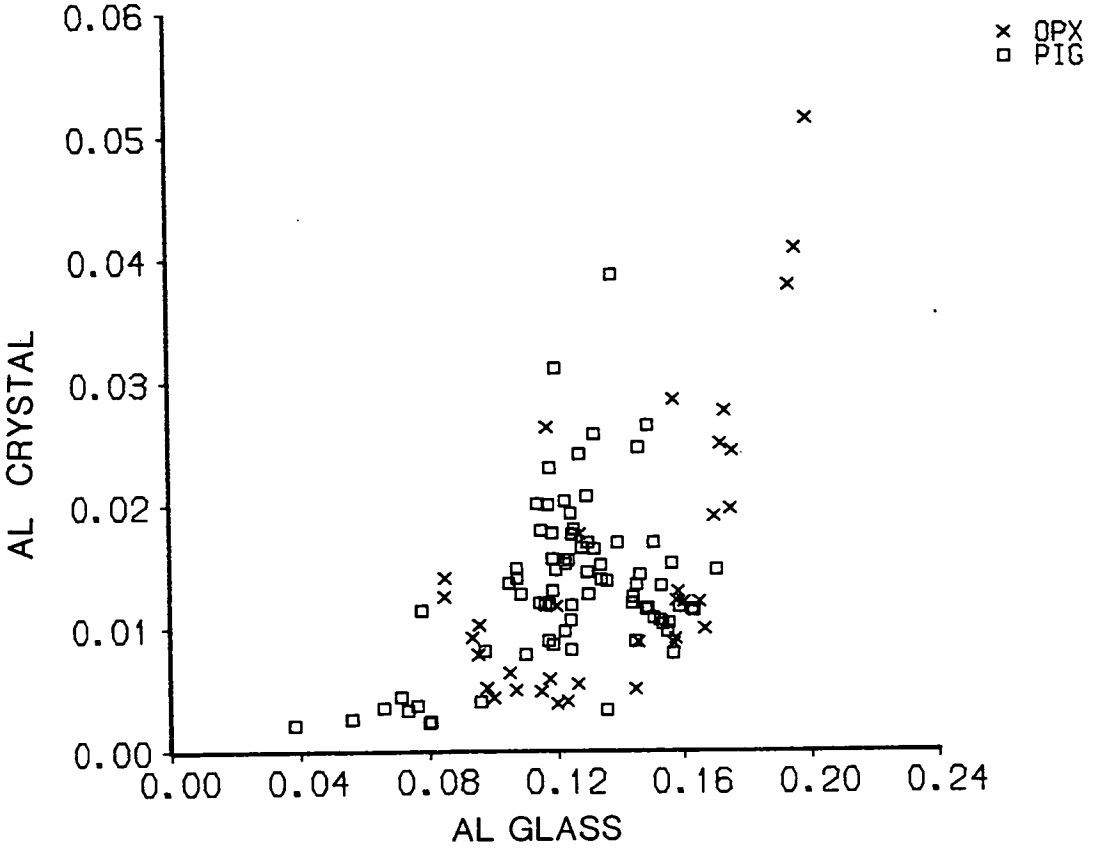

Figure 4.51

Al pyroxene v Al glass for low-calcium pyroxene - liquid pairs from this study (top diagram) and from the literature search (bottom diagram).

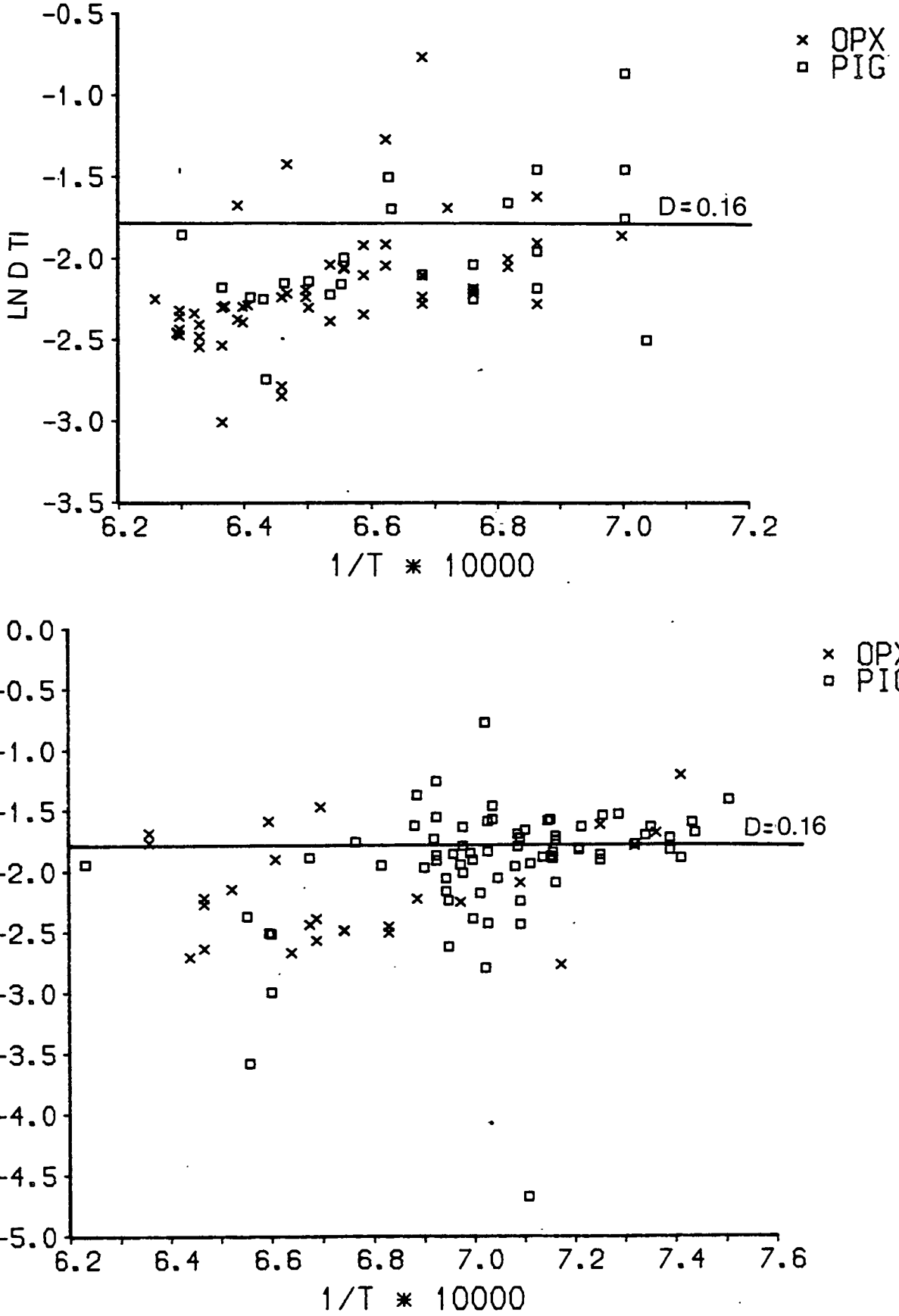

Figure 4.52

ln D_{Ti} v 1/T°K for low-calcium pyroxene - liquid pairs from this study (top diagram) and the literature search (bottom diagram).

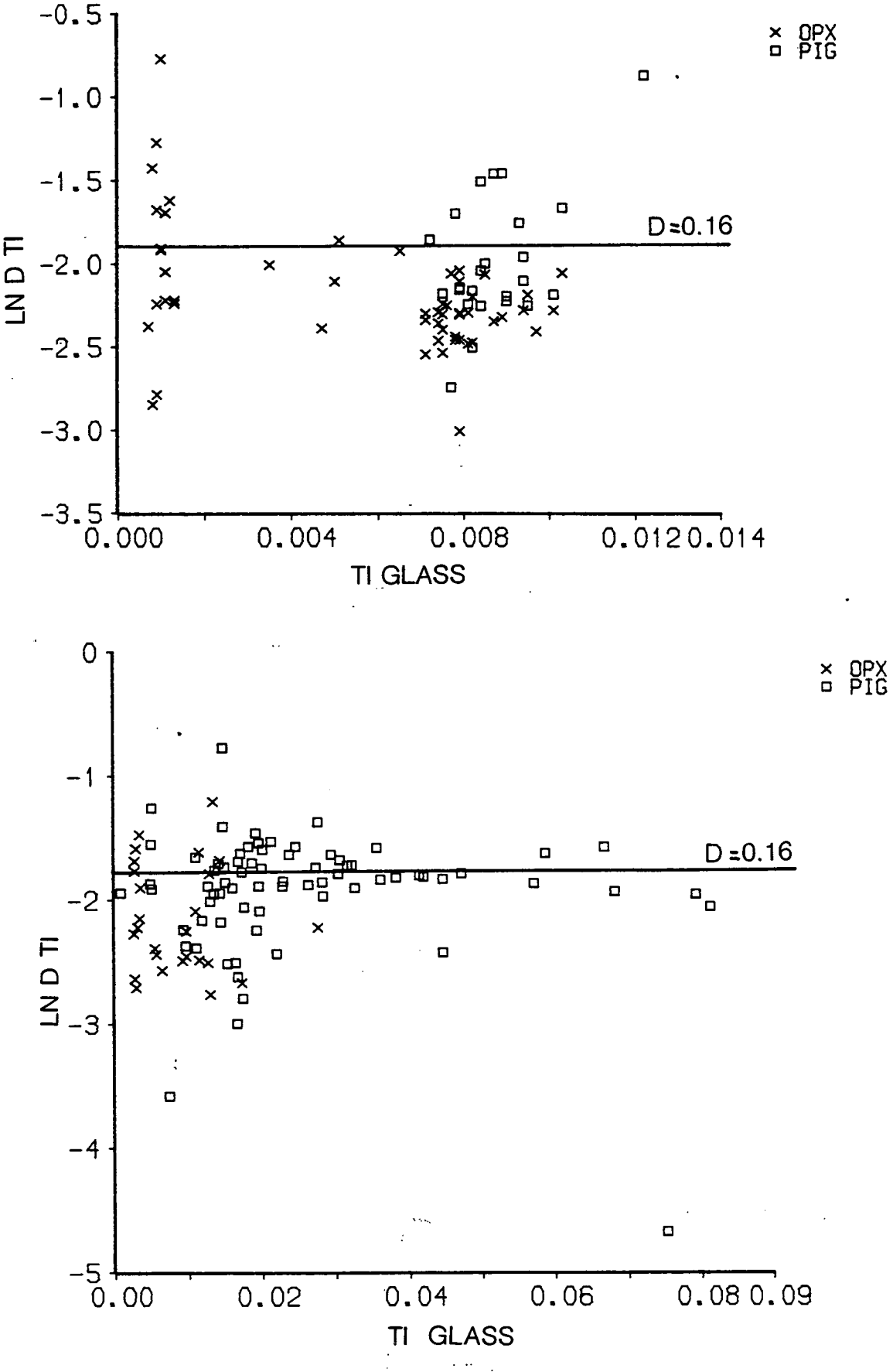

Figure 4.53

ln D_{Ti} v Ti glass for low-calcium pyroxene - liquid pairs from this study (top diagram) and from the literature search (bottom diagram).

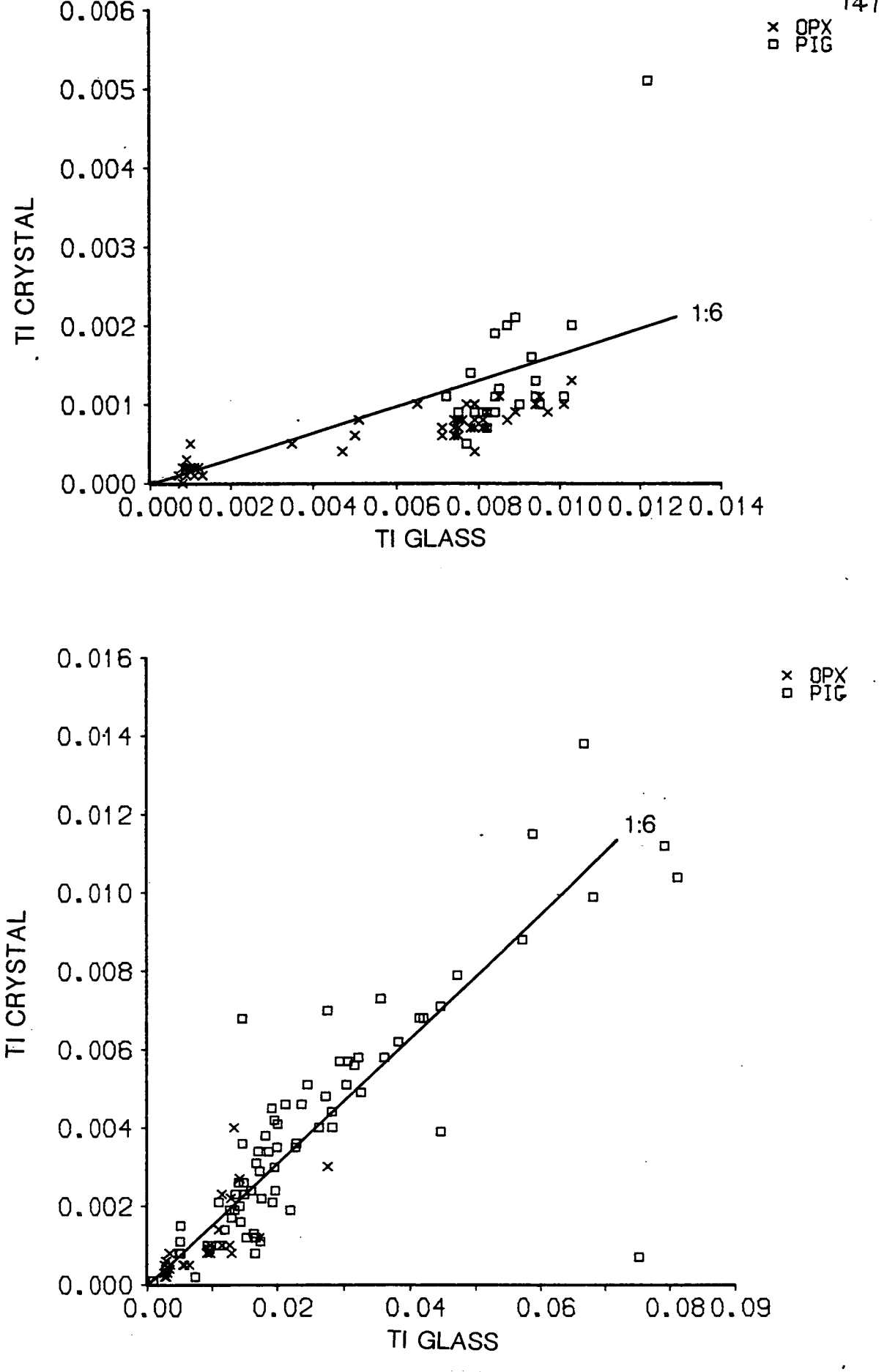

Figure 4.54

Ti pyroxene v Ti glass for low-calcium pyroxene - liquid pairs from this study (top diagram) and the literature search (bottom diagram).

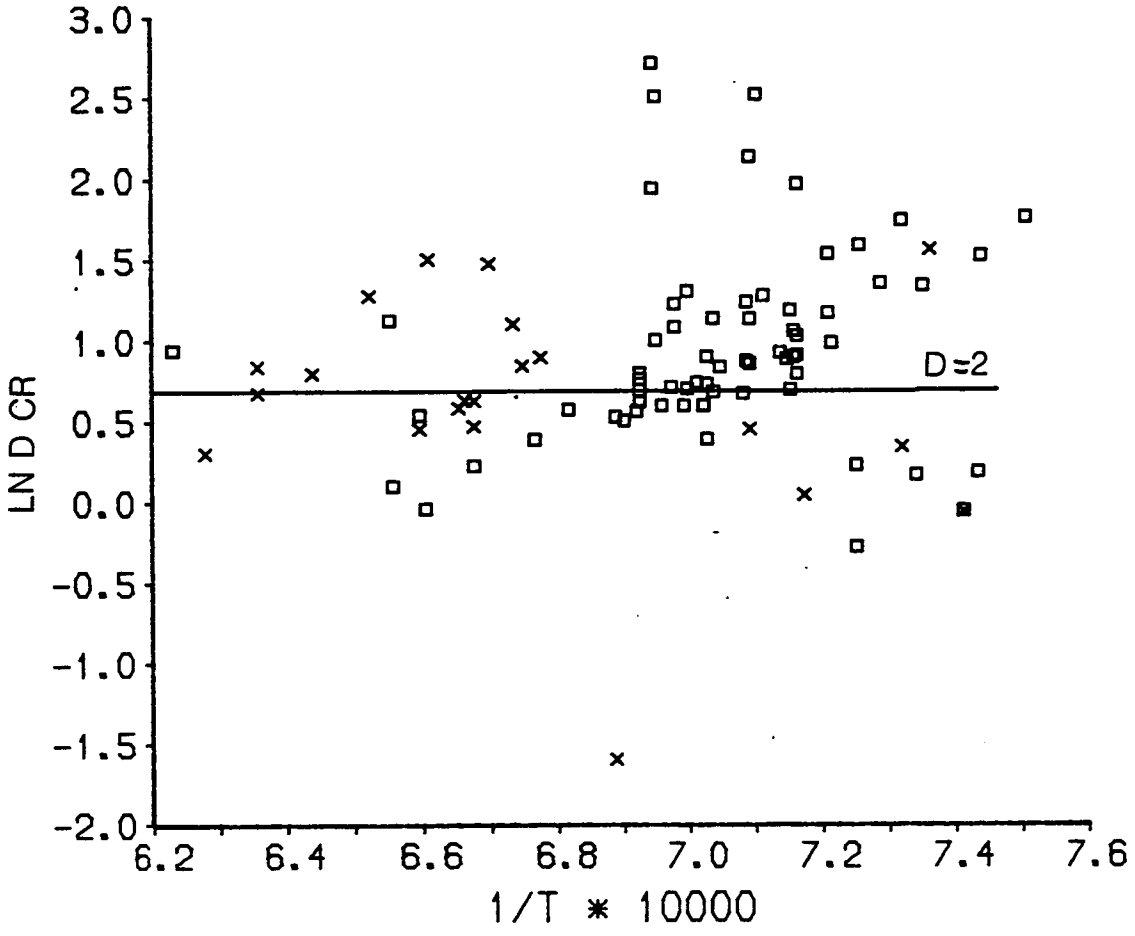

Figure 4.55

ln D_{Cr} v 1/T°K for low-calcium pyroxene - liquid pairs from the literature search.

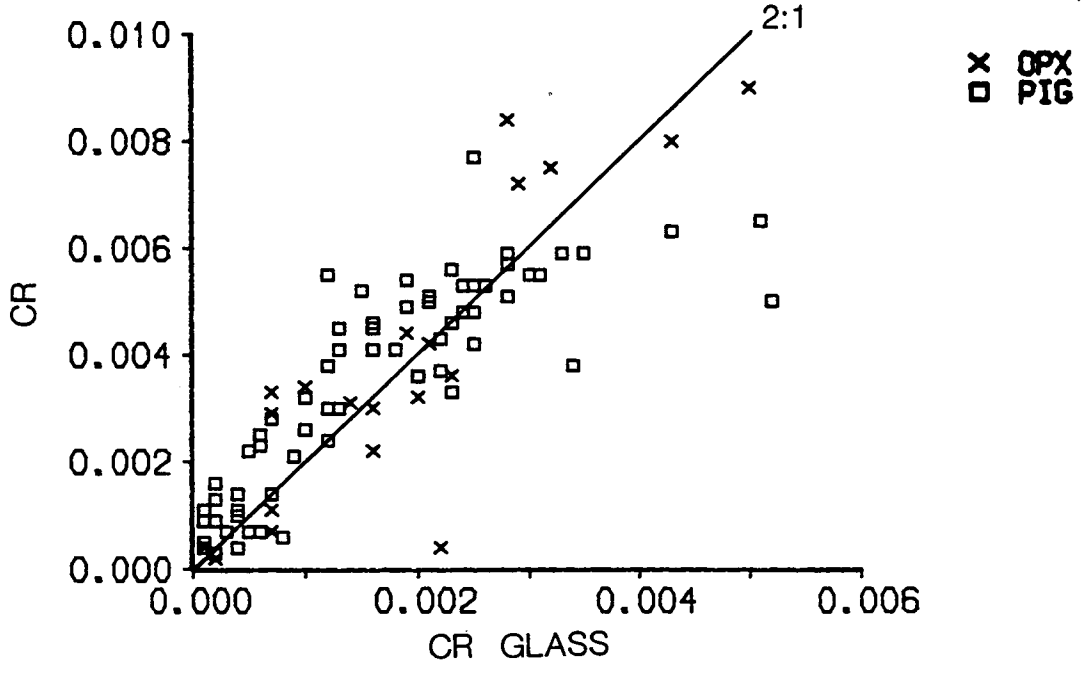

Figure 4.56

Cr pyroxene v Cr glass for low-calcium pyroxene - liquid pairs from the literature search.

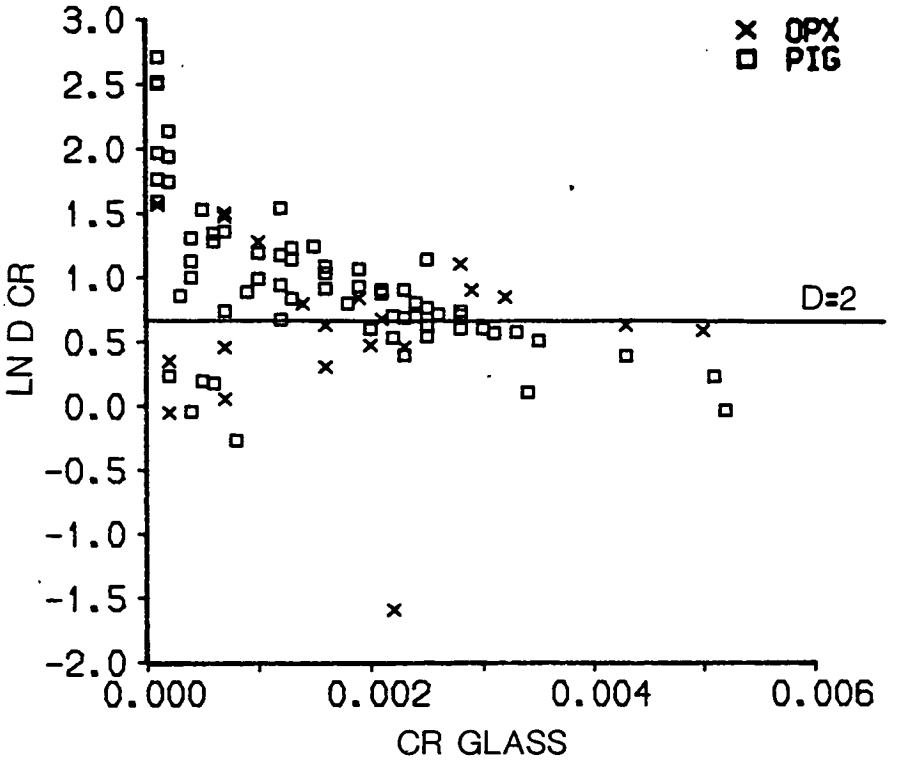

Figure 4.57

ln D_{Cr} v Cr glass for low-calcium pyroxene - liquid pairs from the literature search.

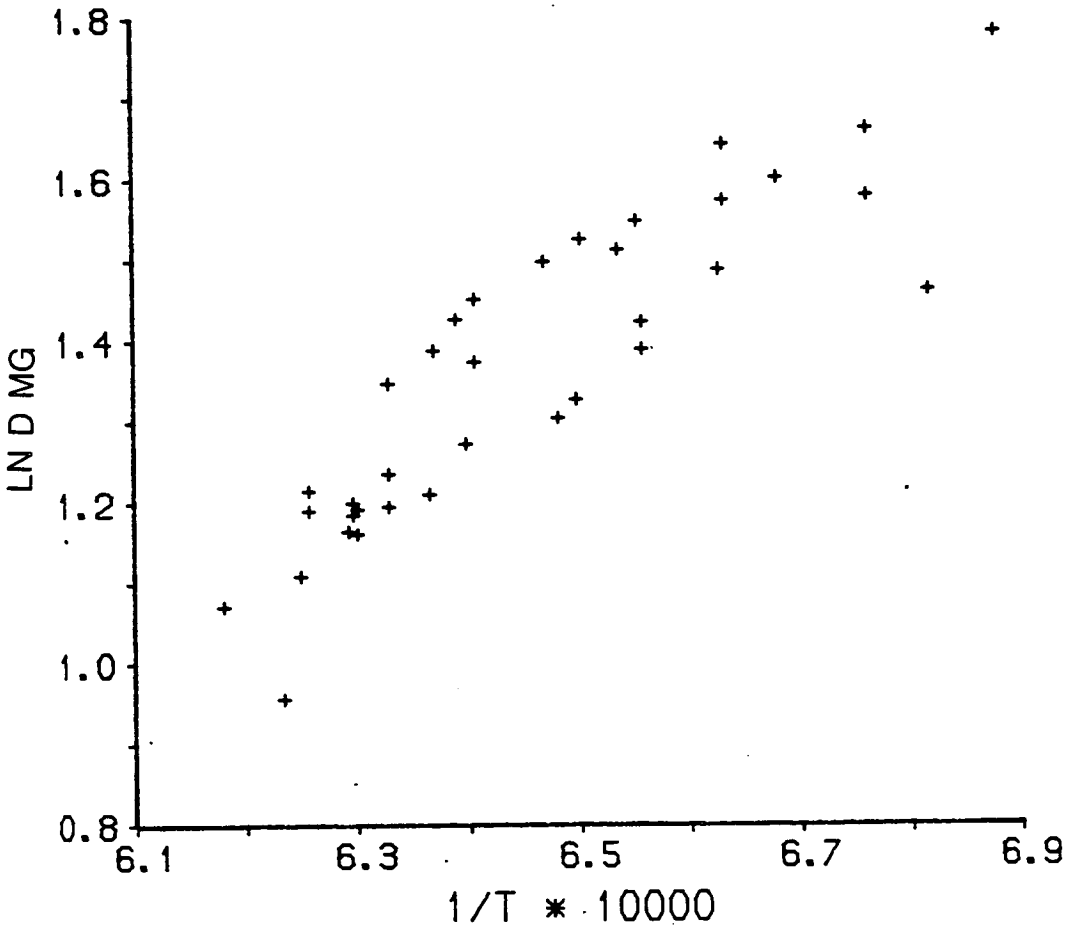

Figure 4.58

ln D_{Mg} v 1/T°K for olivine - liquid pairs from this study.

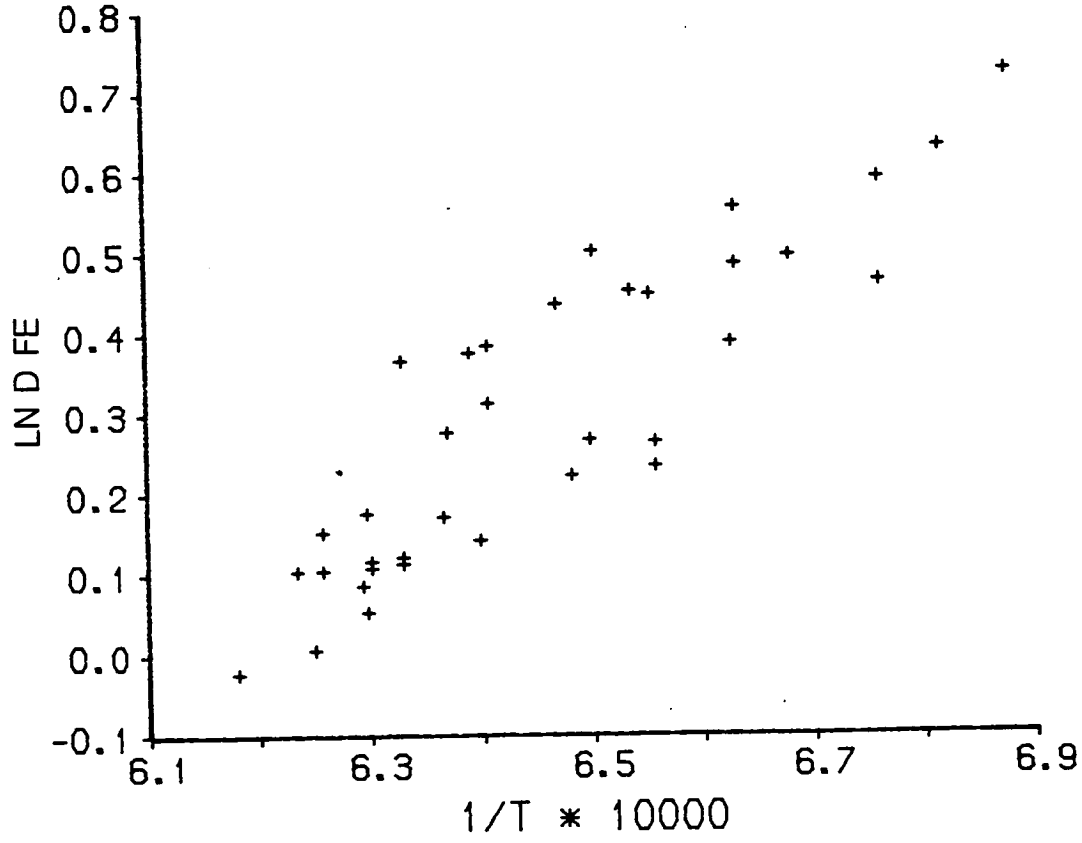

Figure 4.59

ln D_{Fe} v 1/T°K for olivine - liquid pairs from this study.

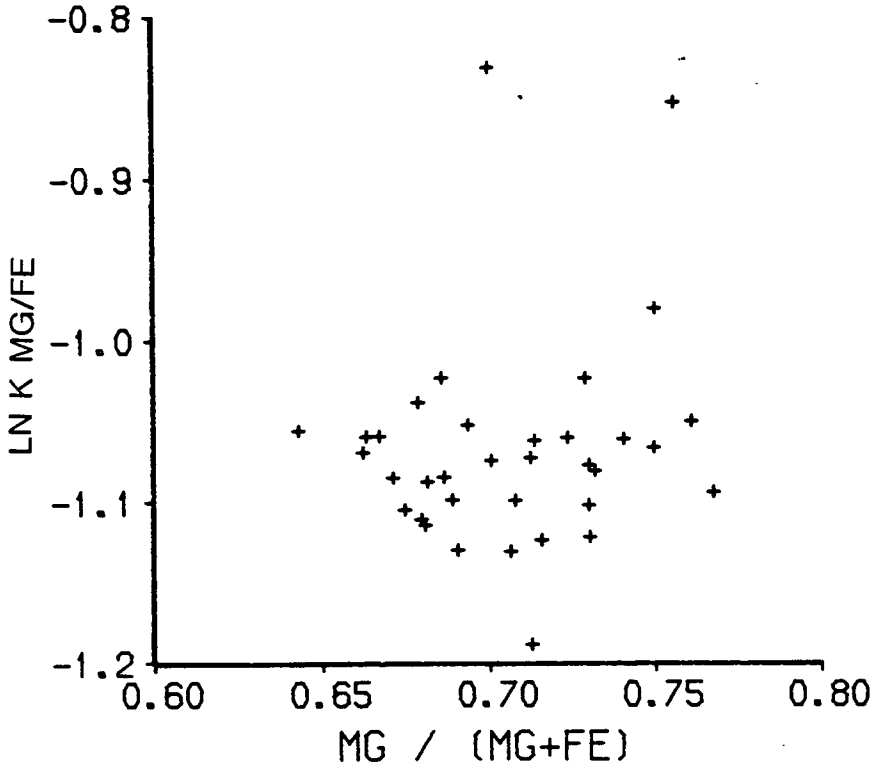

Figure 4.60

ln $K_D^{Fe^{2+}/Mg}$ v Mg/(Mg + Fe) for olivine - liquid pairs from this study.

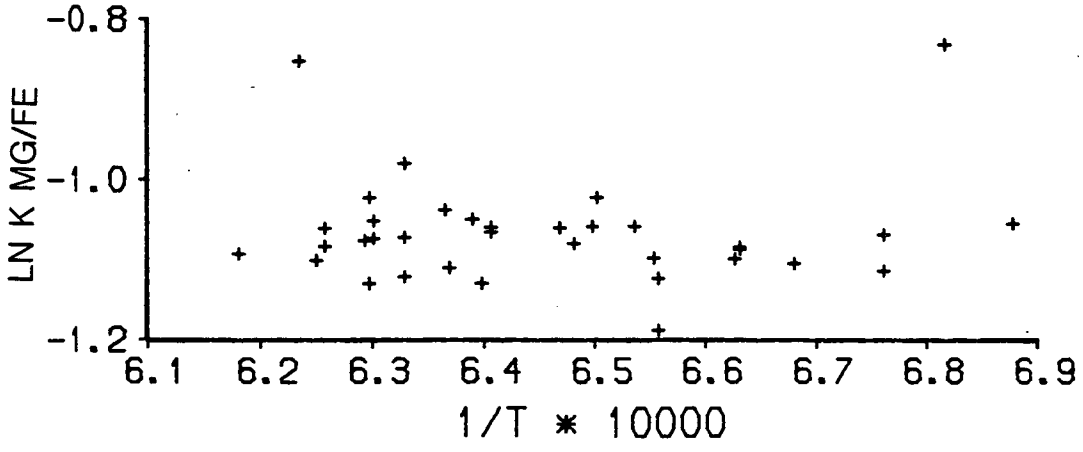

Figure 4.61

ln $K_D^{Fe^{2+}/Mg}$ v 1/T°K for olivine - liquid pairs from this study.

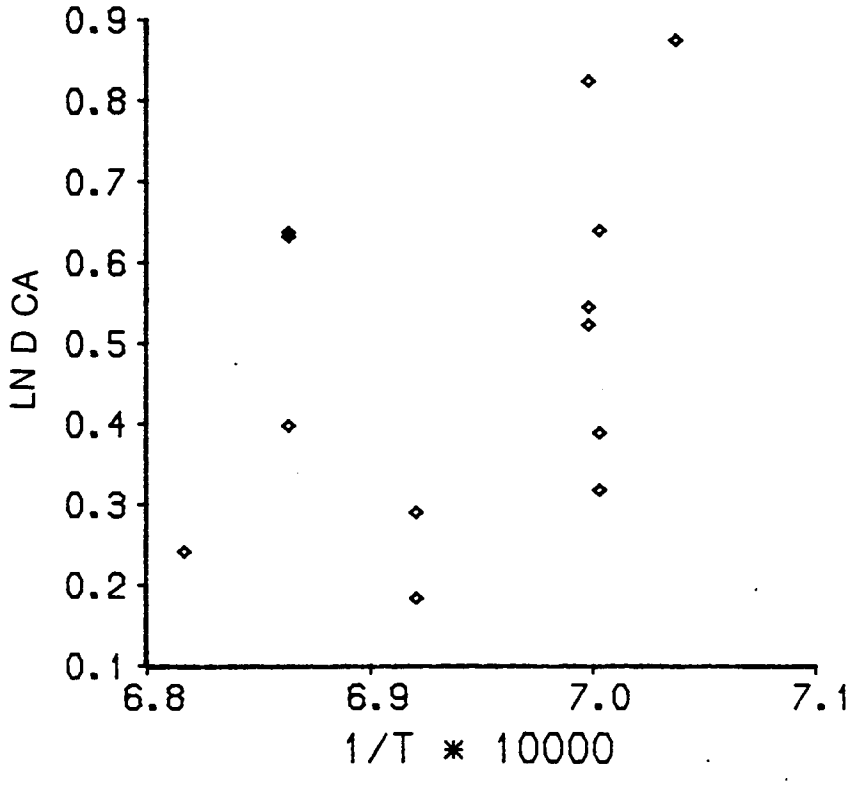

Figure 4.62

ln D_{Ca} v 1/T°K for augite - liquid pairs from this study.

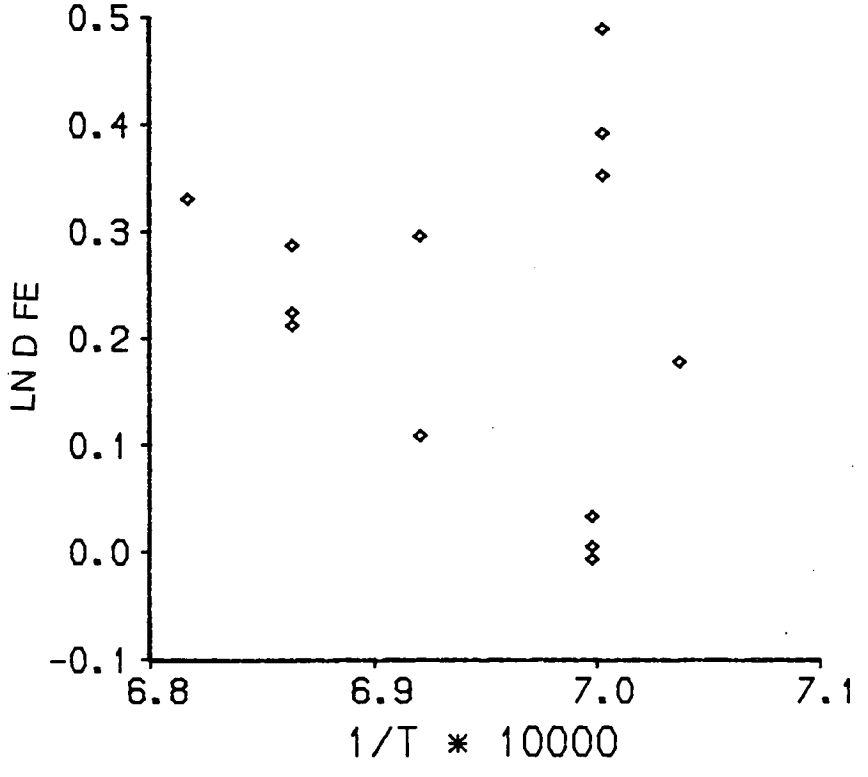

Figure 4.63

ln D_{Fe} v 1/T°K for augite - liquid pairs from this study.

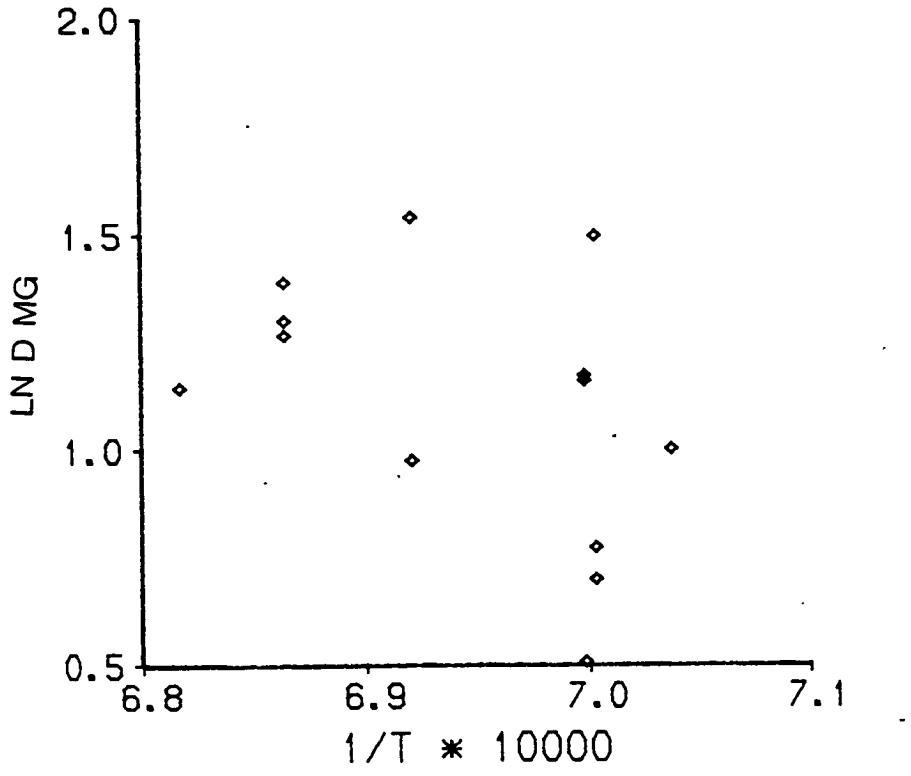

Figure 4.64

ln D_{Mg} v 1/T°K for augite - liquid pairs from this study.

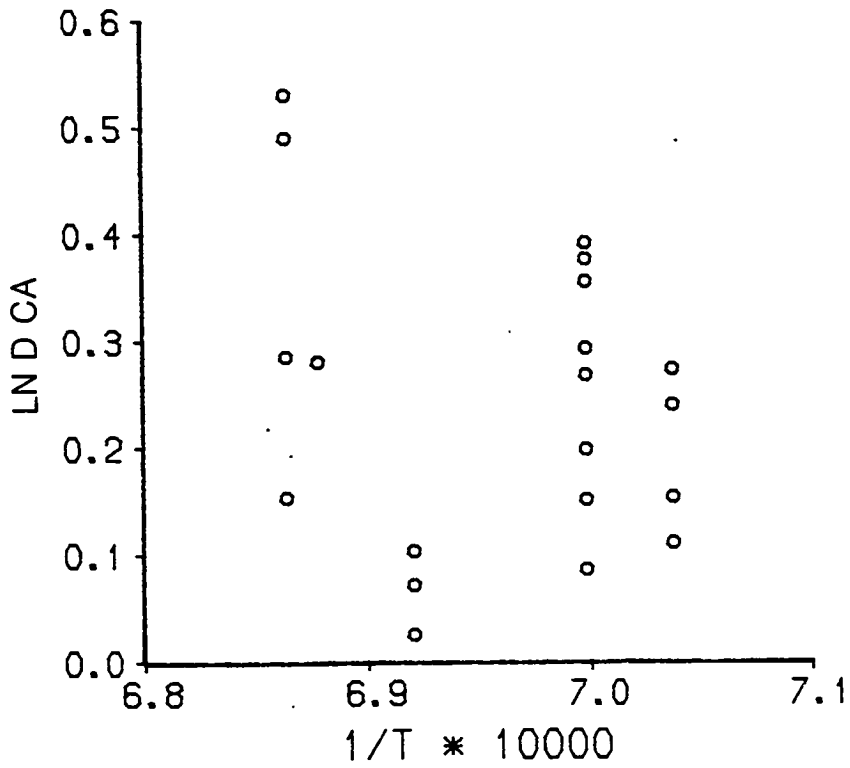

Figure 4.65

ln D_{Ca} v 1/T°K for plagioclase - liquid pairs from this study.

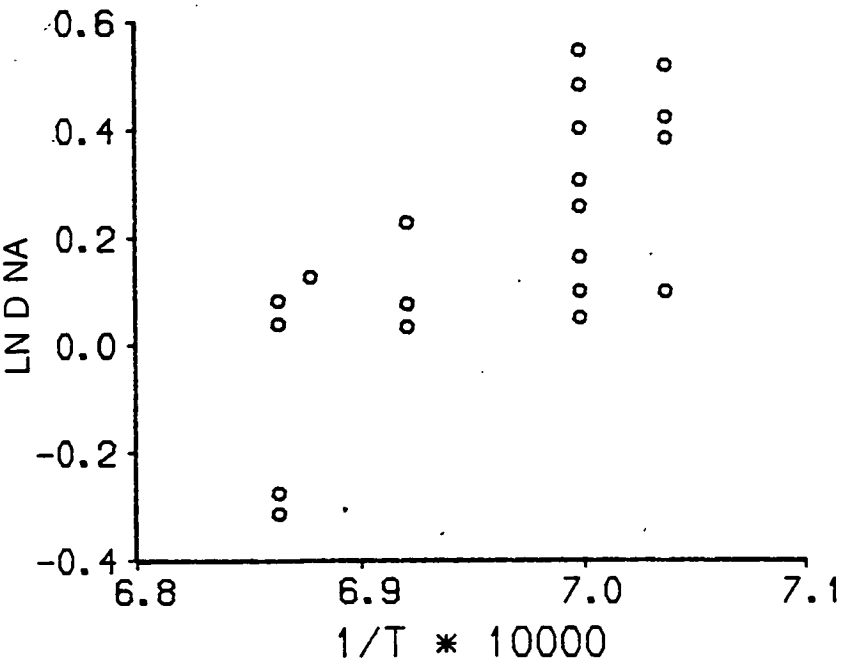

Figure 4.66

ln D_{Na} v 1/T°K for plagioclase - liquid pairs from this study.

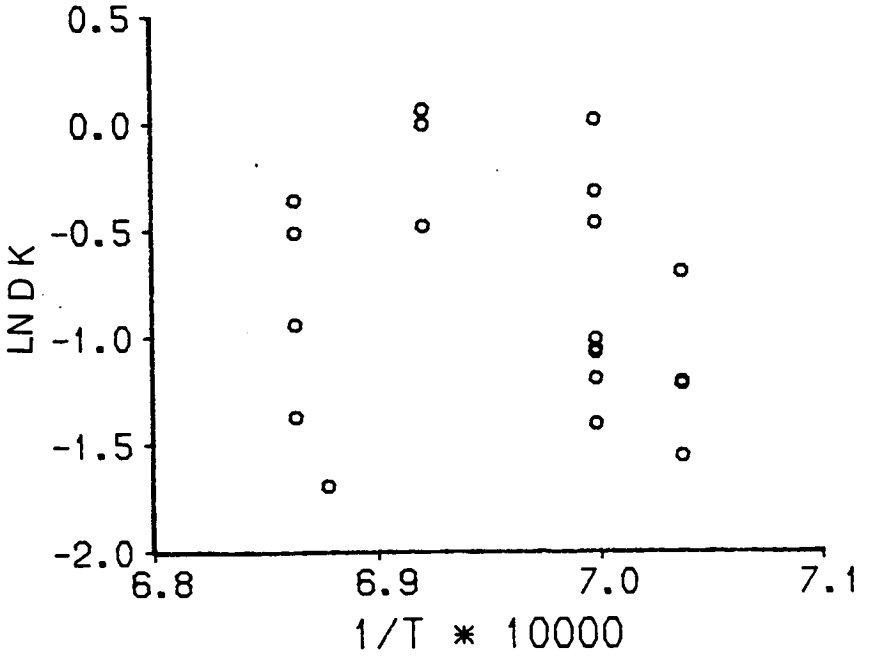

Figure 4.67

ln D_K v 1/T°K for plagioclase - liquid pairs from this study.

CHAPTER 5

LOW-CALCIUM PYROXENE - MELT EQUILIBRIA

5.1 INTRODUCTION

The partial molar free energy (G_i) of a component i in phase α at temperature T, constant pressure and constant ΔCp is given by:-

$$G_i^{\alpha} = H_i^{\circ} - TS_i^{\circ} + RT\ln X_i^{\alpha} + RT\ln \gamma_i^{\alpha} \qquad (1)$$

where H_i° and S_i° are the enthalpy and entropy of component i in the pure phase α, X_i^{α} and γ_i^{α} are the mole fraction and activity coefficient of component i in phase α. Although ΔCp does vary with temperature the change is only marked over a wide range of temperatures. Thus over a restricted temperature range ΔCp can be assumed to be constant. For symmetric solutions activity coefficients are related to composition through an interaction parameter, W.

$$RT\ln\gamma_i^{\alpha} = W(X_j^{\alpha} - X_i^{\alpha}X_j^{\alpha}) \qquad (2)$$

The free energy change (ΔG) of a reaction is given by:-

$$\Delta G = \Delta H - T\Delta S + RT\ln K \qquad (3)$$

where K is an equilibrium constant between component i in the phases of interest:-

$$K = \frac{(X_i^{\alpha} . \gamma_i^{\alpha})}{(X_i^{\beta} . \gamma_i^{\beta})} \qquad (4)$$

for example,

$$Mg_2Si_2O_6^{Px} = 2MgO^{L} + 2SiO_2^{L} \qquad (5)$$

$$K = \frac{X_{Mg_2Si_2O_6}^{Px} . \gamma_{Mg_2Si_2O_6}^{Px}}{(X_{MgO}^{L} . \gamma_{MgO}^{L})^2 . (X_{SiO_2}^{L} . \gamma_{SiO_2}^{L})^2} \qquad (6)$$

At equilibrium $\Delta G = 0$ so

$$-RT\ln K = \Delta H - T\Delta S \qquad (7)$$

Thus in a plot of lnK v 1/T giving a straight line relationship of the form:-

$$\ln K = A/T + B \qquad (8)$$

$$A = -\Delta H/R \qquad (9)$$

$$B = \Delta S/R \qquad (10)$$

As A and B are related to the entropy and enthalpy their signs should be consistent for all components (i, j, k etc.) of phase α. Thus for a four-component pyroxene - liquid model described by equations similar to equation 5 above all four A's should be positive and all four B's negative. If the signs are not consistent then one or other of the phases has not been adequately described by the thermodynamic model under consideration.

5.2 PREVIOUS WORK

5.2.1 Nathan and Van Kirk (1978)

From a data base of liquids in equilibrium with known minerals, mostly in synthetic systems, a set of 8 mineral temperature equations was derived by multiple linear regression analysis. These mineral temperature equations describe the crystallisation temperature of each mineral (ol, hyp, aug, plag, orth, leuc, neph & mag) and are considered to be a smooth function of the composition of the liquid. This is an empirical model used because of the difficulties in describing the thermodynamic properties of liquids. The equations are of the form:-

$$T = a_0 + a_1Al + a_2Ti + a_3Fe^3 + a_4Fe^2 + a_5Mg + a_6Ca + a_7Na + a_8K + a_9(\log_e II) + a_{10}Al(Na + K) \qquad (11)$$

where Al, Ti etc. represent cation fractions in the liquid, a_0 to a_{10} are constants, different for each mineral, derived by multiple linear regression. II is the geometric mean of the fractions of essential cations multiplied according to their ratios in the mineral e.g. for hypersthene $II = \sqrt[2]{(Fe + Mg)(Si)}$. The final term accounts for the effect of coexisting alumina and alkalis to which many minerals are sensitive.

Given a liquid composition of interest the crystallisation temperatures of all 8 minerals are calculated, the mineral with the highest crystallisation temperature is considered to be the liquidus phase. For two minerals to coexist on the liquidus they must have identical crystallisation temperatures. The composition of the mineral crystallising was obtained by assuming simple ionic equilibrium between crystals and liquid e.g.

$$Mg^{2+}_{hyp} + Fe^{2+}_{L} = Mg^{2+}_{L} + Fe^{2+}_{hyp} \qquad (12)$$

giving rise to an equilibrium cation ratio:-

$$\left(\frac{Mg^{2+}}{Fe^{2+}}\right)_{hyp} = k\left(\frac{Mg^{2+}}{Fe^{2+}}\right)_{L} \qquad (13)$$

where for hypersthene k = 2.73. To model fractional crystallisation once the crystallising phase(s) have been determined a small amount of solids of this composition is removed from the liquid and the process repeated with the new liquid composition.

The correlation coefficients obtained during the multiple linear regression are in the range 0.971 (hypersthene) to 0.832 (orthoclase), these figures indicate a fairly small amount of scatter for each equation. The authors admit that with a mean error of 20°C in the mineral temperature equations calculated crystallisation sequences will deviate from nature and that the model has serious deficiencies. In terms of low-calcium pyroxene -liquid equilibria this model has several drawbacks. Firstly it only considers the Mg^{2+} and Fe^{2+} bearing components of "hypersthene", ignoring Ca^{2+} which is a significant component in pigeonites.

Secondly the value of k used in calculating the crystal composition is based on the "monoclinic structure" - i.e. pigeonite. Thirdly it does not differentiate between orthopyroxene and pigeonite which coexist in many natural systems. Finally the data set for hypersthene is biased towards synthetic systems - 48 liquids from synthetic systems were used compared to 3 from the remelting of rocks.

5:2:2 Nielsen and Drake (1979)

Using a data base of 63 coexisting pyroxene - liquid analyses (31 low-calcium pyroxene, 32 high-calcium pyroxene) three thermodynamic models of pyroxene - liquid equilibria were evaluated.

The first model considered was a "macroscopic "M" site mixing model for pyroxene - simple oxide ideal mixing model for liquid". In this model the pyroxene formula was considered in terms of MTO_3 instead of the more usual $M1M2T_2O_6$ by assuming ideal mixing of all octahedrally co-ordinated elements in the single M site. This model also assumes that all Na is coupled with Al, the remaining Al being distributed equally between M and T sites. The activity of end member components is given by equations of the form:-

$$a^{Px}_{MgSiO_3} = X^{M}_{Mg} \,/\, [X^{Px}_{Mg} + X^{Px}_{Fe} + X^{Px}_{Ca} + 2X^{Px}_{Na} + X^{Px}_{Cr} + \ldots\ldots X^{Px}_{Ti} + 1/2(X^{Px}_{Al} - X^{Px}_{Na})] \qquad (14)$$

The liquid was assumed to be composed of ideally mixed free oxides the activities of which are equal to their mole fractions in the melt:-

$$a^{L}_{MgO} = X^{L}_{MgO} \qquad (15)$$

Equilibrium relations for Mg, Fe and Ca bearing end members of the following form were considered:-

$$MgO(L) + SiO_2(L) = Mg^{M}Si^{T}O_3 \qquad (16)$$

together with the Fe-Mg exchange reaction:-

$$Fe^{M}Si^{T}O_3(Px) + MgO(L) = Mg^{M}Si^{T}O_3(Px) + FeO(L) \qquad (17)$$

and the "bulk" reaction:-

$$CaO(L) + FeO(L) + MgO(L) + 3SiO_2(L) = Ca^{M}Si^{T}O_3(Px) + ..$$

$$...Fe^{M}Si^{T}O_3(Px) + Mg^{M}Si^{T}O_3(Px) \qquad (18)$$

Equations of the form:-

$$\ln K = A/T + B \qquad (19)$$

were produced by linear regression where

$$K = \frac{II[products]^n}{II[reactants]^n} \qquad (20)$$

and [] denote activities and n is the molar balance coefficient.

The authors considered that this model would give a good fit about the regression line for low-calcium pyroxenes - which was the case. They were, however, surprised to find that this model also gave a good fit for high-calcium pyroxenes despite the assumption of ideal mixing of Ca between M sites when Ca is known to occupy only the M2 site. The major problem with the model was the failure of the simple oxide ideal mixing model to cope with liquids rich in alkalis, such data points did not plot anywhere near the regression lines for the rest of the data. As a result of this a more complex liquid model was considered.

The second model retained the pyroxene mixing model previously used but adopted a "modified Bottinga-Weill liquid model". In the Bottinga-Weill model the liquid is considered to consist of network-forming Si-O and Al-O tetrahedra together with larger network-modifying cations. In this modified version of the model SiO_2, $KAlO_2$ and $NaAlO_2$ are considered to be network formers (NF) and MgO, CaO, $AlO_{1.5}$ etc. are network modifiers (NM). Activities of components in the melt are given by equations of the form:-

$$a^{L}_{SiO_2} = X^{NF}_{SiO_2} = X^{L}_{SiO_2}/[X^{L}_{NaO_{0.5}} + X^{L}_{KO_{0.5}} + X^{L}_{SiO_2}] \qquad (21)$$

$$a^{L}_{MgO} = X^{NM}_{MgO} = X^{L}_{MgO}/[X^{L}_{MgO} + X^{L}_{FeO} + X^{L}_{CaO} + (X^{L}_{AlO_{1.5}} - \ldots$$

$$\ldots . X^{L}_{NaO_{0.5}} - X^{L}_{KO_{0.5}})] \qquad (22)$$

Pyroxene - liquid relations were described by the equations used in the first model (16-18) but with the new liquid components, thus equation 16 becomes:-

$$MgO^{NM}(L) + SiO_2^{NF}(L) = Mg^{M}Si^{T}O_3(Px) \qquad (23)$$

This model produced a better fit about the regression line than the simple oxide ideal mixing liquid model above and brought the alkali-rich compositions into agreement with the rest of the data set.

For the third model a "multisite pyroxene mixing model" was adopted to describe pyroxene behaviour whilst the modified Bottinga-Weill liquid model was retained. In this model pyroxenes are considered in terms of the formula $M1M2T_2O_6$ where M1 is preferentially occupied by Mg, Fe, Cr, Al and Ti; M2 is preferentially occupied by Ca and Na but also contains Mg and Fe^{2+}. T is occupied by Si and Al, Al distribution between T and M1 is completely disordered. The activity of pyroxene end-member components is given by equations of the form:-

$$a^{Px}_{MgMgSi_2O_6} = X^{M1}_{Mg} X^{M2}_{Mg} (X^{T}_{Si})^2 \qquad (24)$$

where X^{M1}_{Mg} and X^{M2}_{Mg} are the Mg concentrations on the M1 and M2 sites respectively as determined by the relations given in Saxena (1976).

Equilibrium relations of the form:-

$$FeO^{NM}(L) + CaO^{NM}(L) + 2SiO_2^{NF}(L) = Fe^{M1}Ca^{M2}Si_2^{T}O_6 \qquad (25)$$

were considered for the end member components $Mg_2Si_2O_6$, $Fe_2Si_2O_6$, $FeCaSi_2O_6$ and $MgCaSi_2O_6$. The fit about the regression line for these new equations was good and the high and low alkali data were in agreement.

Nielsen and Drake concluded that whilst the modified Bottinga-Weill liquid model was an improvement on a simple oxide ideal mixing model the multisite pyroxene mixing model was no better than the macroscopic M site mixing model for describing pyroxene behaviour.

A model to calculate the liquidus temperature and pyroxene composition of a melt of known composition was suggested utilizing the macroscopic M site pyroxene - modified Bottinga-Weill liquid model. The equilibrium relationship used was the "bulk" reaction (equation 18) into which an assumed value for the mole fraction of Ca in the pyroxene was inserted together with the known liquid composition. The model then calculates the mole fractions of Mg and Fe in the pyroxene and calculates the temperature according to equation 19 (A and B are known from the linear regression). The mole fraction of Ca in the pyroxene was then recalculated using the wollastonite equilibrium (similar to equation 16) together with the calculated temperature and this new value returned to the beginning of the routine. After 20 repeats of this cycle the mole fractions of Mg,Fe and Ca in the pyroxene are given together with the temperature. It was found that the accuracy of the temperature calculations could be improved if aluminium in the M site was considered according to the relationship:-

$$AlO^{NM}_{1.5}(L) = Al^{Px}(Px) \qquad (26)$$

The model given above was able to predict temperatures to within $\pm 20°C$ (1σ). Although this is no more accurate than the Nathan and Van Kirk (1978) model it has its advantages - notably the ability to describe low-calcium pyroxenes in terms of four components (Mg, Fe^{2+}, Ca and Al) rather than two (Mg and Fe^{2+}) and its more rigorous thermodynamic basis. However the data base is small, only 31 pairs of analyses for low-calcium pyroxene; restricted to experiments carried out near the IW buffer and no attempt is made to distinguish between orthopyroxene and pigeonite.

5.2.3 Lindsley and Anderson (1980)

This model is not concerned with mineral-liquid equilibria but with two-pyroxene geothermometry, however it does provide information about pyroxene components so the main points are considered here. The model uses a "phase diagram", based on results in simple synthetic systems, together with recalculation schemes for pyroxene components that are designed to obtain mole fractions of Wo, En and Fs that most closely correspond to the bulk activities of these components. The Wo:En:Fs ratios obtained from the recalculation schemes are then plotted in the "phase diagram" and the temperature determined by eye. Theoretically coexisting pyroxenes will produce identical temperature determinations. The authors consider that for pyroxenes consisting principally of Mg, Fe^{2+} and Ca the thermometer is accurate to $\pm 50°C$, as non-quadrilateral components increase in the pyroxene the uncertainty increases e.g. for a pyroxene containing 91% Wo+En+Fs the accuracy is $\pm 85°C$.

The recalculation schemes used by Lindsley and Anderson (table 5.1) are based on a statistical study of correlations between minor components in pyroxenes and crystal-chemical considerations. All Si is assigned to the tetrahedral site; Ca and Na are restricted to M2; Fe^{3+}, Ti and Cr are restricted to M1; Mg, Fe^{2+} and Mn can go into M1 or M2 and in this model no attempt is made to partition them. Al is distributed amongst M1 and T according to the relationships:-

$$Al^{iv} = 2 - Si \qquad (27)$$

$$Al^{vi} = Al^{tot} - Al^{iv} \qquad (28)$$

If Fe^{3+} is not given in the analysis it is calculated according to the relationship:-

$$Al^{vi} + Fe^{3+} + Cr + 2Ti^{4+} = Al^{iv} + Na \qquad (29)$$

From table 5.1 it can be seen that Lindsley and Anderson consider pigeonite to be more closely related to augite than orthopyroxene in terms of the substitution patterns of non-quadrilateral components. This is particularly interesting as none of the previous models distinguished between orthopyroxene and pigeonite.

5:2:4 Ghiorso et al. (1983)

This model is an expanded regular solution approximation for silicate liquids based on a data base of 557 pairs of analyses covering a large variety of minerals (plag, ol, opx, cpx, sp, lc, ilm, mel, ksp and qtz) over a wide range of temperatures and pressures (1198-1723°K, 0.001-20kb) at fO_2's below the QFM buffer.

The Gibbs free energy of the liquid is described in the following terms:-

$$G^{liquid} = G_o + G_{mix}^{ideal} + G_{mix}^{excess} \qquad (30)$$

which can be expanded to give:-

$$G^{liquid} = \sum_{i=1}^{n} u_i^{\circ} n_i + NRT \sum_{i=1}^{n} X_i \ln X_i + N/2 \sum_{i=1}^{n} \sum_{j=1}^{n} W_{ij} X_i X_j \qquad (31)$$

$$G^{\circ} \qquad G_{mix}^{ideal} \qquad G_{mix}^{excess}$$

where u_i° is the standard state chemical potential of component i, n_i the number of moles of component i, N is the sum of all n_i, X_i the mole fraction of component i and W_{ij} a symmetrical interaction parameter ($W_{ij}=W_{ji}$). It can be shown that with $a_i=X_i$ i

$$RT\ln a_i = RT\ln X_i + RT\ln \gamma_i \qquad (32)$$

and

$$RT\ln \gamma_i = \sum_{j=1}^{n} W_{ij} X_j - 1/2 \sum_{j-1}^{n} \sum_{k=1}^{n} W_{jk} X_j x_k \qquad (33)$$

Minerals in equilibrium with the liquid may be related to the liquid by the reaction:-

$$M = \sum_{i=1}^{n} v_i C_i \qquad (34)$$

where M is an end-member component or a pure mineral, C_i are the liquid components and v_i the stoichiometric numbers of each of these components in the mineral formula. Thus for enstatite:-

$$MgSiO_3 = 1/4 Mg_4Si_2O_8 + 1/8\ Si_4O_8 \qquad (35)$$

The mass action expression corresponding to equation 34 is given by

$$RT\ln K = \sum_{i=1}^{n} v_i RT\ln a_i^{liquid} - RT\ln a_m^{solid} \qquad (36)$$

where K is the equilibrium constant and a_m is the activity of end-member component m in the solid. Equation 36 is combined with equation 33 to give:-

$$RT\ln K + RT\ln a_m^{solid} - \sum_{i=1}^{n} v_i RT\ln X_i = \sum_{i=1}^{n} v_i \sum_{j=1}^{n} W_{ij} X_j - \ldots$$

$$\ldots 1/2 \sum_{i=1}^{n} v_i \sum_{j=1}^{n} \sum_{k=1}^{n} W_{jk} X_j X_k \qquad (37)$$

Each end-member in each solid solution phase will give rise to one statement of this equation; the quantities on the left hand side can be calculated from the mineral-liquid pairs in the data base.

Before applying these equations suitable components for all phases have to be selected. Ghiorso et al. (1983) conclude from structural studies of silicate melts, especially in the feldspar system, that the molecular species present are probably fairly simple and that molecules based on 8 oxygens were most compatible with the regular solution model. As a result, the components selected to describe the liquids were of the "stoichiometric mineral" model developed from Ghiorso & Carmichael (1980) e.g. Si_4O_8, $Al_{16/3}O_8$, $Mg_4Si_2O_8$ and $Na_{16/3}Si_{8/3}O_8$. For each mineral the major component end-members were considered together with appropriate thermodynamic models e.g. a sub-regular solution model for olivine and an ideal site mixing model for clinopyroxene. For low-calcium pyroxene only two end-member components were considered, $MgSiO_3$ and $FeSiO_3$, where according to an ideal site mixing model (table 5.2):-

$$a_{MgSiO_3}^{opx} = (X_{Mg}^{M1} X_{Mg}^{M2})^{1/2} \qquad (38)$$

$$a_{FeSiO_3}^{opx} = (X_{Fe}^{M1} X_{Fe}^{M2})^{1/2} \qquad (39)$$

The site occupancies of Mg and Fe being determined by the authors own system (table 5.2).

Having obtained the values for the left hand side of equation 37 the values of W_{ij} were calculated using least squares regression and matrix inverse theory. By using the calculated values of W_{ij} it is now possible to use equation 37 as a geothermometer and as a model for magmatic crystallisation.

As a geothermometer the model was disappointing - for low-calcium pyroxene in the original data set the error in temperature calculation was $\pm 57°K$ (2σ). However as this model has a rigorous thermodynamic basis it should be possible to apply it to compositions outwith its data base without severe loss of accuracy. This model produces a poorer definition than that of Nielsen & Drake (1979) because it only considers two end-member components. The poor fit is not surprising when the data set is considered in more detail, although there are 557 pairs of analyses 215 are ol-gl pairs and 123 are plag-gl pairs. Low-calcium pyroxene data is particularly sparse, only 21 pairs of analyses over pressure and temperature ranges of 0.001-20 kb and 1198-1723 °K respectively with no differentiation made between orthopyroxene and pigeonite.

5:2:5 Nielsen and Dungan (1983)

Using a data set of mineral-liquid pairs from experiments on natural samples at atmospheric pressure together with some synthetic data and new synthetic spinel-liquid results equations were developed to model the behaviour of pyroxene-, olivine-, plagioclase-, spinel- and ilmenite-liquid equilibria. The model is based on simple equilibrium thermodynamics; at equilibrium

$$G° = -RT\ln K \qquad (40)$$

and at constant pressure

$$-RT\ln K = \Delta H° - T\Delta S° \qquad (41)$$

$$\ln K = \frac{-\Delta H°}{RT} + \frac{\Delta S°}{R} \qquad (42)$$

and

$$K = \frac{[P_i]^n}{[R_i]^n} \qquad (43)$$

where [ ] denotes the activity of product (P_i) and reactant (R_i) components and n is the molar balance coefficient required by stoichiometry. Where activity is unknown it is possible to use a distribution coefficient (K_D) which is related to the temperature by an equation of the form:-

$$\ln K_D = a/T + b \qquad (44)$$

where a and b are constants calculated by linear least squares regression.

For this model Nielsen and Dungan chose the modified Bottinga-Weill melt model given in Nielsen & Drake (1979), see section 5.2.2 equations 19 and 20 above, together with ideal mixing models for the mineral phases. Thus for low-calcium pyroxene the formula $M1M2T_2O_6$ was considered with Mg, Fe, Al, Cr and Ti occupying M1; Ca, Mn, Na, Mg and Fe^{2+} occupying M2; Si and Al occupying T. This model assumes that mixing on the M sites is ideal with complete disorder of Al between M1 and T, thus for enstatite:-

$$a^{Px}_{Mg_2Si_2O_6} = X^{M1}_{Mg} X^{M2}_{Mg} (X^{T}_{Si})^2 \qquad (45)$$

where X^{M1}_{Mg} and X^{M2}_{Mg} are the cation normalized mole fractions of Mg in M1 and M2 respectively as determined by the relationships in Saxena (1976). The authors considered four end-member components, $Mg_2Si_2O_6$, $Fe_2Si_2O_6$, $MgCaSi_2O_6$ and $FeCaSi_2O_6$, together with single oxide distribution coefficients for Ti, Cr and Al as uncertainty in minor element analyses precluded the application of paired substitution models. Equilibrium reactions used were of the form:-

$$MgO^{NM} + CaO^{NM} + 2SiO_2^{NF} = Mg^{M1}Ca^{M2}Si_2O_6^{Px}_{Di} \qquad (46)$$

and

$$AlO^{NM}_{1.5} = AlO^{Px}_{1.5} \qquad (47)$$

To calculate mineral composition and temperature from a given starting composition an initial temperature estimate is inserted into the equations for every mineral component (33 equations in all, 7 for orthopyroxene) and an initial estimate of the cation mole fractions of the mineral end members is made. For mass balance requirements to be met the sum of the cation mole fractions in a mineral must be equal to one, site occupancy and charge balance requirements must be met e.g. in orthopyroxene Mg, Fe, Ca, Al, Ti and Cr must sum to 0.5 and Si must equal 0.5. The initial estimate of cation mole fraction is compared with the mass balance requirements for the mineral concerned and the temperature estimate adjusted upwards or downwards depending on the gradient of the specific mineral equation and whether the estimated cation mole fraction exceeds or falls short of the mass balance requirements. This process is repeated until a temperature at which the mass balance requirements are met is found, this temperature represents the liquidus temperature of the mineral and the cation mole fractions the mineral compositions. The liquidus phase for a given liquid composition is the mineral with the highest calculated liquidus temperature. Crystallisation was modelled by removing small amounts of the liquidus phase(s) from the liquid and calculating the liquidus temperatures for the new liquid composition.

This model reproduces the input data set to within 20°C (1σ) and when tested against experimental results for 52 mafic and intermediate compositions not included in the data set predicted the correct crystallisation sequence for 89.9% of runs, all predictions being within 40°C of the experimental determinations. These results are a considerable improvement on the other models; although the accuracy of the temperature calculations has not improved, this model more accurately defines the resulting mineral compositions. However, there has still been no attempt to differentiate between orthopyroxene and pigeonite.

A summary of these models is given in table 5.3

5:3 APPLICATION OF THE NEW DATA BASE TO OLD MODELS

All of the models previously described in the literature rely on comparatively small low-calcium pyroxene experimental data bases. In this study 111 pairs of analyses found during a literature search (34 opx-gl, 77 pig-gl), listed in appendices III.2 and IV.1, were combined with 80 new pairs of analyses (55 opx-gl, 25 pig-gl), listed in appendices III.4 and IV.3, to give a data set covering a wider T-X-fO_2 range than previously considered. Initially this new data set was applied to some of the previously described models to assess their quality of fit. In all cases the orthopyroxene and pigeonite data were considered separately, this had not been the case in any of the original models, principally due to the lack of data. The model of Nathan & Van Kirk (1978) was not considered because of its poor thermodynamic basis.

5:3:1 Simple Pyroxene - Simple Liquid Model

This model is comparable to the first model considered in Nielsen & Drake (1979). The pyroxene composition was considered in terms of the $M_2T_2O_6$ formula and the liquid in terms of simple oxides. Pyroxene - liquid equilibria was described by the following reactions:-

$$2CaO(L) + 2SiO_2(L) = Ca_2Si_2O_6 \quad (Wo) \qquad (48)$$

$$2MgO(L) + 2SiO_2(L) = Mg_2Si_2O_6 \quad (En) \qquad (49)$$

$$2FeO(L) + 2SiO_2(L) = Fe_2Si_2O_6 \quad (Fs) \qquad (50)$$

giving rise to equations of the form:-

$$\ln K = A/T + B \qquad (51)$$

where A and B are constants determined by linear regression and

$$K = \frac{a^{Px}_{Ca_2Si_2O_6}}{(a^{L}_{CaO})^2 . (a^{L}_{SiO_2})^2} \qquad (52)$$

where $$a^{Px}_{Ca_2Si_2O_6} = Ca/[Ca + Mg + Fe] \quad (53)$$

and Ca, Mg, Fe refer to the normalized cation fractions of Ca^{2+}, Mg^{2+} and Fe^{2+} in the pyroxene formula.

The values obtained for A and B together with the least squares correlation coefficient (r) are given in table 5.4; graphs of lnK v 1/T are given in fig. 5.1a-c.

Although this is a very simple model the fit about the regression line for enstatite is good. However, the fit for ferrosilite is very poor showing that this simple model cannot accurately describe pyroxene-liquid equilibria in iron bearing systems. It is interesting to note that even this simple model is able to detect the difference between pigeonite and orthopyroxene in terms of Mg and Ca content, there being more Ca and less Mg in pigeonite compared with orthopyroxene at a given temperature.

5.3.2 Pyroxene Recalculation Models

5.3.2.1 Lindsley and Anderson (1980)

The pyroxene recalculation scheme given by Lindsley and Anderson (table 5.1) was used to determine the activities of end-member components in pyroxenes assuming ideal mixing in the M sites. The liquid was considered in terms of simple oxides as before. Equilibrium reactions of the following form were considered:-

$$NaO_{0.5} + FeO_{1.5} + 2SiO_2 = NaFe^{3+}Si_2O_6 \quad (pig) \quad (54)$$

$$NaO_{0.5} + (AlO_{1.5} + CrO_{1.5} + FeO_{1.5}) + 2SiO_2 = NaR^{3+}Si_2O_6 \quad (opx) \quad (55)$$

$$2MgO + 2SiO_2 = Mg_2Si_2O_6 \quad (opx \ \& \ pig) \quad (56)$$

giving rise to equilibrium constants of the form:-

$$K = a^{Px}_{NaFe^{3+}Si_2O_6} \ / \ a^{L}_{NaO_{0.5}} \times a^{L}_{FeO_{1.5}} \times (a^{L}_{SiO_2})^2 \quad (57)$$

$$K = a^{Px}_{NaR^{3+}Si_2O_6} \ / \ a^{L}_{NaO_{0.5}} \times a^{L}_{(AlO_{1.5} + CrO_{1.5} + FeO_{1.5})} \times (a^{L}_{SiO_2})^2 \quad (58)$$

$$K = a^{Px}_{Mg_2Si_2O_6} / (a^{L}_{MgO})^2 \times (a^{L}_{SiO_2})^2 \qquad (59)$$

where $a^{Px}_{component} = X^{Px}_{component}$ as calculated from the recalculation scheme and $a^{L}_{SiO_2} = X^{L}_{SiO_2}$ where X is the normalized mole fraction of a component in the liquid.

Equations of the form:-

$$\ln K = A/T + B \qquad (60)$$

were produced for every end-member component by linear regression. Values of A, B and r are given in table 5.5, plots of lnK v 1/T are given for the Wo, En and Fs components of orthopyroxene and pigeonite (fig. 5.2a-c). Initially the Fe_2O_3 content of the pyroxenes were calculated according to the charge balance reaction given in Lindsley & Anderson (1983), equation 29 above. However, the fit about the regression line for the Fe_2O_3 bearing components was very poor, table 5.5a, so the calculations were repeated without Fe_2O_3 in the pyroxenes. The values of A, B and r for this second calculation are given in table 5.5b.

In orthopyroxene there is a marked improvement in the quality of fit of the non-quadrilateral components and some improvement in the fit of ferrosilite. In pigeonite there is no change in the fit of the non-quadrilateral components but some improvement in the fit of wollastonite. Plots of lnK v 1/T are not given for this second calculation because of their similarity to those shown in fig. 5.2a-c. By comparing the values of A and B given in tables 5.5a and 5.5b it can be seen that there is very little change in the position of the regression lines.

From fig. 5.2a-c it can be seen that the Lindsley and Anderson recalculation scheme is very good at distinguishing the activities of quadrilateral components in orthopyroxene and pigeonite. However, the large scatter about the regression line for ferrosilite (fig. 5.7) indicates that this model also fails to describe the behaviour of iron bearing systems. The poor fit for non-quadrilateral components is an effect of the recalculation scheme; for example $NaTiAlSiO_6$ in orthopyroxene is calculated according to the presence of Ti^{4+} or Al^{iv} or any remaining Na^{+} after $NaR^{3+}Si_2O_6$ has been

calculated - whichever is smallest. Thus in some cases $NaTiAlSiO_6$ will have been calculated on the Ti content whilst in others it may depend on Al^{iv} or Na^+. For the purposes of modelling pyroxene-liquid equilibria "multiple choice" components of this nature are no use whatsoever because one can never be sure which element one is dealing with.

5.3.2.2 Cawthorn and Collerson (1974)

The recalculation scheme of Cawthorn and Collerson, table 5.6a, is intended to minimise the significance of Fe_2O_3 contents. A low-calcium pyroxene - liquid equilibria model using a modified version of Cawthorn and Collerson's scheme (Ford, pers. comm.) was considered although the recalculation scheme itself was based on studies of high-calcium pyroxenes. The components used and methods of calculation are given in table 5.6b. By using equilibrium reactions of a similar form to those given in equations 54 to 59 above regression lines were fitted to

$$\ln K = A/T + B \qquad (61)$$

for each component. Values of A, B and r are given in table 5.7.

No acmite component was produced because Na + K was always less than Al; likewise no calcium ferri-tschermak component was produced because Fe_2O_3 was not present in the pyroxene analyses. The fit about the regression line for Mg and Ca bearing end-members was good; however, the fit for ferrosilite was again very poor (fig. 5.3a-d). Even though the non-quadrilateral components are clearly defined in terms of single elements their fits are generally very poor. The good fit for $CaMnSi_2O_6$ and to a lesser extent $CaCrSi_2O_6$ is probably due to the presence of calcium in the components. A similar effect is seen in the quadrilateral components where $Fe_2Si_2O_6$ has a very poor fit but $FeCaSi_2O_6$ gives a reasonable fit about the regression line.

5.3.2.3 Schweitzer et al. (1979)

From a statistical study of clinopyroxenes in deep sea basalts recalculation schemes were proposed for pyroxenes in alkalic and tholeiitic basalts (table 5.8). Low-calcium pyroxene - liquid equilibria were modelled using the scheme for tholeiitic basalts as most of the data set was low in alkalis. Equilibrium reactions of the form given in equations 54 to 60 were considered; values of A, B and r obtained from linear regression are given in table 5.9. Initially the Fe_2O_3 contents of the pyroxenes were calculated according to the charge balance equation of Lindsley & Anderson (1983), equation 29 above; however, the fit for the Fe^{3+} bearing component was very poor. The calculation was repeated without any Fe_2O_3 in the pyroxene and the fit for the wollastonite component was found to improve slightly; the fit for ferrosilite component in orthopyroxene also showed a slight improvement although the fit for ferrosilite in pigeonite deteriorated. The values given in table 5.9 and the plot of lnK v 1/T for quadrilateral components given in fig. 5.4a-c relate to calculations carried out without Fe_2O_3 in the pyroxene analyses. Again the fit for ferrosilite was poor, fig. 5.4c.

5.3.3 Ideal Mixing Pyroxene - Polymer Liquid Model

This model is identical to that given in Nielsen & Dungan (1983). The pyroxene formula is taken to be $M1M2T_2O_6$ and ideal mixing is assumed between cations on the M sites. Nielsen & Dungan calculated the distribution of Mg and Fe^{2+} between the M1 andM2 sites according to the method of Saxena (1976); however, this model is based solely on results in synthetic systems and involves interaction parameters. Ghiorso et al. (1983) presented a method for the calculation of Mg and Fe site occupancy based on the overall Mg/(Mg + Fe) ratio of the pyroxene (table 5.2), this method was preferred to that of Saxena (1976) because of its simplicity and applicability to natural systems. The calculation was adapted to allow for the presence of Mn on both M1 and M2 sites (chapter 3) and for the calculation of more components, e.g.:-

$$X_{Mg}^{M1} = n_{Mg}^{M1} / (n_{Cr} + 1/2n_{Al} + n_{Ti} + 1/2n_{Mn} + n_{Mg}^{M1} + n_{Fe}^{M1}) \quad (62)$$

$$X_{Fe}^{M2} = n_{Fe}^{M2} / (n_{Ca} + 1/2n_{Mn} + n_{Na} + n_{Mg}^{M2} + n_{Fe}^{M2}) \quad (63)$$

$$X_{Ca}^{M2} = n_{Ca} / (n_{Ca} + 1/2n_{Mn} + n_{Na} + n_{Mg}^{M2} + n_{Fe}^{M2}) \quad (64)$$

$$X_{Mn}^{M2} = 1/2n_{Mn} / (n_{Ca} + 1/2n_{Mn} + n_{Na} + n_{Mg}^{M2} + n_{Fe}^{M2}) \quad (65)$$

$$X_{Na}^{M2} = n_{Na} / (n_{Ca} + 1/2n_{Mn} + n_{Na} + n_{Mg}^{M2} + n_{Fe}^{M2}) \quad (66)$$

thus

$$a_{MgCaSi_2O_6}^{Px} = X_{Mg}^{M1} X_{Ca}^{M2} \quad (67)$$

$$a_{Mg_2Si_2O_6}^{Px} = X_{Mg}^{M1} X_{Mg}^{M2} \quad (68)$$

$$a_{Mn_2Si_2O_6}^{Px} = X_{Mn}^{M1} X_{Mn}^{M2} \quad (69)$$

$$a_{NaAlSi_2O_6}^{Px} = \left(X_{Na}^{M2}\right)^2 \quad (70)$$

The liquid was described in terms of the polymer model of Nielsen & Drake (1979) given in section 5.2.2.

Equilibrium reactions of the following form were considered for quadrilateral components:-

$$2MgO^{NM} + 2SiO_2^{NF} = Mg^{M1}Mg^{M2}Si_2O_6 \quad (71)$$

$$MgO^{NM} + CaO^{NM} + 2SiO_2^{NF} = Mg^{M1}Ca^{M2}Si_2O_6 \quad (72)$$

Initially for non-quadrilateral components simple oxide distribution coefficients were considered. Equations of the form:-

$$\ln K = A/T + B \quad (73)$$

were produced for each end-member and the non-quadrilateral components; values of A, B and r are given in table 5.10, plot of lnK v 1/T for the quadrilateral components are given in fig. 5.5a-d

The fit for iron bearing components is a considerable improvement on the previous models tested (see table 5.18 for a summary). There is no improvement in the fit for minor components

using the simple oxide distribution coefficients rather than the components described in the previous models. However the fit for manganese oxide produced similar results to those for the $CaMnSi_2O_6$ component of the Cawthorn & Collerson model (table 5.7)

An attempt was then made to model some of the non-quadrilateral components as end-members, the following reactions were chosen:-

$$2MnO^{NM} + 2SiO_2^{NF} = Mn_2Si_2O_6 \qquad (74)$$

$$NaAlO_2^{NF} + 2SiO_2^{NF} = NaAlSi_2O_6 \qquad (75)$$

However, there was no significant improvement in the goodness of fit for either of these end-members (table 5.10).

5.3.4 Ideal Mixing Pyroxene - "Stoichiometric Mineral" Liquid Model

In this model the "stoichiometric mineral" model of Ghiorso et al.(1983), section 5.2.4, was used in conjunction with an ideal mixing pyroxene model the site occupancies of which were determined by the adapted method of Ghiorso et al. given in table 5.2 and equations 62 to 70 above. Equilibrium reactions of the form:-

$$1/2Mg_4Si_2O_8 + 1/4Si_4O_8 = Mg^{M1}Mg^{M2}Si_2O_6 \qquad (76)$$

$$1/4Mg_4Si_2O_8 + 1/4Ca_4Si_2O_8 + 1/4Si_4O_8 = Mg^{M1}Ca^{M2}Si_2O_6 \qquad (77)$$

$$3/16Na_{16/3}Si_{8/3}O_8 + 3/16Al_{16/3}O_8 + 3/8Si_4O_8 = NaAlSi_2O_6 \qquad (78)$$

were considered and a regression line fitted as above. Values of A, B and r are given in table 5.11a and plots of lnK v 1/T for the quadrilateral components are given in fig. 5.6a-d. Although the fit for iron and manganese components is good compared with the other models the fit for enstatite is very poor. As the pyroxene mixing model gave good results for enstatite with the polymer liquid model the poor fit for enstatite in this case must be related to the Mg bearing component in the liquid model of Ghiorso et al. (1983).

5:3:5 Ideal Mixing Pyroxene = Regular Mixing Liquid Model

The liquid components given in Ghiorso et al. (1983) were intended for use with a set of interaction parameters (W_{ij}'s); thus the activity of the liquid component is now expressed as, for example:-

$$a^{L}_{Mg_2Si_2O_6} = \frac{(X^{L}_{Mg_4Si_2O_8} \times \gamma^{L}_{Mg_4Si_2O_8})^{0.5} \times (X^{L}_{Si_4O_8} \times \gamma^{L}_{Si_4O_8})^{0.25}}{(X^{o}_{Mg_4Si_2O_8} \times \gamma^{o}_{Mg_4Si_2O_8})^{0.5} \times (X^{o}_{Si_4O_8} \times \gamma^{o}_{Si_4O_8})^{0.25}} \quad (79)$$

where X^{L}_{i} and γ^{L}_{i} refer to the mole fraction and activity coefficient of component i in the natural liquid, X^{o}_{i} and γ^{o}_{i} refer to the mole fraction and activity coefficient of component i in a liquid of pure pyroxene component composition. Values of γ were calculated using equations of the form:-

$$RT\ln\gamma_i = nW_{ij}(X_j - X_iX_j) \quad (80)$$

$$RT\ln\gamma^{o}_{Mg} = (Si^{o} - Mg^{o}Si^{o}) \times W_{Mg-Si} \quad (81)$$

$$RT\ln\gamma^{o}_{Si} = (Mg^{o} - Si^{o}Mg^{o}) \times W_{Si-Mg} \quad (82)$$

and as an example

$$RT\ln\gamma^{L}_{Si_4O_8} = [(Ti - SixTi) \times W_{Si-Ti}] + [(Al - SixAl) \times W_{Si-Al}] + \ldots$$
$$\ldots. [(Fe^{3+} - SixFe^{3+}) \times W_{Si-Fe^{3+}}] + [(TixAl) \times W_{Ti-Al}] + \ldots$$
$$\ldots. [(TixFe^{3+}) \times W_{Ti-Fe^{3+}}] + [(NaxK) \times W_{Na-K}] \quad (83)$$

where, for the sake of brevity in equations 81 to 83, $Si^{o} = X^{o}_{Si_4O_8}$, $Si = X^{L}_{Si_4O_8}$ etc. Thus:-

$$K = X^{M1}_{Mg}X^{M2}_{Mg} \;/\; a^{L}_{Mg_2Si_2O_6} \quad (84)$$

and equations of the form:-

$$\ln K = A/T + B \quad (85)$$

were fitted as before, values of A, B and r are given in table 5.11b and plots of lnK v 1/T are given in fig.5.7a-d. The use of the interaction parameters considerably improved the fit for enstatite using this liquid model; however, the fit for ferrosilite and the non-quadrilateral components used was poorer.

5:4 DEVELOPMENT OF NEW MODELS

5:4:1 Regular Mixing Pyroxene - Regular Mixing Liquid Models

Using the liquid interaction parameters given in Ghiorso et al. (1983) a regular mixing model for the low-calcium pyroxenes was developed. In this model the activity of, for example, the $Mg_2Si_2O_6$ component in orthopyroxene is given by:-

$$a_{En}^{opx} = X_{Mg}^{M1} . X_{Mg}^{M2} . \gamma_{En}^{opx} \qquad (86)$$

where $$RT\ln\gamma_{En}^{opx} = W_{ij}(X_i^{opx} - X_i^{opx} . X_j^{opx}) \qquad (87)$$

and $i \neq j$, $i \neq X_{En}$

As six pyroxene components are being considered in this model (En, Fs, Di, Hd, Mn and Jd) and the mixing is symmetrical ($W_{ij}=W_{ji}$) there will be 15 terms in equation 87 and six equations of this form for every opx-lq or pig-lq pair in the data set.

The activities of liquid components in this model have already been defined, equation 79 above, and as:-

$$K = a_{En}^{opx} / a_{En}^{L} \qquad (88)$$

the equation

$$\ln K = A/T + B \qquad (89)$$

can be rearranged so that all the unknowns are on the right hand side, thus:-

$$\ln \frac{(X_{Mg}^{M1} . X_{Mg}^{M2})^{opx}}{a_{En}^{L}} = A/T + B - \ln\gamma_{En}^{opx} \qquad (90)$$

There are 27 unknowns on the right hand side - 6 each of A and B (12) and 15W_{ij}'s (which are the same for all six components). The value of these 27 unknowns was determined by setting up a series of simultaneous equations and solving by least squares method using the NAG fortran routine F04JGF (Lawson & Hanson, 1974).

After the initial calculation of all 27 unknowns those W_{ij}'s that were too small to be significant (less than 100 joules) or that had large standard errors (greater than 100%) were omitted from the equation and the rest recalculated. The omission of interaction parameters of less than 100 joules can be justified by considering the following examples:-

Let $X_i = 0.7$, $X_j = 0.2$, T=1500°K

first with W_{ij} = 100 joules

$RT\ln = 100(0.7 - 0.7 \times 0.2)$

$= 56$

$= \exp(56 / (8.3144 \times 1500))$

$= 1.0045$

second with W_{ij} = 100,000 joules

$RT\ln = 100{,}000(0.7 - 0.7 \times 0.2)$

$= 56{,}000$

$= \exp(56{,}000 / (8.3144 \times 1500))$

$= 89.1394$

From which it can be seen that, once summed, an interaction parameter of less than 1000 joules has very little effect on the total in the presence of interaction parameters of 100,000 joules or more.

Values of W_{ij} for orthopyroxene and pigeonite in equilibrium with Ghiorso et al.'s liquid model are given in table 5.12. Values of A, B and r for this new model are given in table 5.13; plots of lnK v 1/T are given in fig. 5.8a-d.

By comparing tables 5.12 and 5.13 it can be seen that there is very little difference in the fit for quadrilateral components and the fit for manganese and sodium bearing components is slightly worse when using the pyroxene interaction parameters. The fit for enstatite is still not as good as that produced in the other models (table 5.18). A possible cause is the data set used for Ghiorso et al.'s interaction parameters. As discussed in section 5.2.4 this

liquid data set was heavily biased towards plagioclase and olivine bearing glasses and only contained 21 orthopyroxene bearing glasses. A new set of liquid interaction parameters, specific to low-calcium pyroxene bearing glasses was determined using the simultaneous equation and least squares method given above; thus equation 90 becomes:-

$$\ln \frac{X_{Mg}^{M1} . X_{Mg}^{M2}}{(X_{Mg_2Si_4O_8}^{L})^{0.5}(X_{Si_4O_8}^{L})^{0.5}} = A/T + B - \ln \gamma_{En}^{opx} + \ln \gamma_{En}^{L} \quad (91)$$

In this equation there are 99 unknowns - 6 each of A and B for both orthopyroxene and pigeonite (24 in all), 15 W_{ij}'s for both orthopyroxene and pigeonite (30 in all) and 45 W_{ij}'s for the glass.

Values of W_{ij} determined for orthopyroxene, pigeonite and glass are given in table 5.14. Values of A, B and r for the fit of lnK v 1/T using this new set of interaction parameters are given in table 5.15. These new interaction parameters do not significantly improve the fit for any major components, indeed the fit was comparable to that obtained using Ghiorso et al.'s (1983) melt model without any interaction parameters (compare tables 5.15 and 5.11a).

As Ghiorso et al. (1983) chose their liquid components principally on the basis of structural studies in the feldspar system it is possible that these liquid components are not suitable for describing relationships in pyroxene bearing systems. As the polymer melt model of Nielsen & Dungan (1983) gave by far the best fit of all the models considered so far a set of interaction parameters was determined for this model (equations 62-72 & 90) to see if the fit could be improved. Values of W_{ij} determined for orthopyroxene, pigeonite and glass are given in table 5.16; the results of linear regression of lnK v 1/T are given in table 5.17 and plots of lnK v 1/T for the quadrilateral components are given in fig. 5.9a-d. The use of interaction parameters with the Nielsen & Dungan melt model made very little difference to the overall quality of fit (table 5.18).

5.5 SUMMARY & CHOICE OF LOW-CALCIUM PYROXENE - MELT MODEL

The models involving simple oxide melts (models 1-5, table 5.18) give very poor fits for the ferrosilite component. As the ferrosilite component of the pyroxene is calculated by a different method in each model whilst the liquid model remains the same, the simple oxide melt model would appear to be at fault. It has been noted that the simple oxide melt model does not adequately describe behaviour in alkali rich melts (section 5.2.2, Nielsen & Drake, (1979)). It also appears that the simple oxide melt model is incapable of describing low-calcium pyroxene - melt equilibria in iron bearing systems. However, that none of the pyroxene recalculation schemes used adequately describes the behaviour of ferrosilite cannot be discounted.

A variety of non-quadrilateral components containing Ti, Al, Cr, Mn and Na were also considered in models 2-5 (tables 5.1, 5.5-5.9). The only ones that gave reasonable fits were those where a "minor" element was linked to Mg or Ca, e.g. $CaMnSi_2O_6$ for orthopyroxene (Cawthorn & Collerson, table 5.7) and $MgCrSiAlO_6$ for pigeonite (Schwietzer et al., table 5.9). This is because the comparatively small amount of Mn or Cr present in both the pyroxene and the liquid is swamped by the amount of Ca or Mg present in the liquid and the latter's relationship to temperature (chapter 4). The lack of any relationship between these components and the melt is not altogether surprising. Firstly there were no obvious coupled substitutions, e.g. Al^{vi}-Al^{iv}, Cr-Al, Na-Al, in the pyroxenes of the data set (section 3.1.3.2). And secondly single element distribution coefficients for these "minor" elements covered a wide range (section 4.4.2), in some cases due to taking a ratio of two small numbers. For chromium bearing components some of this lack of fit can be attributed to changes in the oxidation state of chromium under different fO_2 conditions which leads to changes in the distribution coefficient of chromium (section 4.4.2).

For models using the "stoichiometric mineral" melt model of Ghiorso et al. (1983); models 7-10, table 5.18; the fit for the ferrosilite component was reasonable. However, the fit for enstatite component was never as good as that obtained from the simple oxide melt models, and in models 7 and 10 there was no fit for enstatite. It is suggested that there are insufficient data to determine accurately the interaction parameters for pyroxene - melt

equilibria on the basis of the following two observations. Firstly, the calculation of interaction parameters for pyroxenes to go with Ghiorso et al.'s melt model made no difference to the quality of fit; models 8 & 9, table 5.18. And secondly, the calculation of interaction parameters for both pyroxenes and liquids produced results no better than the use of Ghiorso et al.'s model without any interaction parameters; models 7 & 10, table 5.18. This is supported by the large number of interaction parameters set to zero because of their large standard errors, which in turn explains why the use of the few interaction parameters remaining has so little effect.

The modified Bottinga-Weill melt model of Nielsen & Dungan (1983); model 6, table 5.18; gave a good fit for all four quadrilateral components. The calculation of interaction parameters for this model did not result in any significant improvement of the fit (model 11, table 5.18), supporting the suggestion that there is insufficient data for the accurate determination of interaction parameters. Nielsen & Dungan (1983) used simple oxide distribution coefficients to describe the non-quadrilateral components, of which only MnO gave a reasonable fit (table 5.10). The $Mn_2Si_2O_6$ and $NaAlSi_2O_6$ components both produced better fits than their simple oxide equivalents, although for $NaAlSi_2O_6$ the fit was still very poor (table 5.10).

The choice of $Mn_2Si_2O_6$ and $NaAlSi_2O_6$ as the only non-quadrilateral components used for models 7-11 (table 5.18) was based on several factors. Firstly, the absence of obvious coupled substitutions for Cr, Al and Ti and the range of simple oxide distribution coefficients for these elements mentioned above. Secondly, for the purposes of calculating interaction parameters the addition of a seventh pyroxene component would have added 8 terms to the equation for pyroxene interaction parameters and 16 terms to the equation for pyroxene and glass interaction parameters. As there appears to have been insufficient data for the calculation of 99 unknowns the determination of 115 unknowns would have produced even worse results. $Mn_2Si_2O_6$ was chosen as a component for three reasons, its simple oxide distribution coefficient produced a good fit, as a divalent cation there is no need for charge balance and at high

temperatures manganese is equally divided between M1 and M2 (chapter 3) so $Mn_2Si_2O_6$ is a possible component. $NaAlSi_2O_6$ was chosen as a component despite the lack of evidence for Na-Al^{vi} substitution (chapter 3) and the low Na^+ content of pyroxenes at atmospheric pressure. Although $NaAlSi_2O_6$ is not an important pyroxene component at atmospheric pressure, knowledge of its' behaviour at atmospheric pressure would provide a basis for any future work involving low-calcium pyroxene - melt equilibria at high pressure. Unfortunately it was not possible to produce a good quality fit for $NaAlSi_2O_6$.

That the fit for ferrosilite is always worse than for the other quadrilateral components is attributable to problems in the accurate determination of the $FeO:Fe_2O_3$ ratio in the glass and the decision not to make any assessment of the Fe_2O_3 content in the pyroxene (chapter 3).

The low-calcium pyroxene - melt model giving the best fit overall was that using the adaptation of Nielsen & Dungan's (1983) model without any interaction parameters; model 6, table 5.18. This model uses ideally mixing pyroxene components, the site occupancy of which was determined by an adaptation of Ghiorso et al.'s (1983) method (table 5.2 and equations 62-70), and the modified Bottinga-Weill melt model of Nielsen & Drake (1979). The pyroxene components used were $Mg_2Si_2O_6$, $Fe_2Si_2O_6$, $MgCaSi_2O_6$, $FeCaSi_2O_6$, $Mn_2Si_2O_6$ and $NaAlSi_2O_6$. Al_2O_3 contents were determined according to the relationship given in table 5.10, although this gave a poor fit it allows some estimation of the Al^{3+} content. For Cr_2O_3 and TiO_2 a constant distribution coefficient was used as suggested by the simple oxide distribution coefficients in chapter 4. Plots of $\ln K_{Cr}$ v Cr glass and $\ln K_{Ti}$ v Ti glass using the low -calcium pyroxene - melt model above are given in figs. 5.10 and 5.11 respectively and these also suggest a constant distribution coefficient, $\ln K_{Cr}=2$ and $\ln K_{Ti}=-0.5$.

5:6 APPLICATIONS OF THE MODEL

5:6:1 As a Geothermometer

By rearranging the equation

$$\ln K = A/T + B \qquad (92)$$

it is possible to use the model to predict the temperature at which a pyroxene - liquid pair is in equilibrium:-

$$T = 1 / [(\ln K - B) / A] \qquad (93)$$

There are six equations for orthopyroxene and pigeonite, one for each of the pyroxene components in the model. Plots of T calculated v T observed for the data set are given for all components in fig. 5.12a-f. The accuracy of the predictions using the four quadrilateral components is as follows:-

component	accuracy (2σ)	
	opx	pig
$Mg_2Si_2O_6$	±35°C	±57°C
$Fe_2Si_2O_6$	±84°C	±150°C
$MgCaSi_2O_6$	±43°C	±47°C
$FeCaSi_2O_6$	±60°C	±60°C

The accuracy of these equations is better than that given for any of the models described in the literature (table 5.3).

Although the $Mn_2Si_2O_6$ equation is only accurate to ±150°C (2σ) this is a reasonable fit given the low level of MnO found in both the pyroxenes and the glasses. However the $NaAlSi_2O_6$ equation is useless as a geothermometer, the total range of temperature predictions was -10,000 to 30,000°C, although admittedly only three points fall outside the range 0-4000°C used for fig. 5.12f.

5.6.2 Calculation of Pyroxene Compositions

By rearranging the equation

$$\ln K = A/T + B \qquad (94)$$

the composition of pyroxene end-members in equilibrium with the liquid at a given temperature can be determined, e.g.

$$a^{px}_{Mg_2Si_2O_6} = \exp\left(A_{En}/T + B_{En} + \ln X^{l}_{En} \right) \qquad (95)$$

as the pyroxene components are a product e.g. $a^{px}_{En} = X^{M1}_{Mg} X^{M2}_{Mg}$ they are not expressed in any units and not constrained by stoichiometry -unlike their constituent parts where, e.g. $X^{M1}_{Mg} + X^{M1}_{Fe} + X^{M1}_{others} = 1$. Thus in plots of a calculated v a observed for the data set, fig. 5.13a-f, the scale serves only as a method of comparing the two values which should, if the model were perfect, be equal. The accuracy with which this model predicts the activity of the quadrilateral components is as follows:-

component	accuracy (2σ)	
	opx	pig
$Mg_2Si_2O_6$	±25%	±38%
$Fe_2Si_2O_6$	±50%	±46%
$MgCaSi_2O_6$	±40%	±50%
$FeCaSi_2O_6$	±50%	±50%

For $Mn_2Si_2O_6$ and $NaAlSi_2O_6$ the amount of end-member present is insignificant so although the errors are large, over 100% in some cases, this will have very little effect on the pyroxene composition.

Of those points showing large deviations from observed = calculated most come from experiments at the lower end of the temperature range suggesting that such experiments may not have equilibrated. A large error in the calculation of one component does not necessarily result in large errors for other components. For example points L and M (fig. 5.13a-c) both show comparatively large errors in the prediction of Di content. However,while the

calculated Hd component for both is close to the observed, point L has a very large error in En content and point M has a large error in Fs content. Both points are from experiments at 1150°C.

5.6.3 Calculating Low-Calcium Pyroxene - Melt Equilibria

By using equation 95 above an initial estimate of the temperature it is possible to calculate the composition of a low-calcium pyroxene in equilibrium with a given melt and the temperature of that equilibrium - the liquidus or saturation temperature. Taking an initial temperature estimate of 1200°C the amount of the four quadrilateral components is calculated, as mentioned above the sum of these components has no stoichiometric value so their constituent components must be evaluated.

$$X_{Di}^{Px} = X_{Mg}^{M1} X_{Ca}^{M2} \qquad (96)$$

$$X_{Hd}^{Px} = X_{Fe}^{M1} X_{Ca}^{M2} \qquad (97)$$

so

$$X_{Ca}^{M2} \left(X_{Fe}^{M1} + X_{Mg}^{M1} \right) = X_{Di}^{Px} + X_{Hd}^{Px} \qquad (98)$$

and as

$$X_{Mg}^{M1} + X_{Fe}^{M1} = 1 \qquad (99)$$

$$X_{Ca}^{M2} = X_{Di}^{Px} + X_{Hd}^{Px} \qquad (100)$$

once X_{Ca}^{M2} is known then the other constituent components, X_{Mg}^{M1}, X_{Fe}^{M1}, X_{Mg}^{M2} and X_{Fe}^{M2} can be calculated. These constituent components should sum to 2, if the sum is less than 2 the initial temperature estimate is too high and is lowered by 75°C, if the sum is greater than 2 the temperature is increased by 75°C. The process is repeated with the new temperature estimate and the temperature adjusted by half that in the last step (37.5°C) and so on down to a final temperature adjustment of 0.5°C. At this stage the pyroxene composition is that in equilibrium with the melt at the final temperature.

Natural pyroxenes are never pure Mg, Ca and Fe so some allowance has to be made for the presence of "minor" elements. As $NaAlSi_2O_6$ is such a minor constituent of pyroxenes it can be ignored, although $Mn_2Si_2O_6$ produced a better fit than any of the other components Mn^{2+} is less important than Al^{3+}, Cr^{3+} or Ti^{4+}.

Thus Al^{3+} is evaluated using the equation given in table 5.10. Although this has a poor fit it does allow for the presence of Al^{3+}. Cr^{3+} and Ti^{4+} are evaluated using the constant values suggested by figs. 5.10 and 5.11 respectively, $\ln K_{Cr}=2$, $\ln K_{Ti}=-0.5$. These "minor" elements are allowed for in the sum, thus:-

$$X^{M1}_{Mg} + X^{M1}_{Fe} + X^{M2}_{Mg} + X^{M2}_{Fe} + X^{M2}_{Ca} = 2 - (Al + Cr + Ti) \quad (101)$$

The use of this "minor" element correction made very little difference to the temperature or pyroxene composition predictions, however, it has been retained because it more accurately describes pyroxene behaviour.

Using the liquid compositions in the data set the accuracy of the temperature and activity predictions is as follows:-

component	accuracy (2σ)	
	opx	pig
T	±30°C	±30°C
$Mg_2Si_2O_6$	±7.5%	±32%
$Fe_2Si_2O_6$	±47%	±45%
$MgCaSi_2O_6$	±40%	±50%
$FeCaSi_2O_6$	±50%	±55%

Plots of calculated v observed are given in fig. 5.14a-e.

TABLE 5.1

Pyroxene Recalculation Scheme of Lindsley & Anderson

Clinopyroxene

$X = Fe^{2+} / (Fe^{2+} + Mg)$

end-member		assessed on the presence of
$NaFe^{3+}Si_2O_6$	(Ac)	Na or Fe^{3+} - whichever is smaller
$NaAl^{vi}Si_2O_6$	(Jd)	Al^{vi} or any remaining Na - whichever is smaller
$CaFe^{3+}AlSiO_6$	(CaFeTs)	remaining Fe^{3+}
$CaCr^{3+}AlSiO_6$	(CaCrTs)	all Cr^{3+}
$CaAl_2O_6$	(CaAlTs)	remaining Al^{vi}
"Ca"		for augite - remaining Ca for pigeonite - 2 - $(Fe^{2+} + Mg)$
$Ca_2Si_2O_6$	(Wo)	["Ca" + Ac - CaAlTs - CaCrTs - CaFeTs] / 2
$Mg_2Si_2O_6$	(En)	(1 - Wo)(1 - X)
$Fe_2Si_2O_6$	(Fs)	(1 - Wo)X

Orthopyroxene

$X = Fe^{2+} / (Fe^{2+} + Mg)$

$R^{3+} = Al^{vi} + Cr^{3+} + Fe^{3+}$

$R^{2+} = [Mg(1 - X) + Fe^{2+}(x)]$

end-member		assessed on the prsence of
$NaR^{3+}Si_2O_6$	(Ac)	Na or R^{3+} - whichever is smaller
$NaTiAlSiO_6$		Ti or Al^{iv} or remaining Na whichever is smaller
$R^{2+}TiAl_2O_6$		remaining Ti or $Al^{iv}/2$ - whichever is smaller
$R^{2+}R^{3+}AlSiO_6$		remaining R^{3+} or Al^{iv}
$Ca_2Si_2O_6$	(Wo)	$Ca/(Ca + Mg + Fe^{2+})$
$Mg_2Si_2O_6$	(En)	$Mg/(Ca + Mg + Fe^{2+})$
$Fe_2Si_2O_6$	(Fs)	$Fe/(Ca + Mg + Fe^{2+})$

TABLE 5.2

Site Occupancy Calculation of Ghiorso et al. (1983)

$$R = n_{Mg} / (n_{Mg} + n_{Fe})$$

$$n_{Mg}^{M1} = R/2 \times (n_{Ca} + n_{Mn} + n_{Na} + n_{Mg} + n_{Fe} - n_{Cr} - n_{Ti} - 1/2n_{Al})$$

$$n_{Mg}^{M2} = n_{Mg} - n_{Mg}^{M1}$$

$$n_{Fe}^{M1} = n_{Mg}^{M1} - (1/R - 1)$$

$$n_{Fe}^{M2} = n_{Fe} - n_{Fe}^{M1}$$

$$X_{Mg}^{M1} = n_{Mg}^{M1} / (n_{Cr} + 1/2n_{Al} + n_{Ti} + n_{Mg}^{M1} + n_{Fe}^{M1})$$

$$X_{Mg}^{M2} = n_{Mg}^{M2} / (n_{Ca} + n_{Mn} + n_{Na} + n_{Mg}^{M2} + n_{Fe}^{M2})$$

$$X_{Fe}^{M1} = n_{Fe}^{M1} / (n_{Cr} + 1/2n_{Al} + n_{Ti} + n_{Mg}^{M1} + n_{Fe}^{M1})$$

$$X_{Fe}^{M2} = n_{Fe}^{M2} / (n_{Ca} + n_{Mn} + n_{Na} + n_{Mg}^{M2} + n_{Fe}^{M2})$$

$$a_{MgSiO_3}^{opx} = (X_{Mg}^{M1} \times X_{Mg}^{M2})^{1/2}$$

$$a_{FeSiO_3}^{opx} = (X_{Fe}^{M1} \times X_{Fe}^{M2})^{1/2}$$

where n_{Mg}, n_{Fe} etc. are the number of atoms of Mg, Fe etc. in the mineral formula, n_{Mg}^{M1} is the number of atoms of Mg in the mineral formula per M1 site, X_{Fe}^{M1} is the site mole fraction of Fe in M1 and $a_{Mg_2Si_2O_6}^{opx}$ is the activity of enstatite in orthopyroxene.

TABLE 5.3

Summary of Low-Calcium Pyroxene - Melt Equilibria Models

Authors	Model	P range	T range	fO_2 range	accuracy
Nathan & Van Kirk 1978	Mineral temperature equations	1 bar	not given		±20°C
Nielsen & Drake 1979	Macroscopic M site pyroxene mixing model - modified Bottinga-Weill melt model	1 bar	1100-1320°C	IW	±20°C(1σ)
Lindsley & Anderson 1980	Pyroxene recalculation	1 bar	800-1300°C	<QFM	±50°C
Nielsen & Dungan 1983	Ideal mixing pyroxene model - modified Bottinga-Weill melt model	1 bar	not given	QFM - IW	±20°C(1σ)
Ghiorso et al. 1983	Ideal mixing pyroxene model - expanded regular solution melt model	0.001-20kb	1198-1723K	<QFM	±57°C(2σ)

TABLE 5.4

Results of Linear Regression for the Simple Pyroxene - Simple Liquid Model

Orthopyroxene

end-member	A	B	r
$Ca_2Si_2O_6$	14555	-7.9928	0.8432
$Mg_2Si_2O_6$	21620	-9.9558	0.9374
$Fe_2Si_2O_6$	3591.8	1.3703	0.1882

Pigeonite

end-member	A	B	r
$Ca_2Si_2O_6$	12978	-6.5165	0.8291
$Mg_2Si_2O_6$	20130	-9.0718	0.9174
$Fe_2Si_2O_6$	-2671.1	5.3871	0.1289

TABLE 5.5a

Results of Linear Regression for the Pyroxene Recalculation Scheme of Lindsley & Anderson (1980) - Simple Liquid Model

Orthopyroxene

end-member	A	B	r
$NaR^{3+}Si_2O_6$	-4272.9	-2.5859	0.2984
$NaTiAlSiO_6$	-4779.8	3.0287	0.1503
$R^{2+}TiAl_2O_6$	-591.33	1.2013	0.01239
$R^{2+}R^{3+}AlSiO_6$	3078.9	-5.1405	0.1327
$Ca_2Si_2O_6$	18364	-10.019	0.8690
$Mg_2Si_2O_6$	21546	-9.9055	0.9414
$Fe_2Si_2O_6$	2500.7	1.9354	0.0939

Pigeonite

end-member	A	B	r
$NaFe^{3+}Si_2O_6$	-1097.5	-43.161	0.01512
$NaAlSi_2O_6$	-16258	7.6739	0.3768
$CaFe^{3+}AlSiO_6$	-1140.4	1.1753	0.02106
$CaCrAlSiO_6$	3049.4	-1.0063	0.1584
$CaAl_2SiO_6$			
$Ca_2Si_2O_6$	10390	-10.645	0.4406
$Mg_2Si_2O_6$	20997	-14.195	0.9280
$Fe_2Si_2O_6$	-2077.1	0.4000	0.1008

TABLE 5.5b

Results of Linear Regression for the Pyroxene Recalculation Scheme of Lindsley & Anderson (1980) - Simple Liquid Model (without Fe_2O_3 in the pyroxene)

Orthopyroxene

end-member	A	B	r
$NaR^{3+}Si_2O_6$	-11212	1.8477	0.5988
$NaTiAlSiO_6$	-24824	15.979	0.5959
$R^{2+}TiAl_2O_6$	-10345	7.4398	0.1965
$R^{2+}R^{3+}AlSiO_6$	-3882.5	-1.4637	0.09439
$Ca_2Si_2O_6$	18105	-10.025	0.8685
$Mg_2Si_2O_6$	21272	-9.7385	0.9353
$Fe_2Si_2O_6$	3244.1	1.5876	0.1701

Pigeonite

end-member	A	B	r
$NaFe^{3+}Si_2O_6$	302.38	-1.3238	0.0046
$NaAlSi_2O_6$	-16258	7.6739	0.3768
$CaFe^{3+}AlSiO_6$			
$CaCrAlSiO_6$	3049.4	-1.0063	0.1584
$CaAl_2SiO_6$			
$Ca_2Si_2O_6$	12719	-12.167	0.6457
$Mg_2Si_2O_6$	20841	-14.103	0.9259
$Fe_2Si_2O_6$	-1960.5	0.3555	0.09587

TABLE 5:6

Pyroxene Recalculation Scheme of Cawthorn & Collerson

end-member		assessed on the presence of
$NaAl^{vi}Si_2O_6$	(Jd)	All Na+k, if Na+K > Al^{vi} then excess produces acmite
$(Na,K)(Fe^{3+}Cr)Si_2O_6$	(Ac)	Na+K, if Fe^{3+} (+Cr) is unknown it is assumed to equal the excess Na+K. If Fe^{3+} (+Cr) is known and less than Na+K then Fe^{2+} is used
$Ca(Fe^{3+}Cr)_2SiO_6$	(CaFeTs)	Fe^{3+} (+Cr) if in excess of Na + K in acmite. If Cr contents are significant $CaCr_2SiO_6$ may be calculated
$CaTiAl_2O_6$	(CaTiTs)	All Ti
$CaAl_2SiO_6$	(CaTs)	Al less Al used in Jd and CaTiTs
$Ca_2Si_2O_6$	(Wo)	Ca less Ca used in CaFeTs, CaTs and CaTiTs
$Mg_2Si_2O_6$	(En)	Mg + Ni
$Fe_2Si_2O_6$	(Fs)	Fe^{2+} + Mn

end-members used for model		assessed on
$(Na,K)AlSi_2O_6$	(Jd)	Na + K, if Na + K < Al
$(Na,K)FeSi_2O_6$	(Ac)	Na, Fe^{2+} converted to Fe^{3+} if Fe^{3+} insufficient or absent
$CaFe_2^{3+}SiO_6$	(CaFeTs)	Fe^{3+} if present
$CaCr_2SiO_6$	(CaCrTs)	Cr^{3+} if present
$CaTi(Al,Fe^{3+})_2O_6$	(CaTiTs)	Ti, Fe^{2+} converted to Fe^{3+} if Al is deficient
$CaAl_2SiO_6$	(CaTs)	Al if remaining
$Ca_2Si_2O_6$	(Ca)	Ca if remaining
$(Mg,Ni)_2Si_2O_6$	(Mg)	Mg
$Fe_2Si_2O_6$	(Fe)	Fe^{2+}
$CaMnSi_2O_6$	(Mn)	Mn if present

$MgCaSi_2O_6$ = Ca x [Mg/(Mg+Fe)]

$FeCaSi_2O_6$ = Ca x [1 - (Mg/(Mg+Fe))]

$Mg_2Si_2O_6$ = Mg - Di

$Fe_2Si_2O_6$ = Fe - Di

TABLE 5.7

Results of Linear Regression for the Pyroxene Recalculation Scheme of Cawthorn & Collerson (1974) - Simple Liquid Model

Orthopyroxene

end-member	A	B	r
$(Na,K)AlSi_2O_6$	-3962.7	-2.0218	0.2693
$(Na,K)Fe^{3+}Si_2O_6$			
$CaFe^{3+}_2SiO_6$			
$CaTi(Al,Fe^{3+})_2O_6$	-1629.6	1.2107	0.09512
$CaAl_2SiO_6$	631.66	-3.1694	0.02613
$Mg_2Si_2O_6$	21258	-14.359	0.9359
$Fe_2Si_2O_6$	3230.2	-3.0331	0.1696
$MgCaSi_2O_6$	26658	-20.906	0.8720
$FeCaSi_2O_6$	25034	-20.968	0.8550
$CaCr_2SiO_6$	16622	-5.4358	0.3801
$CaMnSi_2O_6$	11239	-7.7245	0.8025

Pigeonite

end-member	A	B	r
$(Na,K)AlSi_2O_6$	1932.9	-4.7080	0.04374
$(Na,K)Fe^{3+}Si_2O_6$			
$CaFe^{3+}_2SiO_6$			
$CaTi(Al,Fe^{3+})_2O_6$	-1134.9	1.0289	0.05805
$CaAl_2SiO_6$	-3616.2	-0.6043	0.1333
$Mg_2Si_2O_6$	19110	-13.082	0.9027
$Fe_2Si_2O_6$	-3772.5	1.4297	0.1763
$MgCaSi_2O_6$	21138	-16.489	0.8900
$FeCaSi_2O_6$	17627	-15.257	0.8117
$CaCr_2SiO_6$	25096	-11.670	0.4355
$CaMnSi_2O_6$	7231.3	-5.1241	0.4360

TABLE 5.8

Pyroxene Recalculation Scheme of Schweitzer et al. (1979)

Alkalic Basalts

$CaTiAl_2O_6$
$CaFe^{3+}SiAlO_6$
$NaFe^{3+}Si_2O_6$
$NaTi^{4+}SiAlO_6$
$Ca_2Si_2O_6$
$Mg_2Si_2O_6$
$Fe_2Si_2O_6$

Tholeiitic Basalts

end-member		for modelling assessed on
$CaFe^{3+}SiAlO_6$	(CaFeTs)	Fe^{3+}
$Fe^{2+}TiAl_2O_6$	(FeTiTs)	Ti^{4+}
$NaTiSiAlO_6$	(NaTiTs)	Na^{+}
$NaFe^{3+}Si_2O_6$	(Ac)	Fe^{3+} - not used
$CaAlSiAlO_6$	(CaTs)	Al^{vi} if remaining
$MgCrSiAlO_6$	(MgCrTs)	Cr^{3+}
$Ca_2Si_2O_6$	(Wo)	Ca less Ca used in CaFeTs and CaTs
$Mg_2Si_2O_6$	(En)	Mg less Mg used in MgCrTs
$Fe_2Si_2O_6$	(Fs)	Fe less Fe used in FeTiTs

TABLE 5.9

Results of Linear Regression for the Pyroxene Recalculation Scheme of Schweitzer et al. (1979) -- Simple Liquid Model

Orthopyroxene

end-member	A	B	r
$Fe^{2+}TiAl_2O_6$	-6465.4	4.7817	0.2832
$NaTiSiAlO_6$	-10832	6.5848	0.3047
$CaAlSiAlO_6$			
$MgCrSiAlO_6$	5631.8	-3.1916	0.2655
$Ca_2Si_2O_6$	15364	-8.6490	0.6152
$Mg_2Si_2O_6$	21644	-9.9683	0.9377
$Fe_2Si_2O_6$	3575.9	1.3786	0.1868

Pigeonite

end-member	A	B	r
$Fe^{2+}TiAl_2O_6$	-9471.6	6.9314	0.4061
$NaTiSiAlO_6$	-14330	9.3882	0.4005
$CaAlSiAlO_6$	-17311	8.8937	0.4542
$MgCrSiAlO_6$	14748	-8.9407	0.5917
$Ca_2Si_2O_6$	15202	-8.0997	0.8894
$Mg_2Si_2O_6$	20145	-9.0750	0.9175
$Fe_2Si_2O_6$	-2924	5.5493	0.1401

TABLE 5.10

Results of Linear Regression for the Ideal Mixing Pyroxene - Polymer Liquid Model

Orthopyroxene

end-member	A	B	r
$Mg_2Si_2O_6$	15548	-5.5985	0.9604
$Fe_2Si_2O_6$	12716	-6.0305	0.7940
$MgCaSi_2O_6$	19644	-10.647	0.9481
$FeCaSi_2O_6$	18228	-10.863	0.9031
MnO	8023.5	-5.4428	0.7979
Na_2O	1267.9	-4.5192	0.1023
Cr_2O_3	-7629.3	6.9681	0.3318
TiO_2	3412.5	-3.3095	0.2455
Al_2O_3	3387.8	-4.4098	0.1677
$Mn_2Si_2O_6$	16261	-8.1998	0.8044
$NaAlSi_2O_6$	4532.7	-11.014	0.1856

Pigeonite

end-member	A	B	r
$Mg_2Si_2O_6$	14265	-4.8603	0.9014
$Fe_2Si_2O_6$	7406.4	-2.4836	0.6058
$MgCaSi_2O_6$	19605	-10.029	0.9240
$FeCaSi_2O_6$	16176	-8.8410	0.8863
MnO	6490.7	-4.3074	0.5582
Na_2O	1777.3	-3.7936	0.05207
Cr_2O_3	5553.2	-1.7029	0.2581
TiO_2	5997.5	-4.8922	0.3291
Al_2O_3	8559.5	-7.7675	0.4307
$Mn_2Si_2O_6$	12399	-5.4018	0.5303
$NaAlSi_2O_6$	-4092.3	-3.5482	0.0808

TABLE 5.11a

Results of Linear Regression for the Ideal Mixing Pyroxene - "Stoichiometric Mineral" - Liquid Model

Orthopyroxene

end-member	A	B	r
$Mg_2Si_2O_6$	-55.053	0.80595	0.01576
$Fe_2Si_2O_6$	22029	-16.939	0.8459
$MgCaSi_2O_6$	12130	-9.8539	0.7684
$FeCaSi_2O_6$	23172	-18.726	0.9079
$Mn_2Si_2O_6$	21875	-22.636	0.8655
$NaAlSi_2O_6$	4797.2	-13.564	0.1760

Pigeonite

end-member	A	B	r
$Mg_2Si_2O_6$	-4171.5	3.3863	0.4131
$Fe_2Si_2O_6$	18028	-14.143	0.8665
$MgCaSi_2O_6$	9789.2	-7.6435	0.7683
$FeCaSi_2O_6$	20889	-16.408	0.9049
$Mn_2Si_2O_6$	17564	-19.546	0.7028
$NaAlSi_2O_6$	-10004	-2.2657	0.1427

TABLE 5.11b

Results of Linear Regression for the Ideal Mixing Pyroxene - Regular Mixing Liquid Model of Ghiorso et al. (1983)

Orthopyroxene

end-member	A	B	r
$Mg_2Si_2O_6$	11415	-5.2540	0.8306
$Fe_2Si_2O_6$	17833	-12.549	0.7442
$MgCaSi_2O_6$	17366	-13.039	0.9285
$FeCaSi_2O_6$	21396	-16.687	0.8964
$Mn_2Si_2O_6$	15222.	-21.584	0.7436
$NaAlSi_2O_6$	3517	-13.145	0.1353

Pigeonite

end-member	A	B	r
$Mg_2SI_2O_6$	6181	-1.7727	0.6188
$Fe_2Si_2O_6$	15868	-11.257	0.7656
$MgCaSi_2O_6$	15698	-11.348	0.8706
$FeCaSi_2O_6$	21362	-16.089	0.9002
$Mn_2Si_2O_6$	14932	-21.091	0.5833
$NaAlSi_2O_6$	-9496.7	-3.0513	0.1395

TABLE 5.12

Interaction Parameters to go with Ghiorso et al.'s Liquid Model

Orthopyroxene

	En	Fs	Di	Hd	Mn
Fs	0				
Di	0	0			
Hd	0	0	0		
Mn	-2658.68	7163.23	0	0	
Jd	-8483.03	-165283	110516	-17187.9	0

Pigeonite

	En	Fs	Di	Hd	Mn
Fs	0				
Di	0	0			
Hd	0	0	0		
Mn	0	0	-7379.14	8144.14	
Jd	-3388.68	-71906.9	25699.3	0	0

TABLE 5.13

Results of Linear Regression for the Regular Mixing Pyroxene - Regular Mixing Liquid Model of Ghiorso et al. (1983)

Orthopyroxene

end-member	A	B	r
$Mg_2Si_2O_6$	11415	-5.2542	0.8306
$Fe_2Si_2O_6$	17833	-12.549	0.7441
$MgCaSi_2O_6$	17367	-13.040	0.9285
$FeCaSi_2O_6$	21369	-16.687	0.8964
$Mn_2Si_2O_6$	16288	-22.409	0.7599
$NaAlSi_2O_6$	-1907.1	-9.9388	0.07159

Pigeonite

end-member	A	B	r
$Mg_2Si_2O_6$	6181.2	-1.7728	0.6189
$Fe_2Si_2O_6$	15868	-11.257	0.7653
$MgCaSi_2O_6$	15698	-11.348	0.8706
$FeCaSi_2O_6$	21363	-16.089	0.9002
$Mn_2Si_2O_6$	15123	-21.259	0.5840
$NaAlSi_2O_6$	-13749	-0.3187	0.1886

TABLE 5.14

New Interaction Parameters, Melt Model after Ghiorso et al. (1983)

Orthopyroxene

	En	Fs	Di	Hd	Mn
Fs	0				
Di	0	0			
Hd	0	0	0		
Mn	-107425	-287921	0	0	
Jd	0	0	0	-3201.82	6271.89

Pigeonite

	En	Fs	Di	Hd	Mn
Fs	0				
Di	0	0			
Hd	0	0	0		
Mn	-81599.1	0	0	-153568	
Jd	0	0	0	-253.89	15660.3

Glass

	Si_4O_8	Ti_4O_8	$Al_{16/3}O_8$	$Fe_{16/3}O_8$	$Fe_4Si_2O_8$	$Mn_4Si_2O_8$	$Mg_4Si_2O_8$	$Ca_4Si_2O_8$	$Na_{16/3}O_8/3O_8$
Ti_4O_8	-293.650								
$Al_{16/3}O_8$	0	0							
$Fe_{16/3}O_8$	306.328	0	0						
$Fe_4Si_2O_6$	363.789	0	0	-1291.99					
$Mn_4Si_2O_8$	-416.634	2310.27	-3480.55	0	0				
$Mg_4Si_2O_8$	-13613.2	13542	0	30959.7	17060.5	0			
$Ca_4Si_2O_8$	0	0	0	0	0	-7997.47	0		
$Na_{16/3}Si_{8/3}O_8$	0	0	0	-4300.97	-5534.39	9944.21	0	0	
$K_{16/3}Si_{8/3}O_8$	0	0	299916	-10628.3	0	0	0	0	0

TABLE 5:15

Results of Linear Regression for the Regular Mixing Pyroxene - Regular Mixing Liquid Model using the new Interaction Parameters

Orthopyroxene

end-member	A	B	r
$Mg_2Si_2O_6$	673.17	-0.1586	0.08658
$Fe_2Si_2O_6$	24052	-18.797	0.8678
$MgCaSi_2O_6$	13042	-11.262	0.7714
$FeCaSi_2O_6$	24735	-20.582	0.9175
$Mn_2Si_2O_6$	28234	-33.358	0.8978
$NaAlSi_2O_6$	4833.9	-14.337	0.1774

Pigeonite

end-member	A	B	r
$Mg_2Si_2O_6$	-4296.9	2.9281	0.3345
$Fe_2Si_2O_6$	19700	-15.801	0.8900
$MgCaSi_2O_6$	10232	-8.7859	0.7761
$FeCaSi_2O_6$	22225	-18.147	0.9265
$Mn_2Si_2O_6$	32988	-34.135	0.7947
$NaAlSi_2O_6$	-10113	-2.9346	0.1452

TABLE 5:16

Interaction Parameters, Melt Model after Neilsen & Dungan

Orthopyroxene

	En	Fs	Di	Hd	Mn
Fs	0				
Di	0	0			
Hd	0	0	0		
Mn	-128610	-225044	-231515	-132138	
Jd	0	-2726.61	552.766	0	7792.66

Pigeonite

	En	Fs	Di	Hd	Mn
Fs	0				
Di	0	0			
Hd	0	0	0		
Mn	-80817	0	0	-178302	
Jd	0	0	0	-235.896	0

Glass

	SiO_2	$AlO_{0.5}$	$FeO_{0.5}$	FeO	MgO	CaO	$NaAlO_2$	$KAlO_2$	TiO_2
$AlO_{0.5}$	0								
$FeO_{0.5}$	0	0							
FeO	393.004	0	0						
MgO	527.55	0	0	-977.322					
CaO	-888.20	1406.87	0	0	0				
$NaAlO_2$	0	0	-60509.8	6957.83	0	0			
$KAlO_2$	19137.1	-21468.2	0	0	-4335.85	0	0		
TiO_2	0	0	0	-4235.41	-7065.16	12126.9	0	-128615	
MnO	-43952.2	0	300030	0	0	172334	0	35607.4	0

TABLE 5.17

Results of Linear Regression for the Regular Mixing Pyroxene - Regular Mixing Liquid Model after Nielsen & Dungan (1983)

Orthopyroxene

end-member	A	B	r
$Mg_2Si_2O_6$	16089	-8.6886	0.9602
$Fe_2Si_2O_6$	12629	-8.7139	0.7869
$MgCaSi_2O_6$	19601	-14.795	0.9488
$FeCaSi_2O_6$	17872	-14.808	0.9017
$Mn_2Si_2O_6$	6988.6	-16.733	0.2775
$NaAlSi_2O_6$	4588	-13.124	0.1872

Pigeonite

end-member	A	B	r
$Mg_2Si_2O_6$	15068	-8.1192	0.9070
$Fe_2Si_2O_6$	7518.3	-5.2906	0.6187
$MgCaSi_2O_6$	19523	-14.151	0.9225
$FeCaSi_2O_6$	15742	-12.733	0.8780
$Mn_2Si_2O_6$	21024	-21.785	0.6158
$NaAlSi_2O_6$	-4511.7	-5.3471	0.0899

TABLE 5:18

Correlation Coefficients for the Quadrilateral Components of all the Models Tested

Model	En	Fs	Di	Hd	Wo
1 Simple Pyroxene - Simple Liquid	0.9374 0.9174	0.1882 0.1289			0.8432 0.8291
2 Lindsley & Anderson + Fe_2O_3	0.9414 0.9280	0.0939 0.1008			0.8690 0.4406
3 Lindsley & Anderson - Fe_2O_3	0.9353 0.9259	0.1701 0.0959			0.8685 0.6457
4 Cawthorn & Collerson	0.9359 0.9027	0.1696 0.1763	0.8720 0.8900	0.8550 0.8117	
5 Schweitzer et al.	0.9377 0.9175	0.1868 0.1401			0.6152 0.8894
6 Nielsen & Dungan	0.9604 0.9014	0.7940 0.6058	0.9481 0.9240	0.9031 0.8863	
7 Ghiorso et al. "Stoichiometric Mineral"	0.0158 0.4131	0.8459 0.8665	0.7684 0.7683	0.9079 0.9049	
8 Ghiorso et al. Regular Mixing Liquid	0.8306 0.6188	0.7442 0.7656	0.9285 0.8706	0.8964 0.9002	
9 Ghiorso et al. Regular Mixing Pyroxene & Liquid	0.8306 0.6189	0.7441 0.7653	0.9285 0.8706	0.8964 0.9002	
10 Ghiorso et al. Regular Mixing Pyroxene & New Liquid	0.0866 0.3345	0.8678 0.8900	0.7714 0.7761	0.9175 0.9265	
11 Nielsen & Dungan Regular Mixing Pyroxene & Liquid	0.9602 0.9070	0.7896 0.6187	0.9488 0.9225	0.9017 0.8780	

For all models the uppermost number is the correlation coefficient for orthopyroxene, the lower one is the correlation coefficient for pigeonite.

For all figures in this chapter the key is

× opx

□ pig

Figure 5.1

lnK v 1/T(K) for the quadrilateral components of the simple pyroxene - simple liquid model.

Figure 5.1a $\ln K_{Wo}$ v 1/T

Figure 5.1b $\ln K_{En}$ v 1/T

Figure 5.1c $\ln K_{Fs}$ v 1/T

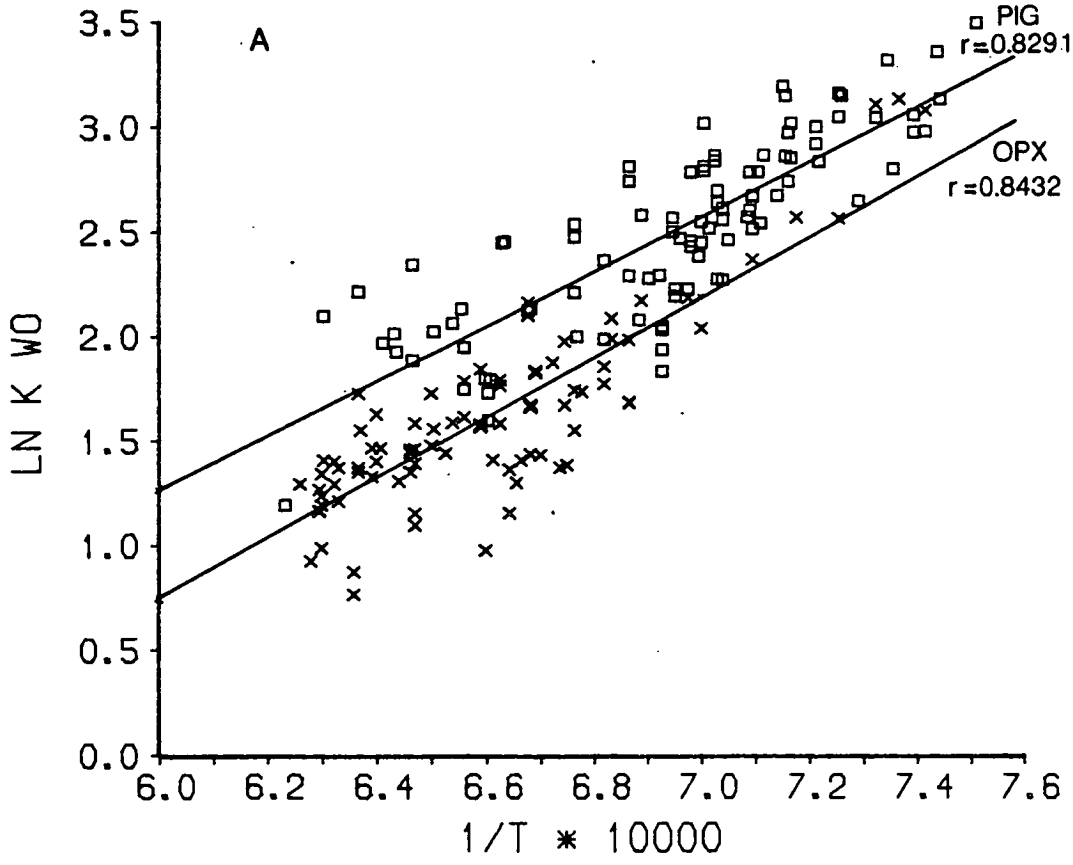

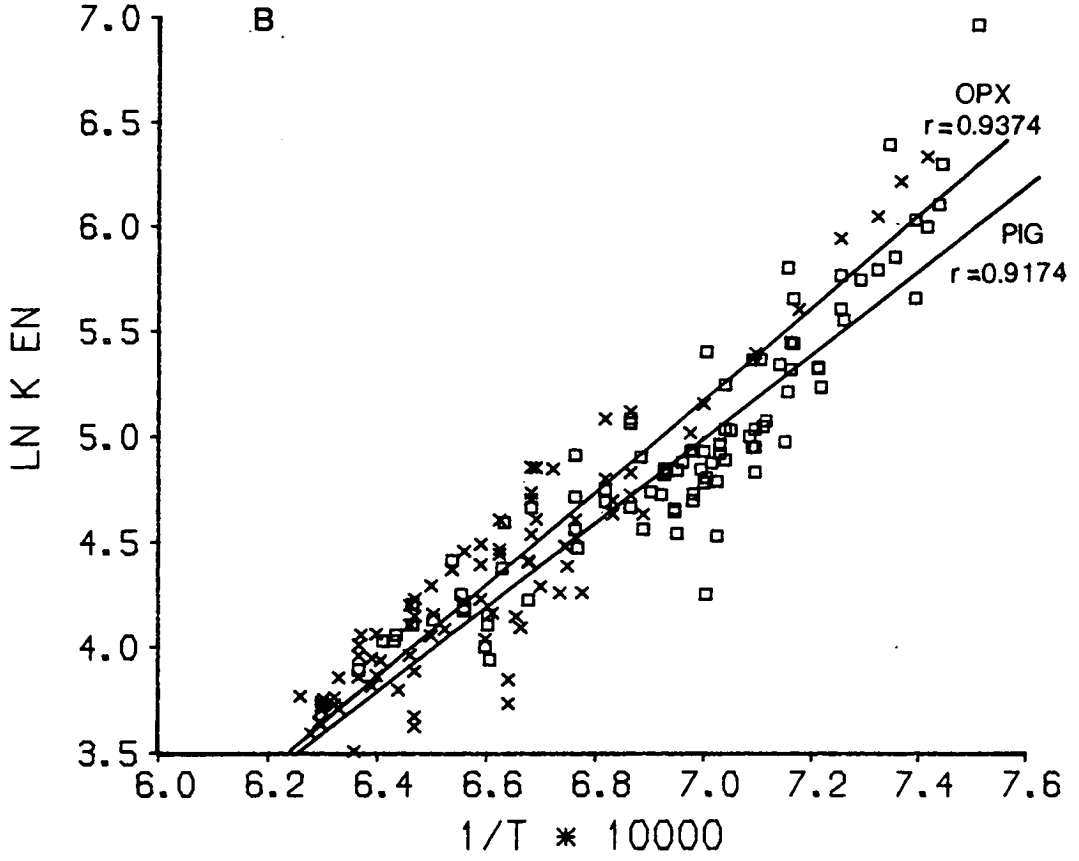
B
OPX
r=0.9374
PIG
r=0.9174
LN K EN
7.0
6.5
6.0
5.5
5.0
4.5
4.0
3.5
6.0
6.2
6.4
6.6
6.8
7.0
7.2
7.4
7.6
1/T * 10000

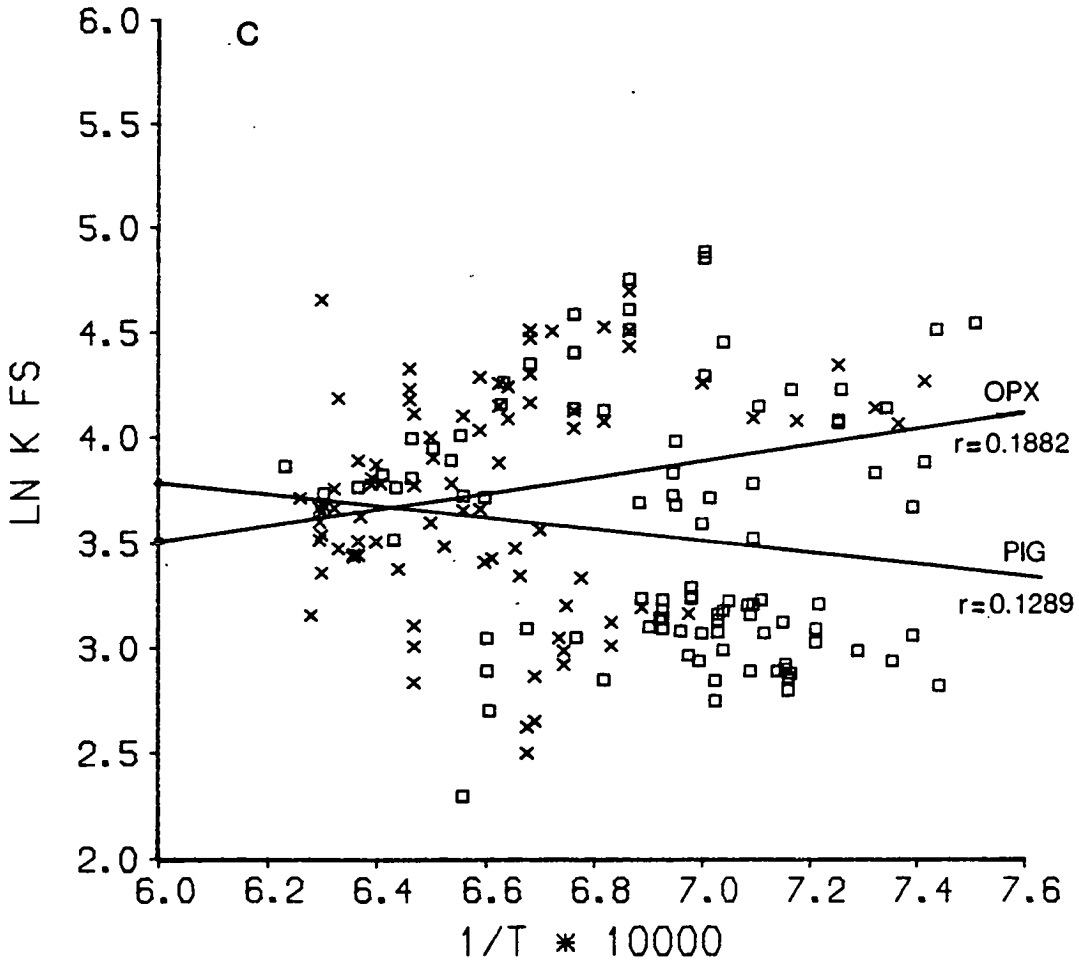
C
OPX
r=0.1882
PIG
r=0.1289
LN K FS
6.0
5.5
5.0
4.5
4.0
3.5
3.0
2.5
2.0
6.0
6.2
6.4
6.6
6.8
7.0
7.2
7.4
7.6
1/T * 10000

Figure 5.2

lnK v 1/T(K) for the quadrilateral components of the Lindsley & Anderson (1980) pyroxene recalculation scheme - simple liquid model.

Figure 5.2a $\ln K_{Wo}$ v 1/T

Figure 5.2b $\ln K_{En}$ v 1/T

Figure 5.2c $\ln K_{Fs}$ v 1/T

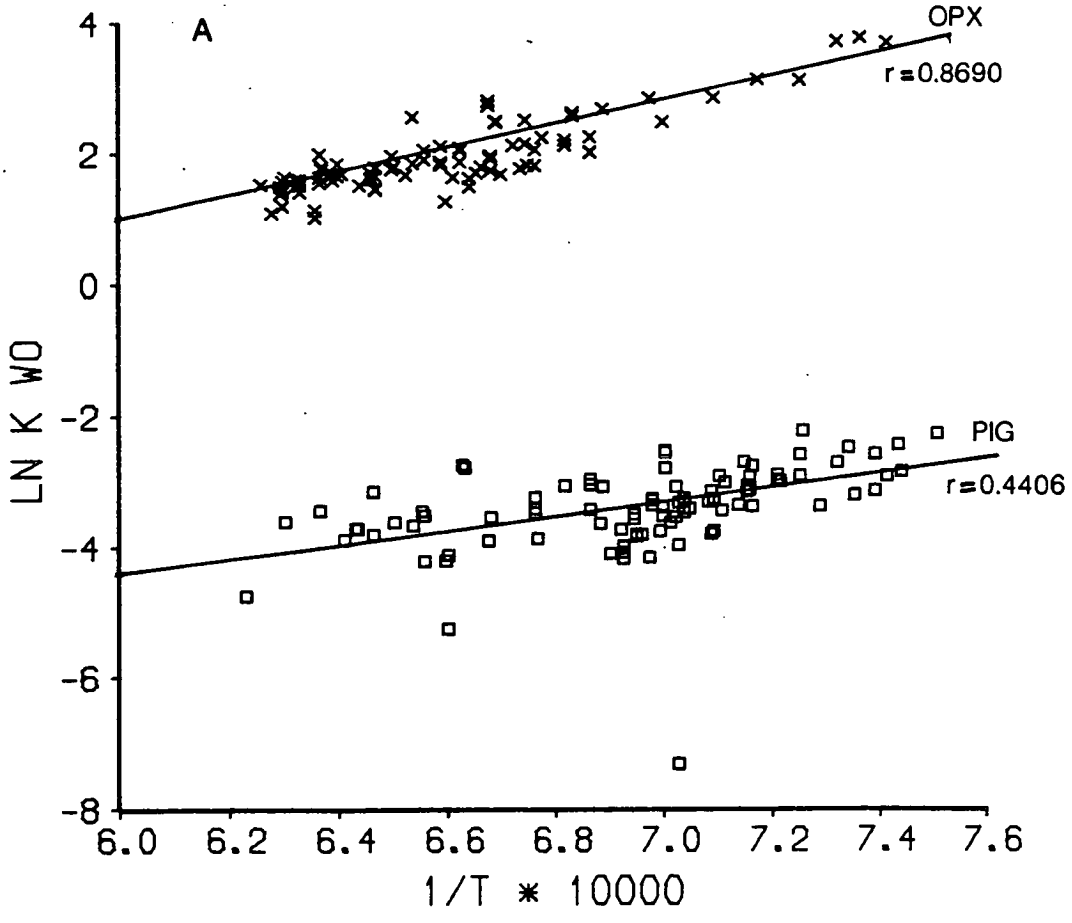

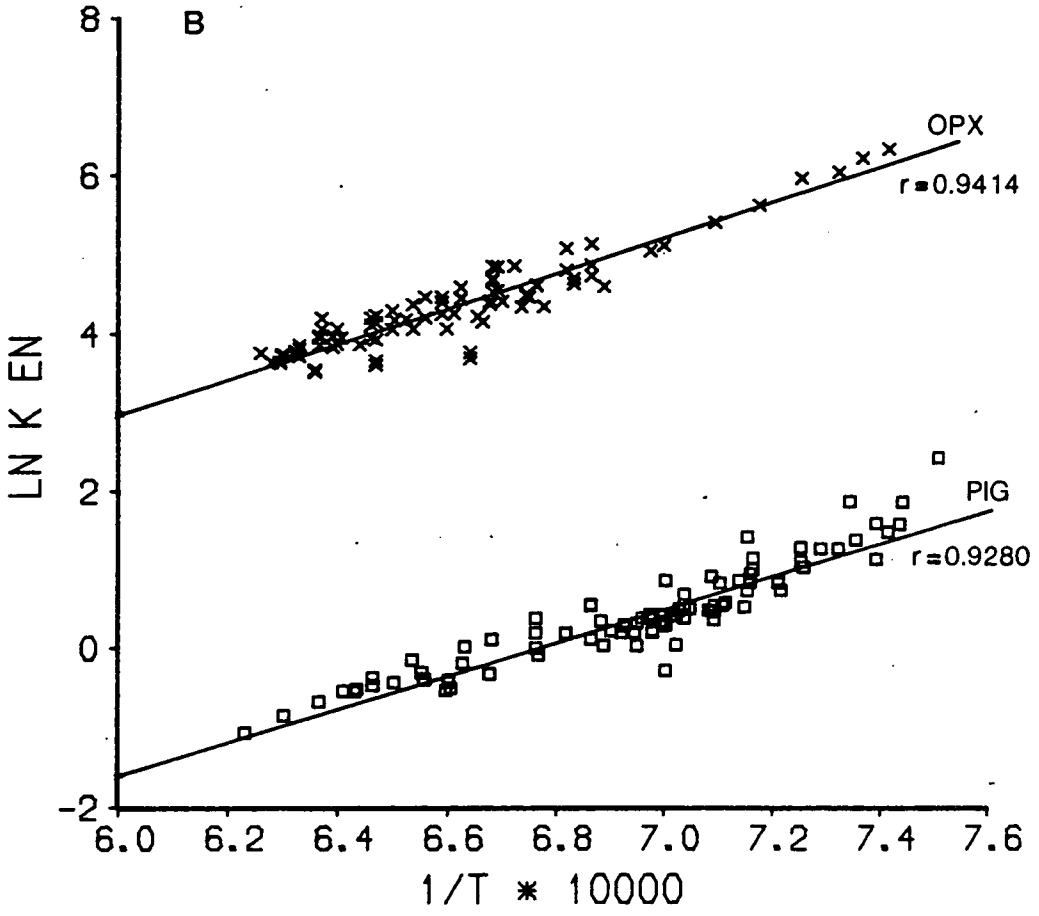
B
OPX
r=0.9414
PIG
r=0.9280
LN K EN
8
6
4
2
0
-2
6.0
6.2
6.4
6.6
6.8
7.0
7.2
7.4
7.6
1/T * 10000

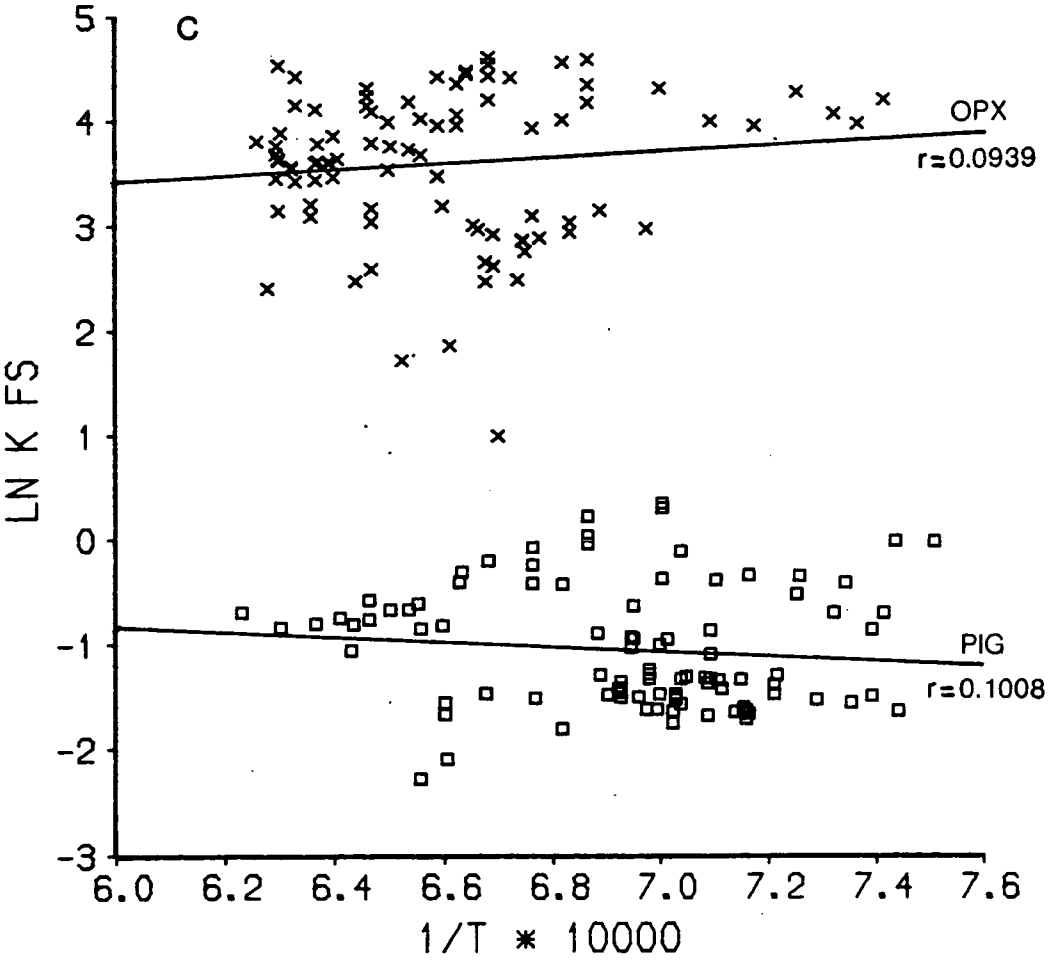
C
OPX
r=0.0939
PIG
r=0.1008
LN K FS
5
4
3
2
1
0
-1
-2
-3
6.0
6.2
6.4
6.6
6.8
7.0
7.2
7.4
7.6
1/T * 10000

Figure 5.3

lnK v 1/T(K) for the quadrilateral components of the Cawthorn & Collerson (1974) pyroxene recalculation scheme - simple liquid model.

Figure 5.3a $\ln K_{En}$ v 1/T

Figure 5.3b $\ln K_{Fs}$ v 1/T

Figure 5.3c $\ln K_{Di}$ v 1/T

Figure 5.3d $\ln K_{Hd}$ v 1/T

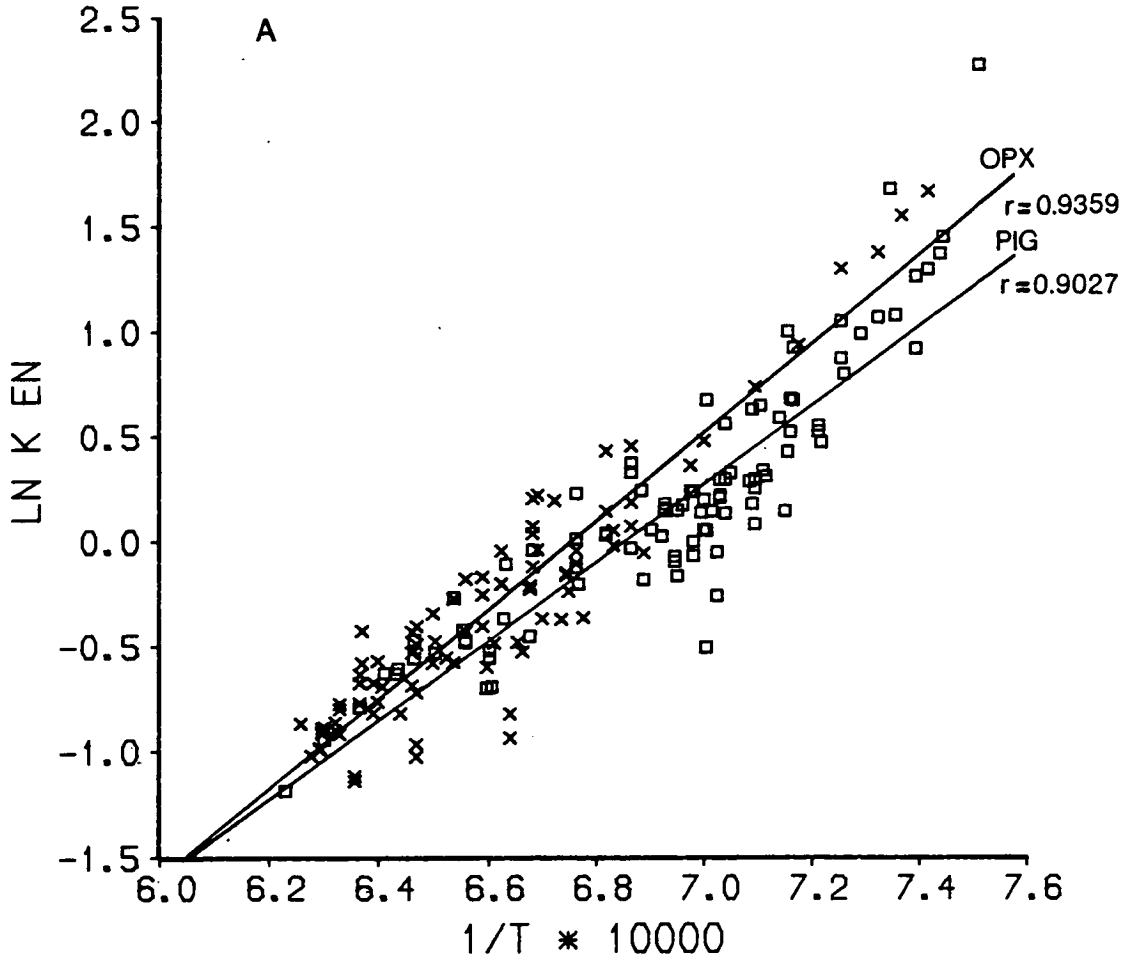
A
OPX
r=0.9359
PIG
r=0.9027
LN K EN
2.5
2.0
1.5
1.0
0.5
0.0
-0.5
-1.0
-1.5
6.0
6.2
6.4
6.6
6.8
7.0
7.2
7.4
7.6
1/T * 10000

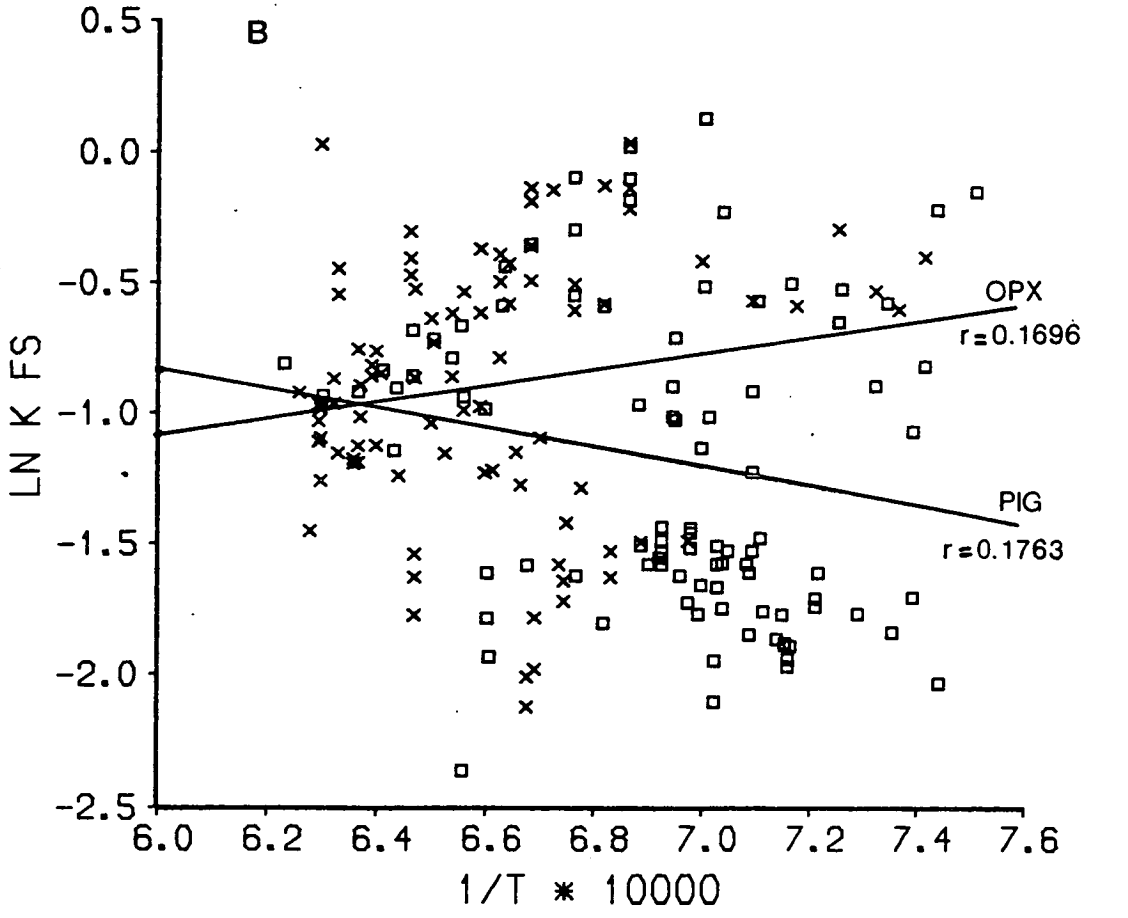
B
OPX
r=0.1696
PIG
r=0.1763
LN K FS
0.5
0.0
-0.5
-1.0
-1.5
-2.0
-2.5
6.0
6.2
6.4
6.6
6.8
7.0
7.2
7.4
7.6
1/T * 10000

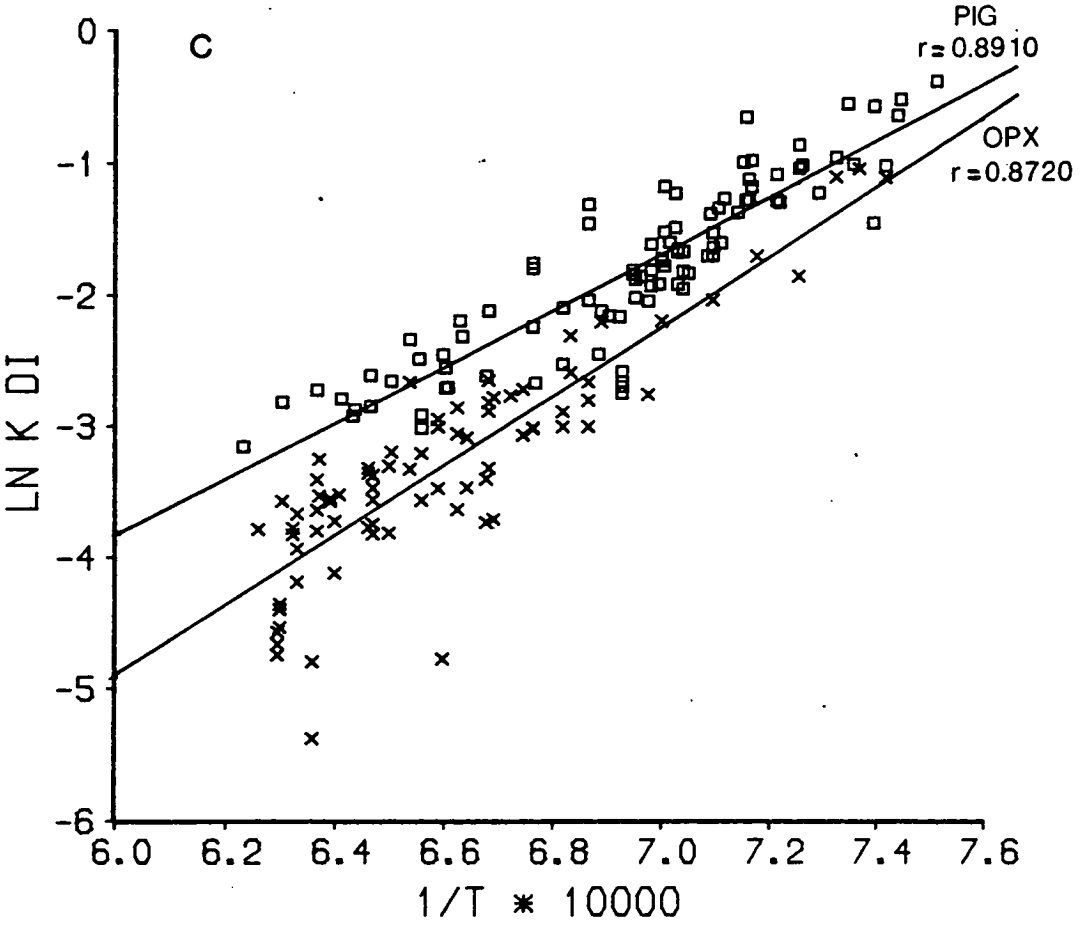
C
PIG
r=0.8910
OPX
r=0.8720
LN K DI
0
-1
-2
-3
-4
-5
-6
6.0
6.2
6.4
6.6
6.8
7.0
7.2
7.4
7.6
1/T * 10000

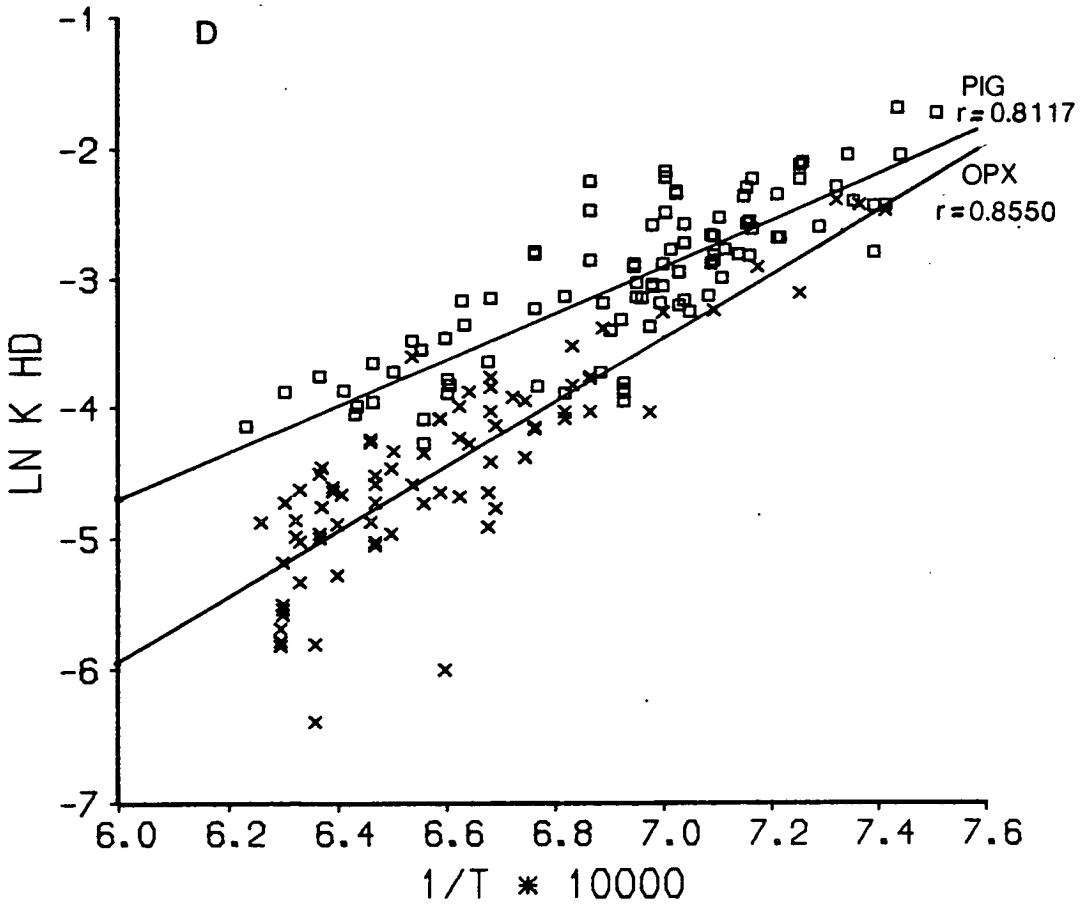
D
PIG
r=0.8117
OPX
r=0.8550
LN K HD
-1
-2
-3
-4
-5
-6
-7
6.0
6.2
6.4
6.6
6.8
7.0
7.2
7.4
7.6
1/T * 10000

Figure 5.4

lnK v 1/T(K) for the quadrilateral components of the Schweitzer et al. (1979) pyroxene recalculation scheme - simple liquid model.

Figure 5.4a $\ln K_{Wo}$ v 1/T

Figure 5.4b $\ln K_{En}$ v 1/T

Figure 5.4c $\ln K_{Fs}$ v 1/T

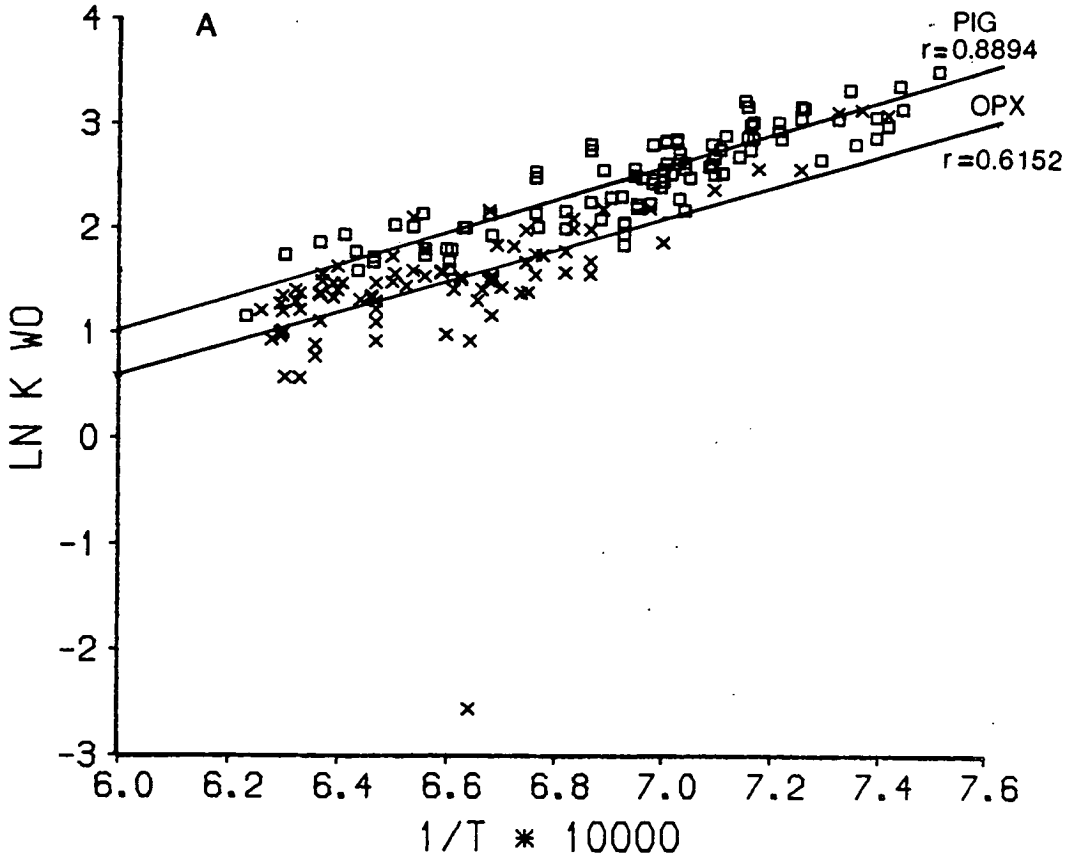

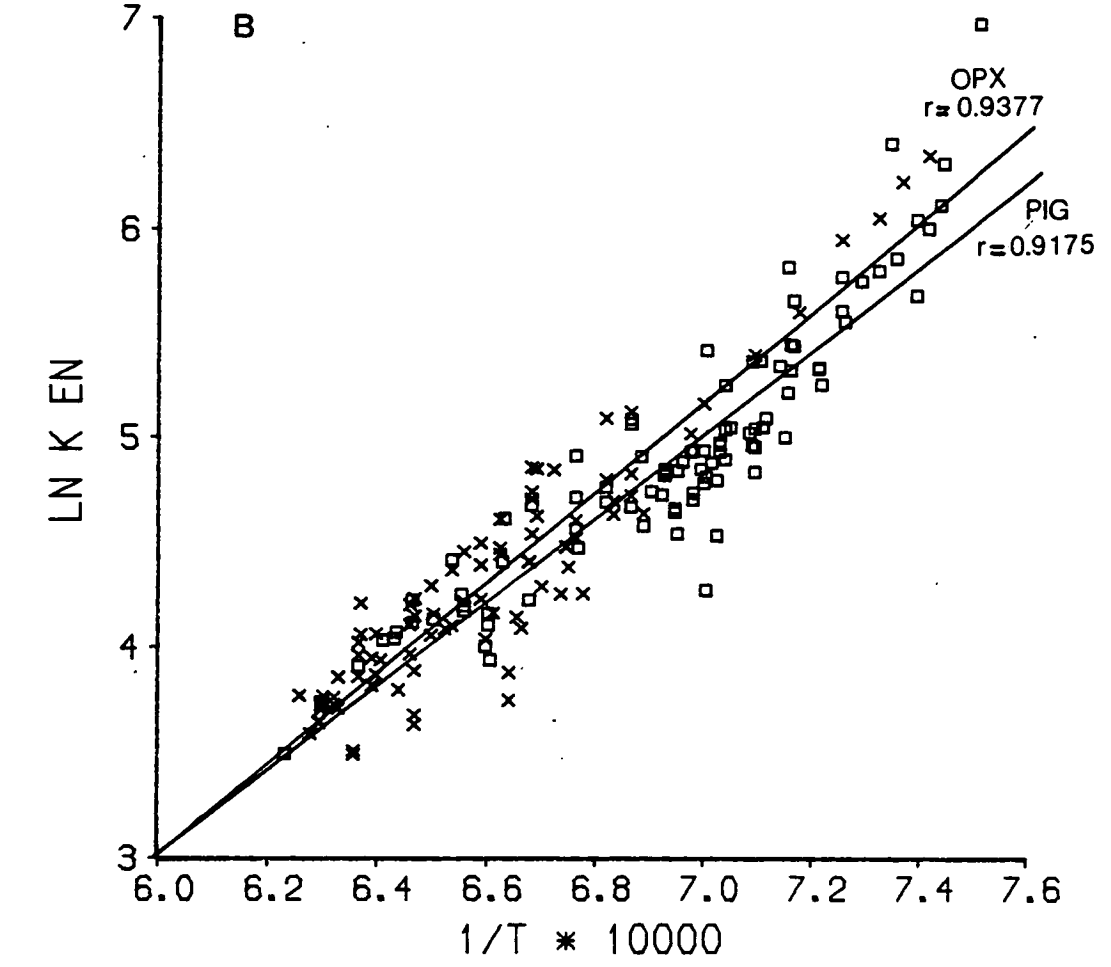
B
OPX
r= 0.9377
PIG
r=0.9175
LN K EN
7
6
5
4
3
6.0
6.2
6.4
6.6
6.8
7.0
7.2
7.4
7.6
1/T * 10000

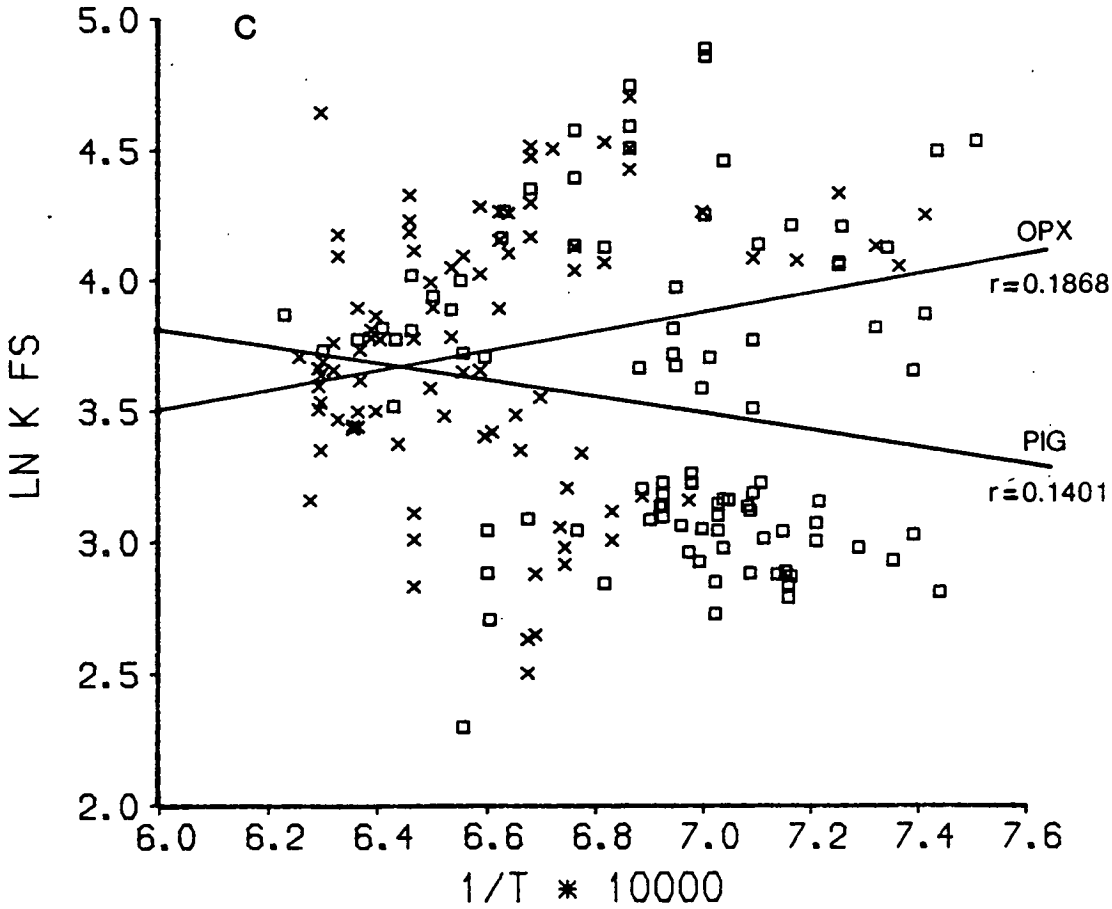
C
OPX
r=0.1868
PIG
r=0.1401
LN K FS
5.0
4.5
4.0
3.5
3.0
2.5
2.0
6.0
6.2
6.4
6.6
6.8
7.0
7.2
7.4
7.6
1/T * 10000

Figure 5.5

lnK v 1/T(K) for the quadrilateral components of the ideal mixing pyroxene - polymer liquid model of Nielsen & Dungan (1983).

Figure 5.5a $\ln K_{En}$ v 1/T

Figure 5.5b $\ln K_{Fs}$ v 1/T

Figure 5.5c $\ln K_{Di}$ v 1/T

Figure 5.5d $\ln K_{Hd}$ v 1/T

Figure 5.5e $\ln K_{Mn}$ v 1/T

Figure 5.5f $\ln K_{Jd}$ v 1/T

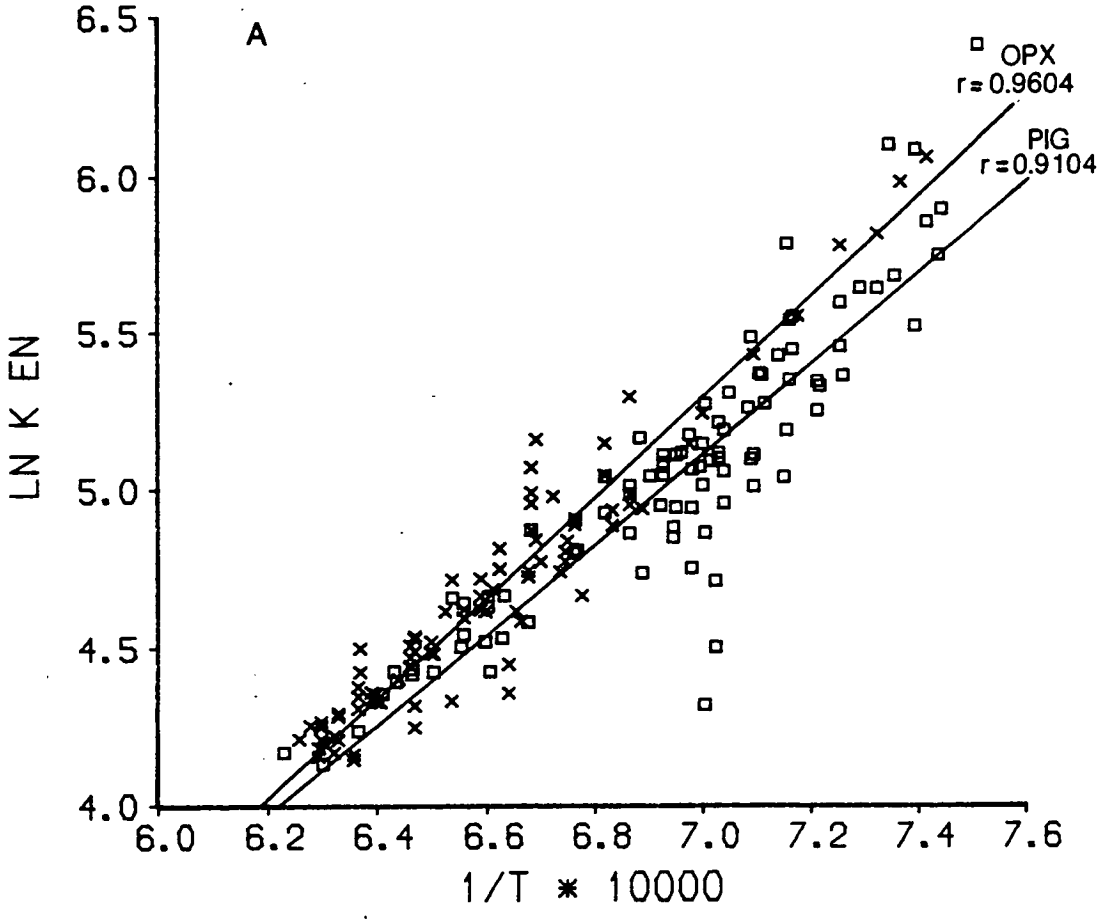
A
OPX
r = 0.9604
PIG
r = 0.9104
LN K EN
6.5
6.0
5.5
5.0
4.5
4.0
6.0
6.2
6.4
6.6
6.8
7.0
7.2
7.4
7.6
1/T * 10000

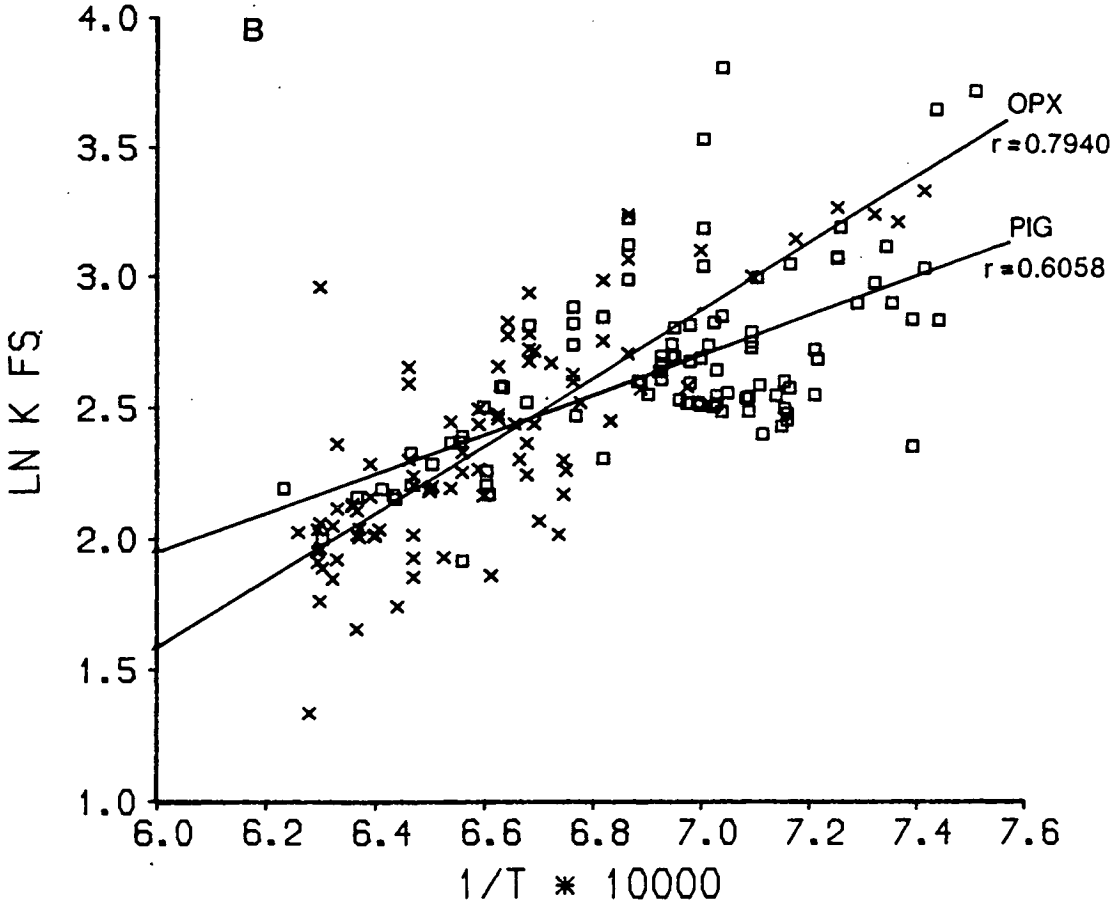
B
OPX
r = 0.7940
PIG
r = 0.6058
LN K FS
4.0
3.5
3.0
2.5
2.0
1.5
1.0
6.0
6.2
6.4
6.6
6.8
7.0
7.2
7.4
7.6
1/T * 10000

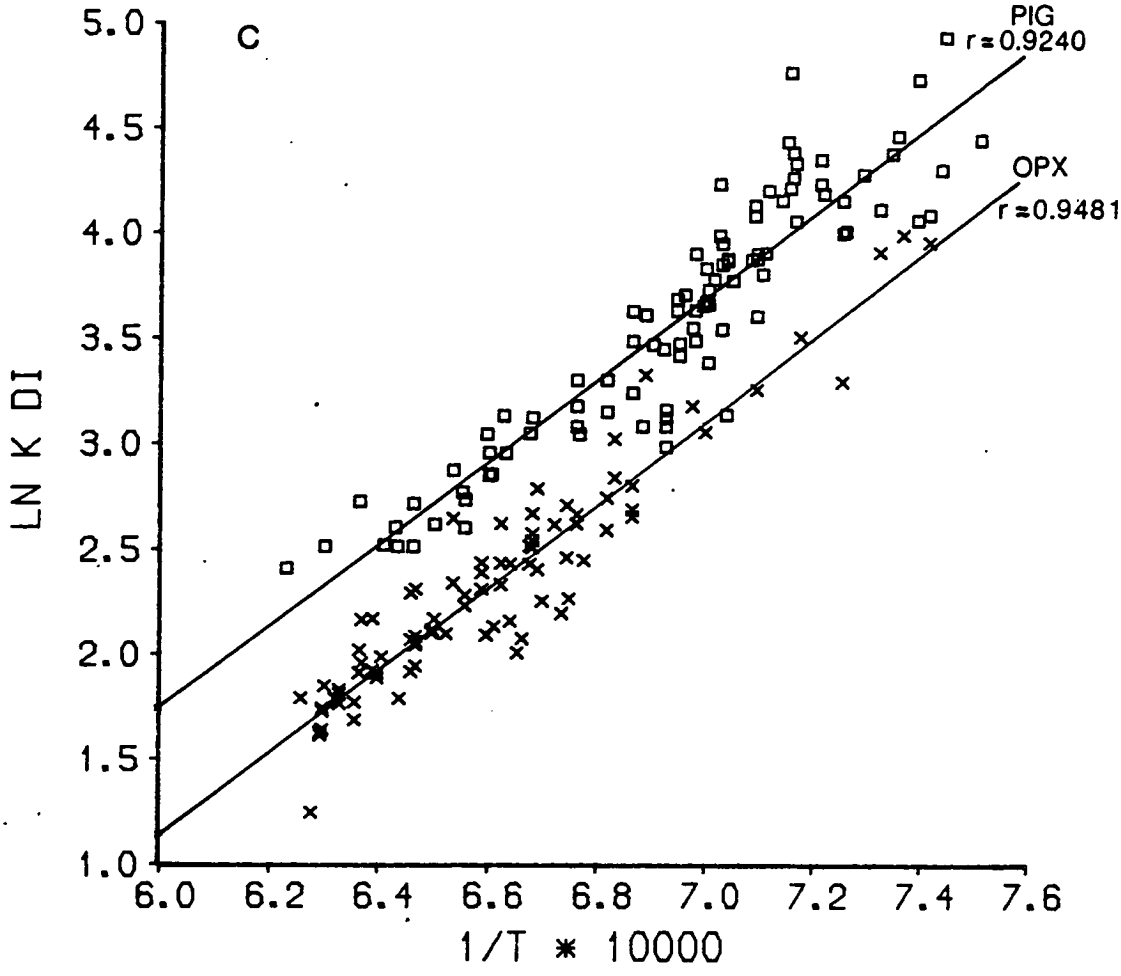
C
PIG
r=0.9240
OPX
r=0.9481
LN K DI
5.0
4.5
4.0
3.5
3.0
2.5
2.0
1.5
1.0
6.0
6.2
6.4
6.6
6.8
7.0
7.2
7.4
7.6
1/T * 10000

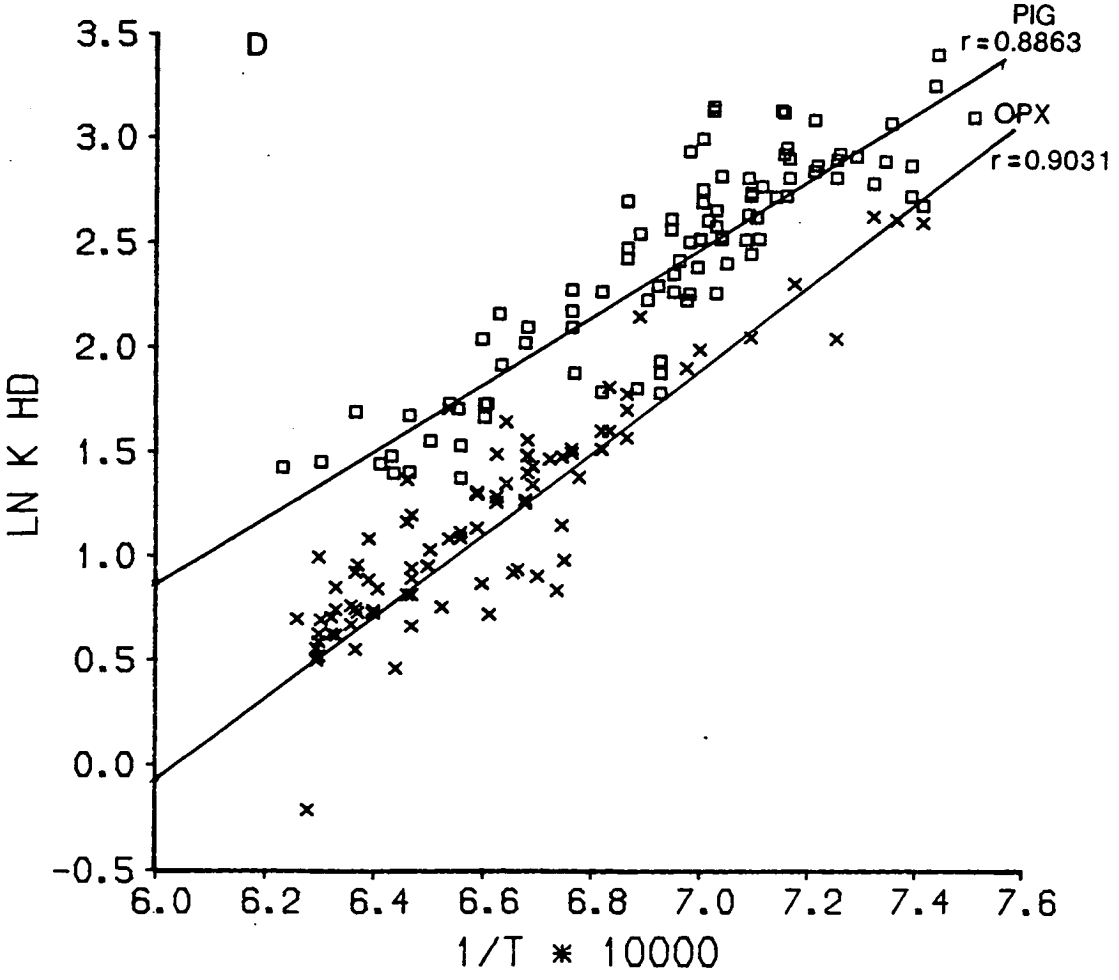
D
PIG
r=0.8863
OPX
r=0.9031
LN K HD
3.5
3.0
2.5
2.0
1.5
1.0
0.5
0.0
-0.5
6.0
6.2
6.4
6.6
6.8
7.0
7.2
7.4
7.6
1/T * 10000

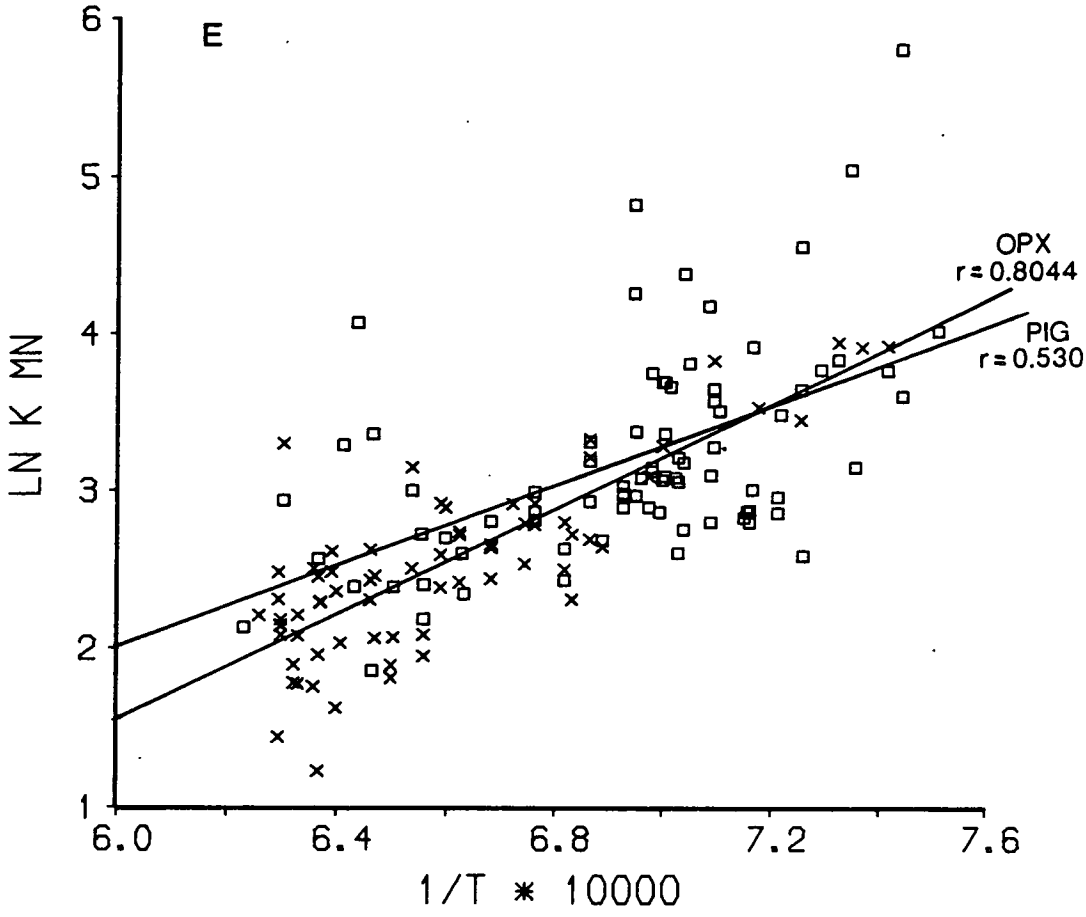
E
LN K MN
1/T * 10000
OPX
r=0.8044
PIG
r=0.5303
6
5
4
3
2
1
6.0
6.4
6.8
7.2
7.6

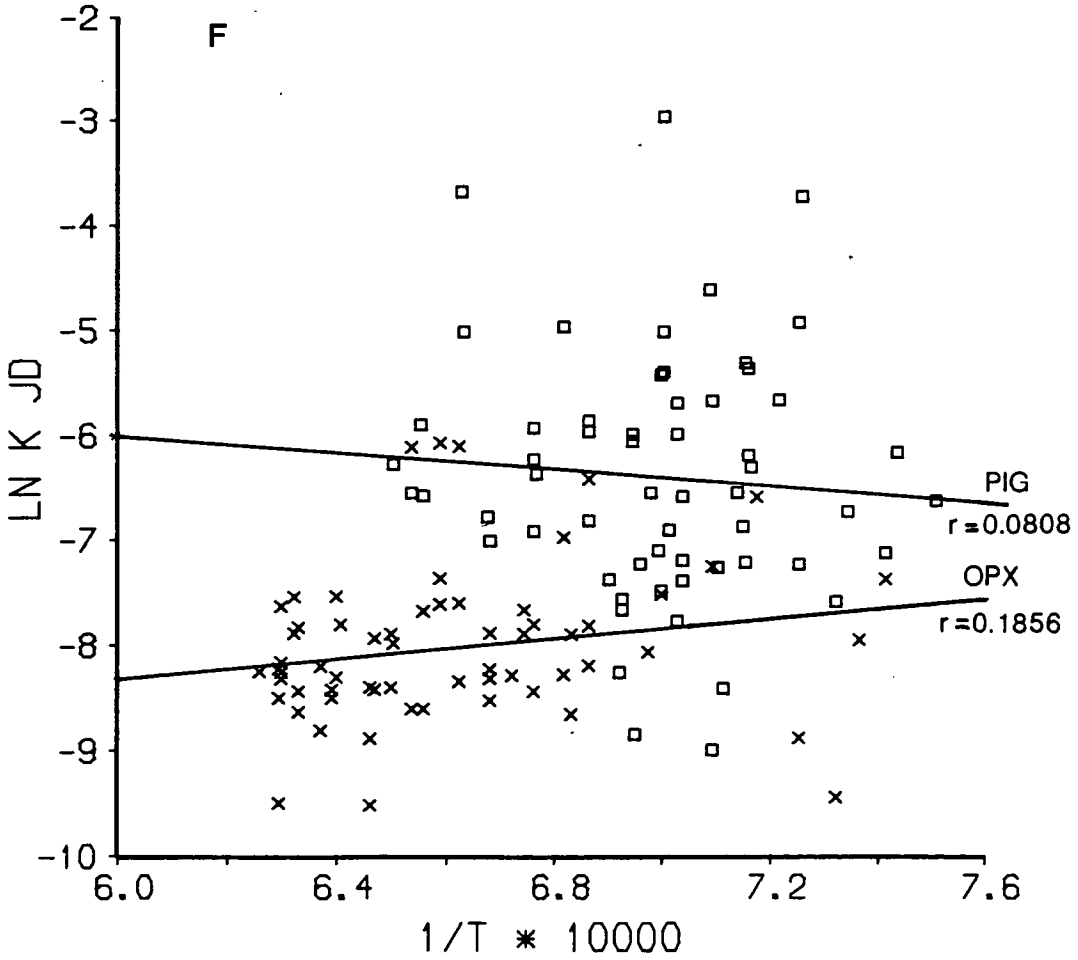
F
LN K JD
1/T * 10000
PIG
r=0.0808
OPX
r=0.1856
-2
-3
-4
-5
-6
-7
-8
-9
-10
6.0
6.4
6.8
7.2
7.6

Figure 5.6

lnK v 1/T(K) for the quadrilateral components of the ideal mixing pyroxene - "stoichiometric mineral" liquid model (after Ghiorso et al., 1983).

Figure 5.6a $\ln K_{En}$ v 1/T

Figure 5.6b $\ln K_{Fs}$ v 1/T

Figure 5.6c $\ln K_{Di}$ v 1/T

Figure 5.6d $\ln K_{Hd}$ v 1/T

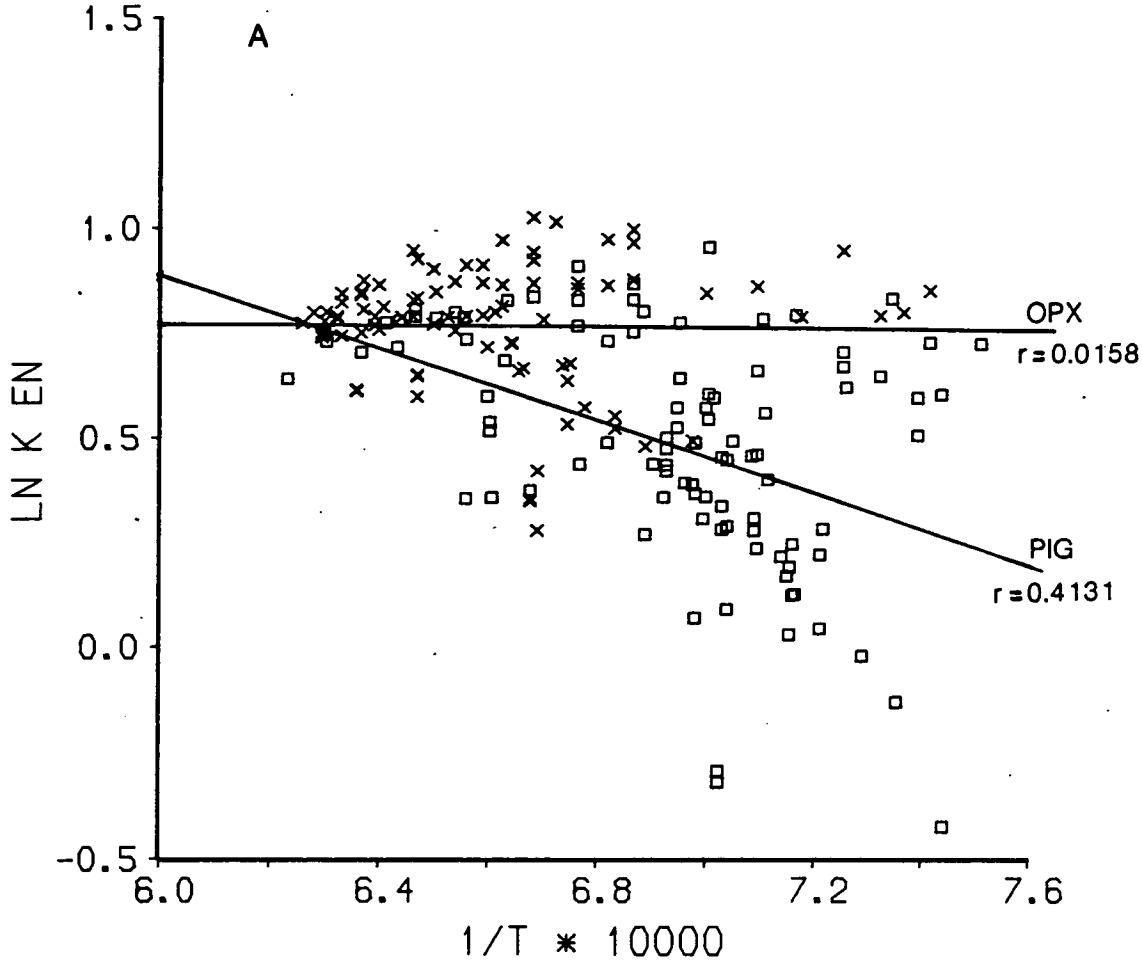
A
1.5
1.0
0.5
0.0
-0.5
LN K EN
6.0
6.4
6.8
7.2
7.6
1/T * 10000
OPX
r=0.0158
PIG
r=0.4131

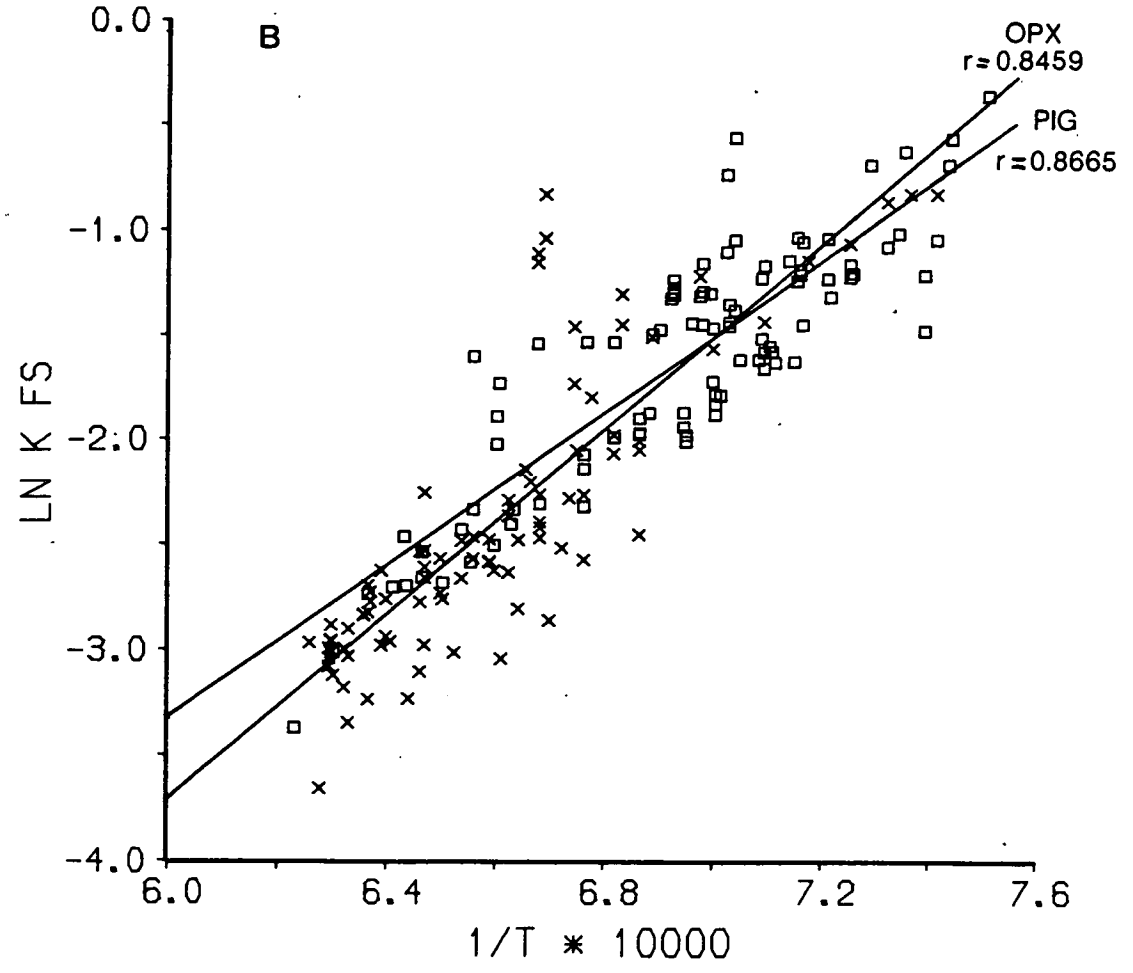
B
0.0
-1.0
-2.0
-3.0
-4.0
LN K FS
6.0
6.4
6.8
7.2
7.6
1/T * 10000
OPX
r=0.8459
PIG
r=0.8665

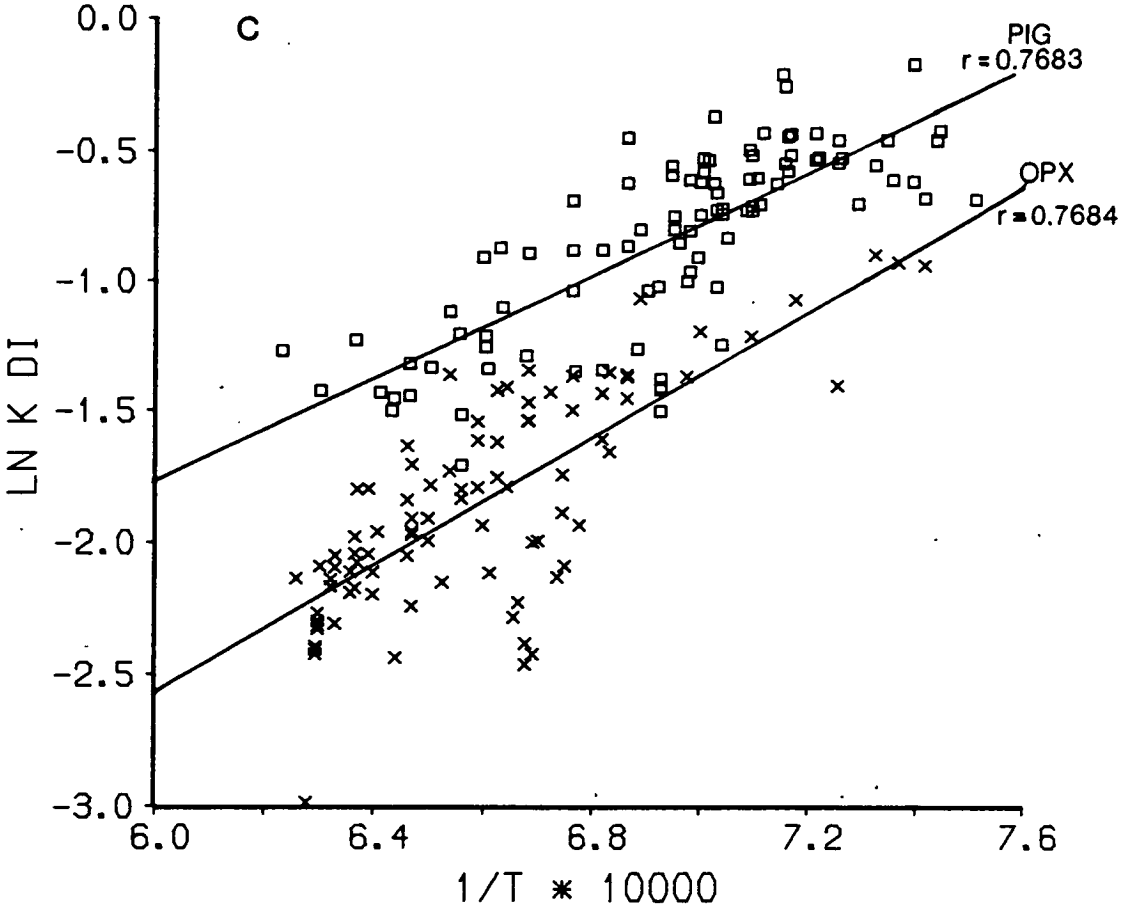
C
PIG
r = 0.7683
OPX
r = 0.7684
LN K DI
0.0
-0.5
-1.0
-1.5
-2.0
-2.5
-3.0
6.0
6.4
6.8
7.2
7.6
1/T * 10000

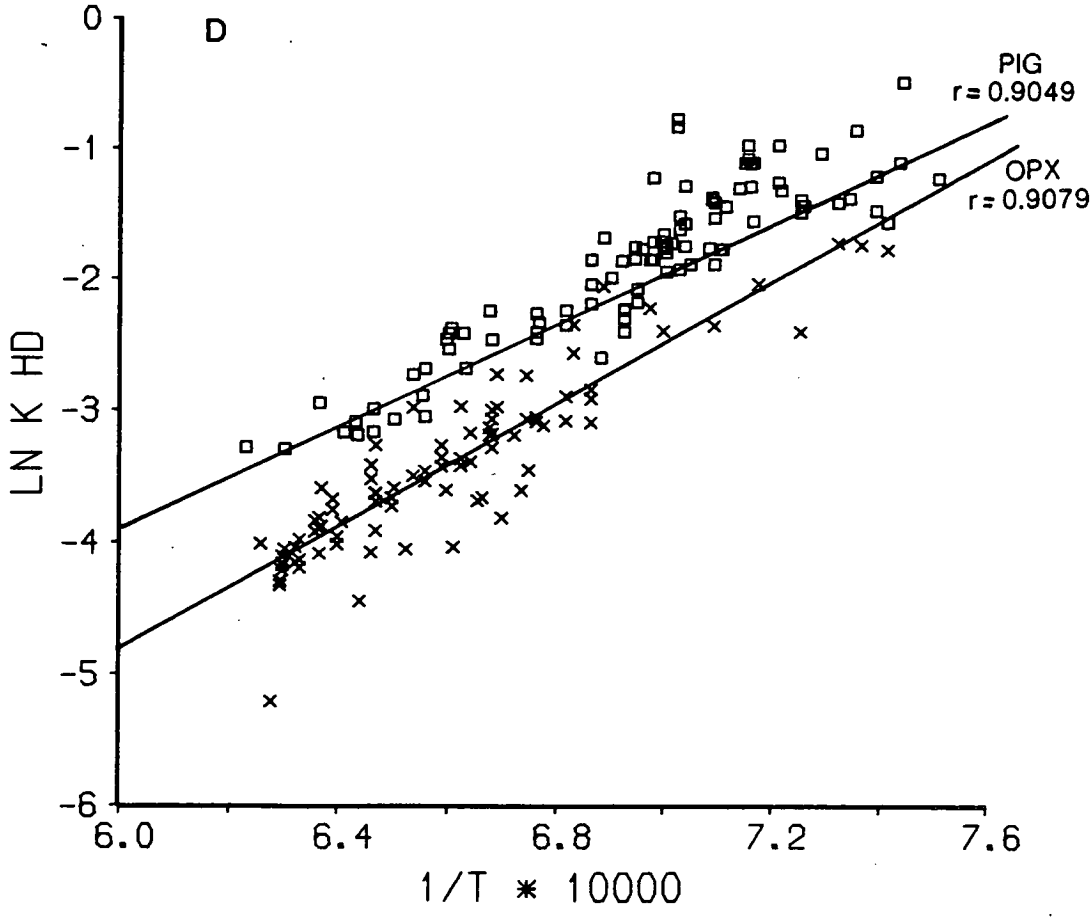
D
PIG
r = 0.9049
OPX
r = 0.9079
LN K HD
0
-1
-2
-3
-4
-5
-6
6.0
6.4
6.8
7.2
7.6
1/T * 10000

Figure 5.7

lnK v 1/T(K) for quadrilateral components of the ideal mixing pyroxene - regular mixing liquid model of Ghiorso et al. (1983).

Figure 5.7a $\ln K_{En}$ v 1/T

Figure 5.7b $\ln K_{Fs}$ v 1/T

Figure 5.7c $\ln K_{Di}$ v 1/T

Figure 5.7d $\ln K_{Hd}$ v 1/T

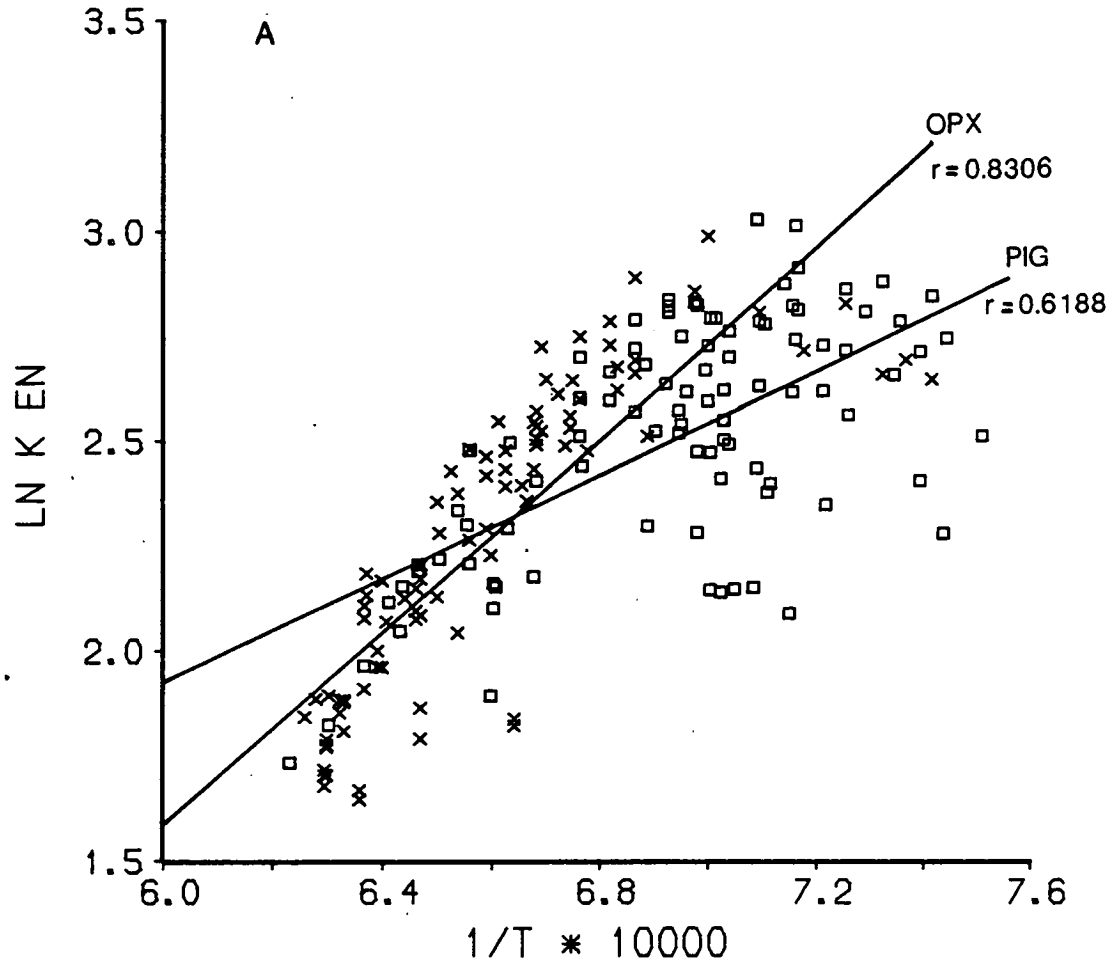
A
OPX
r = 0.8306
PIG
r = 0.6188
LN K EN
3.5
3.0
2.5
2.0
1.5
6.0
6.4
6.8
7.2
7.6
1/T * 10000

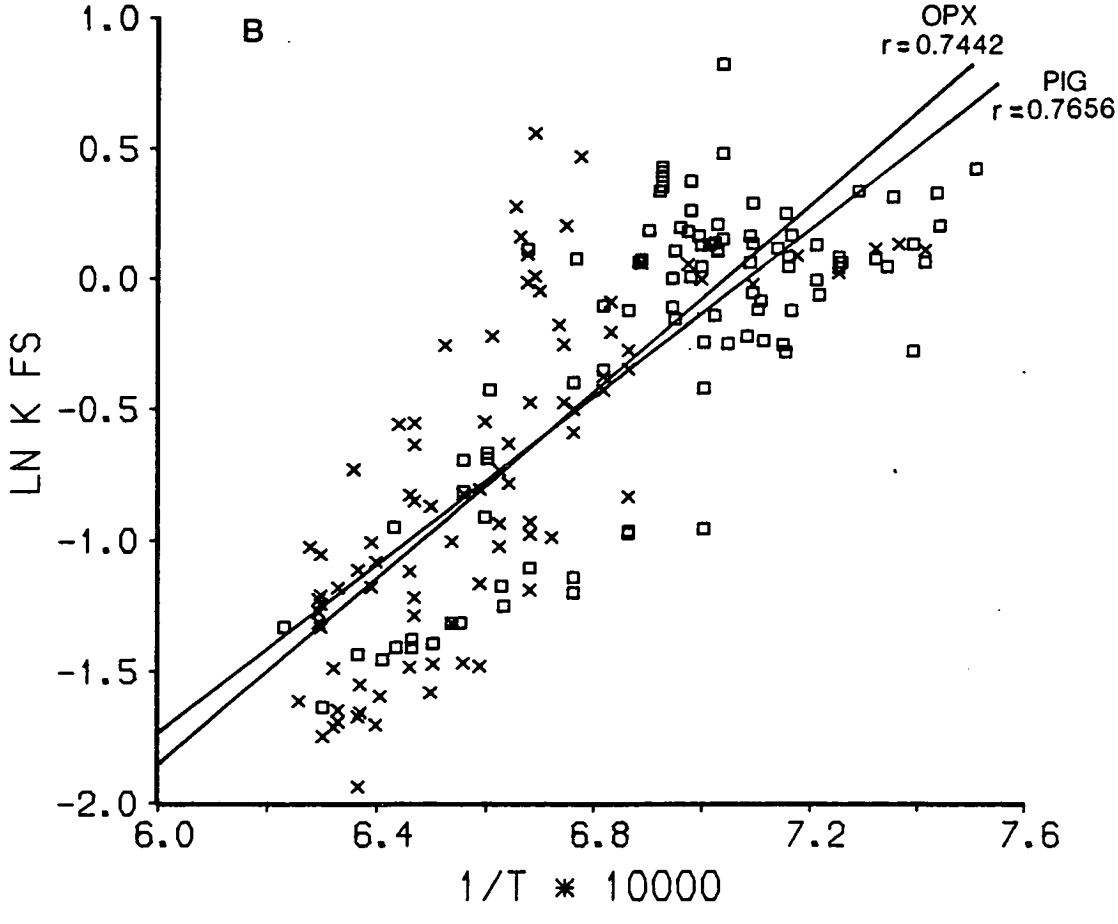
B
OPX
r = 0.7442
PIG
r = 0.7656
LN K FS
1.0
0.5
0.0
-0.5
-1.0
-1.5
-2.0
6.0
6.4
6.8
7.2
7.6
1/T * 10000

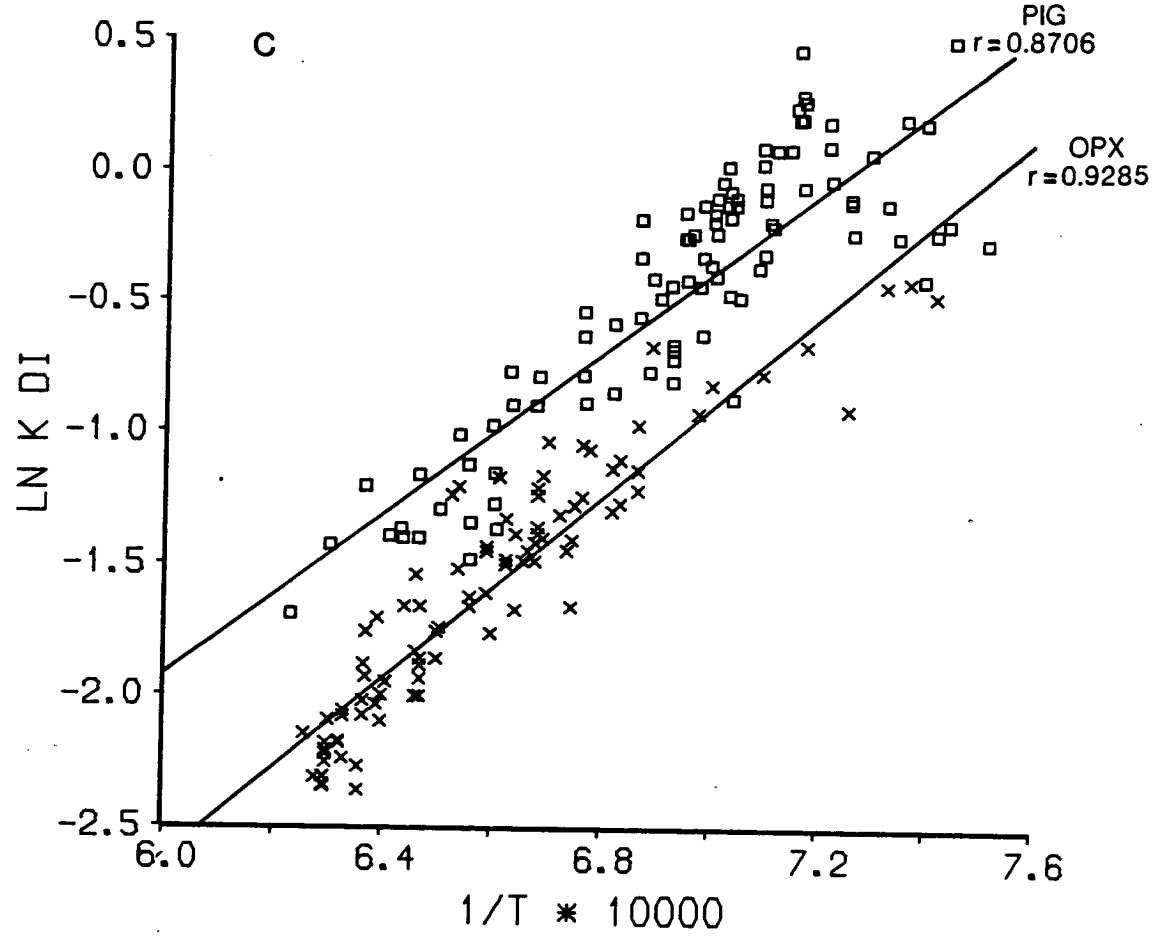
C
PIG
r=0.8706
OPX
r=0.9285
LN K DI
0.5
0.0
-0.5
-1.0
-1.5
-2.0
-2.5
6.0
6.4
6.8
7.2
7.6
1/T * 10000

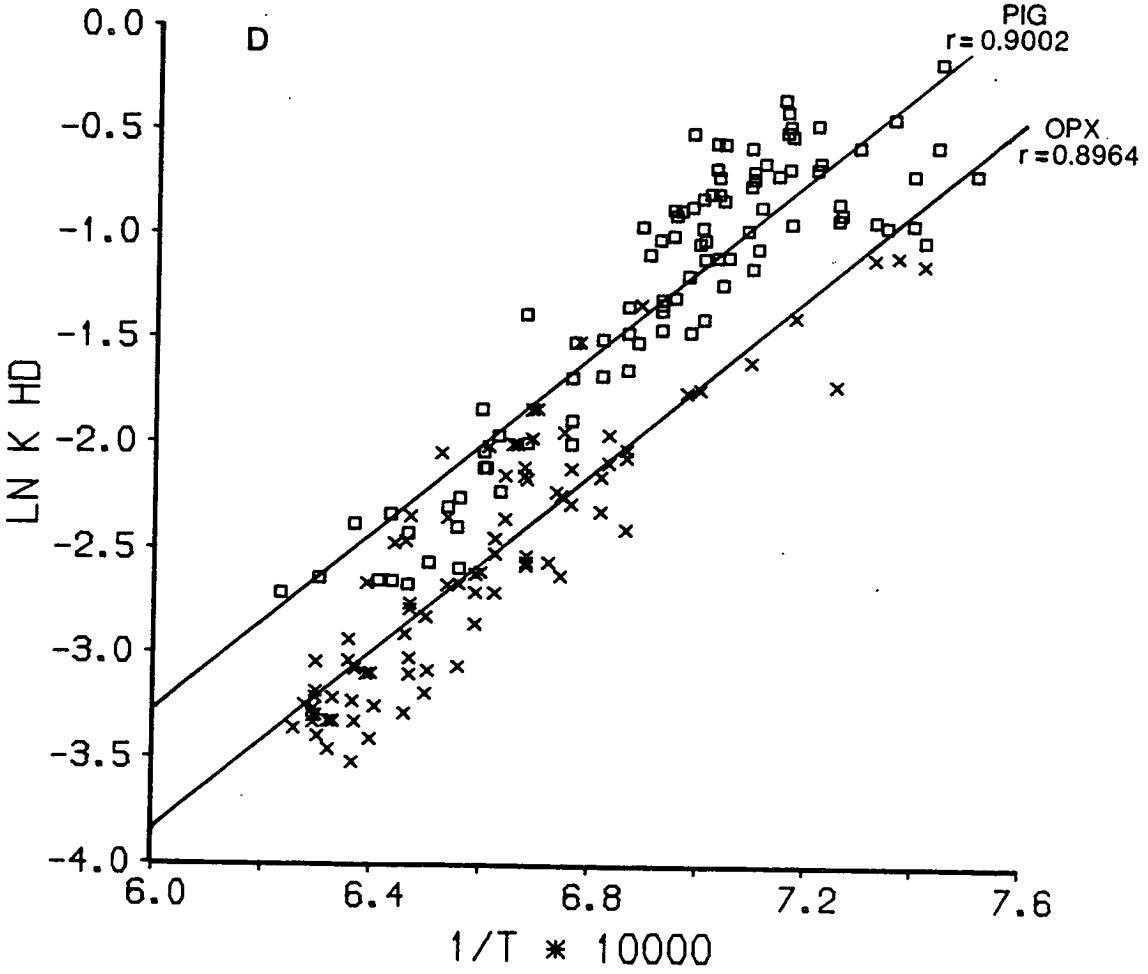
D
PIG
r=0.9002
OPX
r=0.8964
LN K HD
0.0
-0.5
-1.0
-1.5
-2.0
-2.5
-3.0
-3.5
-4.0
6.0
6.4
6.8
7.2
7.6
1/T * 10000

Figure 5.8

lnK v 1/T(K) for quadrilateral components of the regular mixing pyroxene - regular mixing liquid model (after Ghiorso et al., 1983).

Figure 5.8a $\ln K_{En}$ v 1/T

Figure 5.8b $\ln K_{Fs}$ v 1/T

Figure 5.8c $\ln K_{Di}$ v 1/T

Figure 5.8d $\ln K_{Hd}$ v 1/T

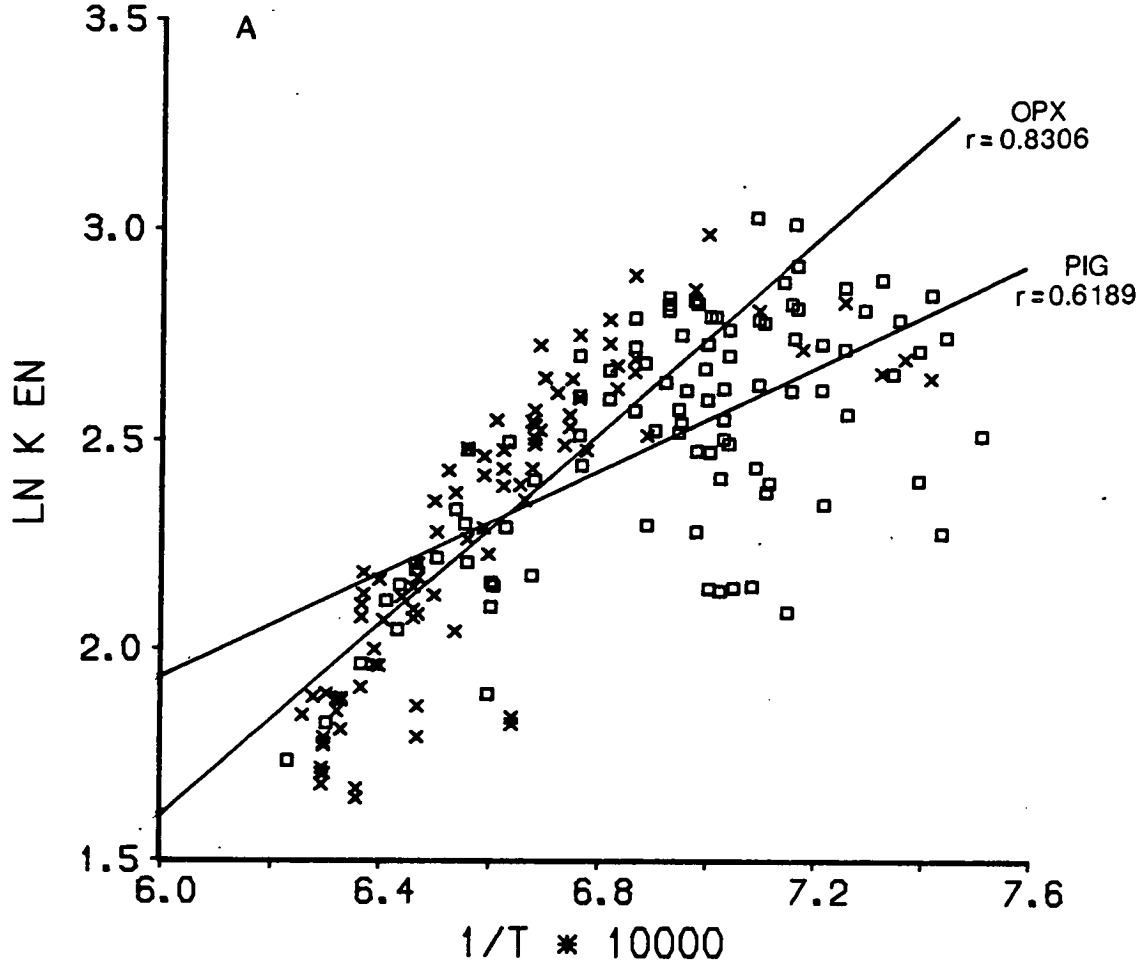
A
OPX
r=0.8306
PIG
r=0.6189
LN K EN
3.5
3.0
2.5
2.0
1.5
6.0
6.4
6.8
7.2
7.6
1/T * 10000

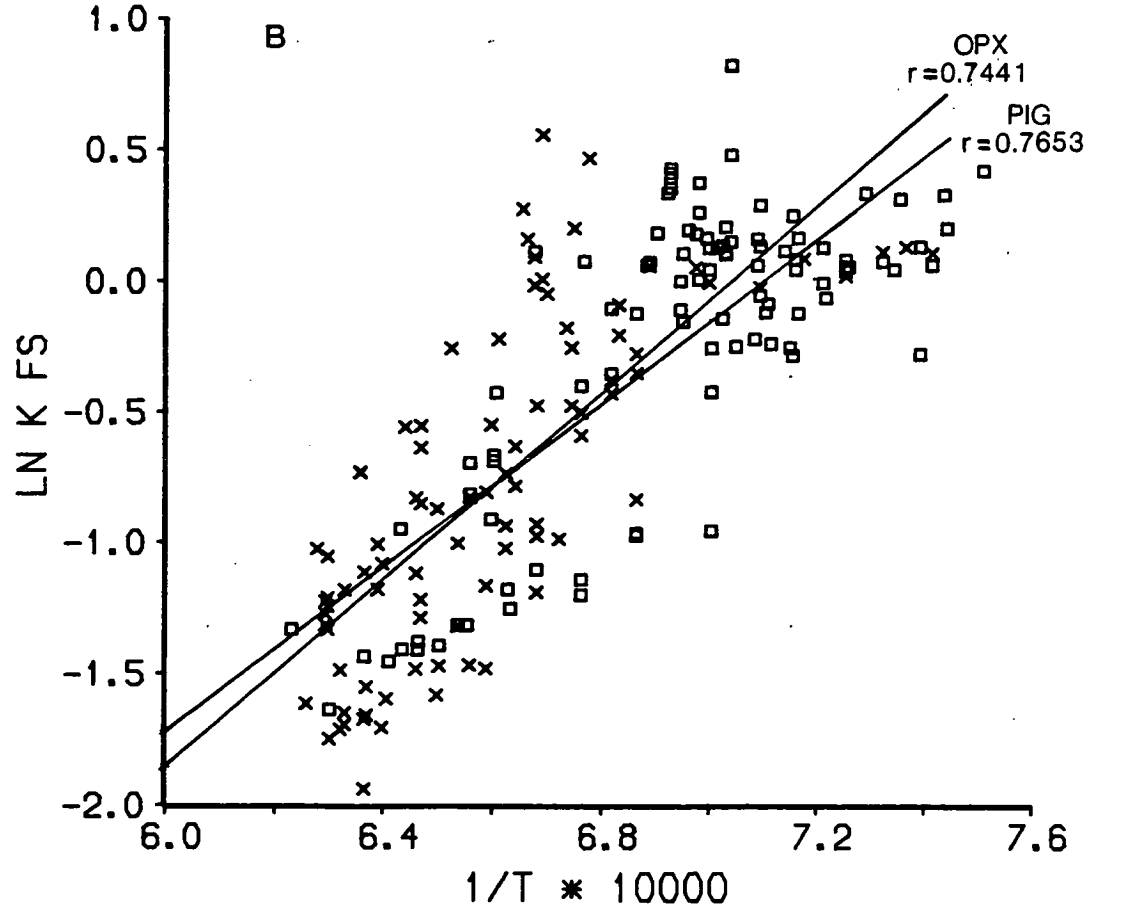
B
OPX
r=0.7441
PIG
r=0.7653
LN K FS
1.0
0.5
0.0
-0.5
-1.0
-1.5
-2.0
6.0
6.4
6.8
7.2
7.6
1/T * 10000

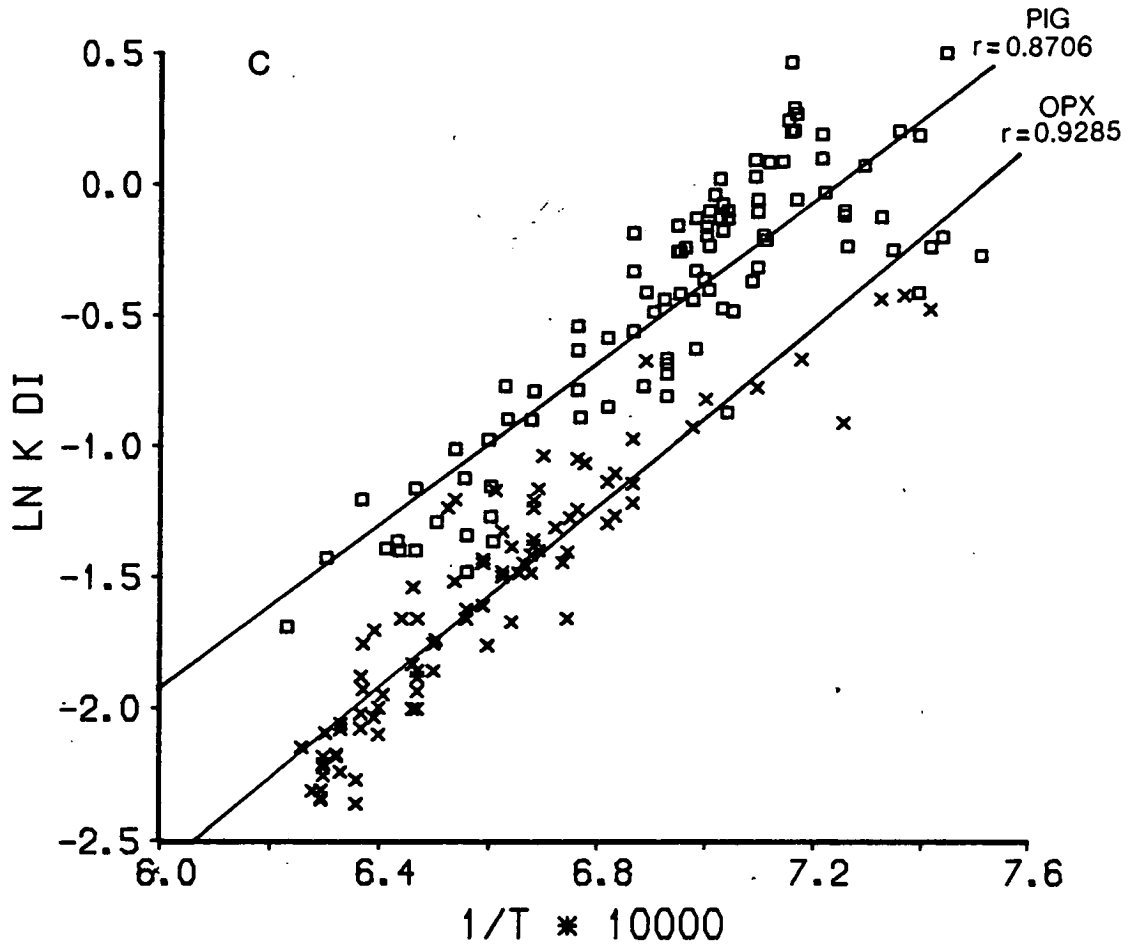
C
PIG
r=0.8706
OPX
r=0.9285
LN K DI
0.5
0.0
-0.5
-1.0
-1.5
-2.0
-2.5
6.0
6.4
6.8
7.2
7.6
1/T * 10000

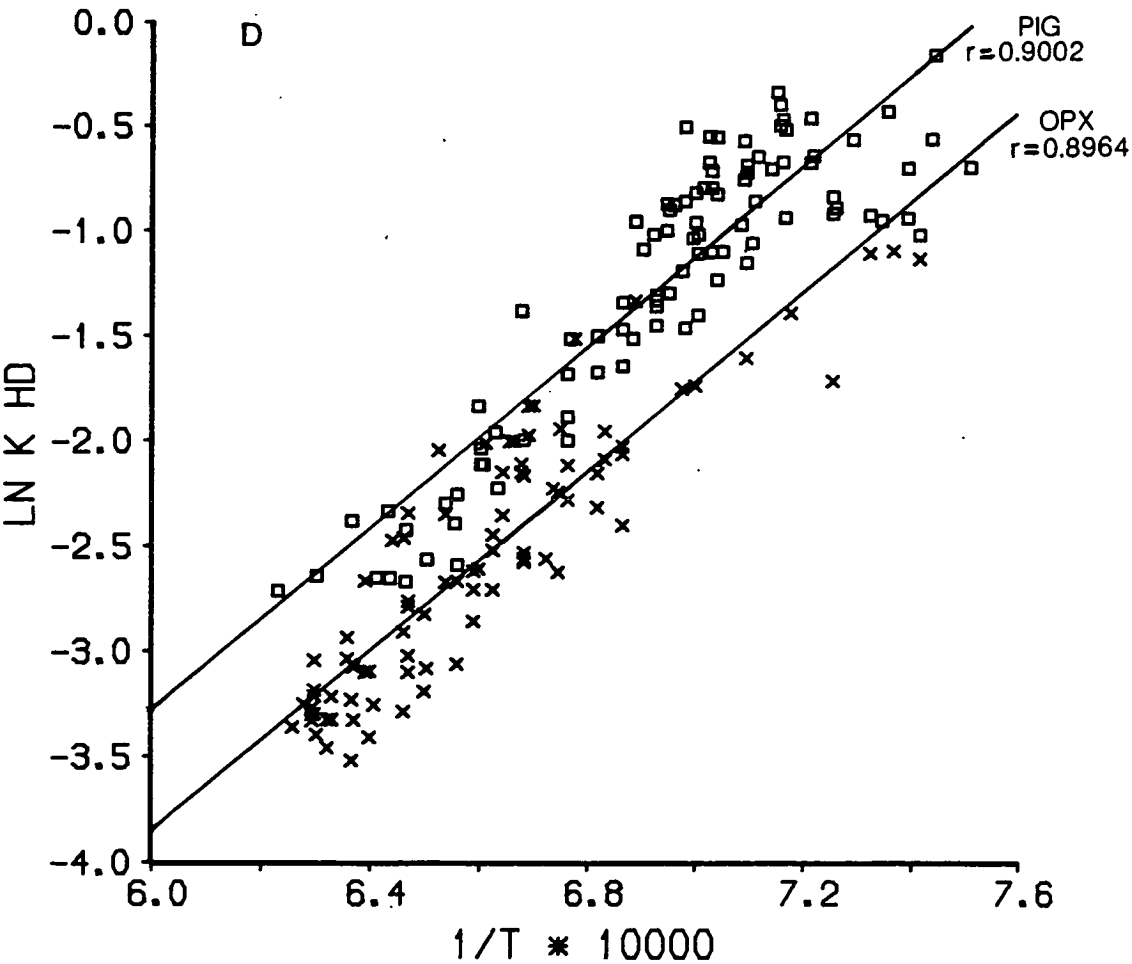
D
PIG
r=0.9002
OPX
r=0.8964
LN K HD
0.0
-0.5
-1.0
-1.5
-2.0
-2.5
-3.0
-3.5
-4.0
6.0
6.4
6.8
7.2
7.6
1/T * 10000

Figure 5.9

lnK v 1/T(K) for quadrilateral components of the regular mixing pyroxene - regular mixing polymer liquid model (after Nielsen & Dungan, 1983).

Figure 5.9a $\ln K_{En}$ v 1/T

Figure 5.9b $\ln K_{Fs}$ v 1/T

Figure 5.9c $\ln K_{Di}$ v 1/T

Figure 5.9d $\ln K_{Hd}$ v 1/T

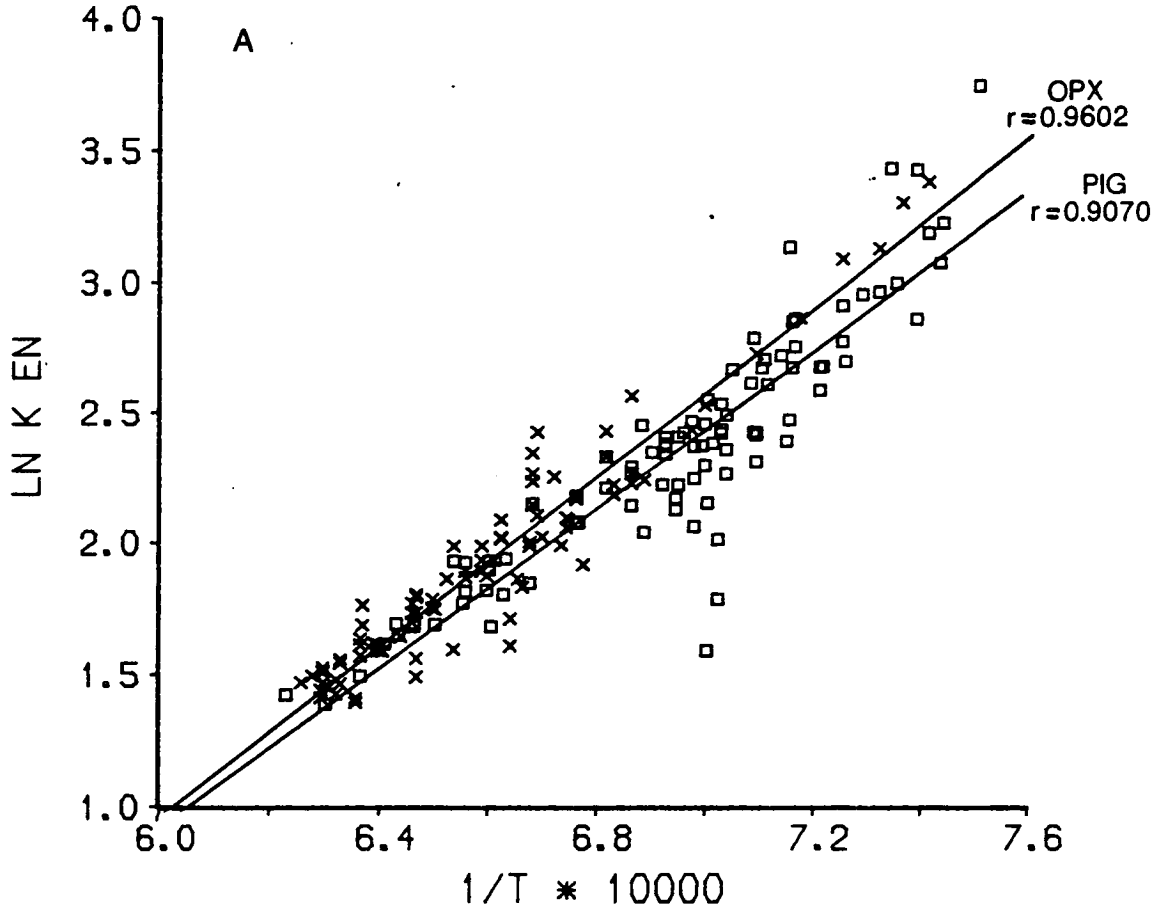
A
OPX
r=0.9602
PIG
r=0.9070
LN K EN
4.0
3.5
3.0
2.5
2.0
1.5
1.0
6.0
6.4
6.8
7.2
7.6
1/T * 10000

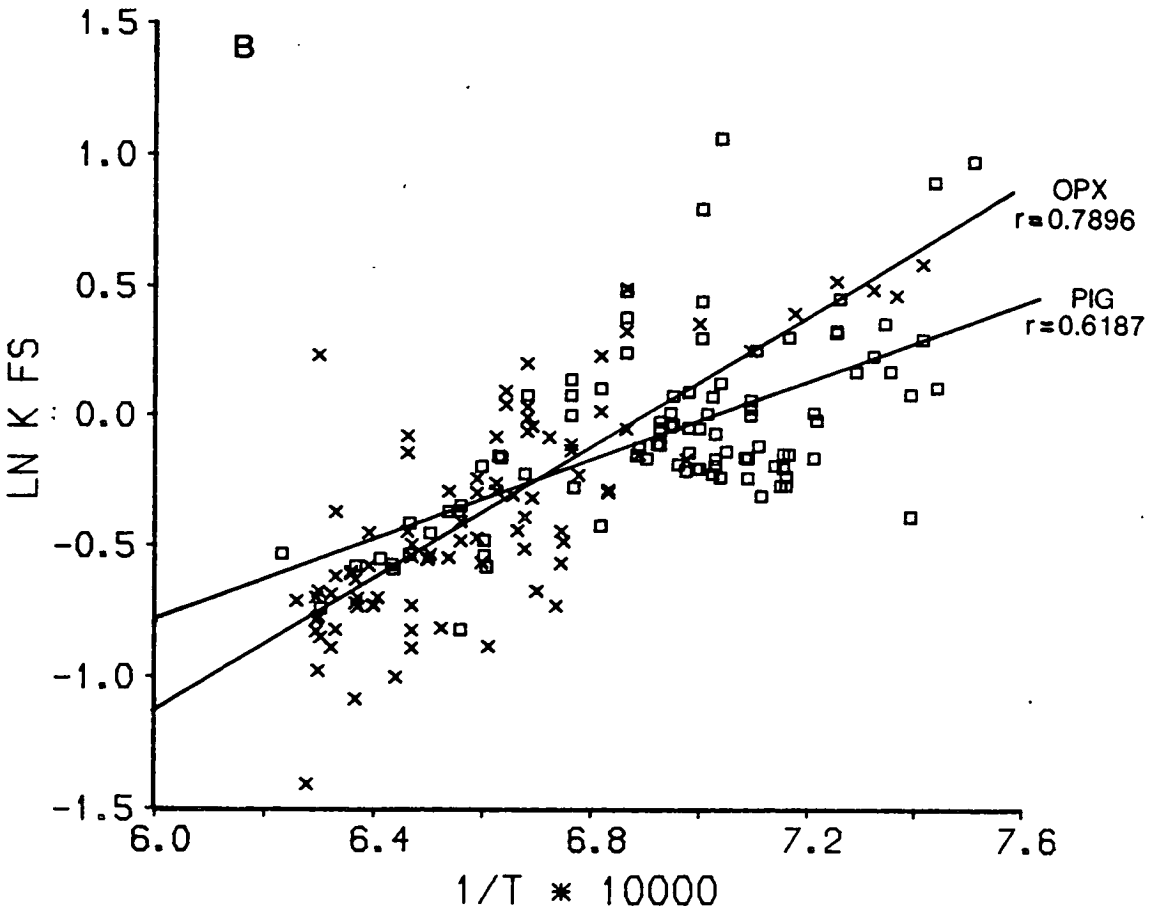
B
OPX
r=0.7896
PIG
r=0.6187
LN K FS
1.5
1.0
0.5
0.0
-0.5
-1.0
-1.5
6.0
6.4
6.8
7.2
7.6
1/T * 10000

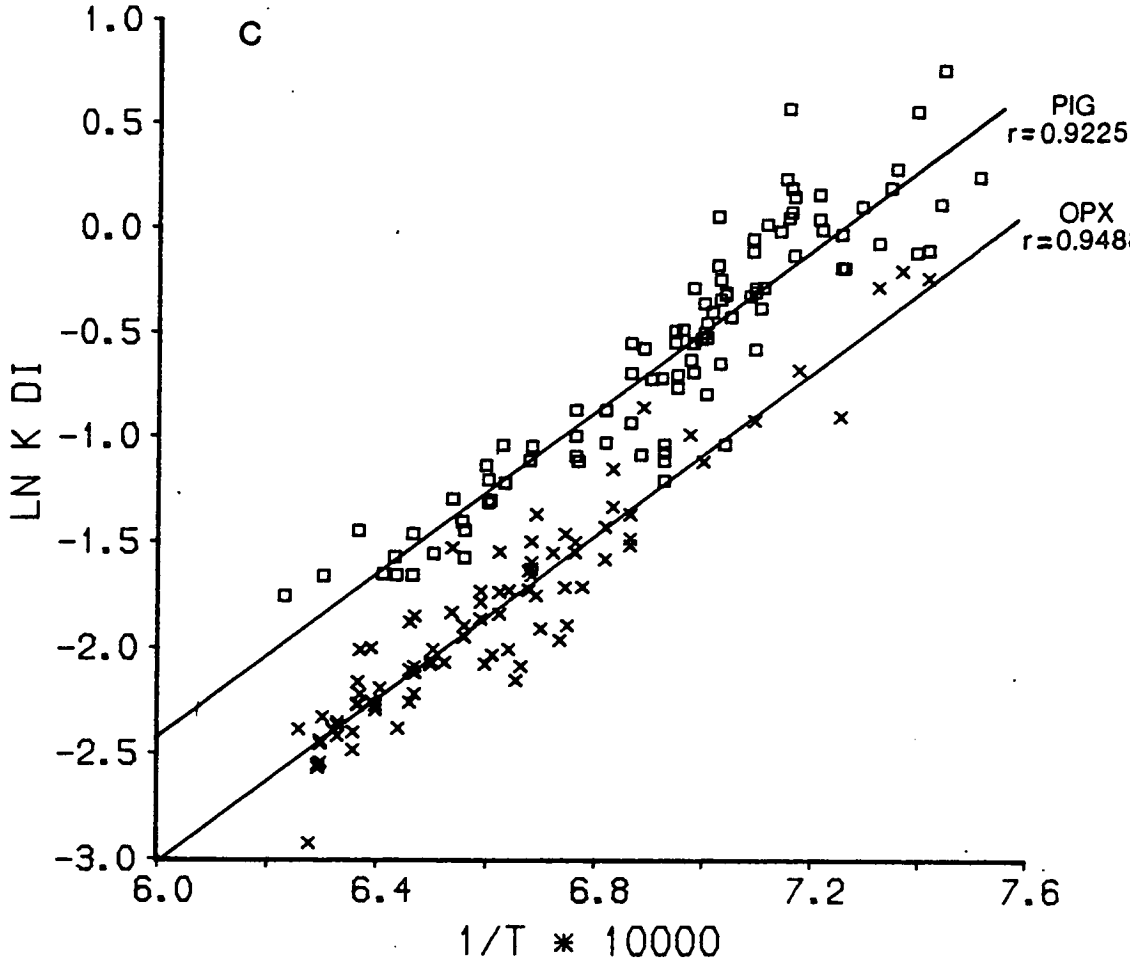
C
PIG
r=0.9225
OPX
r=0.9488
LN K DI
1.0
0.5
0.0
-0.5
-1.0
-1.5
-2.0
-2.5
-3.0
6.0
6.4
6.8
7.2
7.6
1/T * 10000

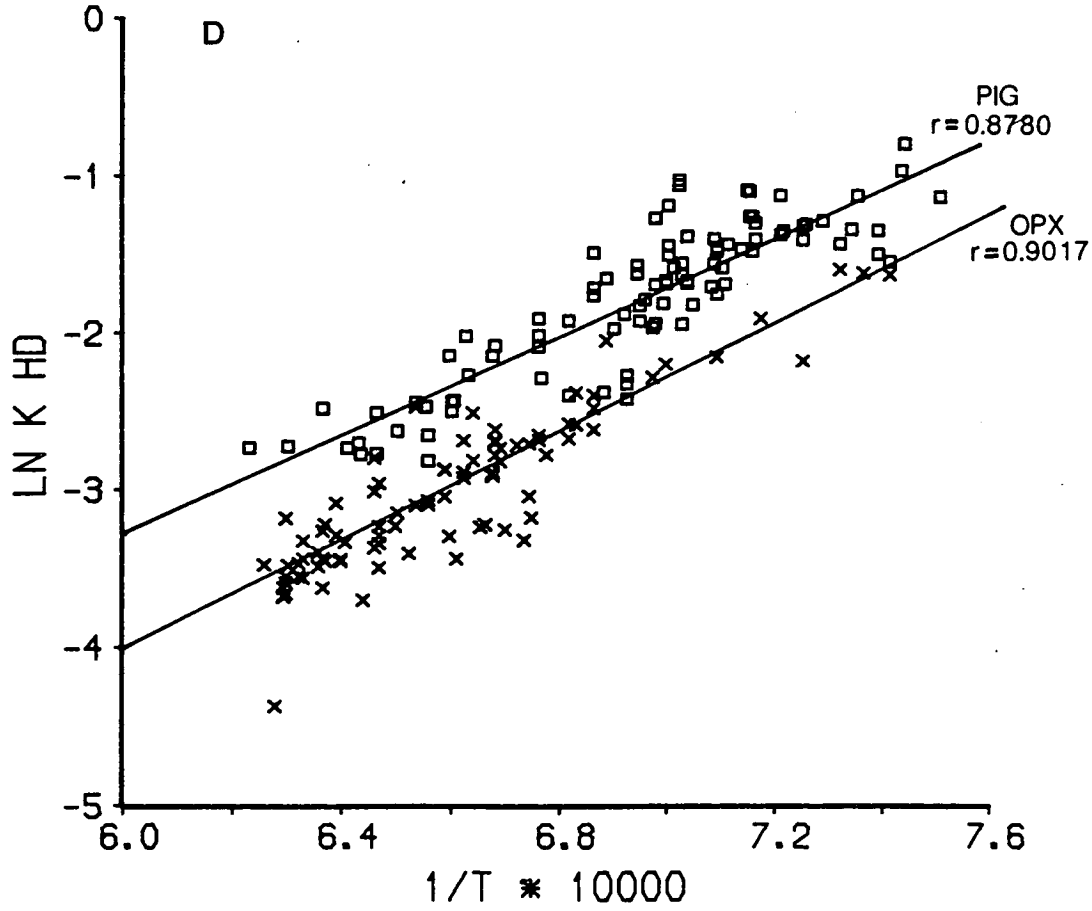
D
PIG
r=0.8780
OPX
r=0.9017
LN K HD
0
-1
-2
-3
-4
-5
6.0
6.4
6.8
7.2
7.6
1/T * 10000

Figure 5.10

$\ln K_{Cr}$ v Cr glass for low-calcium pyroxenes using the polymer melt model of Nielsen & Dungan (1983).

Figure 5.11

$\ln K_{Ti}$ v Ti glass for low-calcium pyroxenes using the polymer melt model of Nielsen & Dungan (1983).

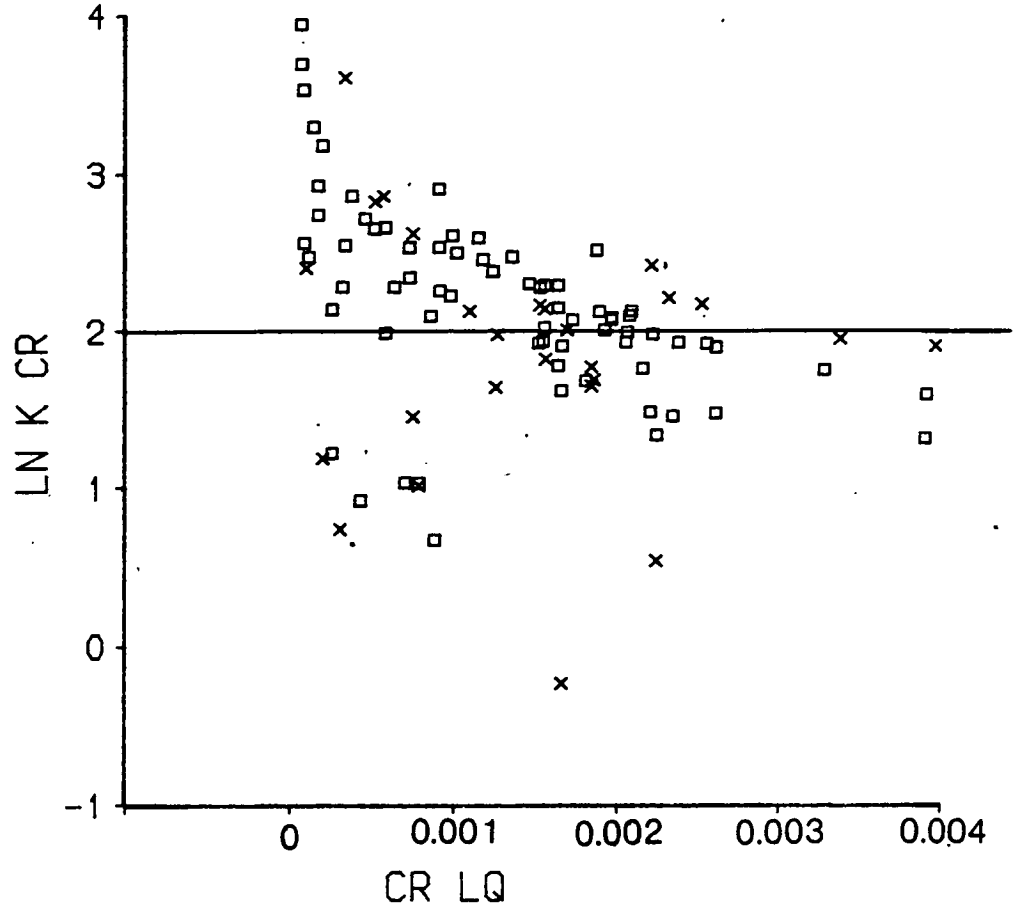
LN K CR
4
3
2
1
0
-1
0
0.001
0.002
0.003
0.004
CR LQ

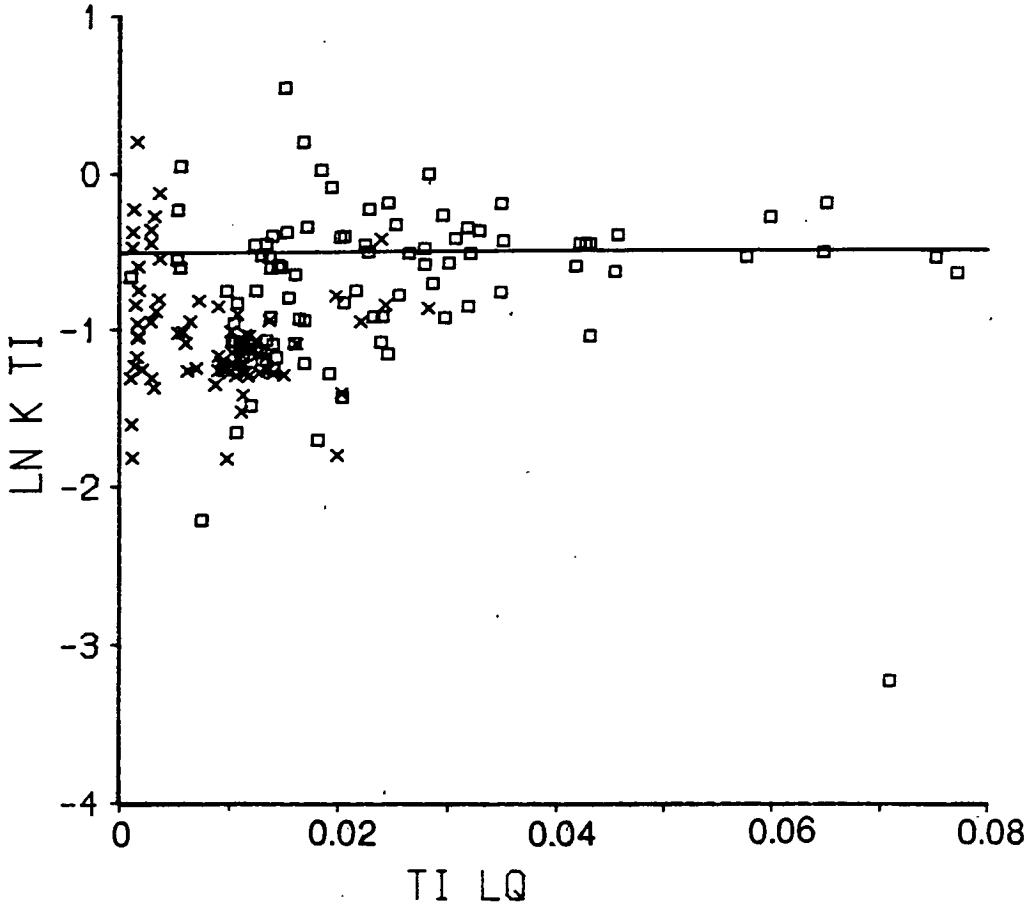
LN K TI
1
0
-1
-2
-3
-4
0
0.02
0.04
0.06
0.08
TI LQ

Figure 5.12

T calculated v T observed for the six low-calcium pyroxene components used in the model. Temperatures are in °C.

Figure 5.12a T calculated v T observed for En

Figure 5.12b T calculated v T observed for Fs

Figure 5.12c T calculated v T observed for Di

Figure 5.12d T calculated v T observed for Hd

Figure 5.12e T calculated v T observed for Mn

Figure 5.12f T calculated v T observed for Jd

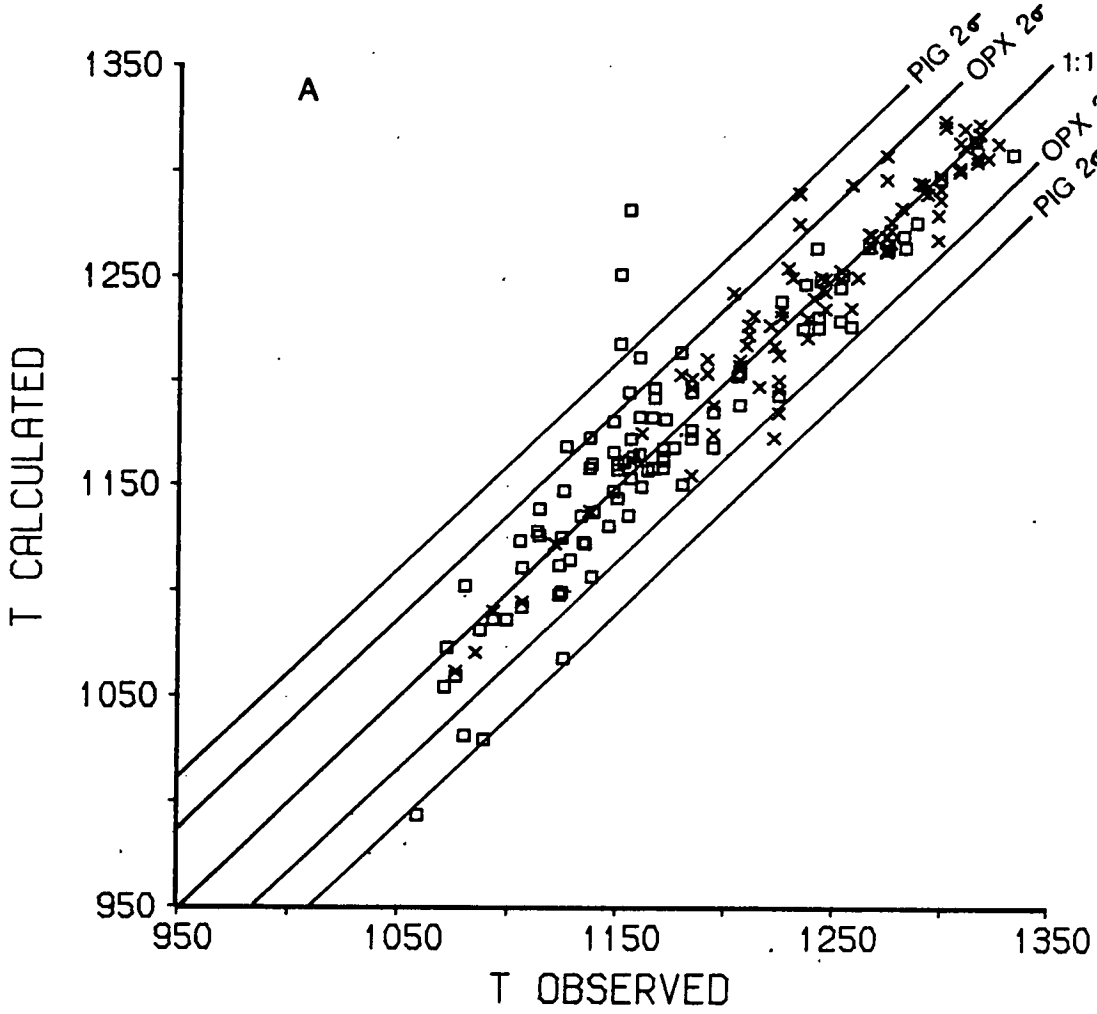
A
PIG 26
OPX 26
1:1
OPX 26
PIG 26
1350
1250
1150
1050
950
950
1050
1150
1250
1350
T CALCULATED
T OBSERVED

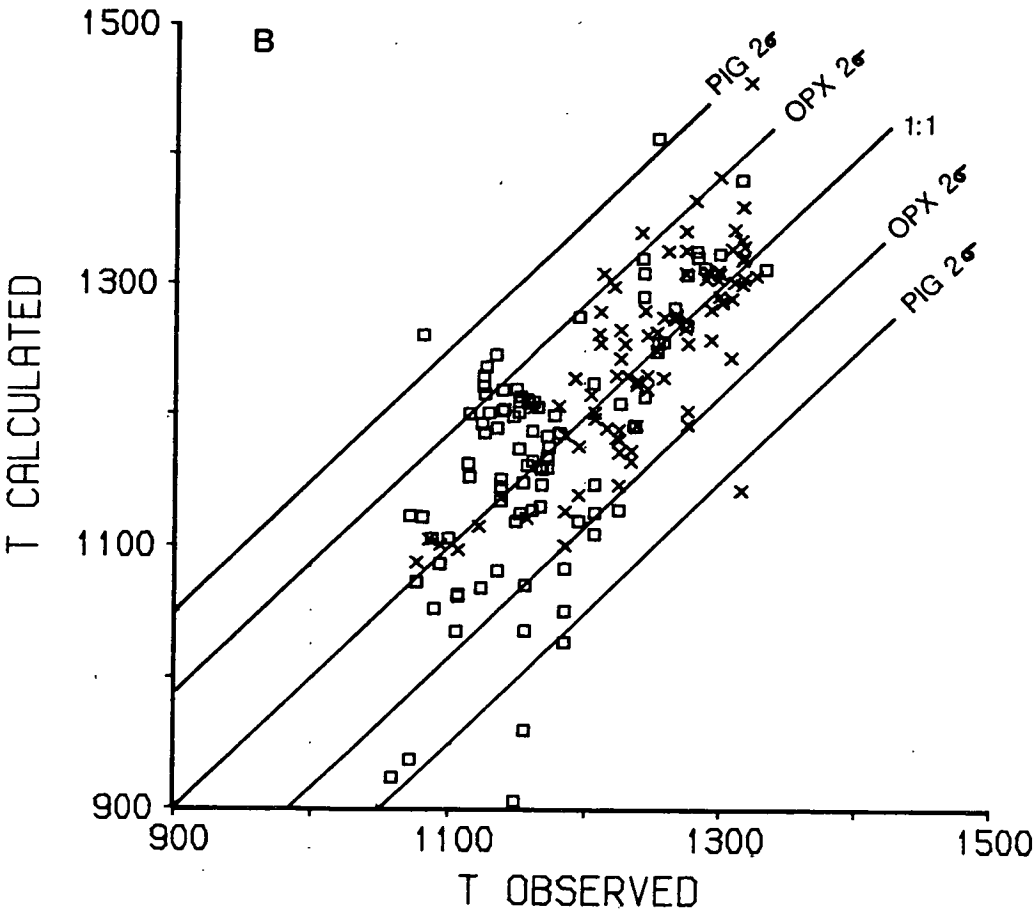
B
PIG 26
OPX 26
1:1
OPX 26
PIG 26
1500
1300
1100
900
900
1100
1300
1500
T CALCULATED
T OBSERVED

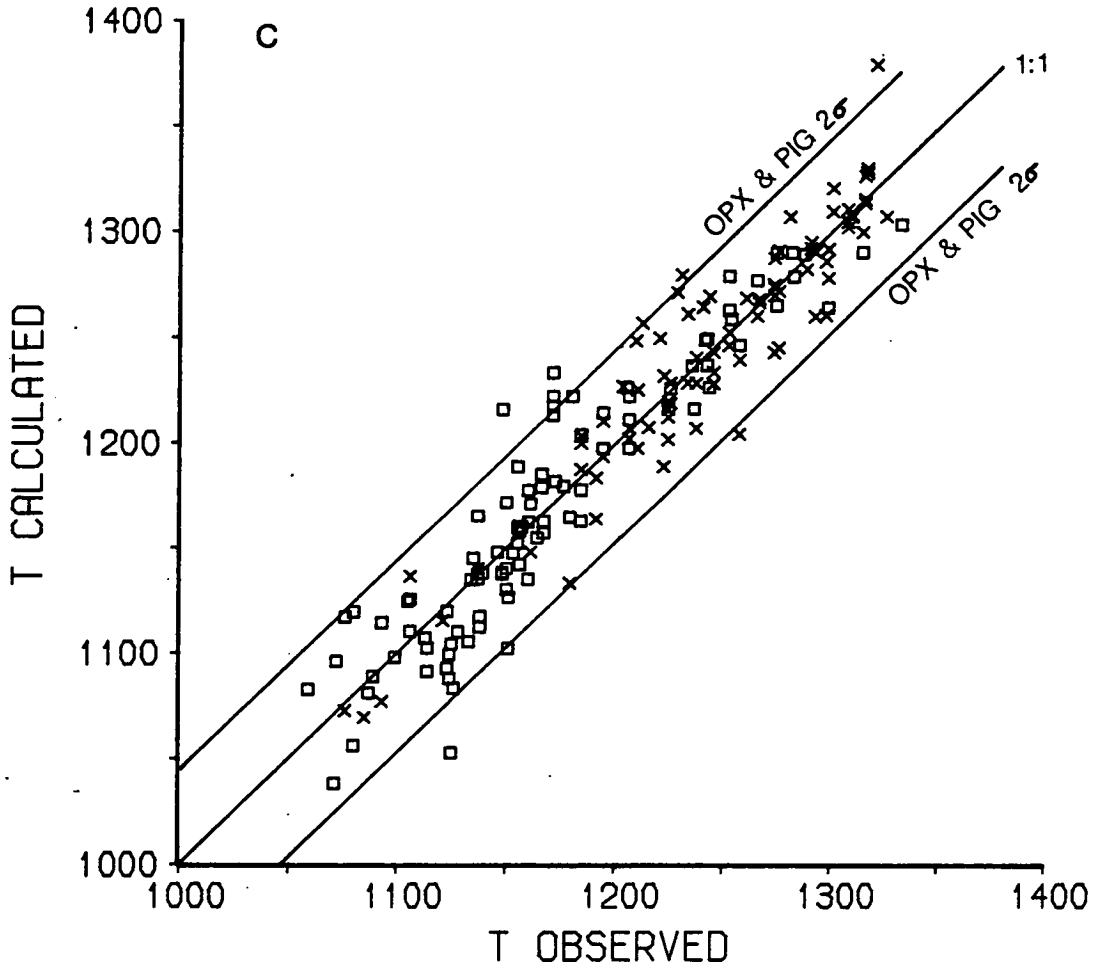
C
1400
1300
1200
1100
1000
T CALCULATED
1000
1100
1200
1300
1400
T OBSERVED
1:1
OPX & PIG 2σ
OPX & PIG 2σ

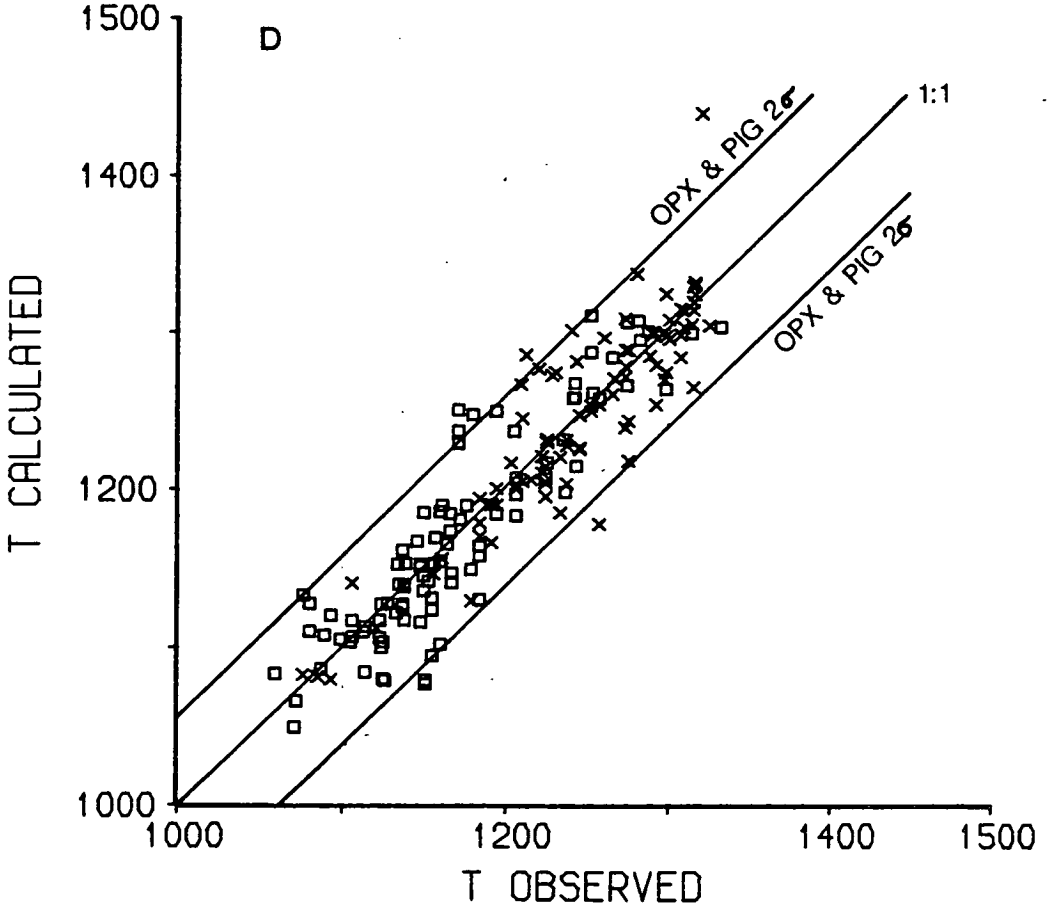
D
1500
1400
1200
1000
T CALCULATED
1000
1200
1400
1500
T OBSERVED
1:1
OPX & PIG 2σ
OPX & PIG 2σ

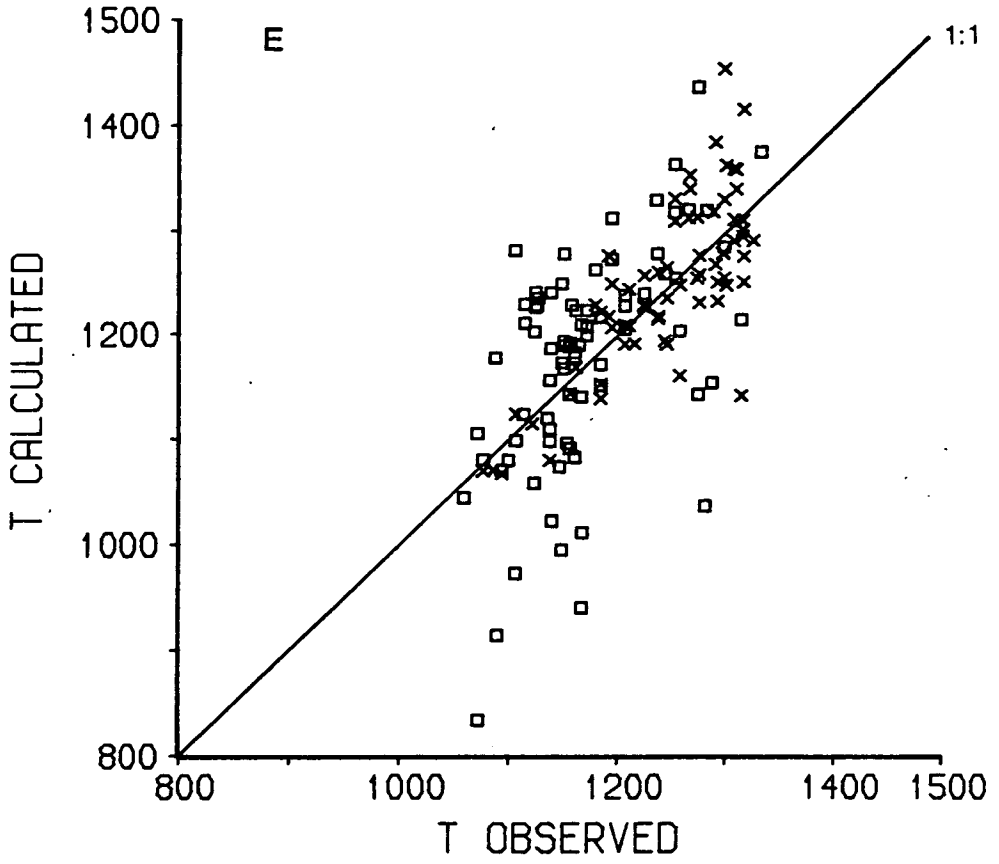
E
1:1
1500
1400
1200
1000
800
T CALCULATED
800
1000
1200
1400
1500
T OBSERVED

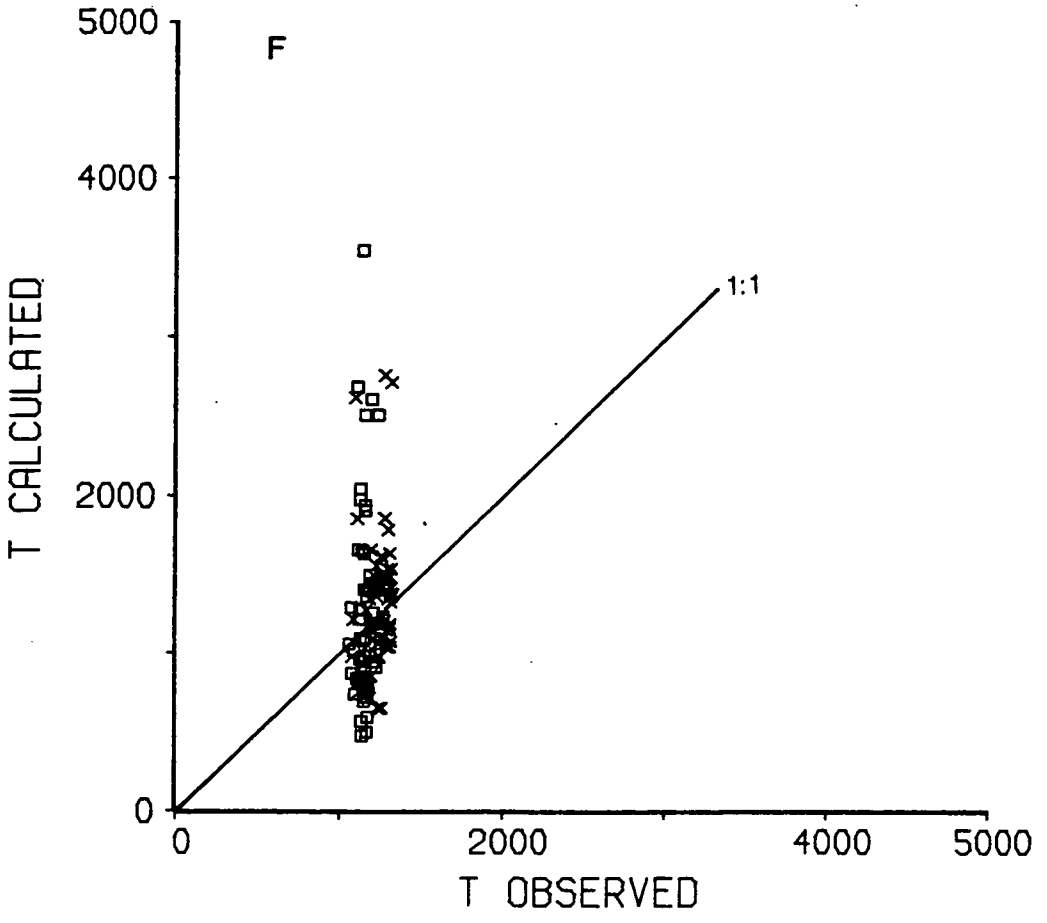
F
1:1
5000
4000
2000
0
T CALCULATED
0
2000
4000
5000
T OBSERVED

Figure 5.13

a^{Px} calculated v a^{px} observed for the quadrilateral components used in the model.

Figure 5.13a a^{Px}_{En} calculated v a^{Px}_{En} observed

Figure 5.13b a^{Px}_{Fs} calculated v a^{Px}_{Fs} observed

Figure 5.13c a^{Px}_{Di} calculated v a^{Px}_{Di} observed

Figure 5.13d a^{Px}_{Hd} calculated v a^{Px}_{Hd} observed

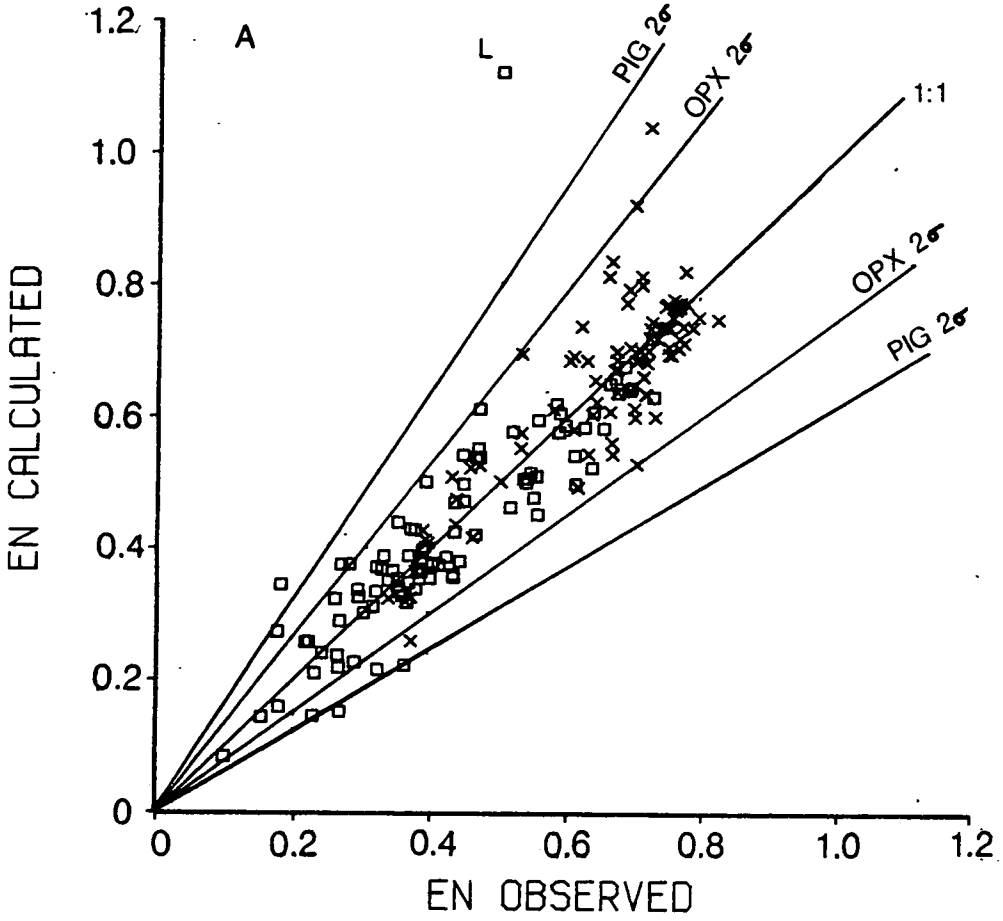
A
L
PIG 26
OPX 26
1:1
OPX 26
PIG 26
EN CALCULATED
EN OBSERVED
0
0.2
0.4
0.6
0.8
1.0
1.2

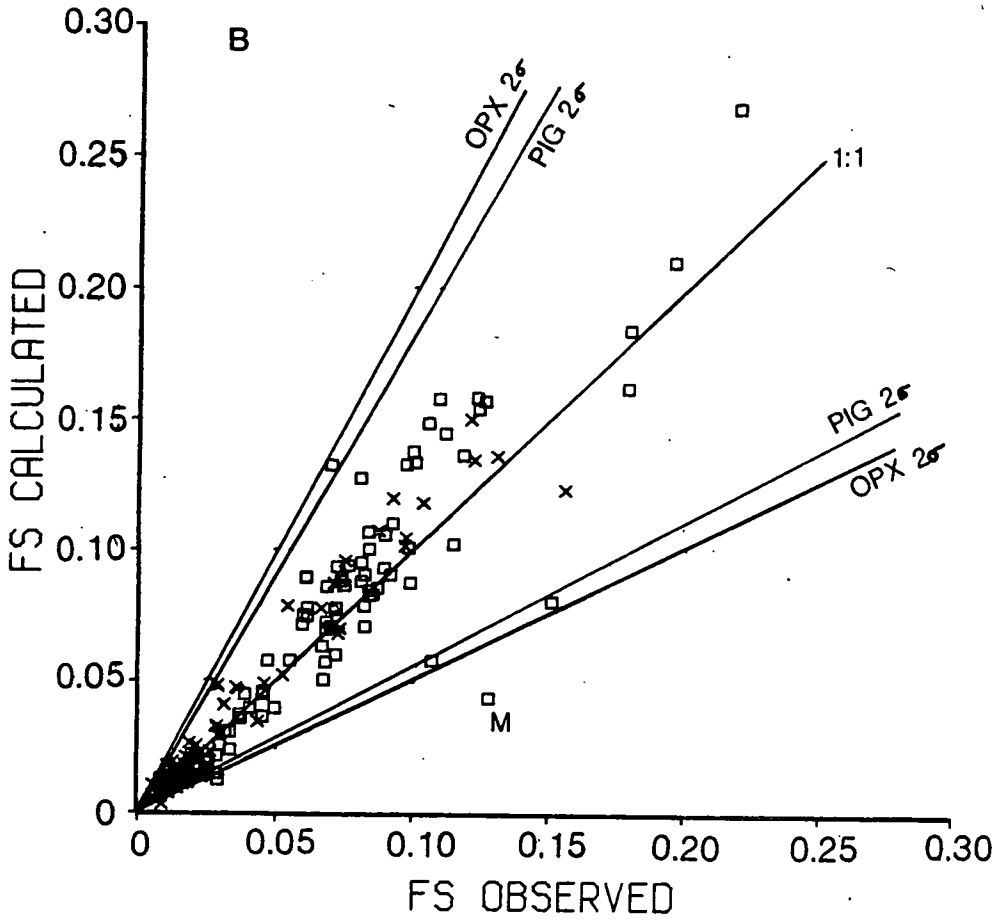
B
OPX 26
PIG 26
1:1
PIG 26
OPX 26
M
FS CALCULATED
FS OBSERVED
0
0.05
0.10
0.15
0.20
0.25
0.30

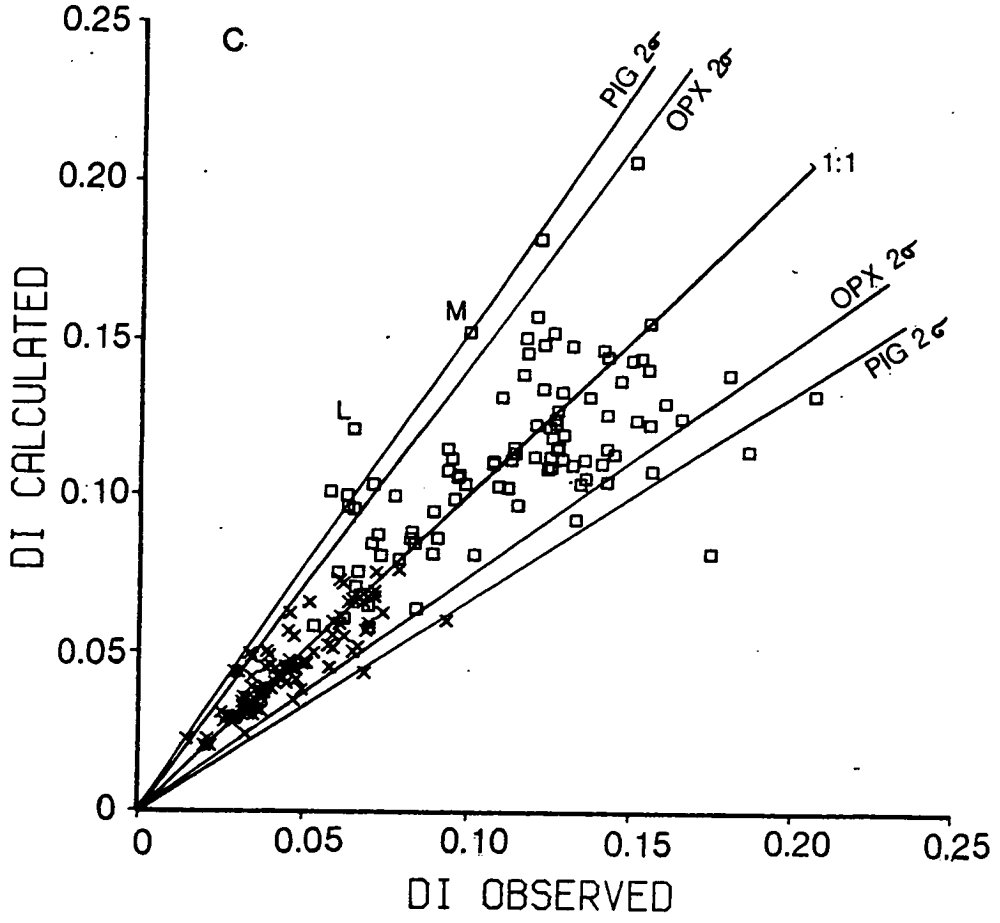
C
PIG 2σ
OPX 2σ
1:1
OPX 2σ
PIG 2σ
M
L
DI CALCULATED
DI OBSERVED
0
0.05
0.10
0.15
0.20
0.25

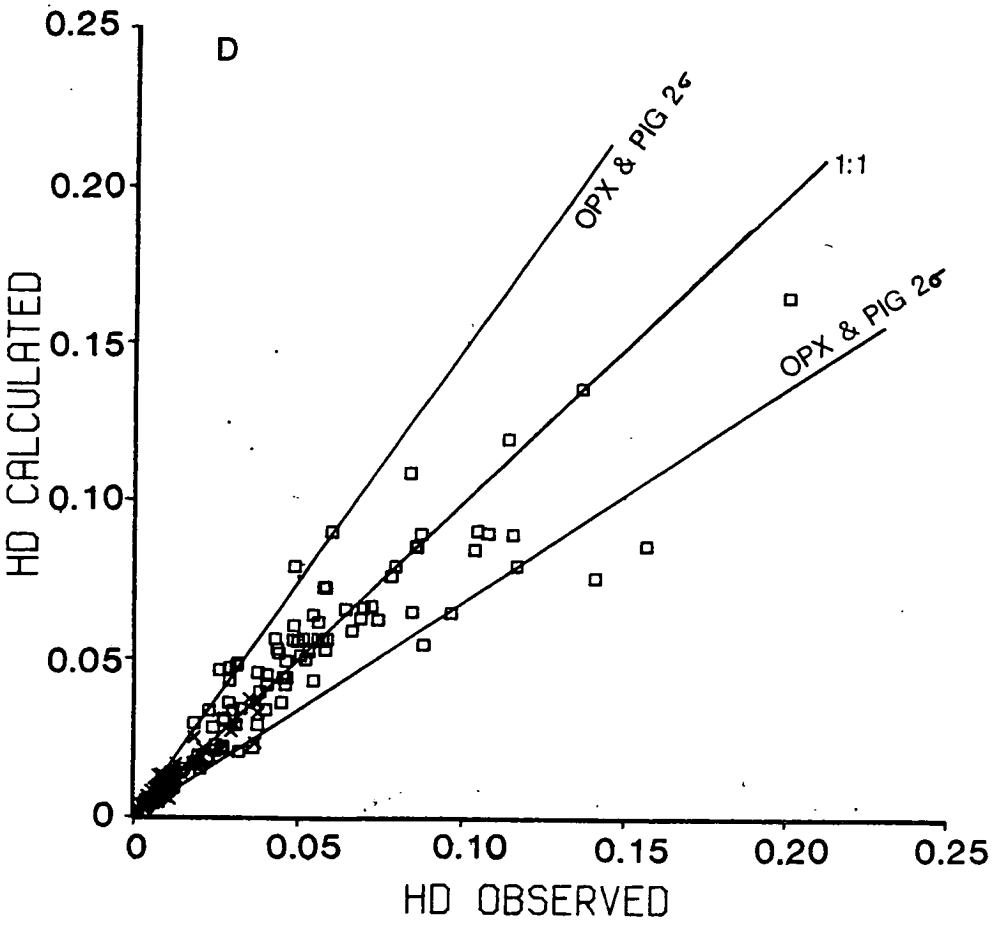
D
OPX & PIG 2σ
1:1
OPX & PIG 2σ
HD CALCULATED
HD OBSERVED
0
0.05
0.10
0.15
0.20
0.25

Figure 5.14

Calculated v observed values for the liquidus temperature and activity determinations.

Figure 5.14a T calculated v T observed (°C)

Figure 5.14b a_{En}^{Px} calculated v a_{En}^{Px} observed

Figure 5.14c a_{Fs}^{Px} calculated v a_{Fs}^{Px} observed

Figure 5.14d a_{Di}^{Px} calculated v a_{Di}^{Px} observed

Figure 5.14e a_{Hd}^{Px} calculated v a_{Hd}^{Px} observed

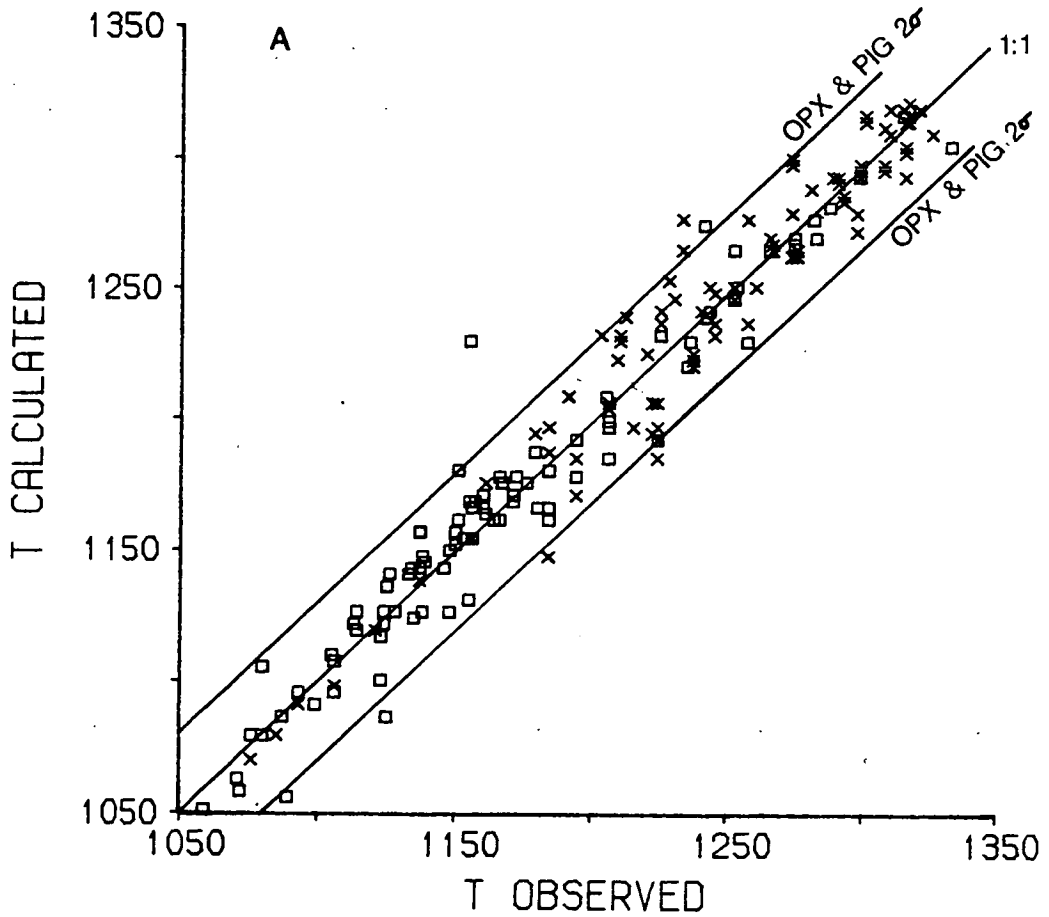

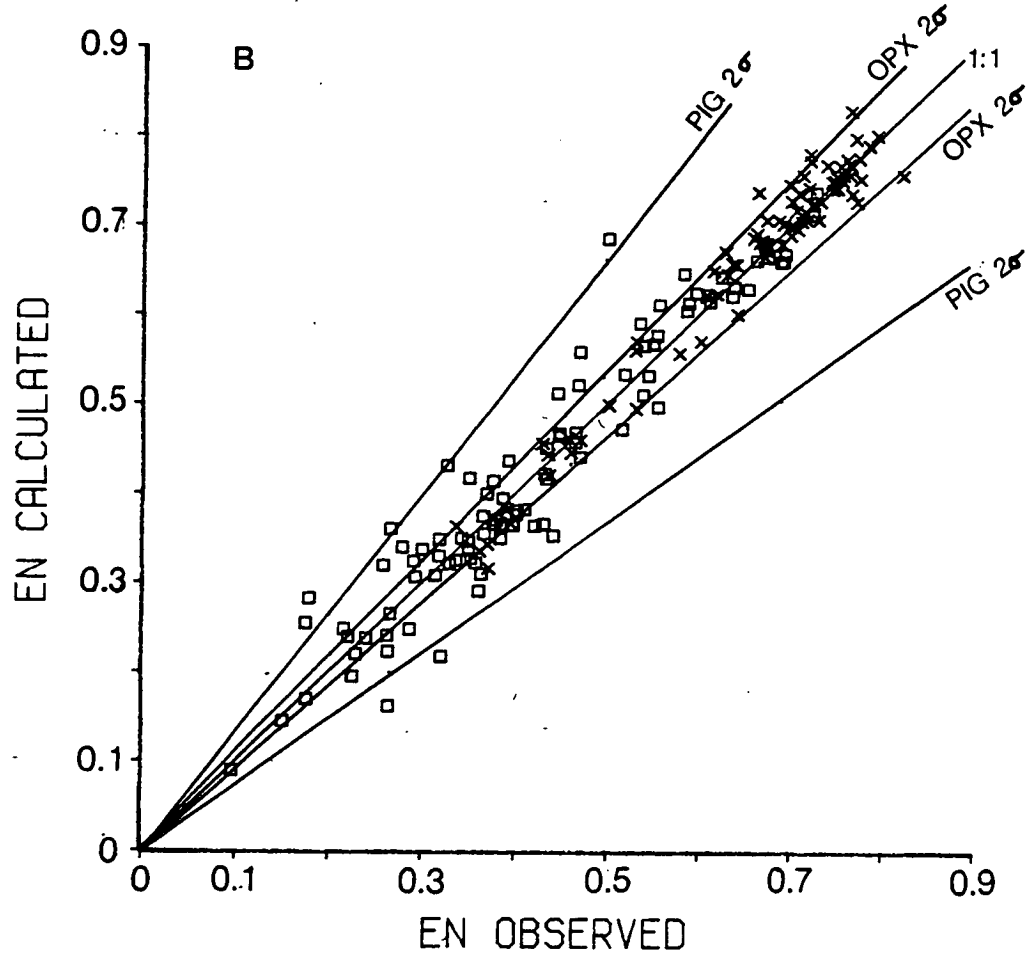
B
PIG 2σ
OPX 2σ
1:1
OPX 2σ
PIG 2σ
EN CALCULATED
EN OBSERVED
0
0.1
0.3
0.5
0.7
0.9

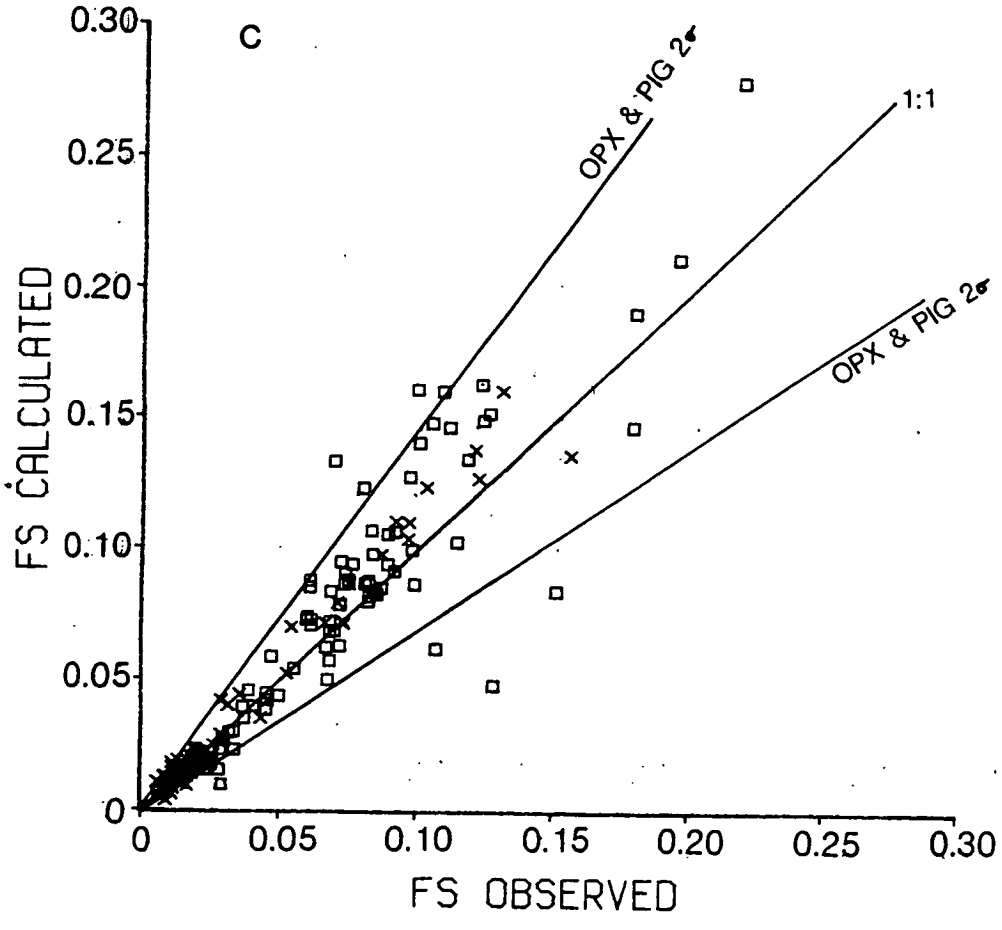
C
OPX & PIG 2σ
1:1
OPX & PIG 2σ
FS CALCULATED
FS OBSERVED
0
0.05
0.10
0.15
0.20
0.25
0.30

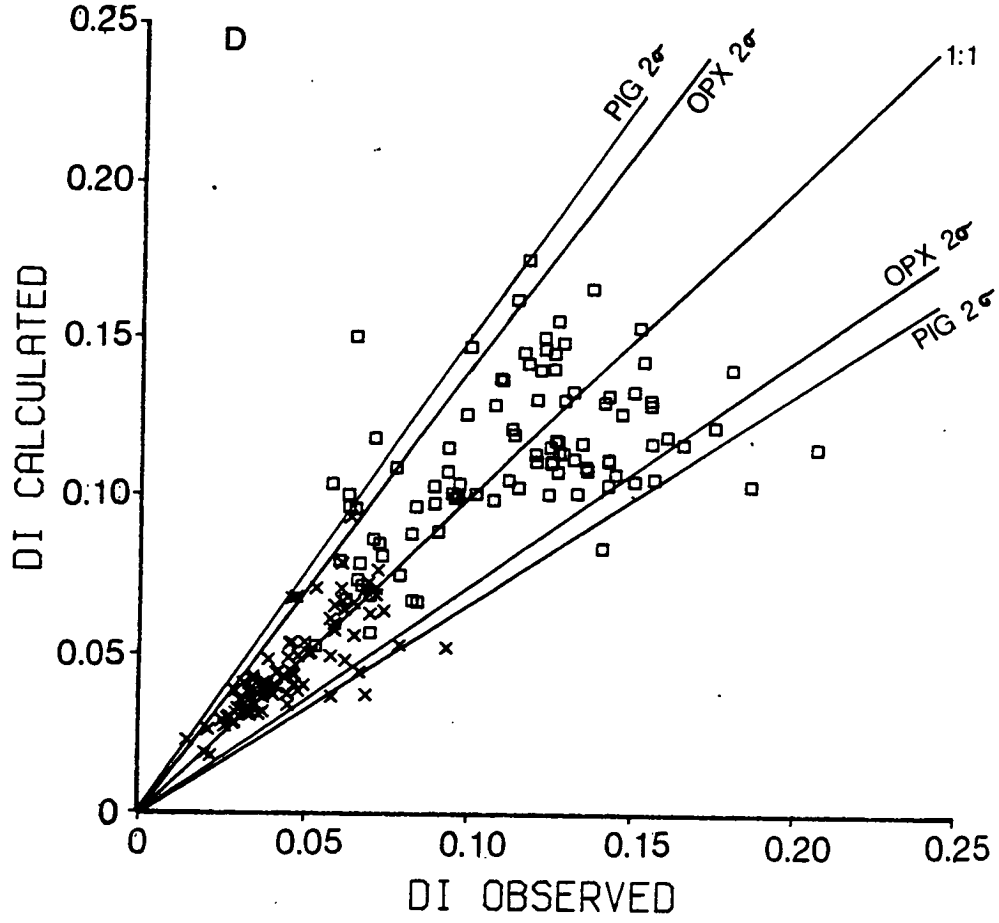
D
PIG 2σ
OPX 2σ
1:1
OPX 2σ
PIG 2σ
DI CALCULATED
DI OBSERVED
0.25
0.20
0.15
0.10
0.05
0
0
0.05
0.10
0.15
0.20
0.25

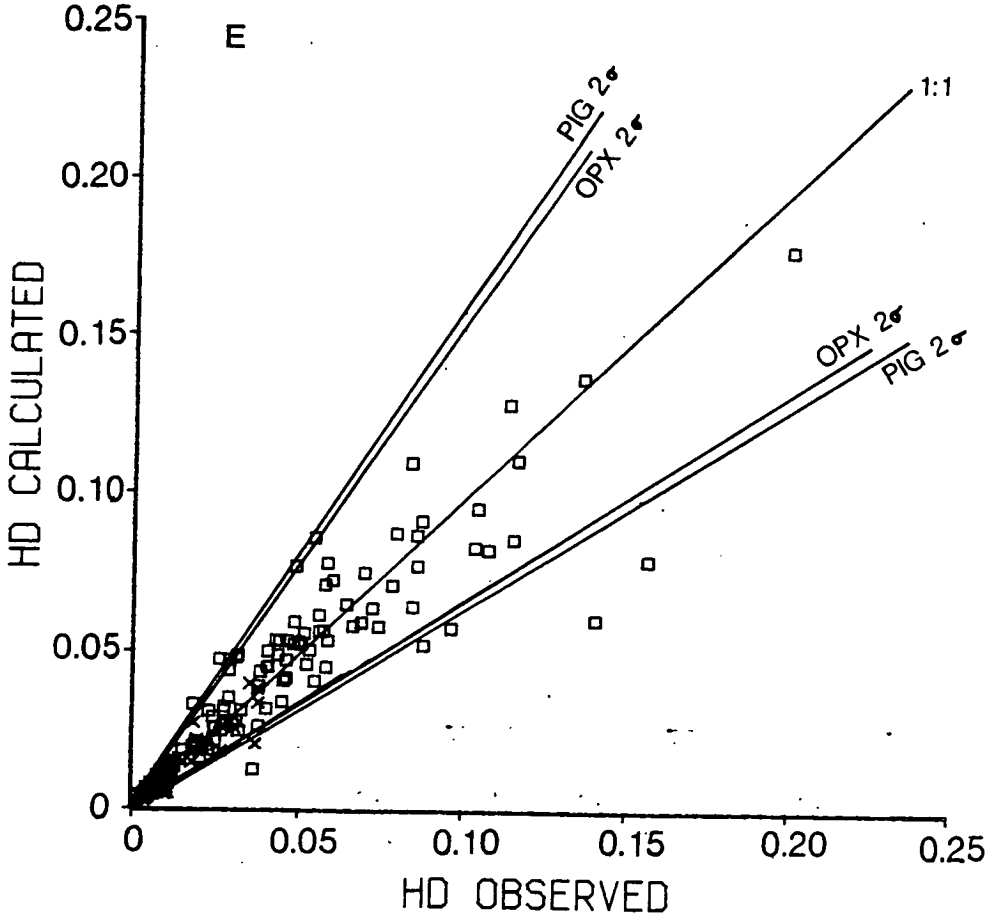
E
PIG 2σ
OPX 2σ
1:1
OPX 2σ
PIG 2σ
HD CALCULATED
HD OBSERVED
0.25
0.20
0.15
0.10
0.05
0
0
0.05
0.10
0.15
0.20
0.25

CHAPTER 6

SUMMARY AND CONCLUSIONS

6.1 MINERAL CHEMISTRY

There are three low-calcium pyroxenes which are stable at high temperatures at atmospheric pressure; in order of increasing CaO content - protopyroxene, orthopyroxene and pigeonite. Protopyroxene is recognised by the presence of its inversion product, clino-enstatite; which together with orthopyroxene and pigeonite is stable at room temperature.

Low-calcium pyroxenes grown under experimental conditions at atmospheric pressure in natural systems may take several days to equilibrate - especially if the starting material contains relict pyroxenes to act as nucleii for growth. Under disequilibrium conditions such as falling temperature or high iron loss proto-pyroxene or pigeonite will grow in preference to orthopyroxene. In this study 55 new analyses of orthopyroxene, 25 of pigeonite and 4 of protopyroxene are presented and considered with 34 orthopyroxene and 77 pigeonite analyses from a literature search. The Fe_2O_3 contents of the pyroxenes has not been determined as formula manipulations are sensitive to the amount of SiO_2 present.

In low-calcium pyroxenes $Ca^{2+} + Fe^{2+} + Mg^{2+} < 2$ cations per six oxygens and as magnesium contents decrease so iron and calcium contents increase; these compositional changes are in part related to temperature. Manganese and sodium contents are both low and tend to increase with iron content. There is more sodium in pigeonite than orthopyroxene due to structural differences. Titanium, chromium and aluminium are also found in low-calcium pyroxenes; titanium contents are low, aluminium and chromium contents are significant (0.5 wt% oxide). For non-divalent cations (Na^{+}, Cr^{3+}, Ti^{4+} and Al^{3+}) coupled substitutions are necessary for charge balance. However, no relationship was found between Na-Al, Cr-Al, etc. As Si + Al > 2 cations per six oxygens there must be some terahedral Al, but there is no evidence for a coupled Al^{vi}-Al^{iv} substitution.

Olivines showed variation in Fo content with temperature, falling from Fo_{90} at 1345°C to Fo_{83} at 1181°C, and to a lesser extent fO_2. There is a slight increase in calcium and manganese with falling temperature. Augites and plagioclase feldspars were found in the lowest temperature experiments but together with coexisting low-calcium pyroxenes are not considered to have reached equilibrium. Opaque oxides, probably of chromite composition, were found in nearly all experiments but were never large enough to probe accurately.

Where olivine and orthopyroxene coexist the olivine contains slightly more magnesium and iron, the distribution coefficients remaining constant with respect to temperature and composition. Manganese, aluminium, chromium and calcium were all concentrated in orthopyroxene. Where pigeonite and orthopyroxene coexist the pigeonite contains more iron and calcium and less magnesium than the orthopyroxene. Manganese shows no preference for orthopyroxene or pigeonite; chromium tends to be concentrated in orthopyroxene; titanium and aluminium tend to be concentrated in pigeonite.

6.2 MELT CHEMISTRY

In experiments where the crystals had not equilibrated with the liquid the compositional variation of the glasses still reflected the phases present suggesting that the crystal margins were in local equilibrium with the liquid. In the projections from olivine onto CS-MS-A and plagioclase onto M_2S-CMS_2-S the liquids in equilibrium with one or more low-calcium pyroxenes ± olivine ± augite ± plagioclase define primary crystallisation volumes similar to those obtained from synthetic systems and from the glasses in equilibrium with the low-calcium pyroxenes found in the literature search.

Grove et al. (1982) suggested a phase diagram for calc-alkaline series rocks based on experimental studies of basaltic andesites of calc-alkaline affinity (fig. 6.1). The crystallisation path of Grove et al.'s low-calcium pyroxene bearing glasses is distinct from that defined by the other data used in this study. This is due to compositional differences which lead to the crystallisation of substantial amounts of plagioclase prior to the crystallisation of low-calcium pyroxene in Grove et al.'s samples. The other samples used in this study typically had olivine or a low-calcium pyroxene

as the liquidus phase and the amounts of plagioclase crystallising, if any, were small. An alternative phase diagram for such samples is given in fig. 6.2.

Single element distribution coefficients have been determined for crystal - liquid pairs where the crystals have equilibrated. A summary of the distribution coefficients obtained from low-calcium pyroxene - liquid pairs is given in table 6.1. Magnesium is always concentrated in the low-calcium pyroxenes. Iron and manganese are concentrated in the liquid at high temperatures and the low-calcium pyroxenes at low temperatures. Iron exhibits this pattern because as temperature falls so the low-calcium pyroxenes contain less magnesium and more iron; manganese exhibits this pattern because the manganese content of a low-calcium pyroxene is related to the iron content. Calcium is always concentrated in the liquid; however, as there is typically more calcium in pigeonite than orthopyroxene the range of distribution coefficients for pigeonites is slightly higher than that for orthopyroxenes. The distribution coefficients for magnesium, iron, manganese and calcium all increase with decreasing temperature.

In these experiments silicon is always concentrated in the liquid and as the amount of silicon in the pyroxene is constrained by stoichiometry the distribution coefficient shows no variation with temperature but falls with increasing silicon content in the liquid. Sodium is always concentrated in the liquid; however, as there is typically more sodium in a pigeonite than an orthopyroxene the range of sodium distribution coefficients for pigeonites is higher than those for orthopyroxenes. The distribution coefficients for sodium and aluminium, which is also concentrated in the liquid, show no definite relationship to temperature or composition; in both cases the data from this study and the literature search suggest different relationships. The distribution coefficients for chromium and titanium both exhibit a large range of values, titanium always being concentrated in the liquid whilst chromium tends to be concentrated in the low-calcium pyroxrene. For both elements the largest range of distribution coefficients was found at lower concentrations, suggesting that much of the variation is due to taking a ratio of two small numbers. At higher concentrations the distribution coefficients for both chromium and titanium appear to be constant.

6:3 LOW-CALCIUM PYROXENE - MELT EQUILIBRIA

Low-calcium pyroxene - melt equilibria models have been proposed by Nathan & Van Kirk (1977), Nielsen & Drake (1979), Ghiorso et al. (1983) and Nielsen & Dungan (1983). The model of Nathan & Van Kirk (1977) is based on a purely empirical relationship between the phases present and the liquid compositions and has no basis in thermodynamics. Nielsen & Drake (1979) considered three pyroxene - liquid models and concluded that a macroscopic M site ideal mixing pyroxene model together with a modified version of the Bottinga-Weill polymer liquid model were best able to describe pyroxene - liquid equilibria. Nielsen & Dungan (1983) retained the modified Bottinga-Weill liquid model but considered the pyroxene in terms of four end-member components, the site occupancies for which were determined according to the model of Saxena (1976), and simple oxide distribution coefficients for $AlO_{1.5}$, $CrO_{1.5}$ and TiO_2. Ghiorso et al. (1983) used a "stoichiometric mineral" melt model developed from Ghiorso & Carmichael (1980) in a regular solution model with interaction parameters determined by least squares regression and matrix inverse theory. For low-calcium pyroxenes Ghiorso et al. considered ideal mixing between $MgSiO_3$ and $FeSiO_3$, the site occupancies for which were determined by thier own method.

All the above models were based on data bases of no more than 50 pairs of low-calcium pyroxene - liquid analyses. Because of this small data base no attempt was made to distinguish between orthopyroxene and pigeonite in any of these models. As orthopyroxene and pigeonite are known to coexist in some rocks a model that fails to distinguish between them cannot accurately describe equilibria in all cases.

The 80 new pairs of low-calcium pyroxene - liquid analyses (55 orthopyroxene - liquid, 25 pigeonite - liquid) produced in this experimental study were combined with 111 pairs of analyses (34 orthopyroxene - liquid, 77 pigeonite - liquid) found in a search of the available literature to give a far larger data set than previously considered. Initially this data set was applied to some simple models based on recalculation schemes for pyroxene components and to some of the previously described models so that the quality of these models could be more accurately compared.

All the models based on pyroxene recalculation schemes used a simple oxide melt model which assumed ideal mixing of all component oxides. The pyroxene recalculation schemes used were those of Lindsley & Anderson (1980), Cawthorn & Collerson (1974) and Schweitzer et al. (1979); a simple model where the wollastonite, enstatite and ferrosilite contents were calculated from the analysis as presented was also considered. All these models produced a good fit for enstatite, a reasonable fit for wollastonite or diopside and hedenbergite and a poor fit for ferrosilite. The poor fit for ferrosilite suggests that either the simple oxide melt model is unable to describe equilibria in iron bearing systems or that the recalculation schemes do not adequately describe the behaviour of ferrosilite. A variety of minor components are considered in these recalculation schemes, only those where the "minor" element was combined with a "major" element produced a good fit, e.g. $MgCrSiAlO_6$ (Schweitzer et al., 1979). This reflects the absence of any obvious coupled substitutions in the pyroxenes of the data set and the low concentrations of many of these "minor" elements in the pyroxenes and/or liquids.

The modified Bottinga-Weill melt model of Nielsen & Drake (1979) and Nielsen & Dungan (1983) was considered with an ideal mixing pyroxene model the site occupancies for which were determined by an adaptation of the method of Ghiorso et al. (1983). This model gave a far better fit for the qudrilateral components than any of the recalculation scheme - simple oxide models above. The fit for ferrosilite was considerably improved although still not as good as the fit for enstatite, diopside and hedenbergite components. For the "minor" elements the use of simple oxides only gave a reasonable fit for MnO. The poor fit for the other oxides can, in part, be attributed to the low concentrations of these oxides in the pyroxenes and/or liquids. The fit for manganese was improved by using a $Mn_2Si_2O_6$ component; however, the fit for a $NaAlSi_2O_6$ component was not significantly better than the fit for Na_2O.

The "stoichiometric mineral" regular solution liquid model of Ghiorso et al. (1983) and the adapted pyroxene site occupancy model gave a reasonable fit for all four quadrilateral components. However, the fit for enstatite, which is the major component in

low-calcium pyroxenes, was not as good as that obtained from any of the other models. The use of the "stoichiometric mineral" liquid model without any interaction parameters gave a particularly poor fit for enstatite, suggesting that the $Mg_4Si_2O_8$ liquid component is not suitable for describing low-calcium pyroxene - melt equilibria.

New interaction parameters were calculated, using a least squares method, for both low-calcium pyroxenes and liquid using the melt models of Ghiorso et al. (1983) and Nielsen & Dungan (1983), in addition interaction parameters were calculated for the pyroxenes alone using the regular mixing melt model of Ghiorso et al. (1983). Models using these interaction parameters did not improve the fit when compared to the same model without the interaction parameters. It appears that there is insufficient data for the accurate calculation of enough interaction parameters to make a difference to these models.

Thus the model that best describes low-calcium pyroxene - melt equilibria is that using the modified Bottinga-Weill polymer melt model of Nielsen & Dungan (1983) and ideally mixing pyroxene components the site occupancy of which was determined by an adaptation of the method of Ghiorso et al. (1983). This model, used as a geothermometer, was able to reproduce the experimental temperatures of the data set to within 35°C (2σ) for orthopyroxene - liquid pairs and 57°C (2σ) for pigeonite - liquid pairs. Used as a liquidus temperature equation it was able to reproduce the experimental temperatures of the data set to within 30°C (2σ) for both orthopyroxene - and pigeonite - liquid pairs. At the same time it was able to reproduce the enstatite activity in the orthopyroxene to within 7.5% (2σ) and in the pigeonite to within 32% (2σ). For the other quadrilateral components the activities calculated were only within 50% (2σ) of the original values; however, as enstatite is the major component of these low-calcium pyroxenes the poor reproducibility for the other components is to be expected.

TABLE 6.1

Summary of Low-calcium Pyroxene - Melt Distribution Coefficients

element	$D^{opx/liq}$	$D^{pig/liq}$	related to
Mg	2.30 - 6.00	2.30 - 6.00	temperature
Fe	0.70 - 2.30	0.70 - 2.30	temperature
Mg/Fe	0.25 - 0.52	0.25 - 0.52	temperature & composition
Ca	0.09 - 0.28	0.20 - 0.60	temperature
Mn	0.50 - 3.10	0.50 - 3.10	temperature
Si	0.80 - 0.97	0.80 - 0.97	composition
Na	0.01 - 0.06	0.02 - 0.24	(composition)
Al	0.025- 0.18	0.025- 0.18	(temeprature & composition)
Ti	0.05 - 0.46	0.05 - 0.40	constant $D_{Ti}=0.16$
Cr	0.22 -12.20	0.22 - 12.20	constant $D_{Cr}=2.0$

Figure 6.1

Phase diagram for calc-alkaline series rocks; fig. 3, Grove et al. (1982).

Figure 6.2

Phase diagram for rocks crystallising olivine + orthopyroxene with minor amounts of plagioclase.

* N.B. These two phase diagrams use different projection schemes (Grove et al., 1982; O'Hara, 1968). However, by comparing figs. 4.4 and 6.1 it can be seen that the trend described by Grove et al.'s (1982) data is the same in both projections.

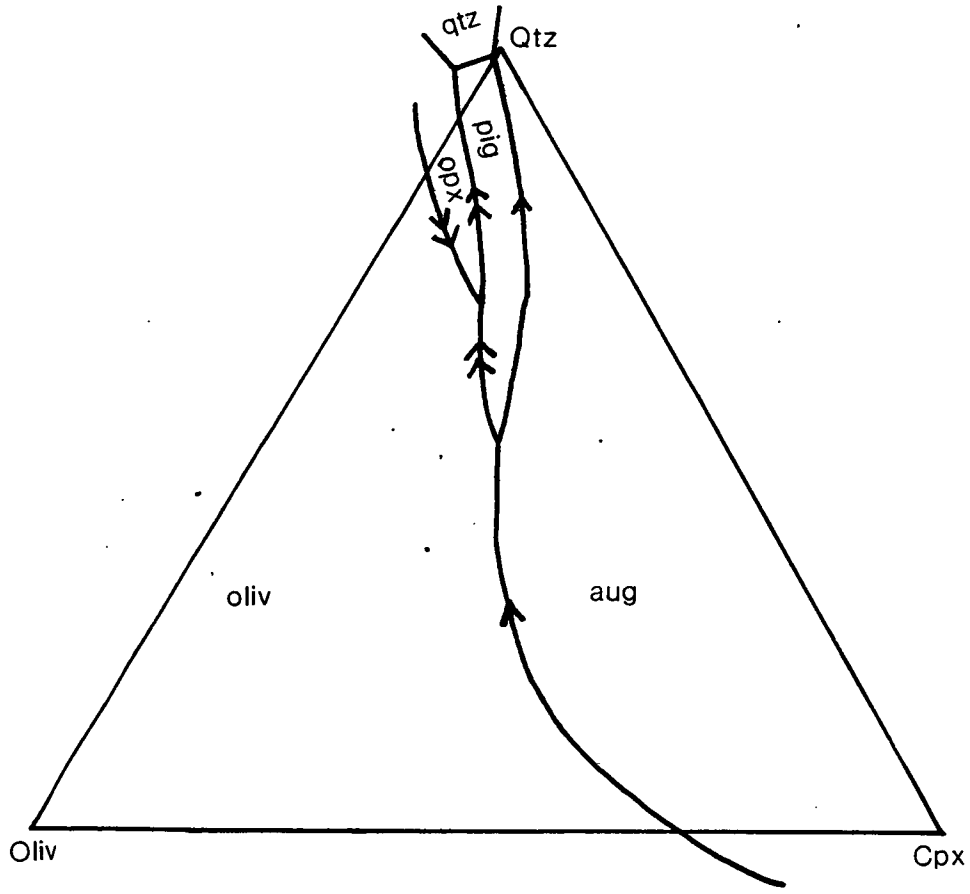
qtz
Qtz
pig
opx
oliv
aug
Oliv
Cpx

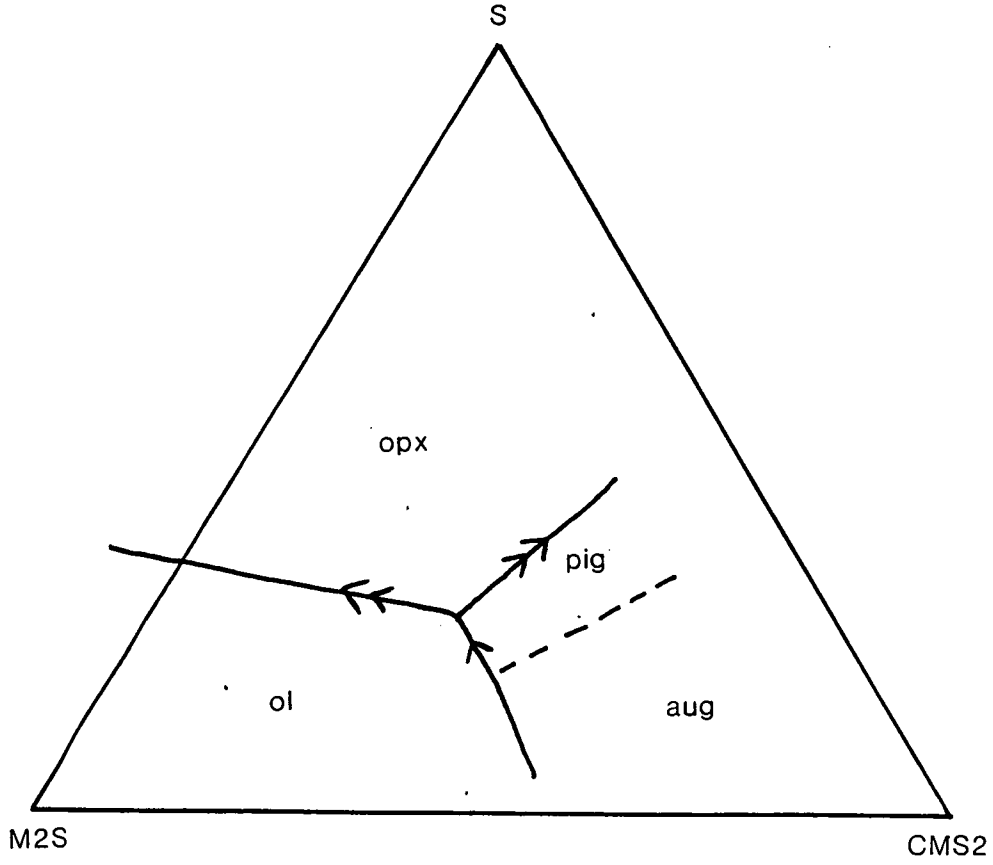
S
opx
pig
ol
aug
M2S
CMS2

ACKNOWLEDGEMENTS

Firstly I would like to thank my supervisors Gordon Biggar and Cliff Ford for their assistance throughout this project. Thanks are also due to Professors Sir Fred Stewart, Gordon Craig and Brian Upton for the use of the departments facilities.

I would also like to thank the probe unit of Pete Hill, Dougie Russell and Elizabeth Cairns for their assistance in producing the numbers on which this thesis is based. Thanks are also due to the technical staff of the department especially Diana Baty for her draughting and photographic skills, and the secretaries Heather, Denise and Patricia for their assistance in the production of the thesis.

I am also grateful to Andy Walker, Bob Cheeney, Cliff Ford and others unknown for many of the computer programs which I have used.

I have had many useful discussions on various topics with Derek Armshaw, John Craven, Steve Elphick, Martin Fisk, Dougie Russell and Mark Welch. I am also grateful for the proof-reading talents of John Craven and Dougie Russell.

Finally I would like to thank my husband Alan for financial and moral support over the years.

This project was carried out during the tenure of a Natural Environment Research Council award.

I would also like to thank J. Mitchell (Aberystwyth) for allowing me to use some of his unpublished analyses.

REFERENCES

ATLAS L. 1952. The polymorphism of $MgSiO_3$ and solid state equilibria in the system $MgSiO_3$-$CaMgSi_2O_6$. J. Geol. **60**, 125-147.

BANCROFT G.M., BURNS R.G. & HOWIE R.A. 1967. Determination of the cation distribution in the orthopyroxene series by the Mossbauer effect. Nature **213**, 1221-1223.

BASALTIC VOLCANISM STUDY PROJECT 1981. Basaltic volcanism on the terrestrial planets. Pergamon Press, Inc. New York

BERMAN R.G. & BROWN T.H. 1984. A thermodynamic model for multicomponent melts, with application to the system CaO-Al_2O_3-SiO_2. Geochim. cosmochim. Acta **48**, 661-678.

BIGGAR G.M. 1970. Molybdenum as a container for melts containing iron-oxide. Bull. Amer. Ceram. Soc. **49**, 286-288.

BIGGAR G.M. 1974. Oxygen partial pressures: control, variation and measurement in quench furnaces at one atmosphere total pressure. Mineralog. Mag. **39**, 580-586.

BIGGAR G.M. 1981a. Na_2O mobility in one atmosphere quench furnaces. Prog. Expt. Petr. **4**, 89-90, NERC Series D No. 18

BIGGAR G.M. 1981b. Melting experiments on ocelli and matrix samples from proterozoic lavas in South Africa. Bull. Mineral. **104**, 369-374.

BIGGAR G.M. 1984a. Calcium poor pyroxenes in the system CaO-MgO-Al_2O_3-SiO_2. Prog. Expt. Petr. **5**, 136-138, NERC Series D No. 25.

BIGGAR G.M. 1984b. The composition of diopside solid solutions, and of liquids, in equilibrium with forsterite, plagioclase and liquid in the system Na_2O-CaO-MgO-Al_2O_3-SiO_2 and remelted rocks from 1bar to 12kb. Mineralog. Mag. **48**, 481-494.

BIGGAR G.M. & O'HARA M.J. 1969. Temperature control and calibration in quench furnaces and some new temperature measurements in the system CaO-MgO-Al_2O_3-SiO_2. Mineralog. Mag. **37**, 1-15.

BIGGAR G.M., O'HARA M.J., PECKETT A. & HUMPHRIES D.J. 1971. Lunar lavas and the achrondrites: petrogenesis of protohypersthene basalts in the maria lava lakes. Proc. Lunar Sci. Conf. 2nd. 617-643.

BOHLEN S.R., BOETTCHER A.L., DOLLASE W.A. & ESSENE E.J. 1980. The effect of manganese on olivine-quartz-orthopyroxene stability. Earth Planet. Sci. Lett. **47**, 11-20.

BOWEN N.L. & SCHAIRER J.F. 1935. The system MgO-FeO-SiO_2. Am. J. Sci. **29**, 151-217.

BOYD F.R. & SCHAIRER J.F. 1964. The system $MgSiO_3$-$CaMgSi_2O_6$. J. Petrol. 5, 275-309.

CAMERON M. & PAPIKE J.J. 1980. Crystal chemistry of silicate pyroxenes. In C.T. Prewitt (Ed.) Pyroxenes. Min. Soc. Am. Reviews in Mineralogy vol. 7, 5-92.

CAMERON W.E., McCULLOCH M.T. & WALKER D.A. 1983. Boninite petrogenesis: Chemical and Nd - Sr isotopic constraints. Earth Planet Sci. Lett. 65, 75-89.

CAMERON W.E., NISBET E.G. & DIETRCH V.J. 1979. Petrographic dissimilarities between ophiolitic and ocean foor basalts. In A. Panayiotou (Ed.) Ophiolites; Proceedings International Ophiolite Symposium. 182-192.

CAMPBELL I.H. & BORELY G.D. 1974. The geochemistry of pyroxenes from the lower layered series of the Jimberlana Intrusion, Western Australia. Contrib. Mineral. Petrol. 47, 281-297.

CAWTHORN R.G. & COLLERSON K.D. 1974. The recalculation of pyroxene end-member parameters and the estimation of ferrous and ferric iron content from electron microprobe analyses. Am. Mineral. 59, 1203-1208.

CAWTHORN R.G. & DAVIES G. 1983. Experimental data at 3kbars pressure on parental magma to the Bushveld Complex. Contrib. Mineral. Petrol. 83, 128-135.

CAWTHORN R.G. & McCARTHY T.S. 1977. Partitioning of nickel between immiscible picritic liquids. Earth Planet. Sci. Lett. 37, 339-346.

CAWTHORN R.G., McIVER J.R., McCARTHY T.S., WYATT B.A., FERGUSON J. & BARNES S.J. 1979. Possible liquid immiscibility textures in high-magnesia basalts from the Ventersdorp Supergroup, South Africa. J. Geol. 87, 105-113.

CORRIGAN G.M. & GIBB F.G.F. 1979. The loss of Fe and Na from a basaltic melt during experiments using the wire loop method. Mineralog. Mag. 43, 121-126.

CRAWFORD A.J. 1980. A clinoenstatite bearing cumulate olivine pyroxenite from Howqua, Victoria. Contrib. Mineral. Petrol. 75, 353-367.

DALLWITZ W.B., GREEN D.H. & THOMPSON J.E. 1966. Clinoenstatite in a volcanic rock from the Cape Vogel area, Papua. J. Petrol. 7, 375-403.

DAVIDSON L.R. 1968. Variation in ferrous iron - magnesium distribution coefficients of metamorphic pyroxenes from Quairading, Western Austraia. Contrib. Mineral. Petrol. 19, 239-259.

DEARING K.M. & BIGGAR G.M. 1984. Liquids in equilibrium with olivine, plagioclase and one or more pyroxenes. Prog. Expt. Petr. vol. 5, 129-134. NERC Series D No. 25.

DEER W.A., HOWIE R.A. & ZUSSMAN J. 1966. An introduction to the rock forming minerals. Longman Group Ltd.

DEINES P. NAFZIGER R.H. ULMER G.C. & WOERMANN E. 1974. Temperature-oxygen fugacity tables for selected gas mixtures in the system C-H-O at one atmosphere total pressure. Bull. 68 of the Earth and Mineral Sciences Experiment Station. The Pennsylvania State University.

DONALDSON C.H. 1979. Composition changes in a basalt melt contained in a wire loop of $Pt_{80}Rh_{20}$: effects of temperature, time and oxygen fugacity. Mineralog. Mag. 43, 115-119.

DRAKE M.J. 1976. Plagioclase - melt equilibria. Geochim. cosmochim. Acta 40, 457-465.

ELTHON D. & SCARFE C.M. 1984. High pressure phase equilibria of a high magnesia basalt and the genesis of primary oceanic basalts. Am. Mineral. 69, 1-15.

ELTHON D., CASEY J.F. & KOMOR S. 1982. Mineral chemistry of ultramafic cumulates from the North Arm Mountain massif of the Bay of Islands Ophiolite: Evidence for high pressure crystal fractionation of oceanic basalts. J. Geophys. Res. 87 B10, 8717-8734.

FLEET M.E. 1974. Partition of major and minor elements and equilibration in coexisting pyroxenes. Contrib. Mineral. Petrol. 44, 259-274.

FORD C.E. 1978. Platinum-iron alloy sample containers for melting experiments on iron bearing rocks, minerals and related systems. Mineralog. Mag. 42, 271-275.

FORD C.E. 1981. Parental liquids of the Skaergaard intrusion cumulates. Nature 291, 21-25.

FORD C.E. & RUSSELL D.G. 1981. Theoretical and experimental studies of magmatic evolution. Prog. Expt. Petr. vol. 4, 116-119. NERC Series D No. 18.

FORD C.E., RUSSELL D.G., CRAVEN J.A. & FISK M.R. 1983. Olivine -liquid equilibria: temperature, pressure and composition dependence of the crystal/liquid cation partition coefficients for Mg, Fe^{2+}, Ca and Mn. J. Petrol. 24, 256-265.

FREER R., CARPENTER M.A., LONG J.V.P. & REED S.J.B. 1982. "Null result" diffusion experiments with diopside: implications for pyroxene equilibria. Earth Planet. Sci. Lett. 58, 285-292.

FRENCH W.J. 1971. The correlation between "anhydrous" crystallisation temperatures and rock composition. Contrib. Mineral. Petrol. 31, 154-158.

FRENCH W.J. & CAMERON E.P. 1981. Calculation of the temperature of crystallisation of silicates from basaltic melts. Mineralog. Mag. 44, 19-26.

FUJII T. & BOUGAULT H. 1983. Melting relations of a magnesian abyssal tholeiite and the origin of MORBs. Earth Planet. Sci. Lett. 62, 283-295.

GANGULY J. & GHOSE S. 1979. Aluminous orthopyroxene: order - disorder, thermodynamic properties, and petrologic implications. Contrib. Mineral. Petrol. 69, 375-385.

GHIORSO M.S. & CARMICHAEL I.S.E. 1980. A regular solution model for met-aluminous silicate liquids:- applications to geothermometry, immiscibility, and the source regions of basic magmas. Contrib. Mineral. Petrol. 71, 323-342.

GHIORSO M.S., CARMICHAEL I.S.E., RIVERS M.L. & SACK R.O. 1983. The Gibbs free energy of mixing of natural silicate liquids; an expanded regular solution approximation for the calculation of magmatic intensive variables. Contrib. Mineral. Petrol. 84, 107-145.

GROVE T.L. & BEATTY D.W. 1980. Classification, experimental petrology and possible volcanic histories of the Apollo 11 high-K basalts. Proc. Lunar Sci. Conf. 11th, 149-177.

GROVE T.L. & BENCE A.E. 1977. Experimental study of pyroxene -liquid interaction in quartz normative basalt 15597. Proc. Lunar Sci. Conf. 8th, 1549-1579.

GROVE T.L. & BRYAN W.B. 1983. Fractionation of pyroxene phyric MORB at low pressure: an experimental study. Contrib. Mineral. Petrol. 84, 293-309.

GROVE T.L. & RAUDSEPP M. 1978. Effects of kinetics on the crystallisation of quartz normative basalt 15597: an experimental study. Proc. Lunar Sci. Conf. 9th, 585-599.

GROVE T.L., GERLACH D.C. & SANDO T.W. 1982. Origin of calc-alkaline series lavas at Medicine Lake Volcano by fractionation, assimilation and mixing. Contrib. Mineral. Petrol. 80, 160-182.

GROVE T.L., WALKER D., LONGHI J., STOLPER E. & HAYS J.F. 1973. Petrology of rock 12002 and origin of picritic basalts at Oceanus Procellarum. Proc. Lunar Sci. Conf. **4th**, 995-1011.

HENSEN B.J. & GRAY D.R. 1979. Clinohypersthene and hypersthene from a coal fire buchite near Ravensworth, N.S.W., Australia. Am. Mineral. **64**, 131-135.

HESS P.C., RUTHERFORD M.J. & CAMPBELL H.W. 1977. Origin and evolution of LKFM basalt. Proc. Lunar Sci. Conf. **8th**, 2357-2373.

HUEBNER J.S. 1980. Pyroxene phase equilibria at low pressure. In C.T. Prewitt (Ed.) Pyroxenes. Min. Soc. Am. Reviews in Mineralogy vol. 7, 213-288.

HUEBNER J.S. & TURNOCK A.C. 1980. The melting relations at 1bar of pyroxenes composed largely of Ca-, Mg- and Fe-bearing components. Am. Mineral. **65**, 225-271.

HUEBNER J.S., LIPIN B.R. & WIGGINS L.B. 1976. Partitioning of chromium between silicate crystals and melts. Proc. Lunar Sci. Conf. **7th**, 1195-1220.

HUMPHRIES D.J. 1975. Phase equilibrium studies of some basalt like compositions in the system CaO-MgO-Al_2O_3-SiO_2-Na_2O-Fe-O_2. Unpublished PhD. Thesis. University of Edinburgh.

IRVINE T.N., KEITH D.W. & TODD S.G. 1983. The J-M platinum-palladium reef of the Stillwater Complex, Montana: II Origin by double diffusive convective magma mixing and implications for the Bushveld Complex. Econ. Geol. **78**, 1287-1334.

JOHANNES W. & BODE B. 1978. Loss of iron to the Pt container in melting experiments with basalts and a method to reduce it. Contrib. Mineral. Petrol. **67**, 221-225.

KOMATSU M. 1980. Clinoenstatite in volcanic rocks from the Bonin Islands. Contrib. Mineral. Petrol. **74**, 329-338.

KUSHIRO I. 1969. The system forsterite - diopside - silica with and without water at high pressures. Am. J. Sci. **267A**, 269-294.

KUSHIRO I. 1972. Determination of liquidus relations in synthetic silicate systems with electron probe analysis: the system forsterite - diopside - silica at 1 atmosphere. Am. Mineral. **57**, 1260-1271.

KUSHIRO I. 1975. On the nature of silicate melt and its significance in magma genesis: regularities in the shift of the liquidus boudaries involving olivine, pyroxene, and silica minerals. Am. J. Sci. **275**, 411-431.

KUSHIRO I. 1980. Changes with pressure of degree of partial melting and K_2O content of liquids in the system Mg_2SiO_4-$KAlSiO_4$-SiO_2. Carnegie Inst. Washington Yearb. 79, 267-271.

LANGMUIR C.H. & HANSON G.N. 1981. Calculating mineral-melt equilibria with stoichiometry, mass balance, and single component distribution coefficients. In Newton R.C. Navrotsky A. & Wood B.J. (Eds.) Thermodynamics of Minerals and Melts. Advances in Physical Geochemistry vol. 1. Springer Verlag. 247-271.

LINDSLEY D.H. & ANDERSON D.J. 1983. A two pyroxene thermometer. Proc. Lunar Sci. Conf. 13th, J. Geophys. Res. 88 Supplement A887-906.

LONGHI J. 1978. Pyroxene stability and the composition of the lunar magma ocean. Proc. Lunar Sci. Conf. 9th, 285-306.

LONGHI J. & BOUDREAU A.E. 1980. The orthoenstatite liquidus field in the system forsterite-diopside-silica at 1 atmosphere. Am. Mineral. 65, 563-573.

LUTH W.C. & TUTTLE O.F. 1963. Externally heated cold-seal pressure vessels for use to 10,000 bars and 750°C. Am. Mineral. 48, 1401-1403.

MATSUI Y. & NISHIZAWA O. 1974. Iron(II)-magnesium exchange equilibrium between olivine and calcium-free pyroxene over a temperature range 800 to 1300°C. Bull. Mineral. 97, 122-130.

Mirchell 1984

MYERS J. & GUNTER W.D. 1979. Measurement of the oxygen fugacity of the cobalt-cobalt oxide buffer assemblage. Am. Mineral. 64, 224-228.

MYSEN B.O. & KUSHIRO I. 1977. Compositional variations of coexisting phases with degree of melting of peridotite in the upper mantle. Am. Mineral. 62, 843-865.

NATHAN H.D. & VAN KIRK C.K. 1978. A model of magmatic crystallisation. J. Petrol. 19, 66-94.

NATLAND J.H. 1982. Crystal morphologies and pyroxene compositions in boninites and tholeiitic basalts from Deep Sea Drilling Project holes 458 and 459b in the Mariana fore-arc region. In Lee M. & Powell R. (Eds.) Initial Reports of the Deep Sea Drilling Project 60, 681-707.

NIELSEN R.L. & DRAKE M.J. 1979. Pyroxene-melt equilibria. Geochim. cosmochim. Acta 43, 1259-1273.

NIELSEN R.L. & DUNGAN M.A. 1983. Low pressure mineral-melt equilibria in natural anhydrous mafic systems. Contrib. Mineral. Petrol. 84, 310-326.

O'HARA M.J. 1968. The bearing of phase equilibria studies in synthetic and natural systems on the origin and evolution of basic and ultrabasic rocks. Earth Science Reviews 4, 69-133.

O'HARA M.J. & HUMPHRIES D.J. 1977. Problems of iron gain and loss during experimentation on natural rocks: the experimental crystallisation of five lunar basalts at low pressures. Phil. Trans. R. Soc. Lond. A286, 313-330.

O'HARA M.J., BIGGAR G.M., HILL P.G., JEFFERIES B. & HUMPHRIES D.J. 1974. Plagioclase saturation in lunar high-titanium basalt. Earth Planet. Sci. Lett. 21, 253-268.

PERFIT M.R. & FORNARI D.J. 1983. Geochemical studies of abyssal lavas recovered by DSRV Alvin from Eastern Galapogos Rift, Inca Transform, and Ecuador Rift 2: Phase chemistry and crystallisation history. J. Geophys. Res. 88 B12, 10530-10550.

PRESNALL D.C., DIXON S.A., DIXON J.R., O'DONNELL T.H., BRENNER N.L., SCHROCK R.L. & DYCUS D.W. 1978. Liquidus phase relations on the join diopside-forsterite-anorthite from 1 atm. to 20 kb: Their bearing on the generation and crystallisation of basaltic magma. Contrib. Mineral. Petrol. 66, 203-220.

PRESNALL D.C., DIXON J.R., O'DONNELL T.H. & DIXON S.A. 1979. Generation of mid-ocean ridge tholeiites. J. Petrol. 20, 3-35.

RHODES J.M. LOFGREN G.E. & SMITH D.P. 1979. One atmosphere melting experiments on ilmenite basalt 12008. Proc. Lunar Sci. Conf. 10th. 407-422.

ROBINSON P. 1980. The compositional space of terrestrial pyroxenes - internal and external limits. In C.T. Prewitt (Ed.) Pyroxenes Min. Soc. Am. Reviews in Mineralogy vol. 7, 419-494.

ROEDER P.L. & EMSLIE R.F. 1970. Olivine - liquid equilibrium. Contrib. Mineral. Petrol. 29, 275-289.

ROSS M. & HUEBNER J.S. 1979. Temperature - composition relationships between naturally occurring augite, pigeonite and orthopyroxene at one bar pressure. Am. Mineral. 64, 1133-1155.

RUSSELL D.G. 1981. Atmospheric pressure experiments with Fe-doped Pt wire hooks. Prog. Expt. Petr. vol. 4, 90-91. NERC Series D No. 18

RUSSELL D.G. 1985. Experimental and petrological studies of phenocryst assemblages in Scottish Permo-Carboniferous basaltic rocks. Unpublished PhD. Thesis, University of Edinburgh.

SACK R.O., CARMICHAEL I.S.E., RIVERS M. & GHIORSO M.S. 1980. Ferric-ferrous equilibria in natural silicate liquids at 1 bar. Contrib. Mineral. Petrol. 75, 369-376.

SAMASHIMA T., PARIS J.-P., BLACK P.M. & HEMING R.F. 1983. Clinoenstatite - bearing lava from Nepoui, New Caledonia. Am. Mineral. 68, 1076-1082.

SAXENA S.K. 1976. Two pyroxene geothermometer: a model with an approximate solution. Am. Mineral. 61, 643-652.

SCARFE C.M., MYSEN B.O. & RAI C.S. 1979. Invariant melting behaviour of mantle material: Partial melting of two lherzolite nodules. Carnegie Inst. Washington Yearb. 78, 498-501.

SCHREIBER H.D. & HASKIN L.A. 1976. Chromium in basalts: Experimental determination of redox states and partitioning among synthetic silicate phases. Proc. Lunar Sci. Conf. 7th, 1221-1259.

SCHWEITZER E.L., PAPIKE J.J. & BENCE A.E. 1979. Statistical analysis of clinopyroxenes from deep-sea basalts. Am. Min. 64, 501-513.

SHARASKIN A.Ya., DOBRETSOV N.L. & SOBOLEV N.V. 1980. Marianites: The clinoenstatite bearing pillow lavas associated with the ophiolite assemblage of Mariana Trench. In A. Panayiotou (Ed.) Ophiolites; Proceedings International Ophiolite Symposium. 473-479.

SHARPE M.R. & IRVINE T.N. 1983. Melting relations of two Bushveld chilled margin rocks and implications for the origin of chromitite. Carnegie Inst. Washington Yearb. 82, 295-300.

SHIRAKI K., KURODA N., URANO H. & MARUYAMA S. 1980. Clinoenstatite in boninites from the Bonin Islands, Japan. Nature 285, 31-32.

SMITH D. & LINDSLEY D.H. 1971. Stable and metastable augite crystallisation trends in a single basalt flow. Am. Mineral. 56, 225-233.

SMYTH J.R. 1974. The high temperature crystal chemistry of clinohypersthene. Am. Mineral. 59, 1069-1082.

SNELLENBURG J.W. 1975. Computer simulation of the distribution of octahedral cations in orthopyroxene. Am. Mineral. 60, 441-447.

STOLPER E. 1977. Experimental petrology of eucritic meteorites. Geochim. cosmochim. Acta 41, 587-611.

STOLPER E. 1980. A phase diagram for mid-ocean ridge basalts:- preliminary results and implications for petrogenesis. Contrib. Mineral. Petrol. **74**, 13-27.

SWEATMAN T.R. & LONG J.V.P. 1969. Quantitative electron probe microanalysis of rock forming minerals. J. Petrol. **10**, 332-379.

THOMPSON R.N. 1972. The 1 atmosphere melting patterns of some basaltic volcanic series. Am. J. Sci. **272**, 901-932.

TILLEY C.E., YODER H.S. & SCHAIRER J.F. 1964. New relations on melting of basalts. Carnegie Inst. Washington Yearb. **63**, 92-97.

VERHOOGEN J. 1962. Distribution of titanium between silicates and oxides in igneous rocks. Am. J. Sci. **260**, 211-220.

VIRGO P. & HAFNER S.S. 1969. Fe^{2+}, Mg order disorder in heated orthopyroxenes. Min. Soc. Am. Spec. Paper 2, 67-81.

WALKER D., KIRKPATRICK R.J., LONGHI J. & HAYS J.F. 1976. Crystallisation history of lunar picritic basalt sample 12002: Phase equilibria and cooling rate studies. Bull. Geol. Soc. Am. **87**, 646-656.

WALKER D., LONGHI J., GROVE T.L., STOLPER E. & HAYS J.F. 1973. Experimental petrology and origin of rocks from the Descartes Highlands. Proc. Lunar Sci. Conf. **4th**, 1013-1032.

WALKER D., LONGHI J., LASAGA A.C., STOLPER E.M., GROVE T.L. & HAYS J.F. 1977. Slowly cooled microgabbros 15555 and 15065. Proc. Lunar Sci. Conf. **8th**, 1521-1547.

WALKER D., SHIBATA T. & DeLONG S.E. 1979. Abyssal tholeiites from the oceanographer fracture zone. II Phase equilibria and melting. Contrib. Mineral. Petrol. **70**, 111-125.

WALSH D. DONNAY G. & DONNAY J.D. 1974. Jahn-Teller effects in ferromagnesian minerals: pyroxenes and olivines. Bull. Mineral. **97**, 170-183.

WEILL D.F. & McKAY G.A. 1975. The partitioning of Mg, Fe, Sr, Ce, Sm, Eu, and Yb in lunar igneous systems and a possible origin of KREEP by equilibrium partial melting. Proc. Lunar Sci. Conf. **6 th**, 1143-1158.

WILSON A.H. 1982. The geology of the Great "Dyke", Zimbabwe: The ultramafic rocks. J. Petrol. **23**, 240-292.

WOOD C.P. 1980. Boninite at a continental margin. Nature **288**, 692-694.

WYLLIE P.J. 1971. The Dynamic Earth. John Wiley & Sons, New York.

YANG H.-Y. 1973. Crystallisation of iron-free pigeonite in the system anorthite - diopside - enstatite - silica at atmospheric pressure. Am. J. Sci. 273, 488-497.

ZVEREV N.D., VAL'TER A.A., ROMANOV V.P. & GOROGOTSKAYA L.I. 1971. Character of Fe^{2+} ion distribution in pyroxenes from eulysite. Lithos 4, 17-21.

APPENDIX I

SAMPLES USED FOR EXPERIMENTS IN THIS STUDY

Description Of Samples

All samples were chosen on the basis of their composition as reported in published work. The whole rock analyses are given in table A I.1, low-calcium pyroxene analyses are given in table A I.2. Brief descriptions of the samples are given below.

M1, C2, C5 and C11 - samples of boninite from the Bonin Islands, Japan provided by M. Komatsu (Komatsu, 1980). They contain phenocrysts of orthopyroxene, clinoenstatite, augite and, in samples M1 and C11, olivine, in a glassy matrix. Many of the crystals exhibit quench textures.

17M, 170 and 120 - samples of matrix (M) and ocelli (O) from the Eagle Brick Quarry, South Africa (Cawthorn & McCarthy, 1977; Cawthorn et al., 1979) provided by G. Cawthorn. As these rocks have been subjected to greenschist facies metamorphism the original, igneous, mineralogy has been destroyed and the rocks are now composed principally of tremolite and chlorite with disseminated grains of pyrite. These samples have previously been studied by Biggar (1981b) when the phase relations were affected by large sodium gains during the experiments.

K1 and K6 - samples of boninite from North Island, New Zealand provided by C.P. Wood (Wood, 1980). They contain phenocrysts of orthopyroxene, pigeonite, augite and olivine in a glassy matrix.

B4 and B5 - samples of sills from near the Bushveld Complex, South Africa (Cawthorn & Davies, 1983), provided by G. Cawthorn. B4 is described as a micropyroxenite containing pseudomorphed olivines and sheaves of bladed orthopyroxenes in a devitrified glass. B5 is described as a medium grained quartz norite. No mineral anlyses are available.

295 - sample from the East Dyke, near the Great Dyke, Zimbabwe (East Dyke Chill sample of Wilson, 1982), provided by S. Tait. Analyses of orthopyroxene in table A I.2 are from Wilson (1982).

T2 - sample from a sill from A Mhoine, Sutherland, Scotland, provided by A. Baxter. Analyses given in table A I.2 are from Baxter (pers. comm.). T2 contains phenocrysts of orthopyroxene (originally thought to be clinoenstatite but they contain too much CaO) in a groundmass of orthopyroxene, pigeonite and feldspar.

TABLE AI.1

	1	2	3	4	5	6	7	8
SiO2	51.49	57:09	55.12	52.79	52.24	52.05	54.19	49.97
TiO2	0.49	0.95	0.89	0.94	0.17	0.17	0.18	0.19
Al2O3	11.40	8.39	9.25	9.21	12.70	12.71	9.57	10.17
Fe2O3	1.38	nd	nd	nd	5.09	2.12	3.30	3.97
Cr2O3	0.33	nd	nd	nd	nd	nd	0.12	0.06
FeO	8.29	9.66	8.47	12.11	4.41	6.65	5.43	3.71
MnO	0.17	0.13	0.09	0.14	0.16	0.17	0.16	0.12
NiO	0.06	nd	nd	nd	nd	nd	nd	nd
MgO	16.00	13.27	10.55	14.70	10.99	10.78	12.79	9.96
CaO	7.08	7.79	6.39	7.49	10.82	10.37	8.54	5.34
Na2O	1.69	1.63	2.74	1.19	1.42	1.77	0.96	1.60
K2O	0.61	0.12	0.19	0.35	0.10	0.09	0.29	0.92
P2O5	0.09	0.12	0.09	0.09	0.09	0.08	0.01	0.01
H2O-	0.08	1.02	6.94	1.82	0.83	1.76	1.91	9.70
H2O+	1.10	nd	nd	nd	1.59	0.82	2.50	4.00
total=	100.26	100.17	100.72	100.83	100.61	99.54	99.95	99.72
qtz	-	8.48	6.88	1.17	7.96	3.88	11.48	11.17
en	28.62	27.18	21.53	32.17	19.25	20.09	25.29	22.01
fs	9.84	13.50	11.68	18.41	2.75	7.85	5.75	3.05
cen	3.62	5.87	4.74	4.44	8.12	6.76	6.56	2.79
cfs	1.24	2.91	2.57	2.54	1.16	2.64	1.49	0.39
cwo	5.28	9.36	7.75	7.37	10.41	10.15	8.91	3.57
fo	5.33	-	-	-	-	-	-	-
fa	2.02	-	-	-	-	-	-	-
or	3.60	0.71	1.12	2.07	0.59	0.53	1.71	5.44
an	21.72	15.22	12.38	18.75	27.98	26.47	20.95	17.85
ab	14.30	13.79	23.18	10.07	12.02	14.98	8.12	13.54
mag	2.00	-	-	-	7.38	3.07	4.78	5.76
ilm	0.93	1.80	1.69	1.79	0.32	0.32	0.34	0.36
ap	0.27	0.36	0.27	0.27	0.27	0.24	0.03	0.03
chr	0.49	-	-	-	-	-	0.18	0.09

1 295 GREAT DYKE,A.H.WILSON J.PET. 23 1982
2 120 EAGLE BRICK,R.G.CAWTHORN & MCCARTHY EPSL 37 1977
3 170 EAGLE BRICK,CAWTHORN R.G. & MCCARTHY EPSL 37 1977
4 17M EAGLE BRICK,R.G.CAWTHORN & MCCARTHY EPSL 37 1977
5 KOPI 1,C.P.WOOD NATURE 288 1980
6 KOPI 6,C.P.WOOD NATURE 288 1980
7 C2 BONIN IS.,KOMATSU M. CMP 74 1980
8 C5 BONIN IS.,KOMATSU M.CMP 74 1980

	9	10	11	12	13
SiO2	55.68	56.31	55.70	54.31	55.01
TiO2	0.20	0.16	0.36	0.57	1.57
Al2O3	12.04	8.23	12.74	15.09	14.90
Fe2O3	2.33	4.08	1.79	2.05	nd
Cr2O3	0.10	0.10	nd	nd	nd
FeO	5.74	5.12	7.17	8.22	10.30
MnO	0.16	0.21	0.09	0.22	0.12
MgO	9.74	11.02	12.44	6.48	6.95
CaO	7.80	7.65	6.96	9.52	7.16
Na2O	1.69	1.46	2.02	2.21	3.10
K2O	0.44	0.49	1.03	0.61	0.64
P2O5	0.01	0.03	nd	nd	nd
H2O-	1.16	1.09	nd	nd	nd
H2O+	2.91	4.31	nd	nd	0.72
total=	100.00	100.26	100.30	99.28	100.47
qtz	12.22	15.45	3.99	7.04	3.60
en	20.09	20.28	27.62	12.15	15.08
fs	7.11	4.55	10.04	9.69	14.41
cen	4.16	7.16	3.36	3.99	2.23
cfs	1.47	1.61	1.22	3.18	2.13
cwo	6.11	9.70	4.96	7.42	4.46
or	2.60	2.90	6.09	3.60	3.78
an	23.97	14.46	22.65	29.45	24.85
ab	14.30	12.35	17.09	18.70	26.23
mag	3.38	5.92	2.60	2.97	-
ilm	0.38	0.30	0.68	1.08	2.98
ap	0.03	0.09	-	-	-
chr	0.15	0.15	-	-	-

9 C11 BONIN IS.,KOMATSU M. CMP 74 1980
10 M1 BONIN IS.,KOMATSU M. CMP 74 1980
11 B4 BUSHVELD,CAWTHORN R.G. ETAL RES.REP. 1979
12 B5 BUSHVELD,CAWTHORN R.G. ETAL RES.REP. 1979
13 T2 BAXTER A.N. PERS. COMM

TABLE AI.2

	1 W	2 W	3 W	4 W	5 W	6 W	7 W	8 W
SiO_2	40.93	55.39	53.75	51.02	55.58	55.89	51.44	51.47
TiO_2	nd	0.09	0.13	0.37	0.04	0.02	0.18	0.08
Al_2O_3	nd	1.57	3.89	4.32	1.74	1.59	5.51	4.67
Cr_2O_3	0.20	0.93	0.30	0.29	0.87	0.53	0.16	0.36
FeO	10.61	7.97	11.45	9.15	7.11	8.30	7.43	6.73
MnO	0.12	0.15	0.34	0.16	0.19	0.18	0.22	0.12
NiO	0.29	0.11	0.35	0.03	0.11	0.09	0.04	0.01
MgO	48.72	31.86	27.56	18.00	32.29	30.80	18.72	16.83
CaO	0.22	1.45	2.60	15.93	1.79	2.87	15.55	20.22
Na_2O	nd	nd	nd	0.20	0.04	0.04	0.08	0.10
K_2O	nd	nd	nd	nd	nd	nd	nd	0.01
total=	101.10	99.52	100.37	99.47	99.76	100.31	99.33	100.60
Si	1.00	1.95	1.91	1.88	1.94	1.96	1.88	1.88
Ti	-	-	-	0.01	-	-	-	-
Al	-	0.07	0.16	0.19	0.07	0.07	0.24	0.20
Cr	-	0.03	-	-	0.02	0.01	-	0.01
Fe_2	0.22	0.23	0.34	0.28	0.21	0.24	0.23	0.21
Mn	-	-	0.01	-	-	-	-	-
Mg	1.77	1.67	1.46	0.99	1.68	1.61	1.02	0.92
Ca	-	0.05	0.10	0.63	0.07	0.11	0.61	0.79
Na	-	-	-	0.01	-	-	-	-
total=	3.00	4.01	4.00	4.01	4.01	4.00	4.00	4.02
oxygens=	[4]	[6]	[6]	[6]	[6]	[6]	[6]	[6]
WO	0.3	2.8	5.2	33.1	3.4	5.5	32.8	41.4
EN	88.9	85.2	76.9	52.0	86.0	82.1	55.0	47.9
FS	10.9	12.0	17.9	14.8	10.6	12.4	12.2	10.7

1 295 GREAT DYKE,WILSON J.PET.23 1982
2 OPX 295 GREAT DYKE,WILSON J.PET.23 1982
3 OPX 295 GREAT DYKE,WILSON J.PET.23 1982
4 CPX 295 GREAT DYKE,WILSON J.PET.23 1982
5 OPX KOPI,WOOD NATURE 288 1980
6 PIG KOPI,WOOD NATURE 288 1980
7 CPX KOPI,WOOD NATURE 288 1980
8 CPX KOPI,WOOD NATURE 288 1980

TABLE AI.2

	9 W	10 W	11 W	12 W	13 W	14 W	15 W	16 W
SiO_2	57.43	56.74	55.94	57.36	57.80	57.27	55.23	55.59
TiO_2	nd	0.03	0.05	nd	0.01	nd	0.03	0.03
Al_2O_3	0.30	0.54	1.27	0.11	0.17	0.32	0.84	0.56
Cr_2O_3	0.46	0.66	1.08	0.28	0.23	0.27	0.36	0.36
FeO	6.64	6.99	8.27	6.32	7.03	7.77	12.35	11.45
MnO	0.08	0.09	0.20	0.09	0.15	0.18	0.21	0.24
MgO	34.78	33.62	31.12	34.97	34.41	33.75	28.51	30.22
CaO	0.32	0.80	1.39	0.26	0.34	0.93	2.51	1.97
Na_2O	0.01	0.05	0.02	nd	0.02	nd	0.01	nd
total=	100.02	99.52	99.34	99.39	100.16	100.49	100.05	100.42
Si	1.98	1.98	1.97	1.99	1.99	1.98	1.97	1.97
Al	0.01	0.02	0.05	-	-	0.01	0.04	0.02
Cr	0.01	0.02	0.03	-	-	-	0.01	0.01
Fe_2	0.19	0.20	0.24	0.18	0.20	0.22	0.37	0.34
Mg	1.79	1.75	1.63	1.81	1.77	1.74	1.52	1.59
Ca	0.01	0.03	0.05	-	0.01	0.03	0.10	0.07
total=	4.00	4.00	3.99	4.00	4.00	4.01	4.01	4.02
oxygens=	[6]	[6]	[6]	[6]	[6]	[6]	[6]	[6]
WO	0.6	1.5	2.7	0.5	0.6	1.7	4.8	3.7
EN	89.8	88.2	84.7	90.4	89.1	87.0	76.5	79.4
FS	9.6	10.3	12.6	9.2	10.2	11.2	18.6	16.9

9 CLINOEN C5 BONIN IS.,KOMATSU CMP 74 1980

10 OPX ASS WITH CLINOEN C5 BONIN IS.,KOMATSU CMP 74 1980

11 OPX C5 BONIN IS.,KOMATSU CMP 74 1980

12 CLINOEN M1 BONIN IS.,KOMATSU CMP 74 1980

13 CLINOEN ASS WITH OL M1 BONIN IS.,KOMATSU CMP 74 1980

14 OPX ASS WITH CLINOEN,HIGH MG,M1 BONIN IS.,KOMATSU CMP 74 1980

15 OPX ASS WITH CLINOEN,LOW MG,M1 BONIN IS.,KOMATSU CMP 74 1980

16 OPX,HIGH MG,M1 BONIN IS.,KOMATSU CMP 74 1980

TABLE AI.2

	17	18	19
	W	W	W
SiO_2	54.73	52.61	53.99
TiO_2	nd	0.02	0.21
Al_2O_3	0.65	1.44	2.52
Cr_2O_3	0.59	0.36	0.47
FeO	14.23	8.90	11.34
MnO	0.32	0.21	0.20
NiO	nd	nd	0.07
MgO	27.66	16.84	29.07
CaO	1.96	19.86	1.55
Na_2O	0.01	0.08	0.06
total=	100.15	100.32	99.48
Si	1.97	1.94	1.93
Al	0.03	0.06	0.11
Cr	0.02	0.01	0.01
Fe_2	0.43	0.28	0.34
Mg	1.48	0.93	1.55
Ca	0.08	0.79	0.06
total=	4.01	4.02	4.01
oxygens=	[6]	[6]	[6]
WO	3.8	39.5	3.0
EN	74.7	46.6	79.5
FS	21.5	13.8	17.4

17 OPX,LOW MG,M1 BONIN IS.,KOMATSU CMP 74 1980
18 CPX M1 BONIN IS.,KOMATSU CMP 74 1980
19 OPX T2,A.N. BAXTER PERS. COMM

APPENDIX II

ELECTRON MICROPROBE OPERATING CONDITIONS

ELECTRON MICROPROBE OPERATING CONDITIONS

Electron microprobe analyses were carried out using a Cambridge Instruments Microscan 5 with 2 wavelength dispersive specrometers (WDS) and fitted with a Link Systems energy dispersive system (EDS). The take - off angle of the instrument is 75°. Most analyses were carried out using the wavelength dispersive spectrometers with QTZ, RAP and LIF crystals. The electron beam was operated at 20kV accelerating potential and 30nA probe current measured at a Faraday cage, yielding a spot nominally 1-2um in diameter. Standards used were wollastonite (Si & Ca), corundum (Al), jadeite (Na), orthoclase (K), apatite (P), periclase (Mg), olivine (Mg), rutile (Ti) and spec. pure metal (Fe, Cr, Mn, Pt). Fully corrected analyses were produced on-line using a ZAF correction procedure after Sweatman & Long (1969). Precision, expressed as a percentage of what's present, and detection limits were determined by the following equations:-

$$\text{detection limit } (3\ ) = \frac{3}{m\sqrt{\frac{R_b}{T_b}}}$$

$$\text{precision} = \frac{100}{\sqrt{T_p}} \cdot \frac{1}{\sqrt{R_p} - \sqrt{R_b}}$$

where m = counts $sec^{-1}\%^{-1}$
R_b = background count rate
T_b = time on background (secs)
R_p = peak count rate
T_p = time on peak (secs)

Precision and detection limits for the phases analysed in this study are given in table AII. These values represent the lowest possible amount of analytical variation, other variables inherent in the day to day operation of the machine tend to have an adverse effect on the precision

Some early analyses (experiments 4/216 to 4/220) were carried out using the EDS system where the beam was operated at 20kV and 6nA. The secondary standard used was cobalt and analyses were based on 100 seconds livetime counting; the ZAF procedure was identical to that used for the WDS system. The EDS system is less precise than the WDS system especially at low concentrations.

ORTHOPYROXENE 17M-3/677

Oxide	wt%	precision 2σ	detection limit
CaO	0.87	0.0710	0.0256
NA_2O	0.03	0.0123	0.0113
TiO_2	0.06	0.0367	0.0359
Cr_2O_3	0.38	0.0463	0.0356
MgO	33.65	0.1704	0.0180
MnO	0.15	0.0397	0.0357
Al_2O_3	0.51	0.0337	0.0215
FeO	7.64	0.1440	0.0447
SiO_2	57.55	0.2931	0.0367

PIGEONITE 120 3/707

Oxide	wt%	precision 2σ	detection limit
CaO	3.02	0.0872	0.0281
Na_2O	0.21	0.0198	0.0054
TiO_2	0.16	0.0396	0.0342
Cr_2O_3	0.50	0.0513	0.0383
MgO	29.78	0.1640	0.0192
MnO	0.16	0.0424	0.0387
Al_2O_3	1.06	0.0433	0.0234
FeO	8.82	0.1515	0.0430
SiO_2	56.21	0.2906	0.0410

CLINOPYROXENE C2MET 3/776

Oxide	wt%	precision 2σ	detection limit
CaO	14.82	0.1407	0.0242
Na_2O	0.12	0.0175	0.0134
TiO_2	0.03	0.0307	0.0311
Cr_2O_3	0.12	0.0305	0.0283
MgO	20.24	0.1406	0.0191
MnO	0.24	0.0362	0.0313
Al_2O_3	1.76	0.0509	0.0221
FeO	8.64	0.1179	0.0349
SiO_2	53.22	0.2752	0.0354

GLASS 120 3/770

Oxide	wt%	precision 2σ	detection limit
K_2O	0.27	0.2400	0.0214
Na_2O	1.96	0.0640	0.0195
CaO	9.53	0.1140	0.0236
P_2O_5	0.23	0.3020	0.3009
TiO_2	1.30	0.0534	0.0279
MgO	6.69	0.0863	0.0177
MnO	0.11	0.0314	0.0298
Al_2O_3	11.18	0.1057	0.0216
FeO	7.26	0.1096	0.0351
SiO_2	59.84	0.2906	0.0365

OLIVINE B4 3/703

Oxide	wt%	precision 2σ	detection limit
CaO	0.60	0.0371	0.0211
MgO	44.14	0.2101	0.0215
MnO	0.16	0.0311	0.0281
Al_2O_3	1.59	0.0521	0.0225
FeO	11.86	0.1296	0.0341
SiO_2	42.34	0.2701	0.0416

PLAGIOCLASE B4 3/744

Oxide	wt%	precision 2σ	detection limit
K_2O	0.73	0.0411	0.0204
Na_2O	3.19	0.0789	0.0216
CaO	11.04	0.1201	0.0236
MgO	3.05	0.0625	0.0192
TiO_2	0.26	0.0328	0.0262
Al_2O_3	22.74	0.1450	0.0226
FeO	4.54	0.0872	0.0333
SiO_2	55.25	0.2937	0.0385

SPINEL 17M-4/237

Oxide	wt%	precision 2σ	detection limit
TiO_2	0.79	0.0544	0.0352
MgO	12.53	0.1270	0.0223
Cr_2O_3	59.31	0.3129	0.0439
Al_2O_3	8.10	0.0714	0.0176
MnO	0.68	0.0599	0.0456
FeO	16.72	0.2023	0.0513
SiO_2	0.11	0.0412	0.0394

APPENDIX III

TABLES

TABLE AIII.1

	1	2	3	4	5	6	7	8
SiO_2	57.90	58.10	58.20	58.40	57.90	58.70	57.49	57.88
TiO_2	0.05	nd	nd	nd	0.06	nd	nd	nd
Al_2O_3	0.08	0.08	0.12	0.14	0.12	0.10	0.44	0.20
Cr_2O_3	0.13	0.33	0.27	0.35	0.58	0.28	0.46	0.34
FeO	4.68	4.29	4.67	4.45	4.64	4.97	7.49	7.03
MnO	0.10	0.12	0.12	0.09	0.15	0.15	0.12	0.14
NiO	0.30	0.10	0.08	0.12	0.08	0.09	nd	nd
MgO	36.00	36.30	35.90	36.10	35.60	36.10	32.63	34.33
CaO	0.37	0.12	0.20	0.11	0.12	0.13	0.49	0.31
total=	99.61	99.44	99.56	99.76	99.25	100.52	99.12	100.23
Si	1.99	2.00	2.00	2.00	2.00	2.00	2.01	2.00
Al	-	-	-	-	-	-	0.02	-
Cr	-	-	-	-	0.02	-	0.01	-
Fe_2	0.13	0.12	0.13	0.13	0.13	0.14	0.22	0.20
Mg	1.85	1.86	1.84	1.84	1.83	1.83	1.70	1.76
Ca	0.01	-	-	-	-	-	0.02	0.01
total=	4.00	4.00	4.00	3.99	3.99	4.00	3.98	4.00
oxygens=	[6]	[6]	[6]	[6]	[6]	[6]	[6]	[6]
WO	0.68	0.22	0.37	0.20	0.22	0.24	0.95	0.58
EN	92.57	93.57	92.85	93.34	92.98	92.61	87.75	89.17
FS	6.75	6.20	6.78	6.46	6.80	7.15	11.30	10.25

1 CRAWFORD A.J. 1980 TABLE 3A1
2 CRAWFORD A.J. 1980 TABLE 3A2
3 CRAWFORD A.J. 1980 TABLE 3B1
4 CRAWFORD A.J. 1980 TABLE 3B2
5 CRAWFORD A.J. 1980 TABLE 3C1
6 CRAWFORD A.J. 1980 TABLE 3C2
7 KOMATSU M. 1980 TABLE 2 C-10 CMP-A
8 KOMATSU M. 1980 TABLE 2 C-10 CMP-B

TABLE AIII.1

	9	10	11	12	13	14	15	16
SiO_2	57.22	56.54	57.36	56.95	57.80	57.75	57.43	57.62
TiO_2	0.01	nd	nd	0.03	0.01	nd	nd	0.02
Al_2O_3	0.56	0.42	0.11	0.16	0.17	0.17	0.30	0.22
Cr_2O_3	0.54	0.78	0.28	0.21	0.23	0.21	0.46	0.39
FeO	7.42	7.54	6.32	6.78	7.03	7.16	6.64	6.85
MnO	0.14	0.14	0.09	0.17	0.15	0.19	0.08	0.16
MgO	34.18	32.72	34.97	34.65	34.41	33.92	34.78	34.60
CaO	0.41	0.43	0.26	0.31	0.34	0.31	0.32	0.32
Na_2O	nd	nd	nd	0.02	0.02	nd	0.01	0.03
total=	100.48	98.57	99.39	99.28	100.16	99.71	100.02	100.21
Si	1.98	1.99	1.99	1.98	1.99	2.00	1.98	1.99
Al	0.02	0.02	-	-	-	-	0.01	-
Cr	0.01	0.02	-	-	-	-	0.01	0.01
Fe_2	0.21	0.22	0.18	0.20	0.20	0.21	0.19	0.20
Mg	1.76	1.72	1.81	1.80	1.77	1.75	1.79	1.78
Ca	0.02	0.02	-	0.01	0.01	0.01	0.01	0.01
total=	4.01	3.99	4.00	4.01	4.00	3.99	4.00	4.00
oxygens=	[6]	[6]	[6]	[6]	[6]	[6]	[6]	[6]
WO	0.76	0.83	0.48	0.58	0.63	0.58	0.59	0.59
EN	88.46	87.82	90.35	89.59	89.15	88.89	89.79	89.47
FS	10.77	11.35	9.16	9.84	10.22	10.53	9.62	9.94

9 KOMATSU M. 1980 TABLE 2 C-10 CMP-C
10 KOMATSU M. 1980 TABLE 2 C-10 CMP-D
11 KOMATSU M. 1980 TABLE 2 M-1 PH1
12 KOMATSU M. 1980 TABLE 2 M-1 PH2
13 KOMATSU M. 1980 TABLE 2 M-1 R
14 KOMATSU M. 1980 TABLE 2 M-1 IR
15 KOMATSU M. 1980 TABLE 2 C-5 PH1
16 KOMATSU M. 1980 TABLE 2 C-5 PH2

TABLE AIII.1

	17	18	19	20	21	22	23	24
SiO_2	56.14	56.70	58.10	58.31	57.79	56.81	58.05	56.78
TiO_2	0.04	nd	nd	nd	0.01	0.01	0.02	0.01
Al_2O_3	0.14	0.54	0.12	0.17	0.36	0.56	0.42	0.52
Cr_2O_3	0.12	0.35	0.29	0.22	0.32	0.37	0.41	0.35
FeO	7.60	6.95	5.25	5.29	5.95	7.40	5.96	7.96
MnO	0.16	0.11	0.12	0.07	0.14	0.16	0.18	0.19
NiO	0.07	nd	0.02	0.02	0.06	0.05	0.06	0.15
MgO	35.72	33.83	35.75	35.82	35.10	34.16	34.84	32.71
CaO	0.25	0.38	0.19	0.22	0.32	0.42	0.33	0.67
Na_2O	0.01	0.05	0.01	0.03	nd	0.01	0.01	0.02
K_2O	0.01	nd	nd	0.01	nd	nd	nd	nd
total=	100.26	98.91	99.85	100.16	100.05	99.95	100.28	99.36
Si	1.95	1.98	1.99	2.00	1.99	1.97	1.99	1.99
Al	-	0.02	-	-	0.01	0.02	0.02	0.02
Cr	-	-	-	-	-	0.01	0.01	-
Fe_2	0.22	0.20	0.15	0.15	0.17	0.21	0.17	0.23
Mg	1.85	1.76	1.83	1.83	1.80	1.77	1.78	1.71
Ca	-	0.01	-	-	0.01	0.02	0.01	0.03
total=	4.05	4.00	4.00	4.00	4.00	4.01	3.99	4.00
oxygens=	[6]	[6]	[6]	[6]	[6]	[6]	[6]	[6]
WO	0.45	0.72	0.35	0.41	0.60	0.78	0.62	1.28
EN	88.93	89.02	92.06	91.97	90.77	88.47	90.68	86.86
FS	10.62	10.26	7.58	7.62	8.63	10.75	8.71	11.86

17 SAMESHIMA T. ETAL 1983 TABLE 1 1
18 SHARASKIN A.YA. ETAL TABLE 3 34
19 SHIRAKI K. ETAL 1980 TABLE 2 1
20 SHIRAKI K. ETAL 1980 TABLE 2 2
21 SHIRAKI K. ETAL 1980 TABLE 2 3C
22 SHIRAKI K. ETAL 1980 TABLE 2 3M
23 SHIRAKI K. ETAL 1980 TABLE 2 5E
24 SHIRAKI K. ETAL 1980 TABLE 2 6E

TABLE AIII.2A

	1	2	3	4	5	6	7	8
SiO2	56.29	53.55	54.29	53.83	53.93	53.27	53.44	54.50
TiO2	0.07	nd	nd	nd	nd	nd	0.43	0.20
Al2O3	1.37	2.31	1.82	2.74	2.39	2.63	1.08	1.14
Cr2O3	0.65	1.27	1.14	1.20	1.07	1.02	0.06	0.15
FeO	8.17	11.65	11.55	11.61	12.89	14.59	16.72	15.20
MnO	0.12	nd	nd	nd	nd	nd	0.25	0.33
MgO	32.73	29.58	30.05	29.69	29.13	27.82	23.81	26.30
CaO	1.23	0.99	1.03	1.17	1.21	1.45	3.39	2.28
Na2O	nd	nd	nd	nd	nd	nd	nd	0.07
total=	100.63	99.35	99.88	100.24	100.62	100.78	99.18	100.17
Si	1.95	1.92	1.93	1.91	1.92	1.91	1.97	1.97
Ti	-	-	-	-	-	-	0.01	-
Al	0.06	0.10	0.08	0.11	0.10	0.11	0.05	0.05
Cr	0.02	0.04	0.03	0.03	0.03	0.03	-	-
Fe2	0.24	0.35	0.34	0.34	0.38	0.44	0.52	0.46
Mn	-	-	-	-	-	-	-	0.01
Mg	1.69	1.58	1.59	1.57	1.54	1.48	1.31	1.42
Ca	0.05	0.04	0.04	0.04	0.05	0.06	0.13	0.09
total=	4.01	4.02	4.01	4.02	4.02	4.02	3.99	4.00
oxygens=	[6]	[6]	[6]	[6]	[6]	[6]	[6]	[6]
temp	1300.00	1230.00	1228.00	1212.00	1209.00	1203.00	1179.00	1137.00
time	44.00	22.00	64.50	137.00	137.00	64.50	5.00	542.50
WO	2.31	1.93	1.98	2.27	2.34	2.81	6.84	4.49
EN	85.69	80.32	80.63	80.14	78.24	75.09	66.83	72.12
FS	12.00	17.75	17.39	17.58	19.43	22.10	26.33	23.39

1 HUEBNER ETAL 1976-OPX,OKB,1300C,44HR,F-11.75,GL+OPX
2 HUEBNER ETAL 1976-OPX,OKB,1230C,22HR,F-13.2,GL+OPX+SP
3 HUEBNER ETAL 1976-OPX,OKB,1228C,64.5HR,F-13.2,GL+OL+OPX+SP
4 HUEBNER ETAL 1976-OPX,OKB,1212C,137HR,F-13.3,GL+OL+PL+OPX+SP
5 HUEBNER ETAL 1976-OPX,OKB,1209C,137HR,F-13.3,GL+OL+PL+OPX+SP
6 HUEBNER ETAL 1976-OPX,OKB,1203C,64.5HR,F-13.4,GL+OL+PL+OPX+SP
7 BIGGAR ETAL 1971 12040-OPX,OKB,1179C,5HR,F-12.1,GL+OL+OPX+SP
8 GROVE ETAL 1982 TABLE 1 79-38B-GL,OKB,1137C,542.5HR,F-9.34,GL+OL+PL+OPX

	9	10	11	12	13	14	15	16
SiO2	53.70	53.10	53.10	52.30	53.20	57.10	56.10	54.90
TiO2	0.12	0.33	0.31	0.38	0.58	nd	0.03	0.06
Al2O3	1.13	0.91	0.80	0.83	1.19	1.20	1.93	3.70
Cr2O3	0.10	nd	0.03	0.05	0.03	0.32	0.45	0.50
FeO	17.80	17.60	20.30	20.90	20.50	5.30	6.50	7.20
MnO	0.34	0.49	0.41	0.52	0.52	nd	nd	nd
MgO	24.30	24.80	22.40	21.90	22.40	35.70	34.20	32.60
CaO	2.65	1.67	2.90	2.78	2.74	0.44	0.78	1.07
Na2O	0.09	0.03	0.02	0.04	0.05	nd	nd	nd
total=	100.23	98.93	100.27	99.70	101.21	100.06	99.99	100.03
Si	1.96	1.96	1.97	1.96	1.95	1.96	1.94	1.91
Ti	-	-	-	0.01	0.02	-	-	-
Al	0.05	0.04	0.03	0.04	0.05	0.05	0.08	0.15
Cr	-	-	-	-	-	-	0.01	0.01
Fe2	0.54	0.54	0.63	0.65	0.63	0.15	0.19	0.21
Mn	0.01	0.02	0.01	0.02	0.02	-	-	-
Mg	1.32	1.37	1.24	1.22	1.23	1.83	1.76	1.69
Ca	0.10	0.07	0.12	0.11	0.11	0.02	0.03	0.04
total=	4.01	4.01	4.01	4.01	4.01	4.01	4.01	4.01
oxygens=	[6]	[6]	[6]	[6]	[6]	[6]	[6]	[6]
temp	1121.00	1106.00	1093.00	1085.00	1076.00	1320.00	1280.00	1260.00
time	793.50	118.50	291.00	237.50	330.00	36.00	36.00	36.00
WO	5.26	3.35	5.81	5.61	5.49	0.81	1.46	2.06
EN	67.14	69.13	62.44	61.47	62.45	91.56	89.04	87.15
FS	27.60	27.53	31.75	32.92	32.06	7.63	9.50	10.80

9 GROVE ETAL 1982 TABLE 1 79-38B-GL,OKB,1121C,793.5HR,F-9.54,GL+OL+PL+OPX
10 GROVE ETAL 1982 TABLE 1 79-9C-GL,OKB,1106C,118.5HR,F-9.66,GL+PL+OPX
11 GROVE ETAL 1982 TABLE 1 79-9C-GL,OKB,1093C,291HR,F-9.94,GL+OL+PL+OPX
12 GROVE ETAL 1982 TABLE 1 79-9C-GL,OKB,1085C,237.5HR,F-9.95,GL+OL+PL+OPX
13 GROVE ETAL 1982 TABLE 1 79-9C-GL,OKB,1076C,330HR,F-10.11,GL+PL+OPX+SP
14 WEILL & MCKAY FMG -OPX,00KB,1320C,36HR,F-12.50,+GL+OPX+OL
15 WEILL & MCKAY FMG -OPX,00KB,1280C,36HR,F-12.50,+GL+OPX+OL
16 WEILL & MCKAY FMG -OPX,00KB,1260C,36HR,F-12.50,+GL+OPX+OL

TABLE AIII.2A

	17	18	19	20	21	22	23	24
SiO2	55.00	54.10	56.29	56.56	56.67	56.08	56.42	58.06
TiO2	0.08	0.12	0.07	0.03	0.05	0.09	0.04	nd
Al2O3	4.00	5.00	1.22	0.48	0.98	1.71	0.88	0.47
Cr2O3	0.48	0.42	0.61	nd	nd	0.52	nd	nd
FeO	7.10	7.70	8.12	12.45	9.83	9.02	9.22	7.05
MnO	nd	nd	0.09	nd	nd	0.20	nd	nd
MgO	32.30	31.30	32.39	31.56	30.59	31.28	31.24	32.07
CaO	1.11	1.29	1.31	1.07	1.83	1.46	1.38	2.35
total=	100.07	99.93	100.10	102.15	99.95	100.36	99.18	100.00
Si	1.91	1.89	1.96	1.97	1.99	1.96	1.99	2.01
Al	0.16	0.21	0.05	0.02	0.04	0.07	0.04	0.02
Cr	0.01	0.01	0.02	-	-	0.01	-	-
Fe2	0.21	0.22	0.24	0.36	0.29	0.26	0.27	0.20
Mg	1.67	1.63	1.68	1.64	1.60	1.63	1.64	1.66
Ca	0.04	0.05	0.05	0.04	0.07	0.05	0.05	0.09
total=	4.00	4.00	4.00	4.02	3.99	4.00	3.99	3.98
oxygens=	[6]	[6]	[6]	[6]	[6]	[6]	[6]	[6]
temp	1240.00	1220.00	1300.00	1273.00	1273.00	1243.00	1273.00	1233.00
time	36.00	36.00	44.00	48.00	48.00	96.00	48.00	24.00
WO	2.15	2.54	2.48	1.95	3.51	2.81	2.65	4.48
EN	87.11	85.64	85.49	80.28	81.75	83.66	83.52	85.04
FS	10.74	11.82	12.02	17.77	14.74	13.54	13.83	10.49

17 WEILL & MCKAY FMG -OPX,00KB,1240C,36HR,F-12.50,+GL+OPX+OL
18 WEILL & MCKAY FMG -OPX,00KB,1220C,36HR,F-12.50,+GL+OPX+OL
19 HUEBENER & TURNOCK 1980 61 SC B -OPX,00KB,1300C,44HR,F-11.75,+GL+OPX+OL
20 HUEBENER & TURNOCK 1980 61 SC B -OPX,00KB,1273C,48HR,F-11.89,+GL+OPX+OL
21 HUEBENER & TURNOCK 1980 61 SC B -OPX,00KB,1273C,48HR,F-11.89,+GL+OPX
22 HUEBENER & TURNOCK 1980 61 SC B -OPX,00KB,1243C,96HR,F-11.94,+GL+OPX+OL
23 HUEBENER & TURNOCK 1980 J-8 -OPX,00KB,1273C,48HR,F-11.89,+GL+OPX
24 NEILSEN & DRAKE TABLE 1 4 -OPX,00KB,1233C,24HR,F-12.00,+GL+OPX

	25	26	27	28	29	30	31	32
SiO2	58.27	53.76	53.34	53.19	53.76	53.94	53.46	53.89
TiO2	0.18	0.07	nd	0.07	0.07	0.14	0.15	0.11
Al2O3	0.56	0.49	0.35	0.36	0.79	0.73	0.40	0.47
Cr2O3	nd	0.41	0.44	nd	nd	nd	0.02	0.01
FeO	8.50	22.22	22.38	23.19	24.41	15.43	17.46	17.87
MnO	nd	nd	nd	nd	nd	0.32	0.31	0.20
MgO	30.92	22.27	22.65	21.89	20.11	27.08	24.79	25.04
CaO	1.56	0.78	0.85	1.30	0.85	1.38	2.40	1.61
Na2O	nd	nd	nd	nd	nd	0.05	0.03	0.04
total=	100.00	100.00	100.00	100.00	100.00	99.07	99.02	99.24
Si	2.02	2.00	1.99	1.99	2.01	1.97	1.98	1.98
Al	0.02	0.02	0.02	0.02	0.03	0.03	0.02	0.02
Cr	-	0.01	0.01	-	-	-	-	-
Fe2	0.25	0.69	0.70	0.72	0.76	0.47	0.54	0.55
Mg	1.60	1.23	1.26	1.22	1.12	1.47	1.37	1.37
Ca	0.06	0.03	0.03	0.05	0.03	0.05	0.10	0.06
total=	3.96	3.99	4.00	4.00	3.97	4.01	4.01	4.00
oxygens=	[6]	[6]	[6]	[6]	[6]	[6]	[6]	[6]
temp	1233.00	1225.00	1225.00	1222.00	1222.00	1210.00	1191.00	1210.00
time	24.00	24.00	24.00	24.00	24.00	19.50	19.90	19.50
WO	3.05	1.59	1.71	2.60	1.78	2.70	4.75	3.19
EN	83.99	63.08	63.22	61.09	58.43	73.73	68.27	69.13
FS	12.96	35.32	35.07	36.31	39.79	23.57	26.98	27.68

25 NEILSEN & DRAKE TABLE 1 5 -OPX,00KB,1233C,24HR,F-12.00,+GL+OPX
26 NEILSEN & DRAKE TABLE 1 6 -OPX,00KB,1225C,24HR,F-12.00,+GL+OPX
27 NEILSEN & DRAKE TABLE 1 7 -OPX,00KB,1225C,24HR,F-12.00,+GL+OPX
28 NEILSEN & DRAKE TABLE 1 8 -OPX,00KB,1222C,24HR,F-12.00,+GL+OPX
29 NEILSEN & DRAKE TABLE 1 9 -OPX,00KB,1222C,24HR,F-12.00,+GL+OPX
30 MITCHELL 1984 ROCK+GEL -OPX,00KB,1210C,19.5HR,F-8.70,+GL+OPX
31 MITCHELL 1984 ROCK+GEL -OPX,00KB,1191C,19.9HR,F-8.80,+GL+OL+OPX
32 MITCHELL 1984 ROCK+GEL -OPX,00KB,1210C,19.5HR,F-8.70,+GL+OL+OPX

TABLE AIII.2A

	33	34
SiO2	53.25	53.29
TiO2	0.12	0.15
Al2O3	0.58	2.46
FeO	19.14	20.06
MnO	0.18	0.22
MgO	23.98	23.01
CaO	1.77	2.50
Na2O	0.04	0.04
total=	99.06	101.73
Si	1.98	1.94
Al	0.03	0.11
Fe2	0.59	0.61
Mg	1.33	1.25
Ca	0.07	0.10
total=	4.01	4.01
oxygens=	[6]	[6]
temp	1191.00	1161.00
time	19.90	19.90
WO	3.53	4.98
EN	66.63	63.81
FS	29.84	31.21

33 MITCHELL 1984 ROCK+GEL -OPX,00KB,1191C,19.9HR,F-8.80,+GL+OL+OPX
34 MITCHELL 1984 ROCK+GEL -OPX,00KB,1161C,19.9HR,F-9.00,+GL+OL+OPX

TABLE AIII.2B

	1	2	3	4	5	6	7	8
SiO2	51.70	51.10	52.50	51.70	57.94	55.58	54.83	50.02
TiO2	0.56	0.62	0.70	1.05	0.02	0.20	0.03	0.95
Al2O3	1.15	1.25	1.55	2.21	0.34	0.38	0.20	1.02
Cr2O3	0.79	0.73	0.78	0.81	0.44	0.60	0.53	0.48
FeO	17.30	17.60	17.70	18.10	5.62	9.12	18.60	23.54
MnO	nd	0.38	0.39	0.35	0.18	0.48	0.38	0.39
MgO	22.90	21.80	21.60	20.70	32.98	29.00	24.39	15.68
CaO	3.60	4.29	4.92	5.59	3.04	4.06	1.97	9.24
Na2O	0.01	0.02	0.05	0.02	nd	nd	nd	nd
total=	98.01	97.79	100.19	100.53	100.56	99.42	100.93	101.32
Si	1.94	1.94	1.94	1.91	1.99	1.98	1.99	1.91
Ti	0.02	0.02	0.02	0.03	-	-	-	0.03
Al	0.05	0.06	0.07	0.10	0.01	0.02	-	0.05
Cr	0.02	0.02	0.02	0.02	0.01	0.02	0.02	0.01
Fe2	0.54	0.56	0.55	0.56	0.16	0.27	0.57	0.75
Mn	-	0.01	0.01	0.01	-	0.01	0.01	0.01
Mg	1.28	1.23	1.19	1.14	1.69	1.54	1.32	0.89
Ca	0.14	0.17	0.19	0.22	0.11	0.15	0.08	0.38
total=	4.00	4.01	4.00	4.00	3.99	4.00	3.99	4.03
oxygens=	[6]	[6]	[6]	[6]	[6]	[6]	[6]	[6]
temp	1176.00	1164.00	1156.00	1150.00	1332.00	1243.00	1252.00	1151.00
time	72.70	45.80	98.70	75.00	71.00	18.00	19.00	45.00
WO	7.35	8.87	10.09	11.52	5.70	7.88	3.91	18.69
EN	65.07	62.72	61.59	59.36	86.07	78.30	67.30	44.13
FS	27.58	28.41	28.32	29.12	8.23	13.82	28.79	37.17

1 WALKER ET.AL.1976-PIG,OKB,1176C,72.7HR,F-12.21,GL+OL+PIG+SP
2 WALKER ET.AL.1976-PIG,OKB,1164C,45.8HR,F-12.37,GL+OL+PIG+SP
3 WALKER ET.AL.1976-PIG,OKB,1156C,98.7HR,F-12.47,GL+OL+PL+PIG+SP
4 WALKER ET.AL.1976-PIG,OKB,1150C,75HR,F-12.56,GL+OL+PL+PIG+SP
5 HUEBNER ETAL 1976-PIG,OKB,1332C,71HR,F-8.26,GL+PIG
6 HUEBNER ETAL 1976-PIG,OKB,1243C,18HR,F-11.77,GL+PIG
7 HUEBNER ETAL 1976-PIG,OKB,1252C,19HR,F-11.42,GL+OL+PIG
8 HUEBNER ETAL 1976-PIG,OKB,1151C,45HR,F-12.65,GL+PIG

	9	10	11	12	13	14	15	16
SiO2	52.90	52.10	51.40	50.80	52.40	53.02	51.64	51.03
TiO2	0.28	0.29	0.44	0.49	1.00	0.73	0.82	0.96
Al2O3	0.83	1.07	1.31	1.61	2.84	1.50	1.88	2.06
Cr2O3	0.82	0.71	0.70	0.60	0.50	0.61	0.56	0.74
FeO	17.90	19.30	20.60	22.50	16.62	17.05	20.21	19.86
MnO	0.28	0.33	0.32	0.37	0.25	0.34	0.33	0.31
MgO	24.50	21.60	19.50	17.20	21.12	21.96	19.49	18.40
CaO	2.68	3.80	5.65	6.46	4.84	4.59	5.27	6.11
total=	100.19	99.20	99.92	100.03	99.57	99.80	100.20	99.47
Si	1.94	1.95	1.94	1.93	1.93	1.96	1.93	1.93
Ti	-	-	0.01	0.01	0.03	0.02	0.02	0.03
Al	0.04	0.05	0.06	0.07	0.12	0.07	0.08	0.09
Cr	0.02	0.02	0.02	0.02	0.01	0.02	0.02	0.02
Fe2	0.55	0.61	0.65	0.72	0.51	0.53	0.63	0.63
Mn	-	0.01	0.01	0.01	-	0.01	0.01	-
Mg	1.34	1.21	1.10	0.98	1.16	1.21	1.09	1.04
Ca	0.11	0.15	0.23	0.26	0.19	0.18	0.21	0.25
total=	4.02	4.00	4.01	4.01	3.97	3.98	4.00	3.99
oxygens=	[6]	[6]	[6]	[6]	[6]	[6]	[6]	[6]
temp	1194.00	1161.00	1138.00	1123.00	1179.00	1160.00	1137.00	1114.00
time	44.80	42.50	73.00	119.00	5.00	5.00	5.00	5.00
WO	5.28	7.77	11.56	13.47	10.25	9.47	10.94	12.94
EN	67.18	61.43	55.52	49.90	62.26	63.06	56.30	54.22
FS	27.54	30.80	32.91	36.63	27.49	27.47	32.76	32.84

9 GROVE & BENCE 1977 15597 -PIG,00KB,1194C,44.8HR,F-11.98,+GL+OL+PIG
10 GROVE & BENCE 1977 15597 -PIG,00KB,1161C,42.5HR,F-12.41,+GL+OL+PIG+SP
11 GROVE & BENCE 1977 15597 -PIG,00KB,1138C,73HR,F-12.72,+GL+OL+PIG+PLAG+SP
12 GROVE & BENCE 1977 15597 -PIG,00KB,1123C,119HR,F-12.92,+GL+PIG+PLAG+SP
13 BIGGAR ETAL 1971 12040 -PIG,00KB,1179C,5HR,F-12.10,+GL+OL+PIG
14 BIGGAR ETAL 1971 12040 -PIG,00KB,1160C,5HR,F-12.30,+GL+OL+PIG
15 BIGGAR ETAL 1971 12038 -PIG,00KB,1137C,5HR,F-12.70,+GL+OL+PIG
16 BIGGAR ETAL 1971 12038 -PIG,00KB,1114C,5HR,F-12.90,+GL+OL+PIG

TABLE AIII.2B

	17	18	19	20	21	22	23	24
SiO2	51.10	50.93	51.62	53.33	52.70	53.45	53.47	53.70
TiO2	0.81	0.95	1.39	0.21	0.15	0.11	0.11	0.28
Al2O3	1.83	1.59	1.06	0.99	1.30	1.06	1.15	0.80
Cr2O3	0.62	0.51	0.31	0.65	0.72	0.66	0.73	0.89
FeO	20.30	21.89	15.81	18.52	19.42	18.87	19.40	16.90
MnO	0.35	0.36	nd	0.68	0.72	0.71	0.73	0.34
MgO	18.66	16.58	21.24	23.18	22.13	23.03	22.55	24.10
CaO	6.22	7.11	6.21	2.18	2.45	2.40	2.53	2.91
Na2O	nd	nd	0.02	0.03	nd	nd	0.03	0.02
total=	99.89	99.92	97.66	99.77	99.59	100.29	100.70	99.94
Si	1.93	1.94	1.95	1.97	1.96	1.97	1.97	1.97
Ti	0.02	0.03	0.04	-	-	-	-	-
Al	0.08	0.07	0.05	0.04	0.06	0.05	0.05	0.03
Cr	0.02	0.02	-	0.02	0.02	0.02	0.02	0.03
Fe2	0.64	0.70	0.50	0.57	0.60	0.58	0.60	0.52
Mn	0.01	0.01	-	0.02	0.02	0.02	0.02	0.01
Mg	1.05	0.94	1.19	1.28	1.23	1.26	1.24	1.32
Ca	0.25	0.29	0.25	0.09	0.10	0.09	0.10	0.11
total=	4.00	3.99	3.99	3.99	4.00	4.00	4.00	4.00
oxygens=	[6]	[6]	[6]	[6]	[6]	[6]	[6]	[6]
temp	1160.00	1114.00	1133.00	1171.00	1171.00	1171.00	1171.00	1225.00
time	5.00	5.00	-	15.30	17.00	15.30	17.00	20.50
WO	12.95	15.04	12.91	4.46	5.06	4.88	5.16	5.86
EN	54.05	48.81	61.43	65.97	63.61	65.16	63.96	67.56
FS	32.99	36.15	25.65	29.57	31.32	29.96	30.88	26.58

17 BIGGAR ETAL 1971 12064 -PIG,00KB,1160C,5HR,F-12.30,+GL+OL+PIG
18 BIGGAR ETAL 1971 12064 -PIG,00KB,1114C,5HR,F-12.90,+GL+OL+PIG
19 O HARA ET AL.1976-PIG,0KB,1133C,0HR,F-13.79,+GL+OL+PL+CPX+SP+OPX+ILM
20 STOLPER 1977 JV14 -PIG,00KB,1171C,15.3HR,F-13.51,+GL+OL+PIG+PL+SP
21 STOLPER 1977 JV18 -PIG,00KB,1171C,17.0HR,F-13.44,+GL+OL+PIG+PL+SP
22 STOLPER 1977 SC54 -PIG,00KB,1171C,15.3HR,F-13.51,+GL+OL+PIG+PL+SP
23 STOLPER 1977 SC58 -PIG,00KB,1171C,17.0HR,F-13.44,+GL+OL+PIG+PL+SP
24 WALKER ETAL 15065 -PIG,00KB,1225C,20.5HR,F-13.00,+GL+OL+SP+PIG

	25	26	27	28	29	30	31	32
SiO2	53.60	53.00	51.30	51.70	50.80	52.40	52.80	51.50
TiO2	0.34	0.38	0.63	0.57	0.66	0.49	0.52	0.72
Al2O3	0.98	1.27	2.32	1.40	1.46	1.40	1.09	1.48
Cr2O3	0.87	0.75	1.04	0.66	0.62	0.69	0.70	0.61
FeO	17.00	18.80	18.40	21.50	22.40	21.10	19.90	21.50
MnO	0.32	0.37	0.34	0.39	0.40	0.38	0.33	0.40
MgO	24.00	22.00	20.00	18.50	16.60	18.40	21.30	18.10
CaO	2.68	3.78	5.08	5.73	6.46	5.82	4.36	5.54
Na2O	0.04	0.02	0.03	0.03	0.03	0.03	0.01	0.02
total=	99.83	100.37	99.14	100.48	99.43	100.71	101.01	99.87
Si	1.97	1.96	1.93	1.94	1.95	1.96	1.95	1.95
Ti	-	0.01	0.02	0.02	0.02	0.01	0.01	0.02
Al	0.04	0.06	0.10	0.06	0.07	0.06	0.05	0.07
Cr	0.03	0.02	0.03	0.02	0.02	0.02	0.02	0.02
Fe2	0.52	0.58	0.58	0.68	0.72	0.66	0.61	0.68
Mn	-	0.01	0.01	0.01	0.01	0.01	0.01	0.01
Mg	1.31	1.21	1.12	1.04	0.95	1.03	1.17	1.02
Ca	0.11	0.15	0.20	0.23	0.27	0.23	0.17	0.22
total=	3.99	4.00	3.99	4.00	3.99	3.99	4.00	3.99
oxygens=	[6]	[6]	[6]	[6]	[6]	[6]	[6]	[6]
temp	1205.00	1172.00	1148.00	1128.00	1125.00	1124.00	1157.00	1148.00
time	22.00	23.70	38.50	70.00	47.20	67.00	46.50	38.50
WO	5.43	7.70	10.75	11.87	13.74	12.15	8.80	11.66
EN	67.67	62.38	58.87	53.34	49.09	53.45	59.83	53.01
FS	26.90	29.91	30.39	34.78	37.17	34.39	31.36	35.33

25 WALKER ETAL 15065 -PIG,00KB,1205C,22HR,F-13.00,+GL+OL+SP+PIG
26 WALKER ETAL 15065 -PIG,00KB,1172C,23.7HR,F-13.00,+GL+OL+SP+PIG
27 WALKER ETAL 15065 -PIG,00KB,1148C,38.5HR,F-13.00,+GL+SP+PIG+PL
28 WALKER ETAL 15065 -PIG,00KB,1128C,70HR,F-13.00,+GL+SP+PIG+PL
29 WALKER ETAL 15065 -PIG,00KB,1125C,47.2HR,F-13.00,+GL+OL+SP+PIG+PL
30 WALKER ETAL 15065 -PIG,00KB,1124C,67HR,F-13.00,+GL+OL+SP+PIG+PL
31 WALKER ETAL 15555 -PIG,00KB,1157C,46.5HR,F-13.00,+GL+OL+SP+PIG
32 WALKER ETAL 15555 -PIG,00KB,1148C,38.5HR,F-13.00,+GL+OL+SP+PIG+PL

TABLE AIII.2B

	33	34	35	36	37	38	39	40
SiO2	51.50	50.32	50.33	51.77	52.27	50.60	49.90	49.80
TiO2	0.81	1.10	1.26	0.57	1.05	0.64	0.63	0.78
Al2O3	1.59	1.57	1.82	0.76	1.82	1.30	1.04	1.18
Cr2O3	0.72	0.67	0.43	0.46	0.78	0.37	0.32	0.29
FeO	20.80	16.77	21.27	19.17	18.55	26.80	27.60	29.60
MnO	0.37	0.32	0.33	0.33	0.31	0.43	0.31	0.38
MgO	17.60	20.29	17.92	23.38	22.44	14.90	13.60	11.00
CaO	6.88	6.27	8.13	3.70	5.31	5.82	6.45	8.47
Na2O	0.03	0.11	0.09	0.08	0.07	nd	nd	nd
total=	100.30	97.42	101.58	100.22	102.60	100.86	99.85	101.50
Si	1.94	1.92	1.89	1.92	1.90	1.94	1.95	1.94
Ti	0.02	0.03	0.04	0.02	0.03	0.02	0.02	0.02
Al	0.07	0.07	0.08	0.03	0.08	0.06	0.05	0.05
Cr	0.02	0.02	0.01	0.01	0.02	0.01	-	-
Fe2	0.66	0.54	0.67	0.60	0.56	0.86	0.90	0.97
Mn	0.01	0.01	0.01	0.01	-	0.01	0.01	0.01
Mg	0.99	1.15	1.00	1.29	1.21	0.85	0.79	0.64
Ca	0.28	0.26	0.33	0.15	0.21	0.24	0.27	0.35
total=	3.99	4.01	4.03	4.04	4.03	4.00	4.00	4.00
oxygens=	[6]	[6]	[6]	[6]	[6]	[6]	[6]	[6]
temp	1124.00	1138.00	1125.00	1150.00	1150.00	1099.00	1087.00	1071.00
time	50.10	40.00	48.50	16.50	16.50	236.00	673.00	361.00
WO	14.46	13.18	16.37	7.23	10.41	12.26	13.75	18.07
EN	51.44	59.32	50.20	63.54	61.20	43.67	40.33	32.64
FS	34.11	27.51	33.43	29.23	28.39	44.07	45.92	49.29

33 WALKER ETAL 15555 -PIG,00KB,1124C,50.1HR,F-13.00,+GL+OL+SP+PIG+PL
34 RHODES ETAL 1979 12045 -PIG,00KB,1138C,40HR,F-13.00,+GL+OL+SP+PIG
35 RHODES ETAL 1979 12008 -PIG,00KB,1125C,48.5HR,F-13.00,+GL+OL+PIG+PL+CPX+SP
36 RHODES ETAL 1979 12008 -PIG,00KB,1150C,16.5HR,F-13.00,+GL+OL+SP+PIG
37 RHODES ETAL 1979 12008 -PIG,00KB,1150C,16.5HR,F-13.00,+GL+OL+SP+PIG
38 GROVE & RAUDSEPP 15597 -PIG,00KB,1099C,236HR,F-13.00,+GL+PLAG+PIG
39 GROVE & RAUDSEPP 15597 -PIG,00KB,1087C,673HR,F-13.00,+GL+PLAG+PIG+QZ
40 GROVE & RAUDSEPP 15597 -PIG,00KB,1071C,361HR,F-13.00,+GL+PLAG+PIG+QZ

	41	42	43	44	45	46	47	48
SiO2	52.90	51.70	51.30	51.70	52.50	55.10	51.80	54.50
TiO2	1.52	1.60	1.98	1.65	0.90	0.50	0.80	0.18
Al2O3	1.38	1.27	1.84	1.42	1.40	1.40	3.50	0.34
Cr2O3	0.41	0.32	0.29	0.35	nd	nd	nd	nd
FeO	16.30	16.00	16.50	19.00	17.80	12.80	17.80	14.11
MnO	0.25	0.21	0.23	0.30	nd	nd	nd	nd
MgO	23.60	22.70	19.80	19.90	21.40	27.90	20.10	26.18
CaO	4.40	4.81	8.56	6.18	7.20	2.40	4.80	3.01
Na2O	nd	nd	0.04	0.08	nd	nd	nd	nd
total=	100.76	98.61	100.54	100.58	101.20	100.10	98.80	98.32
Si	1.93	1.93	1.90	1.92	1.93	1.96	1.93	1.99
Ti	0.04	0.04	0.06	0.05	0.02	0.01	0.02	-
Al	0.06	0.06	0.08	0.06	0.06	0.06	0.15	0.01
Cr	0.01	-	-	0.01	-	-	-	-
Fe2	0.50	0.50	0.51	0.59	0.55	0.38	0.55	0.43
Mg	1.28	1.26	1.09	1.10	1.17	1.48	1.12	1.43
Ca	0.17	0.19	0.34	0.25	0.28	0.09	0.19	0.12
total=	4.00	4.00	4.00	4.00	4.02	3.99	3.97	3.99
oxygens=	[6]	[6]	[6]	[6]	[6]	[6]	[6]	[6]
temp	1146.00	1139.00	1126.00	1113.00	1080.00	1180.00	1080.00	1242.00
time	234.80	316.60	317.10	264.50	48.00	48.00	188.00	26.00
WO	8.81	9.84	17.47	12.69	14.16	4.69	10.29	5.97
EN	65.72	64.61	56.23	56.85	58.53	75.80	59.93	72.20
FS	25.47	25.55	26.29	30.45	27.32	19.51	29.78	21.83

41 GROVE & BEATY 10085 -PIG,00KB,1146C,234.8HR,F-13.00,+GL+PIG+ILM
42 GROVE & BEATY 10085 -PIG,00KB,1139C,316.6HR,F-13.00,+GL+PIG+ILM
43 GROVE & BEATY 10085 -PIG,00KB,1126C,317.1HR,F-13.00,+GL+PIG+CPX+ILM
44 GROVE & BEATY 10085 -PIG,00KB,1113C,264.5HR,F-13.00,+GL+PIG+CPX+PLAG+ILM
45 HESS ETAL LKFM -PIG,00KB,1080C,48HR,F-13.00,+GL+PIG+PLAG+ILM
46 HESS ETAL 15382 -PIG,00KB,1180C,48HR,F-13.00,+GL+PIG+PLAG+SP
47 HESS ETAL 15382 -PIG,00KB,1080C,188HR,F-13.00,+GL+PIG+PLAG+ILM+SP
48 HUEBENER &TURNOCK 1980 12021 -PIG,00KB,1242C,26HR;F-11.96,+GL+PIG

TABLE AIII.2B

	49	50	51	52	53	54	55	56
SiO2	53.52	50.02	53.13	51.42	51.16	52.30	51.29	54.10
TiO2	0.12	0.95	0.15	0.68	0.34	nd	nd	0.24
Al2O3	0.21	1.02	0.30	1.15	0.72	0.39	0.85	1.43
Cr2O3	0.73	0.48	nd	0.55	0.54	nd	nd	0.20
FeO	12.95	23.54	27.05	23.19	24.79	28.44	27.77	13.50
MnO	nd	0.39	nd	0.52	0.96	1.46	1.36	0.37
MgO	27.04	15.68	15.06	17.64	15.91	17.77	17.58	25.10
CaO	2.96	9.24	6.81	6.26	6.55	0.49	0.62	5.34
Na2O	nd	nd	nd	0.04	0.03	nd	nd	0.07
total=	97.53	101.32	102.50	101.45	101.00	100.85	99.47	100.35
Si	1.97	1.91	2.00	1.94	1.95	1.99	1.98	1.95
Ti	-	0.03	-	0.02	-	-	-	-
Al	-	0.05	0.01	0.05	0.03	0.02	0.04	0.06
Cr	0.02	0.01	-	0.02	0.02	-	-	-
Fe2	0.40	0.75	0.85	0.73	0.79	0.91	0.90	0:41
Mn	-	0.01	-	0.02	0.03	0.05	0.04	0.01
Mg	1.49	0.89	0.85	0.99	0.91	1.01	1.01	1.35
Ca	0.12	0.38	0.27	0.25	0.27	0.02	0.03	0.21
total=	4.01	4.03	3.99	4.01	4.01	4.00	4.00	4.01
oxygens=	[6]	[6]	[6]	[6]	[6]	[6]	[6]	[6]
temp	1242.00	1151.00	1151.00	1123.00	1123.00	1226.00	1178.00	1153.00
time	26.00	45.00	45.00	19.00	19.00	54.00	52.00	458.10
WO	5.84	18.69	13.93	12.80	13.64	1.03	1.33	10.51
EN	74.22	44.13	42.87	50.19	46.08	52.14	52.31	68.74
FS	19.94	37.17	43.20	37.02	40.28	46.82	46.36	20.75

49 HUEBENER & TURNOCK 1980 12021 -PIG2,00KB,1242C,26HR,F-11.96,+GL+PIG
50 HUEBENER & TURNOCK 1980 12021 -PIG,00KB,1151C,45HR,F-12.65,+GL+PIG
51 HUEBENER & TURNOCK 1980 12021 -PIG2,00KB,1151C,45HR,F-12.65,+GL+PIG
52 HUEBENER & TURNOCK 1980 12021 -PIG,00KB,1123C,19HR,F-13.49,+GL+PIG+OL
53 HUEBENER & TURNOCK 1980 12021 -PIG2,00KB,1123C,19HR,F-13.49,+GL+PIG+OL+CPX
54 HUEBENER & TURNOCK 1980 223 -PIG,00KB,1226C,54HR,F-11.58,+GL+PIG+OL
55 HUEBENER & TURNOCK 1980 223 -PIG,00KB,1178C,52HR,F-12.06,+GL+PIG
56 GROVE ETAL 1982 79-35G -PIG,00KB,1153C,458.1HR,F-9.10,+GL+OL+PL+CPX+PIG

	57	58	59	60	61	62	63	64
SiO2	53.40	53.30	52.90	53.30	55.20	54.90	52.80	53.90
TiO2	0.28	0.34	0.49	0.59	0.31	0.38	0.60	0.35
Al2O3	1.57	0.96	0.97	0.95	1.08	1.09	1.54	1.25
Cr2O3	0.10	0.08	0.10	0.09	0.13	0.15	0.05	0.04
FeO	15.40	17.70	18.60	21.30	14.10	14.90	16.50	17.10
MnO	0.32	0.38	0.37	0.40	0.38	0.38	0.32	0.44
MgO	23.00	22.70	21.80	20.00	25.30	24.60	21.80	22.80
CaO	5.62	4.84	4.37	4.88	4.25	4.90	4.60	4.56
Na2O	0.12	0.07	0.08	0.09	0.07	0.12	0.41	0.25
K2O	nd	nd	nd	nd	nd	nd	nd	0.03
total=	99.81	100.37	99.68	101.60	100.82	101.42	98.62	100.72
Si	1.96	1.96	1.97	1.97	1.98	1.97	1.97	1.97
Ti	-	-	0.01	0.02	-	0.01	0.02	-
Al	0.07	0.04	0.04	0.04	0.05	0.05	0.07	0.05
Fe2	0.47	0.54	0.58	0.66	0.42	0.45	0.51	0.52
Mn	-	0.01	0.01	0.01	0.01	0.01	0.01	0.01
Mg	1.26	1.24	1.21	1.10	1.35	1.32	1.21	1.24
Ca	0.22	0.19	0.17	0.19	0.16	0.19	0.18	0.18
Na	-	-	-	-	-	-	0.03	0.02
total=	4.00	4.01	4.00	4.00	3.99	4.00	4.00	4.01
oxygens=	[6]	[6]	[6]	[6]	[6]	[6]	[6]	[6]
temp	1137.00	1106.00	1089.00	1072.00	1135.00	1123.00	1105.00	1106.00
time	542.50	306.80	218.00	194.60	148.70	164.30	221.10	118.50
WO	11.32	9.63	8.88	9.89	8.42	9.65	9.62	9.19
EN	64.46	62.86	61.62	56.40	69.76	67.43	63.44	63.92
FS	24.22	27.50	29.50	33.70	21.81	22.91	26.94	26.90

57 GROVE ETAL 1982 79-35G -PIG,00KB,1137C,542.5HR,F-9.34,+GL+OL+PL+CPX+PIG
58 GROVE ETAL 1982 79-38B -PIG,00KB,1106C,306.8HR,F-9.65,+GL+OL+PL+PIG
59 GROVE ETAL 1982 79-38B -PIG,00KB,1089C,218HR,F-9.90,+GL+PL+PIG
60 GROVE ETAL 1982 79-38B -PIG,00KB,1072C,194.6HR,F-10.16,+GL+PL+PIG
61 GROVE ETAL 1982 187 -PIG,00KB,1135C,148.7HR,F-9.28,+GL+OL+PL+PIG
62 GROVE ETAL 1982 187 -PIG,00KB,1123C,164.3HR,F-9.41,+GL+OL+PL+PIG
63 GROVE ETAL 1982 187 -PIG,00KB,1105C,221.1HR,F-9.71,+GL+OL+PL+PIG
64 GROVE ETAL 1982 79-20E -PIG,00KB,1106C,118.5HR,F-9.66,+GL+PL+OL+PIG

TABLE AIII.2B

	65	66	67	68	69	70	71	72
SiO2	53.30	53.20	51.40	53.40	55.90	54.50	53.50	54.80
TiO2	0.42	0.43	0.50	0.20	0.15	0.15	0.33	0.18
Al2O3	0.81	1.07	0.86	2.47	1.13	1.27	2.31	0.74
Cr2O3	0.12	0.05	0.06	0.22	0.15	0.20	0.16	0.13
FeO	18.80	19.30	24.50	12.70	12.10	14.10	12.10	11.50
MnO	0.40	0.50	0.54	0.33	0.24	0.27	0.33	0.34
MgO	21.40	22.10	18.20	24.60	27.40	24.80	25.40	27.60
CaO	4.50	3.89	3.43	5.37	4.43	4.96	5.14	3.79
Na2O	0.06	0.07	0.07	0.11	0.03	0.05	0.11	0.03
K2O	0.03	0.02	0.06	nd	nd	nd	nd	nd
total=	99.84	100.63	99.62	99.40	101.53	100.30	99.38	99.11
Si	1.98	1.96	1.96	1.94	1.97	1.97	1.94	1.98
Ti	0.01	0.01	0.01	-	-	-	-	-
Al	0.04	0.05	0.04	0.11	0.05	0.05	0.10	0.03
Fe2	0.58	0.60	0.78	0.39	0.36	0.43	0.37	0.35
Mn	0.01	0.02	0.02	0.01	-	-	0.01	0.01
Mg	1.18	1.21	1.04	1.33	1.44	1.34	1.37	1.48
Ca	0.18	0.15	0.14	0.21	0.17	0.19	0.20	0.15
total=	3.99	4.01	4.01	4.00	4.00	4.00	4.01	4.00
oxygens=	[6]	[6]	[6]	[6]	[6]	[6]	[6]	[6]
temp	1093.00	1076.00	1059.00	1167.00	1166.00	1156.00	1167.00	1166.00
time	291.00	330.00	628.00	500.90	242.30	244.40	500.90	458.20
WO	9.19	7.83	7.16	10.85	8.52	9.83	10.30	7.41
EN	60.83	61.86	52.89	69.13	73.31	68.36	70.79	75.05
FS	29.98	30.31	39.95	20.03	18.17	21.81	18.92	17.54

65 GROVE ETAL 1982 79-20E -PIG,00KB,1093C,291HR,F-9.94,+GL+OL+PL+PIG
66 GROVE ETAL 1982 79-20E -PIG,00KB,1076C,330HR,F-10.11,+GL+PL+OL+PIG
67 GROVE ETAL 1982 79-9C -PIG,00KB,1059C,628HR,F-10.34,+GL+PL+PIG
68 GROVE & BRYAN 1983 ALV 528 11 -PIG,00KB,1167C,500.9HR,F-9.03,+GL+OL+PL+CPX+PIG
69 GROVE & BRYAN 1983 ALV 528 11 -PIG,00KB,1166C,242.3HR,F-8.98,+GL+OL+PL+CPX+PIG
70 GROVE & BRYAN 1983 ALV 528 11 -PIG,00KB,1156C,244.4HR,F-9.14,+GL+OL+PL+CPX+PIG
71 GROVE & BRYAN 1983 ALV 525 4B -PIG,00KB,1167C,500.9HR,F-9.03,+GL+OL+PL+CPX+PIG
72 GROVE & BRYAN 1983 AII 966 42 -PIG,00KB,1166C,458.2HR,F-9.08,+GL+OL+PL+CPX+PIG

	73	74	75	76	77
SiO2	53.60	52.78	51.84	54.14	53.42
TiO2	0.30	nd	nd	0.10	0.25
Al2O3	1.12	0.24	0.21	1.21	0.71
Cr2O3	0.18	0.70	nd	nd	nd
FeO	14.20	16.95	26.39	16.20	18.49
MnO	0.40	nd	nd	nd	0.38
MgO	25.40	26.28	14.78	23.80	22.55
CaO	4.20	3.06	6.78	4.55	3.52
Na2O	0.03	nd	nd	nd	0.09
total=	99.43	100.00	100.00	100.00	99.41
Si	1.96	1.94	2.00	1.98	1.98
Al	0.05	0.01	-	0.05	0.03
Cr	-	0.02	-	-	-
Fe2	0.43	0.52	0.85	0.49	0.57
Mn	0.01	-	-	-	0.01
Mg	1.38	1.44	0.85	1.29	1.25
Ca	0.16	0.12	0.28	0.18	0.14
total=	4.01	4.05	3.99	4.00	4.00
oxygens=	[6]	[6]	[6]	[6]	[6]
temp	1137.00	1241.00	1151.00	1134.00	1160.00
time	311.40	24.00	24.00	24.00	19.90
WO	8.30	5.78	14.14	9.05	7.14
EN	69.80	69.19	42.90	65.81	63.60
FS	21.90	25.03	42.96	25.14	29.26

73 GROVE & BRYAN 1983 AII 966 42 -PIG,00KB,1137C,311.4HR,F-9.12,+GL+OL+PL+CPX+PIG
74 NEILSEN & DRAKE TABLE 1 1 -PIG,00KB,1241C,24HR,F-10.00,+GL+PIG
75 NEILSEN & DRAKE TABLE 1 3 -PIG,00KB,1151C,24HR,F-10.00,+GL+PIG
76 NEILSEN & DRAKE TABLE 1 10 -PIG,00KB,1134C,24HR,F-10.00,+GL+PIG
77 MITCHELL 1984 ROCK+GEL -PIG,00KB,1160C,19.9HR,F-9.00,+GL+OL+PIG

TABLE AIII.3

17M

Heating experiments at NNO

run no.	T°C	t hrs	fO_2	phases
3/761	1345	24	-6.30	gl
3/764	1327	24	-6.40	gl + ol + sp
3/677	1307	24	-6.65	gl + ol + opx + sp
3/684	1290	24	-6.70	gl + ol + opx + sp
3/692	1266	24	-6.90	gl + ol + opx + sp
3/700	1252	24	-7.05	gl + ol + opx + pig + sp
3/726	1245	48	-7.40	gl + opx + sp (+ ol)
3/706	1235	24	-7.20	gl + ol + opx + pig
3/745	1206	48	-7.60	gl + opx + pig + sp
3/775	1194	96	-7.60	gl + opx + pig
3/743	1184	48	-8.00	gl + opx + pig + sp
3/757	1155	95	-8.15	gl + pig + sp (+ opx)
3/777	1148	95	-8.20	gl + pig + plag

Cooling experiments at NNO

run no.	Ti°C	ti	Tf°C	tf	T°C/hr	fO_2	phases
3/714	1340	5	1317	24	240	-6.40	gl + ol + sp
3/715	1333	5	1313	24	240	-6.40	gl + ol + sp
3/719	1313	24	1266	24	240	-6.60	gl + ol + opx + sp

Heating experiments at CCO

run no.	T°C	t hrs	fO_2	phases
4/214	1352	5	-7.80	gl
4/215	1331	5	-7.85	gl + ol
4/216	1314	5	-8.00	gl + ol + sp
4/217	1298	5	-8.15	gl + ol + opx + sp
4/219	1281	5	-8.31	gl + ol + pig + sp
4/239:2	1309	72	-8.00	gl + ol + opx
4/239:3	1309	72	-8.00	gl + ol + opx
4/239:4	1309	72	-8.00	gl + ol + opx
4/245	1315	24	-8.00	gl + ol + opx + sp
4/248	1316	46	-8.00	gl + ol + opx + sp
4/249:1	1316	102	-8.00	gl + opx + sp
4/249:2	1316	102	-8.00	gl + opx + sp

Cooling experiments at CCO

run no.	Ti°C	ti	Tf°C	tf	T°C/hr	fO_2	phases
4/237	1365	1	1304	69	30	-7.90	gl + ol + sp
4/237A	1365	1	1304	69	30	-7.90	gl + pr + opx + ol
4/238	1327	1	1307	70	20	-8.00	gl + pr + opx
4/238A	1327	1	1307	70	20	-8.00	gl + pr + opx

TABLE AIII.3

17M cont.

Heating experiments at IW

run no.	T°C	t hrs	fO_2	phases
5/757	1314	23	-10.50	gl + pr + opx
5/750	1307	24	-10.45	gl + opx + ol
5/751	1258	45	-11.20	gl + opx (+ ol)
5/760	1325	23	-10.40	gl + ol
5/761	1297	22	-10.70	gl + ol + opx
5/762	1257	48	-11.10	gl + opx + pig

170

Heating experiments at NNO

run no.	T°C	t hrs	fO_2	phases
3/671	1345	24	-6.30	gl + sp
3/674	1327	24	-6.40	gl + sp
3/677	1307	24	-6.65	gl + ol + sp
3/684	1290	24	-6.70	gl + opx + sp
3/692	1266	24	-6.90	gl + opx + sp
3/700	1252	24	-7.05	gl + opx + pig + sp
3/726	1245	48	-7.40	gl + opx + sp
3/706	1235	24	-7.20	gl + pig + sp
3/745	1206	48	-7.60	gl + pig + sp
3/743	1184	48	-8.00	gl + pig + sp
3/757	1155	95	-8.15	gl + pig + cpx + sp

Heating experiments at CCO

run no.	T°C	t hrs	fO_2	phases
4/214	1352	5	-7.80	gl
4/215	1331	5	-7.85	gl + sp
4/216	1314	5	-8.00	gl + opx + sp
4/217	1298	5	-8.15	gl + opx + sp
4/218	1287	5	-8.26	gl + opx + sp
4/220	1274	5	-8.36	gl + pig + sp

Heating experiments at IW

run no.	T°C	t hrs	fO_2	phases
5/757	1314	23	-10.50	gl + pr
5/750	1307	24	-10.45	gl + pr + opx
5/751	1258	45	-11.20	gl + opx
5/760	1325	23	-10.40	gl
5/761	1297	22	-10.70	gl + opx
5/762	1257	48	-11.10	gl + opx (+ pig)

TABLE AIII.3

120

Heating experiments at NNO

run no.	T°C	t hrs	fO_2	phases
3/673	1347	24	-6.25	gl + sp
3/675	1327	23	-6.50	gl + sp
3/681	1309	23	-6.55	gl + opx + sp
3/685	1288	24	-6.70	gl + opx + sp
3/693	1265	25	-6.85	gl + opx + pig +sp
3/703	1253	23	-7.05	gl + pig + sp
3/726	1245	48	-7.40	gl + opx + sp
3/707	1235	23	-7.15	gl + pig + sp
3/770	1224	477	-7.40	gl + opx + pig + sp
3/745	1206	48	-7.60	gl + pig + sp
3/743	1184	48	-8.00	gl + pig + cpx + sp
3/757	1155	95	-8.15	gl + pig + cpx + sp

Cooling experiments at NNO

run no.	Ti°C	ti	Tf°C	tf	T°C/hr	fO_2	phases
3/714	1340	5	1317	24	240	-6.40	gl + pr + opx + sp
3/715	1333	5	1313	24	240	-6.40	gl + opx + sp
3/717	1311	24	1289	24	240	-6.60	gl + opx + sp
3/719	1317	24	1271	24	240	-6.60	gl + opx
3/765	1332	3.5	1225	39	20	-6.80	gl + opx + sp

Heating experiments at CCO

run no.	T°C	t hrs	fO_2	phases
4/214	1352	5	-7.70	gl
4/215	1331	5	-7.70	gl + sp
4/216	1314	5	-7.85	gl + opx + pig + sp
4/217	1298	5	-8.00	gl + opx + pig + sp
4/218	1287	5	-8.10	gl + pig + sp
4/219	1281	5	-8.15	gl + pig + sp
4/220	1274	5	-8.20	gl + pig + sp

Heating experiments at IW

run no.	T°C	t hrs	fO_2	phases
5/757	1314	23	-10.50	gl + pr + opx
5/750	1307	24	-10.45	gl + opx
5/751	1258	45	-11.20	gl + opx + pig
5/760	1325	23	-10.40	gl + opx
5/761	1297	22	-10.70	gl + opx (+ pig)
5/762	1257	48	-11.10	gl + pig (+ opx)

TABLE AIII.3

B4

Heating experiments at NNO

run no.	T°C	t hrs	fO_2	phases
3/673	1347	24	-6.25	gl
3/675	1327	23	-6.50	gl
3/681	1309	23	-6.55	gl
3/685	1288	23	-6.70	gl + ol
3/693	1265	25	-6.85	gl + ol
3/703	1253	24	-7.05	gl + ol + opx + sp
3/708	1235	24	-7.15	gl + ol + opx + sp
3/746	1206	48	-7.50	gl + opx (+ pig)
3/744	1181	48	-7.90	gl + opx + plag + sp
3/756	1156	48	-8.15	gl + opx + plag + quench
3/777	1148	95	-8.20	gl + pig + cpx + plag

B5

Heating experiments at NNO

run no.	T°C	t hrs	fO_2	phases
3/746	1206	48	-7.50	gl
3/775	1194	96	-7.60	gl + opx
3/756	1156	48	-8.15	gl + opx + cpx + plag
3/777	1148	95	-8.20	gl + opx + plag

T2

Heating experiments at NNO

run no.	T°C	t hrs	fO_2	phases
3/703	1253	24	-7.05	gl
3/708	1235	24	-7.15	gl
3/746	1206	48	-7.50	gl + sp
3/744	1181	48	-7.90	gl + ol + sp
3/756	1156	48	-8.15	gl + opx + plag + sp
3/777	1148	95	-8.20	gl + opx + plag

K6

Heating experiments at NNO

run no.	T°C	t hrs	fO_2	phases
3/682	1309	24	-6.50	gl + sp
3/686	1288	24	-6.70	gl + sp
3/694	1270	24	-6.80	gl + ol + sp
3/695	1252	23	-7.05	gl + ol + sp
3/707	1235	24	-7.15	gl + ol + sp
3/743	1184	48	-8.00	gl + opx + plag (+ cpx + ol)

TABLE AIII.3

K1

Heating experiments at NNO

run no.	T°C	t hrs	fO_2	phases
3/682	1309	24	-6.50	gl + sp
3/686	1288	24	-6.70	gl + sp
3/694	1270	24	-6.80	gl + ol + sp
3/695	1252	23	-7.05	gl + ol + sp
3/745	1206	48	-7.60	gl + opx + ol + sp
3/775	1194	96	-7.60	gl + pig + cpx
3/776	1172	93	-7.90	gl + pig + cpx + plag
3/756	1156	48	-8.15	gl + pig + cpx + plag +sp

295

Heating experiments at NNO

run no.	T°C	t hrs	fO_2	phases
3/676	1398	1	-5.65	gl + sp
3/671	1345	24	-6.30	gl + ol + sp
3/674	1327	24	-6.40	gl + ol + sp
3/677	1307	24	-6.65	gl + ol + sp
3/684	1290	24	-6.70	gl + ol + sp
3/692	1266	24	-6.90	gl + ol + sp
3/700	1252	24	-7.05	gl + ol + sp
3/706	1235	24	-7.20	gl + ol + opx + sp
3/770	1224	477	-7.40	gl + ol + opx + sp
3/746	1206	48	-7.50	gl + ol + opx + sp
3/775	1194	96	-7.60	gl + ol + opx + sp
3/744	1181	48	-7.90	gl + ol + opx + plag + sp
3/757	1155	95	-8.15	gl + ol + opx + plag + sp

Heating experiments at IW

run no.	T°C	t hrs	fO_2	phases
5/757	1314	23	-10.50	gl + ol
5/750	1307	24	-10.45	gl + ol + sp (+ opx)
5/751	1258	45	-11.20	gl + ol + opx + pr + sp
5/760	1325	23	-10.40	gl + ol
5/761	1297	22	-10.70	gl + ol
5/762	1257	48	-11.10	gl + ol + opx

TABLE AIII.3

M1

Heating experiments at NNO

run no.	T°C	t hrs	fO_2	phases
3/673	1347	24	-6.25	gl
3/675	1327	23	-6.50	gl + sp
3/716	1312	24	-6.40	gl + opx
3/681	1307	23	-6.55	gl + opx
3/685	1288	23	-6.70	gl + opx
3/693	1265	25	-6.85	gl + opx
3/703	1253	24	-7.05	gl + opx + sp
3/708	1235	24	-7.15	gl + opx

Cooling experiments at NNO

run no.	Ti°C	ti	Tf°C	tf	T°C/hr	fO_2	phases
3/714	1340	5	1317	24	240	-6.40	gl + sp
3/715	1333	5	1313	24	240	-6.40	gl + pr
3/719	1317	24	1271	24	240	-6.60	gl + opx
3/765	1332	3.5	1225	39	20	-6.60	gl + opx

M1MET

Heating experiments at NNO

run no.	T°C	t hrs	fO_2	phases
3/727	1317	24	-6.50	gl
3/752	1292	48	-6.70	gl + opx
3/743	1275	48	-6.85	gl + opx
3/728	1273	24	-7.00	gl + opx
3/750	1237	48	-7.10	gl + opx
3/770	1224	477	-7.40	gl + opx
3/735	1215	48	-7.60	gl + opx + pig
3/742	1184	48	-7.90	gl + opx + pig
3/758	1156	121	-8.15	gl + opx

C2

Heating experiments at NNO

run no.	T°C	t hrs	fO_2	phases
3/673	1347	24	-6.25	gl + sp
3/674	1327	24	-6.40	gl
3/681	1309	23	-6.55	gl + opx
3/684	1290	24	-6.70	gl + opx
3/692	1266	24	-6.90	gl + opx
3/700	1252	24	-7.05	gl + opx (+ pig)
3/706	1235	24	-7.20	gl + opx (+ pig)

TABLE AIII.3

C2MET

Heating experiments at NNO

run no.	T°C	t hrs	fO_2	phases
3/752	1292	48	-6.70	gl + opx
3/743	1275	48	-6.85	gl + opx + sp
3/751	1273	48	-6.70	gl + opx
3/750	1237	48	-7.10	gl + opx
3/735	1215	48	-7.60	gl + opx + sp
3/742	1184	48	-7.90	gl + opx
3/776	1172	93	-7.90	gl + opx + cpx + plag
3/758	1156	121	-8.15	gl + opx + cpx + plag

C5

Heating experiments at NNO

run no.	T°C	t hrs	fO_2	phases
3/682	1309	24	-6.50	gl + ol
3/685	1288	24	-6.70	gl + ol
3/693	1265	25	-6.85	gl + opx
3/694	1270	24	-6.80	gl + opx + sp
3/695	1252	23	-7.05	gl + opx
3/707	1235	24	-7.15	gl + opx
3/744	1181	48	-7.90	gl + opx

C5MET

Heating experiments at NNO

run no.	T°C	t hrs	fO_2	phases
3/752	1292	48	-6.70	gl + ol + sp
3/734	1275	48	-6.85	gl + opx + sp
3/751	1273	48	-6.70	gl + ol + opx
3/750	1237	48	-7.10	gl + opx
3/770	1224	477	-7.40	gl + opx
3/735	1215	48	-7.60	gl + opx
3/742	1184	48	-7.90	gl + opx + sp
3/758	1156	121	-8.15	gl + opx + plag

TABLE AIII.3

C11

Heating experiments at NNO

run no.	T°C	t hrs	fO_2	phases
3/682	1309	24	-6.50	gl + sp
3/686	1288	24	-6.70	gl + sp
3/694	1270	24	-6.80	gl + opx + sp
3/695	1252	23	-7.05	gl + opx + sp
3/707	1236	24	-7.15	gl + opx + sp

C11MET

Heating experiments at NNO

run no.	T°C	t hrs	fO_2	phases
3/734	1275	48	-6.85	gl + sp
3/751	1273	48	-6.70	gl + opx
3/750	1237	48	-7.10	gl + opx + sp
3/742	1184	48	-7.90	gl + opx + plag + sp
3/758	1156	121	-8.15	gl + opx + plag

TABLE AIII.4A

	1	2	3	4	5	6	7	8
SiO2	57.41	57.29	55.59	55.41	54.79	55.68	55.08	55.59
TiO2	0.09	0.11	0.14	0.16	0.12	0.16	0.20	0.15
Al2O3	0.59	0.70	0.82	0.91	0.96	1.15	1.25	0.93
Cr2O3	0.42	0.50	0.49	0.53	0.49	0.54	0.51	0.39
FeO	7.64	8.21	8.79	9.12	9.16	9.82	10.74	10.41
MnO	0.14	0.17	0.16	0.15	0.18	0.20	0.17	0.17
MgO	33.31	32.74	31.21	30.44	30.75	30.26	29.04	29.87
CaO	0.89	0.99	1.19	1.36	1.44	1.90	1.99	1.97
Na2O	0.04	0.04	0.04	0.03	0.05	0.04	0.04	0.05
total=	100.52	100.74	98.41	98.11	97.96	99.76	99.02	99.54
Si	1.98	1.98	1.98	1.98	1.97	1.97	1.97	1.97
Al	0.02	0.03	0.03	0.04	0.04	0.05	0.05	0.04
Cr	0.01	0.01	0.01	0.01	0.01	0.02	0.01	0.01
Fe2	0.22	0.24	0.26	0.27	0.27	0.29	0.32	0.31
Mg	1.72	1.69	1.65	1.62	1.64	1.59	1.55	1.58
Ca	0.03	0.04	0.05	0.05	0.06	0.07	0.08	0.07
total=	4.00	4.00	4.00	3.99	4.01	4.00	3.99	4.00
oxygens=	[6]	[6]	[6]	[6]	[6]	[6]	[6]	[6]
temp	1307.00	1290.00	1266.00	1252.00	1245.00	1206.00	1194.00	1184.00
time	24.00	24.00	24.00	24.00	48.00	48.00	96.00	48.00
WO	1.67	1.87	2.31	2.68	2.81	3.68	3.92	3.80
EN	87.12	86.03	84.36	83.32	83.27	81.49	79.57	80.46
FS	11.21	12.10	13.33	14.01	13.92	14.84	16.51	15.73

1 17M 3:677 -OPXB8,00KB,1307C,24HR,F-6.65,+GL+OL+OPXB+SP
2 17M 3:684 -OPXB10,00KB,1290C,24HR,F-6.70,+GL+OL+OPXB+SP
3 17M 3:693 -OPXB4,00KB,1266C,24HR,F-6.90,+GL+OPXB+OL+SP
4 17M 3:700 -OPXB3,00KB,1252C,24HR,F-7.05,+GL+OPXB+SP+PIG+OL
5 17M 3:726 -OPX12,00KB,1245C,48HR,F-7.40,+GL+OPXB+OL+SP
6 17M 3:745 -OPX3,00KB,1206C,48HR,F-7.60,+GL+OPXB+PIG+SP
7 17M 3:775 -OPXB3,00KB,1194C,96HR,F-7.60,+GL+OPXB+PIG
8 17M 3:743 -OPXB1,00KB,1184C,48HR,F-8.00,+GL+OXB+PIG+SP

	9	10	11	12	13	14	15	16
SiO2	57.40	56.89	56.31	56.68	57.15	56.36	56.24	55.70
TiO2	0.11	0.12	0.15	0.15	0.11	0.11	0.12	0.14
Al2O3	0.58	0.52	0.58	0.90	0.44	0.45	0.44	0.61
Cr2O3	0.51	0.50	0.73	0.51	0.50	0.52	0.45	0.45
FeO	6.97	7.59	8.24	7.80	6.35	6.99	7.66	8.15
MnO	0.11	0.13	0.16	0.18	0.13	0.14	0.14	0.16
MgO	33.43	32.67	32.13	31.36	34.07	33.16	32.65	31.35
CaO	0.98	1.17	1.31	1.57	1.01	1.23	1.44	1.82
Na2O	0.07	0.06	0.07	0.14	0.06	0.06	0.05	0.07
total=	100.16	99.66	99.68	99.28	99.82	99.02	99.20	98.44
Si	1.99	1.99	1.97	1.99	1.98	1.98	1.98	1.98
Al	0.02	0.02	0.02	0.04	0.02	0.02	0.02	0.03
Cr	0.01	0.01	0.02	0.01	0.01	0.01	0.01	0.01
Fe2	0.20	0.22	0.24	0.23	0.18	0.20	0.23	0.24
Mg	1.72	1.70	1.68	1.64	1.76	1.73	1.71	1.66
Ca	0.04	0.04	0.05	0.06	0.04	0.05	0.05	0.07
total=	4.00	4.00	4.00	3.99	4.00	4.01	4.01	4.00
oxygens=	[6]	[6]	[6]	[6]	[6]	[6]	[6]	[6]
temp	1290.00	1266.00	1252.00	1245.00	1309.00	1288.00	1265.00	1245.00
time	24.00	24.00	24.00	48.00	23.50	23.75	25.00	48.00
WO	1.85	2.23	2.51	3.06	1.89	2.32	2.71	3.52
EN	87.88	86.49	85.24	85.07	88.82	87.35	85.97	84.20
FS	10.27	11.27	12.26	11.88	9.29	10.32	11.32	12.28

9 170 3:684 -OPXB8,00KB,1290C,24HR,F-6.70,+GL+OPXB+SP
10 170 3:692 -OPXB10,00KB,1266C,24HR,F-6.90,+GL+OPXB+SP
11 170 3:700 -OPXB5,00KB,1252C,24HR,F-7.05,+GL+OPXB+PIG+SP
12 170 3:726 -OPX10,00KB,1245C,48HR,F-7.40,+GL+OPXB+SP
13 120 3:681 -OPXB9,00KB,1309C,23.5HR,F-6.55,+GL+OPXB+SP
14 120 3:685 -OPXB7,00KB,1288C,23.75HR,F-6.75,+GL+OPXB+SP
15 120 3:693 -OPXB2,00KB,1265C,25HR,F-6.85,+GL+OPXB+SP+PIG
16 120 3:726 -OPX11,00KB,1245C,48HR,F-7.40,+GL+OPXB+SP

TABLE AIII.4A

	17	18	19	20	21	22	23	24
SiO2	55.82	55.96	55.15	54.50	55.26	56.78	56.21	56.60
TiO2	0.14	0.07	0.12	0.02	0.09	nd	0.01	0.01
Al2O3	0.60	1.31	0.92	1.43	1.35	0.50	0.45	0.50
Cr2O3	0.51	0.32	0.15	0.56	0.64	0.24	0.27	0.29
FeO	8.57	10.57	13.60	8.43	8.61	6.89	8.41	8.23
MnO	0.16	0.22	0.34	0.23	0.20	0.18	0.24	0.23
MgO	30.24	29.54	26.63	31.98	30.02	33.62	32.60	32.19
CaO	2.12	1.51	2.41	2.31	1.79	1.04	1.14	1.38
Na2O	0.05	0.09	0.07	0.05	0.03	0.04	0.03	0.03
total=	98.20	99.58	99.38	99.52	97.99	99.27	99.36	99.46
Si	1.99	1.98	1.99	1.93	1.98	1.98	1.98	1.99
Al	0.03	0.05	0.04	0.06	0.06	0.02	0.02	0.02
Cr	0.01	-	-	0.02	0.02	-	-	-
Fe2	0.26	0.31	0.41	0.25	0.26	0.20	0.25	0.24
Mn	-	-	0.01	-	-	-	-	-
Mg	1.61	1.56	1.43	1.69	1.60	1.75	1.71	1.68
Ca	0.08	0.06	0.09	0.09	0.07	0.04	0.04	0.05
total=	3.99	3.99	3.99	4.04	3.99	4.01	4.01	4.00
oxygens=	[6]	[6]	[6]	[6]	[6]	[6]	[6]	[6]
temp	1224.00	1194.00	1156.00	1206.00	1224.00	1309.00	1292.00	1275.00
time	477.00	96.00	48.00	48.00	477.00	23.50	48.00	48.00
WO	4.17	2.98	4.81	4.34	3.55	1.95	2.16	2.63
EN	82.69	80.80	73.98	83.34	83.08	87.94	85.48	85.15
FS	13.15	16.22	21.21	12.32	13.36	10.11	12.37	12.22

17 120 3:770 -OPXB7,00KB,1224C,477HR,F-7.40,+GL+OPXB+PIG+SP
18 B5 3:775 -OPXB3,00KB,1194C,96HR,F-7.60,+GL+OPXB
19 B5 3:756 -OPXB9,00KB,1156C,48HR,F-8.15,+GL+OPXB+CPX+PLAG
20 K1 3:745 -OPXB10,00KB,1206C,48HR,F-7.60,+GL+OL+OPXB+SP
21 295 3:770 -OPXB8,00KB,1224C,477HR,F-7.40,+GL+OPXB+OL+SP
22 M1 3:681 -OPXB8,00KB,1309C,23.5HR,F-6.55,+GL+OPXB
23 M1MET 3:752 -OPXB8,00KB,1292C,48HR,F-6.70,+GL+OPXB
24 M1MET 3:734 -OPX17,00KB,1275C,48HR,F-6.85,+GL+OPXB

	25	26	27	28	29	30	31	32
SiO2	57.15	56.43	55.95	56.53	56.40	57.20	57.40	57.21
TiO2	0.03	0.04	0.07	0.03	0.01	0.02	0.02	0.02
Al2O3	0.50	1.09	0.64	0.78	0.73	0.70	0.75	0.92
Cr2O3	0.25	0.32	0.27	0.40	0.40	0.34	0.33	0.38
FeO	8.44	9.77	8.93	6.91	7.18	5.86	6.52	7.66
MnO	0.23	0.26	0.25	0.16	0.17	0.15	0.16	0.19
MgO	32.21	29.77	30.16	32.89	31.90	33.90	33.53	32.10
CaO	1.27	2.06	1.86	1.51	1.74	1.02	1.12	1.53
Na2O	0.03	0.11	0.03	0.03	0.02	0.02	0.05	0.04
total=	100.11	99.84	98.17	99.22	98.56	99.21	99.88	100.05
Si	1.99	1.99	2.00	1.98	1.99	1.99	1.99	1.99
Al	0.02	0.05	0.03	0.03	0.03	0.03	0.03	0.04
Cr	-	-	-	0.01	0.01	-	-	0.01
Fe2	0.25	0.29	0.27	0.20	0.21	0.17	0.19	0.22
Mg	1.67	1.56	1.60	1.71	1.68	1.76	1.73	1.66
Ca	0.05	0.08	0.07	0.06	0.07	0.04	0.04	0.06
total=	4.00	3.99	3.99	4.00	3.99	3.99	3.99	3.99
oxygens=	[6]	[6]	[6]	[6]	[6]	[6]	[6]	[6]
temp	1273.00	1237.00	1224.00	1292.00	1275.00	1275.00	1273.00	1237.00
time	48.00	48.00	477.00	48.00	48.00	48.00	48.00	48.00
WO	2.42	4.02	3.67	2.86	3.37	1.93	2.12	2.93
EN	85.07	81.05	82.61	86.90	85.80	89.41	88.25	85.61
FS	12.51	14.93	13.72	10.24	10.83	8.66	9.63	11.46

25 M1MET 3:751 -OPXB11,00KB,1273C,48HR,F-6.70,+GL+OPXB
26 M1MET 3:750 -OPXB12,00KB,1237C,48HR,F-7.10,+GL+OPXB
27 M1MET 3:770 -OPXB8,00KB,1224C,477HR,F-7.40,+GL+OPXB
28 C2MET 3:752 -OPXB11,00KB,1292C,48HR,F-6.70,+GL+OPXB
29 C2MET 3:734 -OPX10,00KB,1275C,48HR,F-6.85,+GL+OPXB+SP
30 C5 3:734 -OPX5,00KB,1275C,48HR,F-6.85,+GL+OPXB+SP
31 C5MET 3:751 -OPXB5,00KB,1273C,48HR,F-6.70,+GL+OL+OPXB
32 C5MET 3:750 -OPXB7,00KB,1237C,48HR,F-7.10,+GL+OPXB

TABLE AIII.4A

	33	34	35	36	37	38	39	40
SiO2	55.84	55.93	55.77	55.88	55.37	56.89	56.71	56.44
TiO2	0.02	0.03	0.02	0.02	0.03	0.13	0.12	0.15
Al2O3	0.91	1.10	1.14	1.32	1.93	0.58	0.38	0.74
Cr2O3	0.26	0.31	0.32	0.41	0.39	0.47	0.50	0.52
FeO	7.92	7.80	8.25	9.03	10.10	5.21	7.88	8.55
MnO	0.16	0.18	0.21	0.24	0.25	0.13	0.15	0.19
MgO	31.20	31.38	31.72	30.80	29.15	33.28	32.41	30.43
CaO	1.61	1.80	1.94	1.44	2.05	1.03	1.02	2.12
Na2O	0.04	0.04	0.05	0.05	0.10	0.03	0.04	0.13
total=	97.96	98.57	99.42	99.19	99.39	97.76	99.19	99.26
Si	1.99	1.98	1.96	1.97	1.96	2.00	1.99	1.99
Al	0.04	0.05	0.05	0.06	0.08	0.02	0.02	0.03
Cr	-	-	-	0.01	0.01	0.01	0.01	0.01
Fe2	0.24	0.23	0.24	0.27	0.30	0.15	0.23	0.25
Mg	1.65	1.65	1.66	1.62	1.54	1.74	1.70	1.60
Ca	0.06	0.07	0.07	0.05	0.08	0.04	0.04	0.08
total=	3.99	4.00	4.01	3.99	3.99	3.98	3.99	3.99
oxygens=	[6]	[6]	[6]	[6]	[6]	[6]	[6]	[6]
temp	1224.00	1215.00	1184.00	1237.00	1184.00	1307.00	1297.00	1257.00
time	477.00	48.00	48.00	48.00	48.00	24.50	22.00	48.00
WO	3.15	3.50	3.70	2.80	4.06	2.01	1.94	4.16
EN	84.77	84.69	84.04	83.47	80.33	90.08	86.29	82.79
FS	12.08	11.81	12.26	13.74	15.62	7.91	11.77	13.05

33 C5MET 3:770 -OPXB11,00KB,1224C,477HR,F-7.40,+GL+OPXB
34 C5 3:735 -OPX5,00KB,1215C,48HR,F-7.60,+GL+OPXB+PIG
35 C5 3:742 -OPXB6,00KB,1184C,48HR,F-7.90,+GL+OPXB+PIG
36 C11MET 3:750 -OPXB8,00KB,1237C,48HR,F-7.10,+GL+OPXB+SP
37 C11MET 3:742 -OPX14,00KB,1184C,48HR,F-7.90,+GL+OPXB+PLAG+SP
38 17M 5:750 -OPXB5,00KB,1307C,24.5HR,F-10.45,+GL+OPXB+OL
39 170 5:761 -OPXB2,00KB,1297C,22HR,F-10.70,+GL+OPXB
40 170 5:762 -OPXB2,00KB,1257C,48HR,F-11.10,+GL+OPXB+PIG

	41	42	43	44	45	46	47	48
SiO2	56.66	57.01	56.38	56.07	56.85	56.70	55.79	55.96
TiO2	0.10	0.12	0.12	0.06	0.10	0.11	0.13	0.11
Al2O3	0.34	0.36	0.39	0.74	0.61	0.63	0.69	0.59
Cr2O3	0.46	0.48	0.49	0.68	0.54	0.56	0.59	0.56
FeO	6.29	6.98	7.85	8.10	7.18	7.13	6.36	7.24
MnO	0.13	0.13	0.15	0.20	0.15	0.15	0.16	0.15
MgO	33.49	33.00	32.08	31.57	32.77	32.99	33.11	33.21
CaO	1.13	1.05	1.44	1.48	0.88	0.90	0.94	0.87
Na2O	0.05	0.04	0.05	0.04	0.03	0.03	0.04	0.04
total=	98.65	99.18	98.96	98.93	99.10	99.19	97.81	98.72
Si	1.99	1.99	1.99	1.98	1.99	1.98	1.97	1.97
Al	0.01	0.01	0.02	0.03	0.02	0.03	0.03	0.02
Cr	0.01	0.01	0.01	0.02	0.01	0.02	0.02	0.02
Fe2	0.18	0.20	0.23	0.24	0.21	0.21	0.19	0.21
Mg	1.75	1.72	1.68	1.66	1.71	1.72	1.75	1.74
Ca	0.04	0.04	0.05	0.06	0.03	0.03	0.04	0.03
total=	4.00	3.99	4.00	4.00	3.99	4.00	4.00	4.01
oxygens=	[6]	[6]	[6]	[6]	[6]	[6]	[6]	[6]
temp	1307.00	1325.00	1297.00	1257.00	1315.00	1315.00	1315.00	1315.00
time	24.50	23.00	22.00	48.00	72.00	72.00	72.00	24.00
WO	2.16	2.00	2.75	2.86	1.68	1.72	1.81	1.64
EN	88.52	87.60	85.50	84.92	87.56	87.65	88.64	87.63
FS	9.32	10.40	11.75	12.22	10.76	10.63	9.56	10.72

41 120 5:750 -OPXB3,00KB,1307C,24.5HR,F-10.45,+GL+OPXB
42 120 5:760 -OPXB6,00KB,1325C,23HR,F-10.40,+GL+OPXB
43 120 5:761 -OPXB3,00KB,1297C,22HR,F-10.70,+GL+OPXB+PIG
44 295 5:762 -OPXB2,00KB,1257C,48HR,F-11.10,+GL+OL+OPXB
45 17M 4:239:2 -OPXB5,00KB,1315C,72HR,F-8.00,+GL+OPXB+OL
46 17M 4:239:3 -OPXB14,00KB,1315C,72HR,F-8.00,+GL+OPXB
47 17M 4:239:4 -OPXB8,00KB,1315C,72HR,F-8.00,+GL+OPXB
48 17M 4:245 -OPXB5,00KB,1315C,24HR,F-8.00,+GL+OPXB+OL

TABLE AIII.4A

	49	50	51	52	53	54	55
SiO2	56.75	57.54	57.47	57.20	57.47	57.69	57.24
TiO2	0.10	0.10	0.10	0.06	0.09	nd	0.12
Al2O3	0.60	0.57	0.65	0.35	0.32	0.27	0.25
Cr2O3	0.54	0.54	0.59	0.49	0.45	0.18	0.63
FeO	7.15	6.74	6.81	8.55	7.23	6.38	6.19
MnO	0.10	0.17	0.17	0.19	0.11	0.21	0.14
NiO	nd	nd	nd	0.21	0.26	nd	0.08
MgO	33.33	33.59	33.41	32.45	32.46	33.29	33.62
CaO	0.79	0.81	0.82	1.02	1.11	1.05	1.11
Na2O	0.02	0.03	0.03	nd	nd	nd	nd
total=	99.38	100.08	100.06	100.50	99.51	99.07	99.38
Si	1.98	1.99	1.99	1.99	2.00	2.01	1.99
Al	0.02	0.02	0.03	0.01	0.01	0.01	0.01
Cr	0.01	0.01	0.02	0.01	0.01	-	0.02
Fe2	0.21	0.19	0.20	0.25	0.21	0.19	0.18
Mg	1.73	1.73	1.72	1.68	1.69	1.73	1.74
Ca	0.03	0.03	0.03	0.04	0.04	0.04	0.04
total=	4.00	3.99	3.99	4.00	3.98	3.98	3.99
oxygens=	[6]	[6]	[6]	[6]	[6]	[6]	[6]
temp	1316.00	1316.00	1316.00	1298.00	1298.00	1314.00	1298.00
time	48.00	102.00	102.00	5.00	5.00	5.00	5.00
WO	1.50	1.53	1.56	1.92	2.14	2.01	2.12
EN	87.91	88.50	88.34	85.44	86.98	88.48	88.72
FS	10.59	9.96	10.10	12.63	10.88	9.51	9.16

49 17M 4:248 -OPXB5,00KB,1316C,48HR,F-8.00,+GL+OPXB+OPXA+OL
50 17M 4:249PT -OPXB4,00KB,1316C,102HR,F-8.00,+GL+OPXB
51 17M 4:249PTFE -OPXB6,00KB,1316C,102HR,F-8.00,+GL+OPXB
52 17M 4:217 -OPXB3,00KB,1298C,05HR,F-8.00,+GL+SP+OL+OPXB
53 170 4:217 -OPXB4,00KB,1298C,05HR,F-8.00,+GL+SP+OPXB
54 120 4:216 -OPXB5,00KB,1314C,05HR,F-7.85,+GL+SP+OPXB+PIG
55 120 4:217 -OPXB2,00KB,1298C,05HR,F-8.00,+GL+SP+OPXB+PIG

TABLE AIII.4B

	1	2	3	4	5	6	7	8
SiO2	56.32	56.63	57.32	56.96	56.31	56.87	56.57	55.05
TiO2	0.15	0.13	nd	0.17	0.13	0.07	0.14	0.17
Al2O3	0.45	0.61	0.71	0.24	0.80	0.50	0.47	1.12
Cr2O3	0.50	0.50	0.39	0.40	0.54	0.45	0.45	0.35
FeO	9.06	9.41	8.25	6.64	7.63	7.89	8.01	9.64
MnO	0.18	0.17	0.26	0.17	0.15	0.19	0.09	0.17
NiO	nd	nd	0.21	nd	0.12	0.21	0.35	nd
MgO	29.90	30.24	30.40	31.69	30.05	30.95	30.89	29.29
CaO	2.77	1.95	2.11	2.06	2.53	1.99	2.01	1.88
Na2O	0.11	nd	nd	nd	nd	nd	nd	0.09
total=	99.43	99.65	99.65	98.33	98.25	99.13	98.97	97.76
Si	1.99	1.99	2.01	2.01	2.00	2.00	2.00	1.98
Al	0.02	0.03	0.03	-	0.03	0.02	0.02	0.05
Cr	0.01	0.01	0.01	0.01	0.02	0.01	0.01	-
Fe2	0.27	0.28	0.24	0.20	0.23	0.23	0.24	0.29
Mg	1.58	1.59	1.59	1.67	1.59	1.62	1.63	1.57
Ca	0.11	0.07	0.08	0.08	0.10	0.07	0.08	0.07
total=	3.99	3.98	3.97	3.98	3.97	3.98	3.98	3.99
oxygens=	[6]	[6]	[6]	[6]	[6]	[6]	[6]	[6]
temp	1257.00	1282.00	1274.00	1314.00	1298.00	1281.00	1274.00	1252.00
time	48.00	5.00	5.00	5.00	5.00	5.00	5.00	24.00
WO	5.39	3.80	4.15	4.01	5.03	3.88	3.93	3.75
EN	80.87	81.90	83.18	85.89	83.12	84.10	83.88	81.25
FS	13.74	14.30	12.67	10.10	11.85	12.02	12.20	15.00

1	120	5:762 -PIG7,00KB,1257C,48HR,F-11.10,+GL+PIG+OPX
2	17M	4:219 -PIG5,00KB,1282C,05HR,F-8.15,+GL+SP+OL+PIG
3	170	4:220 -PIG1,00KB,1274C,05HR,F-8.20,+GL+SP+PIG
4	120	4:216 -PIG1,00KB,1314C,05HR,F-7.85,+GL+SP+OPXB+PIG
5	120	4:217 -PIG6,00KB,1298C,05HR,F-8.00,+GL+SP+OPXB+PIG
6	120	4:219 -PIG7,00KB,1281C,05HR,F-8.15,+GL+SP+PIG
7	120	4:220 -PIG5,00KB,1274C,05HR,F-8.20,+GL+SP+PIG
8	17M	3:700 -PIG1,00KB,1252C,24HR,F-7.05,+GL+OPXB+SP+PIG+OL

	9	10	11	12	13	14	15	16
SiO2	56.24	55.22	55.81	54.50	55.48	54.90	54.71	56.26
TiO2	0.15	0.29	0.17	0.76	0.21	0.16	0.30	0.24
Al2O3	0.91	1.74	1.00	1.51	1.48	0.73	0.79	0.88
Cr2O3	0.37	0.35	0.35	0.38	0.38	0.38	0.40	0.36
FeO	10.71	10.95	11.15	12.14	8.69	9.48	10.37	10.41
MnO	0.19	0.18	0.19	0.23	0.17	0.17	0.19	0.22
MgO	28.73	26.67	27.87	25.49	28.40	29.03	27.48	27.27
CaO	3.02	3.48	3.58	4.86	2.55	3.09	4.01	4.03
Na2O	0.08	0.22	0.09	0.61	0.25	0.17	0.17	0.20
total=	100.40	99.10	100.20	100.48	97.61	98.12	98.39	99.87
Si	1.98	1.98	1.98	1.95	1.99	1.98	1.98	2.00
Ti	-	-	-	0.02	-	-	-	-
Al	0.04	0.07	0.04	0.06	0.06	0.03	0.03	0.04
Cr	0.01	-	-	0.01	0.01	0.01	0.01	0.01
Fe2	0.32	0.33	0.33	0.36	0.26	0.29	0.31	0.31
Mg	1.51	1.43	1.47	1.36	1.52	1.56	1.48	1.44
Ca	0.11	0.13	0.14	0.19	0.10	0.12	0.16	0.15
Na	-	0.02	-	0.04	0.02	0.01	0.01	0.01
total=	3.99	3.98	3.99	4.01	3.97	4.00	4.00	3.98
oxygens=	[6]	[6]	[6]	[6]	[6]	[6]	[6]	[6]
temp	1206.00	1194.00	1184.00	1155.00	1235.00	1206.00	1184.00	1155.00
time	48.00	96.00	48.00	95.00	24.00	48.00	48.00	95.00
WO	5.89	7.08	7.01	9.76	5.21	6.08	7.96	8.05
EN	77.83	75.52	75.94	71.21	80.90	79.37	75.96	75.73
FS	16.28	17.40	17.05	19.03	13.90	14.55	16.08	16.22

9	17M	3:745 -PIG6,00KB,1206C,48HR,F-7.60,+GL+OPXB+PIG+SP
10	17M	3:775 -PIG1,00KB,1194C,96HR,F-7.60,+GL+OPXB+PIG
11	17M	3:743 -PIG3,00KB,1184C,48HR,F-8.00,+GL+OPXB+PIG+SP
12	17M	3:757 -PIG1,00KB,1155C,95HR,F-8.15,+GL+PIG+SP
13	170	3:706 -PIG3,00KB,1235C,24HR,F-7.20,+GL+PIG+SP
14	170	3:745 -PIG4,00KB,1206C,48HR,F-7.60,+GL+PIG+SP
15	170	3:743 -PIG4,00KB,1184C,48HR,F-8.00,+GL+PIG+SP
16	170	3:757 -PIG1,00KB,1155C,95HR,F-8.15,+GL+PIG+CPX+SP

TABLE AIII.4B

	17	18	19	20	21	22	23	24
SiO2	56.08	56.48	56.45	55.93	54.57	53.21	54.35	52.90
TiO2	0.14	0.14	0.28	0.17	0.15	0.19	0.30	0.10
Al2O3	0.61	0.76	1.99	0.73	0.69	0.75	1.12	0.50
Cr2O3	0.44	0.45	0.38	0.49	0.43	0.42	0.39	0.06
FeO	7.84	8.26	8.64	8.85	8.81	9.80	10.77	22.49
MnO	0.17	0.18	0.16	0.17	0.17	0.19	0.21	0.59
MgO	31.16	30.81	27.50	28.65	28.61	26.12	25.03	20.12
CaO	2.24	2.56	3.56	3.34	3.98	4.66	4.75	2.60
Na2O	0.13	0.16	0.45	0.07	0.14	0.17	0.22	0.07
total=	98.80	99.79	99.42	98.41	97.54	95.50	97.14	99.44
Si	1.98	1.98	1.99	2.00	1.98	1.98	2.00	2.00
Al	0.03	0.03	0.08	0.03	0.03	0.03	0.05	0.02
Cr	0.01	0.01	0.01	0.01	0.01	0.01	0.01	-
Fe2	0.23	0.24	0.26	0.26	0.27	0.31	0.33	0.71
Mn	-	-	-	-	-	-	-	0.02
Mg	1.64	1.61	1.45	1.53	1.54	1.45	1.37	1.13
Ca	0.08	0.10	0.13	0.13	0.15	0.19	0.19	0.11
Na	-	0.01	0.03	-	-	0.01	0.02	-
total=	4.00	4.00	3.97	3.98	4.00	3.99	3.97	3.99
oxygens=	[6]	[6]	[6]	[6]	[6]	[6]	[6]	[6]
temp	1265.00	1253.00	1236.00	1224.00	1206.00	1184.00	1155.00	1148.00
time	25.00	23.50	23.60	477.00	48.00	48.00	95.00	95.00
WO	4.34	4.93	7.32	6.67	7.85	9.58	9.90	5.40
EN	83.83	82.64	78.79	79.55	78.57	74.70	72.58	58.13
FS	11.83	12.43	13.89	13.78	13.58	15.73	17.52	36.47

17 120 3:693 -PIG4,00KB,1265C,25HR,F-6.85,+GL+OPXB+PIG+SP
18 120 3:703 -PIG9,00KB,1253C,23.5HR,F-7.05,+GL+PIG+SP
19 120 3:707 -PIG10,00KB,1236C,23.6HR,F-7.15,+GL+PIG+SP
20 120 3:770 -PIG6,00KB,1224C,477HR,F-7.40,+GL+OPXB+PIG+SP
21 120 3:745 -PIG4,00KB,1206C,48HR,F-7.60,+GL+PIG+SP
22 120 3:743 -PIG2,00KB,1184C,48HR,F-8.00,+GL+PIG+CPX+SP
23 120 3:757 -PIG2,00KB,1155C,95HR,F-8.15,+GL+PIG+CPX+SP
24 B4 3:777 -PIG2,00KB,1148C,95HR,F-8.20,+GL+PIG+PLAG+CPX

	25
SiO2	56.77
TiO2	0.13
Al2O3	0.34
Cr2O3	0.48
FeO	7.92
MnO	0.18
NiO	0.24
MgO	31.51
CaO	2.06
total=	99.62
Si	1.99
Al	0.01
Cr	0.01
Fe2	0.23
Mg	1.65
Ca	0.08
total=	3.99
oxygens=	[6]
temp	1287.00
time	5.00
WO	3.95
EN	84.18
FS	11.87

25 120 4:218 -PIG6,00KB,1287C,05HR,F-8.10,+GL+SP+PIG

TABLE AIII.5

	1	2	3	4	5	6	7	8
SiO2	40.51	40.06	39.93	39.62	39.92	40.55	38.50	41.45
Al2O3	0.18	0.12	0.09	0.22	0.08	0.46	0.36	0.84
FeO	10.63	11.75	12.24	13.55	10.65	10.92	11.61	12.15
MnO	0.14	0.15	0.13	0.15	0.17	0.15	0.18	0.17
MgO	48.53	47.73	47.38	43.93	47.77	46.25	39.51	45.24
CaO	0.25	0.24	0.26	0.35	0.28	0.34	0.38	0.43
total=	100.23	100.04	100.04	97.82	98.86	98.66	90.54	100.26
Si	0.99	0.99	0.99	1.01	0.99	1.01	1.05	1.02
Al	-	-	-	-	-	0.01	0.01	0.02
Fe2	0.22	0.24	0.25	0.29	0.22	0.23	0.26	0.25
Mg	1.78	1.76	1.75	1.67	1.77	1.72	1.60	1.66
Ca	-	-	-	-	-	-	0.01	0.01
total=	3.00	3.01	3.01	2.99	3.00	2.98	2.95	2.97
oxygens=	[4]	[4]	[4]	[4]	[4]	[4]	[4]	[4]
temp	1327.00	1307.00	1290.00	1266.00	1307.00	1288.00	1265.00	1253.00
time	24.00	24.00	24.00	24.00	24.00	23.75	25.00	24.00

1 OL 17M 3:674 -OL3,00KB,1327C,24HR,F-6.40,+GL+OL+SP
2 OL 17M 3:677 -OL3,00KB,1307C,24HR,F-6.65,+GL+OL+OPXB+SP
3 OL 17M 3:684 -OL3,00KB,1290C,24HR,F-6.70,+GL+OL+OPXB+SP
4 OL 17M 3:692 -OL1,00KB,1266C,24HR,F-6.90,+GL+OPXB+OL+SP
5 OL 170 3:677 -OL3,00KB,1307C,24HR,F-6.65,+GL+OL+SP
6 OL B4 3:685 -OL4,00KB,1288C,23.75HR,F-6.70,+GL+OL
7 OL B4 3:693 -OL1,00KB,1265C,25HR,F-6.85,+GL+OL
8 OL B4 3:703 -OL2,00KB,1253C,24HR,F-7.05,+GL+OPXB+OL

	9	10	11	12	13	14	15	16
SiO2	41.24	41.32	40.35	40.80	40.03	39.97	40.74	40.59
Al2O3	0.32	0.35	0.27	0.26	0.20	0.10	0.23	0.07
FeO	13.15	10.63	11.61	10.59	10.87	12.65	8.90	10.40
MnO	0.24	0.19	0.20	0.17	0.18	0.20	0.16	0.19
MgO	44.57	48.55	47.33	47.73	47.22	46.11	49.26	48.45
CaO	0.38	0.42	0.41	0.43	0.35	0.39	0.28	0.20
total=	99.90	101.46	100.17	99.97	98.84	99.42	99.57	99.89
Si	1.02	1.00	1.00	1.00	1.00	1.00	1.00	1.00
Fe2	0.27	0.22	0.24	0.22	0.23	0.26	0.18	0.21
Mg	1.65	1.75	1.74	1.75	1.76	1.72	1.80	1.78
Ca	0.01	0.01	0.01	0.01	-	0.01	-	-
total=	2.97	2.99	3.00	2.99	3.00	3.00	3.00	3.00
oxygens=	[4]	[4]	[4]	[4]	[4]	[4]	[4]	[4]
temp	1235.00	1252.00	1236.00	1270.00	1252.00	1206.00	1345.00	1307.00
time	24.00	23.00	23.60	23.75	23.00	48.00	24.00	24.00

9 OL B4 3:708 -OL1,00KB,1235C,24HR,F-7.15,+GL+OPXB+OL+SP
10 OL K6 3:695 -OL2,00KB,1252C,23HR,F-7.05,+GL+OL+SP
11 OL K6 3:707 -OL4,00KB,1236C,23.6HR,F-7.15,+GL+OL+SP
12 OL K1 3:694 -OL2,00KB,1270C,23.75HR,F-6.80,+GL+OL+SP
13 OL K1 3:695 -OL2,00KB,1252C,23HR,F-7.05,+GL+OL+SP
14 OL K1 3:745 -OL1,00KB,1206C,48HR,F-7.60,+GL+OPXB+OL+SP
15 OL 295 3:671 -OL4,00KB,1345C,24HR,F-6.30,+GL+OL+SP
16 OL 295 3:677 -OL2,00KB,1307C,24HR,F-6.65,+GL+OL+SP

TABLE AIII.5

	17	18	19	20	21	22	23	24
SiO2	38.91	39.60	39.21	39.15	40.82	40.53	40.71	39.41
Al2O3	0.08	0.08	0.22	0.23	0.33	0.10	0.07	0.08
FeO	12.82	12.95	13.96	14.99	9.80	9.40	10.32	14.63
MnO	0.20	0.21	0.23	0.24	0.14	0.15	0.16	0.23
MgO	45.63	45.48	44.71	43.50	47.84	48.00	47.76	43.93
CaO	0.26	0.27	0.33	0.39	0.31	0.24	0.27	0.33
total=	97.90	98.58	98.66	98.49	99.24	98.42	99.29	98.61
Si	0.99	1.00	0.99	1.00	1.01	1.01	1.01	1.00
Fe2	0.27	0.27	0.30	0.32	0.20	0.20	0.21	0.31
Mg	1.73	1.71	1.69	1.66	1.76	1.78	1.76	1.67
Ca	-	-	-	0.01	-	-	-	-
total=	3.01	3.00	3.00	3.00	2.99	2.99	2.99	3.00
oxygens=	[4]	[4]	[4]	[4]	[4]	[4]	[4]	[4]
temp	1235.00	1224.00	1206.00	1181.00	1288.00	1292.00	1273.00	1194.00
time	24.00	477.00	48.00	48.00	23.75	48.00	48.00	96.00

17 OL 295 3:706 -OL1,00KB,1235C,24HR,F-7.20,+GL+OL+OPXB+SP
18 OL 295 3:770 -OL2,00KB,1224C,477HR,F-7.40,+GL+OPXB+OL+SP
19 OL 295 3:746 -OL3,00KB,1206C,48HR,F-7.50,+GL+OL+OPXB+SP
20 OL 295 3:744 -OL2,00KB,1181C,48HR,F-7.90,+GL+OL+OPXB+SP
21 OL C5 3:685 -OL6,00KB,1288C,23.75HR,F-6.70,+GL+OL
22 OL C5MET 3:752 -OL3,00KB,1292C,48HR,F-6.70,+GL+OL+SP
23 OL C5MET 3:751 -OL1,00KB,1273C,48HR,F-6.70,+GL+OL+OPXB
24 295 3:775 -OL1,00KB,1194C,96HR,F-7.60,+GL+OL+OPXB

	25	26	27	28	29	30	31	32
SiO2	40.15	40.34	39.86	39.47	40.29	41.62	41.73	39.91
Al2O3	0.05	0.18	0.16	0.09	0.07	0.59	0.84	0.06
FeO	12.60	11.44	12.52	13.93	11.27	11.97	12.73	10.94
MnO	0.17	0.16	0.19	0.21	0.18	0.16	nd	0.14
NiO	nd	nd	nd	nd	0.36	0.49	0.64	0.16
MgO	45.77	46.25	45.24	44.39	45.98	43.51	42.59	45.87
CaO	0.22	0.28	0.31	0.28	0.37	0.75	0.91	0.25
total=	98.94	98.65	98.28	98.36	98.51	99.09	99.44	97.34
Si	1.01	1.01	1.01	1.00	1.01	1.04	1.04	1.01
Al	-	-	-	-	-	0.02	0.02	-
Fe2	0.26	0.24	0.26	0.30	0.24	0.25	0.27	0.23
Ni	-	-	-	-	-	-	0.01	-
Mg	1.71	1.72	1.70	1.68	1.72	1.62	1.58	1.73
Ca	-	-	-	-	-	0.02	0.02	-
total=	2.99	2.99	2.99	3.00	2.99	2.95	2.95	2.99
oxygens=	[4]	[4]	[4]	[4]	[4]	[4]	[4]	[4]
temp	1325.00	1325.00	1297.00	1257.00	1331.00	1314.00	1298.00	1315.00
time	23.00	23.00	22.00	48.00	5.00	5.00	5.00	72.00

25 OL 17M 5:760 -OL2,00KB,1325C,23HR,F-10.40,+GL+OL
26 OL 295 5:760 -OL1,00KB,1325C,23HR,F-10.40,+GL+OL
27 OL 295 5:761 -OL1,00KB,1297C,22HR,F-10.70,+GL+OL
28 OL 295 5:762 -OL4,00KB,1257C,48HR,F-11.10,+GL+OPXB+OL
29 17M 4:215 -OL2,00KB,1331C,05HR,F-7.70,+GL+SP+OL
30 17M 4:216 -OL3,00KB,1314C,05HR,F-7.85,+GL+SP+OL
31 17M 4:217 -OL2,00KB,1298C,05HR,F-8.00,+GL+SP+OL+OPXB
32 17M 4:239:2 -OL2,00KB,1315C,72HR,F-8.00,+GL+OPXB+OL

	33	34	35
SiO2	41.52	41.17	40.21
Al2O3	0.15	0.09	0.18
FeO	11.52	10.92	12.14
MnO	0.14	0.14	0.13
NiO	0.20	0.12	0.39
MgO	48.14	48.62	46.63
CaO	0.31	0.29	0.34
total=	101.98	101.35	100.03
Si	1.00	1.00	1.00
Fe2	0.23	0.22	0.25
Mg	1.74	1.76	1.72
total=	2.99	3.00	3.00
oxygens=	[4]	[4]	[4]
temp	1315.00	1316.00	1314.00
time	24.00	48.00	5.00

33 17M 4:245 -OL7,00KB,1315C,24HR,F-8.00,+GL+OPXB+OL
34 17M 4:248 -OL10,00KB,1316C,48HR,F-8.00,+GL+OPXB+OL+OPXA
35 17M 4:216 -OL10,00KB,1314C,05HR,F-7.85,+GL+OL+SP

TABLE AIII.6

	1	2	3	4	5	6	7	8
SiO2	55.40	53.70	54.29	53.60	52.66	53.81	53.25	52.73
TiO2	0.40	0.43	0.24	0.66	0.14	0.18	0.24	0.07
Al2O3	2.22	1.13	1.25	1.80	0.86	1.60	2.34	2.32
Cr2O3	0.42	0.64	0.29	0.43	0.08	0.32	0.41	0.87
FeO	7.93	6.41	6.92	6.48	11.79	8.77	8.57	6.80
MnO	0.18	0.14	0.15	0.16	0.29	0.26	0.24	0.20
MgO	19.97	19.91	21.81	19.22	12.81	18.34	18.21	19.34
CaO	12.70	15.69	12.43	15.75	21.16	16.13	16.57	16.33
Na2O	0.50	0.31	0.35	0.33	0.20	0.20	0.21	0.16
total=	99.72	98.36	97.73	98.43	99.99	99.61	100.04	98.82
Si	2.00	1.98	1.99	1.97	1.98	1.98	1.95	1.94
Ti	0.01	0.01	-	0.02	-	-	-	-
Al	0.09	0.05	0.05	0.08	0.04	0.07	0.10	0.10
Cr	0.01	0.02	-	0.01	-	-	0.01	0.03
Fe2	0.24	0.20	0.21	0.20	0.37	0.27	0.26	0.21
Mg	1.07	1.09	1.19	1.05	0.72	1.00	0.99	1.06
Ca	0.49	0.62	0.49	0.62	0.85	0.63	0.65	0.64
Na	0.03	0.02	0.02	0.02	0.01	0.01	0.01	0.01
total=	3.96	3.99	3.98	3.98	4.00	3.99	4.00	4.00
oxygens=	[6]	[6]	[6]	[6]	[6]	[6]	[6]	[6]
temp	1155.00	1184.00	1184.00	1184.00	1148.00	1156.00	1156.00	1194.00
time	95.00	48.00	48.00	48.00	95.00	48.00	48.00	96.00
WO	27.21	32.42	25.80	33.13	43.91	33.26	34.10	33.64
EN	59.53	57.24	62.98	56.24	36.99	52.62	52.13	55.43
FS	13.26	10.34	11.21	10.64	19.10	14.12	13.77	10.93

1 170 3:757 -CPX1,00KB,1155C,95HR,F-8.15,+GL+PIG+CPX+SP
2 120 3:743 -CPX1,00KB,1184C,48HR,F-8.00,+GL+PIG+CPX+SP
3 120 3:743 -CPX2,00KB,1184C,48HR,F-8.00,+GL+PIG+CPX+SP
4 120 3:743 -CPX3,00KB,1184C,48HR,F-8.00,+GL+PIG+CPX+SP
5 B4 3:777 -CPX1,00KB,1148C,95HR,F-8.20,+GL+PIG+PLAG+CPX
6 B5 3:756 -CPX1,00KB,1156C,48HR,F-8.15,+GL+OPXB+CPX+PLAG
7 B5 3:756 -CPX2,00KB,1156C,48HR,F-8.15,+GL+OPXB+CPX+PLAG
8 K1 3:775 -CPX1,00KB,1194C,96HR,F-7.60,+GL+PIG+CPX

	9	10	11	12	13
SiO2	52.37	53.22	52.26	56.09	54.40
TiO2	0.06	0.03	0.09	0.41	0.48
Al2O3	3.17	1.76	2.99	3.90	5.85
Cr2O3	0.21	0.12	0.20	0.51	0.26
FeO	7.68	8.64	7.59	7.61	7.57
MnO	0.20	0.24	0.22	0.17	0.15
MgO	20.26	20.24	17.62	18.10	16.07
CaO	14.46	14.82	17.91	13.18	11.74
Na2O	0.10	0.12	0.16	0.78	0.43
total=	98.51	99.19	99.04	100.75	96.95
Si	1.93	1.96	1.93	2.00	2.00
Ti	-	-	-	0.01	0.01
Al	0.14	0.08	0.13	0.16	0.25
Cr	-	-	-	0.01	-
Fe2	0.24	0.27	0.23	0.23	0.23
Mg	1.11	1.11	0.97	0.96	0.88
Ca	0.57	0.58	0.71	0.50	0.46
Na	-	-	0.01	0.05	0.03
total=	4.00	4.01	4.00	3.93	3.88
oxygens=	[6]	[6]	[6]	[6]	[6]
temp	1172.00	1172.00	1156.00	1155.00	1155.00
time	93.00	93.00	121.00	95.00	95.00
WO	29.73	29.81	37.04	29.75	29.35
EN	57.95	56.63	50.70	56.84	55.88
FS	12.32	13.56	12.25	13.41	14.77

9 K1 3:776 -CPX1,00KB,1172C,93HR,F-7.90,+GL+PIG+CPX+PLAG
10 C2M 3:776 -CPX1,00KB,1172C,93HR,F-7.90,+GL+OPXB+CPX+PLAG
11 C2MET 3:758 -CPX1,00KB,1156C,121HR,F-8.15,+GL+OPXB+CPX+PLAG
12 120 3:757 -CPX1,00KB,1155C,95HR,F-8.15,+GL+PIG+CPX+SP
13 120 3:757 -CPX2,00KB,1155C,95HR,F-8.15,+GL+PIG+CPX+SP

TABLE AIII.7

	1	2	3	4	5	6	7	8
SiO2	55.09	53.34	53.48	54.80	54.61	57.45	53.39	54.89
TiO2	0.02	0.01	nd	nd	0.01	0.36	0.39	0.03
Al2O3	27.11	28.54	27.73	28.96	27.84	25.52	26.90	28.30
FeO	0.39	0.53	0.41	0.32	1.30	1.58	1.69	0.55
MgO	0.06	0.09	0.09	0.05	0.05	0.88	0.97	0.16
CaO	10.59	11.96	11.45	11.35	10.54	9.51	11.25	11.24
Na2O	5.16	4.52	4.65	4.73	5.00	5.28	4.06	4.52
K2O	0.28	0.20	0.28	0.18	0.25	0.28	0.26	0.23
total=	98.70	99.19	98.09	100.39	99.60	100.86	98.91	99.92
Si	10.07	9.75	9.87	9.85	9.93	10.29	9.82	9.92
Ti	-	-	-	-	-	0.05	0.05	-
Al	5.84	6.15	6.03	6.14	5.97	5.39	5.83	6.03
Fe2	0.06	0.08	0.06	0.05	0.20	0.24	0.26	0.08
Mg	0.02	0.02	0.02	0.01	0.01	0.23	0.27	0.04
Ca	2.07	2.34	2.26	2.19	2.05	1.82	2.22	2.18
Na	1.83	1.60	1.66	1.65	1.76	1.83	1.45	1.58
K	0.07	0.05	0.07	0.04	0.06	0.06	0.06	0.05
total=	19.96	20.00	19.98	19.93	19.99	19.92	19.96	19.88
oxygens=	[32]	[32]	[32]	[32]	[32]	[32]	[32]	[32]
temp	1148.00	1148.00	1148.00	1156.00	1156.00	1156.00	1156.00	1156.00
time	95.00	95.00	95.00	48.00	48.00	48.00	48.00	48.00

1 B4 3:777 -PLAG1,00KB,1148C,95HR,F-8.20,+GL+PIG+PLAG+CPX
2 B4 3:777 -PLAG2,00KB,1148C,95HR,F-8.20,+GL+PIG+PLAG+CPX
3 B4 3:777 -PLAG3,00KB,1148C,95HR,F-8.20,+GL+PIG+PLAG+CPX
4 B5 3:756 -PLAG1,00KB,1156C,48HR,F-8.15,+GL+OPXB+CPX+PLAG
5 B5 3:756 -PLAG2,00KB,1156C,48HR,F-8.15,+GL+OPXB+CPX+PLAG
6 T2 3:756 -PLAG1,00KB,1156C,48HR,F-8.15,+GL+OPXB+PLAG
7 T2 3:756 -PLAG3,00KB,1156C,48HR,F-8.15,+GL+OPXB+PLAG
8 T2 3:756 -PLAG4,00KB,1156C,48HR,F-8.15,+GL+OPXB+PLAG

	9	10	11	12	13	14	15	16
SiO2	54.19	50.34	50.11	51.91	52.88	53.10	56.16	57.90
TiO2	0.39	0.06	0.05	0.17	0.22	0.09	0.14	0.20
Al2O3	26.39	27.27	29.60	22.62	20.51	29.55	20.23	17.32
FeO	1.93	2.30	1.46	5.41	6.91	4.06	5.81	6.58
MgO	0.62	1.63	0.84	3.53	3.53	1.45	3.38	3.75
CaO	11.15	14.01	14.83	12.71	12.06	14.08	12.05	10.93
Na2O	4.67	2.68	2.83	2.40	2.49	2.93	1.76	1.80
K2O	0.26	0.07	0.03	0.15	0.24	0.17	0.48	0.66
total=	99.60	98.36	99.75	98.90	98.84	105.43	100.01	99.14
Si	9.92	9.42	9.23	9.78	10.02	9.33	10.38	10.79
Ti	0.05	-	-	0.02	0.03	0.01	0.02	0.03
Al	5.69	6.01	6.43	5.02	4.58	6.12	4.41	3.80
Fe2	0.30	0.36	0.22	0.85	1.09	0.60	0.90	1.03
Mg	0.17	0.45	0.23	0.99	1.00	0.38	0.93	1.04
Ca	2.19	2.81	2.93	2.56	2.45	2.65	2.39	2.18
Na	1.66	0.97	1.01	0.88	0.91	1.00	0.63	0.65
K	0.06	0.02	-	0.04	0.06	0.04	0.11	0.16
total=	20.04	20.06	20.06	20.14	20.14	20.12	19.77	19.68
oxygens=	[32]	[32]	[32]	[32]	[32]	[32]	[32]	[32]
temp	1148.00	1184.00	1184.00	1172.00	1172.00	1181.00	1172.00	1156.00
time	95.00	48.00	48.00	93.00	93.00	48.00	93.00	121.00

9 T2 3:777 -PLAG1,00KB,1148C,95HR,F-8.20,+GL+OPXB+PLAG
10 K6 3:743 -PLAG1,00KB,1184C,48HR,F-8.00,+GL+OL+OPXB+CPX+PLAG
11 K6 3:743 -PLAG2,00KB,1184C,48HR,F-8.00,+GL+OL+OPXB+CPX+PLAG
12 K1 3:776 -PLAG1,00KB,1172C,93HR,F-7.90,+GL+PIG+CPX+PLAG
13 K1 3:776 -PLAG2,00KB,1172C,93HR,F-7.90,+GL+PIG+CPX+PLAG
14 295 3:744 -PLAG1,00KB,1181C,48HR,F-7.90,+GL+OL+OPXB+PLAG+SP
15 C2M 3:776 -PLAG1,00KB,1172C,93HR,F-7.90,+GL+OPXB+CPX+PLAG
16 C2MET 3:758 -PL1,00KB,1156C,121HR,F-8.15,+GL+OPXB+CPX+PLAG

TABLE AIII.7

	17	18	19	20
SiO2	57.56	57.77	55.23	52.75
TiO2	0.11	0.14	0.12	0.07
Al2O3	21.00	20.88	19.88	26.13
FeO	4.27	4.42	5.20	2.50
MgO	3.39	2.64	4.05	2.18
CaO	10.40	10.07	11.47	13.32
Na2O	2.82	2.94	2.24	2.38
K2O	1.22	1.40	0.37	0.21
total=	100.77	100.26	98.56	99.54
Si	10.48	10.57	10.34	9.71
Ti	0.02	0.02	0.02	-
Al	4.51	4.50	4.39	5.67
Fe2	0.65	0.68	0.81	0.38
Mg	0.92	0.72	1.13	0.60
Ca	2.03	1.97	2.30	2.63
Na	1.00	1.04	0.81	0.85
K	0.28	0.33	0.09	0.05
total=	19.89	19.84	19.90	19.90
oxygens=	[32]	[32]	[32]	[32]
temp	1156.00	1156.00	1184.00	1184.00
time	121.00	121.00	48.00	48.00

17 C5MET 3:758 -PLAG1,00KB,1156C,121HR,F-8.15,+GL+OPXB+PLAG
18 C5MET 3:758 -PLAG2,00KB,1156C,121HR,F-8.15,+GL+OPXB+PLAG
19 C11MET 3:742 -PLAG1,00KB,1184C,48HR,F-7.90,+GL+OPXB+PLAG+SP
20 C11MET 3:742 -PLAG2,00KB,1184C,48HR,F-7.90,+GL+OPXB+PLAG+SP

TABLE AIII.8

	1	2	3	4	5	6	7
SiO_2	0.11	0.10	23.05	2.73	12.64	1.03	1.80
TiO_2	0.79	0.75	1.10	0.12	0.41	0.35	0.35
Al_2O_3	8.10	8.02	8.99	13.90	9.69	11.48	12.10
Cr_2O_3	59.31	59.56	33.48	46.87	41.49	53.41	50.66
FeO	16.72	16.65	16.46	20.07	18.72	19.29	19.00
MnO	0.68	0.68	0.49	0.64	0.61	0.25	0.24
NiO	nd	nd	nd	nd	nd	0.20	0.20
MgO	12.53	12.53	8.77	12.04	16.14	13.09	15.36
total=	98.24	98.29	92.34	96.37	99.70	99.10	99.71
Si	0.03	0.03	5.65	0.72	3.05	0.27	0.46
Ti	0.16	0.15	0.20	0.02	0.07	0.07	0.07
Al	2.56	2.53	2.60	4.33	2.76	3.54	3.66
Cr	12.58	12.63	6.49	9.79	7.92	11.05	10.27
Fe_2	3.75	3.73	3.37	4.44	3.78	4.22	4.08
Mn	0.15	0.15	0.10	0.14	0.12	0.06	0.05
Ni	-	-	-	-	-	0.04	0.04
Mg	5.01	5.01	3.20	4.74	5.81	5.11	5.87
total=	24.24	24.24	21.61	24.19	23.53	24.36	24.50
oxygens=	[32]	[32]	[32]	[32]	[32]	[32]	[32]
temp	1310.00	1310.00	1224.00	1206.00	1224.00	1290.00	1290.00
time	72.00	72.00	477.00	48.00	477.00	24.00	24.00

1 17M 4:237 -SP1,00KB,1310C,72HR,F-8.00,+GL+OL+SP
2 17M 4:237 -SP3,00KB,1310C,72HR,F-8.00,+GL+OL+SP
3 120 3:770 -SP1,00KB,1224C,477HR,F-7.40,+GL+OPXB+PIG+SP
4 K1 3:745 -SP2,00KB,1206C,48HR,F-7.60,+GL+OPXB+OL+SP
5 295 3:770 -SP1,00KB,1224C,477HR,F-7.40,+GL+OPXB+OL+SP
6 C2 3:684 -SP1,00KB,1290C,24HR,F-6.70,+GL+SP+OPX
7 C2 3:684 -SP3,00KB,1290C,24HR,F-6.70,+GL+SP+OPX

APPENDIX IV

TABLE AIV.1A

	1	2	3	4	5	6	7	8
SiO2	53.62	51.71	51.09	49.90	49.39	50.96	47.23	56.80
TiO2	0.38	nd	nd	nd	nd	nd	3.76	1.53
Al2O3	7.70	16.00	15.25	13.66	15.08	15.53	10.40	14.70
Fe2O3	0.14	0.10	0.10	0.13	0.12	0.12	0.47	1.47
Cr2O3	0.26	0.68	0.57	0.36	0.42	0.39	0.28	0.09
FeO	9.84	12.36	12.84	14.34	14.39	14.51	17.29	9.08
MnO	0.12	nd	nd	nd	nd	nd	0.25	0.13
MgO	14.29	10.57	10.68	9.39	8.97	9.46	7.53	4.66
CaO	12.89	9.47	8.94	9.31	9.68	9.00	11.46	7.36
Na2O	0.04	nd	nd	nd	nd	nd	0.72	2.26
K2O	nd	nd	nd	nd	nd	nd	0.02	1.27
total=	99.28	100.89	99.47	97.08	98.05	99.97	99.41	99.35
qtz	5.79	6.08	5.91	5.94	4.78	5.97	2.38	12.30
en	24.27	25.60	26.01	21.65	21.03	23.12	13.13	9.61
fs	11.97	22.00	22.97	24.28	24.77	26.05	17.94	10.91
cen	11.31	0.73	0.59	1.74	1.31	0.44	5.62	1.99
cfs	5.58	0.62	0.52	1.95	1.54	0.50	7.68	2.26
cwo	18.00	1.39	1.14	3.72	2.87	0.95	13.26	4.30
or	-	-	-	-	-	-	0.12	7.50
an	20.83	43.66	41.61	37.27	41.15	42.37	25.09	26.21
ab	0.34	-	-	-	-	-	6.09	19.12
mag	0.21	0.14	0.14	0.18	0.18	0.17	0.68	2.13
ilm	0.72	-	-	-	-	-	7.14	2.91
chr	0.38	1.00	0.84	0.53	0.62	0.57	0.41	0.13
temp	1300.00	1230.00	1228.00	1212.00	1209.00	1203.00	1179.00	1137.00
time	44.00	22.00	64.50	137.00	137.00	64.50	5.00	542.50

1 HUEBNER ETAL 1976-GL,0KB,1300C,44HR,F-11.75,GL+0PX
2 HUEBNER ETAL 1976-GL,0KB,1230C,22HR,F-13.2,GL+0PX+SP
3 HUEBNER ETAL 1976-GL,0KB,1228C,64.5HR,F-13.2,GL+0L+0PX+SP
4 HUEBNER ETAL 1976-GL,0KB,1212C,137HR,F-13.3,GL+0L+PL+0PX+SP
5 HUEBNER ETAL 1976-GL,0KB,1209C,137HR,F-13.3,GL+0L+PL+0PX+SP
6 HUEBNER ETAL 1976-GL,0KB,1203C,64.5HR,F-13.4,GL+0L+PL+0PX+SP
7 BIGGAR ETAL 1971 12040-GL,0KB,1179C,5HR,F-12.1,GL+0L+0PX+SP
8 GROVE ETAL 1982 TABLE 1 79-38B -GL,0KB,1137C,542.5HR,F-9.34,GL+0L+PL+0PX

	9	10	11	12	13	14	15	16
SiO2	57.80	60.30	60.50	60.80	63.20	52.30	52.00	50.80
TiO2	1.80	1.58	1.75	1.95	1.84	0.39	0.42	0.48
Al2O3	13.90	14.60	13.60	13.70	13.90	14.80	16.10	17.70
Fe2O3	1.61	1.41	1.57	1.73	1.53	0.06	0.07	0.09
Cr2O3	0.09	0.01	0.02	0.01	0.03	0.22	0.19	0.13
FeO	9.55	7.92	9.18	9.74	8.50	9.65	9.63	9.82
MnO	0.15	0.20	0.13	0.17	0.16	nd	nd	nd
MgO	3.90	3.17	2.79	2.55	2.37	15.10	13.40	11.60
CaO	6.93	5.26	5.15	5.01	4.98	7.50	8.30	9.30
Na2O	1.99	2.33	1.82	1.67	1.47	nd	nd	nd
K2O	1.44	1.47	1.67	1.67	1.82	nd	nd	nd
total=	99.16	98.25	98.19	99.00	99.80	100.02	100.12	99.92
qtz	15.98	20.28	22.78	23.99	28.20	5.97	6.53	5.76
en	8.02	7.71	6.72	6.35	5.90	37.61	33.37	28.89
fs	11.17	10.87	12.49	13.55	11.60	17.03	16.94	17.17
cen	1.69	0.18	0.23	-	-	-	-	-
cfs	2.35	0.26	0.43	-	-	-	-	-
cwo	4.02	0.44	0.64	-	-	-	-	-
or	8.51	8.69	9.87	9.87	10.75	-	-	-
an	24.74	25.04	24.01	24.85	24.71	37.21	41.18	46.14
ab	16.84	19.72	15.40	14.13	12.44	-	-	-
mag	2.33	2.05	2.28	2.52	2.23	0.08	0.11	0.12
ilm	3.42	3.00	3.32	3.70	3.49	0.74	0.80	0.91
crn	-	-	-	0.04	0.46	1.16	1.01	0.79
chr	0.13	0.01	0.03	0.01	0.04	0.32	0.28	0.19
temp	1121.00	1106.00	1093.00	1085.00	1076.00	1320.00	1280.00	1260.00
time	793.50	118.50	291.00	237.50	330.00	36.00	36.00	36.00

9 GROVE ETAL 1982 TABLE 1 79-38B -GL,0KB,1121C,793.5HR,F-9.54,GL+0L+PL+0PX
10 GROVE ETAL 1982 TABLE 1 79-9C -GL,0KB,1106C,118.5HR,F-9.66,GL+PL+0PX
11 GROVE ETAL 1982 TABLE 1 79-9C -GL,0KB,1093C,291HR,F-9.94,GL+0L+PL+0PX
12 GROVE ETAL 1982 TABLE 1 79-9C -GL,0KB,1085C,237.5HR,F-9.95,GL+0L+PL+0PX
13 GROVE ETAL TABLE 1 79-9C -GL,0KB,1076C,330HR,F-10.11,GL+PL+0PX+SP
14 WEILL &MCKAY FMG -GL,00KB,1320C,36HR,F-12.50,+GL+0PX+0L
15 WEILL & MCKAY FMG -GL,00KB,1280C,36HR,F-12.50,+GL+0PX+0L
16 WEILL & MCKAY FMG -GL,00KB,1260C,36HR,F-12.50,+GL+0PX+0L

TABLE AIV.1A

	17	18	19	20	21	22	23	24
SiO2	50.20	50.40	54.04	50.74	52.30	52.16	52.36	58.22
TiO2	0.50	0.49	0.38	0.37	0.42	0.40	0.35	1.30
Al2O3	17.90	18.20	7.74	9.28	8.39	11.22	8.09	10.43
Fe2O3	0.10	0.12	0.15	0.22	0.18	0.19	0.19	0.12
Cr2O3	0.10	0.09	0.29	nd	nd	0.30	nd	nd
FeO	10.21	9.90	9.97	15.79	12.44	10.39	12.34	5.74
MnO	nd	nd	0.13	nd	nd	0.16	nd	nd
MgO	11.30	10.40	14.49	11.12	12.68	10.59	12.20	11.83
CaO	9.80	10.40	12.73	9.76	10.81	12.47	10.67	12.37
Na2O	nd	nd	0.05	nd	nd	nd	nd	nd
total=	100.11	99.99	99.96	97.28	97.23	97.88	96.20	100.01
qtz	4.23	5.17	5.89	5.39	6.85	7.95	7.99	17.40
en	28.14	25.44	25.00	23.00	24.33	19.03	23.20	19.68
fs	17.84	16.96	12.33	23.43	16.96	13.39	16.74	5.54
cen	-	0.46	11.09	4.70	7.25	7.34	7.19	9.79
cfs	-	0.31	5.47	4.78	5.05	5.17	5.19	2.76
cwo	-	0.81	17.64	9.64	12.83	13.05	12.89	13.75
an	48.62	49.66	20.89	25.32	22.89	30.61	22.07	28.46
ab	-	-	0.42	-	-	-	-	-
mag	0.15	0.17	0.21	0.32	0.27	0.27	0.27	0.17
ilm	0.95	0.93	0.72	0.70	0.80	0.76	0.66	2.47
crn	0.08	-	-	-	-	-	-	-
chr	0.15	0.13	0.43	-	-	0.44	-	-
temp	1240.00	1220.00	1300.00	1273.00	1273.00	1243.00	1273.00	1233.00
time	36.00	36.00	44.00	48.00	48.00	96.00	48.00	24.00

17 WEILL & MCKAY FMG -GL,00KB,1240C,36HR,F-12.50,+GL+OPX+OL
18 WEILL & MCKAY FMG -GL,00KB,1220C,36HR,F-12.50,+GL+OPX+OL
19 HUEBENER & TURNOCK 1980 61 SC B -GL,00KB,1300C,44HR,F-11.75,+GL+OPX+OL
20 HUEBENER & TURNOCK 1980 61 SC B -GL,00KB,1273C,48HR,F-11.89,+GL+OPX+OL
21 HUEBENER & TURNOCK 1980 61 SC B -GL,00KB,1273C,48HR,F-11.89,+GL+OPX
22 HUEBENER & TURNOCK 1980 61 SC B -GL,00KB,1243C,96HR,F-11.94,+GL+OPX+OL
23 HUEBENER & TURNOCK 1980 J-8 -GL,00KB,1273C,48HR,F-11.89,+GL+OPX
24 NEILSEN & DRAKE TABLE 1 4 -GL,00KB,1233C,24HR,F-12.00,+GL+OPX

	25	26	27	28	29	30	31	32
SiO2	57.82	49.76	49.20	50.47	49.06	50.59	50.21	49.67
TiO2	2.45	0.77	0.08	0.87	0.75	1.57	1.72	1.24
Al2O3	10.58	10.91	10.31	10.54	12.59	8.30	8.60	8.43
Fe2O3	0.14	0.35	0.37	0.41	0.35	2.10	2.31	2.17
Cr2O3	nd	0.21	0.26	nd	nd	nd	nd	nd
FeO	6.82	24.94	26.62	24.22	23.88	17.08	16.74	19.04
MnO	nd	nd	nd	nd	nd	0.26	0.26	0.19
MgO	11.00	7.68	7.72	5.87	6.79	8.03	7.03	7.75
CaO	11.22	5.36	5.43	7.61	6.62	8.72	9.21	8.09
Na2O	nd	0.05	0.05	nd	nd	1.52	1.51	1.23
K2O	nd	nd	nd	nd	nd	0.53	0.54	0.46
P2O5	nd	nd	nd	nd	nd	0.38	nd	0.30
total=	100.01	100.03	100.04	100.00	100.03	99.08	98.13	98.57
qtz	19.37	6.38	3.68	7.91	5.47	3.49	3.70	3.26
en	19.54	19.13	19.23	13.60	16.91	15.45	12.37	15.84
fs	5.97	44.24	48.45	39.75	42.34	21.25	18.71	25.84
cen	7.85	-	-	1.01	-	4.55	5.13	3.46
cfs	2.40	-	-	2.95	-	6.26	7.76	5.64
cwo	11.19	-	-	3.76	-	10.77	12.78	8.97
or	-	-	-	-	-	3.13	3.19	2.72
an	28.86	26.58	26.95	28.75	32.84	14.26	15.09	16.12
ab	-	0.44	0.44	-	-	12.86	12.78	10.41
mag	0.20	0.51	0.53	0.60	0.51	3.05	3.35	3.14
ilm	4.65	1.46	0.15	1.66	1.41	2.98	3.27	2.36
crn	-	1.09	0.34	-	0.55	-	-	-
ap	-	-	-	-	-	1.14	-	0.90
chr	-	0.30	0.38	-	-	-	-	-
temp	1233.00	1225.00	1225.00	1222.00	1222.00	1210.00	1191.00	1210.00
time	24.00	24.00	24.00	24.00	24.00	19.50	19.90	19.50

25 NILSEN &DRAKE TABLE 1 5 -GL,00KB,1233C,24HR,F-12.00,+GL+OPX
26 NEILSEN & DRAKE TABLE 1 6 -GL,00KB,1225C,24HR,F-12.00,+GL+OPX
27 NEILSEN & DRAKE TABLE 1 7 -GL,00KB,1225C,24HR,F-12.00,+GL+OPX
28 NEILSEN & DRAKE TABLE 1 8 -GL,00KB,1222C,24HR,F-12.00,+GL+OPX
29 NEILSEN & DRAKE TABLE 1 9 -GL,00KB,1222C,24HR,F-12.00,+GL+OPX
30 MITCHELL 1984 ROCK+GEL -GL,00KB,1210C,19.5HR,F-8.70,+GL+OPX
31 MITCHELL 1984 ROCK+GEL -GL,00KB,1191C,19.9HR,F-8.80,+GL+OL+OPX
32 MITCHELL 1984 ROCK+GEL -GL,00KB,1210C,19.5HR,F-8.70,+GL+OL+OPX

TABLE AIV.1A

	33	34
SiO2	49.30	49.11
TiO2	1.31	1.30
Al2O3	9.00	9.97
Fe2O3	2.36	2.57
FeO	18.82	17.68
MnO	0.19	0.15
MgO	6.80	5.62
CaO	8.43	9.00
Na2O	1.25	1.44
K2O	0.48	0.54
P2O5	0.45	0.43
total=	98.39	97.81
qtz	4.03	4.33
en	13.83	10.90
fs	25.16	22.17
cen	3.10	3.10
cfs	5.64	6.30
cwo	8.56	9.13
or	2.84	3.19
an	17.53	19.15
ab	10.58	12.18
mag	3.42	3.72
ilm	2.49	2.47
ap	1.35	1.29
temp	1191.00	1161.00
time	19.90	19.90

33 MITCHELL 1984 ROCK+GEL -GL,00KB,1191C,19.9HR,F-8.80,+GL+OL+OPX
34 MITCHELL 1984 ROCK+GEL -GL,00KB,1161C,19.9HR,F-9.00,+GL+OL+OPX

TABLE AIV.1B

	1	2	3	4	5	6	7	8
SiO2	46.00	45.60	45.60	44.90	57.28	55.94	48.49	48.93
TiO2	3.79	3.76	4.38	4.74	0.13	2.24	0.97	1.96
Al2O3	11.10	11.40	11.10	10.80	6.04	8.34	3.20	6.61
Fe2O3	0.44	0.46	0.48	0.50	0.57	0.21	0.59	0.64
Cr2O3	0.45	0.38	0.36	0.36	0.16	0.32	0.43	0.25
FeO	18.40	18.89	19.16	19.35	6.35	8.15	25.58	23.72
MnO	0.32	0.31	0.32	0.36	0.21	0.39	0.41	0.30
MgO	7.00	6.41	6.26	6.03	13.87	9.45	8.58	5.23
CaO	11.20	11.20	11.60	11.50	15.68	12.56	9.68	12.56
Na2O	0.04	0.14	0.14	0.23	0.08	0.02	nd	0.01
total=	98.74	98.54	99.41	98.77	100.37	97.62	97.93	100.20
qtz	4.19	3.59	3.80	3.37	10.68	18.00	2.65	5.36
en	13.28	12.14	11.35	10.75	16.74	13.19	15.97	8.26
fs	21.15	21.80	20.50	20.01	5.51	6.63	34.12	25.59
cen	4.15	3.82	4.24	4.27	17.80	10.35	5.40	4.76
cfs	6.61	6.87	7.65	7.96	5.85	5.20	11.54	14.76
cwo	10.63	10.47	11.64	11.95	25.75	16.55	16.41	18.50
an	30.11	30.48	29.66	28.44	16.12	22.67	8.73	17.99
ab	0.34	1.18	1.18	1.95	0.68	0.17	-	0.08
mag	0.64	0.66	0.70	0.72	0.82	0.30	0.85	0.93
ilm	7.20	7.14	8.32	9.00	0.25	4.25	1.84	3.72
chr	0.66	0.56	0.53	0.53	0.24	0.47	0.63	0.37
temp	1176.00	1164.00	1156.00	1150.00	1332.00	1243.00	1252.00	1151.00
time	72.70	45.80	98.70	75.00	71.00	18.00	19.00	45.00

1 WALKER ET.AL.1976-GL,00KB,1176C,72.7HR,F-12.21,GL+OL+PIG+SP
2 WALKER ET.AL.1976-GL,00KB,1164C,45.8HR,F-12.37,GL+OL+PIG+SP
3 WALKER ET.AL.1976-GL,00KB,1156C,98.7HR,F-12.47,GL+OL+PL+PIG+SP
4 WALKER ET.AL.1976-GL,00KB,1150C,75HR,F-12.56,GL+OL+PL+PIG+SP
5 HUEBNER ETAL 1976-GL,00KB,1332C,71HR,F-8.26,GL+PIG
6 HUEBNER ETAL 1976-GL,00KB,1243C,18HR,F-11.77,GL+PIG
7 HUEBNER ETAL 1976-GL,00KB,1252C,19HR,F-11.42,GL+OL+PIG
8 HUEBNER ETAL 1976-GL,00KB,1151C,45HR,F-12.65,GL+PIG

	9	10	11	12	13	14	15	16
SiO2	48.10	47.30	46.70	46.60	47.23	46.86	46.24	45.08
TiO2	1.83	1.92	2.24	2.63	3.76	4.17	4.35	5.58
Al2O3	10.10	10.70	11.00	10.50	10.40	11.50	11.14	9.97
Fe2O3	0.48	0.50	0.54	0.57	0.47	0.47	0.52	0.63
Cr2O3	0.43	0.33	0.19	0.20	0.28	0.17	0.17	0.15
FeO	20.37	20.45	21.72	22.49	17.29	17.15	19.16	20.86
MnO	0.30	0.29	0.29	0.30	0.25	0.20	0.24	0.28
MgO	7.10	6.06	4.59	4.09	7.53	7.10	5.66	4.78
CaO	10.70	11.60	11.60	10.80	11.46	11.93	11.32	10.82
Na2O	0.16	0.22	0.21	0.26	0.72	0.51	0.78	0.85
K2O	0.04	0.05	0.07	nd	0.02	0.07	nd	0.13
total=	99.61	99.42	99.15	98.44	99.41	100.14	99.58	99.13
qtz	3.46	2.59	3.19	4.61	2.38	2.82	2.57	2.71
en	13.86	11.21	8.40	7.69	13.13	12.37	9.89	8.03
fs	27.07	25.63	26.66	27.95	17.94	17.21	19.67	19.63
cen	3.83	3.88	3.03	2.50	5.62	5.31	4.20	3.87
cfs	7.47	8.88	9.62	9.09	7.68	7.39	8.35	9.46
cwo	11.01	12.31	11.98	10.90	13.26	12.65	12.22	12.81
or	0.24	0.30	0.41	-	0.12	0.41	-	0.77
an	26.72	28.06	28.86	27.48	25.09	28.88	26.89	23.00
ab	1.35	1.86	1.78	2.20	6.09	4.32	6.60	7.19
mag	0.69	0.72	0.79	0.82	0.68	0.68	0.75	0.92
ilm	3.48	3.65	4.25	4.99	7.14	7.92	8.26	10.60
chr	0.63	0.49	0.28	0.29	0.41	0.25	0.25	0.22
temp	1194.00	1161.00	1138.00	1123.00	1179.00	1160.00	1137.00	1114.00
time	44.80	42.50	73.00	119.00	5.00	5.00	5.00	5.00

9 GROVE & BENCE 1977-GL,00KB,1194C,44.8HR,F-11.98,+GL+OL+PIG
10 GROVE & BENCE 1977-GL,00KB,1161C,42.5HR,F-12.41,+GL+OL+PIG+SP
11 GROVE & BENCE 1977-GL,00KB,1138C,73HR,F-12.72,+GL+OL+PL+PIG+SP
12 GROVE & BENCE 1977-GL,00KB,1123C,119HR,F-12.92,+GL+PIG+SP+PL
13 BIGGAR ETAL 1971 12040-GL,00KB,1179C,5HR,F-12.10,+GL+OL+PIG+SP
14 BIGGAR ETAL 1971 12040-GL,00KB,1160C,5HR,F-12.30,+GL+OL+PL+PIG+SP
15 BIGGAR ETAL 1971 12038-GL,00KB,1137C,5HR,F-12.70,+GL+OL+PL+PIG+SP+CPX
16 BIGGAR ETAL 1971 12038-GL,00KB,1114C,5HR,F-12.90,+GL+PL+PIG+SP+CPX

TABLE AIV.1B

	17	18	19	20	21	22	23	24
SiO2	46.35	45.41	42.48	49.39	49.08	49.38	48.90	48.00
TiO2	3.97	5.50	8.93	0.70	0.68	0.70	0.67	1.72
Al2O3	10.56	9.75	9.70	13.07	12.78	12.85	12.48	10.20
Fe2O3	0.52	0.66	0.33	0.21	0.23	0.21	0.23	0.19
Cr2O3	0.20	0.15	0.08	0.33	0.31	0.31	0.32	0.66
FeO	18.89	21.09	18.61	17.16	18.82	17.69	18.92	17.62
MnO	0.28	0.31	nd	0.57	0.58	0.57	0.59	nd
MgO	6.57	4.50	5.94	6.41	6.50	6.44	6.40	8.96
CaO	11.64	11.15	11.45	10.47	10.28	10.39	10.19	10.50
Na2O	0.45	0.86	0.43	0.53	0.51	0.44	0.47	0.09
K2O	0.07	0.08	nd	nd	nd	nd	nd	nd
total=	99.50	99.46	97.95	98.84	99.77	98.98	99.17	97.95
qtz	2.61	3.07	4.84	4.12	2.74	4.28	3.08	3.58
en	11.50	7.28	8.93	13.26	13.65	13.40	13.40	17.87
fs	19.84	19.27	11.56	25.95	28.94	26.92	29.05	23.51
cen	4.86	3.93	5.87	2.70	2.54	2.63	2.54	4.45
cfs	8.39	10.40	7.59	5.29	5.39	5.29	5.49	5.85
cwo	13.01	13.70	13.47	7.79	7.69	7.71	7.77	10.30
or	0.41	0.47	-	-	-	-	-	-
an	26.59	22.51	24.54	33.28	32.58	33.09	31.94	27.43
ab	3.81	7.28	3.64	4.48	4.32	3.72	3.98	0.76
mag	0.76	0.96	0.48	0.30	0.33	0.31	0.34	0.28
ilm	7.54	10.45	16.96	1.33	1.29	1.33	1.27	3.27
chr	0.29	0.22	0.12	0.49	0.46	0.46	0.47	0.97
temp	1160.00	1114.00	1133.00	1171.00	1171.00	1171.00	1171.00	1225.00
time	5.00	5.00	-	15.30	17.00	15.30	17.00	20.50

17 BIGGAR ETAL 1971 12064-GL,00KB,1160C,5HR,F-12.30,+GL+PIG+SP
18 BIGGAR ETAL 1971 12064-GL,00KB,1114C,5HR,F-12.90,+GL+PL+PIG+SP+CPX
19 O HARA ET.AL.(1976)-GL,00KB,1133C,0HR,F-13.79,+GL+OL+PL+CPX+SP+OPX+ILM
20 STOLPER TABLE 3 JV14GL,00KB,1171C,15.3HR,F-13.51,+OL+PL+PIG+SP
21 STOLPER TABLE 3 JV18GL,00KB,1171C,17.0HR,F-13.44,+OL+PL+PIG+SP
22 STOLPER TABLE 3 SC54GL,00KB,1171C,15.3HR,F-13.51,+OL+PL+PIG+SP
23 STOLPER TABLE 3 SC58GL,00KB,1171C,17.0HR,F-13.44,+OL+PLAG+PIG+SP
24 WALKER ETAL 15065 -GL,00KB,1225C,20.5HR,F-13.00,+GL+OL+SP+PIG

	25	26	27	28	29	30	31	32
SiO2	47.80	47.20	46.10	45.60	45.80	45.90	46.40	45.80
TiO2	1.84	2.02	2.53	3.44	2.40	3.01	3.09	3.26
Al2O3	10.70	11.70	11.10	10.20	10.30	10.40	10.10	10.80
Fe2O3	0.24	0.30	0.39	0.53	0.54	0.55	0.40	0.40
Cr2O3	0.55	0.40	0.31	0.24	0.27	0.26	0.36	0.29
FeO	18.19	18.63	19.75	22.03	22.92	23.21	21.44	19.64
MnO	nd	nd	0.32	nd	nd	0.34	0.30	0.31
MgO	7.96	6.85	5.55	4.49	4.65	4.32	6.40	5.74
CaO	10.80	11.30	11.40	11.20	11.10	11.10	11.70	11.70
Na2O	0.24	0.40	0.17	0.16	0.33	0.05	0.03	0.14
total=	98.31	98.80	97.62	97.88	98.30	99.14	100.22	98.08
qtz	3.16	2.11	3.51	4.49	2.15	3.97	2.52	3.58
en	15.57	13.10	10.31	8.11	8.63	8.12	11.76	10.31
fs	23.69	23.52	24.14	24.88	28.07	28.53	25.46	22.31
cen	4.26	3.96	3.51	3.08	2.95	2.64	4.17	3.98
cfs	6.48	7.10	8.21	9.45	9.61	9.29	9.03	8.61
cwo	10.63	10.83	11.29	11.88	11.88	11.24	12.78	12.19
an	28.12	30.13	29.52	27.11	26.62	28.15	27.42	28.84
ab	2.03	3.38	1.44	1.35	2.79	0.42	0.25	1.18
mag	0.34	0.44	0.57	0.76	0.78	0.80	0.58	0.58
ilm	3.49	3.84	4.80	6.53	4.56	5.72	5.87	6.19
chr	0.81	0.59	0.46	0.35	0.40	0.38	0.53	0.43
temp	1205.00	1172.00	1148.00	1128.00	1125.00	1124.00	1157.00	1148.00
time	22.00	23.70	38.50	70.00	47.20	67.00	46.50	38.50

25 WALKER ETAL 15065 -GL,00KB,1205C,22HR,F-13.00,+GL+OL+SP+PIG
26 WALKER ETAL 15065 -GL,00KB,1172C,23.7HR,F-13.00,+GL+OL+SP+PIG
27 WALKER ETAL 15065 -GL,00KB,1148C,38.5HR,F-13.00,+GL+SP+PIG+PL
28 WALKER ETAL 15065 -GL,00KB,1128C,70HR,F-13.00,+GL+SP+PIG+PL
29 WALKER ETAL 15065 -GL,00KB,1125C,47.2HR,F-13.00,+GL+OL+SP+PIG+PL
30 WALKER ETAL 15065 -GL,00KB,1124C,67HR,F-13.00,+GL+OL+SP+PIG+PL
31 WALKER ETAL 15555 -GL,00KB,1157C,46.5HR,F-13.00,+GL+OL+SP+PIG
32 WALKER ETAL 15555 -GL,00KB,1148C,38.5HR,F-13.00,+GL+OL+SP+PIG+PL

TABLE AIV.1B

	33	34	35	36	37	38	39	40
SiO2	44.10	44.82	45.57	44.53	44.53	49.00	48.70	47.40
TiO2	4.71	6.38	7.51	6.03	6.03	2.79	3.09	3.98
Al2O3	9.85	10.75	9.81	10.72	10.72	9.98	9.53	8.70
Fe2O3	0.56	0.44	0.61	0.41	0.41	0.68	0.78	1.01
Cr2O3	0.23	0.27	0.12	0.29	0.29	0.09	0.08	0.06
FeO	22.89	18.62	21.48	19.32	19.32	22.09	23.10	25.89
MnO	0.35	0.27	0.28	0.25	0.25	0.23	0.23	0.23
MgO	4.61	6.27	3.50	6.51	6.51	3.11	2.83	2.08
CaO	11.00	12.15	10.50	11.70	11.70	10.80	10.60	10.50
Na2O	0.11	0.31	0.39	0.43	0.43	0.05	0.03	nd
K2O	nd	nd	nd	nd	nd	0.08	0.10	0.13
total=	98.42	100.28	99.77	100.19	100.19	98.90	99.07	99.98
qtz	3.42	3.78	9.10	2.21	2.21	10.10	10.15	9.03
en	8.38	10.21	5.81	11.18	11.18	5.60	5.10	3.69
fs	25.15	15.56	18.05	17.69	17.69	25.92	26.84	28.90
cen	3.10	5.40	2.91	5.03	5.03	2.14	1.95	1.49
cfs	9.30	8.23	9.02	7.96	7.96	9.90	10.25	11.67
cwo	11.77	13.50	11.30	12.83	12.83	11.19	11.28	12.00
or	-	-	-	-	-	0.47	0.59	0.77
an	26.38	27.94	25.02	27.32	27.32	26.77	25.57	23.35
ab	0.93	2.62	3.30	3.64	3.64	0.42	0.25	-
mag	0.82	0.64	0.88	0.59	0.59	0.99	1.13	1.46
ilm	8.95	12.12	14.26	11.45	11.45	5.30	5.87	7.56
chr	0.34	0.40	0.18	0.43	0.43	0.13	0.12	0.09
temp	1124.00	1138.00	1125.00	1150.00	1150.00	1099.00	1087.00	1071.00
time	50.10	40.00	48.50	16.50	16.50	236.00	673.00	361.00

33 WALKER ETAL 15555 -GL,00KB,1124C,50.1HR,F-13.00,+GL+OL+SP+PIG+PL
34 RHODES ETAL 12045 -GL,00KB,1138C,40HR,F-13.00,+GL+OL+SP+PIG
35 RHODES ETAL 12008 -GL,00KB,1125C,48.5HR,F-13.00,+GL+OL+PIG+PL+CPX+SP
36 RHODES ETAL 12008 -GL,00KB,1150C,16.5HR,F-13.00,+GL+OL+SP+PIG
37 RHODES ETAL 12008 -GL,00KB,1150C,16.5HR,F-13.00,+GL+OL+SP+PIG
38 GROVE & RAUDSEPP 15597 -GL,00KB,1099C,236HR,F-13.00,+GL+PLAG+PIG
39 GROVE & RAUDSEPP 15597 -GL,00KB,1087C,673HR,F-13.00,+GL+PLAG+PIG+QZ
40 GROVE & RAUDSEPP 15597 -GL,00KB,1071C,361HR,F-13.00,+GL+PLAG+PIG+QZ

	41	42	43	44	45	46	47	48
SiO2	43.20	42.90	44.10	45.70	51.60	51.10	50.60	52.32
TiO2	10.70	10.40	8.87	7.76	5.20	2.40	4.20	2.03
Al2O3	9.02	8.99	9.65	9.97	11.60	15.30	11.70	6.44
Fe2O3	0.45	0.47	0.51	0.56	0.71	0.19	0.55	0.33
Cr2O3	0.16	0.15	0.11	0.12	nd	nd	nd	nd
FeO	17.10	17.28	18.18	17.89	17.16	11.43	12.90	15.65
MnO	0.14	0.10	0.21	0.19	nd	nd	nd	nd
MgO	6.25	6.28	5.91	4.99	3.20	6.90	3.80	8.48
CaO	11.50	11.50	11.20	10.90	9.70	9.80	8.40	11.41
Na2O	0.15	0.15	0.36	0.46	0.40	1.30	1.10	nd
K2O	0.27	0.28	0.24	0.27	1.80	1.00	2.20	nd
P2O5	nd	nd	nd	nd	nd	0.70	2.00	nd
total=	98.93	98.50	99.34	98.82	101.37	100.12	97.45	96.66
qtz	8.46	7.76	6.58	8.54	11.75	5.40	12.91	12.23
en	8.22	8.41	8.93	7.60	5.25	15.17	8.79	13.72
fs	7.19	7.72	11.34	12.18	14.73	14.89	15.14	16.31
cen	7.35	7.23	5.79	4.83	2.72	2.02	0.67	7.40
cfs	6.43	6.63	7.36	7.75	7.61	1.98	1.16	8.79
cwo	14.16	14.21	13.18	12.41	9.85	4.07	1.80	16.30
or	1.60	1.65	1.42	1.60	10.64	5.91	13.00	-
an	23.14	23.03	24.01	24.34	24.54	32.96	20.49	17.57
ab	1.27	1.27	3.05	3.89	3.38	11.00	9.31	-
mag	0.65	0.68	0.75	0.81	1.03	0.28	0.80	0.49
ilm	20.32	19.75	16.85	14.74	9.88	4.56	7.98	3.86
ap	-	-	-	-	-	2.09	5.98	-
chr	0.24	0.22	0.16	0.18	-	-	-	-
temp	1146.00	1139.00	1126.00	1113.00	1080.00	1180.00	1080.00	1242.00
time	234.80	316.60	317.10	264.50	48.00	48.00	188.00	26.00

41 GROVE & BEATY 10085 -GL,00KB,1146C,234.8HR,F-13.00,+GL+PIG+ILM
42 GROVE & BEATY 10085 -GL,00KB,1139C,316.6HR,F-13.00,+GL+PIG+ILM
43 GROVE & BEATY 10085 -GL,00KB,1126C,317.1HR,F-13.00,+GL+PIG+CPX+ILM
44 GROVE & BEATY 10085 -GL,00KB,1113C,264.5HR,F-13.00,+GL+PIG+CPX+PLAG+ILM
45 HESS ETAL LKFM -GL,00KB,1080C,48HR,F-13.00,+GL+PIG+PLAG+ILM
46 HESS ETAL 15382 -GL,00KB,1180C,48HR,F-13.00,+GL+PIG+PLAG+SP
47 HESS ETAL 15382 -GL,00KB,1080C,188HR,F-13.00,+GL+PIG+PLAG+ILM+SP
48 HUEBENER & TURNOCK 1980 12021 -GL1,00KB,1242C,26HR,F-11.96,+GL+PIG

TABLE AIV.1B

	49	50	51	52	53	54	55	56
SiO2	51.98	48.93	49.08	45.59	47.13	45.84	46.61	50.50
TiO2	2.20	1.96	2.25	3.59	2.54	0.08	0.02	2.00
Al2O3	6.76	6.61	6.04	9.13	8.00	5.82	9.95	13.90
Fe2O3	0.31	0.64	0.59	0.43	0.46	0.63	0.56	1.71
Cr2O3	nd	0.25	nd	0.23	0.20	0.01	nd	0.09
FeO	13.94	23.72	23.43	21.95	22.12	36.66	30.04	11.56
MnO	nd	0.30	nd	1.29	1.72	1.57	1.33	0.20
MgO	8.89	5.23	5.69	5.28	4.13	4.87	3.81	6.61
CaO	12.16	12.56	10.15	11.19	11.07	3.52	4.92	11.70
Na2O	nd	0.01	nd	0.10	0.08	0.02	nd	1.35
K2O	nd	nd	nd	nd	nd	nd	nd	0.14
total=	96.24	100.20	97.23	98.77	97.45	99.02	97.25	99.76
qtz	11.82	5.36	8.48	3.28	6.14	-	4.36	5.24
en	13.49	8.26	10.21	9.54	7.19	11.76	9.49	11.07
fs	13.23	25.59	27.97	26.43	27.44	67.47	57.15	11.36
cen	8.65	4.76	3.96	3.61	3.09	0.11	-	5.39
cfs	8.49	14.76	10.86	9.99	11.80	0.65	-	5.53
cwo	17.49	18.50	14.14	12.96	13.97	0.70	-	11.10
fo	-	-	-	-	-	0.18	-	-
fa	-	-	-	-	-	1.14	-	-
or	-	-	-	-	-	-	-	0.83
an	18.45	17.99	16.48	24.46	21.47	15.79	24.41	31.45
ab	-	0.08	-	0.85	0.68	0.17	-	11.42
mag	0.44	0.93	0.85	0.62	0.67	0.91	0.81	2.48
ilm	4.18	3.72	4.27	6.82	4.82	0.15	0.04	3.80
crn	-	-	-	-	-	-	1.00	-
chr	-	0.37	-	0.34	0.29	0.01	-	0.13
temp	1242.00	1151.00	1151.00	1123.00	1123.00	1226.00	1178.00	1153.00
time	26.00	45.00	45.00	19.00	19.00	54.00	52.00	458.10

49 HUEBENER & TURNOCK 1980 12021 -GL2,00KB,1242C,26HR,F-11.96,+GL+PIG
50 HUEBENER & TURNOCK 1980 12021 -GL1,00KB,1151C,45HR,F-12.65,+GL+PIG
51 HUEBENER & TURNOCK 1980 12021 -GL2,00KB,1151C,45HR,F-12.65,+GL+PIG
52 HUEBENER & TURNOCK 1980 12021 -GL1,00KB,1123C,19HR,F-13.49,+GL+PIG+OL
53 HUEBENER & TURNOCK 1980 12021 -GL2,00KB,1123C,19HR,F-13.49,+GL+PIG+OL+CPX
54 HUEBENER & TURNOCK 1980 223 -GL,00KB,1226C,54HR,F-11.58,+GL+PIG+OL
55 HUEBENER & TURNOCK 1980 223 -GL,00KB,1178C,52HR,F-12.06,+GL+PIG
56 GROVE ETAL 1982 79-35G -GL,00KB,1153C,458.1HR,F-9.10,+GL+OL+PL+CPX+PIG

	57	58	59	60	61	62	63	64
SiO2	49.40	56.90	58.70	61.00	57.40	58.00	57.30	55.50
TiO2	3.02	2.08	2.56	2.74	1.55	2.00	2.75	2.22
Al2O3	12.20	13.70	13.30	13.30	14.70	14.70	13.50	13.50
Fe2O3	2.02	1.83	1.86	1.53	1.50	1.60	1.74	1.85
Cr2O3	0.04	0.10	0.08	0.07	0.01	0.02	0.01	0.03
FeO	13.68	9.75	9.23	7.81	8.62	8.46	9.13	9.84
MnO	0.18	0.10	0.07	0.05	0.18	0.14	0.24	0.19
MgO	6.51	3.54	2.43	2.56	4.71	3.99	4.06	3.97
CaO	11.20	7.11	5.98	5.90	8.28	7.87	7.33	7.54
Na2O	1.18	2.31	1.97	1.42	2.32	2.64	2.59	2.93
K2O	0.12	1.80	2.64	2.24	1.09	1.40	1.80	1.16
total=	99.55	99.22	98.82	98.62	100.36	100.82	100.45	98.73
qtz	5.84	13.01	17.71	25.06	12.49	12.61	12.03	9.62
en	10.86	6.52	4.56	5.32	8.81	7.04	6.89	6.82
fs	12.59	9.72	8.52	7.21	9.29	7.92	7.66	9.12
cen	5.35	2.30	1.49	1.06	2.92	2.90	3.22	3.07
cfs	6.21	3.42	2.79	1.44	3.08	3.26	3.58	4.10
cwo	11.66	5.67	4.18	2.49	6.10	6.23	6.88	7.16
or	0.71	10.64	15.60	13.24	6.44	8.27	10.64	6.85
an	27.64	21.70	19.65	23.30	26.48	24.13	19.89	20.26
ab	9.98	19.55	16.67	12.02	19.63	22.34	21.92	24.79
mag	2.93	2.66	2.69	2.22	2.17	2.32	2.52	2.68
ilm	5.74	3.95	4.86	5.20	2.94	3.80	5.22	4.22
chr	0.06	0.15	0.12	0.10	0.01	0.03	0.01	0.04
temp	1137.00	1106.00	1089.00	1072.00	1135.00	1123.00	1105.00	1106.00
time	542.50	306.80	218.00	194.60	148.70	164.30	221.10	118.50

57 GROVE ETAL 1982 79-35G -GL,00KB,1137C,542.5HR,F-9.34,+GL+OL+PL+CPX+PIG
58 GROVE ETAL 1982 79-38B -GL,00KB,1106C,306.8HR,F-9.65,+GL+OL+PL+PIG
59 GROVE ETAL 1982 79-38B -GL,00KB,1089C,218HR,F-9.90,+GL+PL+PIG
60 GROVE ETAL 1982 79-38B -GL,00KB,1072C,194.6HR,F-10.16,+GL+PL+PIG
61 GROVE ETAL 1982 187 -GL,00KB,1135C,148.7HR,F-9.28,+GL+OL+PL+PIG
62 GROVE ETAL 1982 187 -GL,00KB,1123C,164.3HR,F-9.41,+GL+OL+PL+PIG
63 GROVE ETAL 1982 187 -GL,00KB,1105C,221.1HR,F-9.71,+GL+OL+PL+PIG
64 GROVE ETAL 1982 79-20E -GL,00KB,1106C,118.5HR,F-9.66,+GL+PL+OL+PIG

TABLE AIV.1B

	65	66	67	68	69	70	71	72
SiO2	55.10	57.20	64.10	51.10	51.90	50.40	51.10	52.00
TiO2	2.36	2.71	1.99	1.65	1.28	1.51	2.43	2.33
Al2O3	12.60	13.10	13.40	13.20	13.90	12.60	12.90	13.90
Fe2O3	2.06	2.05	1.56	1.55	1.34	1.72	1.49	1.32
Cr2O3	0.02	0.05	0.01	0.03	0.05	0.05	0.01	0.01
FeO	11.54	11.15	7.93	11.11	10.39	12.05	10.16	9.01
MnO	0.16	0.20	0.15	0.10	0.18	0.14	0.13	0.20
MgO	3.46	3.11	1.53	7.32	7.62	6.61	7.30	6.81
CaO	7.42	6.97	4.44	11.40	11.70	11.20	11.40	11.00
Na2O	2.47	2.11	1.53	1.39	nd	1.25	1.47	1.79
K2O	1.33	1.48	2.11	0.18	0.14	0.14	0.23	0.30
total=	98.53	100.14	98.75	99.02	98.50	97.67	98.62	98.67
qtz	11.11	15.74	30.65	5.34	11.99	6.20	6.33	6.79
en	6.00	5.87	3.81	12.41	14.49	11.17	11.61	10.96
fs	11.06	11.13	10.27	11.28	12.36	12.54	8.71	7.74
cen	2.62	1.87	-	5.82	4.49	5.29	6.58	6.00
cfs	4.83	3.55	-	5.30	3.83	5.94	4.94	4.24
cwo	7.28	5.29	-	11.40	8.57	11.36	11.96	10.67
or	7.86	8.75	12.47	1.06	0.83	0.83	1.36	1.77
an	19.36	21.90	22.03	29.25	37.51	28.36	27.92	29.01
ab	20.90	17.85	12.95	11.76	-	10.58	12.44	15.15
mag	2.99	2.98	2.26	2.25	1.95	2.49	2.16	1.92
ilm	4.48	5.15	3.78	3.13	2.43	2.87	4.62	4.43
crn	-	-	0.53	-	-	-	-	-
chr	0.03	0.07	0.01	0.04	0.07	0.07	0.01	0.01
temp	1093.00	1076.00	1059.00	1167.00	1166.00	1156.00	1167.00	1166.00
time	291.00	330.00	628.00	500.90	242.30	244.40	500.90	458.20

65 GROVE ETAL 1982 79-20E -GL,00KB,1093C,291HR,F-9.94,+GL+OL+PL+PIG
66 GROVE ETAL 1982 79-20E -GL,00KB,1076C,330HR,F-10.11,+GL+PL+OL+PIG
67 GROVE ETAL 1982 79-9C -GL,00KB,1059C,628HR,F-10.34,+GL+PL+PIG
68 GROVE & BRYAN 1983 ALV 528 11 -GL,00KB,1167C,500.9HR,F-9.03,+GL+OL+PL+CPX+PIG
69 GROVE & BRYAN 1983 ALV 528 11 -GL,00KB,1166C,242.3HR,F-8.98,+GL+OL+PL+CPX+PIG
70 GROVE & BRYAN 1983 ALV 528 11 -GL,00KB,1156C,244.4HR,F-9.14,+GL+OL+PL+CPX+PIG
71 GROVE & BRYAN 1983 ALV 525 48 -GL,00KB,1167C,500.9HR,F-9.03,+GL+OL+PL+CPX+PIG
72 GROVE & BRYAN 1983 AII 966 42 -GL,00KB,1166C,458.2HR,F-9.08,+GL+OL+PL+CPX+PIG

	73	74	75	76	77
SiO2	51.20	49.78	49.98	43.09	49.10
TiO2	2.66	1.04	2.42	10.05	1.75
Al2O3	12.60	4.89	6.82	10.10	9.43
Fe2O3	1.97	0.39	0.82	0.76	2.62
Cr2O3	0.02	0.68	nd	0.33	nd
FeO	11.03	20.66	23.76	17.49	16.66
MnO	0.21	nd	nd	nd	0.26
MgO	6.16	10.37	5.73	6.40	5.90
CaO	10.00	12.23	10.55	11.57	9.63
Na2O	2.12	nd	nd	0.29	1.70
K2O	0.34	nd	nd	nd	0.56
P2O5	nd	nd	nd	nd	0.28
total=	98.31	100.04	100.08	100.07	97.89
qtz	5.86	1.99	8.37	7.02	3.06
en	9.96	17.53	10.33	9.37	10.24
fs	9.49	24.37	28.17	8.76	18.14
cen	5.39	8.29	3.95	6.57	4.45
cfs	5.13	11.53	10.79	6.14	7.89
cwo	10.75	19.75	14.07	13.00	12.09
or	2.01	-	-	-	3.31
an	23.86	13.35	18.61	26.25	16.45
ab	17.94	-	-	2.45	14.38
mag	2.85	0.57	1.19	1.11	3.80
ilm	5.05	1.98	4.60	19.09	3.32
ap	-	-	-	-	0.84
chr	0.03	1.00	-	0.49	-
temp	1137.00	1241.00	1151.00	1134.00	1160.00
time	311.40	24.00	24.00	24.00	19.90

73 GROVE & BRYAN 1983 AII 966 42 -GL,00KB,1137C,311.4HR,F-9.12,+GL+OL+PL+CPX+PIG
74 NEILSEN & DRAKE TABLE 1 1 -GL,00KB,1241C,24HR,F-10.00,+GL+PIG
75 NEILSEN & DRAKE TABLE 1 3 -GL,00KB,1151C,24HR,F-10.00,+GL+PIG
76 NEILSEN & DRAKE TABLE 1 10 -GL,00KB,1134C,24HR,F-10.00,+GL+PIG
77 MITCHELL 1984 ROCK+GEL -GL,00KB,1160C,19.9HR,F-9.00,+GL+OL+PIG

TABLE AIV.2

	1	2	3	4	5	6	7	8
SiO2	54.63	54.60	54.99	54.78	53.11	54.03	53.93	53.97
TiO2	0.98	0.96	1.01	1.06	1.14	1.19	1.22	1.23
Al2O3	9.07	9.06	9.50	10.04	10.58	11.25	11.43	11.81
Fe2O3	1.33	1.58	1.70	1.83	1.92	2.01	1.75	2.02
FeO	8.22	9.27	9.07	9.33	9.20	9.21	9.18	8.79
MnO	0.17	0.15	0.15	0.16	0.19	0.18	0.15	0.19
MgO	14.85	14.04	12.70	11.66	10.34	9.54	9.49	8.72
CaO	7.43	7.53	7.87	8.20	8.62	8.73	9.13	8.91
Na2O	1.51	1.43	1.58	1.64	1.58	1.80	1.73	1.91
K2O	0.30	0.29	0.32	0.33	0.38	0.42	0.37	0.42
P2O5	0.02	0.02	nd	0.02	0.05	0.02	0.00	nd
total=	98.50	98.94	98.89	99.04	97.12	98.38	98.39	97.98
qtz	5.20	5.91	7.04	7.28	7.20	7.56	7.48	8.02
en	31.37	29.55	25.90	23.38	20.20	18.29	17.90	16.28
fs	10.77	12.17	11.36	11.40	10.81	10.49	10.36	9.59
cen	5.60	5.42	5.72	5.66	5.56	5.48	5.74	5.43
cfs	1.92	2.23	2.51	2.76	2.97	3.14	3.32	3.20
cwo	8.17	8.23	8.83	8.97	9.05	9.11	9.57	9.10
or	1.76	1.73	1.92	1.95	2.23	2.50	2.16	2.50
an	17.13	17.47	17.88	19.05	20.67	21.35	22.31	22.40
ab	12.73	12.06	13.34	13.88	13.34	15.26	14.68	16.19
mag	1.93	2.30	2.46	2.65	2.79	2.91	2.54	2.93
ilm	1.86	1.83	1.92	2.02	2.17	2.26	2.32	2.34
ap	0.05	0.07	-	0.05	0.16	0.05	0.01	-
temp	1345.00	1327.00	1307.00	1290.00	1266.00	1252.00	1245.00	1235.00
time	24.00	24.00	24.00	24.00	24.00	24.00	48.00	24.00

1	17M	3:671 -GL4,00KB,1345C,24HR,F-6.30,+GL
2	17M	3:674 -GL4,00KB,1327C,24HR,F-6.40,+GL+OL+SP
3	17M	3:677 -GL4,00KB,1307C,24HR,F-6.55,+GL+OL+OPXB+SP
4	17M	3:684 -GL4,00KB,1290C,24HR,F-6.70,+GL+OL+OPXB+SP
5	17M	3:692 -GL3,00KB,1266C,24HR,F-6.90,+GL+OPXB+OL+SP
6	17M	3:700 -GL3,00KB,1252C,24HR,F-7.05,+GL+OPXB+SP+PIG+OL
7	17M	3:726 -GL4,00KB,1245C,48HR,F-7.40,+GL+OPXB+OL+SP
8	17M	3:706 -GL3,00KB,1235C,24HR,F-7.20,+GL+OPXB+PIG+OL

	9	10	11	12	13	14	15	16
SiO2	54.29	53.87	54.49	55.25	59.36	58.95	59.24	59.88
TiO2	1.32	1.44	1.42	1.69	0.96	0.96	1.01	1.07
Al2O3	12.93	13.18	14.06	13.58	9.34	9.38	9.95	10.50
Fe2O3	1.85	2.11	1.51	1.96	1.42	1.38	1.56	1.66
FeO	7.78	8.02	6.60	7.57	6.63	6.53	6.66	6.48
MnO	0.14	0.15	0.13	0.14	0.13	0.12	0.13	0.13
MgO	7.74	6.89	7.24	6.37	11.17	10.99	9.93	8.70
CaO	9.57	9.65	10.03	8.89	6.48	6.47	6.79	7.02
Na2O	2.20	2.24	2.25	2.31	2.85	2.99	3.04	3.24
K2O	0.46	0.46	0.46	0.61	0.17	0.17	0.19	0.19
P2O5	0.05	nd	0.03	0.03	nd	nd	nd	nd
total=	98.36	98.01	98.20	98.41	98.50	97.95	98.50	98.88
qtz	7.88	8.18	8.35	10.72	11.52	10.72	11.63	12.80
en	13.46	11.47	12.07	11.20	22.12	21.54	18.95	15.85
fs	7.56	7.28	5.87	6.88	7.69	7.47	7.28	6.58
cen	5.81	5.69	5.96	4.66	5.69	5.84	5.79	5.83
cfs	3.27	3.61	2.90	2.87	1.98	2.02	2.22	2.42
cwo	9.60	9.76	9.45	7.92	8.33	8.54	8.65	8.88
or	2.75	2.75	2.72	3.59	0.98	1.00	1.10	1.12
an	24.01	24.53	26.90	24.90	12.18	11.65	12.94	13.56
ab	18.66	18.97	19.04	19.52	24.13	25.34	25.74	27.39
mag	2.69	3.05	2.19	2.85	2.05	2.01	2.26	2.41
ilm	2.52	2.73	2.69	3.22	1.83	1.82	1.93	2.03
ap	0.16	-	0.08	0.09	-	-	-	-
temp	1206.00	1194.00	1184.00	1155.00	1327.00	1307.00	1290.00	1266.00
time	48.00	96.00	48.00	95.00	24.00	24.00	24.00	24.00

9	17M	3:745 -GL1,00KB,1206C,48HR,F-7.60,+GL+OPXB+PIG+SP
10	17M	3:775 -GL4,00KB,1194C,96HR,F-7.60,+GL+OPXB+PIG
11	17M	3:743 -GL4,00KB,1184C,48HR,F-8.00,+GL+OPXB+PIG+SP
12	17M	3:757 -GL4,00KB,1155C,95HR,F-8.15,+GL+PIG+SP
13	170	3:674 -GL4,00KB,1327C,24HR,F-6.40,+GL+SP
14	170	3:677 -GL4,00KB,1307C,24HR,F-6.65,+GL+OL+SP
15	170	3:684 -GL5,00KB,1290C,24HR,F-6.70,+GL+OPXB+SP
16	170	3:692 -GL4,00KB,1266C,24HR,F-6.90,+GL+OPXB+SP

TABLE AIV.2

	17	18	19	20	21	22	23	24
SiO2	59.66	60.97	59.95	61.14	59.62	63.77	57.36	57.16
TiO2	1.09	1.12	1.10	1.19	1.20	1.31	0.99	1.00
Al2O3	10.68	11.14	11.20	11.93	12.07	13.67	8.14	8.36
Fe2O3	1.71	1.33	1.76	1.57	1.53	1.42	1.42	1.53
FeO	6.36	5.60	6.23	5.31	5.43	4.70	7.04	7.20
MnO	0.14	0.11	0.13	0.10	0.09	0.08	0.13	0.14
MgO	7.89	7.60	7.17	5.91	5.22	4.33	12.87	12.10
CaO	7.15	7.52	7.37	7.47	7.59	6.48	7.48	7.86
Na2O	3.45	3.05	3.51	3.73	3.75	3.32	2.21	2.32
K2O	0.19	0.20	0.20	0.21	0.19	0.24	0.09	0.10
P2O5	0.02	0.01	0.03	0.02	nd	0.01	0.05	0.07
total=	98.34	98.64	98.66	98.56	96.69	99.32	97.78	97.84
qtz	12.70	16.19	13.35	15.54	14.67	23.02	9.73	9.52
en	13.68	13.09	11.99	8.89	7.32	8.08	24.91	22.64
fs	6.07	5.20	5.66	4.03	3.88	4.07	8.05	7.94
cen	5.98	5.85	5.86	5.83	5.69	2.70	7.14	7.50
cfs	2.65	2.32	2.77	2.64	3.02	1.36	2.31	2.63
cwo	9.25	8.81	9.22	9.07	9.23	4.32	10.29	10.99
or	1.12	1.18	1.18	1.22	1.12	1.39	0.55	0.59
an	13.11	16.11	14.24	15.18	15.54	21.69	11.99	12.10
ab	29.17	25.81	29.68	31.59	31.73	28.11	18.73	19.63
mag	2.48	1.92	2.55	2.27	2.22	2.06	2.06	2.22
ilm	2.08	2.13	2.09	2.26	2.28	2.49	1.88	1.90
ap	0.07	0.03	0.09	0.05	-	0.03	0.16	0.20
temp	1252.00	1245.00	1235.00	1206.00	1184.00	1155.00	1327.00	1309.00
time	24.00	48.00	24.00	48.00	48.00	95.00	23.00	23.50

17 170 3:700 -GL3,00KB,1252C,24HR,F-7.05,+GL+OPXB+PIG+SP
18 170 3:726 -GL4,00KB,1245C,48HR,F-7.40,+GL+OPXB+SP
19 170 3:706 -GL3,00KB,1235C,24HR,F-7.20,+GL+PIG+SP
20 170 3:745 -GL3,00KB,1206C,48HR,F-7.60,+GL+PIG+SP
21 170 3:743 -GL1,00KB,1184C,48HR,F-8.00,+GL+PIG+SP
22 170 3:757 -GL5,00KB,1155C,95HR,F-8.15,+GL+PIG+CPX
23 120 3:675 -GL3,00KB,1327C,23HR,F-6.40,+GL+SP
24 120 3:681 -GL4,00KB,1309C,23.5HR,F-6.55,+GL+OPXB+SP

	25	26	27	28	29	30	31	32
SiO2	57.95	57.93	58.32	56.76	59.01	59.76	59.46	61.01
TiO2	1.05	1.12	1.16	0.91	1.20	1.30	1.26	1.33
Al2O3	8.97	9.44	10.02	11.07	10.41	11.07	11.02	12.23
Fe2O3	1.62	1.83	1.80	1.52	1.90	1.58	1.68	1.45
FeO	7.06	6.92	6.92	6.78	6.75	5.74	5.70	5.06
MnO	0.14	0.14	0.12	0.13	0.13	0.11	0.10	0.09
MgO	10.67	9.43	8.88	8.33	8.09	6.62	6.60	5.30
CaO	8.32	8.55	8.69	9.72	8.99	9.42	8.88	8.14
Na2O	2.41	2.74	2.84	2.39	2.86	1.97	3.30	3.68
K2O	0.11	0.12	0.11	0.11	0.11	0.27	0.12	0.12
P2O5	0.03	0.07	0.20	nd	0.12	0.25	0.08	0.12
total=	98.33	98.28	99.06	97.73	99.58	98.10	98.19	98.54
qtz	11.23	11.27	11.81	10.94	13.05	19.98	14.15	16.41
en	18.82	15.59	14.74	13.05	12.55	9.99	8.73	7.07
fs	7.20	6.38	6.36	6.25	5.65	4.42	3.82	3.25
cen	7.75	7.90	7.37	7.69	7.60	6.49	7.70	6.12
cfs	2.97	3.23	3.18	3.69	3.42	2.87	3.37	2.81
cwo	11.58	11.98	11.32	12.15	11.81	10.04	11.88	9.56
or	0.62	0.68	0.63	0.65	0.63	1.63	0.72	0.73
an	13.31	13.12	14.31	19.14	15.24	20.55	14.90	16.50
ab	20.43	23.16	23.99	20.24	24.24	16.69	27.88	31.14
mag	2.35	2.65	2.61	2.20	2.76	2.29	2.43	2.10
ilm	1.99	2.12	2.21	1.73	2.28	2.47	2.39	2.53
ap	0.09	0.22	0.60	-	0.37	0.76	0.25	0.36
temp	1288.00	1265.00	1253.00	1245.00	1236.00	1224.00	1206.00	1184.00
time	23.75	25.00	23.50	48.00	23.66	477.00	48.00	48.00

25 120 3:685 -GL4,00KB,1288C,23.75HR,F-6.75,+GL+OPXB+SP
26 120 3:693 -GL4,00KB,1265C,25HR,F-6.85,+GL+OPXB+PIG+SP
27 120 3:703 -GL4,00KB,1253C,23.5HR,F-7.05,+GL+PIG+SP
28 120 3:726 -GL4,00KB,1245C,48HR,F-7.40,+GL+OPXB+SP
29 120 3:707 -GL4,00KB,1236C,23.66HR,F-7.15,+GL+PIG+SP
30 120 3:770 -GL4,00KB,1224C,477HR,F-7.40,+GL+OPXB+PIG+SP
31 120 3:745 -GL4,00KB,1206C,48HR,F-7.60,+GL+PIG+SP
32 120 3:743 -GL3,00KB,1184C,48HR,F-8.00,+GL+PIG+SP

TABLE AIV.2

	33	34	35	36	37	38	39	40
SiO2	60.26	56.43	56.70	57.11	57.55	57.46	57.33	58.14
TiO2	1.27	0.37	0.38	0.42	0.39	0.41	0.43	0.55
Al2O3	11.38	11.87	12.46	12.88	13.18	13.68	14.59	13.39
Fe2O3	1.44	1.37	1.44	1.61	1.54	1.65	1.60	1.75
FeO	5.18	7.42	7.23	6.88	6.86	6.71	6.31	6.45
MnO	0.11	0.17	0.16	0.17	0.13	0.15	0.14	0.15
MgO	8.10	11.60	10.50	8.41	8.52	7.68	6.74	5.99
CaO	8.65	6.52	6.78	7.34	7.23	7.54	7.89	7.43
Na2O	2.76	1.99	2.07	2.24	2.34	2.41	2.60	2.58
K2O	0.11	0.89	0.93	1.03	1.04	1.13	1.18	1.55
P2O5	0.02	nd	0.01	nd	0.00	nd	nd	0.01
total=	99.28	98.64	98.67	98.08	98.78	98.83	98.80	98.00
qtz	15.60	7.08	8.09	10.02	9.71	9.77	9.42	11.48
en	13.09	25.72	23.02	17.24	17.72	15.51	13.16	10.96
fs	4.17	10.86	10.34	8.99	9.14	8.56	7.68	7.18
cen	7.09	3.16	3.13	3.70	3.49	3.62	3.62	3.95
cfs	2.26	1.33	1.41	1.93	1.80	2.00	2.11	2.59
cwo	10.19	4.83	4.86	5.99	5.62	5.96	6.05	6.86
or	0.66	5.29	5.51	6.07	6.15	6.68	6.96	9.14
an	18.36	20.80	21.94	22.06	22.36	23.15	24.66	20.37
ab	23.31	16.88	17.53	18.95	19.82	20.41	22.00	21.86
mag	2.08	1.98	2.09	2.33	2.24	2.39	2.33	2.54
ilm	2.42	0.71	0.73	0.79	0.73	0.78	0.82	1.05
ap	0.05	-	0.03	-	0.01	-	-	0.03
temp	1155.00	1309.00	1288.00	1265.00	1253.00	1235.00	1206.00	1156.00
time	95.00	23.50	23.75	25.00	23.50	24.00	48.00	48.00

33 120 3:757 -GL4,00KB,1155C,95HR,F-8.15,+GL+PIG+CPX+SP
34 B4 3:681 -GL4,00KB,1309C,23.5HR,F-6.55,+GL
35 B4 3:685 -GL4,00KB,1288C,23.75HR,F-6.70,+GL+OL
36 B4 3:693 -GL3,00KB,1265C,25HR,F-6.85,+GL+OL
37 B4 3:703 -GL4,00KB,1253C,23.5HR,F-7.05,+GL+OPXB+OL+SP
38 B4 3:708 -GL4,00KB,1235C,24HR,F-7.15,+GL+OPXB+OL+SP
39 B4 3:746 -GL3,00KB,1206C,48HR,F-7.50,+GL+OPXB
40 B4 3:756 -GL3,00KB,1156C,48HR,F-8.15,+GL+OPXB+PLAG

	41	42	43	44	45	46	47	48
SiO2	54.56	57.10	55.00	63.66	55.04	55.26	55.63	55.84
TiO2	1.14	0.50	0.62	0.82	1.57	1.57	1.61	1.83
Al2O3	12.99	15.03	16.21	14.36	14.51	14.55	15.11	14.76
Fe2O3	2.78	1.70	1.87	1.54	1.92	1.92	1.84	2.04
FeO	9.68	6.36	7.15	4.65	7.71	7.81	7.57	7.59
MnO	0.19	0.14	0.15	0.08	0.14	0.14	0.13	0.15
MgO	4.62	6.02	4.80	2.98	6.90	6.91	5.99	5.18
CaO	8.66	8.06	9.68	5.90	7.24	7.26	7.47	7.42
Na2O	2.93	2.68	2.80	2.63	3.23	3.15	3.15	3.36
K2O	0.90	1.22	0.67	2.59	0.62	0.61	0.64	0.73
P2O5	nd	1.49	0.01	nd	0.04	0.10	0.01	0.04
total=	98.45	100.30	98.97	99.20	98.92	99.28	99.15	98.94
qtz	7.31	12.07	7.28	20.67	6.25	6.81	7.96	8.60
en	7.12	14.50	8.04	5.30	14.12	14.40	12.11	9.80
fs	8.64	9.41	7.31	4.32	8.42	8.71	8.08	7.23
cen	4.37	0.48	3.90	2.12	3.05	2.81	2.82	3.10
cfs	5.31	0.31	3.54	1.73	1.82	1.70	1.88	2.29
cwo	9.73	0.83	7.63	3.98	5.14	4.76	4.92	5.61
or	5.34	7.18	3.97	15.30	3.65	3.60	3.78	4.31
an	19.63	25.41	29.67	19.73	23.28	23.74	25.22	23.01
ab	24.79	22.68	23.71	22.25	27.31	26.70	26.64	28.45
mag	4.03	2.46	2.72	2.23	2.78	2.79	2.66	2.96
ilm	2.17	0.94	1.18	1.56	2.99	2.99	3.06	3.48
ap	-	4.47	0.02	-	0.12	0.31	0.02	0.13
temp	1148.00	1194.00	1156.00	1148.00	1235.00	1206.00	1181.00	1156.00
time	95.00	96.00	48.00	95.00	24.00	48.00	48.00	48.00

41 B4 3:777 -GL3,00KB,1148C,95HR,F-8.20,+GL+PIG+PLAG+CPX
42 B5 3:775 -GL4,00KB,1194C,96HR,F-7.60,+GL+OPXB
43 B5 3:756 -GL5,00KB,1156C,48HR,F-8.15,+GL+OPXB+CPX+PLAG
44 B5 3:777 -GL1,00KB,1148C,95HR,F-8.20,+GL+OPXB+PLAG
45 T2 3:708 -GL4,00KB,1235C,24HR,F-7.15,+GL
46 T2 3:746 -GL4,00KB,1206C,48HR,F-7.50,+GL+SP
47 T2 3:744 -GL6,00KB,1181C,48HR,F-7.90,+GL+OL+SP
48 T2 3:756 -GL4,00KB,1156C,48HR,F-8.15,+GL+OPXB+SP

TABLE AIV.2

	49	50	51	52	53	54	55	56
SiO2	53.90	52.76	52.87	52.92	52.87	53.15	52.32	53.36
TiO2	1.17	0.17	0.17	0.17	0.20	0.19	0.21	0.29
Al2O3	21.37	12.69	12.67	12.81	13.03	14.16	17.29	18.29
Fe2O3	1.28	1.38	1.42	1.52	1.53	1.56	1.19	1.72
FeO	4.45	7.30	7.44	7.47	7.38	7.00	4.66	6.69
MnO	0.08	0.19	0.19	0.19	0.19	0.17	0.15	0.14
MgO	2.19	11.74	11.77	11.43	10.41	8.37	5.87	4.23
CaO	9.77	10.86	10.82	10.85	11.10	11.75	12.23	11.69
Na2O	4.14	1.36	1.37	1.45	1.48	1.62	1.94	2.30
K2O	0.51	0.14	0.14	0.15	0.14	0.15	0.17	0.24
P2O5	nd	nd	0.00	0.01	0.02	nd	nd	nd
total=	98.86	98.59	98.87	98.97	98.35	98.12	96.04	98.93
qtz	3.46	3.49	3.45	3.49	4.57	6.12	6.91	7.00
en	3.33	22.18	22.31	21.50	18.94	13.90	8.73	6.63
fs	3.25	9.35	9.56	9.47	8.99	7.72	4.48	6.72
cen	2.12	7.05	6.99	6.97	7.00	6.95	5.89	3.90
cfs	2.07	2.97	2.99	3.07	3.32	3.86	3.02	3.95
cwo	4.28	10.77	10.72	10.77	11.02	11.43	9.48	7.99
or	3.01	0.81	0.81	0.89	0.84	0.89	1.02	1.42
an	38.22	28.09	28.00	27.98	28.50	30.91	37.95	38.88
ab	35.03	11.55	11.63	12.29	12.52	13.73	16.42	19.44
mag	1.86	2.01	2.06	2.21	2.22	2.26	1.73	2.49
ilm	2.22	0.33	0.33	0.32	0.37	0.36	0.41	0.54
ap	-	-	0.01	0.02	0.07	-	-	-
temp	1148.00	1309.00	1288.00	1270.00	1252.00	1206.00	1194.00	1172.00
time	95.00	24.00	24.00	23.75	23.00	48.00	96.00	93.00

49 T2 3:777 -GL1,00KB,1148C,95HR,F-8.20,+GL+OPXB+PLAG
50 K1 3:682 -GL4,00KB,1309C,24HR,F-6.50,+GL+SP
51 K1 3:686 -GL4,00KB,1288C,24HR,F-6.70,+GL+SP
52 K1 3:694 -GL4,00KB,1270C,23.75HR,F-6.80,+GL+OL+SP
53 K1 3:695 -GL4,00KB,1252C,23HR,F-7.05,+GL+OL+SP
54 K1 3:745 -GL3,00KB,1206C,48HR,F-7.60,+GL+OPXB+SP
55 K1 3:775 -GL4,00KB,1194C,96HR,F-7.60,+GL+PIG+CPX
56 K1 3:776 -GL4,00KB,1172C,93HR,F-7.90,+GL+PIG+CPX+PLAG

	57	58	59	60	61	62	63	64
SiO2	53.29	53.37	53.56	53.86	53.33	60.07	52.02	53.02
TiO2	0.19	0.18	0.19	0.18	0.17	1.43	0.51	0.56
Al2O3	13.02	13.11	13.30	13.63	13.65	12.24	10.58	11.12
Fe2O3	1.38	1.42	1.49	1.54	1.57	1.50	1.30	1.21
FeO	7.39	7.37	7.26	7.35	6.88	5.26	8.46	8.06
MnO	0.20	0.19	0.18	0.19	0.16	0.10	0.18	0.18
MgO	11.78	11.63	11.22	10.23	9.34	5.44	16.05	14.94
CaO	10.66	10.43	10.56	10.76	11.04	8.45	7.02	7.47
Na2O	1.37	1.75	1.75	1.85	1.87	3.61	1.61	1.45
K2O	0.16	0.13	0.13	0.13	0.12	0.12	0.60	0.54
P2O5	nd	nd	nd	nd	0.00	0.05	0.16	0.13
total=	99.44	99.58	99.64	99.72	98.13	98.28	98.51	98.69
qtz	3.78	2.57	3.26	4.06	4.91	15.06	-	1.65
en	22.80	22.38	21.35	18.90	16.34	6.96	32.25	33.33
fs	9.71	9.59	9.26	9.11	7.98	3.22	11.26	11.84
cen	6.54	6.59	6.60	6.57	6.91	6.58	3.89	3.89
cfs	2.78	2.82	2.86	3.17	3.37	3.04	1.36	1.38
cwo	10.02	10.10	10.16	10.40	10.96	10.29	5.70	5.71
fo	-	-	-	-	-	-	2.69	-
fa	-	-	-	-	-	-	1.03	-
or	0.95	0.77	0.78	0.80	0.72	0.68	3.52	3.16
an	28.90	27.53	28.05	28.48	28.47	16.84	19.86	22.24
ab	11.61	14.82	14.81	15.65	15.87	30.59	13.67	12.31
mag	2.01	2.06	2.16	2.23	2.27	2.17	1.89	1.75
ilm	0.35	0.35	0.36	0.35	0.32	2.72	0.97	1.06
ap	-	-	-	-	0.01	0.16	0.48	0.40
temp	1309.00	1288.00	1270.00	1252.00	1236.00	1184.00	1398.00	1345.00
time	24.00	24.00	23.75	23.00	23.60	48.00	1.00	24.00

57 K6 3:682 -GL4,00KB,1309C,24HR,F-6.50,+GL+SP
58 K6 3:686 -GL4,00KB,1288C,24HR,F-6.70,+GL+SP
59 K6 3:694 -GL4,00KB,1270C,23.75HR,F-6.80,+GL+OL+SP
60 K6 3:695 -GL4,00KB,1252C,23HR,F-7.05,+GL+OL+SP
61 K6 3:707 -GL4,00KB,1236C,23.6HR,F-7.15,+GL+OL+SP
62 K6 3:743 -GL2,00KB,1184C,48HR,F-8.00,+GL+OPXB+CPX+PLAG(+OL)
63 295 3:676 -GL4,00KB,1398C,1HR,F-5.65,+GL+SP
64 295 3:671 -GL4,00KB,1345C,24HR,F-6.30,+GL+OL+SP

TABLE AIV.2

	65	66	67	68	69	70	71	72
SiO2	53.66	55.12	55.23	53.89	55.32	53.96	55.16	55.78
TiO2	0.58	0.60	0.62	0.70	0.66	0.68	0.68	1.14
Al2O3	11.82	12.44	13.12	14.50	13.88	13.79	14.65	14.16
Fe2O3	1.39	1.61	1.66	1.50	1.72	1.64	1.63	1.89
FeO	8.16	7.53	7.06	6.98	6.93	7.06	6.55	6.60
MnO	0.18	0.17	0.16	0.17	0.16	0.17	0.14	0.15
MgO	12.39	9.90	8.47	8.11	7.62	9.23	6.62	5.11
CaO	7.98	8.55	9.00	9.77	9.44	9.20	9.84	8.47
Na2O	1.70	1.92	2.11	1.56	2.21	2.13	2.39	2.73
K2O	0.62	0.68	0.74	0.62	0.79	0.77	0.86	1.57
P2O5	0.13	0.06	0.04	0.07	0.04	nd	0.06	nd
total=	98.60	98.57	98.20	97.87	98.77	98.63	98.58	97.60
qtz	3.70	7.11	7.78	8.48	7.71	4.52	7.44	8.42
en	26.58	19.72	15.87	15.80	13.67	17.71	11.12	7.96
fs	11.38	9.47	8.18	8.38	7.57	8.33	6.63	5.60
cen	4.27	4.92	5.23	4.41	5.31	5.28	5.36	4.76
cfs	1.83	2.36	2.69	2.34	2.94	2.48	3.20	3.35
cwo	6.55	7.77	8.42	7.17	8.74	8.29	9.02	8.46
or	3.63	4.03	4.34	3.65	4.64	4.55	5.06	9.31
an	22.80	23.32	24.18	30.72	25.63	25.79	26.71	21.73
ab	14.38	16.25	17.83	13.24	18.72	18.02	20.22	23.10
mag	2.02	2.33	2.40	2.17	2.49	2.38	2.36	2.74
ilm	1.11	1.13	1.18	1.34	1.26	1.29	1.30	2.17
ap	0.38	0.17	0.11	0.20	0.10	-	0.18	-
temp	1307.00	1266.00	1235.00	1224.00	1206.00	1194.00	1181.00	1155.00
time	24.00	24.00	24.00	477.00	48.00	96.00	48.00	95.00

65 295 3:677 -GL4,00KB,1307C,24HR,F-6.65,+GL+OL+SP
66 295 3:692 -GL4,00KB,1266C,24HR,F-6.90,+GL+OL+SP
67 295 3:706 -GL4,00KB,1235C,24HR,F-7.20,+GL+OL+OPXB+SP
68 295 3:770 -GL4,00KB,1224C,477HR,F-7.40,+GL+OPXB+OL+SP
69 295 3:746 -GL4,00KB,1206C,48HR,F-7.50,+GL+OL+OPXB+SP
70 295 3:775 -GL4,00KB,1194C,96HR,F-7.60,+GL+OL+OPXB
71 295 3:744 -GL3,00KB,1181C,48HR,F-7.90,+GL+OL+OPXB+SP
72 295 3:757 -GL2,00KB,1155C,95HR,F-8.15,+GL+OPXB+OL+PLAG+SP

	73	74	75	76	77	78	79	80
SiO2	57.85	59.35	58.92	58.68	59.20	59.46	59.05	60.49
TiO2	0.95	0.10	0.10	0.11	0.11	0.12	0.10	0.11
Al2O3	7.98	9.03	9.40	10.08	10.46	10.85	9.65	10.38
Fe2O3	1.45	1.45	1.58	1.80	1.76	1.86	1.61	1.39
FeO	7.09	6.94	7.20	7.27	7.07	6.85	7.44	5.84
MnO	0.14	0.20	0.20	0.19	0.18	0.17	0.19	0.19
MgO	12.88	11.45	10.32	8.93	8.22	7.43	10.23	9.21
CaO	7.57	8.16	8.39	8.81	9.03	9.26	8.37	8.93
Na2O	2.27	1.49	1.56	1.68	1.72	1.82	1.51	1.53
K2O	0.10	0.49	0.52	0.56	0.59	0.61	0.50	0.52
P2O5	0.03	0.00	nd	0.02	0.04	0.07	0.00	0.01
total=	98.30	98.65	98.19	98.11	98.37	98.50	98.66	98.61
qtz	9.79	14.10	14.30	14.62	15.64	16.35	14.55	17.58
en	24.57	21.93	19.21	15.79	14.08	12.13	19.31	16.31
fs	8.05	9.04	9.07	8.54	8.03	7.32	9.49	6.94
cen	7.50	6.58	6.49	6.44	6.40	6.36	6.16	6.62
cfs	2.46	2.71	3.07	3.48	3.65	3.84	3.03	2.82
cwo	10.85	10.00	10.21	10.52	10.62	10.73	9.79	10.14
or	0.57	2.88	3.05	3.31	3.49	3.58	2.98	3.10
an	11.30	16.51	17.16	18.31	19.08	19.64	18.06	19.92
ab	19.22	12.61	13.16	14.23	14.53	15.44	12.75	12.92
mag	2.10	2.10	2.29	2.62	2.55	2.70	2.34	2.01
ilm	1.80	0.19	0.19	0.20	0.21	0.22	0.19	0.21
ap	0.09	0.01	-	0.07	0.11	0.21	0.01	0.04
temp	1327.00	1309.00	1288.00	1265.00	1253.00	1235.00	1292.00	1275.00
time	23.00	23.50	23.75	25.00	23.50	24.00	48.00	48.00

73 M1 3:675 -GL4,00KB,1327C,23HR,F-6.40,+GL+SP
74 M1 3:681 -GL4,00KB,1309C,23.5HR,F-6.55,+GL+OPXB
75 M1 3:685 -GL8,00KB,1288C,23.75HR,F-6.75,+GL+OPXB
76 M1 3:693 -GL4,00KB,1265C,25HR,F-6.85,+GL+OPXB
77 M1 3:703 -GL4,00KB,1253C,23.5HR,F-7.05,+GL+OPXB+SP
78 M1 3:708 -GL4,00KB,1235C,24HR,F-7.15,+GL+OPXB
79 M1MET 3:752 -GL4,00KB,1292C,48HR,F-6.70,+GL+OPXB
80 M1MET 3:734 -GL4,00KB,1275C,48HR,F-6.85,+GL+OPXB

TABLE AIV.2

	81	82	83	84	85	86	87	88
SiO2	59.65	59.12	61.65	60.24	61.09	62.03	58.60	55.64
TiO2	0.12	0.13	0.14	0.12	0.13	0.14	0.99	0.11
Al2O3	10.20	10.93	11.69	11.30	12.39	13.52	8.20	10.35
Fe2O3	1.89	2.07	1.42	1.60	1.67	1.64	1.25	1.16
FeO	7.62	7.85	5.28	6.43	6.01	5.61	6.22	6.76
MnO	0.19	0.18	0.17	0.17	0.14	0.12	0.13	0.14
MgO	9.25	7.66	6.38	6.94	5.14	4.19	12.97	14.11
CaO	8.60	9.17	9.73	9.26	9.18	8.59	7.74	9.07
Na2O	1.55	1.72	1.50	1.77	2.12	2.18	2.14	0.96
K2O	0.50	0.58	0.58	0.62	0.71	0.77	0.10	0.31
P2O5	0.09	0.02	0.04	0.06	0.06	0.02	0.05	0.02
total=	99.66	99.42	98.57	98.52	98.64	98.80	98.39	98.63
qtz	15.95	15.47	21.86	18.04	19.43	21.60	11.44	7.95
en	17.30	13.14	9.62	11.29	7.57	6.59	24.71	28.86
fs	9.44	8.83	5.21	6.92	5.74	5.64	6.89	9.47
cen	5.74	5.94	6.26	6.00	5.23	3.84	7.59	6.29
cfs	3.13	3.99	3.39	3.68	3.97	3.29	2.12	2.06
cwo	9.40	10.39	10.23	10.18	9.55	7.33	10.65	9.09
or	2.97	3.41	3.46	3.64	4.20	4.56	0.59	1.81
an	19.37	20.42	23.45	21.05	22.17	24.83	12.48	23.05
ab	13.14	14.53	12.67	15.01	17.96	18.40	18.11	8.10
mag	2.74	3.00	2.06	2.32	2.42	2.38	1.81	1.68
ilm	0.23	0.24	0.27	0.23	0.25	0.27	1.88	0.20
ap	0.28	0.06	0.10	0.19	0.18	0.07	0.14	0.07
temp	1273.00	1237.00	1224.00	1215.00	1184.00	1156.00	1347.00	1327.00
time	48.00	48.00	477.00	48.00	48.00	121.00	24.00	24.00

81 M1MET 3:751 -GL3,00KB,1273C,48HR,F-6.70,+GL+OPXB
82 M1MET 3:750 -GL3,00KB,1237C,48HR,F-7.10,+GL+OPXB
83 M1MET 3:770 -GL4,00KB,1224C,477HR,F-7.40,+GL+OPXB
84 M1MET 3:735 -GL5,00KB,1215C,48HR,F-7.60,+GL+OPXB+PIG
85 M1MET 3:742 -GL4,00KB,1184C,48HR,F-7.90,+GL+OPXB+PIG
86 M1MET 3:758 -GL4,00KB,1156C,121HR,F-8.15,+GL+OPXB
87 C2 3:673 -GL4,00KB,1347C,24HR,F-6.25,+GL
88 C2 3:674 -GL4,00KB,1327C,24HR,F-6.40,+GL

	89	90	91	92	93	94	95	96
SiO2	55.11	55.21	56.11	55.29	56.05	55.13	53.70	55.41
TiO2	0.11	0.12	0.13	0.13	0.12	0.13	0.14	0.14
Al2O3	10.58	11.19	12.27	11.35	12.04	11.84	12.78	13.48
Fe2O3	1.31	1.40	1.34	1.41	1.26	1.60	1.76	1.42
FeO	7.24	7.31	6.20	7.50	6.15	7.38	7.73	6.50
MnO	0.14	0.13	0.14	0.13	0.14	0.13	0.13	0.13
MgO	13.19	11.99	10.44	12.02	10.82	11.00	9.22	8.06
CaO	9.44	9.90	10.79	9.83	10.44	10.26	10.86	11.48
Na2O	1.01	1.00	1.11	1.01	1.03	1.04	1.14	1.17
K2O	0.33	0.33	0.37	0.32	0.36	0.34	0.36	0.40
P2O5	nd	0.02	nd	0.01	0.08	nd	nd	0.01
total=	98.45	98.60	98.90	99.00	98.48	98.84	97.80	98.21
qtz	7.57	8.68	10.51	8.52	10.97	9.09	8.35	11.33
en	26.26	23.31	18.76	23.60	20.26	20.87	16.58	13.29
fs	9.83	9.62	7.45	9.96	7.75	9.33	9.20	7.14
cen	6.59	6.55	7.24	6.32	6.70	6.52	6.38	6.78
cfs	2.47	2.70	2.87	2.67	2.56	2.92	3.54	3.64
cwo	9.80	9.96	10.91	9.66	10.00	10.12	10.50	11.06
or	1.96	1.98	2.16	1.90	2.10	1.99	2.11	2.38
an	23.37	25.08	27.42	25.52	27.19	26.66	28.72	30.37
ab	8.50	8.42	9.39	8.50	8.69	8.77	9.60	9.87
mag	1.89	2.04	1.94	2.05	1.83	2.32	2.55	2.06
ilm	0.20	0.22	0.25	0.26	0.23	0.26	0.27	0.27
ap	-	0.06	-	0.03	0.23	-	-	0.03
temp	1309.00	1290.00	1266.00	1292.00	1275.00	1273.00	1237.00	1215.00
time	23.50	24.00	24.00	48.00	48.00	48.00	48.00	48.00

89 C2 3:681 -GL4,00KB,1309C,23.5HR,F-6.55,+GL+OPXB
90 C2 3:684 -GL4,00KB,1290C,24HR,F-6.70,+GL+OPXB
91 C2 3:692 -GL7,00KB,1266C,24HR,F-6.90,+GL+OPXB
92 C2MET 3:752 -GL4,00KB,1292C,48HR,F-6.70,+GL+OPXB
93 C2MET 3:734 -GL4,00KB,1275C,48HR,F-6.85,+GL+OPXB+SP
94 C2MET 3:751 -GL4,00KB,1273C,48HR,F-6.70,+GL+OPXB
95 C2MET 3:750 -GL4,00KB,1237C,48HR,F-7.10,+GL+OPXB
96 C2MET 3:735 -GL4,00KB,1215C,48HR,F-7.60,+GL+OPXB+PIG+SP

TABLE AIV.2

	97	98	99	100	101	102	103	104
SiO2	55.86	56.34	58.18	58.53	58.16	58.35	58.45	58.59
TiO2	0.15	0.14	0.14	0.15	0.14	0.15	0.16	0.14
Al2O3	13.80	15.07	11.74	12.08	12.36	12.85	14.64	12.21
Fe2O3	1.58	1.50	1.24	1.30	1.44	1.49	1.47	1.21
FeO	6.79	6.29	6.06	5.91	6.06	6.18	5.35	5.77
MnO	0.12	0.12	0.15	0.13	0.13	0.14	0.11	0.14
MgO	7.06	7.47	11.17	9.93	9.13	8.25	5.38	10.31
CaO	10.89	10.84	7.27	7.37	7.60	7.78	8.45	7.37
Na2O	1.37	1.40	1.86	2.08	2.17	2.32	2.72	1.99
K2O	0.50	0.45	1.16	1.27	1.33	1.40	1.63	1.22
P2O5	0.07	nd	0.03	0.04	0.08	0.11	0.06	nd
total=	98.19	99.62	99.01	98.78	98.60	99.02	98.42	98.96
qtz	12.37	11.80	9.51	10.21	9.98	10.03	10.57	10.20
en	11.90	13.45	23.43	20.19	18.15	16.04	8.92	21.23
fs	7.54	7.45	8.55	7.98	7.94	7.92	5.69	7.95
cen	5.69	5.15	4.40	4.54	4.60	4.51	4.49	4.44
cfs	3.60	2.85	1.61	1.79	2.01	2.22	2.87	1.66
cwo	9.75	8.47	6.50	6.83	7.09	7.17	7.72	6.60
or	2.94	2.66	6.85	7.49	7.86	8.27	9.63	7.19
an	30.04	33.51	20.25	19.88	20.08	20.53	22.91	20.77
ab	11.59	11.85	15.76	17.60	18.34	19.61	23.02	16.88
mag	2.29	2.17	1.80	1.89	2.10	2.16	2.13	1.76
ilm	0.28	0.27	0.26	0.28	0.26	0.28	0.30	0.28
ap	0.22	-	0.09	0.11	0.23	0.32	0.19	-
temp	1184.00	1172.00	1309.00	1288.00	1270.00	1252.00	1181.00	1292.00
time	48.00	93.00	24.00	23.75	23.75	23.00	48.00	48.00

97 C2MET 3:742 -GL3,00KB,1184C,48HR,F-7.90,+GL+OPXB+PIG
98 C2M 3:776 -GL3,00KB,1172C,93HR,F-7.90,+GL+OPXB+CPX+PLAG
99 C5 3:682 -GL3,00KB,1309C,24HR,F-6.50,+GL+OL
100 C5 3:685 -GL3,00KB,1288C,23.75HR,F-6.70,+GL+OL
101 C5 3:694 -GL3,00KB,1270C,23.75HR,F-6.80,+GL+OPXB+SP
102 C5 3:695 -GL3,00KB,1252C,23HR,F-7.05,+GL+OPXB
103 C5 3:744 -GL3,00KB,1181C,48HR,F-7.90,+GL+OPXB
104 C5MET 3:752 -GL4,00KB,1292C,48HR,F-6.70,+GL+OL+SP

	105	106	107	108	109	110	111	112
SiO2	59.60	57.13	57.45	59.28	59.31	57.61	59.44	57.48
TiO2	0.13	0.15	0.16	0.19	0.15	0.14	0.20	0.14
Al2O3	12.67	12.60	13.44	14.31	14.00	13.95	14.18	12.83
Fe2O3	1.11	1.40	1.52	1.26	1.30	1.35	1.44	1.39
FeO	4.92	5.85	5.86	5.12	5.24	5.30	5.18	6.46
MnO	0.12	0.15	0.15	0.12	0.11	0.11	0.12	0.17
MgO	9.44	9.36	7.57	6.41	6.65	6.62	5.77	9.93
CaO	7.66	7.58	7.94	8.48	8.29	8.02	7.53	8.27
Na2O	2.06	2.11	2.34	1.85	2.56	2.63	2.60	1.80
K2O	1.25	1.30	1.43	1.21	1.52	1.55	1.89	0.45
P2O5	0.06	0.03	nd	0.12	0.18	0.02	nd	nd
total=	99.03	97.67	97.86	98.36	99.32	97.29	98.35	98.92
qtz	12.29	8.94	9.51	15.79	11.45	9.38	12.05	11.19
en	18.98	18.85	14.31	12.35	12.04	11.86	10.36	20.55
fs	6.55	7.77	7.23	6.41	6.18	6.18	5.93	8.96
cen	4.54	4.47	4.54	3.61	4.51	4.63	4.00	4.18
cfs	1.57	1.84	2.29	1.88	2.32	2.41	2.29	1.82
cwo	6.63	6.79	7.27	5.83	7.26	7.47	6.64	6.44
or	7.40	7.66	8.42	7.15	8.99	9.18	11.15	2.65
an	21.64	21.08	21.96	27.14	22.20	21.68	21.44	25.60
ab	17.41	17.87	19.82	15.70	21.70	22.23	22.02	15.25
mag	1.61	2.03	2.21	1.83	1.88	1.95	2.09	2.02
ilm	0.25	0.29	0.30	0.35	0.29	0.27	0.38	0.28
ap	0.17	0.09	-	0.35	0.54	0.07	-	-
temp	1275.00	1273.00	1237.00	1224.00	1215.00	1184.00	1156.00	1270.00
time	48.00	48.00	48.00	477.00	48.00	48.00	121.00	23.75

105 C5 3:734 -GL4,00KB,1275C,48HR,F-6.85,+GL+OPXB+SP
106 C5MET 3:751 -GL4,00KB,1273C,48HR,F-6.70,+GL+OL+OPXB
107 C5MET 3:750 -GL4,00KB,1237C,48HR,F-7.10,+GL+OPXB
108 C5MET 3:770 -GL4,00KB,1224C,477HR,F-7.40,+GL+OPXB
109 C5 3:735 -GL4,00KB,1215C,48HR,F-7.60,+GL+OPXB+PIG
110 C5 3:742 -GL3,00KB,1184C,48HR,F-7.90,+GL+PIG+OPXB
111 C5MET 3:758 -GL4,00KB,1156C,121HR,F-8.15,+GL+OPXB+PLAG
112 C11 3:694 -GL6,00KB,1270C,23.75HR,F-6.80,+GL+OPXB+SP

TABLE AIV.2

	113	114	115	116	117
SiO2	57.80	58.40	57.63	57.96	62.93
TiO2	0.16	0.15	0.15	0.16	0.24
Al2O3	13.52	12.93	13.47	15.57	13.89
Fe2O3	1.43	1.04	1.62	1.34	1.43
FeO	6.55	5.02	6.83	5.47	4.81
MnO	0.17	0.14	0.17	0.13	0.15
MgO	8.84	10.19	8.16	5.63	4.28
CaO	8.55	8.43	8.69	9.81	8.78
Na2O	1.88	1.66	1.84	2.15	2.23
K2O	0.47	0.42	0.46	0.53	0.75
total=	99.36	98.40	99.01	98.74	99.50
qtz	11.91	13.36	12.73	13.73	22.34
en	18.00	20.97	16.29	9.80	6.45
fs	8.91	6.92	9.03	6.23	4.56
cen	4.02	4.40	4.05	4.22	4.20
cfs	1.99	1.45	2.24	2.68	2.97
cwo	6.41	6.37	6.66	7.25	7.47
or	2.78	2.49	2.70	3.12	4.45
an	27.05	26.57	27.14	31.29	25.67
ab	15.93	14.06	15.54	18.18	18.84
mag	2.07	1.51	2.35	1.94	2.07
ilm	0.30	0.29	0.28	0.31	0.46
temp	1252.00	1275.00	1237.00	1184.00	1156.00
time	23.00	48.00	48.00	48.00	121.00

113 C11 3:695 -GL4,00KB,1252C,23HR,F-7.05,+GL+OPXB+SP
114 C11MET 3:734 -GL4,00KB,1275C,48HR,F-6.85,+GL+SP
115 C11MET 3:750 -GL4,00KB,1237C,48HR,F-7.10,+GL+OPXB+SP
116 C11MET 3:742 -GL5,00KB,1184C,48HR,F-7.90,+GL+OPXB+PLAG+SP
117 C11MET 3:758 -GL3,00KB,1156C,121HR,F-8.15,+GL+OPXB+PLAG

TABLE AIV.3A

	1	2	3	4	5	6	7	8
SiO2	54.99	54.78	53.11	54.03	53.93	54.29	53.87	54.49
TiO2	1.01	1.06	1.14	1.19	1.22	1.32	1.44	1.42
Al2O3	9.50	10.04	10.58	11.25	11.43	12.93	13.18	14.06
Fe2O3	1.63	1.83	1.92	2.01	1.75	1.85	2.11	1.51
FeO	9.14	9.33	9.20	9.21	9.18	7.78	8.02	6.60
MnO	0.15	0.16	0.19	0.18	0.15	0.14	0.15	0.13
MgO	12.70	11.66	10.34	9.54	9.49	7.74	6.89	7.24
CaO	7.87	8.20	8.62	8.73	9.13	9.57	9.65	10.03
Na2O	1.58	1.64	1.58	1.80	1.73	2.20	2.24	2.25
K2O	0.32	0.33	0.38	0.42	0.37	0.46	0.46	0.46
P2O5	nd	0.02	0.05	0.02	0.00	0.05	nd	0.03
total=	98.88	99.04	97.12	98.38	98.39	98.36	98.01	98.20
qtz	6.96	7.28	7.20	7.56	7.48	7.88	8.18	8.35
en	25.92	23.38	20.20	18.29	17.90	13.46	11.47	12.07
fs	11.51	11.40	10.81	10.49	10.36	7.56	7.28	5.87
cen	5.70	5.66	5.56	5.48	5.74	5.81	5.69	5.96
cfs	2.53	2.76	2.97	3.14	3.32	3.27	3.61	2.90
cwo	8.83	8.97	9.05	9.11	9.57	9.60	9.76	9.45
or	1.92	1.95	2.23	2.50	2.16	2.75	2.75	2.72
an	17.88	19.05	20.67	21.35	22.31	24.01	24.53	26.90
ab	13.34	13.88	13.34	15.26	14.68	18.66	18.97	19.04
mag	2.36	2.65	2.79	2.91	2.54	2.69	3.05	2.19
ilm	1.92	2.02	2.17	2.26	2.32	2.52	2.73	2.69
ap	-	0.05	0.16	0.05	0.01	0.16	-	0.08
temp	1307.00	1290.00	1266.00	1252.00	1245.00	1206.00	1194.00	1184.00
time	24.00	24.00	24.00	24.00	48.00	48.00	96.00	48.00

1	17M	3:677 -GL4,00KB,1307C,24HR,F-6.65,+GL+OL+OPXB+SP
2	17M	3:684 -GL4,00KB,1290C,24HR,F-6.70,+GL+OL+OPXB+SP
3	17M	3:692 -GL3,00KB,1266C,24HR,F-6.90,+GL+OPXB+OL+SP
4	17M	3:700 -GL3,00KB,1252C,24HR,F-7.05,+GL+OPXB+SP+PIG+OL
5	17M	3:726 -GL4,00KB,1245C,48HR,F-7.40,+GL+OPXB+OL+SP
6	17M	3:745 -GL4,00KB,1206C,48HR,F-7.60,+GL+OPXB+PIG+SP
7	17M	3:775 -GL4,00KB,1194C,96HR,F-7.60,+GL+OPXB+PIG
8	17M	3:743 -GL4,00KB,1184C,48HR,F-8.00,+GL+OPXB+PIG+SP

	9	10	11	12	13	14	15	16
SiO2	59.24	59.88	59.66	60.97	57.16	57.95	57.93	56.76
TiO2	1.01	1.07	1.09	1.12	1.00	1.05	1.12	0.91
Al2O3	9.95	10.50	10.68	11.14	8.36	8.97	9.44	11.07
Fe2O3	1.56	1.66	1.71	1.33	1.53	1.62	1.83	1.52
FeO	6.66	6.48	6.36	5.60	7.20	7.06	6.92	6.78
MnO	0.13	0.13	0.14	0.11	0.14	0.14	0.14	0.13
MgO	9.93	8.70	7.89	7.60	12.10	10.67	9.43	8.33
CaO	6.79	7.02	7.15	7.52	7.86	8.32	8.55	9.72
Na2O	3.04	3.24	3.45	3.05	2.32	2.41	2.74	2.39
K2O	0.19	0.19	0.19	0.20	0.10	0.11	0.12	0.11
P2O5	nd	nd	0.02	0.01	0.07	0.03	0.07	nd
total=	98.50	98.88	98.34	98.64	97.84	98.33	98.28	97.73
qtz	11.63	12.80	12.70	16.19	9.52	11.23	11.27	10.94
en	18.95	15.85	13.68	13.09	22.64	18.82	15.59	13.05
fs	7.28	6.58	6.07	5.20	7.94	7.20	6.38	6.25
cen	5.79	5.83	5.98	5.85	7.50	7.75	7.90	7.69
cfs	2.22	2.42	2.65	2.32	2.63	2.97	3.23	3.69
cwo	8.65	8.88	9.25	8.81	10.99	11.58	11.98	12.15
or	1.10	1.12	1.12	1.18	0.59	0.62	0.68	0.65
an	12.94	13.56	13.11	16.11	12.10	13.31	13.12	19.14
ab	25.74	27.39	29.17	25.81	19.63	20.43	23.16	20.24
mag	2.26	2.41	2.48	1.92	2.22	2.35	2.65	2.20
ilm	1.93	2.03	2.08	2.13	1.90	1.99	2.12	1.73
ap	-	-	0.07	0.03	0.20	0.09	0.22	-
temp	1290.00	1266.00	1252.00	1245.00	1309.00	1288.00	1265.00	1245.00
time	24.00	24.00	24.00	48.00	23.50	23.75	25.00	48.00

9	170	3:684 -GL5,00KB,1290C,24HR,F-6.70,+GL+OPXB+SP
10	170	3:692 -GL4,00KB,1266C,24HR,F-6.90,+GL+OPXB+SP
11	170	3:700 -GL3,00KB,1252C,24HR,F-7.05,+GL+OPXB+PIG+SP
12	170	3:726 -GL4,00KB,1245C,48HR,F-7.40,+GL+OPXB+SP
13	120	3:681 -GL4,00KB,1309C,23.5HR,F-6.55,+GL+OPXB+SP
14	120	3:685 -GL4,00KB,1288C,23.75HR,F-6.75,+GL+OPXB+SP
15	120	3:693 -GL4,00KB,1265C,25HR,F-6.85,+GL+OPXB+PIG+SP
16	120	3:726 -GL4,00KB,1245C,48HR,F-7.40,+GL+OPXB+SP

TABLE AIV.3A

	17	18	19	20	21	22	23	24
SiO2	59.76	57.10	55.31	53.15	53.89	59.35	59.05	60.49
TiO2	1.30	0.50	0.71	0.19	0.70	0.10	0.10	0.11
Al2O3	11.07	15.03	13.93	14.16	14.50	9.03	9.65	10.38
Fe2O3	1.58	1.70	2.20	1.56	1.50	1.45	1.61	1.39
FeO	5.74	6.36	8.23	7.00	6.98	6.94	7.44	5.84
MnO	0.11	0.14	0.19	0.17	0.17	0.20	0.19	0.19
MgO	6.62	6.02	5.52	8.37	8.11	11.45	10.23	9.21
CaO	9.42	8.06	9.28	11.75	9.77	8.16	8.37	8.93
Na2O	1.97	2.68	2.78	1.62	1.56	1.49	1.51	1.53
K2O	0.27	1.22	0.70	0.15	0.62	0.49	0.50	0.52
P2O5	0.25	1.49	nd	nd	0.07	0.00	0.00	0.01
total=	98.10	100.30	98.84	98.12	97.87	98.65	98.66	98.61
qtz	19.98	12.07	7.55	6.12	8.48	14.10	14.55	17.58
en	9.99	14.50	8.92	13.90	15.80	21.93	19.31	16.31
fs	4.42	9.41	8.10	7.72	8.38	9.04	9.49	6.94
cen	6.49	0.48	4.82	6.95	4.41	6.58	6.16	6.62
cfs	2.87	0.31	4.37	3.86	2.34	2.71	3.03	2.82
cwo	10.04	0.83	9.43	11.43	7.17	10.00	9.79	10.14
or	1.63	7.18	4.14	0.89	3.65	2.88	2.98	3.10
an	20.55	25.41	23.46	30.91	30.72	16.51	18.06	19.92
ab	16.69	22.68	23.52	13.73	13.24	12.61	12.75	12.92
mag	2.29	2.46	3.19	2.26	2.17	2.10	2.34	2.01
ilm	2.47	0.94	1.35	0.36	1.34	0.19	0.19	0.21
ap	0.76	4.47	-	-	0.20	0.01	0.01	0.04
temp	1224.00	1194.00	1156.00	1206.00	1224.00	1309.00	1292.00	1275.00
time	477.00	96.00	48.00	48.00	477.00	23.50	48.00	48.00

17 120 3:770 -GL4,00KB,1224C,477HR,F-7.40,+GL+OPXB+PIG+SP
18 B5 3:775 -GL4,00KB,1194C,96HR,F-7.60,+GL+OPXB
19 B5 3:756 -GL5,00KB,1156C,48HR,F-8.15,+GL+OPXB+CPX+PLAG
20 K1 3:745 -GL3,00KB,1206C,48HR,F-7.60,+GL+OPXB+SP
21 295 3:770 -GL4,00KB,1224C,477HR,F-7.40,+GL+OPXB+OL+SP
22 M1 3:681 -GL4,00KB,1309C,23.5HR,F-6.55,+GL+OPXB
23 M1MET 3:752 -GL4,00KB,1292C,48HR,F-6.70,+GL+OPXB
24 M1MET 3:734 -GL1,00KB,1275C,48HR,F-6.85,+GL+OPXB

	25	26	27	28	29	30	31	32
SiO2	59.65	59.12	61.65	55.29	56.05	59.60	57.13	57.45
TiO2	0.12	0.13	0.14	0.13	0.12	0.13	0.15	0.16
Al2O3	10.20	10.93	11.69	11.35	12.04	12.67	12.60	13.44
Fe2O3	1.89	2.07	1.42	1.41	1.26	1.11	1.40	1.52
FeO	7.62	7.85	5.28	7.50	6.15	4.92	5.85	5.86
MnO	0.19	0.18	0.17	0.13	0.14	0.12	0.15	0.15
MgO	9.25	7.66	6.38	12.02	10.82	9.44	9.36	7.57
CaO	8.60	9.17	9.73	9.83	10.44	7.66	7.58	7.94
Na2O	1.55	1.72	1.50	1.01	1.03	2.06	2.11	2.34
K2O	0.50	0.58	0.58	0.32	0.36	1.25	1.30	1.43
P2O5	0.09	0.02	0.04	0.01	0.08	0.06	0.03	nd
total=	99.66	99.42	98.57	99.00	98.48	99.03	97.67	97.86
qtz	15.95	15.47	21.86	8.52	10.97	12.29	8.94	9.51
en	17.30	13.14	9.62	23.60	20.26	18.98	18.85	14.31
fs	9.44	8.83	5.21	9.96	7.75	6.55	7.77	7.23
cen	5.74	5.94	6.26	6.32	6.70	4.54	4.47	4.54
cfs	3.13	3.99	3.39	2.67	2.56	1.57	1.84	2.29
cwo	9.40	10.39	10.23	9.66	10.00	6.63	6.79	7.27
or	2.97	3.41	3.46	1.90	2.10	7.40	7.66	8.42
an	19.37	20.42	23.45	25.52	27.19	21.64	21.08	21.96
ab	13.14	14.53	12.67	8.50	8.69	17.41	17.87	19.82
mag	2.74	3.00	2.06	2.05	1.83	1.61	2.03	2.21
ilm	0.23	0.24	0.27	0.26	0.23	0.25	0.29	0.30
ap	0.28	0.06	0.10	0.03	0.23	0.17	0.09	-
temp	1273.00	1237.00	1224.00	1292.00	1275.00	1275.00	1273.00	1237.00
time	48.00	48.00	477.00	48.00	48.00	48.00	48.00	48.00

25 M1MET 3:751 -GL3,00KB,1273C,48HR,F-6.70,+GL+OPXB
26 M1MET 3:750 -GL3,00KB,1237C,48HR,F-7.10,+GL+OPXB
27 M1MET 3:770 -GL4,00KB,1224C,477HR,F-7.40,+GL+OPXB
28 C2MET 3:752 -GL4,00KB,1292C,48HR,F-6.70,+GL+OPXB
29 C2MET 3:734 -GL4,00KB,1275C,48HR,F-6.85,+GL+OPXB+SP
30 C5 3:734 -GL4,00KB,1275C,48HR,F-6.85,+GL+OPXB+SP
31 C5MET 3:751 -GL4,00KB,1273C,48HR,F-6.70,+GL+OL+OPXB
32 C5MET 3:750 -GL4,00KB,1237C,48HR,F-7.10,+GL+OPXB

TABLE AIV.3A

	33	34	35	36	37	38	39	40
SiO2	59.28	59.31	57.61	57.63	57.96	57.29	60.52	60.88
TiO2	0.19	0.15	0.14	0.15	0.16	1.38	1.11	1.12
Al2O3	14.31	14.00	13.95	13.47	15.57	10.91	10.29	10.43
Fe2O3	1.26	1.30	1.35	1.62	1.34	0.16	0.23	0.21
FeO	5.12	5.24	5.30	6.83	5.47	5.39	7.32	6.58
MnO	0.12	0.11	0.11	0.17	0.13	0.16	0.12	0.10
MgO	6.41	6.65	6.62	8.16	5.63	11.58	8.80	9.11
CaO	8.48	8.29	8.02	8.69	9.81	8.55	7.09	7.09
Na2O	1.85	2.56	2.63	1.84	2.15	1.97	2.58	2.49
K2O	1.21	1.52	1.55	0.46	0.53	0.33	0.17	0.20
P2O5	0.12	0.18	0.02	nd	nd	0.12	nd	nd
total=	98.36	99.32	97.29	99.01	98.74	97.83	98.23	98.21
qtz	15.79	11.45	9.38	12.73	13.73	10.49	15.40	16.15
en	12.35	12.04	11.86	16.29	9.80	22.40	16.99	17.73
fs	6.41	6.18	6.18	9.03	6.23	6.03	9.03	8.00
cen	3.61	4.51	4.63	4.05	4.22	6.45	4.92	4.97
cfs	1.88	2.32	2.41	2.24	2.68	1.74	2.62	2.24
cwo	5.83	7.26	7.47	6.66	7.25	8.99	8.00	7.73
or	7.15	8.99	9.18	2.70	3.12	1.96	1.00	1.21
an	27.14	22.20	21.68	27.14	31.29	19.94	15.99	16.64
ab	15.70	21.70	22.23	15.54	18.18	16.69	21.83	21.11
mag	1.83	1.88	1.95	2.35	1.94	0.24	0.33	0.30
ilm	0.35	0.29	0.27	0.28	0.31	2.62	2.10	2.13
ap	0.35	0.54	0.07	-	-	0.34	-	-
temp	1224.00	1215.00	1184.00	1237.00	1184.00	1307.00	1297.00	1257.00
time	477.00	48.00	48.00	48.00	48.00	24.50	22.00	48.00

33 C5MET 3:770 -GL4,00KB,1224C,477HR,F-7.40,+GL+OPXB
34 C5 3:735 -GL4,00KB,1215C,48HR,F-7.60,+GL+OPXB+PIG
35 C5 3:742 -GL3,00KB,1184C,48HR,F-7.90,+GL+PIG+OPXB
36 C11MET 3:750 -GL4,00KB,1237C,48HR,F-7.10,+GL+OPXB+SP
37 C11MET 3:742 -GL5,00KB,1184C,48HR,F-7.90,+GL+OPXB+PLAG+SP
38 17M 5:750 -GL4,00KB,1307C,24.5HR,F-10.45,+GL+OPXB+OL
39 170 5:761 -GL2,00KB,1297C,22HR,F-10.70,+GL+OPXB
40 170 5:762 -GL1,00KB,1257C,48HR,F-11.10,+GL+OPXB+PIG

	41	42	43	44	45	46	47	48
SiO2	59.97	58.78	57.98	55.07	55.66	55.21	57.68	54.53
TiO2	1.14	1.08	1.13	0.66	1.10	1.14	1.24	1.04
Al2O3	9.50	8.78	9.32	12.98	10.10	10.25	11.22	9.46
Fe2O3	0.18	0.21	0.25	0.23	0.74	0.69	0.40	0.81
Cr2O3	nd	nd	nd	nd	nd	nd	0.05	nd
FeO	5.28	7.24	8.02	7.89	8.44	7.85	4.31	9.31
MnO	0.12	0.12	0.14	0.17	0.15	0.16	0.16	0.15
MgO	10.76	11.48	9.77	8.71	12.28	12.05	11.76	12.56
CaO	8.77	8.31	8.55	8.94	8.23	8.41	9.17	7.80
Na2O	1.91	2.03	2.43	1.94	1.20	1.13	0.82	1.54
K2O	0.18	0.10	0.10	0.64	0.28	0.27	0.16	0.31
P2O5	0.00	nd	0.02	0.04	nd	nd	nd	nd
total=	97.82	98.14	97.72	97.26	98.19	97.18	96.98	97.51
qtz	15.50	12.13	10.82	7.33	9.82	10.25	16.58	6.61
en	18.93	21.22	17.14	17.00	25.32	24.61	23.32	25.81
fs	5.58	8.60	9.09	10.60	11.04	10.05	4.66	12.38
cen	7.87	7.37	7.20	4.69	5.28	5.40	5.96	5.47
cfs	2.32	2.98	3.82	2.93	2.30	2.21	1.19	2.62
cwo	11.15	11.15	11.69	8.01	8.13	8.20	7.95	8.63
or	1.08	0.59	0.60	3.78	1.64	1.60	0.95	1.83
an	16.80	14.52	14.21	24.82	21.37	22.09	26.46	18.00
ab	16.16	17.22	20.56	16.41	10.13	9.60	6.93	13.01
mag	0.25	0.31	0.36	0.33	1.07	1.00	0.58	1.18
ilm	2.17	2.05	2.15	1.25	2.10	2.17	2.35	1.97
ap	0.01	-	0.07	0.12	-	-	-	-
chr	-	-	-	-	-	-	0.07	-
temp	1307.00	1325.00	1297.00	1257.00	1315.00	1315.00	1315.00	1315.00
time	24.50	23.00	22.00	48.00	72.00	72.00	72.00	24.00

41 120 5:750 -GL3,00KB,1307C,24.5HR,F-10.45,+GL+OPXB
42 120 5:760 -GL4,00KB,1325C,23HR,F-10.40,+GL+OPXB
43 120 5:761 -GL5,00KB,1297C,22HR,F-10.70,+GL+OPXB+PIG
44 295 5:762 -GL3,00KB,1257C,48HR,F-11.10,+GL+OL+OPXB
45 17M 4:239:2 -GL9,00KB,1315C,72HR,F-8.00,+GL+OPXB
46 17M 4:239:3 -GL7,00KB,1315C,72HR,F-8.00,+GL+OPXB
47 17M 4:239:4 -GL8,00KB,1315C,72HR,F-8.00,+GL+OPXB
48 17M 4:245 -GL6,00KB,1315C,24HR,F-8.00,+GL+OPXB+OL

TABLE AIV.3A

	49	50	51	52	53	54	55
SiO2	54.13	56.50	56.90	55.57	60.26	58.66	58.14
TiO2	1.03	1.11	1.13	1.12	1.06	1.03	1.07
Al2O3	9.61	9.98	10.14	9.81	9.56	8.54	8.94
Fe2O3	0.72	0.69	0.66	0.95	0.79	0.80	0.89
Cr2O3	nd	nd	nd	0.27	0.22	0.30	0.20
FeO	8.49	7.97	7.68	9.61	6.65	7.19	7.64
MnO	0.15	0.16	0.16	0.22	0.16	0.12	0.12
MgO	12.88	13.00	12.89	11.38	9.94	11.82	10.64
CaO	7.66	8.26	8.24	8.24	6.80	8.02	8.43
Na2O	1.45	1.25	1.08	1.39	2.86	2.30	2.44
K2O	0.32	0.28	0.26	0.30	0.15	0.05	0.02
total=	96.44	99.19	99.12	98.87	98.45	98.84	98.53
qtz	6.83	9.75	11.37	9.31	13.59	11.08	10.73
en	26.83	26.76	26.80	22.93	19.01	21.87	18.82
fs	11.36	10.36	10.00	12.47	7.76	8.22	8.34
cen	5.25	5.62	5.29	5.41	5.76	7.56	7.68
cfs	2.22	2.18	1.98	2.95	2.35	2.84	3.40
cwo	8.03	8.42	7.87	8.86	8.73	11.25	11.88
or	1.89	1.64	1.52	1.77	0.89	0.27	0.15
an	18.76	20.81	22.04	19.66	12.81	12.85	13.35
ab	12.27	10.55	9.16	11.72	24.17	19.47	20.65
mag	1.05	1.00	0.96	1.38	1.15	1.16	1.29
ilm	1.95	2.10	2.14	2.13	2.01	1.96	2.03
chr	-	-	-	0.40	0.33	0.44	0.30
temp	1316.00	1316.00	1316.00	1298.00	1298.00	1314.00	1298.00
time	48.00	102.00	102.00	5.00	5.00	5.00	5.00

49	17M	4:248	-GL6,00KB,1316C,48HR,F-8.00,+GL+OPXB+OPXA+OL
50	17M	4:249PT	-GL3,00KB,1316C,102HR,F-8.00,+GL+OPXB
51	17M	4:249PTFE	-GL4,00KB,1316C,102HR,F-8.00,+GL+OPXB
52	17M	4:217	-GL3,00KB,1298C,05HR,F-8.00,+GL+SP+OL+OPXB
53	170	4:217	-GL3,00KB,1298C,05HR,F-8.00,+GL+SP+OPXB
54	120	4:216	-GL8,00KB,1314C,05HR,F-7.85,+GL+SP+OPXB+PIG
55	120	4:217	-GL4,00KB,1298C,05HR,F-8.00,+GL+SP+OPXB+PIG

TABLE AIV.3B

	1	2	3	4	5	6	7	8
SiO2	59.07	55.23	59.85	58.66	58.14	57.60	58.06	54.03
TiO2	1.26	1.19	1.14	1.03	1.07	1.09	1.11	1.19
Al2O3	10.40	10.43	10.64	8.54	8.94	9.46	9.34	11.25
Fe2O3	0.26	1.04	0.87	0.80	0.89	0.94	0.95	2.01
Cr2O3	nd	0.22	0.20	0.30	0.20	0.24	0.28	nd
FeO	7.40	9.90	6.93	7.19	7.64	7.70	7.50	9.21
MnO	0.11	0.16	0.13	0.12	0.12	0.07	0.10	0.18
MgO	7.76	10.28	8.97	11.82	10.64	9.86	9.51	9.54
CaO	9.01	8.44	7.07	8.02	8.43	8.55	8.69	8.73
Na2O	2.53	1.72	3.09	2.30	2.44	2.60	2.58	1.80
K2O	0.12	0.33	0.21	0.05	0.02	0.09	0.10	0.42
P2O5	nd	nd	nd	nd	nd	nd	nd	0.02
total=	97.90	98.93	99.10	98.84	98.53	98.20	98.22	98.38
qtz	13.85	8.19	12.27	11.08	10.73	9.96	11.08	7.56
en	12.37	20.16	16.86	21.87	18.82	17.00	15.87	18.29
fs	7.35	12.34	7.82	8.22	8.34	8.09	7.60	10.49
cen	6.96	5.44	5.48	7.56	7.68	7.56	7.80	5.48
cfs	4.14	3.33	2.54	2.84	3.40	3.60	3.74	3.14
cwo	11.70	9.23	8.57	11.25	11.88	11.91	12.32	9.11
or	0.69	1.95	1.24	0.27	0.15	0.53	0.57	2.50
an	16.67	19.76	14.54	12.85	13.35	13.89	13.60	21.35
ab	21.41	14.55	26.15	19.47	20.65	21.97	21.86	15.26
mag	0.37	1.51	1.26	1.16	1.29	1.36	1.38	2.91
ilm	2.39	2.25	2.17	1.96	2.03	2.07	2.10	2.26
ap	-	-	-	-	-	-	-	0.05
chr	-	0.32	0.29	0.44	0.30	0.35	0.42	-
temp	1257.00	1282.00	1274.00	1314.00	1298.00	1281.00	1274.00	1252.00
time	48.00	5.00	5.00	5.00	5.00	5.00	5.00	24.00

1	120	5:762 -GL5,00KB,1257C,48HR,F-11.10,+GL+OPXB+PIG
2	17M	4:219 -GL3,00KB,1282C,05HR,F-8.15,+GL+SP+OL+PIG
3	170	4:220 -GL1,00KB,1274C,05HR,F-8.20,+GL+SP+PIG
4	120	4:216 -GL8,00KB,1314C,05HR,F-7.85,+GL+SP+OPXB+PIG
5	120	4:217 -GL4,00KB,1298C,05HR,F-8.00,+GL+SP+OPXB+PIG
6	120	4:219 -GL4,00KB,1281C,05HR,F-8.15,+GL+SP+PIG
7	120	4:220 -GL3,00KB,1274C,05HR,F-8.20,+GL+SP+PIG
8	17M	3:700 -GL3,00KB,1252C,24HR,F-7.05,+GL+OPXB+SP+PIG+OL

	9	10	11	12	13	14	15	16
SiO2	54.29	53.87	54.49	55.25	59.95	61.14	59.62	63.77
TiO2	1.32	1.44	1.42	1.69	1.10	1.19	1.20	1.31
Al2O3	12.93	13.18	14.06	13.58	11.20	11.93	12.07	13.67
Fe2O3	1.85	2.11	1.51	1.96	1.76	1.57	1.53	1.42
FeO	7.78	8.02	6.60	7.57	6.23	5.31	5.43	4.70
MnO	0.14	0.15	0.13	0.14	0.13	0.10	0.09	0.08
MgO	7.74	6.89	7.24	6.37	7.17	5.91	5.22	4.33
CaO	9.57	9.65	10.03	8.89	7.37	7.47	7.59	6.48
Na2O	2.20	2.24	2.25	2.31	3.51	3.73	3.75	3.32
K2O	0.46	0.46	0.46	0.61	0.20	0.21	0.19	0.24
P2O5	0.05	nd	0.03	0.03	0.03	0.02	nd	0.01
total=	98.36	98.01	98.20	98.41	98.66	98.56	96.69	99.32
qtz	7.88	8.18	8.35	10.72	13.35	15.54	14.67	23.02
en	13.46	11.47	12.07	11.20	11.99	8.89	7.32	8.08
fs	7.56	7.28	5.87	6.88	5.66	4.03	3.88	4.07
cen	5.81	5.69	5.96	4.66	5.86	5.83	5.69	2.70
cfs	3.27	3.61	2.90	2.87	2.77	2.64	3.02	1.36
cwo	9.60	9.76	9.45	7.92	9.22	9.07	9.23	4.32
or	2.75	2.75	2.72	3.59	1.18	1.22	1.12	1.39
an	24.01	24.53	26.90	24.90	14.24	15.18	15.54	21.69
ab	18.66	18.97	19.04	19.52	29.68	31.59	31.73	28.11
mag	2.69	3.05	2.19	2.85	2.55	2.27	2.22	2.06
ilm	2.52	2.73	2.69	3.22	2.09	2.26	2.28	2.49
ap	0.16	-	0.08	0.09	0.09	0.05	-	0.03
temp	1206.00	1194.00	1184.00	1155.00	1235.00	1206.00	1184.00	1155.00
time	48.00	96.00	48.00	95.00	24.00	48.00	48.00	95.00

9	17M	3:745 -GL4,00KB,1206C,48HR,F-7.60,+GL+OPXB+PIG+SP
10	17M	3:775 -GL4,00KB,1194C,96HR,F-7.60,+GL+OPXB+PIG
11	17M	3:743 -GL4,00KB,1184C,48HR,F-8.00,+GL+OPXB+PIG+SP
12	17M	3:757 -GL4,00KB,1155C,95HR,F-8.15,+GL+PIG+SP
13	170	3:706 -GL3,00KB,1235C,24HR,F-7.20,+GL+PIG+SP
14	170	3:745 -GL3,00KB,1206C,48HR,F-7.60,+GL+PIG+SP
15	170	3:743 -GL1,00KB,1184C,48HR,F-8.00,+GL+PIG+SP
16	170	3:757 -GL5,00KB,1155C,95HR,F-8.15,+GL+PIG+CPX

TABLE AIV.3B

	17	18	19	20	21	22	23	24
SiO2	57.93	58.32	59.01	59.76	59.46	61.01	60.26	54.56
TiO2	1.12	1.16	1.20	1.30	1.26	1.33	1.27	1.14
Al2O3	9.44	10.02	10.41	11.07	11.02	12.23	11.38	12.99
Fe2O3	1.83	1.80	1.90	1.58	1.68	1.45	1.44	2.78
FeO	6.92	6.92	6.75	5.74	5.70	5.06	5.18	9.68
MnO	0.14	0.12	0.13	0.11	0.10	0.09	0.11	0.19
MgO	9.43	8.88	8.09	6.62	6.60	5.30	8.10	4.62
CaO	8.55	8.69	8.99	9.42	8.88	8.14	8.65	8.66
Na2O	2.74	2.84	2.86	1.97	3.30	3.68	2.76	2.93
K2O	0.12	0.11	0.11	0.27	0.12	0.12	0.11	0.90
P2O5	0.07	0.20	0.12	0.25	0.08	0.12	0.02	nd
total=	98.28	99.06	99.58	98.10	98.19	98.54	99.28	98.45
qtz	11.27	11.81	13.05	19.98	14.15	16.41	15.60	7.31
en	15.59	14.74	12.55	9.99	8.73	7.07	13.09	7.12
fs	6.38	6.36	5.65	4.42	3.82	3.25	4.17	8.64
cen	7.90	7.37	7.60	6.49	7.70	6.12	7.09	4.37
cfs	3.23	3.18	3.42	2.87	3.37	2.81	2.26	5.31
cwo	11.98	11.32	11.81	10.04	11.88	9.56	10.19	9.73
or	0.68	0.63	0.63	1.63	0.72	0.73	0.66	5.34
an	13.12	14.31	15.24	20.55	14.90	16.50	18.36	19.63
ab	23.16	23.99	24.24	16.69	27.88	31.14	23.31	24.79
mag	2.65	2.61	2.76	2.29	2.43	2.10	2.08	4.03
ilm	2.12	2.21	2.28	2.47	2.39	2.53	2.42	2.17
ap	0.22	0.60	0.37	0.76	0.25	0.36	0.05	-
temp	1265.00	1253.00	1236.00	1224.00	1206.00	1184.00	1155.00	1148.00
time	25.00	23.50	23.60	477.00	48.00	48.00	95.00	95.00

17 120 3:693 -GL4,00KB,1265C,25HR,F-6.85,+GL+OPXB+PIG+SP
18 120 3:703 -GL4,00KB,1253C,23.5HR,F-7.05,+GL+PIG+SP
19 120 3:707 -GL4,00KB,1236C,23.6HR,F-7.15,+GL+PIG+SP
20 120 3:770 -GL4,00KB,1224C,477HR,F-7.40,+GL+OPXB+PIG+SP
21 120 3:745 -GL4,00KB,1206C,48HR,F-7.60,+GL+PIG+SP
22 120 3:743 -GL3,00KB,1184C,48HR,F-8.00,+GL+PIG+SP
23 120 3:757 -GL4,00KB,1155C,95HR,F-8.15,+GL+PIG+CPX+SP
24 84 3:777 -GL3,00KB,1148C,95HR,F-8.20,+GL+PIG+PLAG+CPX

	25
SiO2	57.83
TiO2	1.13
Al2O3	9.16
Fe2O3	0.90
Cr2O3	0.30
FeO	7.33
MnO	0.10
MgO	9.88
CaO	8.35
Na2O	2.65
K2O	0.06
total=	97.70
qtz	10.71
en	16.94
fs	7.60
cen	7.66
cfs	3.43
cwo	11.89
or	0.37
an	12.93
ab	22.40
mag	1.30
ilm	2.15
chr	0.44
temp	1287.00
time	5.00

25 120 4:218 -GL3,00KB,1287C,05HR,F-8.10,+GL+SP+PIG